NEA/CSNI/R(94)24 Part I

OECD
OCDE
NEA

ISP33

OECD/NEA/CSNI International Standard Problem No.33

PACTEL Natural Circulation
Stepwise Coolant Inventory Reduction Experiment

Comparison Report

VOLUME I

December 1994

COMMITTEE ON THE SAFETY OF NUCLEAR INSTALLATIONS
OECD NUCLEAR ENERGY AGENCY
Le Seine Saint Germain - 12, Boulevard des Iles
F-92130 Issy-les-Moulineaux (France)
Tel. (33-1)45 24 82 00 Fax (33-1)45 24 11 10
Electronic mail : NEA@FRNEAB51

OECD/NEA/CSNI International Standard Problem No. 33 (ISP 33)

PACTEL Natural Circulation Stepwise Coolant Inventory Reduction Experiment

Comparison Report

Volume I

December 1994

H. Purhonen

J. Kouhia

H. Holmström

VTT ENERGY, Nuclear Energy

In 1948, the United States offered Marshall Plan aid to europe, provided the war-torn European countries worked together for their own recovery. This they did in the Organisation for European Economic Cooperation (OEEC). In 1960, Europe's fortunes had been restored; her standard of living was higher than ever before. On both sides of the Atlantic the interdependence of the industrialised countries of the Western World was now widely recognised. Canada and the United States joined the European countries of the OEEC to create a new organisation, the Organisation for the Economic Co-operation and Development. The Convention establishing the OECD was signed in Paris on 14th December 1960.

Pursuant to article 1 of the Convention, which came into force on 30th September 1961, the OECD shall promote policies designed:

- to achieve the highest sustainable economic growth and employment and a rising standard of living in Member countries, while maintaining financial stability, and this to contribute to the development of the world economy;

- to contribute to sound economic expansion in Member as well as non-member countries in the process of economic development; and

- to contribute to the expansion of world trade on a multilateral, non-discriminatory basis in accordance with international obligations.

The original Signatories of the Convention were Austria, Belgium, Canada, Denmark, France, the Federal Republic of Germany, Greece, Iceland, Italy, Luxembourg, the Netherlands, Norway, Portugal, Spain, Sweden, Switzerland, Turkey, the United Kingdom and the United States. The following countries acceded subsequently to the Convention (the dates are those on which the instruments of accession were deposited): Japan (28th April 1964), Finland (28th January 1969), Australia (7th June 1971), New Zealand (29th May 1973) and Korea. The Commission of the European Communities takes part in the work of the OECD (Article 13 of the OECD Convention).

The OECD Nuclear Energy Agency (NEA) was established on 1st February 1958 under the name of the OEEC European Nuclear Energy Agency. It received its present designation on April 20th, 1972, when Japan became its first non-European full Member. NEA membership today consists of all European Member countries of OECD as well as Australia, Canada, the Republic of Korea and the United States. The Commission of the European Communities takes part in the work of the Agency.

The primary objective of NEA is to promote co-operation among the government of its participating countries in furthering the development of nuclear power as a safe, environmentally acceptable and economic energy source.

This is achieved by:

- encouraging harmonization of national regulatory policies and practices, with particular reference to the safety of nuclear installations, protection of man against ionising radiation and preservation of the environment, radioactive waste management, and nuclear third party liability and insurance;

- assessing the contribution of nuclear power to the overall energy supply by keeping under review the technical and economic aspects of nuclear power growth and forecasting demand and supply for the different phases of the nuclear fuel cycle;

- developing exchanges of scientific and technical information on nuclear energy, particularly through participation in common services;

- setting up international research and development programmes and joint undertakings.

In these and related tasks, NEA works in close collaboration with the International Atomic Energy Agency in Vienna, with which it has concluded a Co-operation Agreement, as well as with other international organisations in the nuclear field.

CSNI

The NEA Committee on the Safety of Nuclear Installations (CSNI) in an international committee made up of scientists and engineers. It was set up in 1973 to develop and coordinate the activities of the Nuclear Energy Agency concerning the technical aspects of the design, construction and operation of nuclear installations insofar as they affect the safety of such installations. The Committee's purpose is to foster international co-operation in nuclear safety amongst the OECD Member countries.

CSNI constitutes a forum for the exchange of the technical information and for collaboration between organisations which can contribute, from their respective backgrounds in research, development, engineering or regulation, to these activities and to the definition of its programme of work. It also reviews the safety assessment, including operating experience. It initiates and conducts programmes identified by these reviews and assessments in order to overcome discrepancies, develop improvements and reach international consensus on technical issues of common interest. It promotes the coordination of work in different Member countries including the establishment of co-operative research projects and international standard problems, and assists in the feedback of the results to participating organisations. Full use is also made of traditional methods of co-operation, such as information exchanges, establishment of working groups, and organisation of conferences and specialist meeting.

The greater part of CSNI's current programme of work is concerned with safety technology of water reactors. The principal areas covered are operating experience and the human factor, reactor coolant system behaviour, various aspects of reactor component integrity, the phenomenology of radioactive releases in reactor accidents and their confinement, containment performance, risk assessment, and severe accidents. The Committee also studies the safety of the fuel cycle, conducts periodic surveys of reactor safety research programmes and operates an international mechanism for exchanging reports on nuclear power plant incidents.

In implementing its programme CSNI establishes co-operative mechanisms with NEA's Committee on Nuclear Regulatory Activities (CNRA), responsible for the activities of the Agency concerning the regulation, licensing and inspection of nuclear installations with regard to safety. It also co-operates with NEA's Committee on Radiation Protection and Public Health and NEA's Radioactive Waste management Committee on matters of common interest.

LIST OF CONTENTS

VOLUME I

LIST OF CONTENTS

VOLUME II

ABBREVIATIONS

BARC	Bhabha Atomic Research Centre (India)
CEA	Commissariat a l'Energie Atomique (France)
CL	Cold Leg
CSNI	OECD/NEA Committee on the Safety of Nuclear Installations
DC	Downcomer
DP	Differential pressure
ECN	Netherlands Energy Research Foundation (The Netherlands)
FRG/FZR	Research Centre Rossendorf (Germany)
GRS	Gesellschaft für Anlagen- und Reaktorsicherheit (GRS) mbH (Germany)
HL	Hot Leg
IJS	Institute "Jozef Stefan" (Slovenia)
ISP	International Standard Problem
JAERI	Japan Atomic Energy Research Institute (Japan)
LOCA	Loss of Coolant Accident
LP	Lower Plenum
NEA	Nuclear Energy Agency (OECD)
NRI	Nuclear Research Institute (Czech Republic)
NPPRI	Nuclear Power Plant Research Institute (Slovakia)
OECD	Organisation for Economic Co-operation and Development
PACTEL	PArallel Channel TEst Loop
PSI	Paul Sherrer Institute (Switzerland)
PWR	Pressurized Water Reactor
PZ	Pressurizer
RRC KI	Russian Research Centre Kurchatov Institute (Russia)
RSC KI	Russian Scientific Centre Kurchatov Institute (Russia)
SG	Steam Generator
SEMAR LEACS	Centre de Cadarache (France)
STUDSVIK	Studsvik EcoSafe (Sweden)
TAEK	Turkish Atomic Energy Authority (Turkey)
THZ	Hochshule für Technik und Wirtschaft Zittau/Görlitz (FH) (Germany)
UP-DCMN	University of Pisa, Department of Mechanical and Nuclear Engineering (Italy)
UP	Upper Plenum
VTT	Technical Research Centre of Finland

1. INTRODUCTION

The OECD/NEA/CSNI International Standard Problems (ISPs) have been organized in the areas relevant to the safety of nuclear installations. Particular attention has been paid to thermal-hydraulic behaviour of light water reactors during loss-of-coolant accidents (LOCAs) and transients.

This is the comparison report of the CSNI ISP No. 33 (ISP 33), which is based on a natural circulation experiment with various coolant inventories conducted in PACTEL facility. The PACTEL is owned and operated by the Technical Research Centre of Finland and located at the Lappeenranta University of Technology (LTKK) in Lappeenranta. It is a 1/305 volumetrically scaled, full-height simulator of a Russian type VVER-440 pressurized water reactor.

ISP 33 was approved by the CSNI in 1991 as a double-blind standard problem (i.e., no experimental data from the facility were released before the deadline of calculations). It was also decided to open the ISP for non-OECD participation.

The first workshop for ISP 33 was held in Lappeenranta on February 18-19, 1992 with participants from twelve countries. Finally fourteen organizations from eleven countries submitted fifteen calculations before the deadline of November 30, 1992 (original deadline was November 1, 1992). In addition, five calculations were submitted later within a month. The Second Workshop of ISP 33 was arranged on May 17-19, 1993 in Lappeenranta with participants from eleven countries and nineteen organizations.

Since this ISP was a double-blind problem, the participants had neither the results of the ISP experiment nor any earlier PACTEL experiments. Only the results of the characterization test were given to the participants to make it easier for them to adjust their input decks for the test facility.

This report presents all submitted blind calculational results including those which have been submitted after the deadline, and all posttest results. The mailing date is the labelled date on the envelope and is mentioned in the table of participants. If missing, the date of receipt is used.

The fifteen calculations that were sent before the deadline of the blind calculations were those of RSC KI (1) (Russia), TAEK (Turkey), THZ (Germany), GRS & RSC KI (Germany & Russia), PSI (Switzerland), IJS (1&2) (Slovenia), NPPRI (Slovakia), BARC (1&2&3) (India), NRI Rez (Czech Republic), CEA CE Cadarache (France), STUDSVIK (Sweden) and ECN (The Netherlands). There were five calculations which were sent after the deadline. These were UP-DCMN (Italy), RSC KI (2) Russia, RRC KI (Russia), OKB Gidropress (1&2) (Russia). No results were sent to the organizations before receiving the readable diskettes. RSC KI was an exception: one group got the results soon after the deadline. Three results from RSC KI and RRC KI were received after sending the first set of experimental data to the institute. FZR sent their results in March 1993.

The codes used for the blind calculations were ATHLET Mod 1.0, CATHARE2, DINAMIKA-5, RELAP4/MOD6, RELAP5/MOD2, RELAP5/MOD2.5, RELAP5/MOD3, SCDAP/RELAP5/MOD2 and TECH-M-4.

All posttest calculations which were either presented at the second workshop or submitted separately are included in the posttest part of this report.

Twenty posttest calculations were received from fifteen organisations (THZ, SEMAR LEACS, TAEK, NRI Rez, NPPRI, FZR, IJS, Siemens, ECN, GRS, STUDSVIK, PSI, UP-DCMN, JAERI and RRC KI).

The codes used for the posttest calculations were ATHLET Mod 1.0, CATHARE2, RELAP5/MOD2, RELAP5/MOD3 and SCDAP/RELAP5/MOD2.

This report presents the results of all the calculations and compares them with the experimental data. Chapter 2 describes the PACTEL facility and the ISP 33 experiment, and summarizes the objectives of this ISP and the requested variables. Chapter 3 presents the summaries of the participants, the computer codes and the nodalizations used for the blind calculations. The blind calculations are compared with the experimental data in Chapter 4. Participants for the posttest calculations are listed in Chapter 5. Posttest calculations are compared with experimental data in Chapter 6. Overall conclusions are drawn in Chapter 7. Reports of the participants are presented in Part II of the report.

The experiment was conducted twice: The first experiment (base case) was terminated when the cladding temperatures exceeded a specific limit. In the second one (variation case) the secondary side control valve was opened after core heatup to decrease the secondary and primary pressure to cause flashing and cooling of the core. Due to the stepwise coolant inventory reduction the secondary side pressure reduction in the optional variation case was not as effective as it would be in continuous coolant inventory reduction. This is why only the experimental results of this pressure reduction are included in the report, but not the comparisons with the calculations.

This ISP addresses the specific features of VVER-440 reactors, but also has general interest in code assessment and development. A large primary volume, horizontal steam generators, loop seals in both hot and cold legs affect the natural circulation in degraded primary inventory situations. At the second workshop there was a general consensus that this ISP was beneficial for the participants and produced valuable VVER related experimental data.

Three main problems with respect to the experiment were noticed during the ISP:

The core power measurement is not very accurate at low power levels. A core power level of 165 kW (instead of 155 kW) was proposed to be used in the post-test calculations. The measured temperature difference over the core cannot be directly used when estimating the actual core power.

The safety valve on the top of the upper plenum leaked during the pressure peaks. The coolant mass lost through the valve is estimated having been about 10 kg.

Steam generator tubes seem to hold some amount of water inside them during the transient, but there was no instrumentation to measure it directly.

2. FACILITY AND EXPERIMENT DESCRIPTION

2.1 Facility Description

PACTEL is a volumetrically scaled (1:305), out of pile model of Russian design VVER-440 pressurized water reactors used in Finland, Figure 2.1.

The maximum operating pressures on the primary and secondary sides are 8 MPa and 4.6 MPa respectively, while the corresponding values in VVER-440 are 12.3 MPa and 4.6 MPa. The reactor vessel is simulated with a U-tube construction including separate downcomer and core sections. The core itself consists of 144 full-height, electrically heated fuel rod simulators with a chopped cosine axial power distribution and a maximum total power output of 1 MW, 22 % of scaled full power. The fuel rod pitch (12.2 mm) and diameter (9.1 mm) are identical to those of the reference reactor. The rods are divided into three roughly triangular-shaped parallel channels representing the intersection of the corners of three hexagonal VVER rod bundles.

Component heights and relative elevations correspond to those of the full-scale reactor to match the natural circulation gravitational heads in the reference system. The hot and cold leg elevations of the reference plant have been maintained, including the loop seals. The hot leg loop seals are a result of the steam generator locations, which are at roughly the same elevation as the hot leg connections to the upper plenum. The hot and cold leg connections to the steam generators are at the bottom of each collector, and a U-shaped pipe must be used. The cold leg loop seals are result from the elevation difference between the inlets and outlets of the reactor coolant pumps, just like in other PWRs.

For practical reasons, the total hot and cold leg pipe lengths of the reference plant were not maintained in the PACTEL facility, but were shortened by almost a factor of two. As a result, the pipe cross-sectional area was increased to preserve the volume scaling factor used for the remainder of the facility and preserve the time scale for energy transport from the heat source to the sinks. As a consequence of the increased cross-sections the Froude number in the loop seals becomes closer to that of the full-scale plant.

Three coolant loops with double capacity steam generators are used to model the six loops of the reference power plant. The U-tube lengths and diameters of the PACTEL steam generators correspond to those of the full-scale models, but the overall height is smaller. The horizontal orientation of these steam generators is one of the unique features of the VVER design. One consequence of this geometry is a reduced driving head for natural circulation. Another notable feature is the relatively large secondary side water inventory, which tends to slow down the progression of transients.

The facility includes a pressurizer, high and low pressure emergency core cooling systems, and an accumulator. The primary pumps were installed later in the beginning of 1993.

2.2 Instrumentation

There are about 400 channels available for instrumentation in the data acquisition system of the facility. The instrumentation consists of temperature, pressure, differential pressure and flow measurements. Also the core power is measured with a built-in instrument of power supply.

Temperatures are measured by K-type mineral insulated thermocouples and Pt100 resistance thermometers. All the thermocouples are ungrounded, the outer diameter varies from 0.5 to 3.0 mm depending on the locations. Cladding temperatures are measured using two different methods: spotwelded thermocouples on the outer surface of the cladding and thermocouples inside the cladding. Only the outer surface thermocouples were used in this ISP.

System pressures are measured using pressure transducers in the pressurizer, in the upper plenum and in the secondary side of the steam generators.

Differential pressures are measured along the whole facility to obtain a satisfactory overall pressure loss distribution. The DP transducers are used also for collapsed level measurements.

The downcomer and loop mass flows are measured by venturi tubes and the draining mass flow is measured by a vortex type flow meter. Electromagnetic flow meters are used to measure the mass flows in the ECCS and the feed water to the steam generators.

The locations of the temperature, pressure and differential pressure measurements are presented in Figures 2.2 and 2.3 The accuracies of the measurements are presented in Tables 2.2 through 2.6. The accuracy of the temperature measurements is ±3.0 K, except for the saturated temperature SAT_TEMP (±1.5 K).

2.3 Objective of ISP 33

In a typical standard problem an expected accident scenario of the reference plant is simulated as a complete transient. The VVER-440 type reactor is addressed for the first time by a CSNI international standard problem. That is why a natural circulation experiment was considered particularly suitable. In a typical LOCA event the transitions between different two-phase flow natural circulation modes are continuous and dominate the scenarios. Many standard problems have indicated the difficulties in calculating the natural circulation well.

The main goal of ISP33 and the corresponding experiment was to study natural circulation in a VVER plant including several single- and two-phase natural circulation modes. The heat generated in the core is transported by the coolant to the steam generator. The steam generator secondary side conditions were held constant, eliminating disturbances caused by the secondary pressure variation. The primary coolant mass was reduced stepwise in the liquid form, and the amount of the drained water was given as a boundary condition. The expected periods were:

- single-phase natural circulation,

- two-phase natural circulation with continuous liquid flow

- natural circulation of reflux boiling type. Heat is transported by saturated steam to steam generators and condensed there. The resulting water is then returned to the pressure vessel via the cold legs and the downcomer.

- cooling of the uncovered core with partially superheated steam. The steam generators are still capable of removing heat from primary circuit.

The draining period is very short compared to the stabilizing period. That is why the different natural circulation mechanisms are clearly identified during the experiment. If the primary coolant inventory is exactly known, even limited instrumentation provides sufficient information about the distribution of coolant in different natural circulation modes. It was expected that the characteristics of natural circulation at constant pressure is mostly dependent on the primary coolant inventory and the core power level.

2.4 Experiment Conditions

2.4.1 Initial conditions

1) The heating power was adjusted to be suitable for the experiment. The power recommended to the blind predictions was 155 kW and 165 kW for the open calculations.

2) The liquid mass drained in a single step was adjusted to give different physical characteristics for the natural circulation modes.

3) Two kinds of experiments were conducted varying the end of the experiment:

   A) Experiments which were terminated by switching the core power off when the core temperature started to increase.

   B) Experiments which were continued by reducing the secondary pressure. The core power was switched off after the core heat-up began again.

4) After it was demonstrated that the experiments could be repeated, one type experiment (of type B) was selected as the basis for ISP 33.

Before the experiment initiation the facility was operating at steady state conditions, at 165 kW power level. The pressurizer heaters were on and the secondary pressure was controlled by control valves.

The initial conditions at 0.0 s were:

Pressurizer pressure	P02PZ_16490	7.39 MPa
Steam generator pressure	P04SG1_9800	4.18 MPa
Downcomer flow	FDC	1.47 kg/s
Pressurizer level	LEPZ	5.18 m
Steam generator levels	LESG1	0.271 m
	LESG2	0.272 m
	LESG3	0.263 m
SG feedwater temperature		32 °C
Pressurizer heater power	E_HEATERS	2 kW

2.4.2 Experiment

During the whole experiment the steam generator level control was maintained. The secondary pressure was controlled by a PI controller. The different steps during the experiment were:

Time (s)	Event
0.0	Start of the experiment and the data gathering.
1200	~60 kg water is drained in 180 seconds from the lower plenum. The pressurizer heaters are switched off at the same time to protect the heating elements.
2100	~60 kg water is drained in 60 seconds from the lower plenum.
3000	~60 kg water is drained again in 60 seconds from the lower plenum .
	The draining procedure is continued after this in the same way with 900 second intervals. Each time 60 kg water is drained from the lower plenum.

The secondary pressure was reduced by opening the steam line control valve after the core began to heat-up for the first time. The experiment was terminated after the core temperatures began to rise again.

2.4.3 Boundary conditions

The pressurizer heater power was cycling with 2 kW and 6 kW power, setpoints for switching were 7.36 MPa and 7.50 MPa.

The experiment also included a reduction of the secondary side pressure by opening the relief valve on the secondary side, for reducing the primary side pressure and for causing the water level to rise in the core and to cool it.

The maximum used capacity for one steam generator feedwater injection was 0.063 kg/s, the initial feedwater mass flow to one steam generator being 0.018 kg/s. The injection was adjusted manually for maintaining a constant steam generator water level. During the experiment typical level variation was 0.263 ... 0.284 m. Due to the large water inventory in the secondary side no fast automatic control was needed.

The estimated temperature of the surrounding athmosphere was 36 °C during the ISP 33. The heat losses were about 3 kW from the pressurizer, 20 kW from the primary side (excluding the pressurizer) and 7.5 kW from the secondary sides. The pressurizer heaters were tripped off at 1200 s of the transient due to the low water level in the pressurizer.

2.5 Summary of Experimental Results

The ISP 33 experiment was performed to investigate natural circulation flow behaviour under quasi-steady state conditions at several different primary side inventory levels. Core power level of 3.7% of the scaled nominal power was selected for this test. Before the experiment the facility was heated until it reached the selected temperature and pressure, and a steady state was established at these conditions. The primary coolant was drained from the lower plenum in several steps, allowing the system to restabilize for 900 seconds between each step. For the duration of the test, the secondary side conditions were maintained near the nominal full power operating conditions of the reference plant. The main events during the ISP 33 experiment are listed in Table 2.1. The plots of measured parameters are presented in Figures 2.4 through 2.49.

The effect of the first draining was a rapid decrease of the primary pressure until saturated conditions were reached at the core outlet. Almost all the water in the pressurizer flowed into the hot leg of loop one. The fluid temperature in the hot leg decreased temporarily when the subcooled water slug from the pressurizer surge line reached the hot leg. Vapour started to accumulate at the top of the upper plenum. The flow in the downcomer remained single-phase with a nearly constant flow rate.

During the second draining the amount of vapour in the upper plenum increased rapidly. The loop and the downcomer mass flow rates increased. When the swell level in the upper plenum fell below the hot leg nozzles, voiding also began in the the hot legs. The flow rate dropped and became stagnant. The loop seals prevented the vapour to reach the steam generators. This flow stagnation was observed in all three loops simultaneously. The system pressure rose sharply since energy transfer to the steam generators was interrupted. Fluid temperatures in the upper plenum, hot legs and at the core outlet rose.

When the pressure increased, water flowed back into the pressurizer. After about two minutes of flow stagnation and a continued increase in the pressurizer water level, all three loop seals cleared and a surge of two-phase flow into the steam generators reduced the pressure. As the pressure dropped, a fraction of the water in the pressurizer returned to the loop and the flow stagnated again initiating another system pressure increase. This was repeated two additional times, with the peak water level in the pressurizer decreasing with each cycle. During the highest pressure peaks approximately 10 kg of coolant escaped through the safety valve leak at the top of the upper plenum.

During the next draining the primary pressure dropped quickly. Temperatures in the upper plenum followed the saturation temperatures. The pressurizer was depleted again and primary mass flow rates increased. When the draining stopped a relatively steady two-phase flow was

established between 3000 s and 4000 s. The bulk of this flow took place through one loop, though none of the loops was totally stagnant. The two loops with low flow rates had partially filled hot leg loop seals while the third loop seal was clear.

Table 2.1. The main events in ISP 33 experiments.

0 s	P_{core} = 165 kW, p_{prim} = 7.39 MPa, $P_{pzheaters}$ = 2 kW, p_{sec} = 4.18 MPa
420 s	$P_{pzheaters}$ = 6 kW, p_{prim} = 7.36 MPa
680 s	$P_{pzheaters}$ = 2 kW, p_{prim} = 7.50 MPa
1200 s	$P_{pzheaters}$ = 0 kW, - 1st draining 58.0 kg, - pressurizer almost empty after draining, - no significant voiding in upper plenum, - saturation pressure reached, - slightly increased mass flow rate
2100 s	- 2nd draining 64.5 kg, - upper plenum voiding, - swell level near hot leg connections, - stagnant periods, - flow through single loop, - pressure rise, - increasing pressure pushes coolant to the pressurizer
3000 s	- 3rd draining 61.8 kg, - pressure drops, - pressurizer empty, - two-phase flow through the 3rd loop, - single-phase flow in cold legs
3900 s	- 4th draining 58.9 kg
4800 s	- 5th draining 58.6 kg
5700 s	- 6th draining 60.3 kg
6600 s	- 7th draining 58.5 kg
6660 s	- cladding temperatures start to rise

As the inventory was reduced further the water level in the two filled loop seals dropped and the flow rates continued to decline, finally becoming nearly stagnant. The heat transfer mechanism from primary to secondary changed to a boiler-condenser mode. Steam was condensed in the steam generators, collected in the cold legs, and returned to the core via the downcomer. The downcomer flow rate was quite low although the energy was transferred efficiently. Reflux condensation was not observed because of the steam generator and hot leg loop seal geometries. Condensation took place in the horizontal U-tubes, but there was no driving force for back flow towards the hot leg and the upper plenum. Moreover, it is apparent that a steady flow of condensate back into the hot leg would eventually fill the loop seal and block the steam flow.

It is noted that the ability of the steam generator to retain significant amounts of condensate has a tendency to shorten the time available before the core heat-up starts.

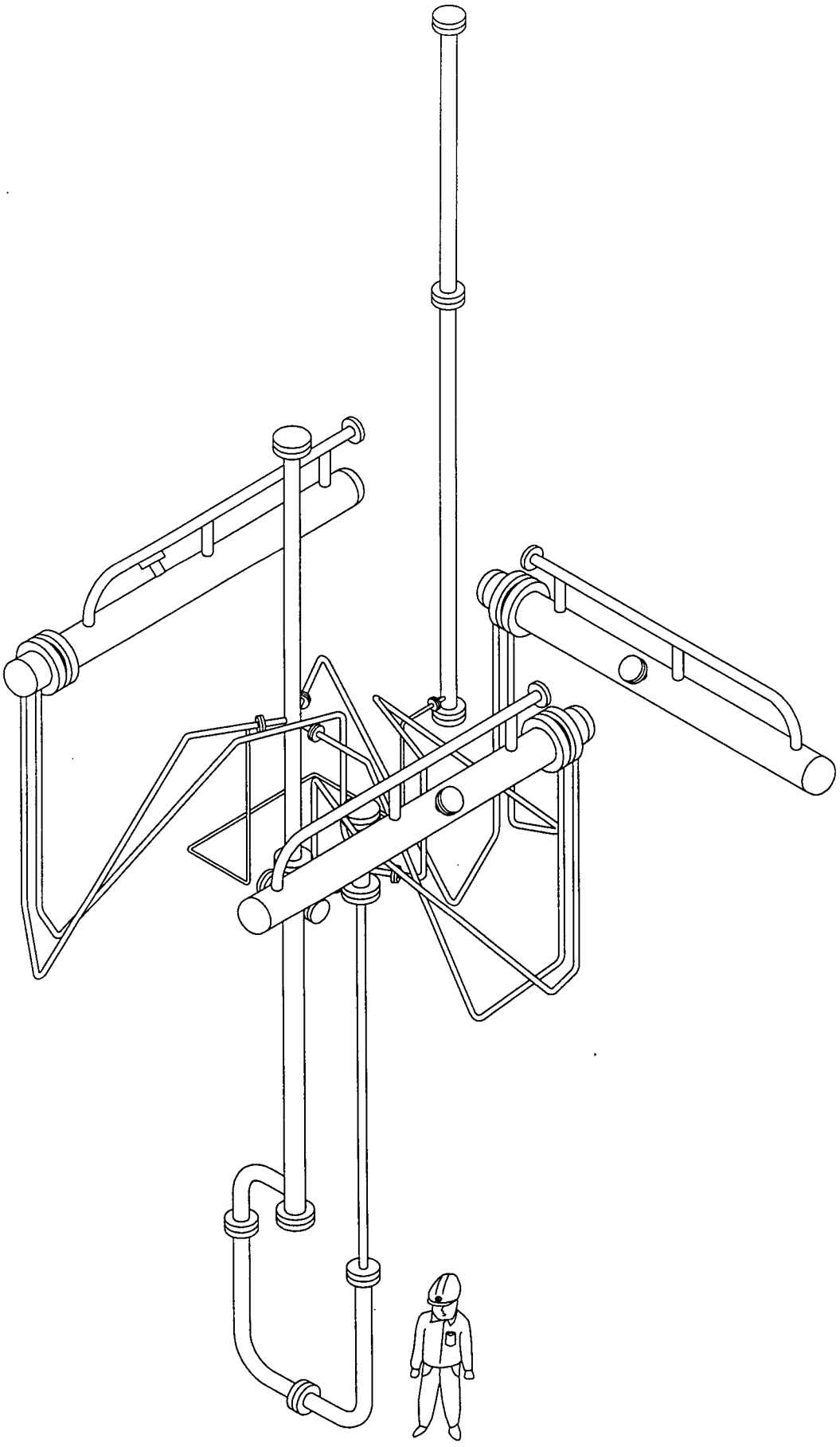

Figure 2.1. PACTEL facility.

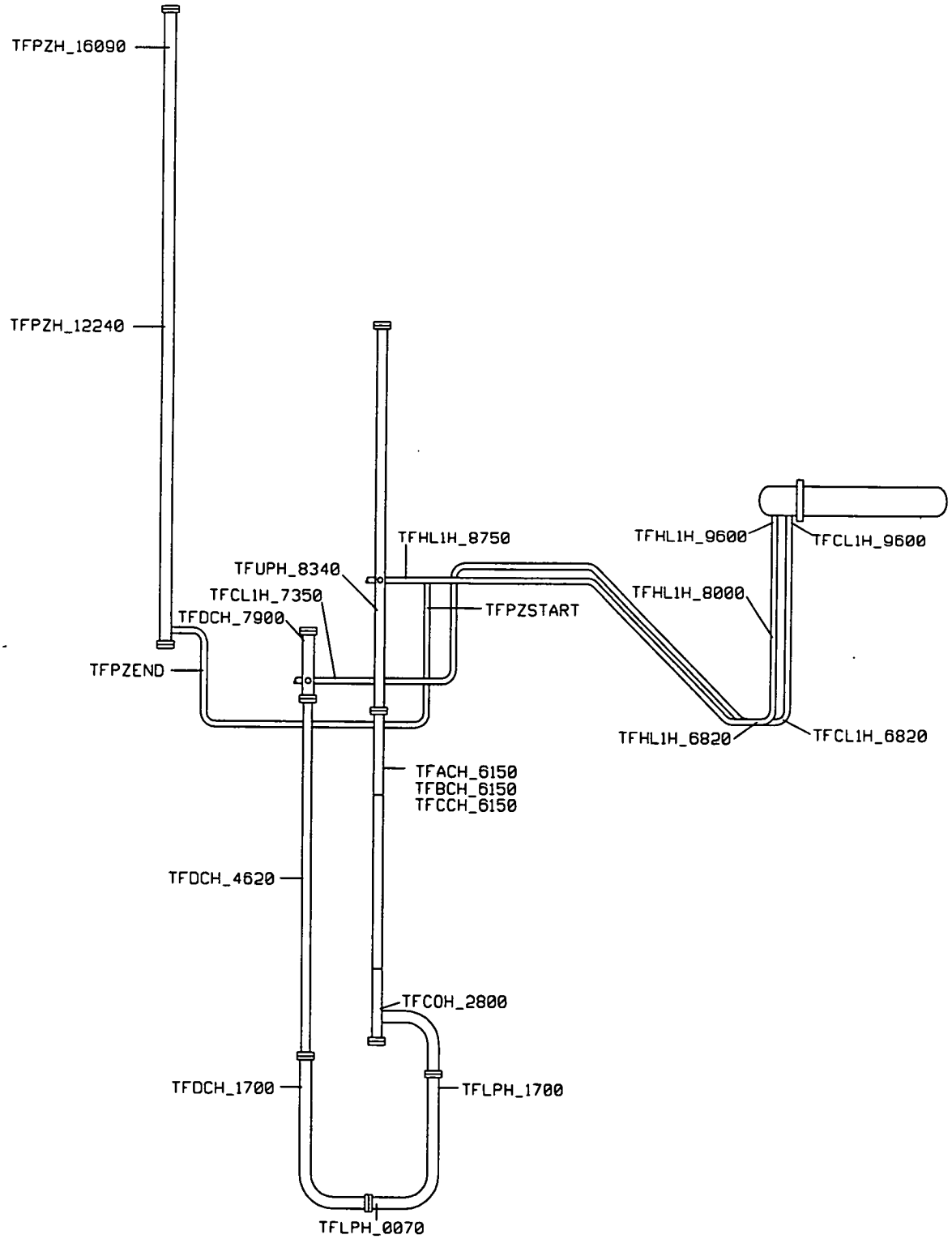

Figure 2.2. Fluid temperature measurements in the PACTEL facility.

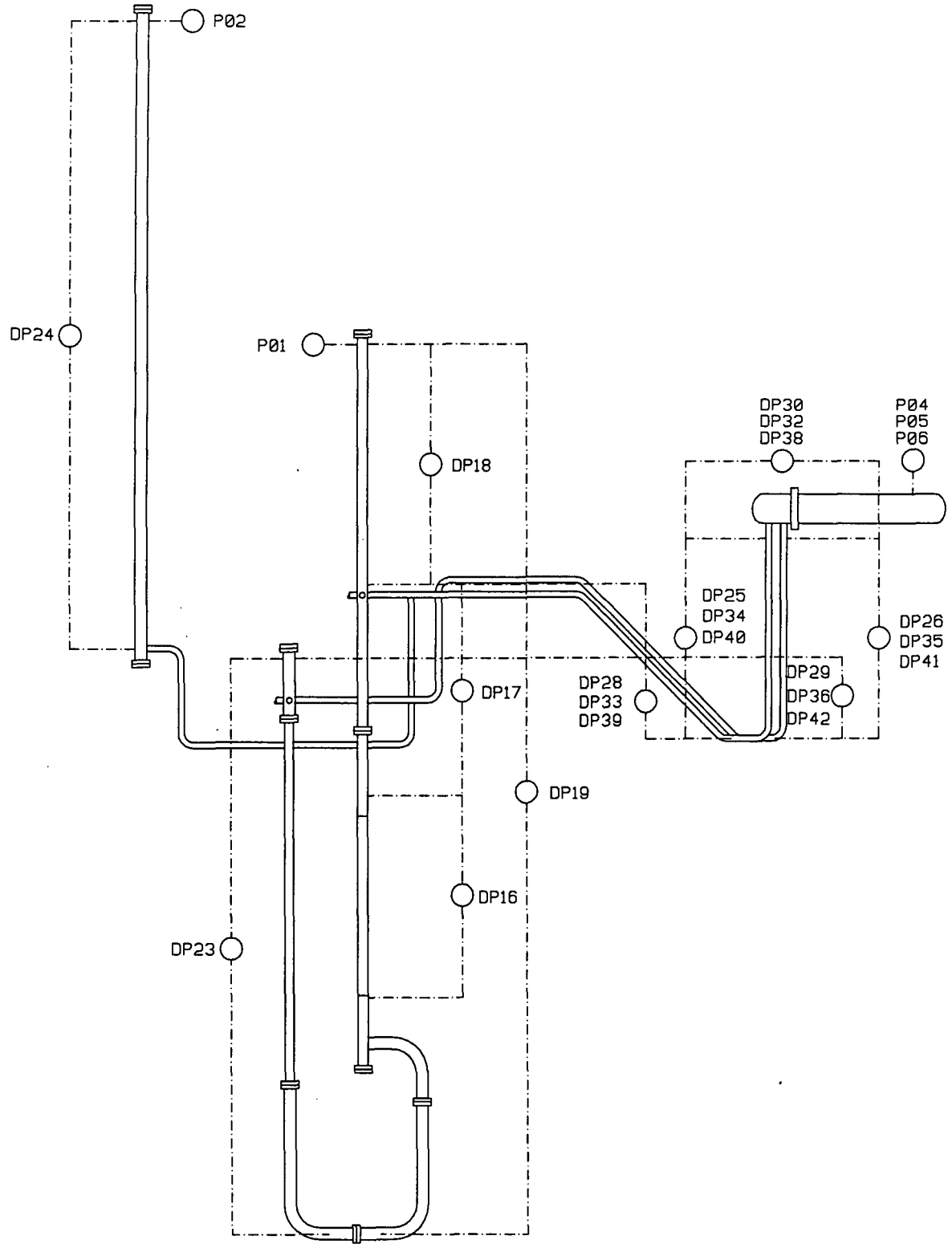

Figure 2.3. Differential pressure and pressure measurements in the PACTEL facility.

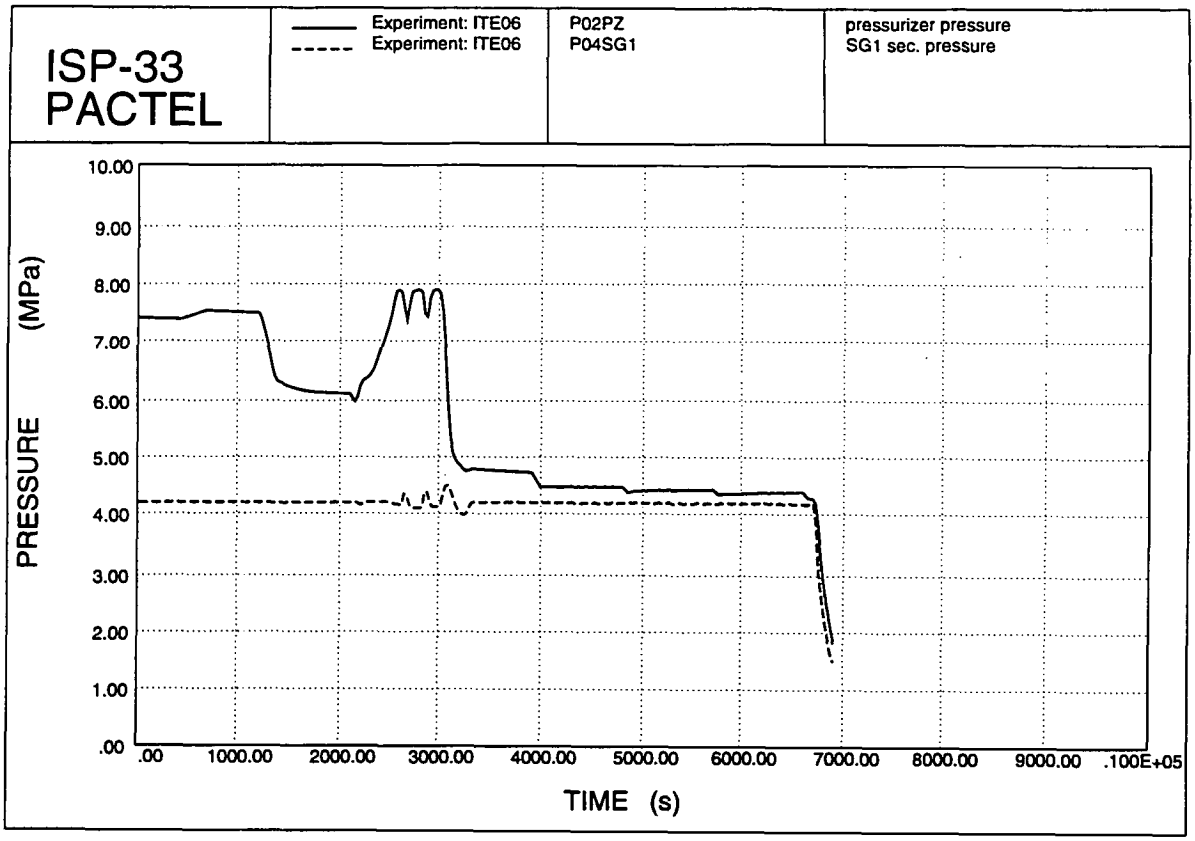

Figure 2.4. Primary and secondary pressures.

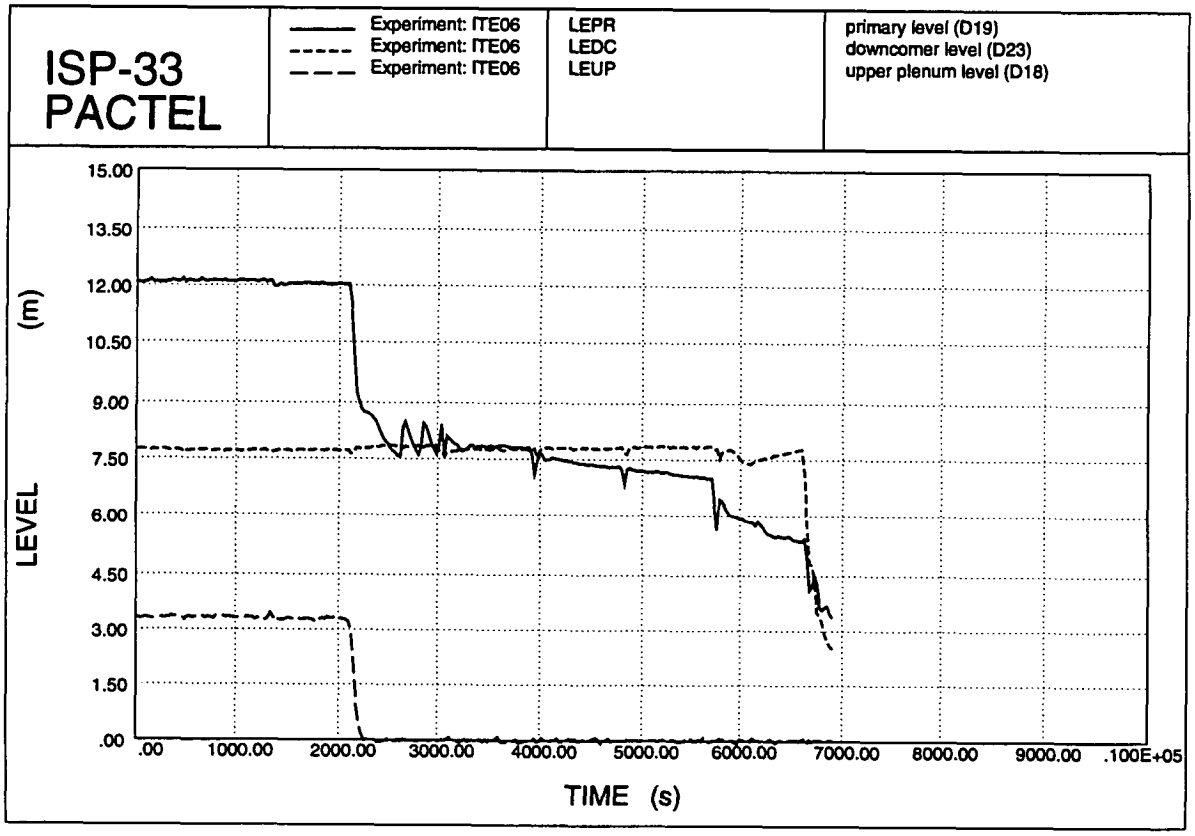

Figure 2.5. Primary levels.

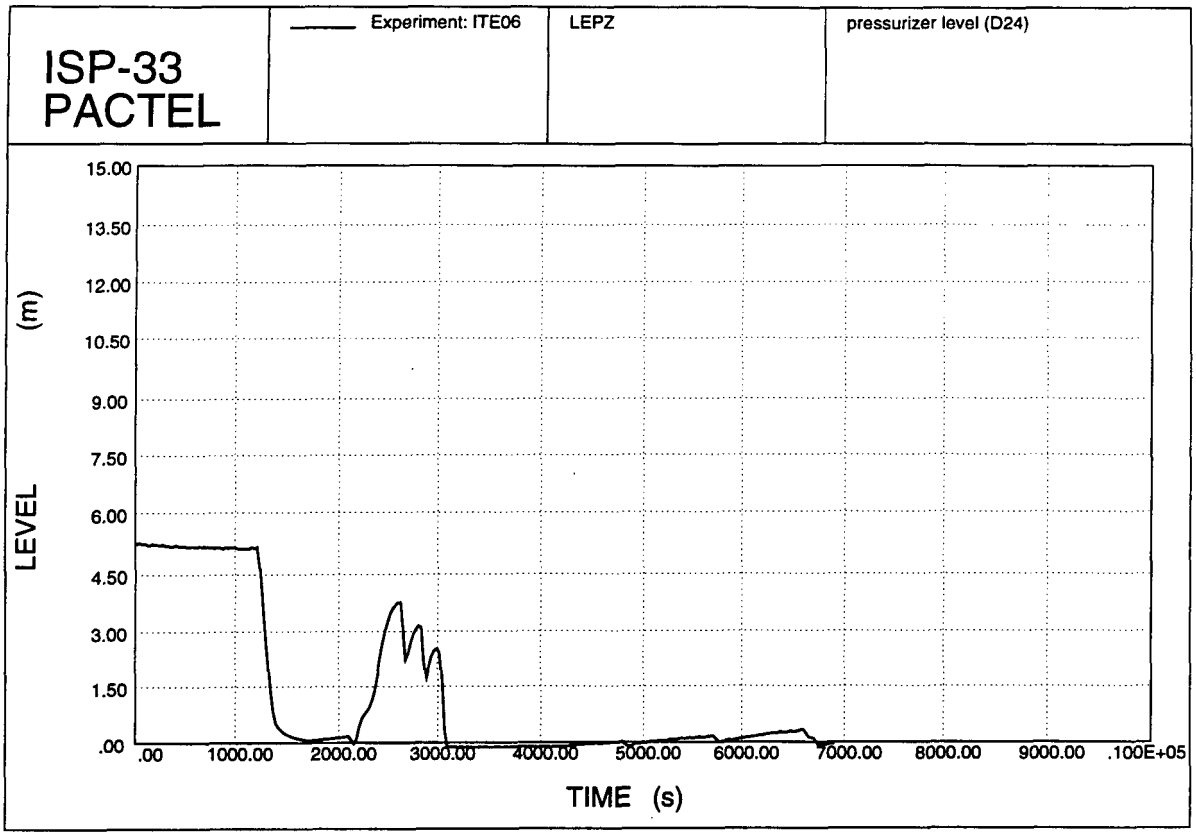

Figure 2.6. Pressurizer level.

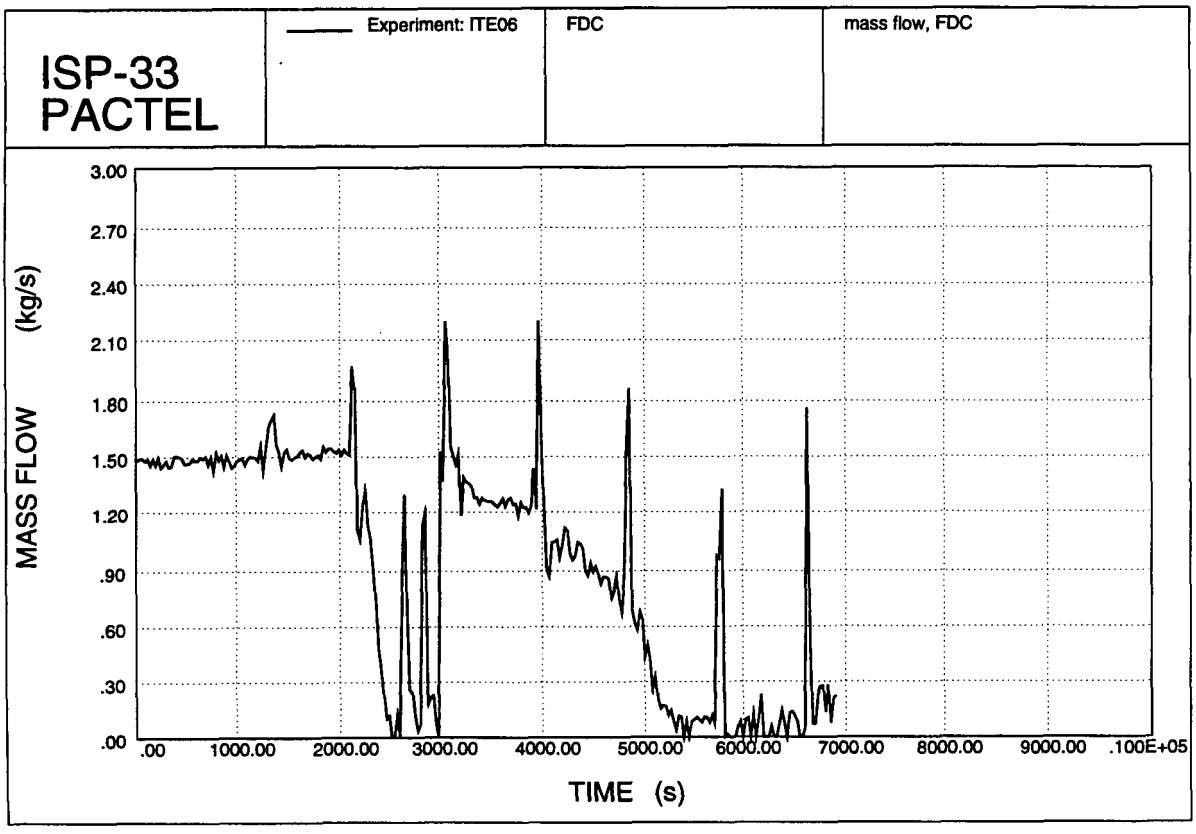

Figure 2.7. Downcomer mass flow rate.

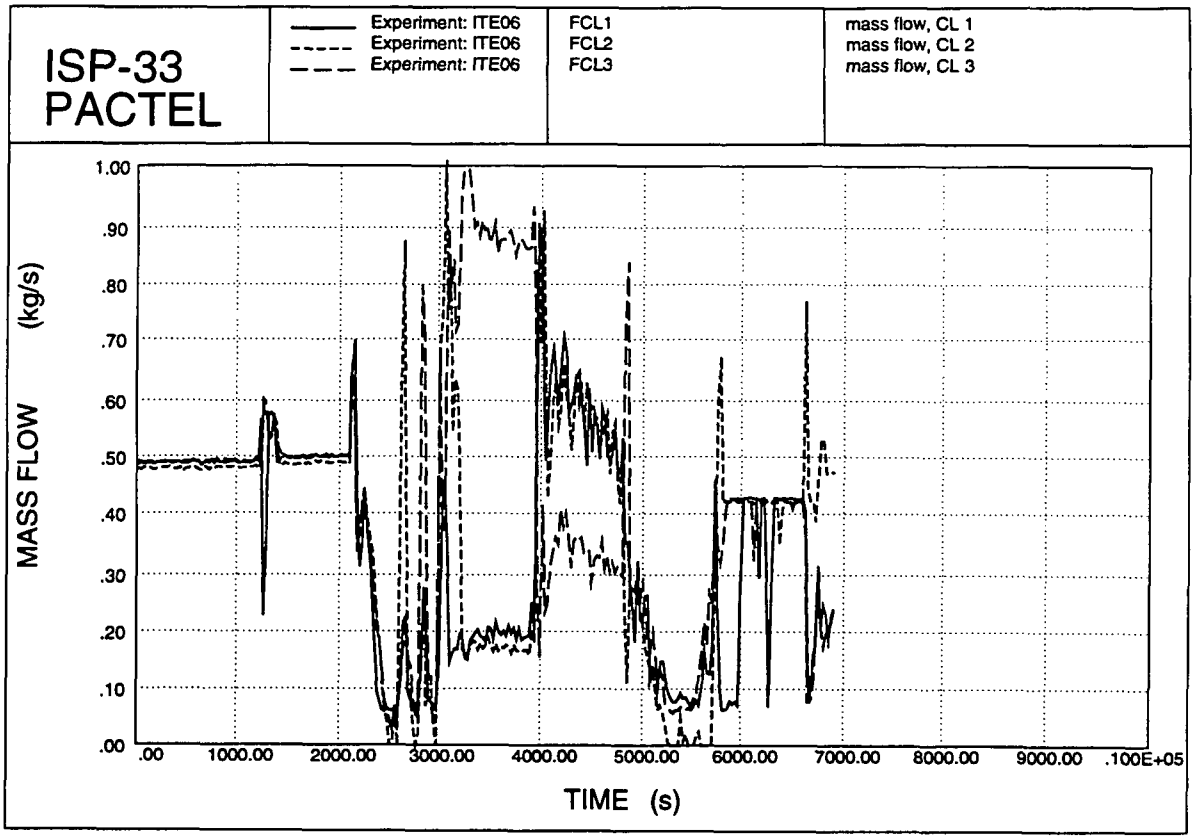

Figure 2.8. Cold leg mass flow rates.

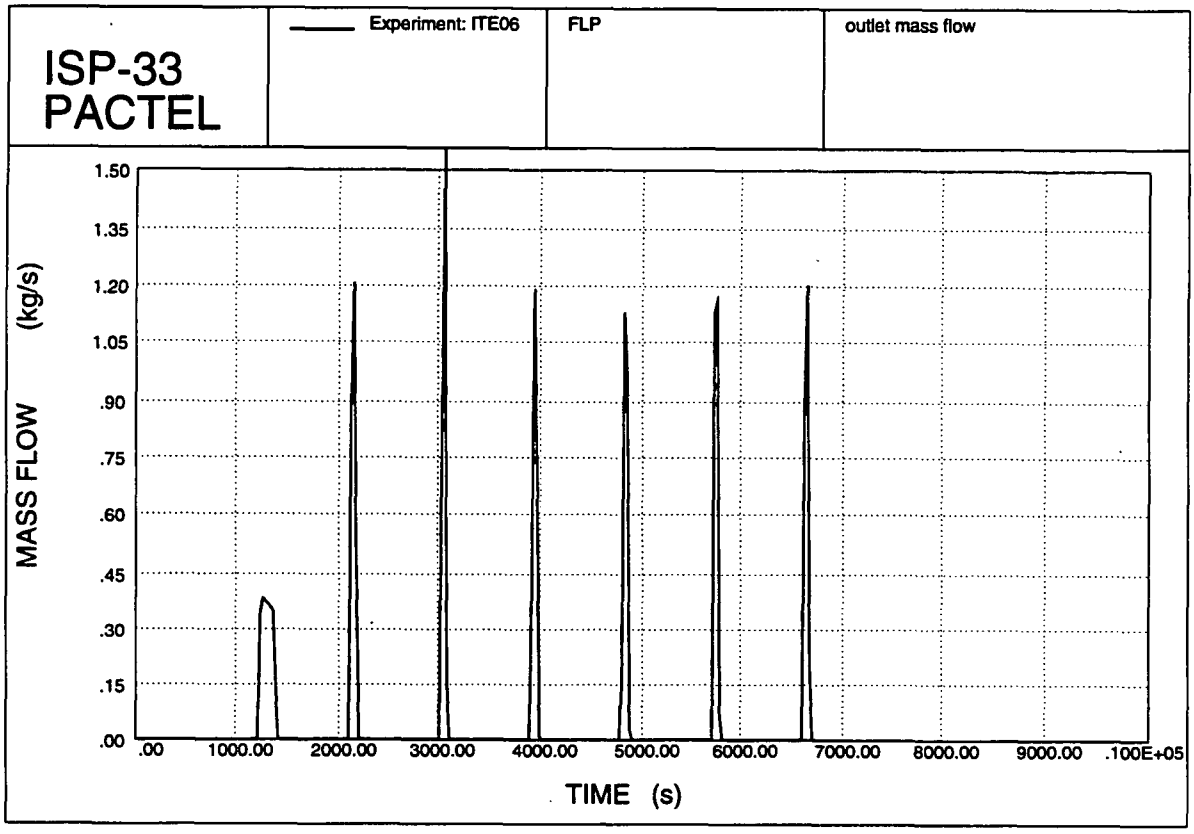

Figure 2.9. Drained mass-flow from the downcomer.

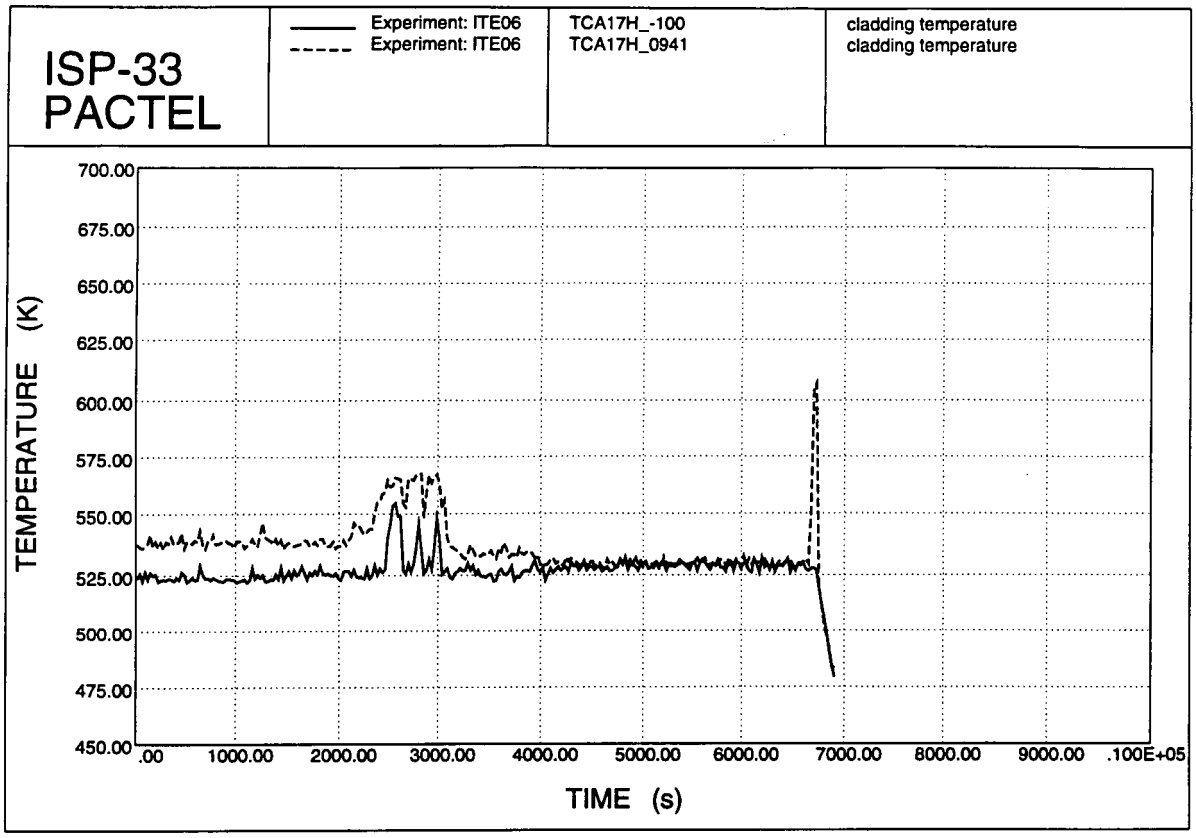

Figure 2.10. Rod 17 cladding temperatures.

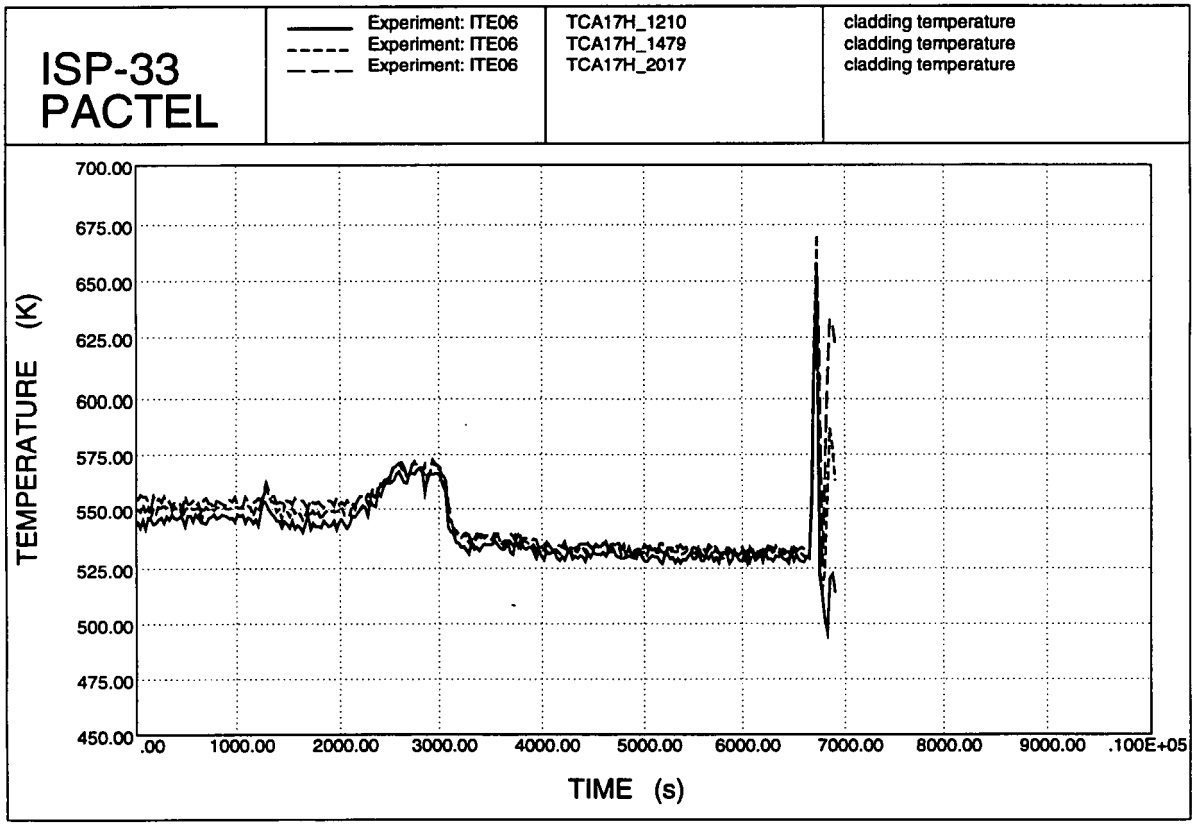

Figure 2.11. Rod 17 cladding temperatures.

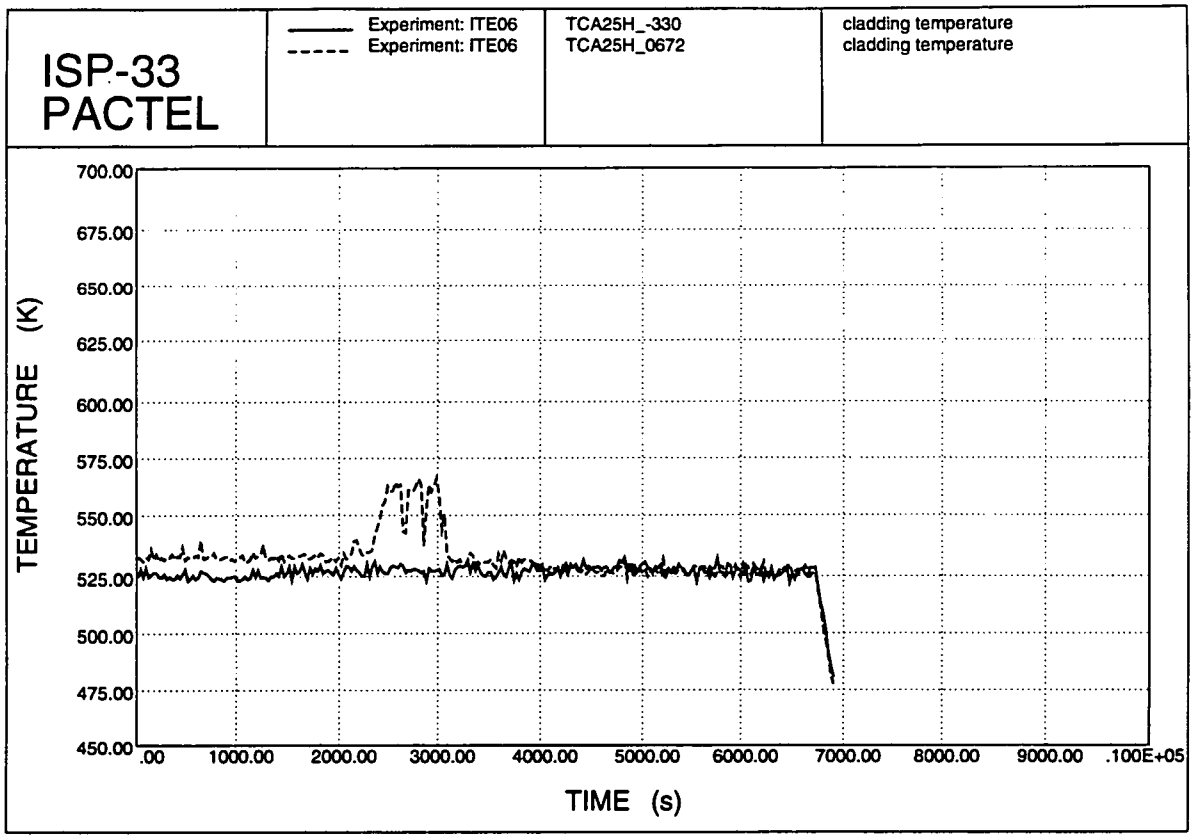

Figure 2.12. Rod 25 cladding temperatures.

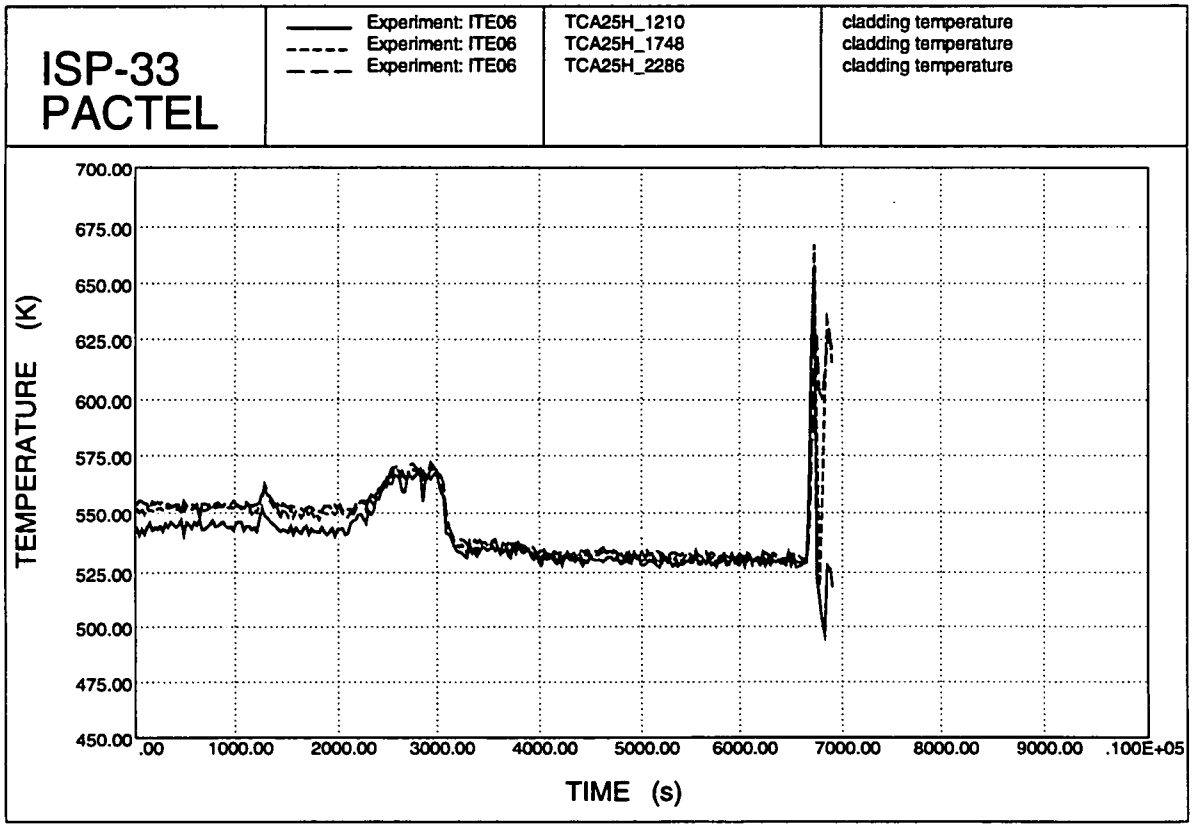

Figure 2.13. Rod 25 cladding temperatures.

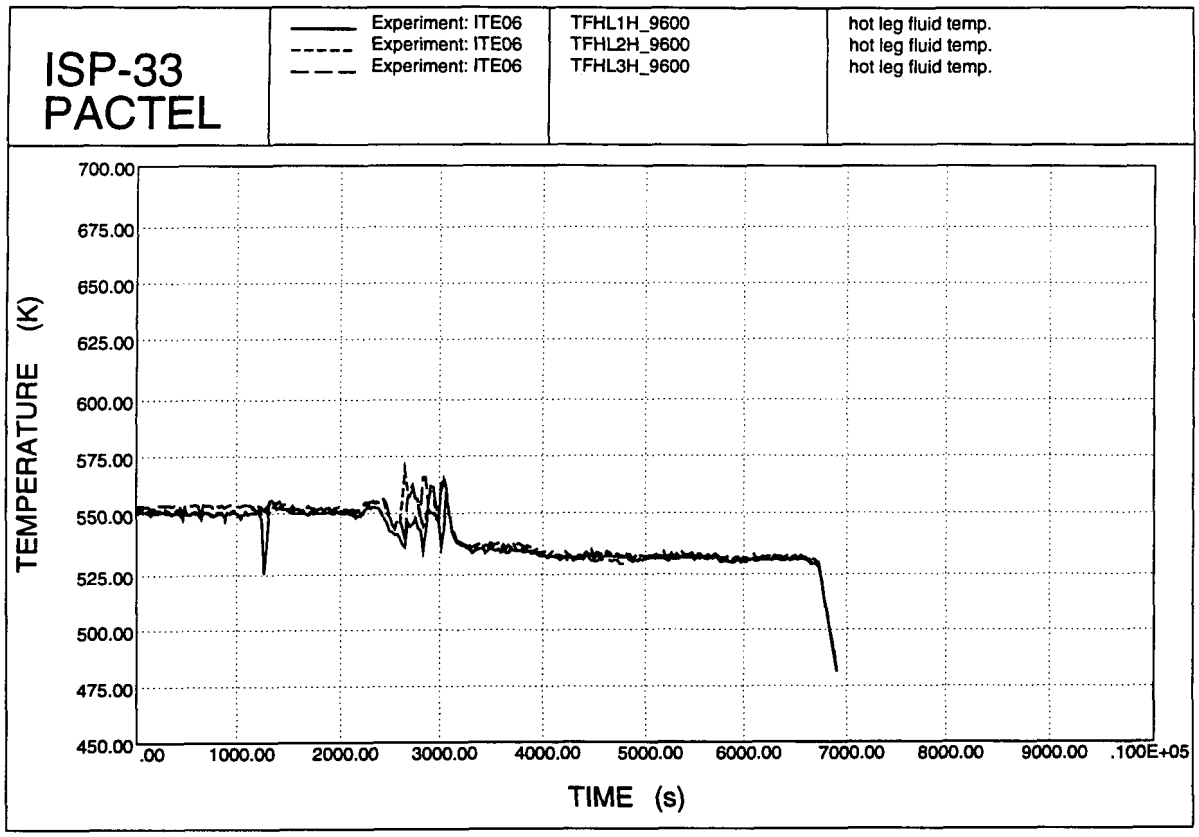

Figure 2.14. Hot leg coolant temperatures.

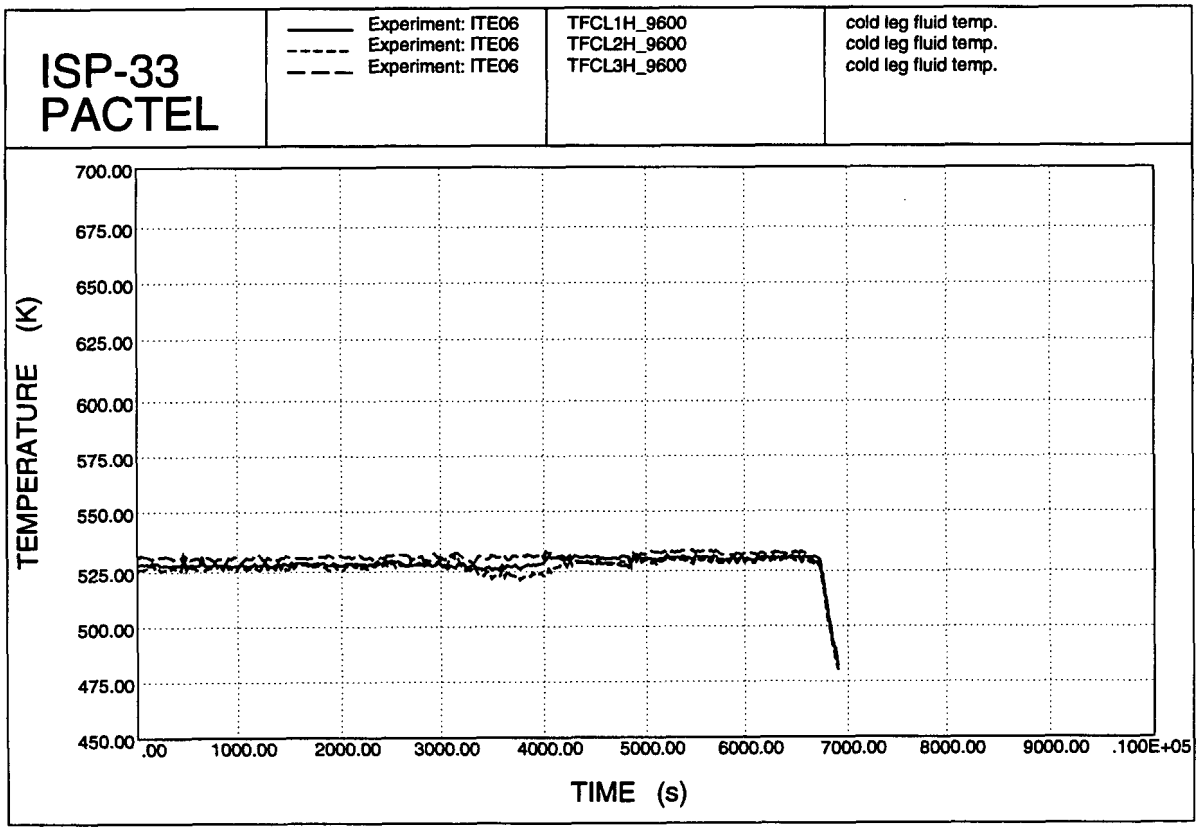

Figure 2.15. Cold leg coolant temperatures.

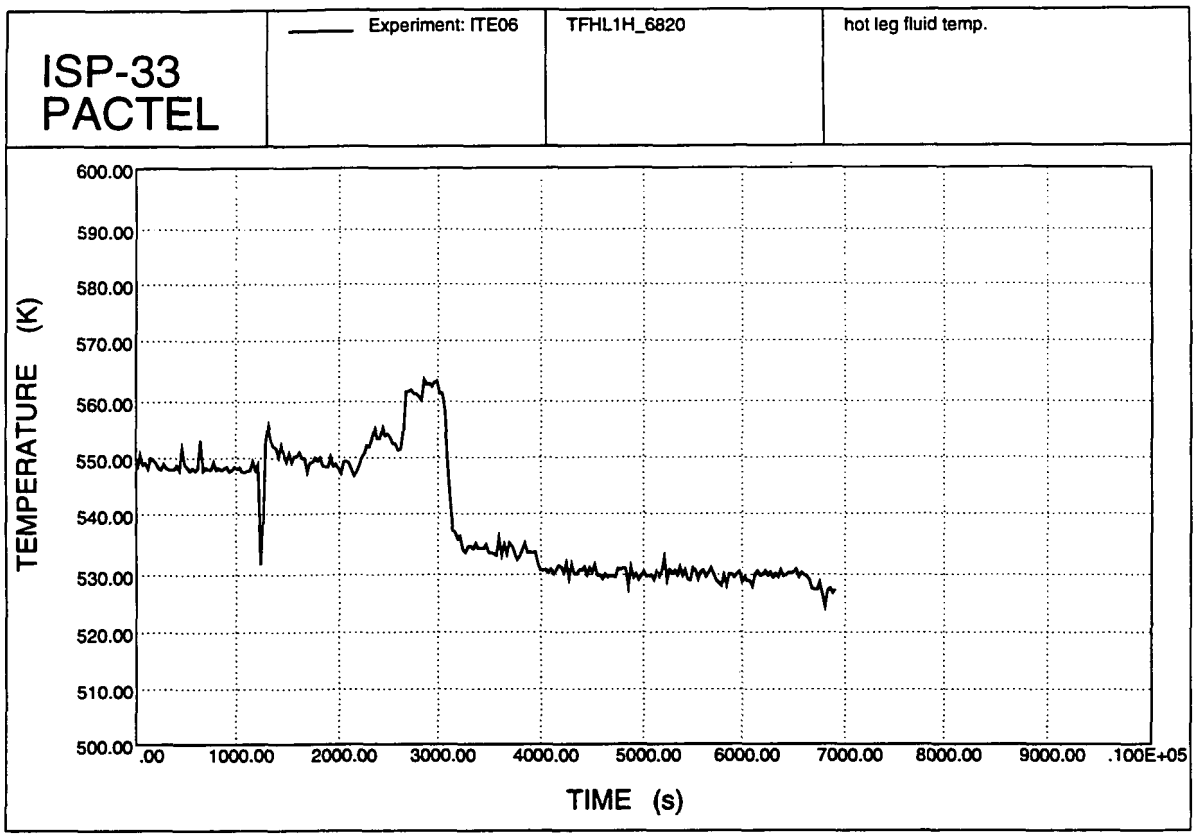

Figure 2.16. Loop 1 coolant temperatures.

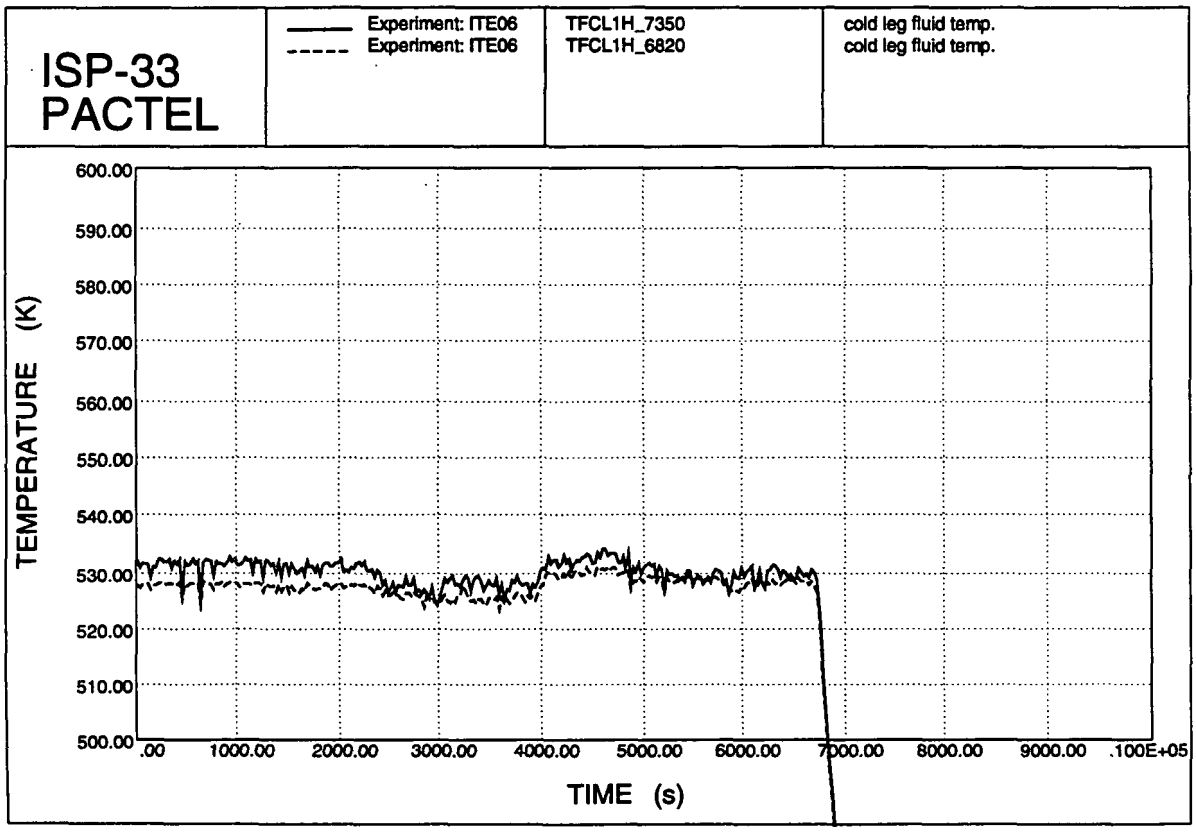

Figure 2.17. Loop 1 coolant temperatures.

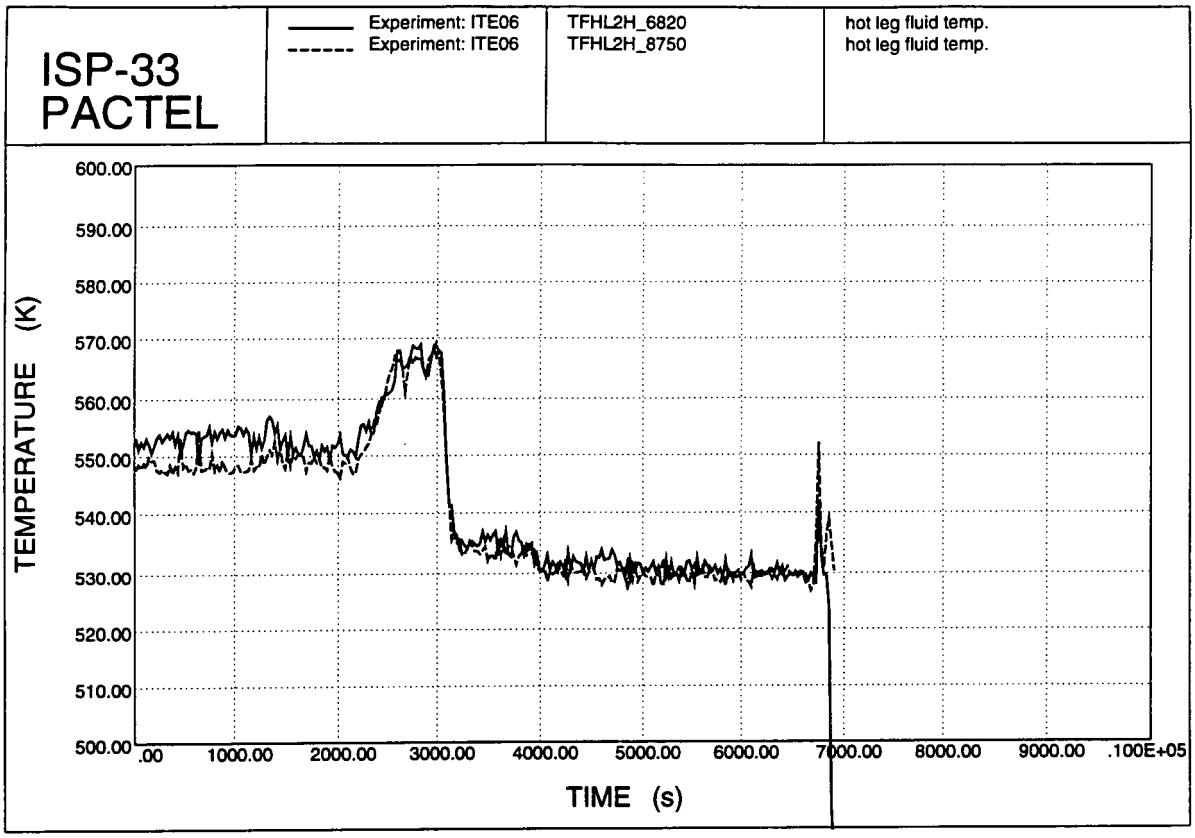

Figure 2.18. Loop 2 coolant temperatures.

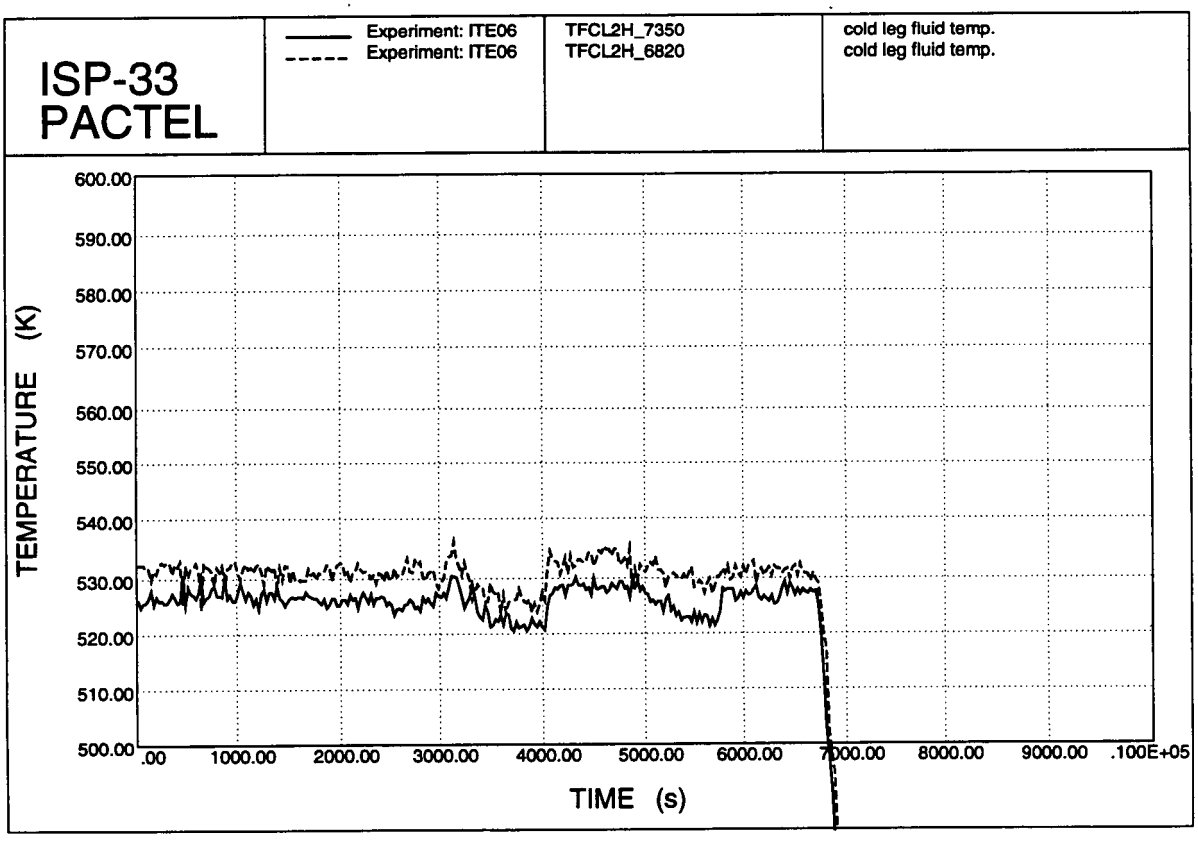

Figure 2.19. Loop 2 coolant temperatures.

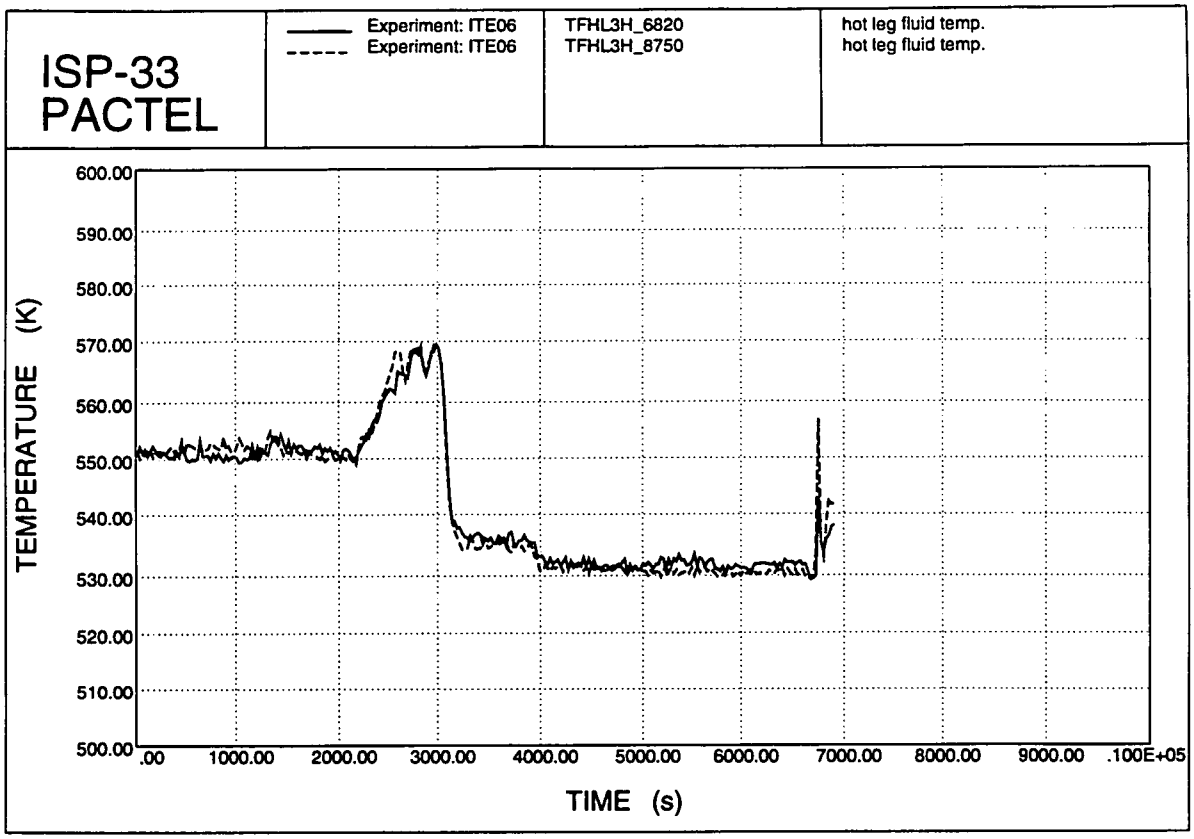

Figure 2.20. Loop 3 coolant temperatures.

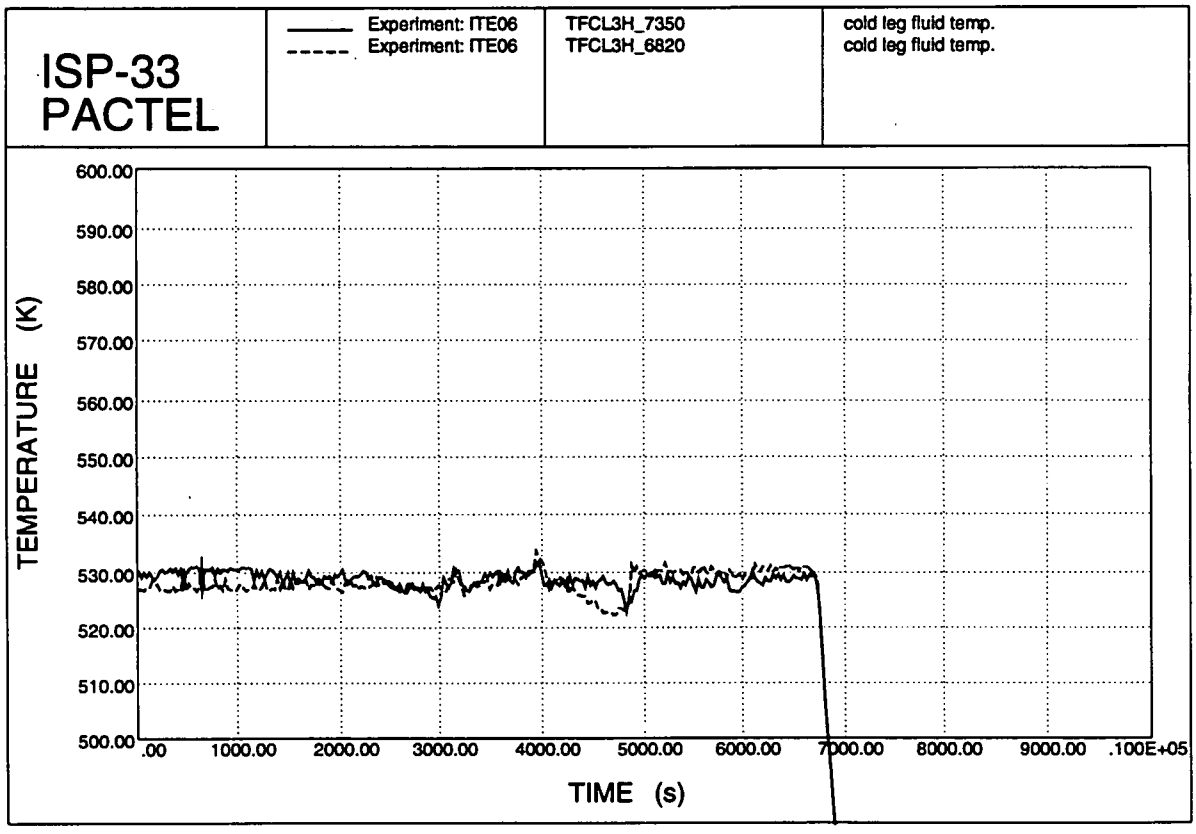

Figure 2.21. Loop 3 coolant temperatures.

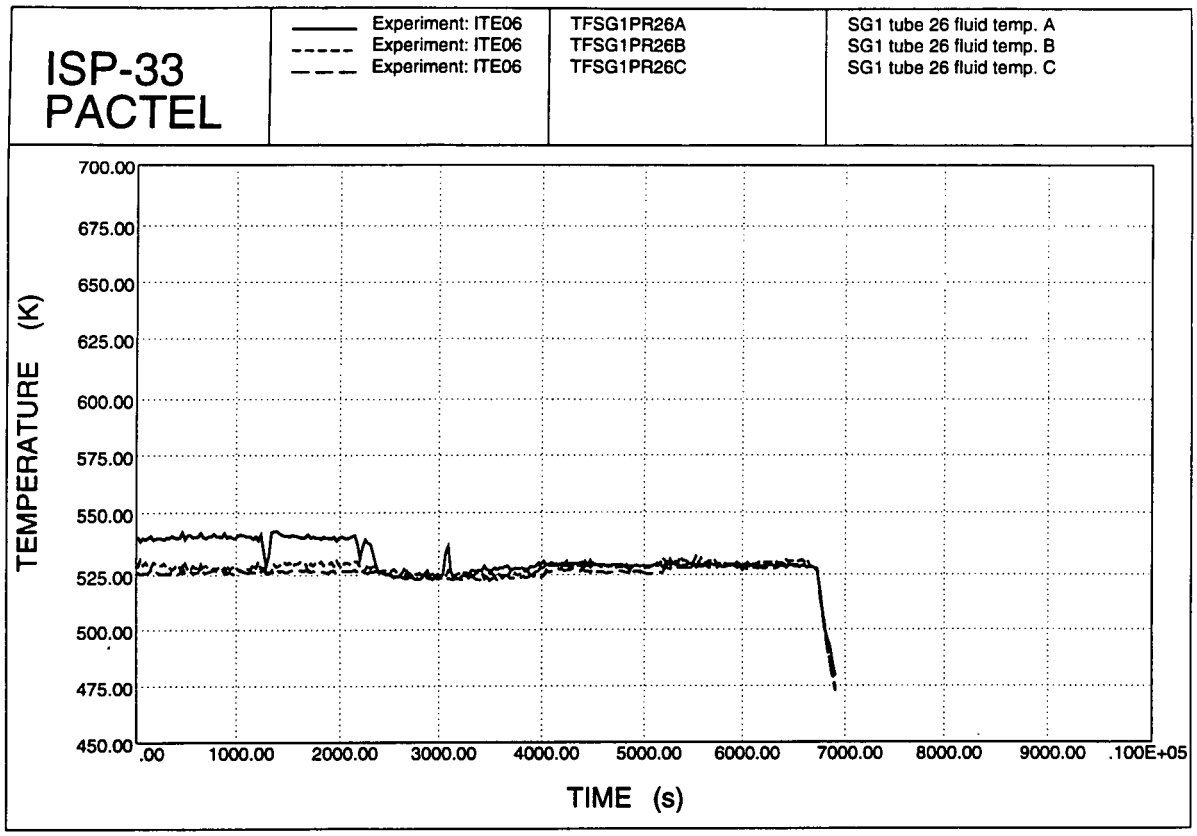

Figure 2.22. SG1 tube primary fluid temperatures.

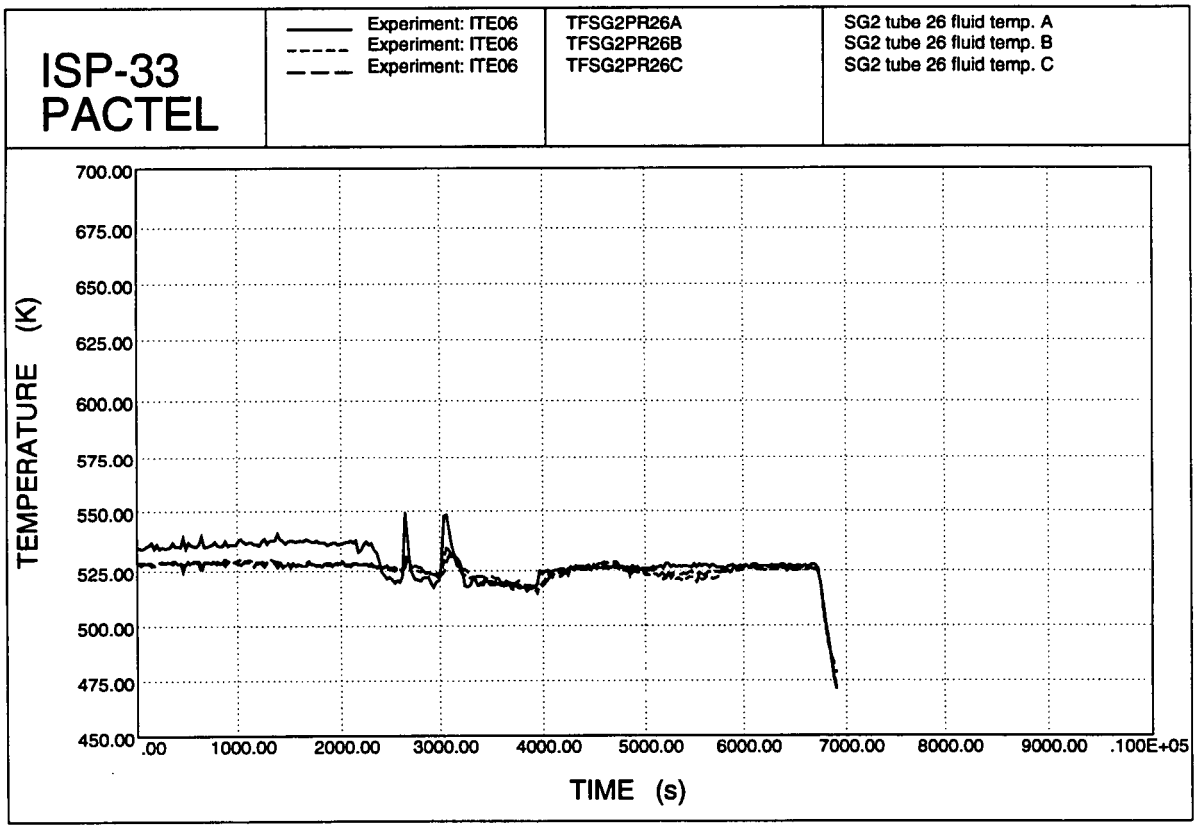

Figure 2.23. SG2 tube primary fluid temperatures.

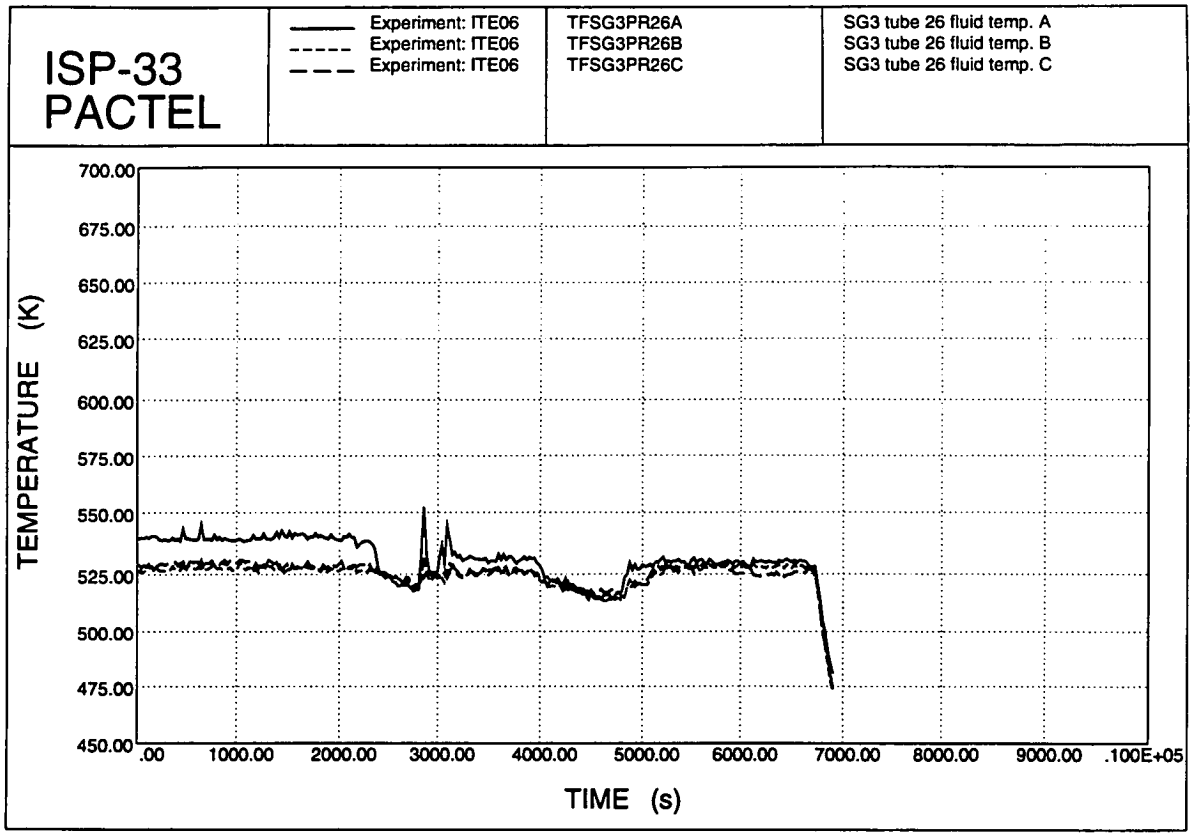

Figure 2.24. SG3 tube primary fluid temperatures.

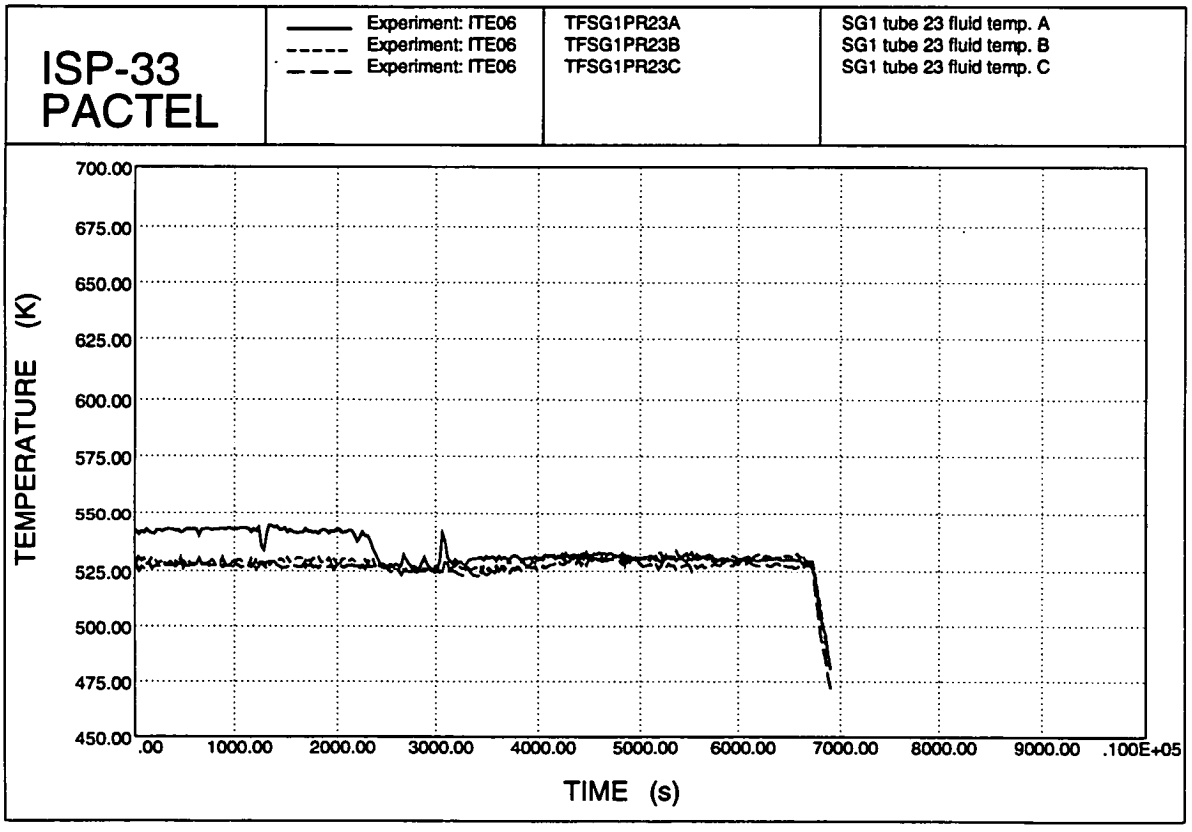

Figure 2.25. SG1 tube primary fluid temperatures.

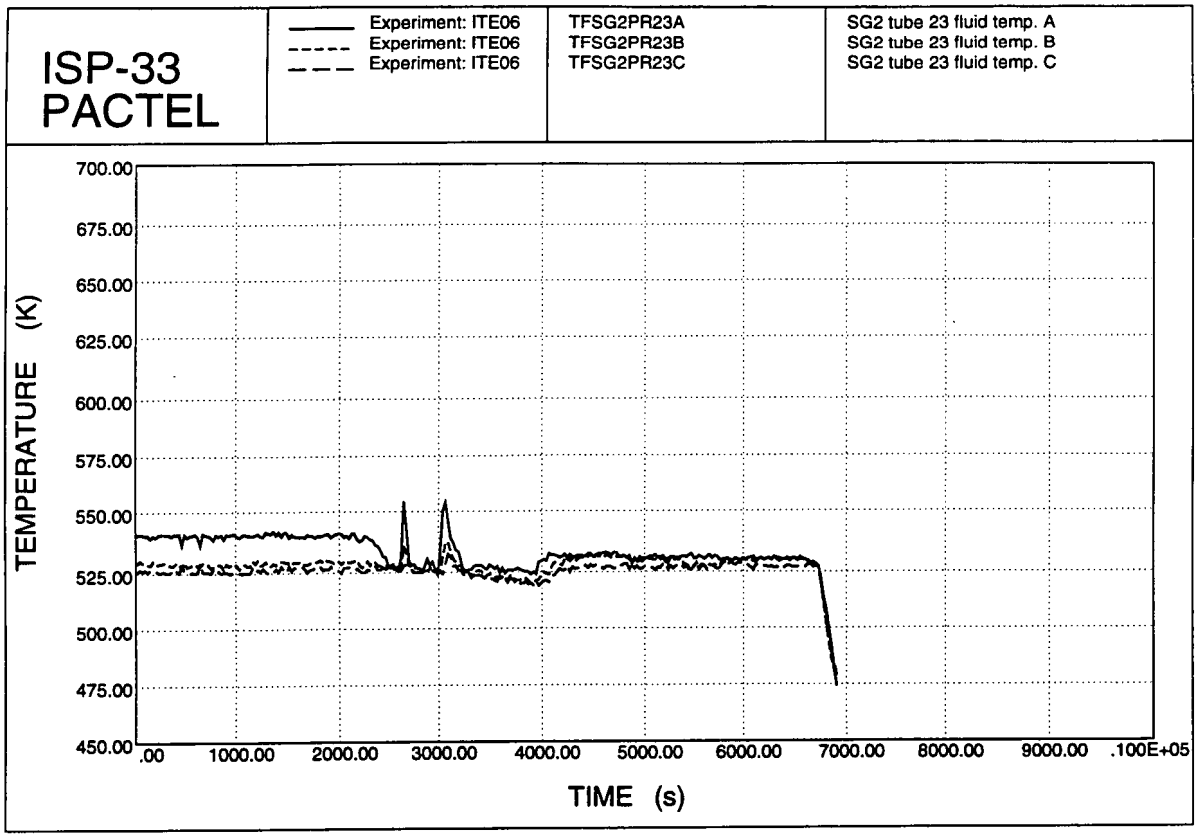

Figure 2.26. SG2 tube primary fluid temperature.

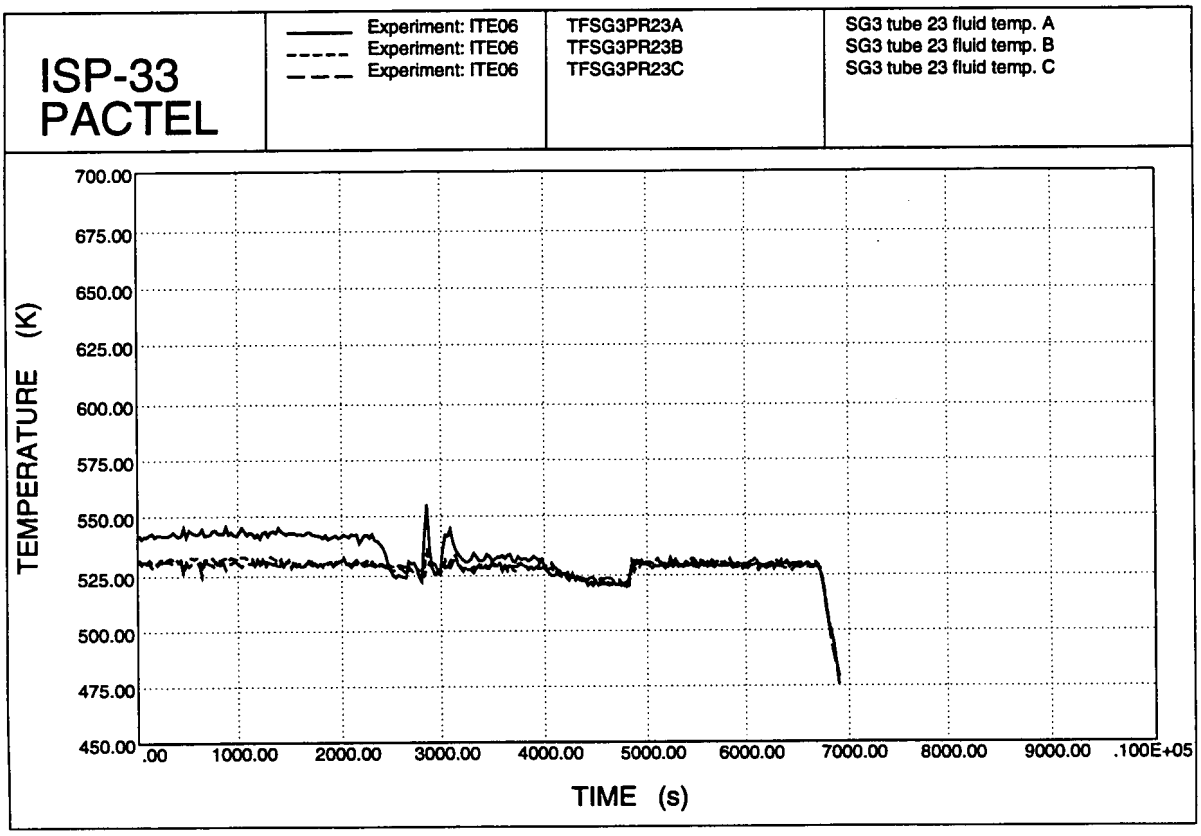

Figure 2.27. SG3 tube primary fluid temperature.

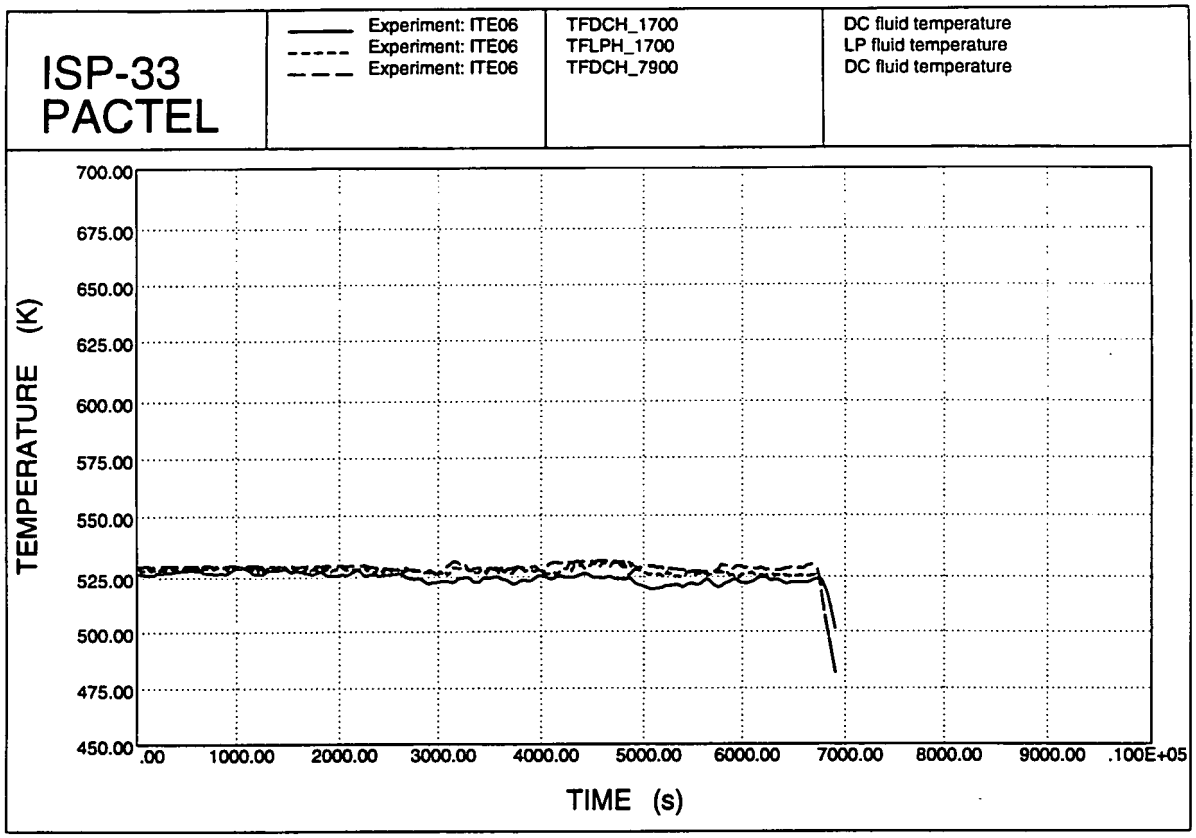

Figure 2.28. Primary fluid temperatures.

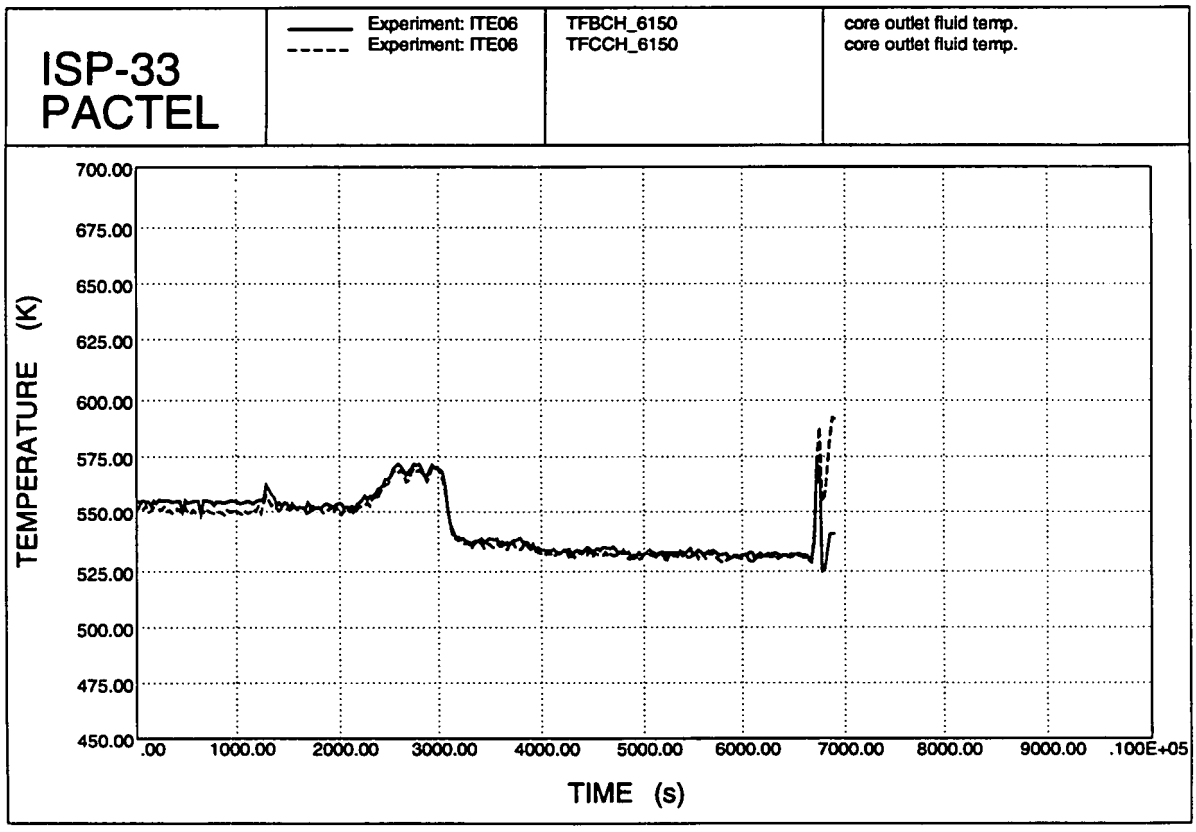

Figure 2.29. Core outlet temperatures.

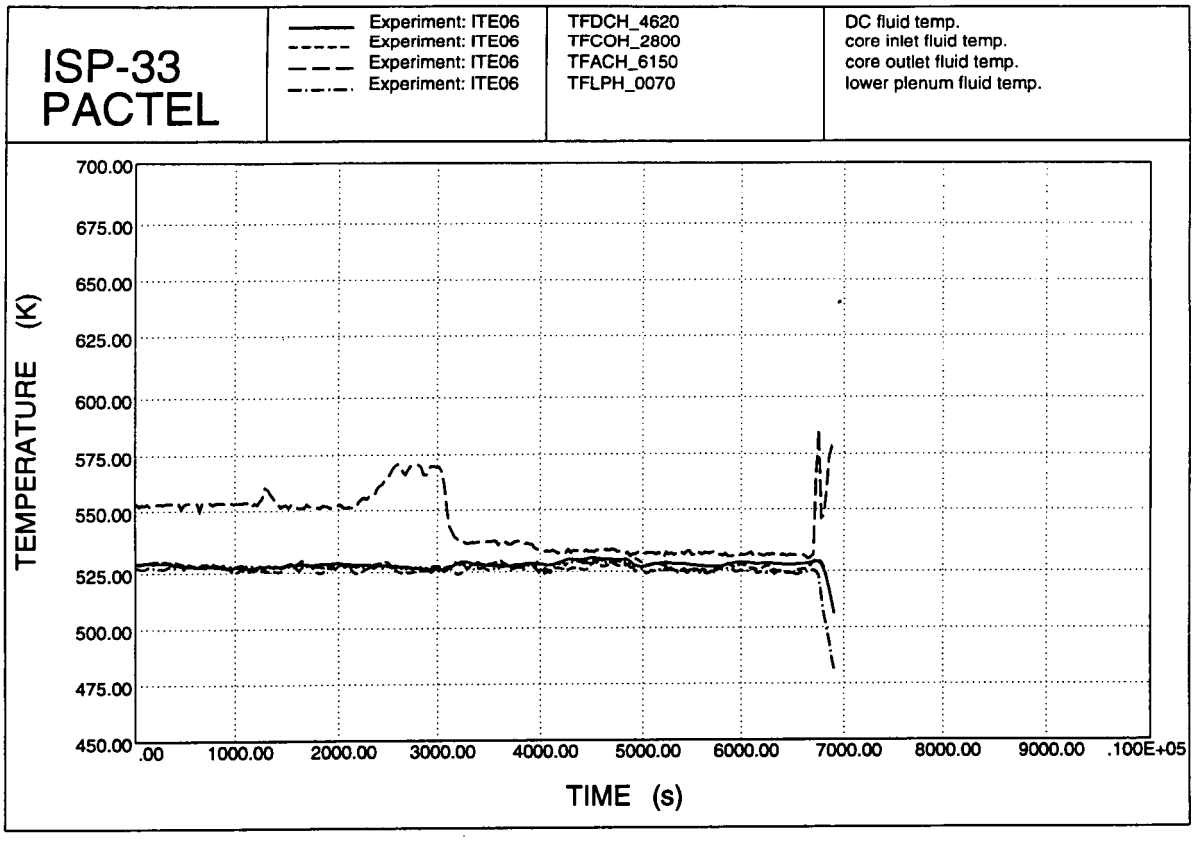

Figure 2.30. Primary fluid temperatures.

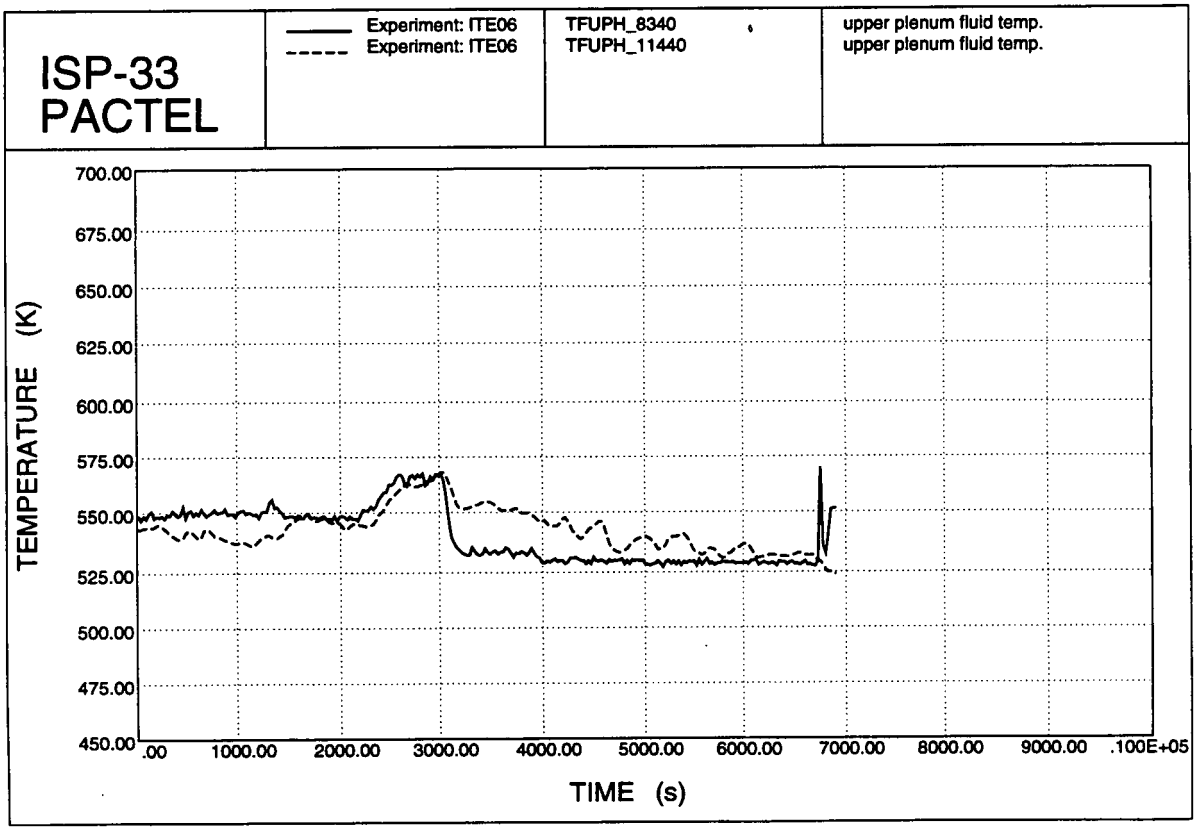

Figure 2.31. Upper plenum fluid temperatures.

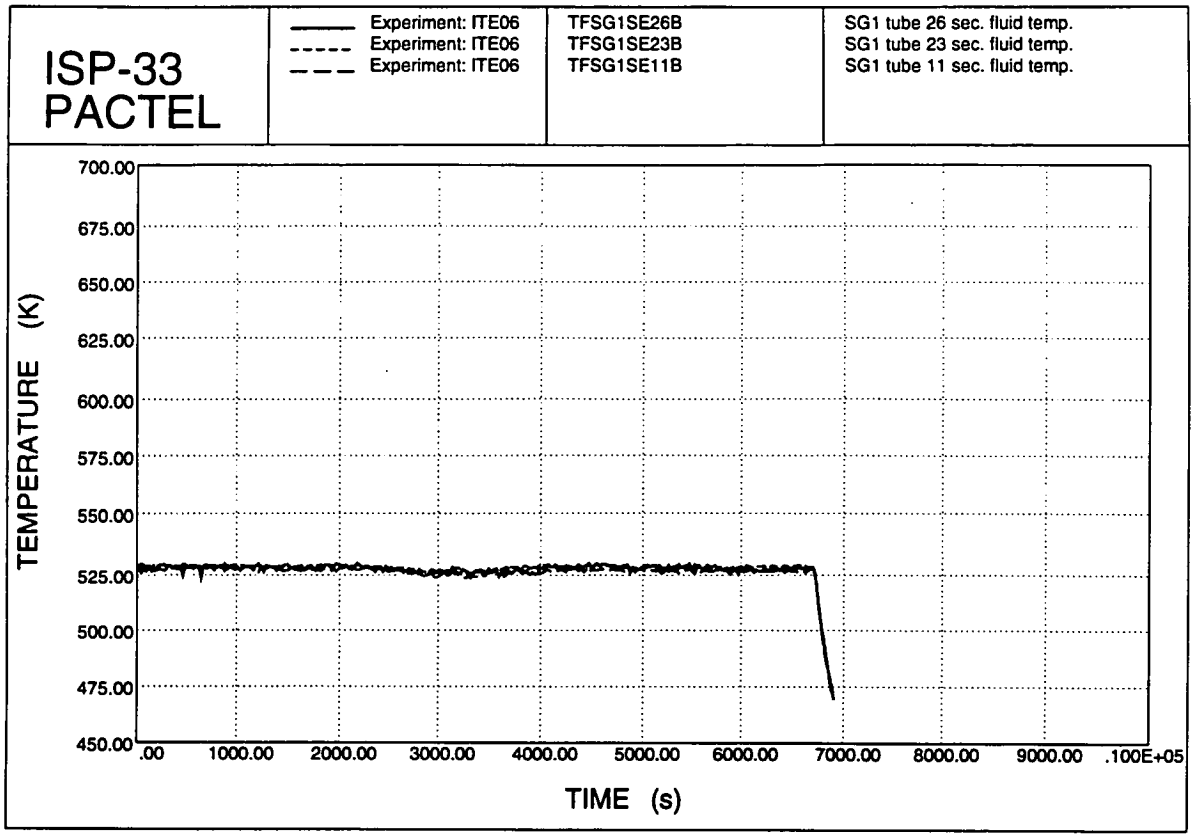

Figure 3.1. SG1 secondary fluid temperatures.

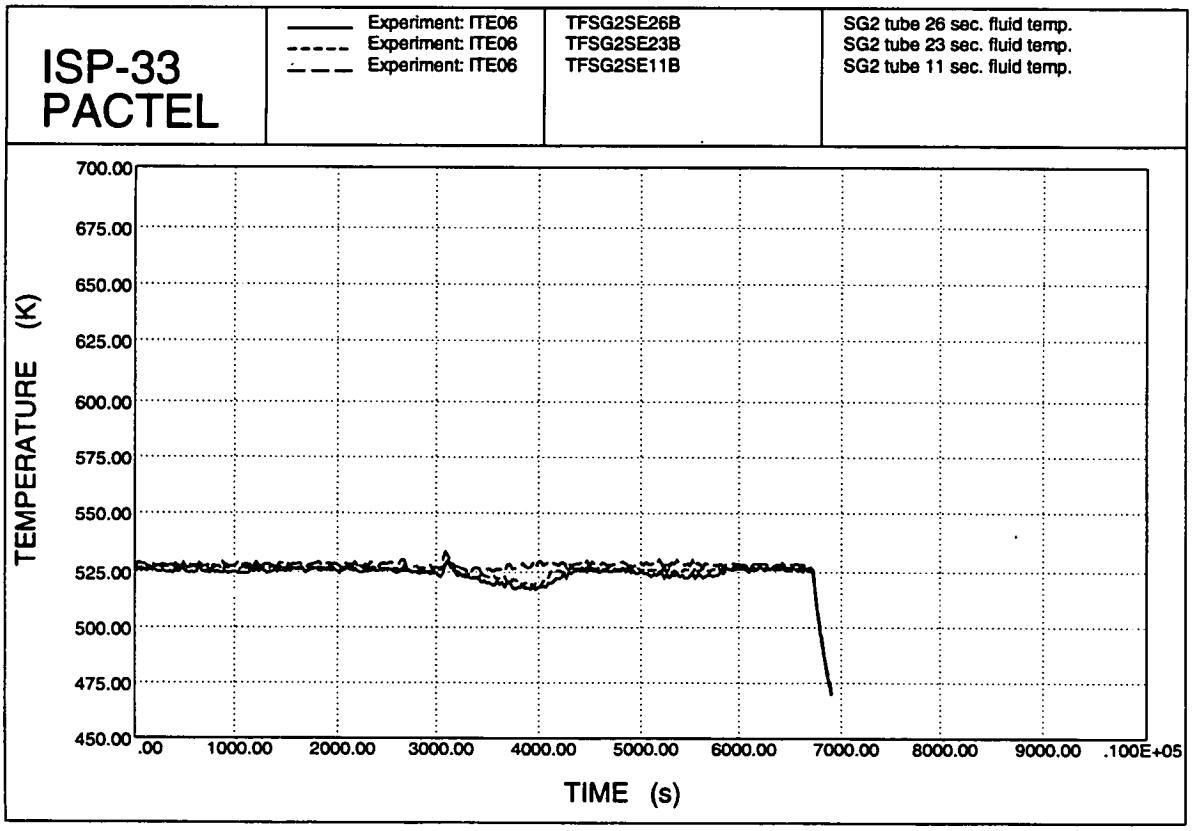

Figure 2.32. SG2 secondary fluid temperatures.

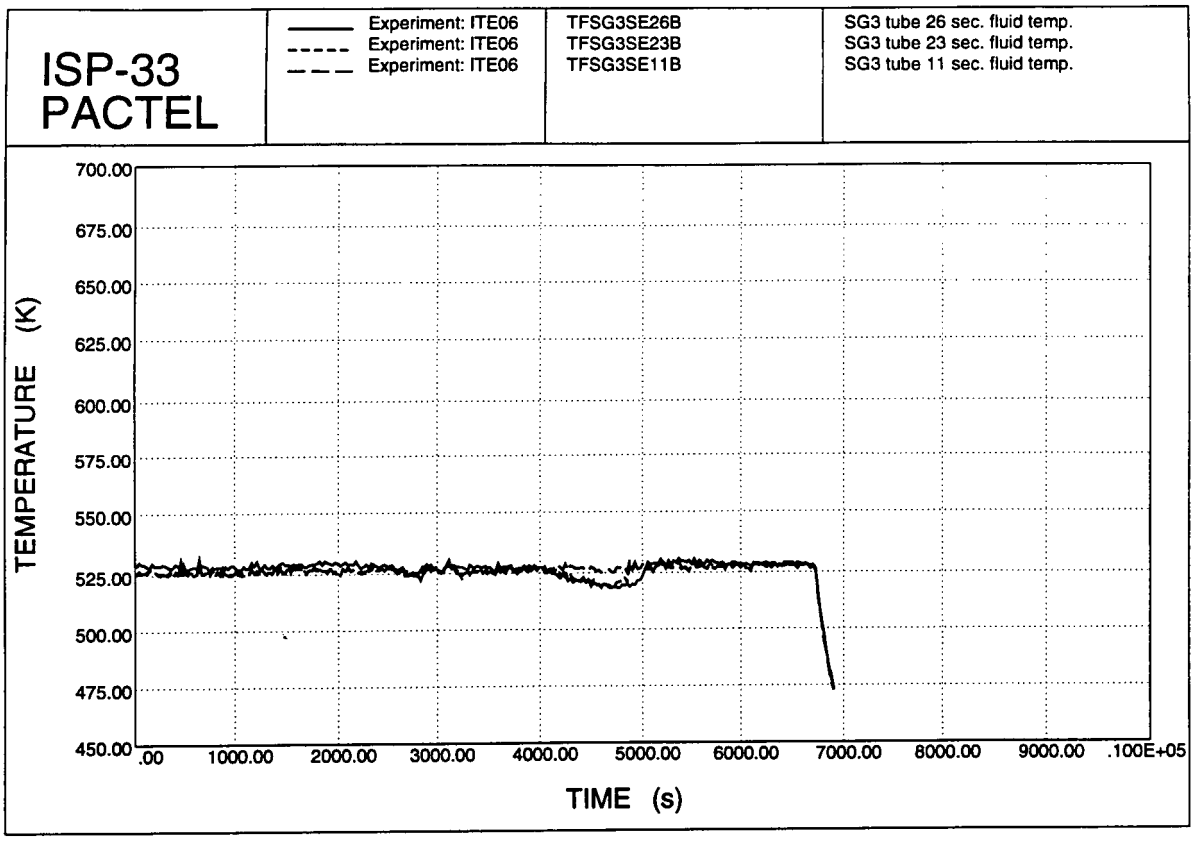

Figure 2.33. SG3 secondary fluid temperatures.

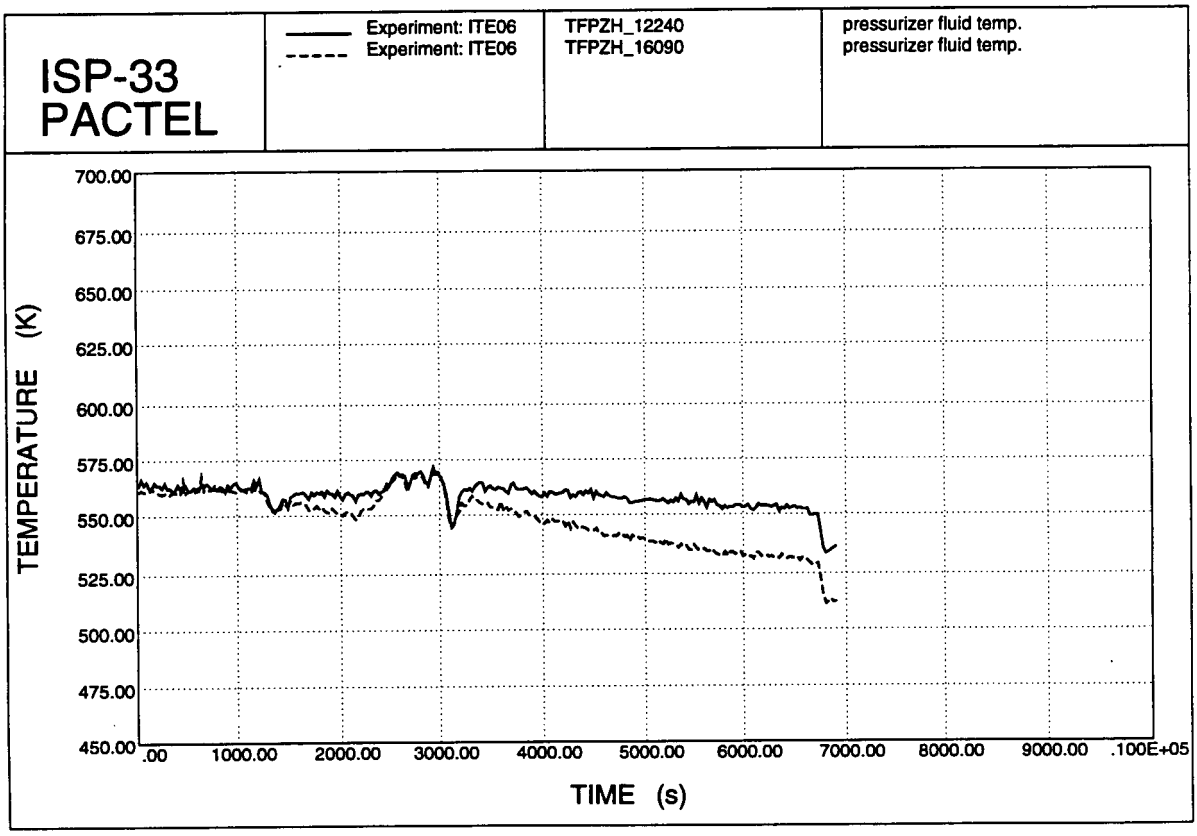

Figure 2.34. Pressurizer fluid temperatures.

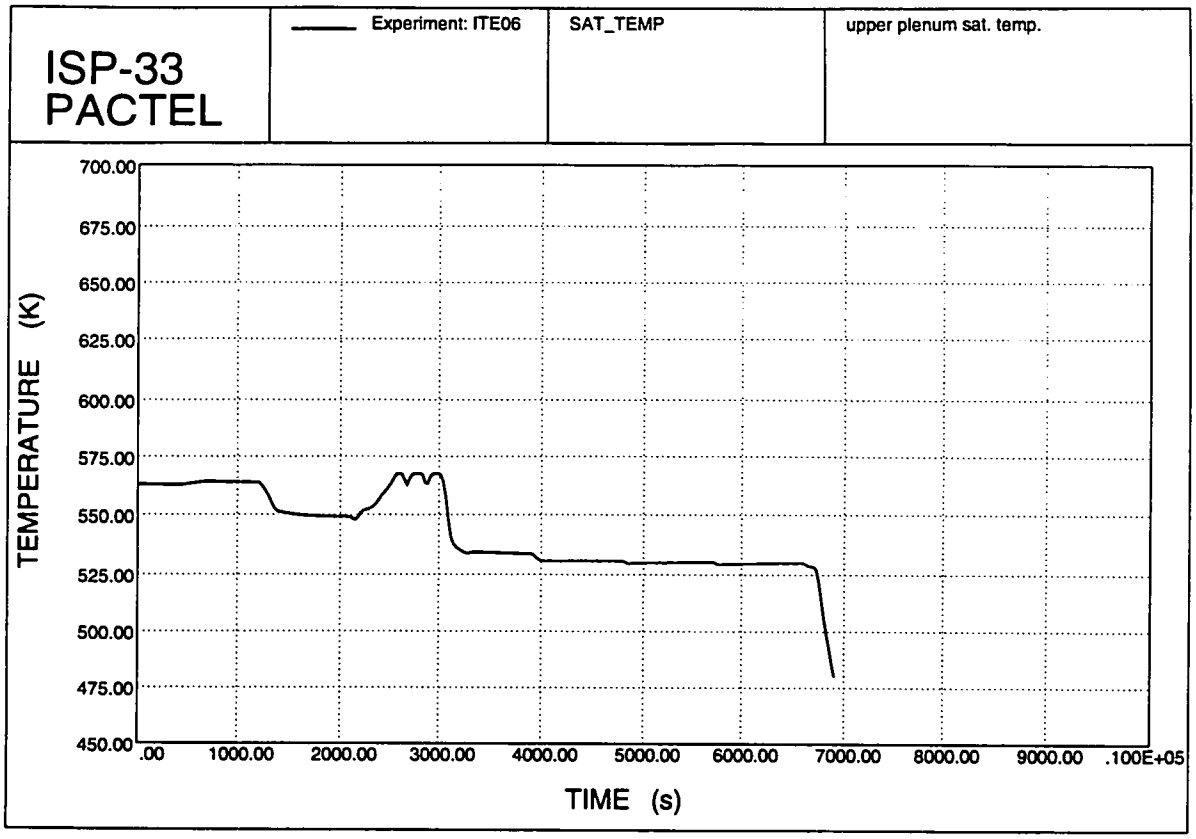

Figure 2.35. Upper plenum saturation temperature.

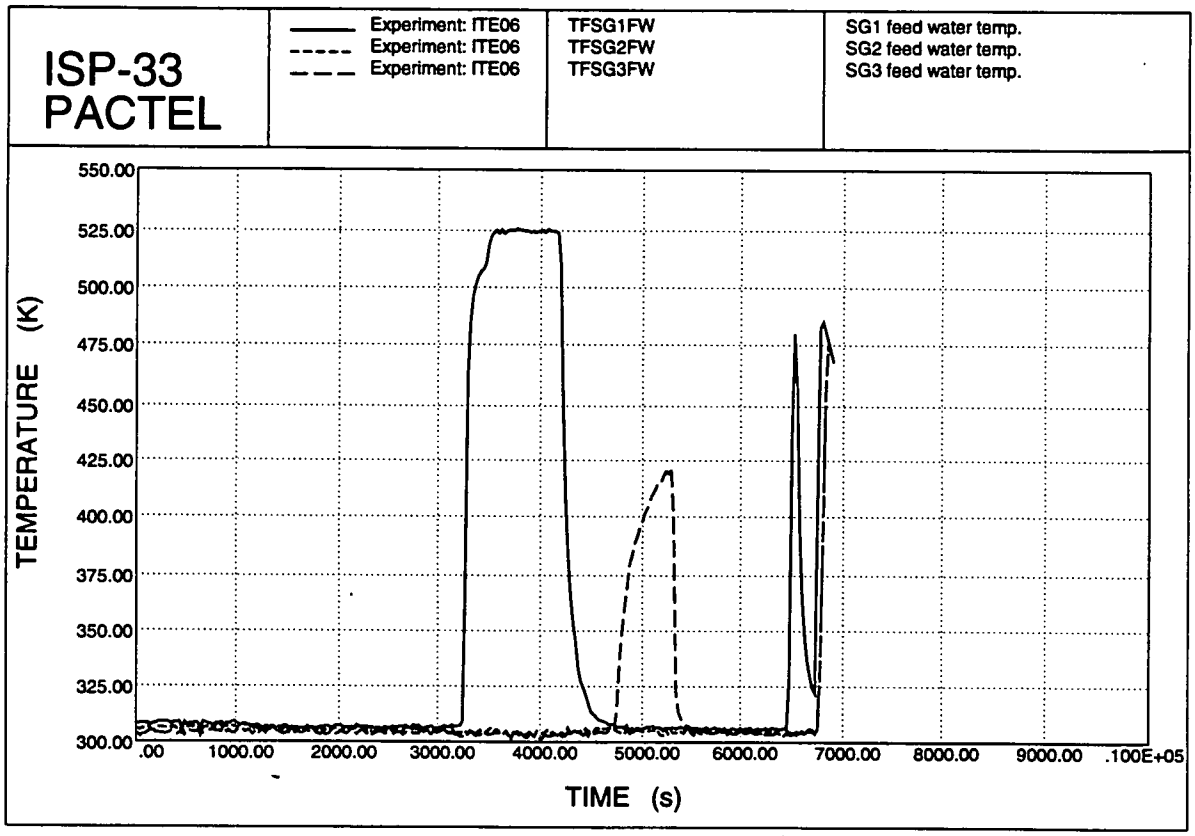

Figure 2.36. SG feed water temperatures. (Temperature rise is due to stopped injection).

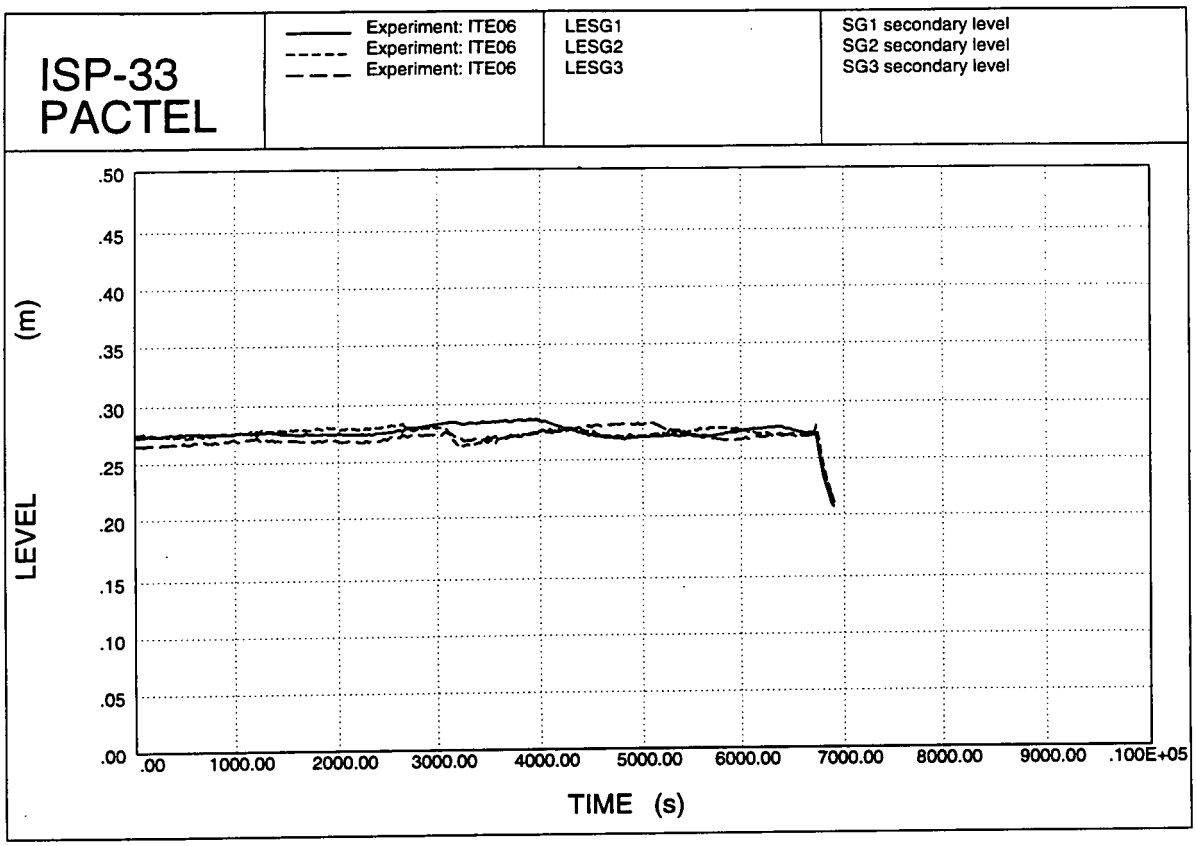

Figure 2.37. SG seconday levels.

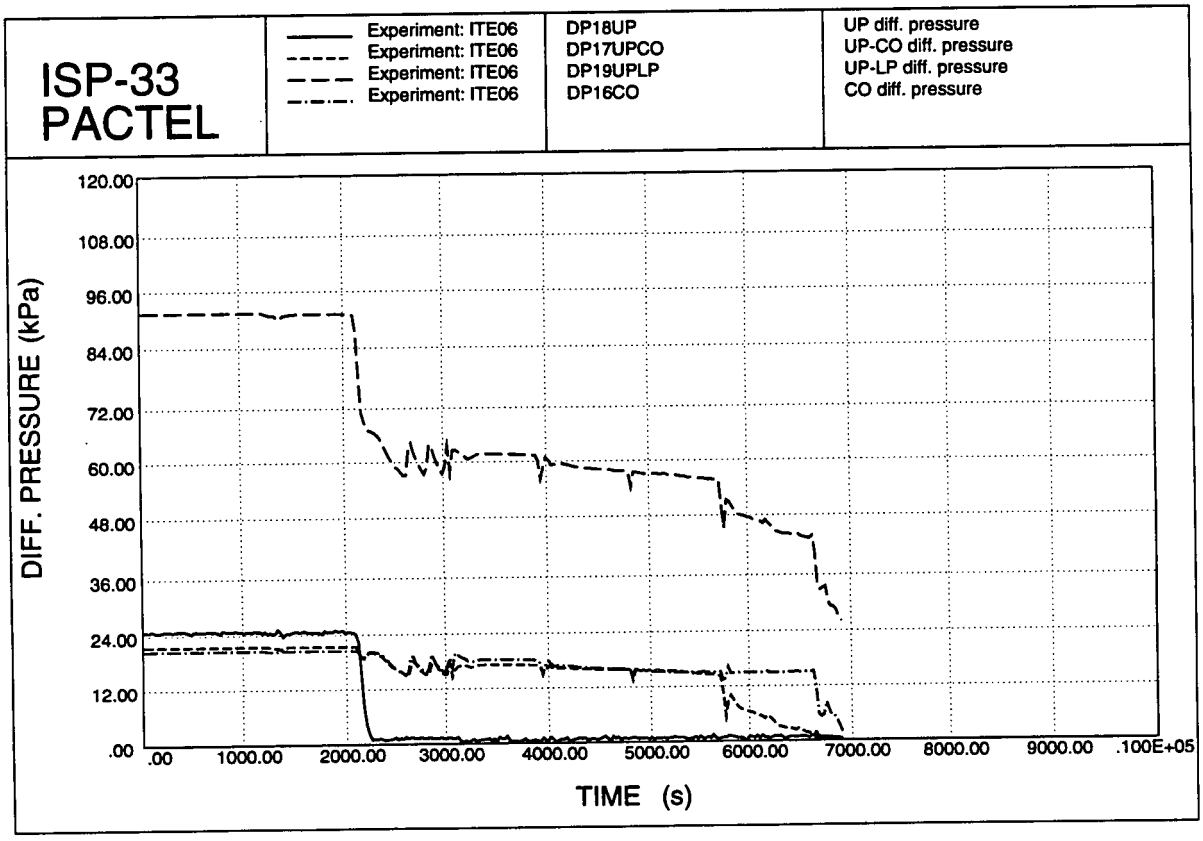

Figure 2.38. Primary differential pressures.

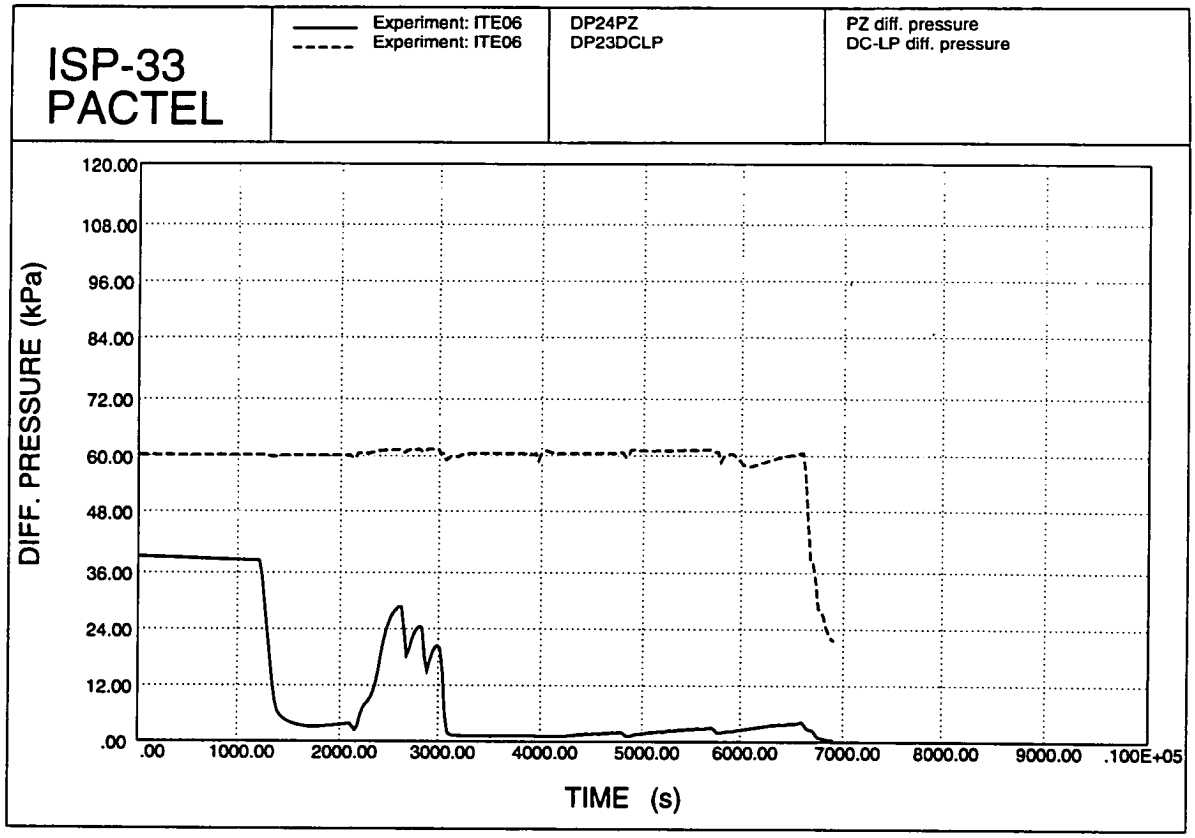

Figure 2.39. Differential pressures.

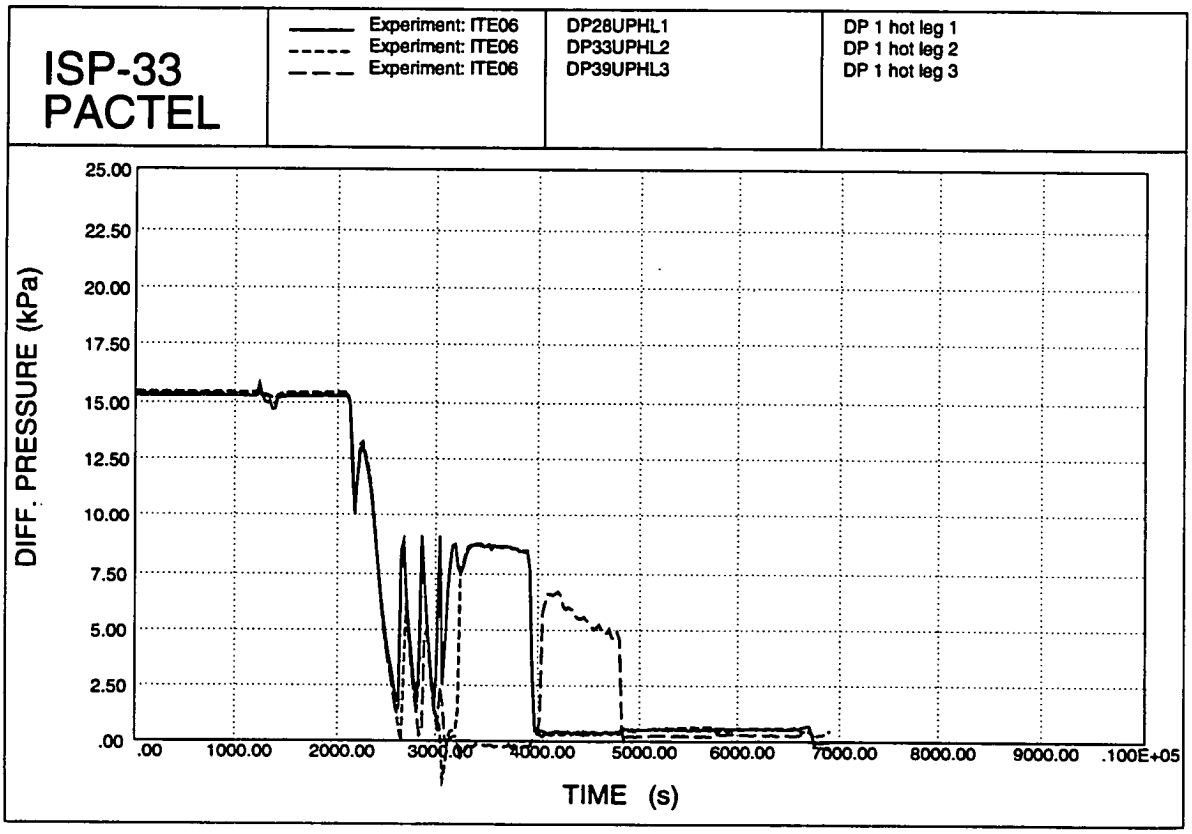

Figure 2.40. Hot leg differential pressures.

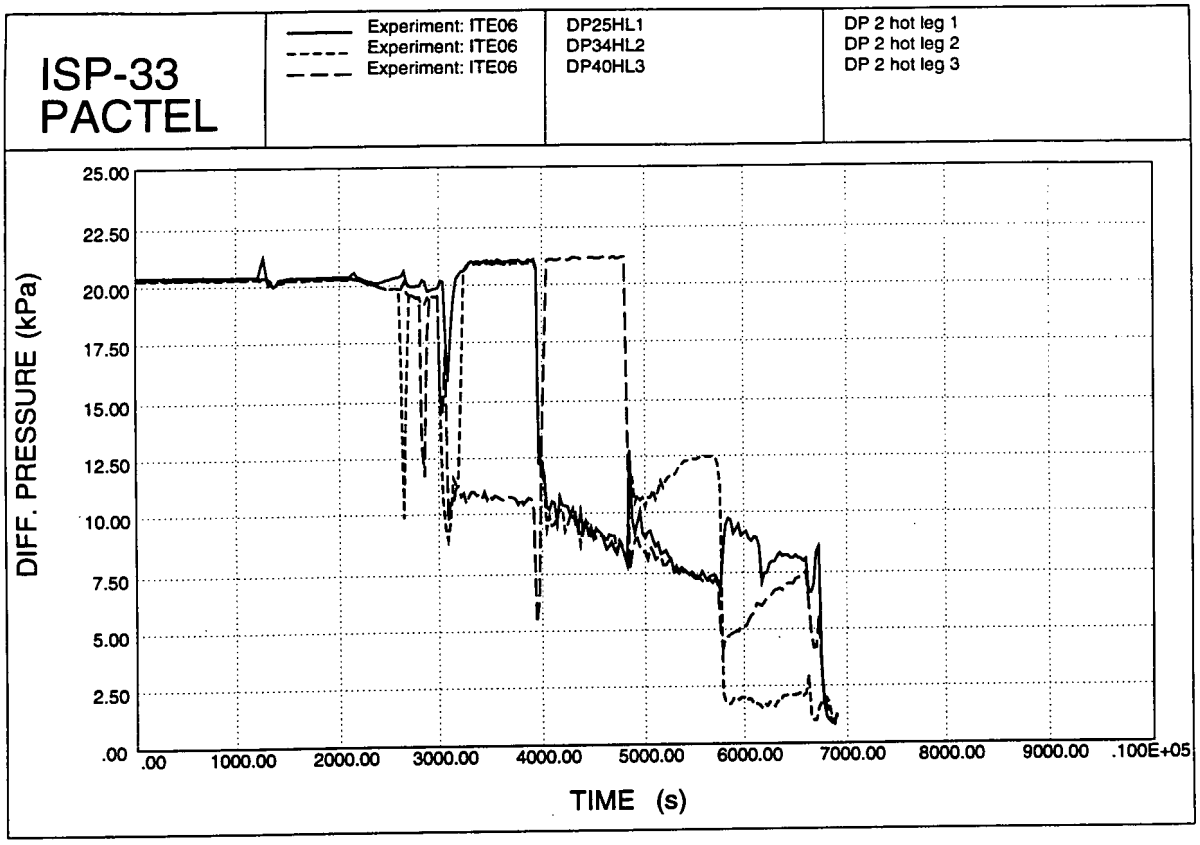

Figure 2.41. Hot leg differential pressures.

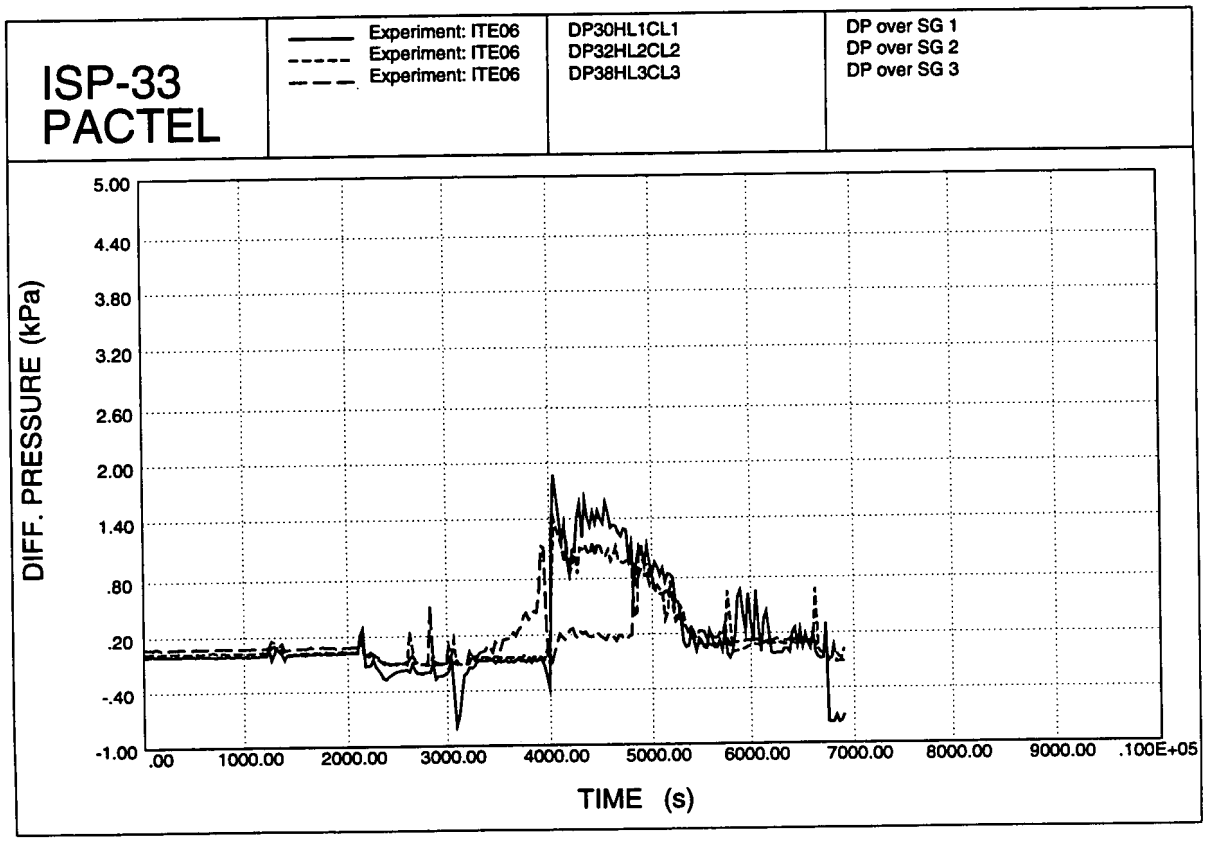

Figure 2.42. Differential pressures over SGs.

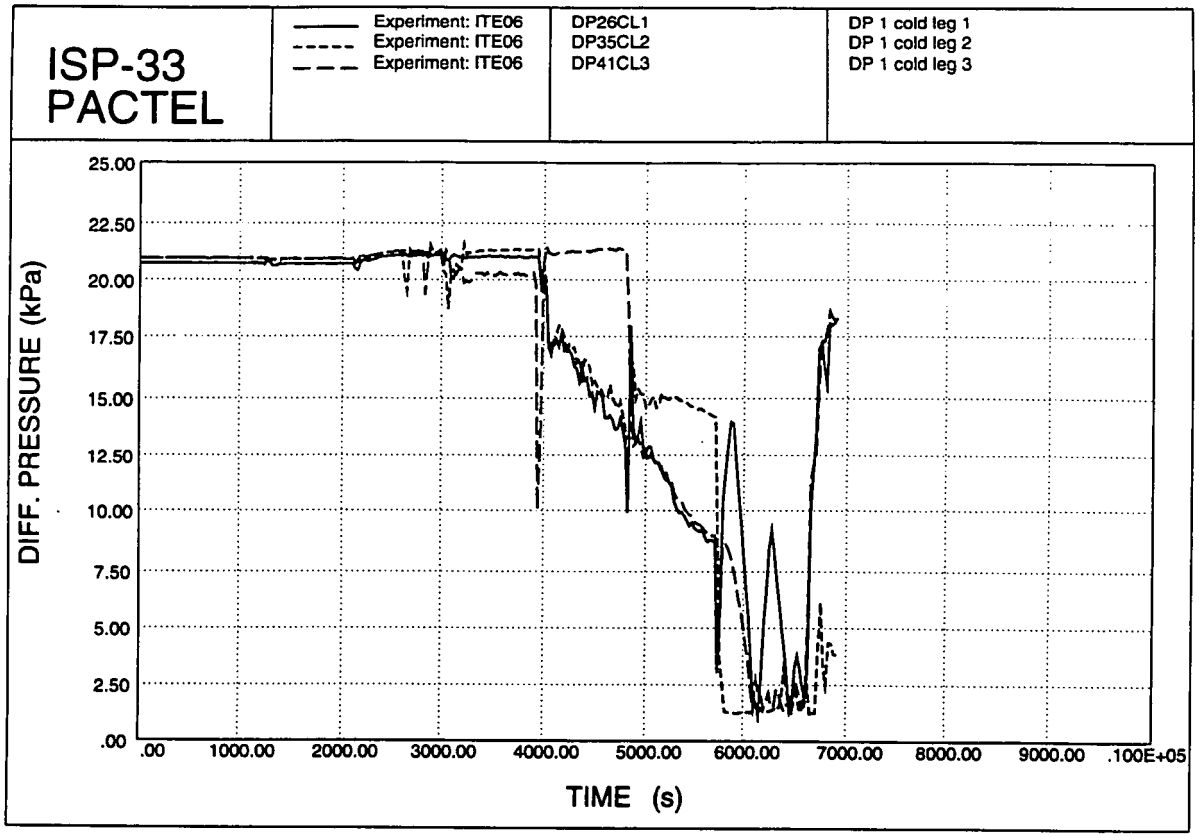

Figure 2.43. Cold leg differential pressures.

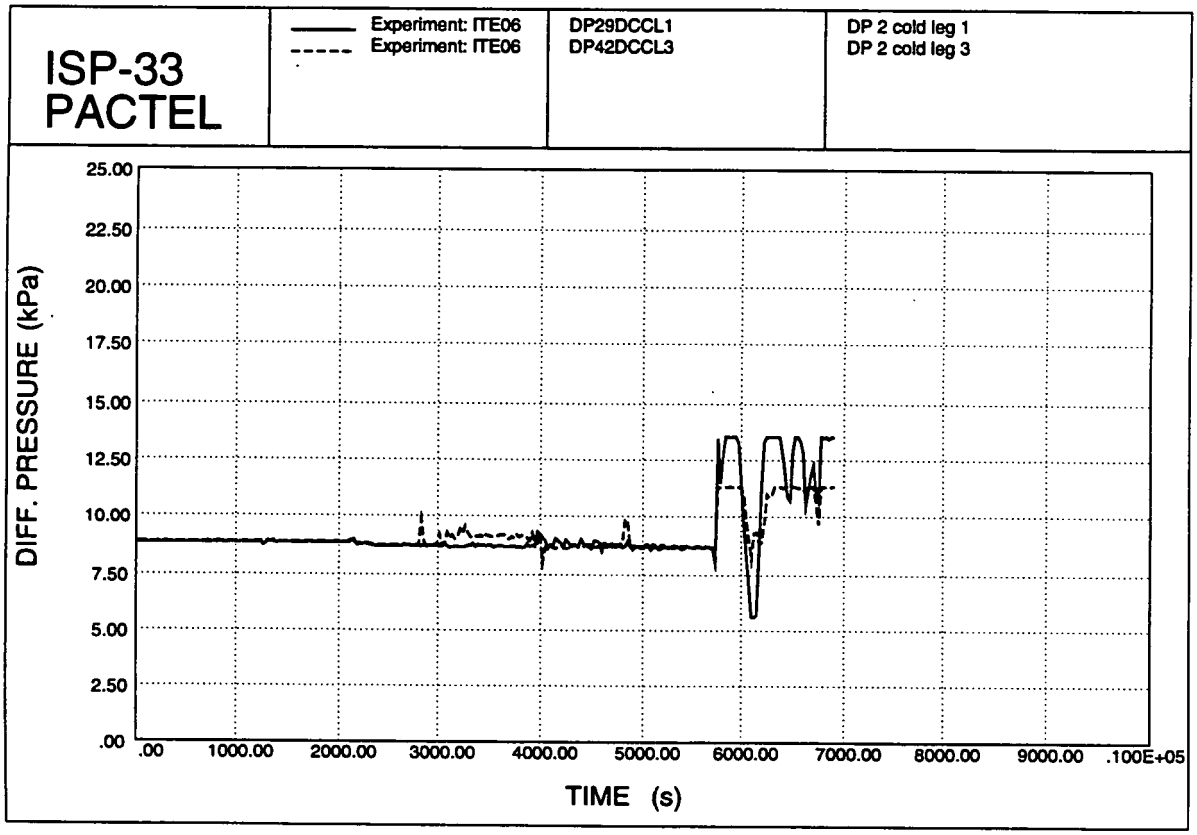

Figure 2.44. Cold leg differential pressures.

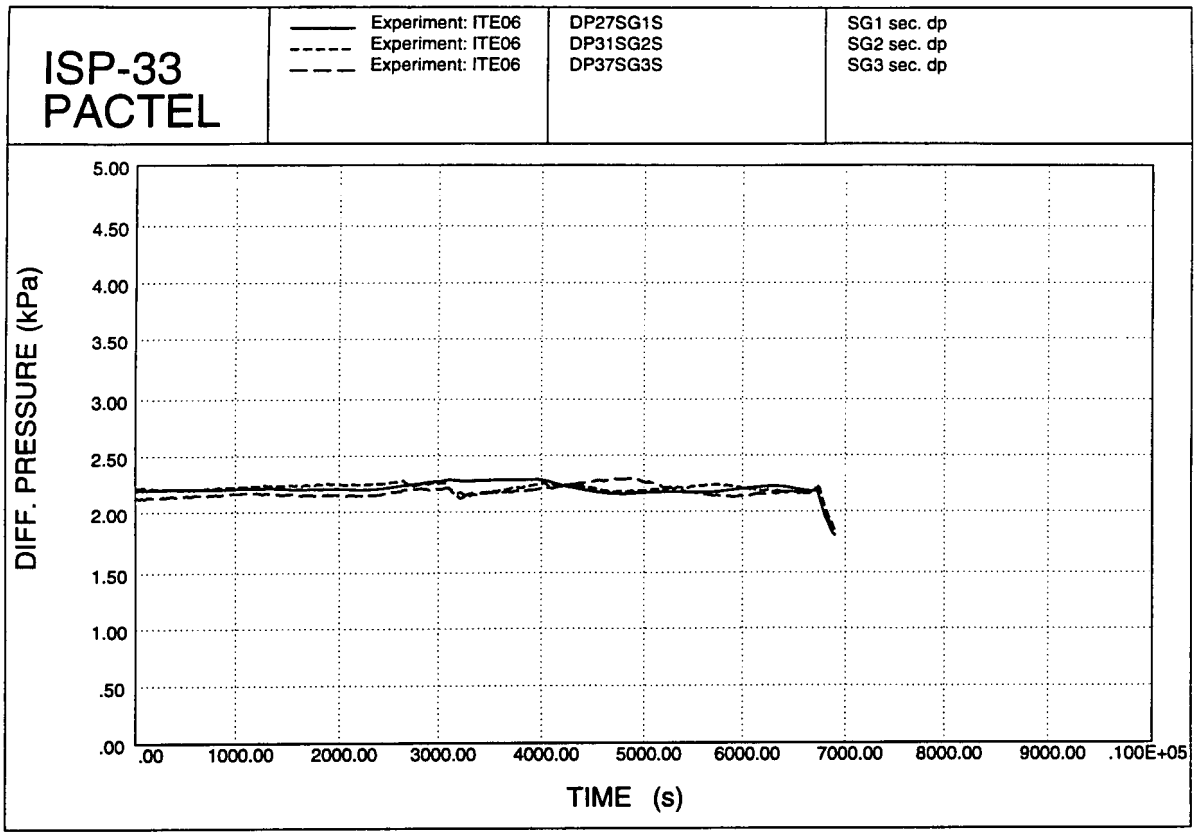

Figure 2.45. SG secondary differential pressures.

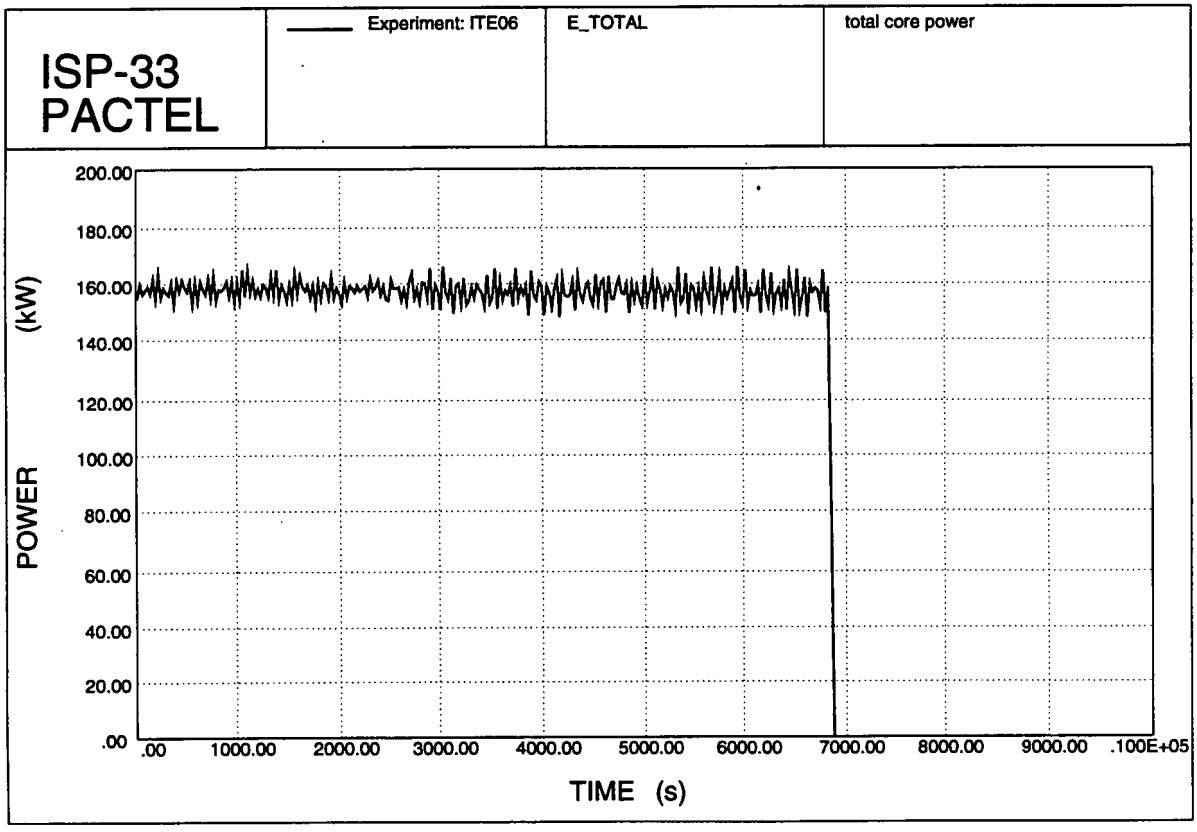

Figure 2.46. Core power.

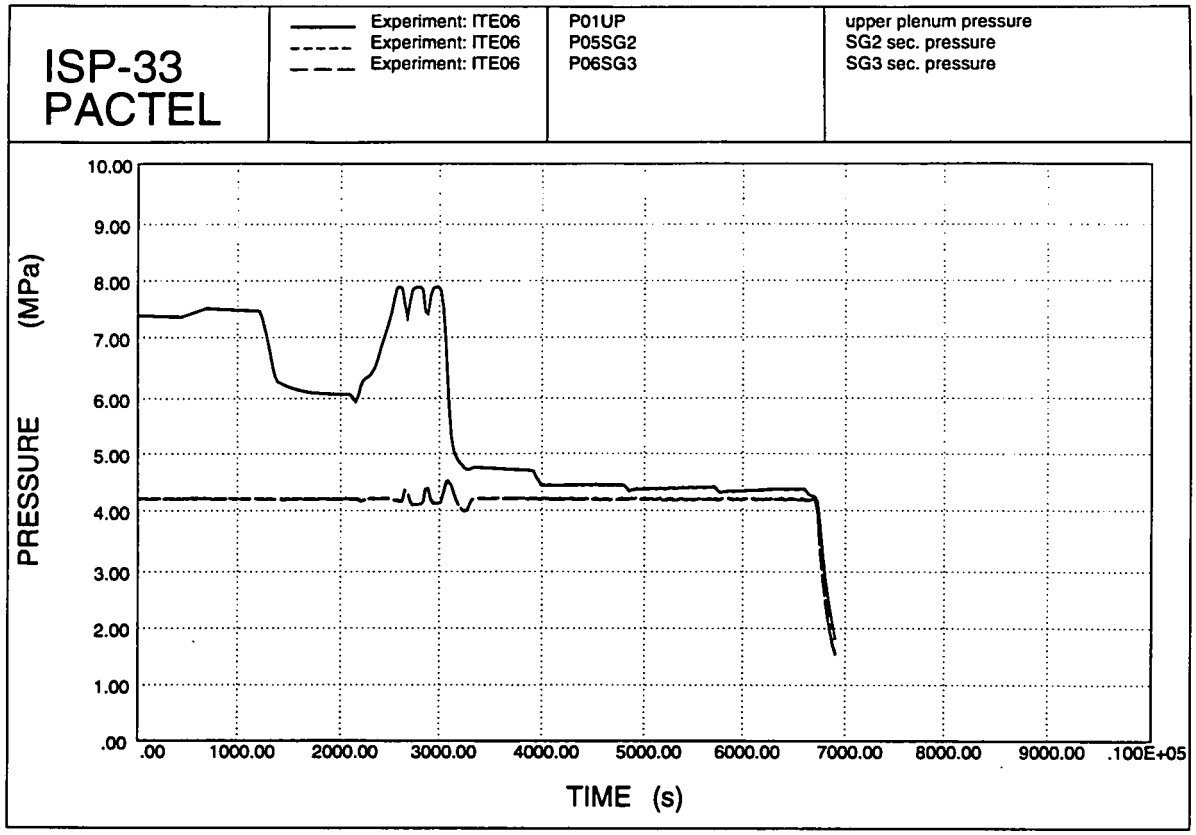

Figure 2.47. Upper plenum and secondary pressures.

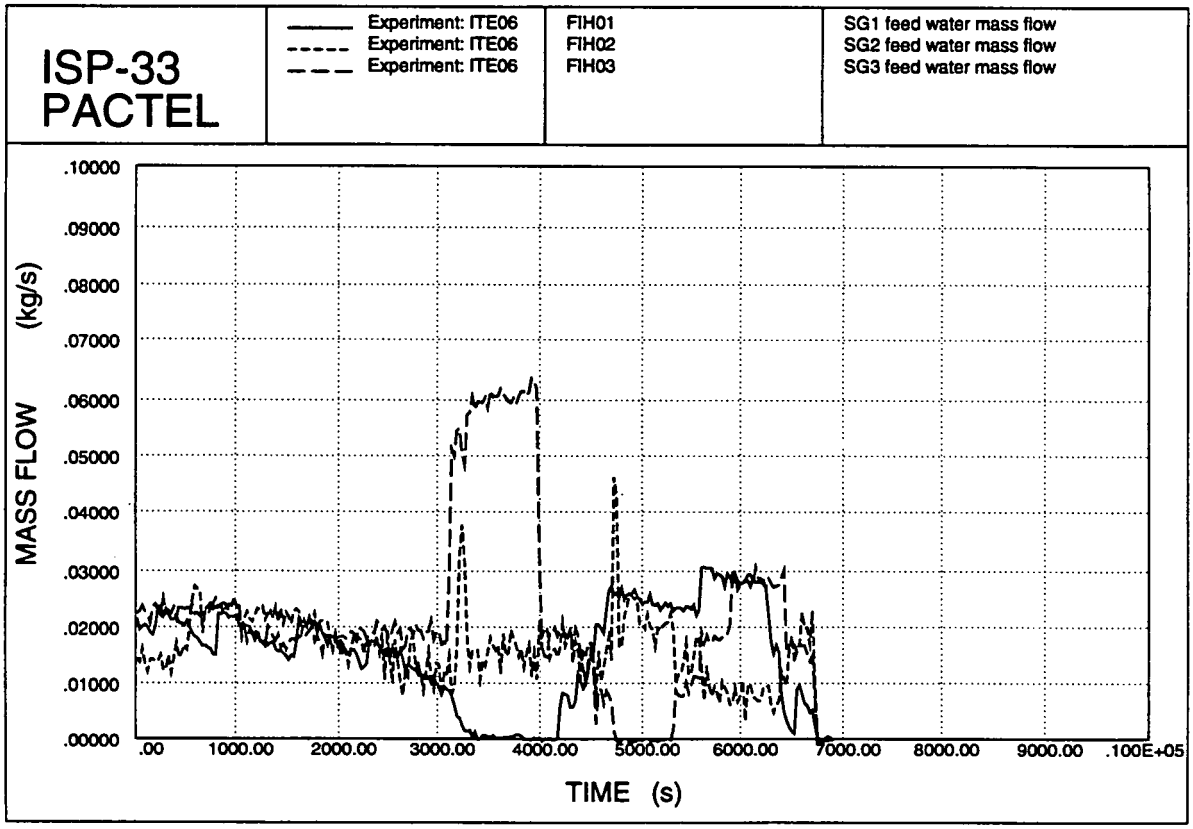

Figure 2.48. SG feed water mass flows.

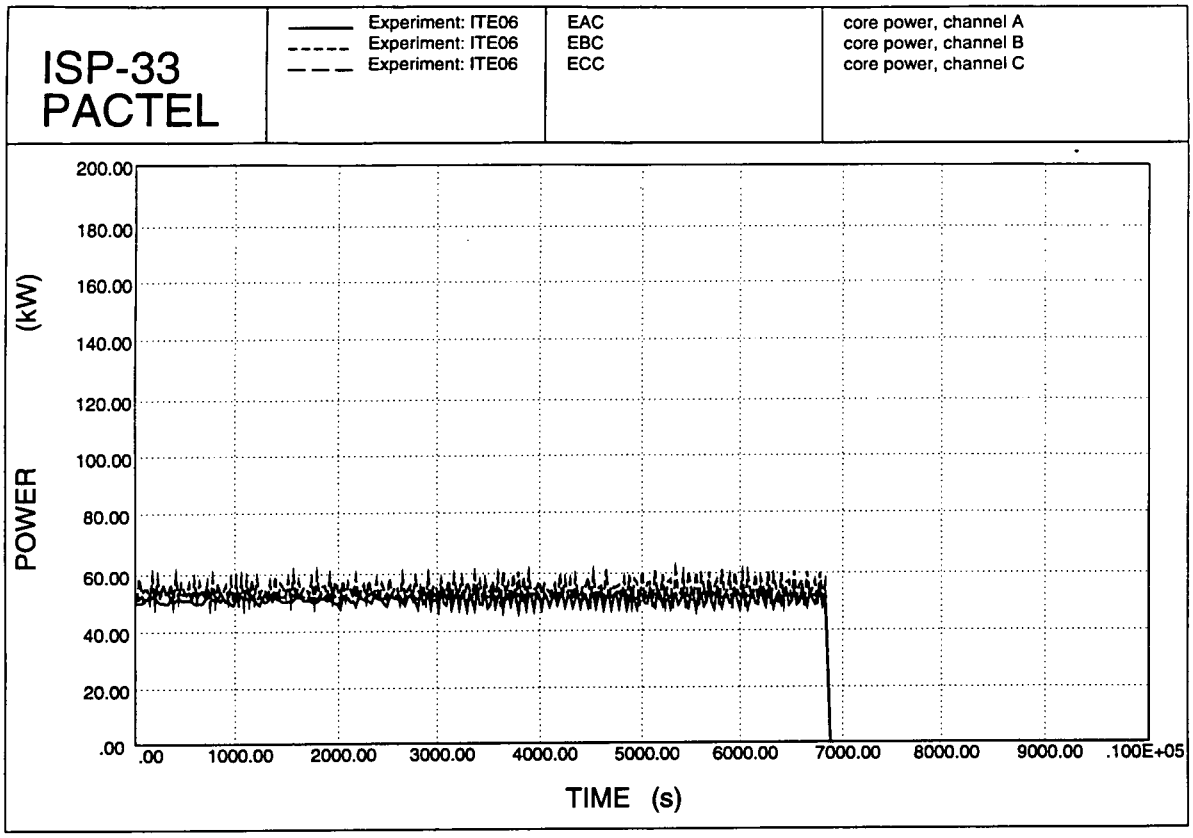

Figure 2.49. Core channel powers.

Table 2.2. The accuracy of differential pressure measurements.

transducer	span [kPa]	error [kPa]
DP18UP	0..60	±0.397
DP17UPCO	0..30	±0.241
DP19UPLP	0..130	±0.985
DP16CO	0..50	±0.339
DP23DCLP	0..90	±0.701
DP24PZ	0..100	±0.765
DP28UPHL1	0..30	±0.230
DP25CL1	0..30	±0.239
DP30HL1CL1	0..10	±0.050
DP26HL1	0..30	±0.239
DP29DCCL1	0..30	±0.219
DP33UPHL2	0..32	±0.240
DP34HL2	0..32	±0.249
DP32HL2CL2	0..10	±0.050
DP35CL2	0..32	±0.249
DP36DCCL2	0..32	not valid
DP39UPHL3	0..32	±0.240
DP40HL3	0..32	±0.249
DP38HL3CL3	0..10	±0.050
DP41CL3	0..32	±0.249
DP42DCCL3	0..32	±0.225
DP27SG1S	0..9	±0.083
DP31SG2S	0..10	±0.088
DP37SG3S	0..10	±0.088

Table 2.3. The accuracy of the pressure measurements.

transducer	range (abs)[MPa]	error [MPa]
P02PZ	0.1..10.1	±0.030
P04SG1	0.1..6.5	±0.020
P01UP	0.1..10.1	±0.030
P05SG2	0.1..6.5	±0.010
P06SG3	0.1..6.5	±0.010

Table 2.4. The accuracy of flowmeters.

transducer	range [kg/s]	error [kg/s]
FCL1	0.1..1.0	±0.015
FCL2	0.1..1.0	±0.015
FCL3	0.1..1.0	±0.015
FDC	0.3..3.0	±0.025
FLP	0.2..2.0	±0.020

Table 2.5. The accuracy of level measurements.

measurement	Δh [m]	Δl [m]
LEPR	12.060	±0.266
LEPZ	8.500	±0.141
LEDC	7.825	±0.142
LEUP	3.240	±0.078
LESG1	0.591	±0.014
LESG2	0.591	±0.014
LESG3	0.591	±0.014

Table 2.6. The accuracy of heating power measurement.

measurement	range [kW]	error [kW]
E_TOTAL	0..1000	±9
EAC	0..333	±3
EBC	0..333	±3
ECC	0..333	±3

3. PARTICIPANTS, CODES AND NODALIZATIONS FOR BLIND CALCULATIONS

3.1 Participants

Fifteen foreign organizations participated in the pretest calculations of ISP33. A list of participants is presented in Table 3.1. This table also includes some statistics of the calculations. The nodalizations used by the participants are presented in figures 3.1 through 3.24. Coolant level/inventory graphs are presented in figures 3.25 through 3.31.

TIME SCHEDULE FOR ISP 33	
18.-19. 2. 1992	First ISP33 Workshop
1. 11. 1992	Deadline for blind calculations (original)
30. 11. 1992	Deadline for blind calculations (changed)
1. 4. 1993	Preliminary Comparison Report completed
17.-19. 5. 1993	Second ISP33 Workshop, deadline for post-test calculations
1. 9. 1993	Final Comparison Report completed

BARC (Bhabha Atomic Research Centre, India) submitted three different calculations, case-I and case-II with ATHLET MOD1 CYCLE D and case-III calculation with RELAP4/MOD6. ECN (The Netherlands) used RELAP5/MOD2.5. CEA CE Cadarache (France) participated jointly with CENG (Grenoble) using CATHARE2 code. GRS (Germany) submitted ATHLET calculations together with RSC KI (Russia). IJS (Institute "Jozef Stefan", Slovenia) sent in two calculations, RELAP5/MOD3 and RELAP5/MOD2. NPPRI (Slovakia) used RELAP5/MOD2 for their calculations. NRI Rez (Czech Republic) used RELAP5/MOD2.5. PSI (Switzerland) used RELAP5/MOD2.5. OKB Gidropress (Russia) sent in calculations performed with DINAMIKA-5 and TECH-M-4 codes. SIEMENS (Germany) participated jointly with RRC KI (Russia) using RELAP5/MOD3. University of Pisa (Italy) submitted CATHARE2 calculations and RSC KI (Russia) participated with SCDAP/RELAP5/MOD2 and RELAP5/MOD3. FZR (Germany) did not submit their pretest results until March 1993.

3.2 Computer code descriptions

3.2.1 ATHLET Mod1.0 Cycle E /3.1/

The ATHLET code is being developed by GRS. The code has been verified by GRS and applied by GRS and other national and international institutions.

ATHLET MOD 1 originated from the implementation of models from the GRS thermalhylraulic codes ALMOD4 and DRUFAN-02 (4-equation system) within a new structure. It was supplemented by a high level language for the simulation of the reactor control system. Development and implementation of a 5-equation model is completed. A 6-equation model with inclusion of equations for non-condensible gases is presently under development. A new condensation model as well as models from the reflood code FLUT will

be implemented. The objective of this development is to obtain a thermalhydraulic code with a wide field of application covering anticipated and abnormal transients, small, intermediate and large break accidents through all relevant phases (blowdown, refill and reflood) in PWR and BWR systems.

ATHLET has a strictly modular structure. The four main modules in accordance with the most important processes are

- thermofluid dynamics (TFO)
- heat conduction and heat transfer (HECU)
- neutron kinetics (NEUKIN)
- general control simulation module (GCSM)

By using of a general interface (GUSER) it is possible to couple additional "independent" modules to the main program. The configuration is defined by the user's input data. The coolant system is simulated by a network of thermofluid "objects" (TFO). The input structure is organized according to those objects. Renodalization within special objects is very convenient for the user.

ATHLET Mod1.0 Cycle E offers basic models with 4 and 5 conservation equations. The ordinary differential equation system, which remains after the spatial approximation by means of the lumped parameter concept, includes a separated mass balance for liquid and vapour as well as an overall momentum balance and an energy balance for the dominant phase. The entire range of fluid conditions from subcooled liquid to superheated vapour including thermodynamic non-equilibrium is considered, assuming the non-dominant phase to be saturated. For the calculation of the relative velocity between the phases a full range drift-flux model which is based on semi-empirical counter-current flow conditions is provided. With this drift-flux model the simulation of cocurrent as well as counter-current flows is possible. The model comprises all flow patterns from homogeneous to separated flow occurring in vertical and horizontal two-phase flow. It also refers to the limitation of water penetration through a vertical flow duct against vapour upflow in different geometrical configurations.

In single-phase as well as in two-phase flow the irreversible pressure loss in a flow channel is considered. Irreversible frictional losses can be calculated as a function of Reynolds number and wall roughness. The increase of the losses in two-phase flow was considered by the Martinelli-Nelson two-phase multiplier. The form losses were input values for forward and reverse flow.

For the four equation system two control volume types are available. Within the ordinary control volume a homogeneous mass and energy distribution is assumed. Within the "non-homogeneous" control volume a mixture level is modeled. Above the mixture level steam with water droplets, below the mixture level liquid with vapour bubbles may exist. The combination of ordinary and non-homogeneous control volumes provides the option to simulate the motion of a mixture level through a vertical component.

The heat transfer packages available for the distinct basic equation systems cover a wide range of single-phase and two-phase flow conditions. The package for the 4-equation model is organized in four levels: condensation, nucleate boiling, transition boiling, and film boiling. It includes a whole range of mass flows (stagnation, natural convection, forced convection)

and an entire enthalpy range (subcooled water, liquid stem mixture, superheated steam). In addition, the heat transfer model was adapted to the drift-flux model (velocity differences between steam and liquid).

The ATHLET assessment is based on a set of separate effect tests, integral system tests and plant data, preferring separate effects tests in full or at least in large scale test facilities that permit the quantification of uncertainties in the simulation of the physical phenomena expected to occur in the full-scale geometry of a PWR or a BWR.

3.2.2 CATHARE2 V1.2E /3.2/

CATHARE (Code Avancè de Thermo-Hydraulic pour les Accidents des Reacteur a'Eau) has been developed by CEA in order to perform best estimate calculations of PWR accidents. It includes several independent modules that take into account mechanical and thermal non-equilibrium which can occur during PWR loss of coolant accidents (large or small break). CATHARE is based on a six partial differential equations (mass, energy and momentum balance equations) model which is solved by a completely implicit method.

The definition of further models concerning mass, energy and momentum exchanges between liquid and vapor and each phase with the wall has to be added to the main system. In order to obtain the model correlation, the classic correlation and experimental data derived from "separate effects" experiment performed in several facilities, have been extensively used.

Three types of thermal exchanges are considered: wall-fluid, liquid-interface and vapor-interface.

1) Wall to fluid heat transfer

According to the general boiling curve three main regions can be distinguished:

1a) Wet wall zone: this region is characterized by the presence of liquid in contact with the wall. The model takes into account forced convection and nucleate boiling. The first one is described by classical laminar and turbulent heat transfer correlation (Colburn); the second one is described by Thom correlation (applied when $T_w > T_{sat}$). Moreover, in accordance to the model of net vapor generation of Zuber and Saha, a distribution of the heat flux between liquid and interface is proposed.

1b) Transition zone: it focuses on the region between a wet and a dry wall and is delimited by the Critical Heat Flux (CHF) value and the Minimum stable film boiling temperature (T_{MIN}). The CHF is based on the Zuber-Griffith and Biasi correlations (with some correction factors applied by the T_{MIN} the Groeneveld-Stervald correlation has been introduced in the code).

1c) Dry wall zone: it is characterized by the contact of the vapor with the wall. Four kinds of heat transfer regimes are assumed: pool boiling (Berenson correlation modified by Groeneveld), forced convection (Hadaller correlation), natural convection and radiative heat transfer (Deruaz model)

2) Liquid interface heat transfer

Two main regions are taken into account:

2a) Boiling region (where $H_L > H_{Lsat}$): A correlation is derived from the analysis of data of the Moby-Dick and Super Moby-Dick experiments.

2b) Condensation region (where $H_L < H_{Lsat}$): A flow with separated phases (Saha correlation) and a droplet flow (rate of entrainment in analogy with Steen-Wallis model) are considered.

3) Vapor interface heat transfer

Both for boiling and condensation situation, the vapor heat transfer is provided by a classical correlation which expresses the conductive and convective heat exchange on droplets for dispersed flows, and laminar or turbulent heat exchange on the liquid core for inverted annular flows.

With wall shear and interfacial friction are included in the friction models.

1) Wall shear

The pressure gradient due to the wall shear is expressed by a relation in which single phase conditions are assumed and the usual friction factors for liquid and vapor are chosen as the maximum values between laminar and turbulent shear coefficient. For the vapor phase the flow regime factor is equal to the void fraction; for the liquid phase the coefficient is equal to the value of the fraction of the perimeter in contact with the liquid (stratified flow), and it is based on the analysis of separate effect experiments in case of non stratified flow.

2) Interfacial friction

A distinction between different flow regimes is made. For each flow regime a specific correlation has been developed, on the basis of experimental data.

a) Non stratified flow

i) Slug flow: the Zuber-Findlay model has been used for the tube geometry. For the rod bundle geometry the correlation is derived from G2 and Pericles experiments.

ii) Annular flow-mist flow: a correlation has been obtained taking into account the Wallis correlation for annular flow, the Steen-Wallis model of entrainment and the data from the Rebeka experiment.

b) Stratified flow

The data of the Echtor experiment have been utilized.

c) Transition flow

The interfacial shear is selected from the range between stratified and non-stratified regimes, using the degree of stratification as weighting factor.

3.2.3 CATHARE2 V1.3E /3.3/

The CATHARE code version V1.3E is the french system code developed in cooperation by CEA, EDF and Framatome. It is based on a two-fluid model leading to a 6-equation system in 1-D elements. Mass, momentum and energy equations are written for each phase. The numerical scheme is a finite difference methodusing the staggered meshing and the first order upwind differencing. The time discretization is fully implicit. Several modules are available to represent the different components of a reactor circuit.

The basic module is the 1-D pipe module; it can be used for hot legs, surge line, SG tubes, intermediate legs, cold legs, downcomer, core and core bypass. The so called "volume module" is a two node module with a moving mixture level, it allows the description of vertical stratification and phase separation effects at the junctions with pipes. It can also be used in the secondary side of SGs to represent the volume above the horizontal tube bundle. The Tee module allows connection of a branch to a main pipe. It is a one node module provided with specific phase separation correlations.

The constitutive relations in the CATHARE code are either taken from the literature developed from the analysis of a large experimental program associated to the code. For example, wall friction models and interfacial friction models have been developed for the following flow patterns: stratified or non stratified, with or without drop entrainment. The stratification criterion takes into account the Kelvin-Helmholtz instability and the liquid turbulence effects. The condensation model used in the SG tubes is derived from the Shah correlation. Convective heat transfers uses the classical Colburn correlation.

3.2.4 DINAMIKA-5

No description submitted.

3.2.5 RELAP4/MOD6 (excerpt from code manual) /3.4/

RELAP4/MOD6 was developed to describe the thermal-hydraulic conditions attendant to postulated transients in light water reactor systems. Those versions of RELAP4 up to and including RELAP4/MOD5 were intended primarily as blowdown and refill codes. That is, they were designed to calculate system phenomena from initial operating conditions at the time of pipe rupture, through system decompression, and up to the initiation of core recovery with emergency core coolant. RELAP5/MOD6 extends the calculational capabilities of RELAP4 from blowdown and refill through reflood for PWR systems.

Approximately 18 000 update cards, including some 50 new subroutines, have been added to RELAP4/MOD5 to provide the RELAP4 reflood calculational capability. This development effort has culminated in RELAP4/MOD6, which contains the RELAP4/MOD5 options, new PWR reflood models, and other program improvements. Major improvements include the following:

(1) Core superheat model for reflood

(2) Moving heat transfer mesh model

(3) Implicit and explicit entrainment models

(4) Upper plenum deentrainment model

(5) Fallback model for core/upper plenum junction

(6) Local mass flux model

(7) New blowdown heat transfer correlation set

(8) Reflood heat transfer correlation set

(9) Steam generator natural convection heat transfer correlation

(10) New heat transfer logic

(11) Extension in dynamic storage capabilities

(12) Best estimate fuel models

RELAP4-EM (Evaluation Model) is available on an optional basis in RELAP4/MOD6, as it was in RELAP4/MOD5. The RELAP4-FLOOD and RELAP4-CONTAINMENT options are also available in RELAP4/MOD6.

3.2.6 RELAP5/MOD2 /3.5/

The RELAP5/MOD2 code is based on a nonhomogeneous nonequilibrium model for the two-phase system that is solved by a fast, partially-implicit numerical scheme to permit economical calculation of system transients. The objective of the development effort from the outset has been to produce a code that includes important first-order effects necessary for accurate prediction of system transients, but is sufficiently simple and cost effective such that parametric sensitivity studies are possible.

The code includes many generic component models from which general systems can be simulated. The component models include pumps, valves, pipes, heat structures, reactor point kinetics, electric heaters, jet pumps, turbines, separators, accumulators, and control system components. In addition, special process models are included for effects such as form loss, flow at an abrupt area change, branching, choked flow, boron tracking, and noncondensible gas.

The system mathematical models are coupled into an efficient code structure. The code includes an extensive input checking capability to help the user discover input errors and inconsistencies. Also included are free format input, internal plot capability, restart, renodalization, and variable output edit features. These user conveniences were developed in recognition that generally the major cost associated with the use of a system transient code is in the engineering labor and time involved accumulating system data and developing system models, while the computer cost associated with generation of the final result is usually small.

The development of RELAP5 has spanned over ten years from the early stages of numerical scheme development to the present. RELAP5 represents the aggregate accumulation of experience in modelling two-phase processes, and LWR systems in particular. The code development has benefitted from extensive application and comparison to experimental data in the LOFT and Semiscale programs. Additional experience has been gained through use of the code by many research and development institutions in the U.S. and in several foreign countries.

3.2.7 RELAP5/MOD2.5

No special description available for RELAP5/MOD2.5. Basicly like RELAP5/MOD2 with some features of MOD3 (see below).

3.2.8 RELAP5/MOD3 /3.6/

RELAP5 was developed at the Idaho National Engineering Laboratory (INEL) for the U.S. Nuclear Regulatory Commission (NRC). The MOD3 version of RELAP5 was developed jointly by the NRC and a consortium consisting of several of the countries and domestic organizations which were members of the International Code Assessment and Applications Program (ICAP). The mission of the RELAP5/MOD3 development program was to develop a code version suitable for the analysis of all transients and postulated accidents in PWR systems, including both large- and small-break loss-of-coolant accidents (LOCAs) as well as the full range of operational transients.

The RELAP5/MOD3 code is based on a nonhomogeneous nonequilibrium model for the two-phase system that is solved by a fast, partially implicit numerical scheme.

Several new models, improvements to existing models and user conveniences have been added. The new models include:

- the Bankoff counter-current flow limiting correlation
- the ECCMIX component for modelling of the mixing of subcooled emergency core cooling system (ECCS) liquid and the resulting interfacial condensation
- a zirconium-water reaction model
- a radiation heat transfer model

Improvements to existing models include:

- new correlations for interfacial friction for all types of geometry in bubbly-slug flow regime in vertical flow passages
- an improved model for vapor pullthrough and liquid entrainment in horizontal pipes to obtain correct computation of the fluid state convected through the break
- a new critical heat flux correlation for rod bundles
- improved stratification models
- a modified reflood heat transfer model
- the extension of water packing logic to horizontal volumes
- the addition of a simple plastic strain model with clad burst criterion to the fuel mechanical model
- the addition of the radiation heat transfer term to the gap conductance model
- modifications to the noncondensible gas model
- improvements to the downcomer penetration, ECCS bypass, and upper plenum deentrainment capabilities
- modifications that take place both the vertical stratification and water packing models under user control so they can be deactivated.

3.2.9 SCDAP/RELAP5/MOD2 /3.7/

No special description available. When used for thermal hydraulic calculations similar to RELAP5/MOD2.

3.2.10 TECH-M-4

No description submitted.

Table 3.1 ISP33 Participants of blind calculations (1/4).

Participant	BARC (India)	ECN (The Netherlands)
Name	H. G. Lele, S. K. Gupta,	L. Winters
	V. Venkat Raj, S. K. Mehta	
Organization	Bhabha Atomic Research Centre	Netherlands Energy Research
		Foundation ECN
Address	Trombay	P.O. Box 1
City/State	Bombay-400 085	1755 ZG Petten
Zip Code		
Country	India	The Netherlands
Phone Number	+91 22 551 3971	+31 2246 4551
Fax Number	+91 22 556 0750	+31 2246 3490
Telex	011 - 72322	57211 REACP NL
Computer	**ND-570**	***IBM RS6000, type 320H***
CPU / Real Time	89000 s/ 7995.0s (11.13)	54848 s/ 7846 s (6.99)
Code	**ATHLET MOD1 CYCLE - D**	**RELAP5/MOD2.5**
Model Descr.		
Volumes	66	306
Junctions	46	313
Heat slabs	32	385
Mailing date	25.Nov.92	30.Nov.92
Participant	**BARC (India)**	**GRS (Germany) & RSC KI (Russia)**
Name	S. K. Mehta	S. Nikonov, J. Steinborn
Organization	Bhabha Atomic Research Centre	Gesellschaft für Anlagen- und
		Reaktorsicherheit (GRS) mbH
Address	Trombay	Kurfürstendamm 200
City/State	Bombay-400 085	1000 Berlin 15
Zip Code		
Country	India	Germany
Phone Number	+91 22 551 3971	+0 30 88 41 89 26
Fax Number	+91 22 556 0750	+0 30 88 23 655
Telex	011 - 72322	
Computer	**MAGNUM MULTIRISC**	**IBM ES/9000**
CPU / Real Time	750000 s/ 4845.02 s (154.80)	327000 s/ 7680.3 s (42.58)
Code	**ATHLET MOD1 CYCLE - D**	**ATHLET Mod 1.0 Cycle E**
Model Descr.		
Volumes	180	212
Junctions	150	232
Heat slabs	137	228
Mailing date	25.Nov.92	30.Oct.92
Participant	**BARC (India)**	**IJS (Slovenia)**
Name	P. Dolas, S. Sengupta, S. Gupta, D. Kumar,	I. Parzer, S. Petelin, O. Gortnar, B. Mavko,
	R.B. Grover, V. Venkat Raj, S. K. Mehta	M. Zeljko
Organization	Bhabha Atomic Research Centre	Institute "Jozef Stefan"
Address	Trombay	Jamova 39
City/State	Bombay-400 085	61111 Ljubljana
Zip Code		
Country	India	Slovenia
Phone Number	+91 22 551 3971	+3861 371 321
Fax Number	+91 22 556 0750	+3861 374 919
Telex	011 - 72322	31296 YU JOSTIN
Computer	**WIPRO, LANDMARK-860**	**SUN Sparc 2**
CPU / Real Time	72000 s/7500.0 s (9.60)	89975 s/ 7863.1 s (11.44)
Code	**RELAP4/MOD6**	**RELAP5/MOD2/36.05**
Model Descr.		
Volumes	28 (1 Time dependent volume)	220
Junctions	37 (5 Fills, 1 Leak)	237
Heat slabs	14 (9 Core , 5 SG)	259 (1263 Mesh points)
Mailing date	25.Nov.92	31.Oct.92

Table 3.2 ISP33 Participants of blind calculation (2/4).

Participant	IJS (Slovenia)	OKB Gidropress (Russia)
Name	I. Parzer, S. Petelin, O. Gortnar, B. Mavko, M. Zeljko	S. I. Zaytzev
Organization	Institute "Jozef Stefan"	OKB Gidropress
Address	Jamova 39	Street Ordzonikidze, 21
City/State	61111 Ljubljana	142103 Moscow district, Podolsk
Zip Code		
Country	Slovenia	Russia
Phone Number	+3861 371 321	+7 095 137 91 08
Fax Number	+3861 374 919	
Telex	31296 YU JOSTIN	
Computer	**SUN Sparc 2**	**IBM-PC/AT/386/33**
CPU / Real Time	107550 s/7869.8 s (13.67)	360000 s/8000 s (45.00)
Code	**RELAP5/MOD3 5m5**	**DINAMIKA-5**
Model Descr.		
Volumes	220	
Junctions	237	
Heat slabs	259 (1263 Mesh points)	
Mailing date	31.Oct.92	none, received 29.Dec.92
Participant	**NPPRI (CSFR)**	**OKB Gidropress (Russia)**
Name	P. Matejovic	S. I. Zaytzev
Organization	Nuclear Power Plant Research Institute	OKB Gidropress
Address	Okruzna 5	Street Ordzonikidze, 21
City/State	918 64 Trnava	142103 Moscow district, Podolsk
Zip Code		
Country	Czechoslovakia	Russia
Phone Number	+42 805 41741	+7 095 137 91 08
Fax Number	+42 805 25396	
Telex	Cs-93851	
Computer	**PC PPS (INTEL486/33)**	**CYBER-962**
CPU / Real Time	185783 s/7893.8 s (23.54)	125000 s/ 7740 s (16.15)
Code	**RELAP5/MOD2/RMA**	**TECH-M-4**
Model Descr.		
Volumes	276	
Junctions	291	
Heat slabs	311 (1903 Mesh points)	
Mailing date	3.Nov.92	none, received 29.Dec.92
Participant	**NRI Rez (CSFR)**	**PSI (Switzerland)**
Name	P. Král	F. De Pasquale
Organization	Nuclear Research Institute	Paul Scherrer Institute
Address		Würenlingen and Villigen
City/State	25068 Rez	CH-5232 Villigen
Zip Code		
Country	Czechoslovakia	Switzerland
Phone Number	+42 2 685 8351	+056 99 27 26
Fax Number	+42 2 685 7567	+056 98 23 27
Telex		827417 psi ch
Computer	**HP-VECTRA**	**CRAY-YMP**
CPU / Real Time	231660 s/7844 s (29.53)	10564 s/ 7884 s (1.34)
Code	**RELAP5/MOD2.5/SRL**	**RELAP5/Mod2.5**
Model Descr.		
Volumes	273	216 (183 prim. / 33 sec.)
Junctions	310	234 (138 prim./ 36 sec)
Heat slabs	360 (1545 Mesh points)	230 (221 prim./ 9 sec.)
Mailing date	25.Nov.92	30.Oct.92

Table 3.3 ISP33 Participants of blind calculation (3/4).

Participant	RRC KI (Russia)	SEMAR LEACS (France)
Name	J. Stolchnev, S. Kichev	E. Laugier, L. Sabotinov
Organization	Russian Research Centre	Centre de Cadarache
	"Kurchatov Institute" (RRC KI)	
Address	Kurchatov Square	13108 Saint-Paul -Lez-Durance CEDEX
City/State	123182 Moscow	
Zip Code		
Country	Russia	France
Phone Number	+7 095 196 1702	+33 42 25 39 47, +33 42 25 78 60
Fax Number	+7 095 196 1702	+ 33 42 25 63 99
Telex	411594 Shuga	440 678 F
Computer	**IBM PC-386**	**CRAY-XMP**
CPU / Real Time	353350 s/ 7067.4 s (50.00)	7018 s/ 7891 s (0.89)
Code	**RELAP5/MOD3**	**CATHARE2 V1.3e**
Model Descr.		
Volumes		325
Junctions		52
Heat slabs		41
Mailing date	8.Dec.92	27.Nov.92
Participant	**RSC KI (Russia)**	**STUDS (Sweden)**
Name	A. Nikonov, S. Spolitak	J. Eriksson
Organization	Russian Scientific Centre Kurchatov Institute	Studsvik EcoSafe
	RSC KI	
Address	Dept. of Nucl. Reactors, Kurchatov Square, 1	
City/State	123182 Moscow	S-611 82 Nyköping
Zip Code		
Country	Russia	Sweden
Phone Number	+7 095 196 61 72	+46 155 221 827
Fax Number	+7 095 196 61 72	+46 155 221 616
Telex	411594 shuga	
Computer	**Cyber-963**	**SUN Server 630 Sparc10**
CPU / Real Time	37053 s/ 6770 s (5.47)	67800 s/ 7749 s (8.75)
Code	**SCDAP/RELAP5/MOD2**	**RELAP5/Mod3/V5m5**
Model Descr.		
Volumes	146	292
Junctions	150	357
Heat slabs	183 (549 Mesh points)	359 (2628 Mesh points)
Mailing date	14.Sep.92	30.Nov.92
Participant	**RSC KI (Russia)**	**TAEK (Turkey)**
Name	A. S. Devkin, E.D. Derbyshire	A. Tanrikut
Organization	Russian Science Centre "Kurchatov Institute"	Turkish Atomic Energy Authority
	(RSC KI)	
Address	Kurchatov Square	PK 249, Kavaklidere
City/State	123182 Moscow	06693 Ankara
Zip Code		
Country	Russia	Turkey
Phone Number	+7 095 196 61 72	+90 312 212 76 65
Fax Number	+7 095 196 66 39	+90 312 223 44 39
Telex	411594 shuga	
Computer	**IBM PC/AT-386 "GEO" model**	**IBM RISC 6000 - Model 320**
CPU / Real Time	458588 s/ 8819 s (52.00)	99900 s/ 7756 s (12.88)
Code	**RELAP5/MOD3 version 5m5**	**RELAP5/MOD3 (v5m5)**
Model Descr.		
Volumes	261	161
Junctions	276	166
Heat slabs	223	155
Mailing date	15.Dec.92	17.Oct.92

Table 3.4 ISP33 Participants of blind calculation (4/4).

Participant	**THZ (Germany)**
Name	B. Vandreier
Organization	Hochschule für Technik und Wirtschaft
	Zittau/Görlitz (FH)
Address	Theodor-Körner-Allee 16
City/State	FGE 7, Zittau
Zip Code	O-8800
Country	Germany
Phone Number	+03583 61674
Fax Number	+03583 61627
Telex	
Computer	**IBM RISC 6000 MOD 320**
CPU / Real Time	1311304 s/ 8000 s (163.91)
Code	**ATHLET Mod 1.0 Cycle E**
Model Descr.	
Volumes	379
Junctions	313
Heat slabs	342
Mailing date	25.Oct.92
Participant	**UP-DCMN (Italy)**
Name	W. Ambrosini, S. Barsotti, S. Belsito,
	F. D'Auria, M. Frogheri
Organization	University of Pisa, Department of
	Mechanical and Nuclear Engineering
Address	Via Diotisalvi 2
City/State	56126 Pisa
Zip Code	
Country	Italy
Phone Number	+39 50 585 253
Fax Number	+39 50 585 265
Telex	500104 (I)
Computer	**IBM 9121/440**
CPU / Real Time	117000 s/ 6993 s (16.73)
Code	**CATHARE 2 V1.2E**
Model Descr.	
Volumes	47 hydr. compon. 644 hydr. meshes
Junctions	50
Heat slabs	42
Mailing date	5.Dec.92
Participant	**FRG/FZR (Germany)**
Name	E. Krepper
Organization	Research Center Rossendorf Inc.
Address	POB 19
City/State	D-O-8051 Dresden
Zip Code	
Country	Germany
Phone Number	(0351) 591/3460
Fax Number	(0351)4605812
Telex	
Computer	**Sun Sparc 2**
CPU / Real Time	1000000 s/ 7660 s (130.55)
Code	**ATHLET mod 1.0 E**
Model Descr.	
Volumes	316
Junctions	262
Heat slabs	256
Mailing date	9. Mar. 93

Table 3.2 Comparison of events in blind calculation (1/6)

	EXPERIMENT		ISP 33 SUBMISSIONS : CALCULATED EVENTS							
FEATURE	ISP 33		BARC (I)	ATHLET	BARC (II)	ATHLET	BARC (III)	R4M6	ECN	R5M2.5
Pressurizer heater cycling										
	2 kW	0 s	2 kW	0.0 s	2 kW	0 s	0 kW	0 s	1 kW	0 s
	6 kW	420 s	6 kW	39 .6 s	4 kW	200 s			5 kW	180 s
	2 kW	680 s	2 kW	1152.0 s	4 kW	400 s			1 kW	300 s
	0 kW	1200 s	0 kW	1200 s	4 kW	600 s			5 kW	780 s
					4 kW	1000s			1 kW	900 s
									0 kW	1200 s
Drainings	Drained	Mass left	Drained	Mass left	Drained	Mass left	Drained	Mass left	Drained	Mass left
		650.0 kg		660 kg		669.8 kg		665.4 kg		650 kg
1 (1200 s)	58.0 kg	592.0 kg	60 kg	600 kg	60 kg	607.6 kg	60.0 kg	605.4 kg	60.0 kg	590 kg
2 (2100 s)	64.5 kg	527.5 kg	60 kg	540 kg	60 kg	543.2 kg	60.0 kg	545.4 kg	60.0 kg	530 kg
3 (3000 s)	61.8 kg	465.7 kg	60 kg	480 kg	60 kg	476.3 kg	60.0 kg	485.4 kg	60.0 kg	470 kg
4 (3900 s)	58.9 kg	406.8 kg	60 kg	420 kg	60 kg	442.3 kg	60.0 kg	425.4 kg	60.0 kg	410 kg
5 (4800 s)	58.6 kg	348.2 kg	60 kg	360 kg	45 kg	366.6 kg	60.0 kg	365.4 kg	60.0 kg	350 kg
6 (5700 s)	60.3 kg	287.9 kg	60 kg	300 kg			60.0 kg	305.4 kg	60.0 kg	290 kg
7 (6600 s)	58.5 kg	229.4 kg	60 kg	240 kg			60.0 kg	245.4 kg	60.0 kg	230 kg
8 (7500 s)			60 kg	180 kg			60.0 kg	185.4 kg	60.0 kg	170 kg
9 (8400 s)										
Void exists (void > 5%)										
Upper head	-		1315 s		2120 s		1300 s		2000 s	
Hot leg	-		1308 s		2125 s	loop 2	3000 s		3060 s	
SG tubes	-		2141 s	hot coll.	3017 s	loop 3	6600 s		5760 s	
Cold leg	-		3303 s		3080 s	loop 2	3000 s		4860 s	
Core top	-		3000 s		2250 s		3900 s		3060 s	
Natural circulation modes										
Single phase NC			0 - 3000 s		-		0 - 3000 s		0 - 3000 s	
Two-phase NC			3300 - 7605 s		-		3000 - 5800 s		3000 - 5760 s	
Stalled Two-phase NC			7605 - 7626 s		-		5800 - 6100 s		5760 - 7500 s	
Steam heat-up in core			7626 - 7916 s		-		6100 - 7500 s		7500 - 7845 s	
Core temperatures										
350 C reached	6690 s		7626 s		4845 s		6100 s		7591 s	
900 C reached			7916 s (750 C)		-		7500 s (670 C)		7846 s	

Table 3.2 Comparison of events in blind calculation (2/6)

	EXPERIMENT		ISP 33 SUBMISSIONS : CALCULATED EVENTS							
FEATURE	ISP 33		GRS	ATHLET	IJS	R5M2	IJS	R2M3	NPPRI	R5M2
Pressurizer heater cycling										
	2 kW	0 s	2 kW	0 s	2 kW	0 s	2 kW	0 s	0 kW	1200 s
	6 kW	420 s	6 kW	168 s	6 kW	380 s	6 kW	no		
	2 kW	680 s	2 kW	394 s	2 kW	580 s	2 kW	no		
	0 kW	1200 s	6 kW	994 s	0 kW	1200 s	0 kW	1200 s		
			0 kW	1200 s						
Drainings	Drained	Mass left	Drained	Mass left	Drained	Mass left	Drained	Mass left	Drained	Mass left
		650.0 kg		644.9 kg		647.3 kg		647.2 kg		
1 (1200 s)	58.0 kg	592.0 kg	60.2 kg	584.7 kg	60.0 kg	587.3 kg	60.0 kg	587.1 kg	60.0 kg	
2 (2100 s)	64.5 kg	527.5 kg	59.9 kg	524.7 kg	60.0 kg	527.5 kg	60.0 kg	527.5 kg	60.0 kg	
3 (3000 s)	61.8 kg	465.7 kg	60.1 kg	464.7 kg	60.0 kg	468.2 kg	60.0 kg	469.0 kg	60.0 kg	
4 (3900 s)	58.9 kg	406.8 kg	63.5 kg	401.2 kg	60.0 kg	411.0 kg	60.0 kg	411.7 kg	60.0 kg	
5 (4800 s)	58.6 kg	348.2 kg	59.8 kg	341.4 kg	60.0 kg	351.0 kg	60.0 kg	352.5 kg	60.0 kg	
6 (5700 s)	60.3 kg	287.9 kg	59.7 kg	281.7 kg	60.0 kg	288.8 kg	60.0 kg	288.5 kg	60.0 kg	
7 (6600 s)	58.5 kg	229.4 kg	60.0 kg	221.7 kg	60.0 kg	228.9 kg	60.0 kg	228.0 kg	60.0 kg	
8 (7500 s)			60.7 kg	161.0 kg	60.0 kg	169 kg	60.0 kg	167.0 kg	60.0 kg	
9 (8400 s)										
Void exists (void > 5%)										
Upper head	-		2115 s		2100 s		2100 s			
Hot leg	-		2717 s		2100 s		2100 s			
SG tubes	-		3290 s		3000 s		3000 s			
Cold leg	-		5700 s		5700 s		5700 s			
Core top	-		3010 s		2100 s		2100 s			
Natural circulation modes										
Single phase NC			0 - 3000 s		0 - 2100 s		0 - 2100 s			
Two-phase NC			3000 - 5700 s		2100 - 5700 s		2100 - 5700 s			
Stalled Two-phase NC			5700 - 7667 s		5700 - 7500 s		5700 - 7500 s			
Steam heat-up in core			7500 - 7667 s		7500 -		7500 -			
Core temperatures										
350 C reached	6690 s		7525 s		7563 s		7564 s			
900 C reached			7591 s		7863 s		7869 s			

Table 3.2 Comparison of events in blind calculation (3/6)

	EXPERIMENT		ISP 33 SUBMISSIONS : CALCULATED EVENTS							
FEATURE	ISP 33		NRI Rez	R5M2.5	OKB G	DIN.	OKB G	T-M-4	UP -DCMN	CAT
Pressurizer heater cycling										
	2 kW	0 s	2 kW	0 s	2 kW	0 s	2 kW	0 s	2 kW	0 s
	6 kW	420 s	6 kW	560 s	6 kW	150 s	6 kW	100 s	6 kW	215 s
	2 kW	680 s	2 kW	680 s	2 kW	430 s	2 kW	270 s	2 kW	253 s
	0 kW	1200 s	0 kW	1200 s	0 kW	1200 s	6 kW	830 s	0 kW	1200 s
							2 kW	1000 s		
								1200 s		
Drainings	Drained	Mass left	Drained	Mass left	Drained	Mass left	Drained	Mass left	Drained	Mass left
		650.0 kg		650.8 kg						630 kg
1 (1200 s)	58.0 kg	592.0 kg	60.6 kg	590.2 kg	60.0 kg		60.0 kg		58 kg	572 kg
2 (2100 s)	64.5 kg	527.5 kg	60,9 kg	528.0 kg	60.0 kg		60.0 kg		60 kg	512 kg
3 (3000 s)	61.8 kg	465.7 kg	54.4 kg	469.8 kg	60.0 kg		60.0 kg		61 kg	451 kg
4 (3900 s)	58.9 kg	406.8 kg	58.0 kg	409.9 kg	60.0 kg		60.0 kg		61 kg	390 kg
5 (4800 s)	58.6 kg	348.2 kg	63.9 kg	350.1 kg	60.0 kg		60.0 kg		68 kg	322 kg
6 (5700 s)	60.3 kg	287.9 kg	61.0 kg	289.9 kg	60.0 kg		60.0 kg		61 kg	261 kg
7 (6600 s)	58.5 kg	229.4 kg	61.8 kg	230.0 kg	60.0 kg		60.0 kg		61 kg	200 kg
8 (7500 s)			64.2 kg	169.9 kg	60.0 kg		60.0 kg			
9 (8400 s)										
Void exists (void > 5%)										
Upper head	-		1380 s		2100 s		1400 s		1220 s	
Hot leg	-		2130 s	temporary	2800 s		2200 s		2250 s	
SG tubes	-		3930 s		3200 s		3100 s		3000 s	
Cold leg	-		4830 s		3950 s		3500 s		4000 s	
Core top	-		2130 s		3050 s		2300 s		2800 s	
Natural circulation modes										
Single phase NC				0 - 1320 s		0 - 2800 s		0 - 2200 s		0 - 3000 s
Two-phase NC				1320 - 7500 s		2800 - 5750 s		2200 - 4800 s		3000 - 4800 s
Stalled Two-phase NC				2890 - 3000 s		5750 - 8000 s		4800 - 5800 s		4800 - 6993 s
Steam heat-up in core				7500 - 7844 s		7575 - 8000 s		5740 - 5800 s		6635 s
Core temperatures										
350 C reached	6690 s		7574 s		7593 s		5765 s		6683 s	
900 C reached			7844 s		8240 s		6760 s		6993 s	

Table 3.2 Comparison of events in blind calculation (4/6)

	EXPERIMENT		ISP 33 SUBMISSIONS : CALCULATED EVENTS							
FEATURE	ISP 33		PSI	R5M2.5	RRC KI St	R5M3	RSC KI Ni	SR5M2	RSC KI De	R5M3
Pressurizer heater cycling										
	2 kW	0 s	2 kW	0 s	0 kW	1200 s	2 kW	0 s	2 kW	0 s
	6 kW	420 s	6 kW	250 s			0 kW	1200 s	6 kW	30 s
	2 kW	680 s	2 kW	450 s					2 kW	610 s
	0 kW	1200 s	0 kW	1200 s					0 kW	1200 s
Drainings	Drained	Mass left	Drained	Mass left	Drained	Mass left	Drained	Mass left	Drained	Mass left
		650.0 kg		651 kg				648.4 kg		
1 (1200 s)	58.0 kg	592.0 kg	60.0 kg	591 kg	60.0 kg		60.0 kg	588.4 kg	60.0 kg	
2 (2100 s)	64.5 kg	527.5 kg	60.0 kg	531 kg	60.0 kg		60.0 kg	528.2 kg	60.0 kg	
3 (3000 s)	61.8 kg	465.7 kg	60.0 kg	471 kg	60.0 kg		60.0 kg	467.7 kg	60.0 kg	
4 (3900 s)	58.9 kg	406.8 kg	60.0 kg	411 kg	60.0 kg		60.0 kg	405.8 kg	60.0 kg	
5 (4800 s)	58.6 kg	348.2 kg	60.0 kg	359 kg	60.0 kg		60.0 kg	345.3 kg	60.0 kg	
6 (5700 s)	60.3 kg	287.9 kg	60.0 kg	316 kg	60.0 kg		60.0 kg	284.9 kg	60.0 kg	
7 (6600 s)	58.5 kg	229.4 kg	60.0 kg	263 kg	60.0 kg		60.0 kg	224.7 kg	60.0 kg	
8 (7500 s)			60.0 kg	205 kg			60.0 kg	165.4 kg	60.0 kg	
9 (8400 s)									60.0 kg	
Void exists (void > 5%)										
Upper head	-		2145 s		1400 s		1800 s		1379 s	
Hot leg	-		1323 s		2100 s		2400 s		1209 s	
SG tubes	-		4833 s				3100 s		3020 s	
Cold leg	-		5778 s				4860 s		3990 s	
Core top	-		2100 s				2600 s		1329 s	
Natural circulation modes										
Single phase NC								0 - 1380 s		0 - 1300 s
Two-phase NC								1380 s -		1300 - 6000 s
Stalled Two-phase NC								3000 s -		6000 - 8000 s
Steam heat-up in core								7560 s -		7960 - 8081 s
Core temperatures										
350 C reached	6690 s		7582 s				7576 s		7850 s	
900 C reached			7884 s				7871 s		8081 s	

Table 3.2 Comparison of events in blind calculation (5/6)

	EXPERIMENT		ISP 33 SUBMISSIONS : CALCULATED EVENTS							
FEATURE	ISP 33		STUDS	R5M3	SEMAR	CAT	TAEK	R5M3	THZ	ATHLET
Pressurizer heater cycling										
	2 kW	0 s	2 kW	0 s	2 kW	0 s	2 kW	0 s	2 kW	0 s
	6 kW	420 s	4 kW	221 s	4 kW	238 s	1 kW	10 s	6 kW	362 s
	2 kW	680 s	2 kW	441 s	2 kW	443 s	0 kW	1200 s	2 kW	554 s
	0 kW	1200 s	0 kW	1200 s	0 kW	1200 s			0 kW	1200 s
Drainings	Drained	Mass left	Drained	Mass left	Drained	Mass left	Drained	Mass left	Drained	Mass left
		650.0 kg		637 kg		660.3 kg		639 kg		648.3 kg
1 (1200 s)	58.0 kg	592.0 kg	60.0 kg	577 kg	59.9 kg	600.4 kg	60.0 kg	579 kg	60.0 kg	588.3 kg
2 (2100 s)	64.5 kg	527.5 kg	60.0 kg	517 kg	61.8 kg	538.6 kg	60.0 kg	519 kg	60.0 kg	528.3 kg
3 (3000 s)	61.8 kg	465.7 kg	60.0 kg	457 kg	61.8 kg	467.8 kg	60.0 kg	459 kg	60.0 kg	469.0 kg
4 (3900 s)	58.9 kg	406.8 kg	60.0 kg	397 kg	60.6 kg	416.1 kg	60.0 kg	399 kg	60.0 kg	409.3 kg
5 (4800 s)	58.6 kg	348.2 kg	60.0 kg	338 kg	61.1 kg	355.0 kg	60.0 kg	339 kg	60.0 kg	348.6 kg
6 (5700 s)	60.3 kg	287.9 kg	60.0 kg	279 kg	61.4 kg	293.6 kg	60.0 kg	279 kg	60.0 kg	288.2 kg
7 (6600 s)	58.5 kg	229.4 kg	60.0 kg	228 kg	60.2 kg	233.4 kg	60.0 kg	219 kg	60.0 kg	227.8 kg
8 (7500 s)			60.0 kg	162 kg	60.5 kg	172.8 kg	60.0 kg	159 kg	60.0 kg	167.4 kg
9 (8400 s)										
Void exists (void > 5%)										
Upper head	-		1382 s		2100 s		1290 s		1365 s	
Hot leg	-		2406 s		2100 s		1260 s		2160 s	
SG tubes	-		3065 s		3000 s		3930 s		3060 s	
Cold leg	-		6640 s		3170 s		4860 s		3960 s	
Core top	-		2901 s		2100 s		1230 s		3060 s	
Natural circulation modes										
Single phase NC			0 - 3960 s		0 - 2750 s		0 - 1260 s		0 -3060 s	
Two-phase NC			3960 - 4980 s		2750 - 3960 s		1260 - 5760 s		3060 - 7560 s	
Stalled Two-phase NC			4980 s -		3960 - 7890 s		5760 - 7560 s		7560 - 8000 s	
Steam heat-up in core			7550 s -		7530 - 7890 s		7560 - 7750 s		7555 - 8000 s	
Core temperatures										
350 C reached	6690 s		7584 s		7620 s		7513 s		7582 s	
900 C reached			7749 s		7890 s		7756 s		7911 s	

Table 3.2 Comparison of events in blind calculation (6/6)

	EXPERIMENT		ISP 33 SUBMISSIONS : CALCULATED EVENTS	
FEATURE	ISP 33		FZR	ATHLET
Pressurizer heater cycling				
	2 kW 0 s 6 kW 420 s 2 kW 680 s 0 kW 1200 s		2 kW 0 s 4 kW 380 s 0 kW 1200 s	
Drainings	Drained	Mass left	Drained	Mass left
		650.0 kg		
1 (1200 s)	58.0 kg	592.0 kg	60.0 kg	
2 (2100 s)	64.5 kg	527.5 kg	60.0 kg	
3 (3000 s)	61.8 kg	465.7 kg	60.0 kg	
4 (3900 s)	58.9 kg	406.8 kg	60.0 kg	
5 (4800 s)	58.6 kg	348.2 kg	60.0 kg	
6 (5700 s)	60.3 kg	287.9 kg	60.0 kg	
7 (6600 s)	58.5 kg	229.4 kg	60.0 kg	
8 (7500 s)			60.0 kg	
9 (8400 s)				
Void exists (void > 5%)				
Upper head	-		1380 s	
Hot leg	-			
SG tubes	-			
Cold leg	-			
Core top	-			
Natural circulation modes				
Single phase NC				
Two-phase NC				
Stalled Two-phase NC				
Steam heat-up in core				
Core temperatures				
350 C reached	6690 s		7592 s	
900 C reached			7660 s (500 C)	

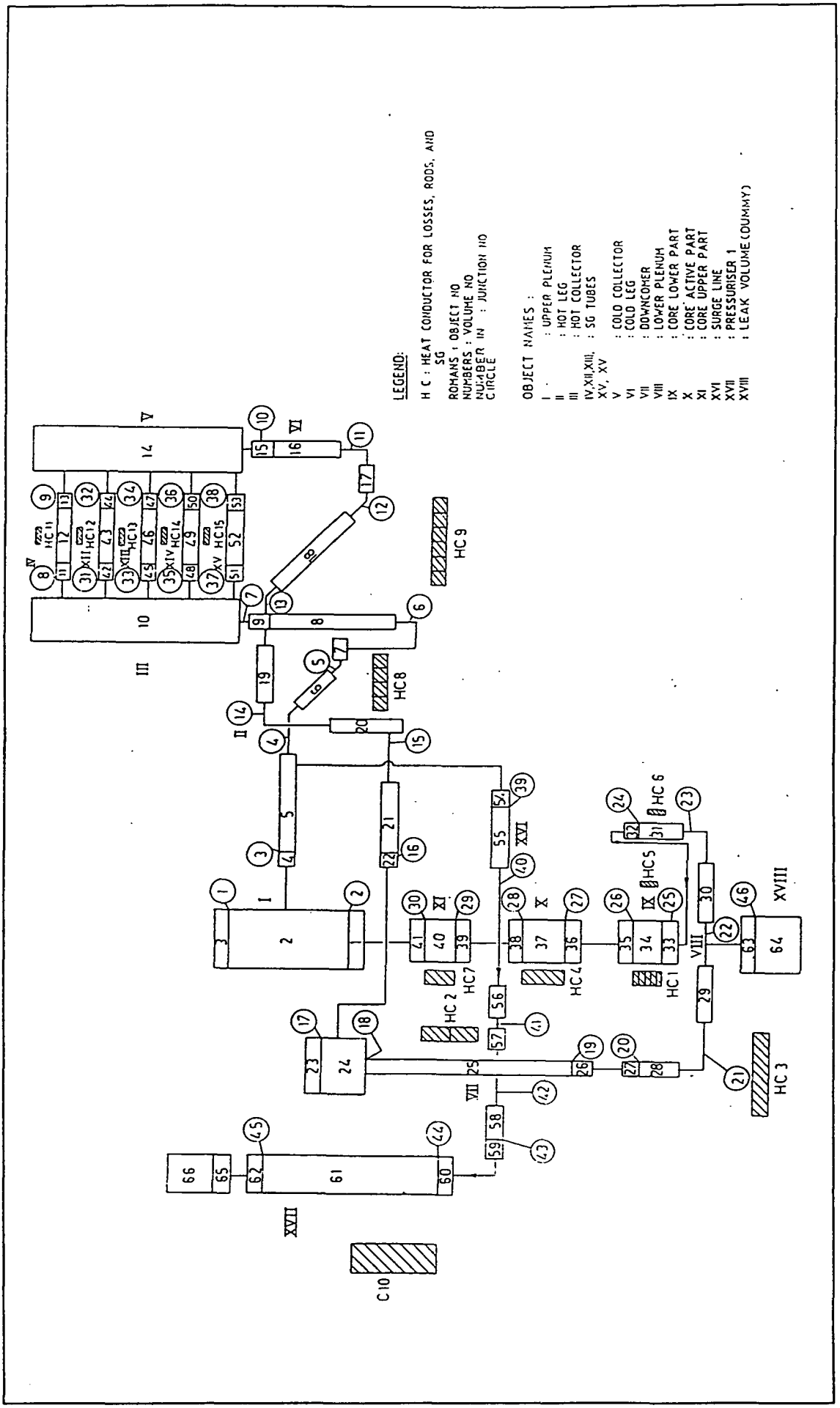

Figure 3.1. ATHLET nodalization for ISP33 by BARC, (Case I).

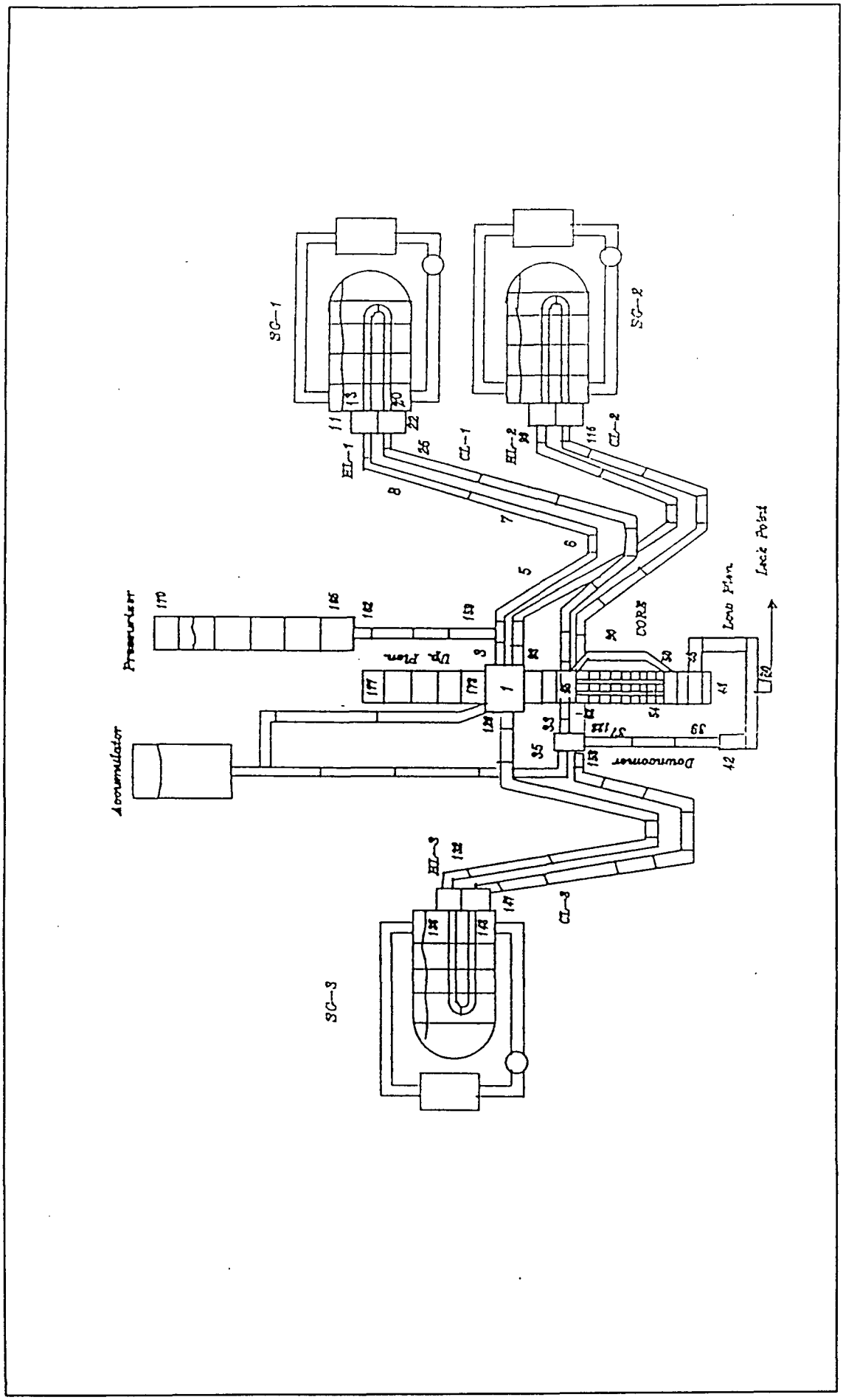

Figure 3.2. ATHLET nodalization for ISP33 by BARC, (Case II).

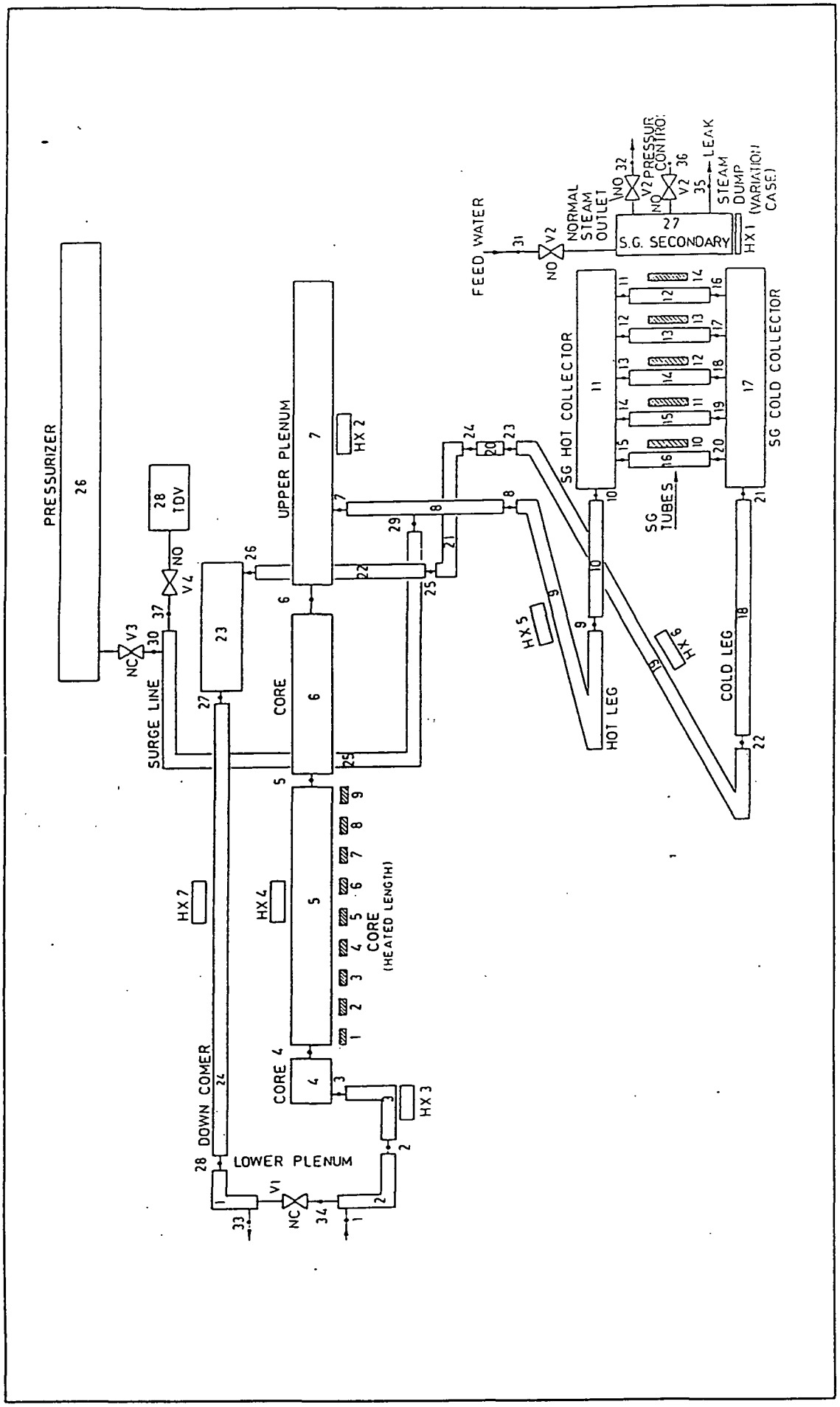

Figure 3.3. RELAP4/MOD6 nodalization for ISP33 by BARC, (Case III).

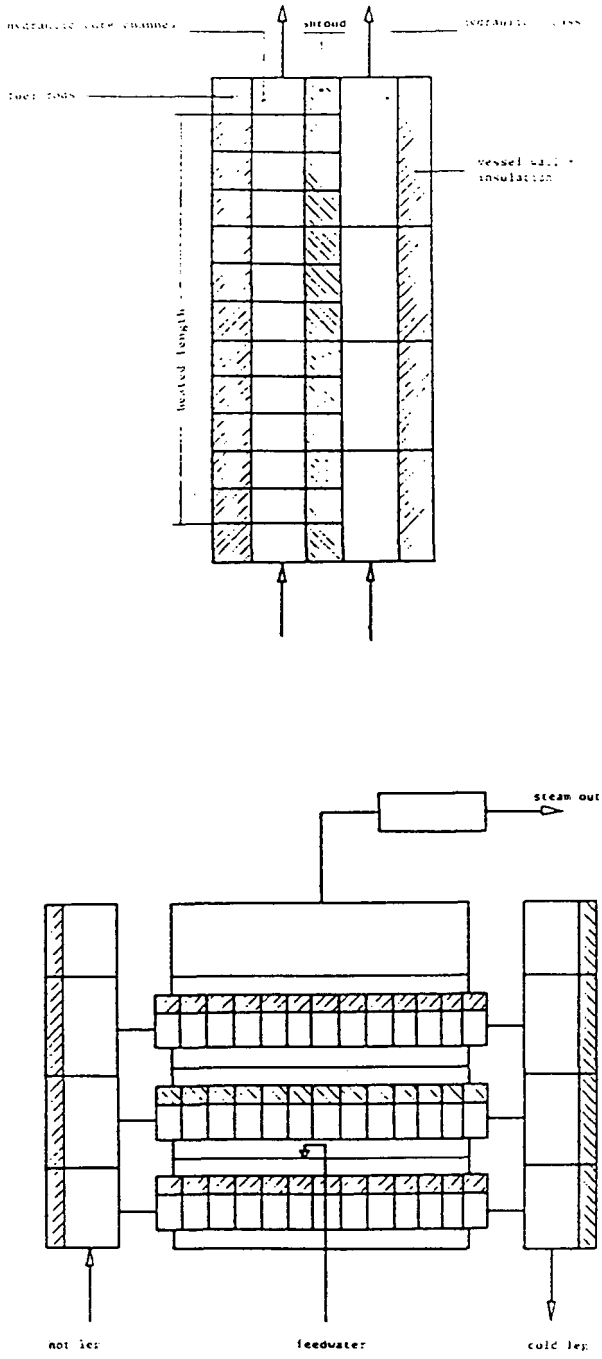

Figure 3.4. RELAP5/MOD2.5 core and steam generator nodalizations for ISP33 by ECN.

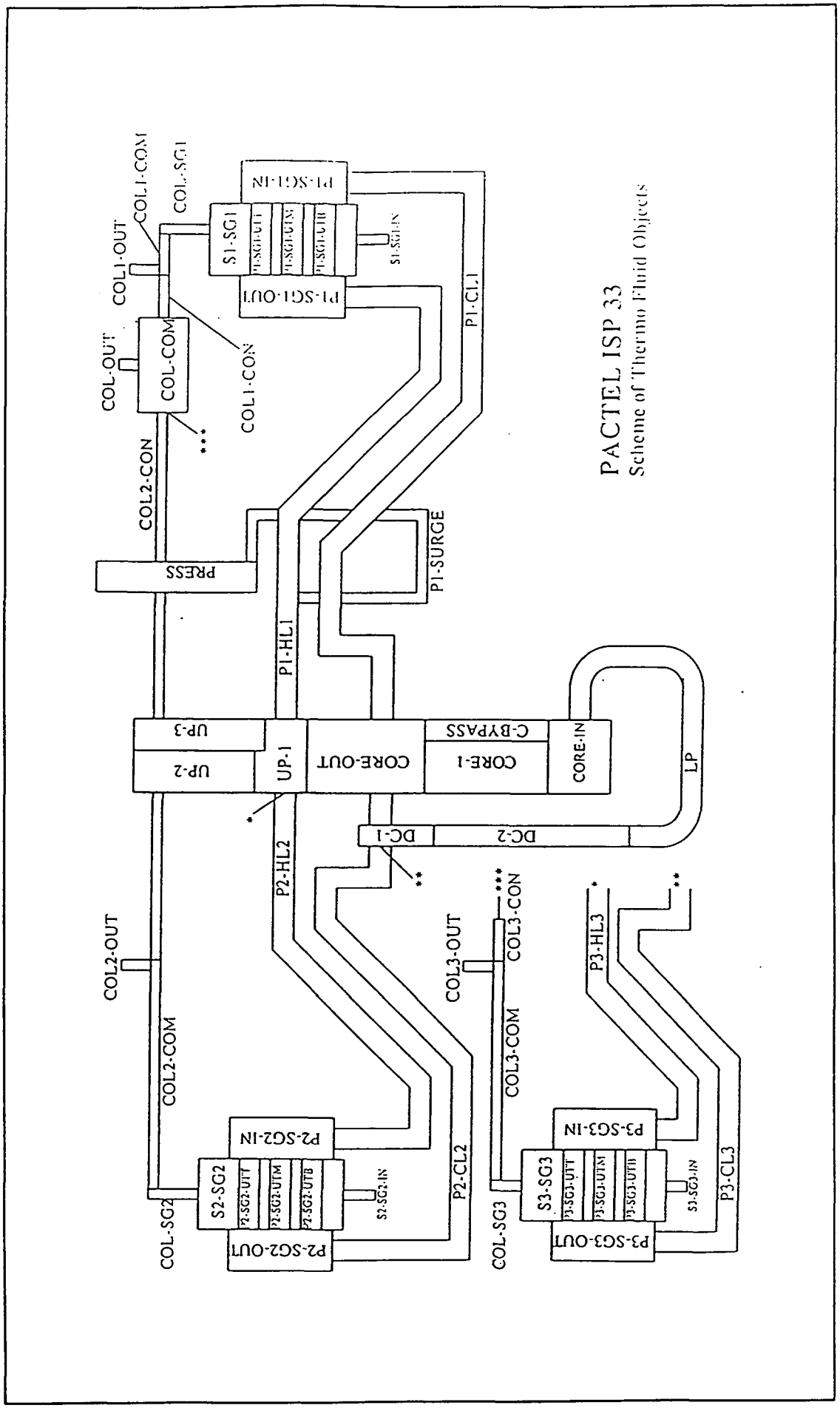

Figure 3.5. ATHLET nodalization for ISP33 by GRS.

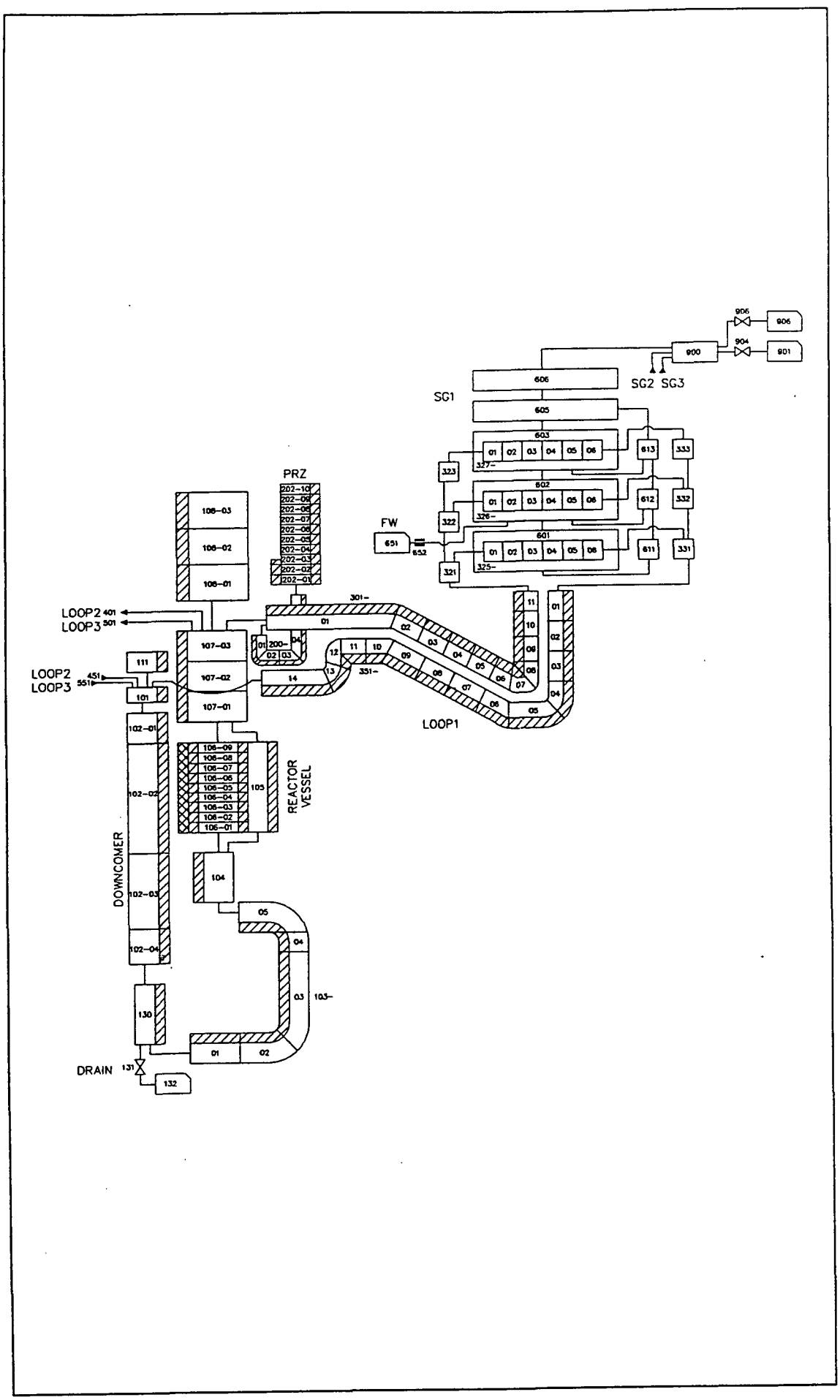

Figure 3.6. RELAP nodalization for ISP33 by IJS, (MOD2 and MOD3).

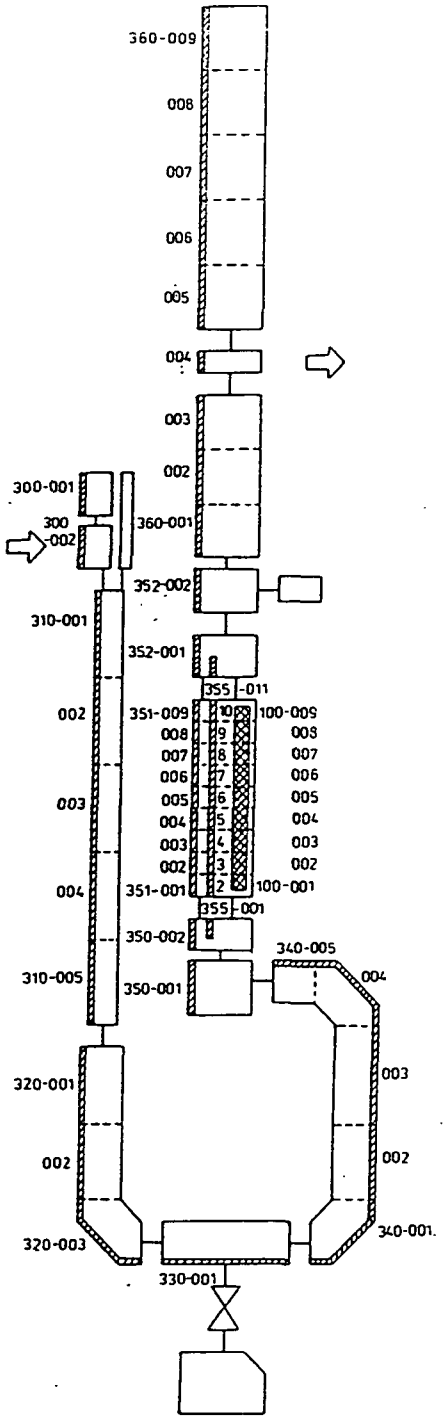

Figure 3.7. RELAP5/MOD2 nodalization for ISP33 by NPPRI, (LP, DC core and UP).

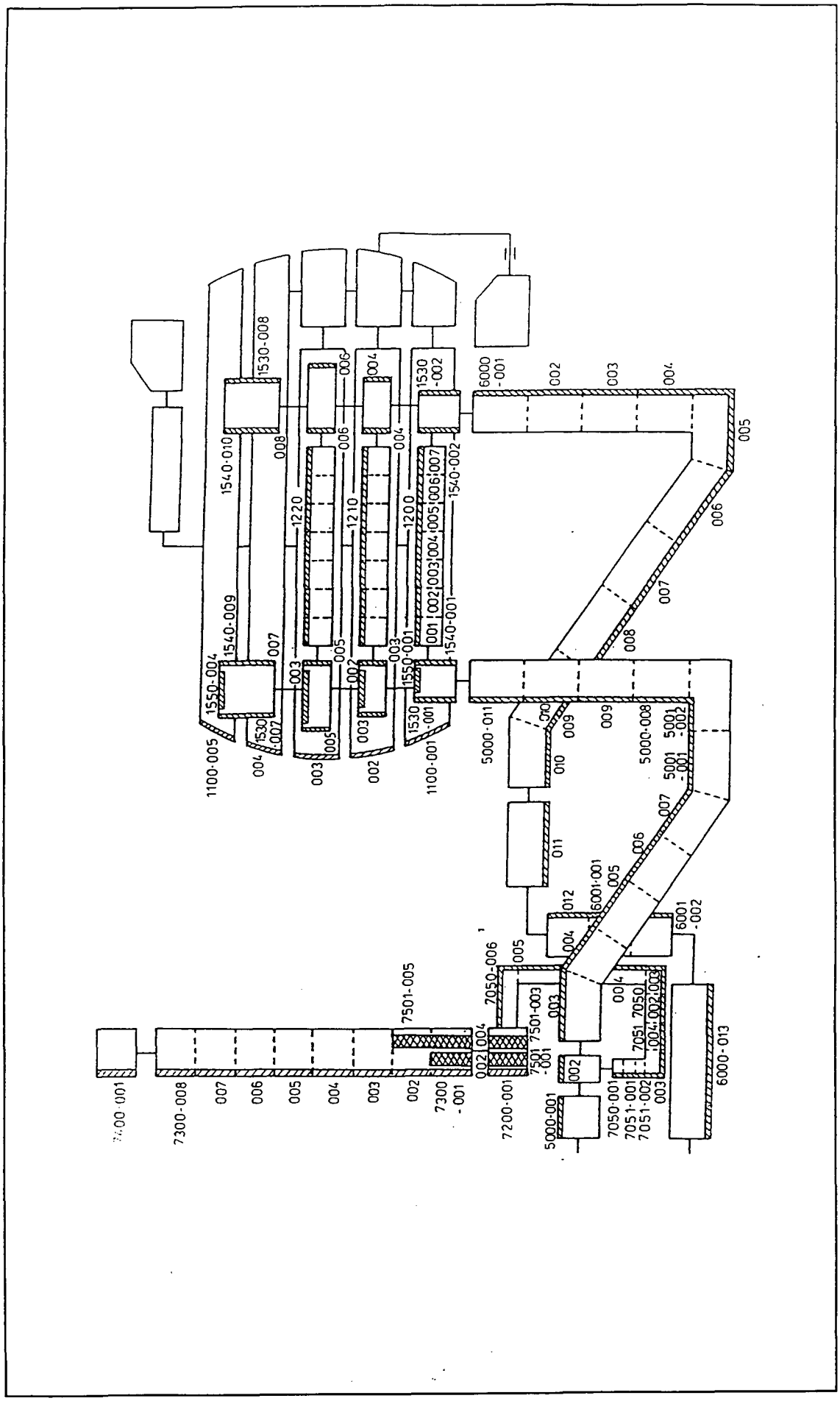

Figure 3.8. RELAP5/MOD2 nodalization for ISP33 by NPPRI, (loop 1).

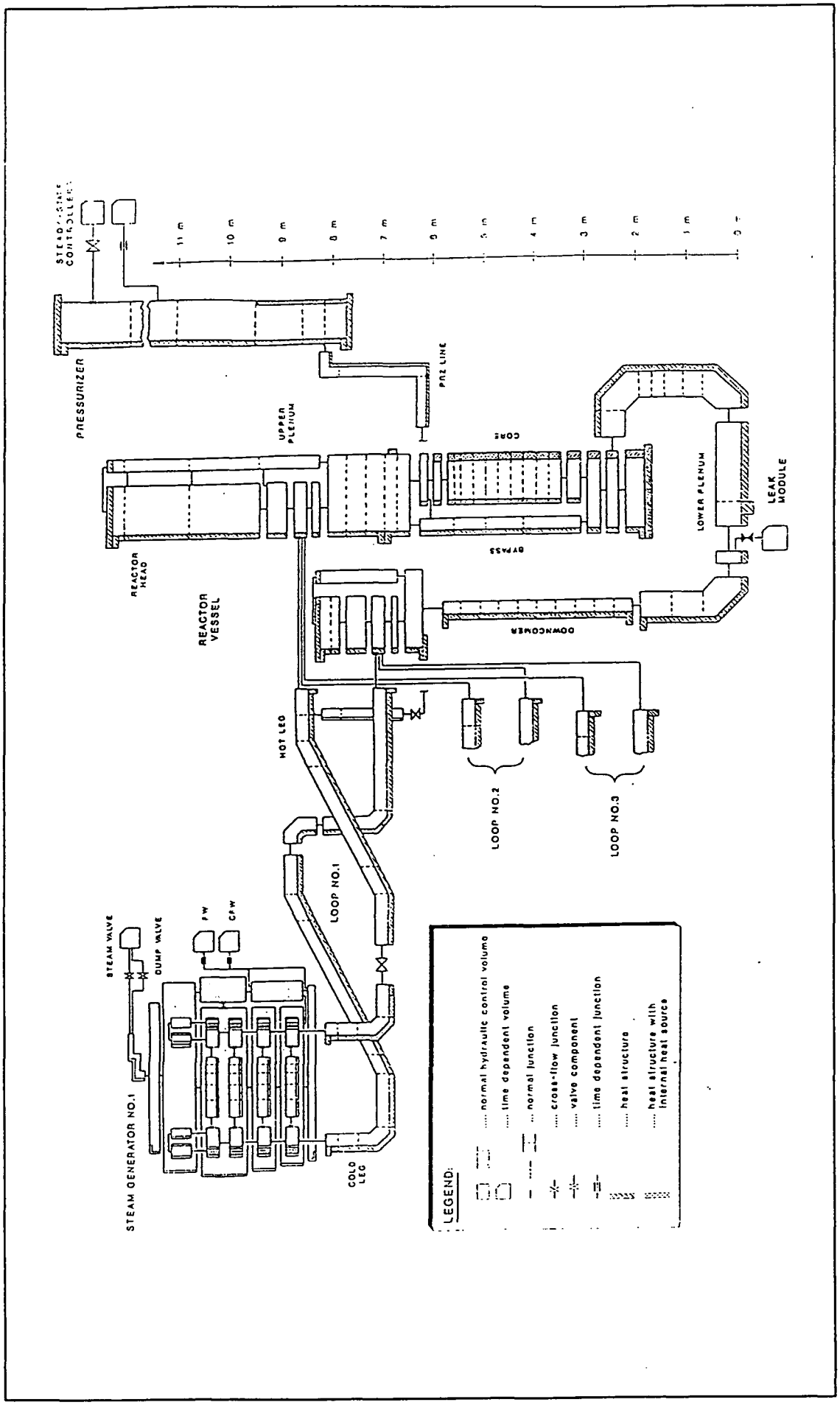

Figure 3.9. RELAP5/MOD2.5 nodalization for ISP33 by NRI Rez.

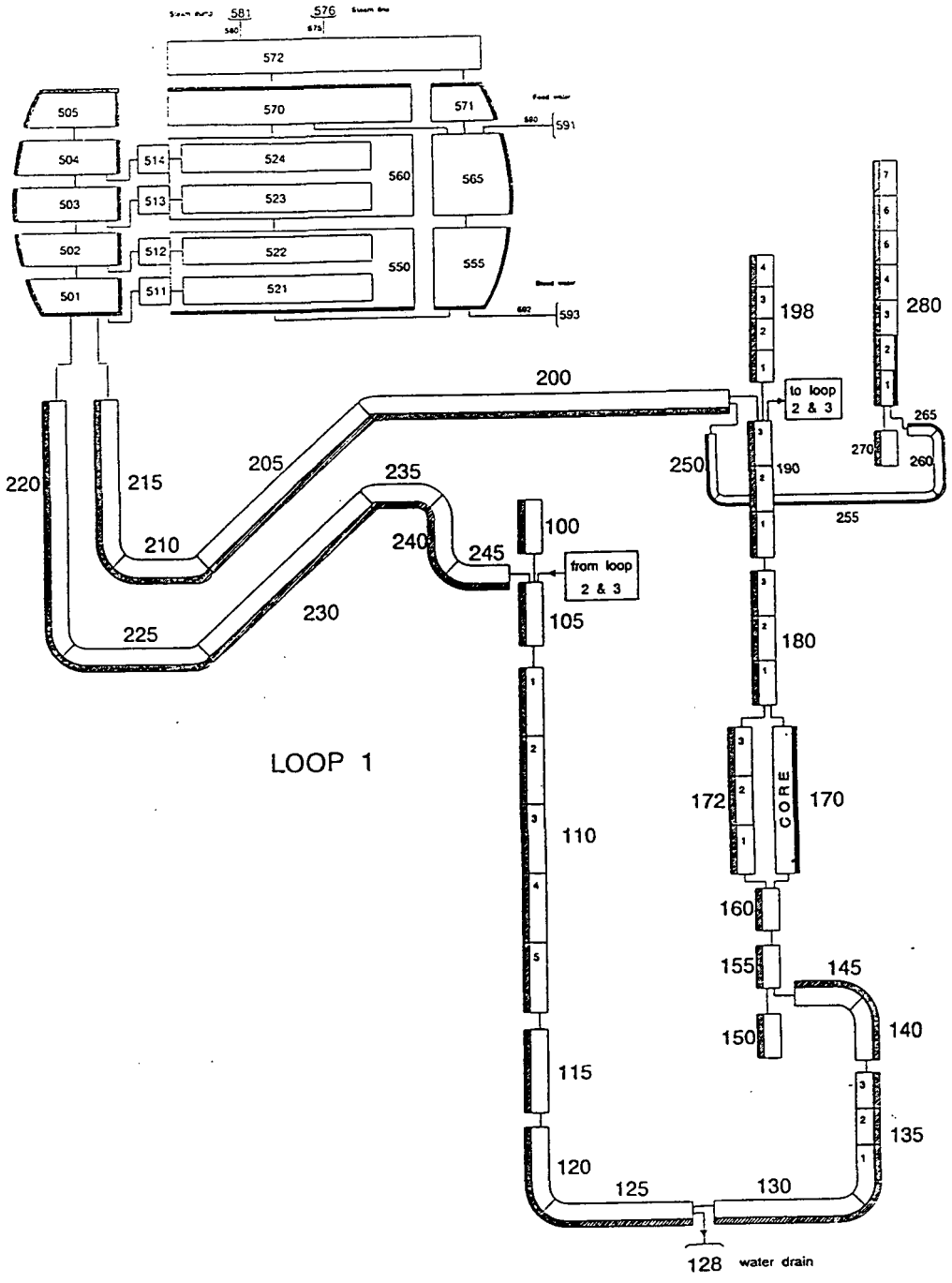

Figure 3.10. RELAP5/MOD2.5 nodalization for ISP33 by PSI.

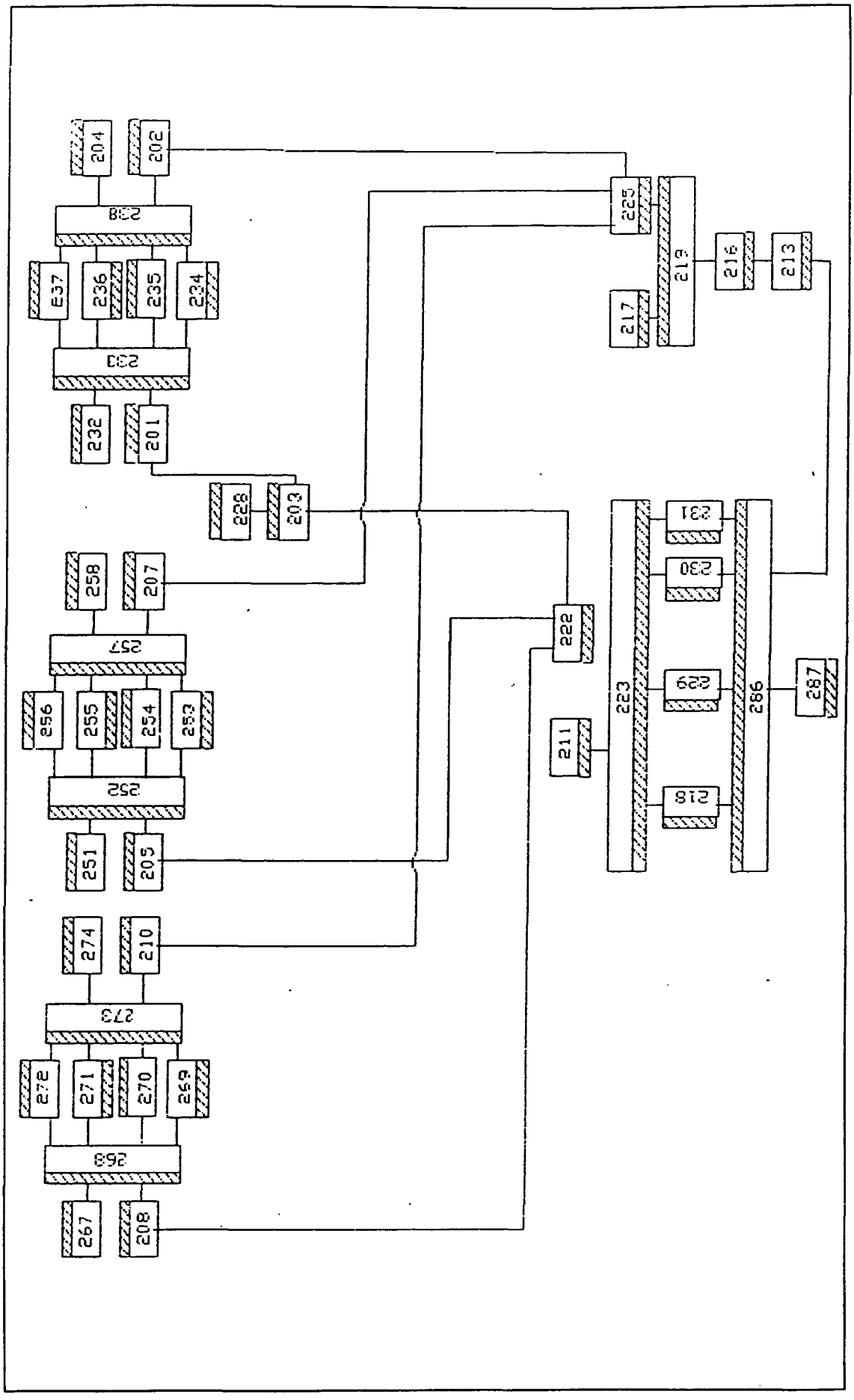

Figure 3.11. RELAP5/MOD3 PACTEL primary circuit nodalization for ISP33 by RRC KI (Stolchnev).

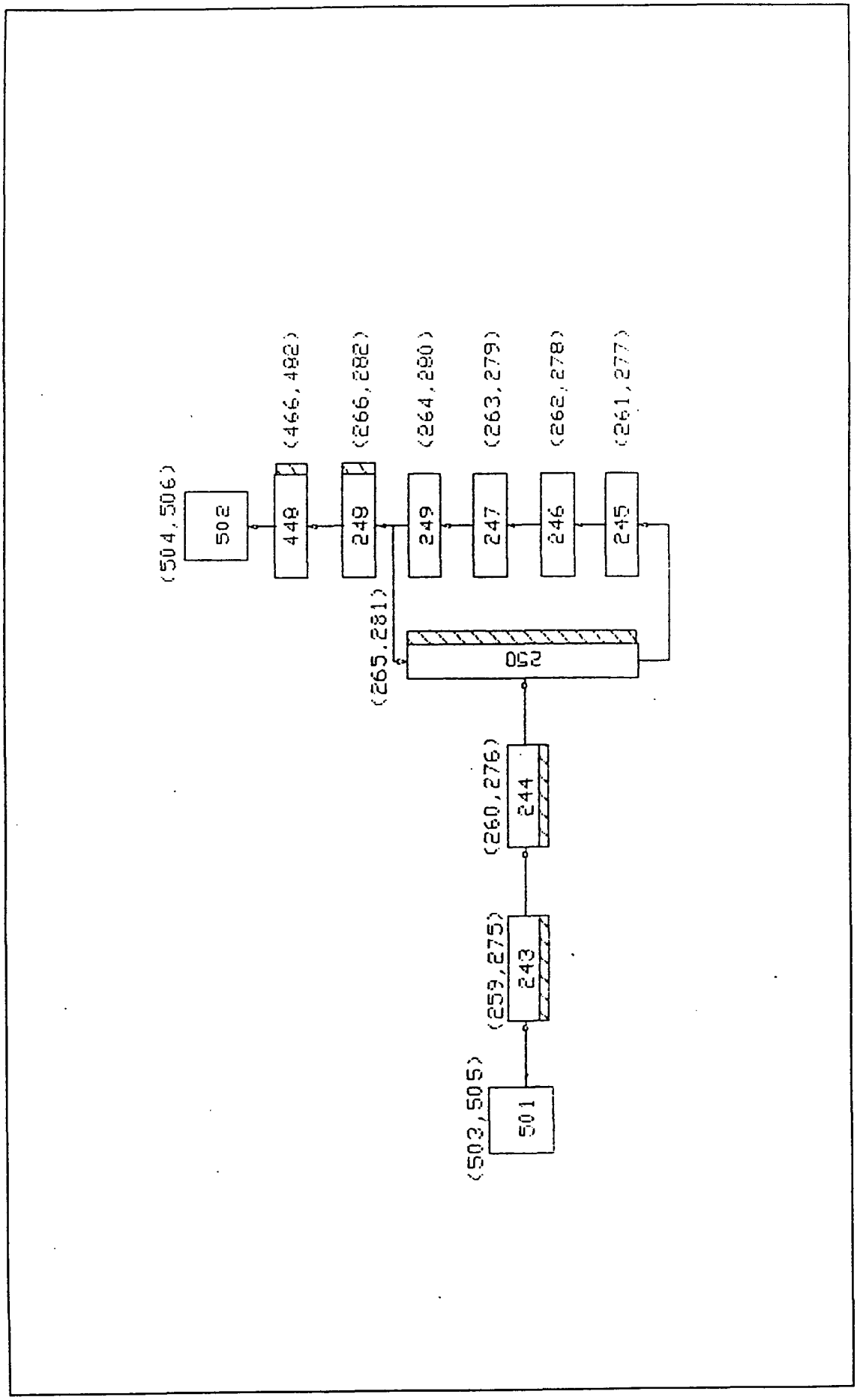

Figure 3.12. RELAP5/MOD3 PACTEL secondary circuit nodalization for ISP33 by RRC KI (Stolchnev).

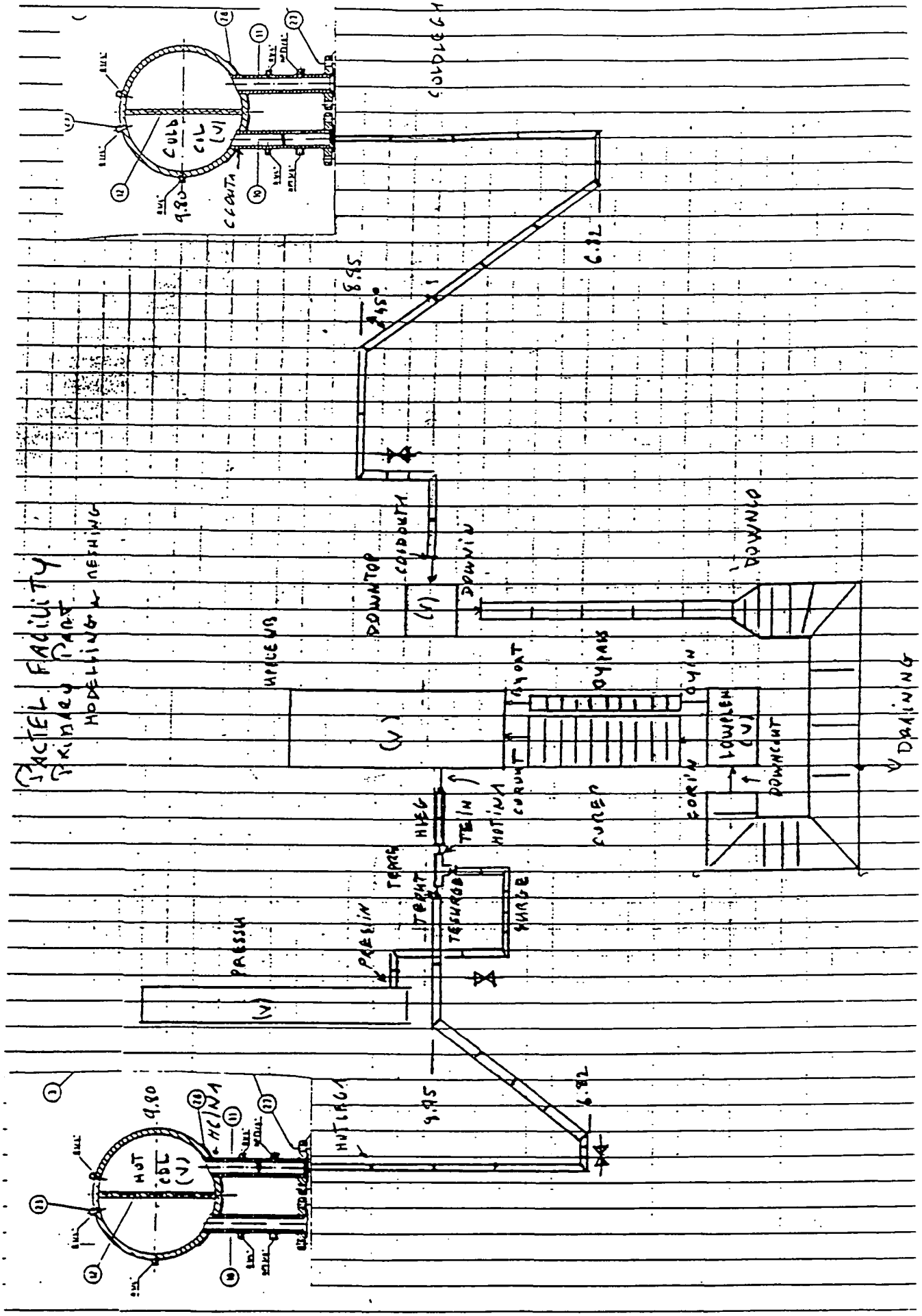

Figure 3.13. CATHARE2 primary part nodalization for ISP33 by SEMAR LEACS.

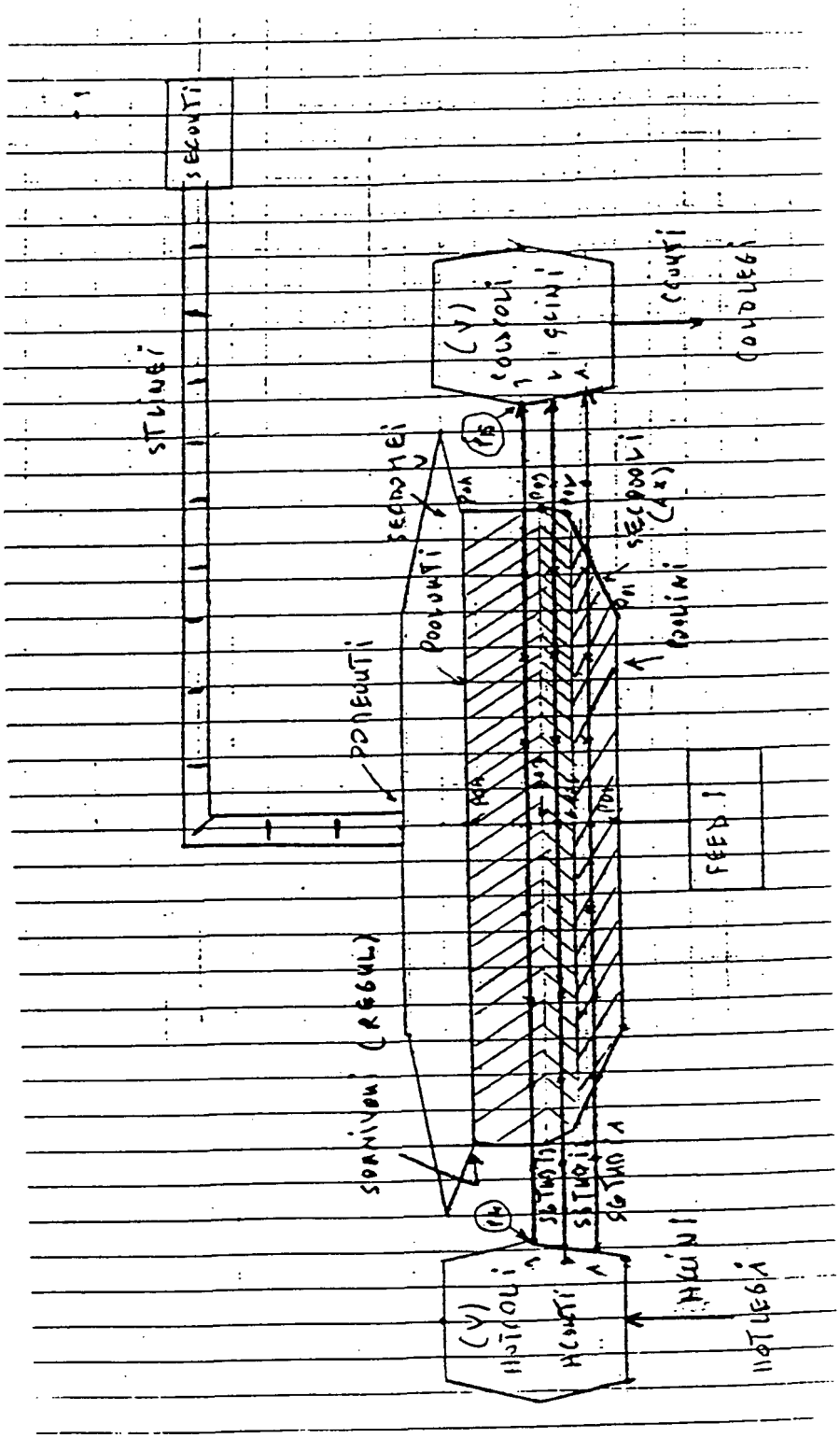

Figure 3.14. CATHARE2, steam generator primary and secondary part nodalization for ISP33 by SEMAR LEACS.

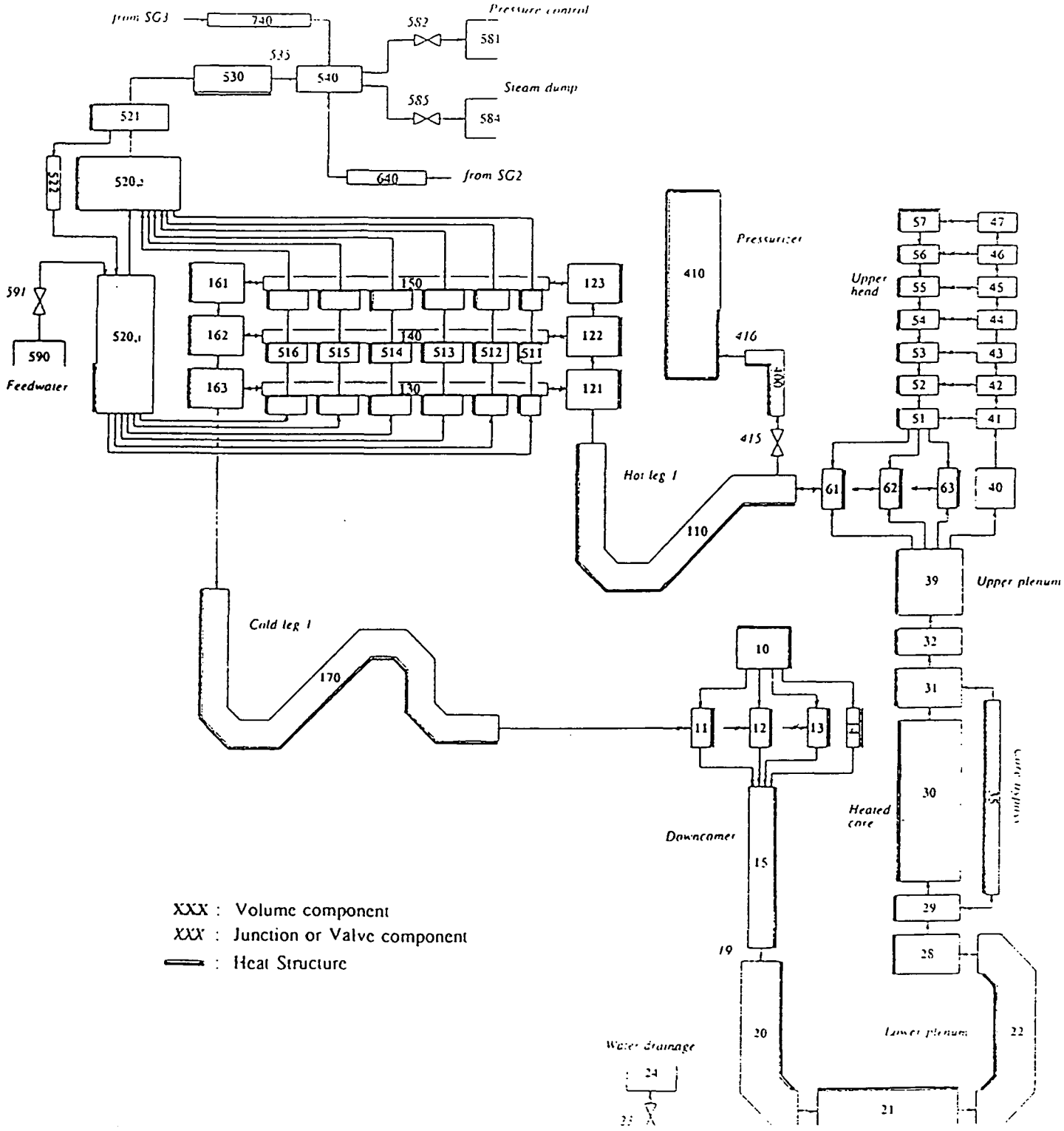

Figure 3.15. RELAP5/MOD3 nodalization for ISP33 by STUDS.

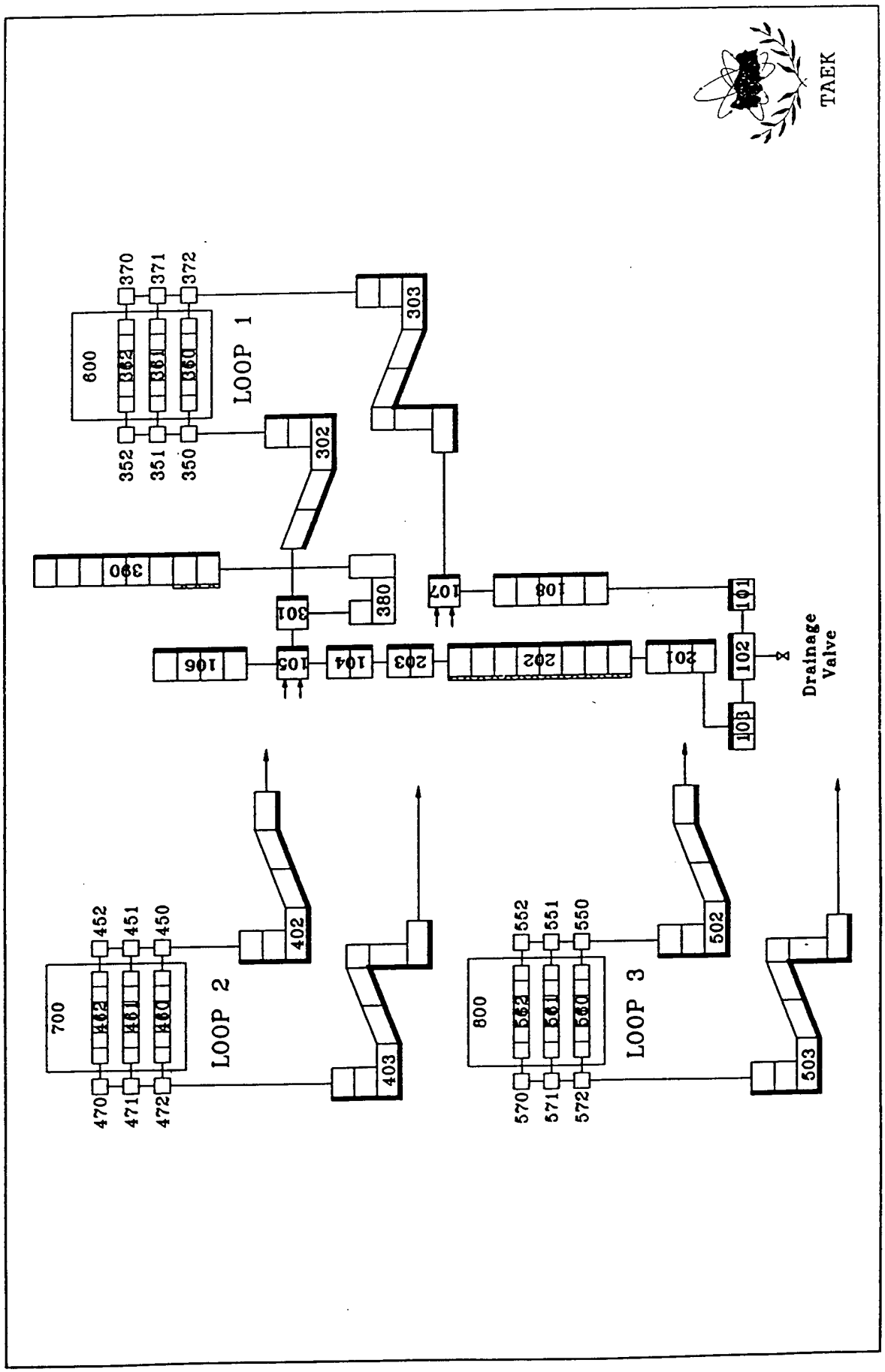

Figure 3.16. RELAP5/MOD3 nodalization for ISP33 by TAEK.

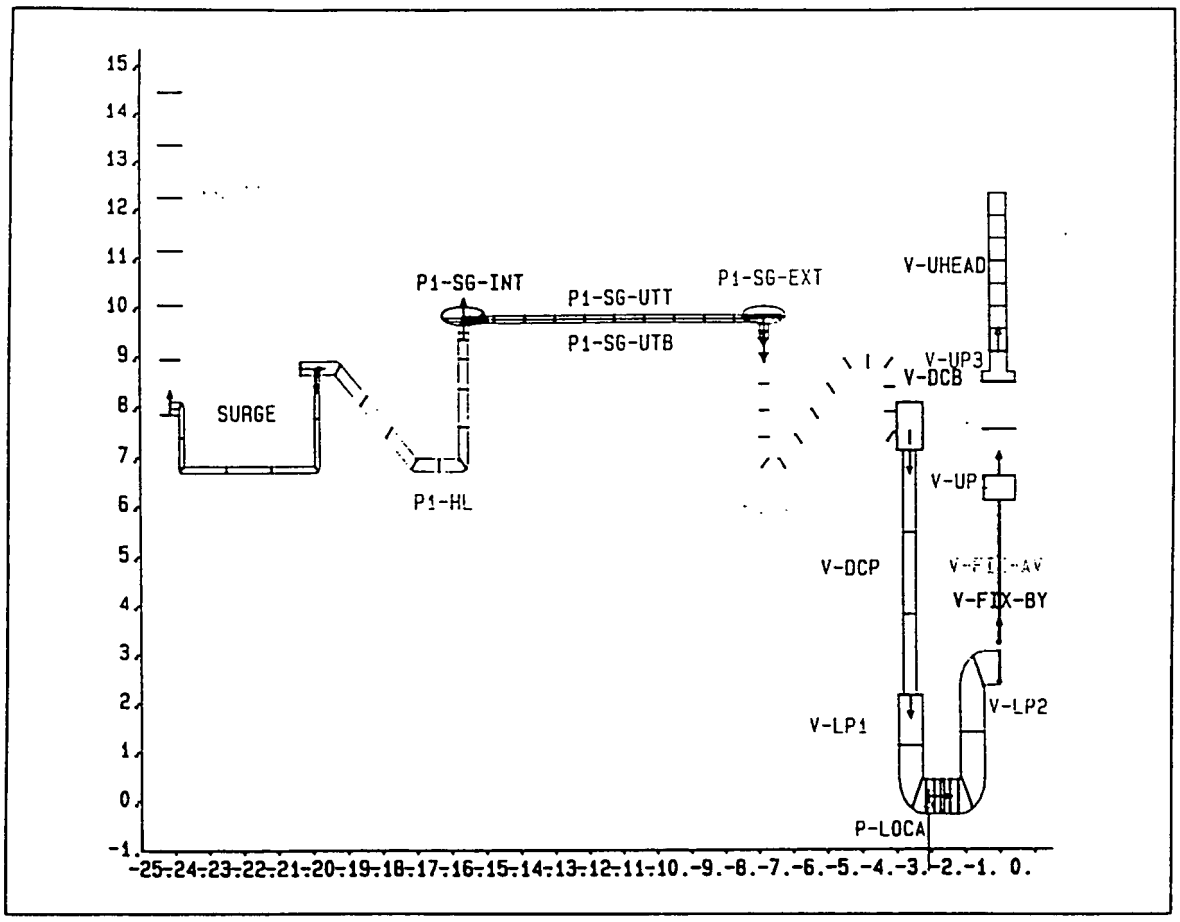

Figure 3.17. ATHLET primary circuit nodalization for ISP33 by THZ.

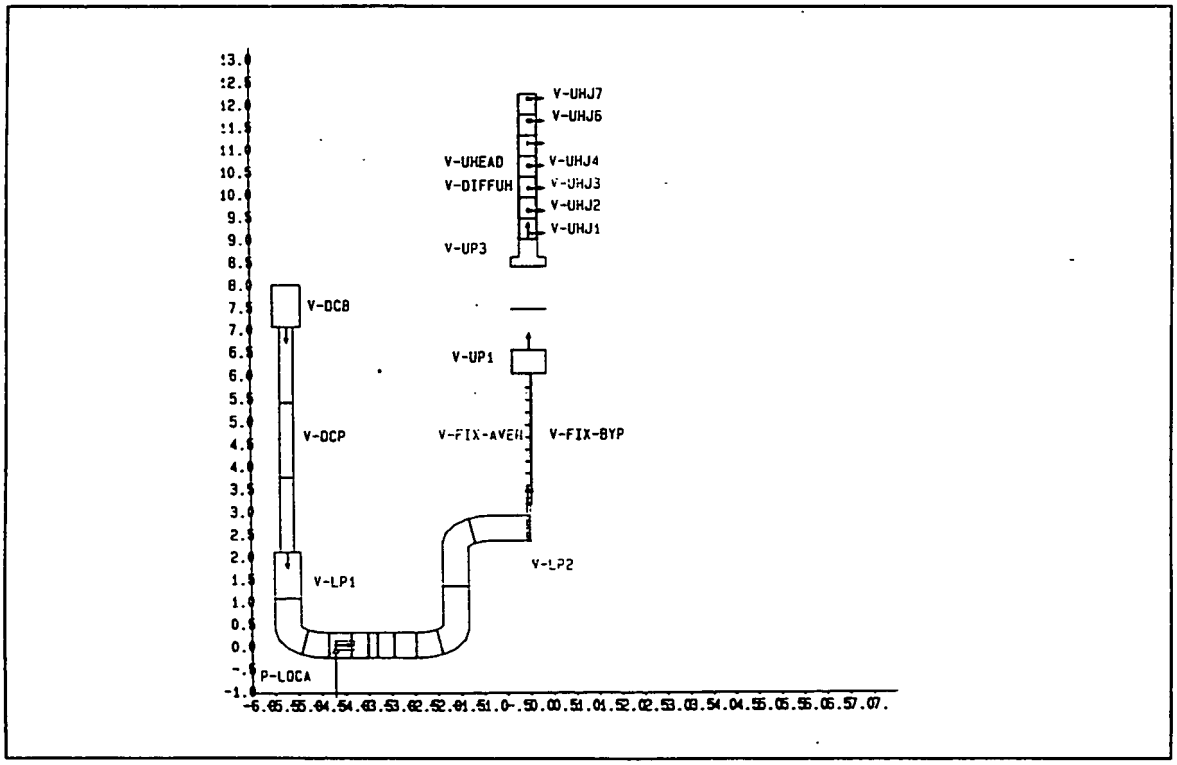

Figure 3.18. ATHLET reactor vessel nodalization for ISP33 by THZ.

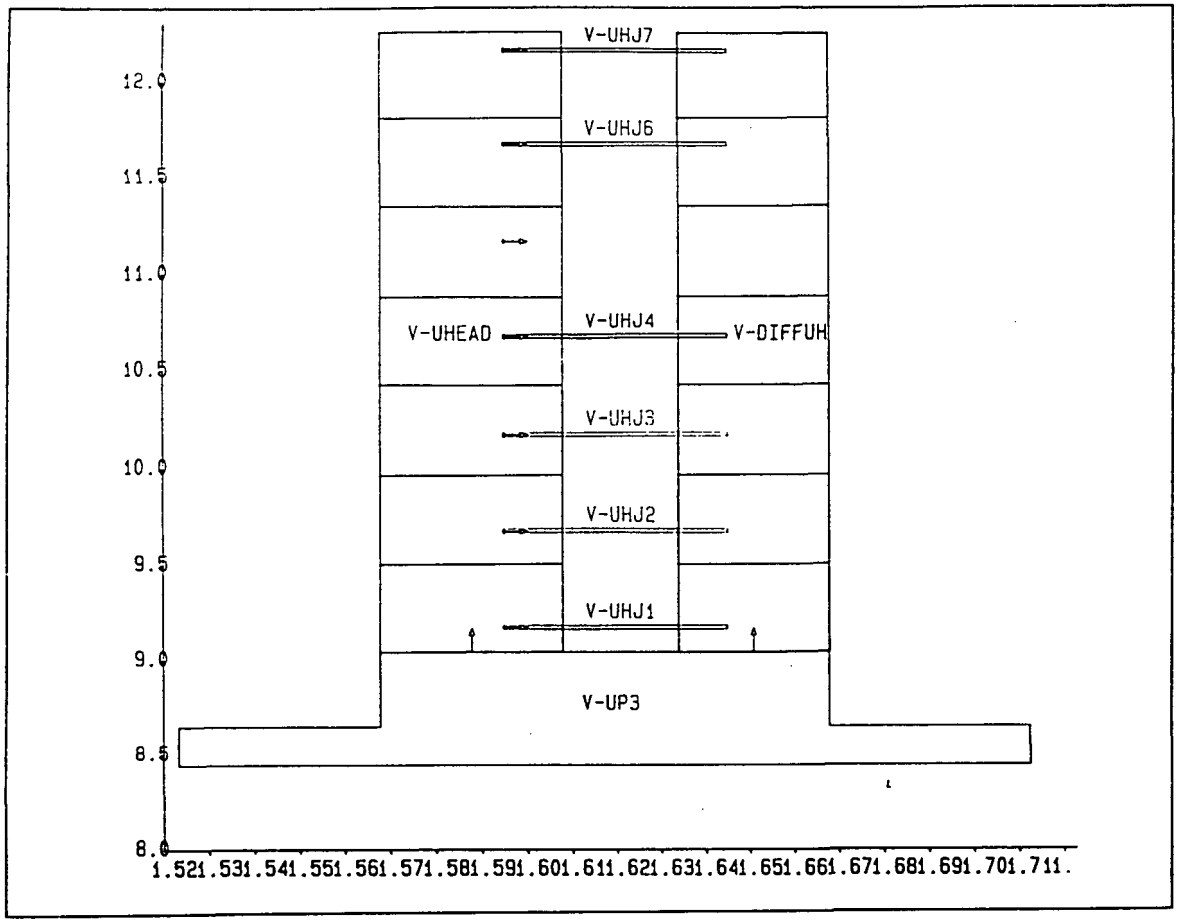

Figure 3.19. ATHLET upper head nodalization for ISP33 by THZ.

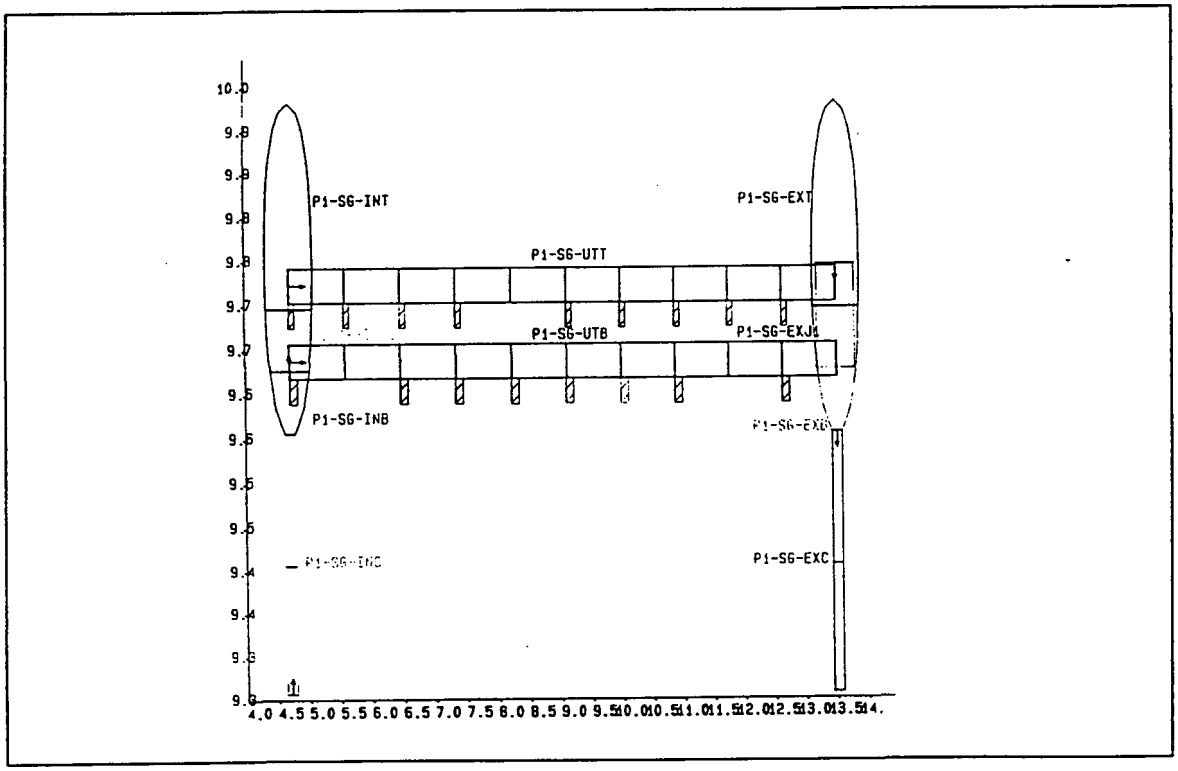

Figure 3.20. ATHLET SG primary side nodalization for ISP33 by THZ.

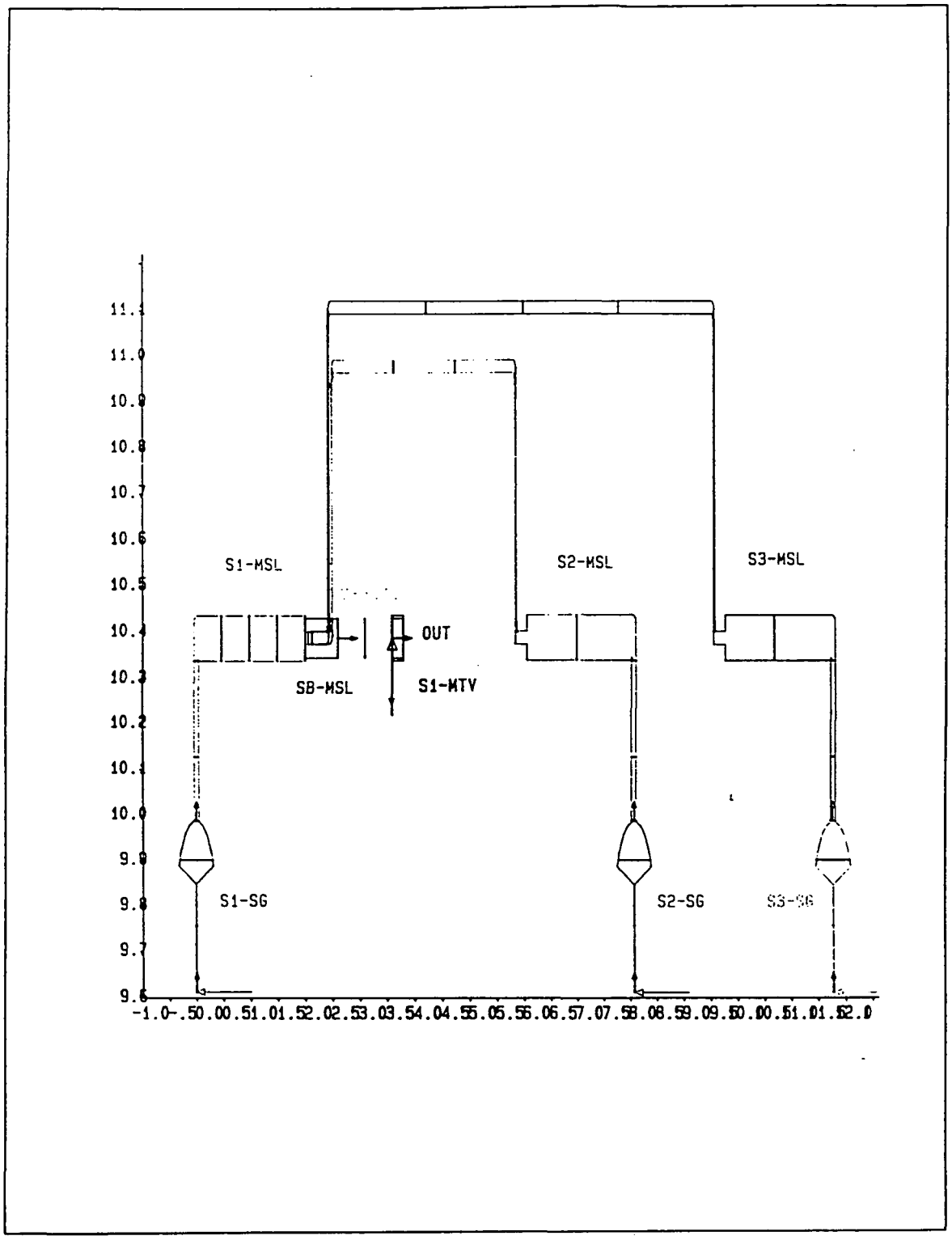

Figure 3.21. ATHLET secondary side nodalization for ISP33 by THZ.

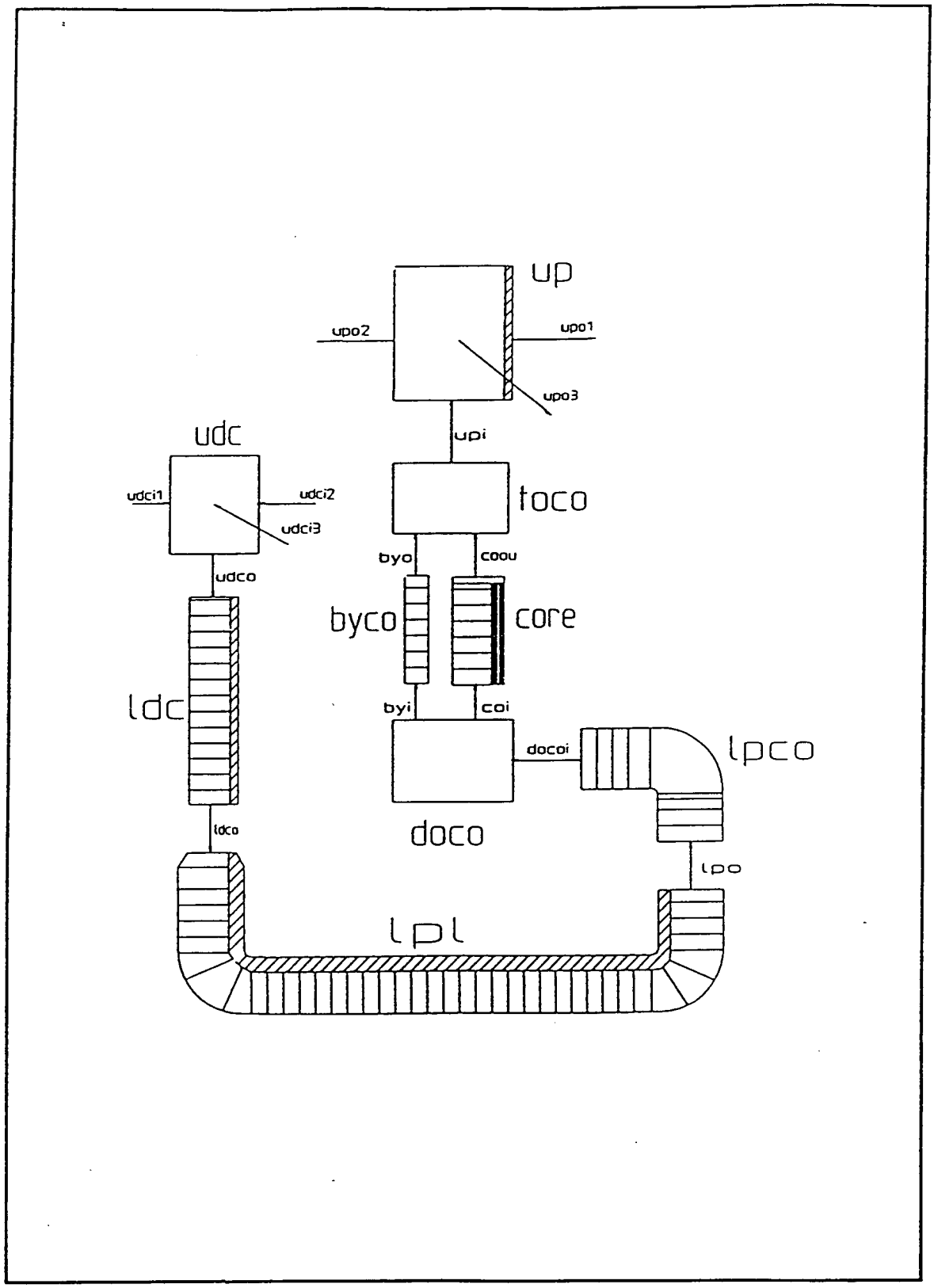

Figure 3.22. CATHARE2 vessel nodalization for ISP33 by Univ. of Pisa.

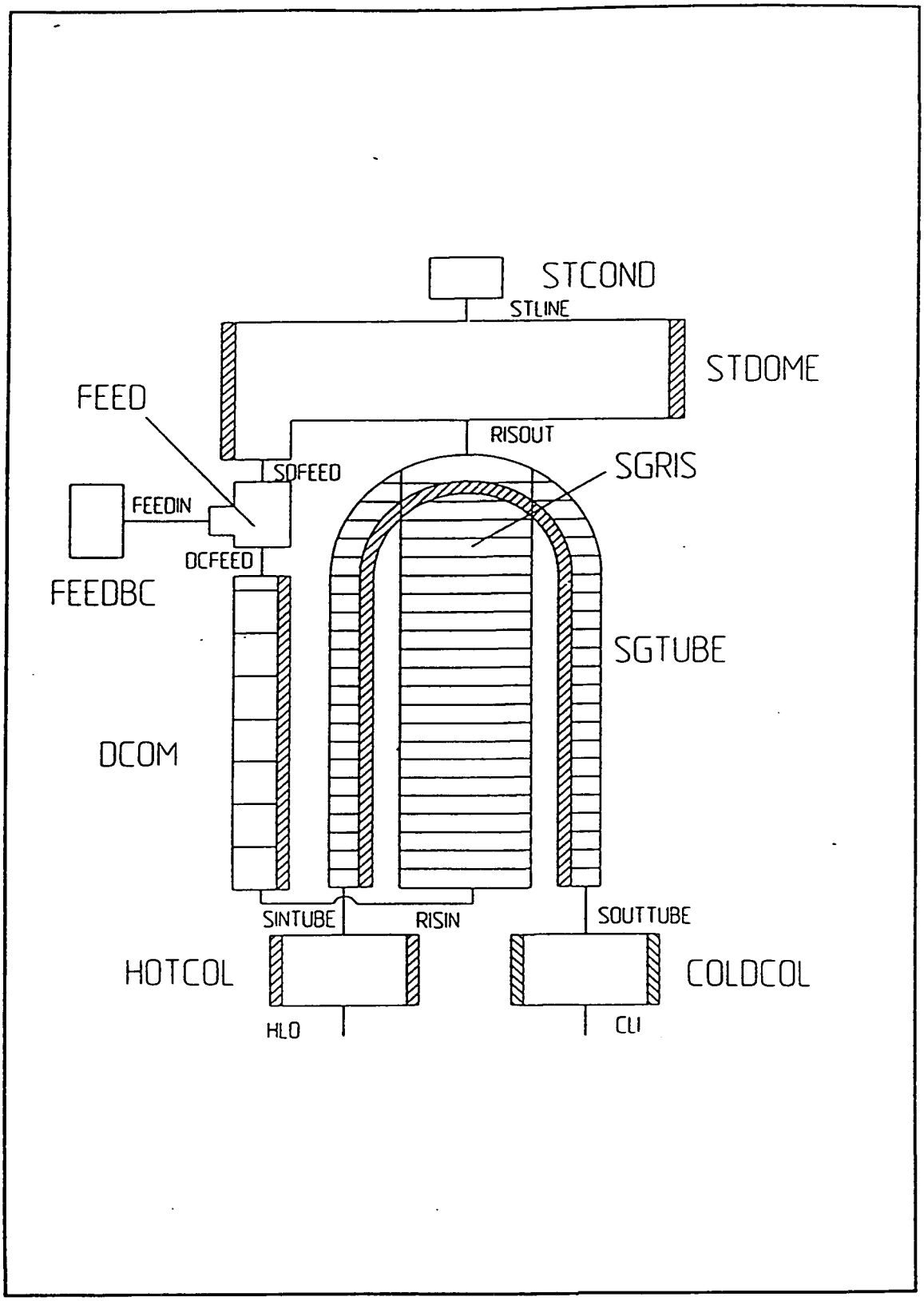

Figure 3.23. CATHARE2 SG nodalization for ISP33 by Univ. of Pisa.

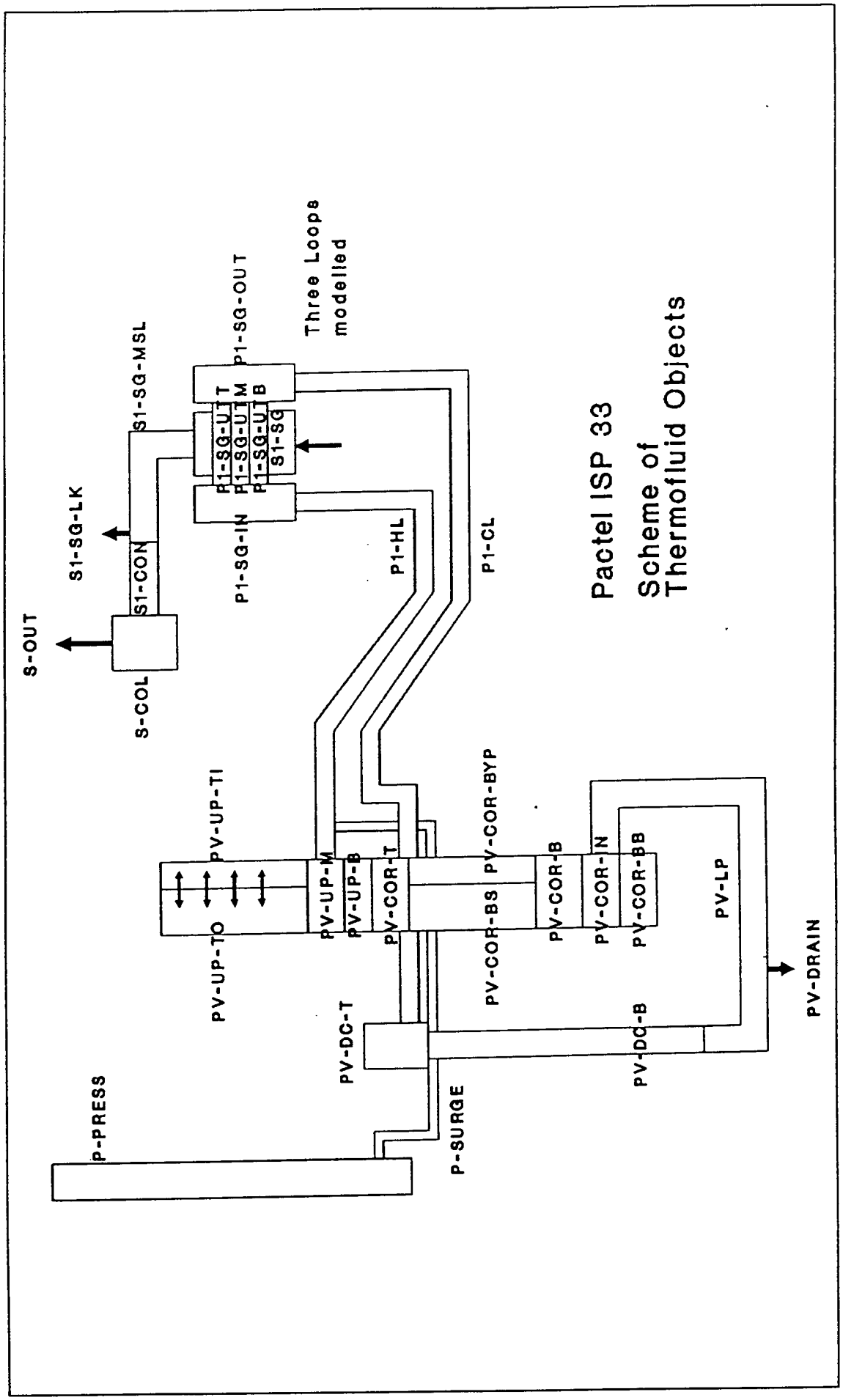

Figure 3.24. ATHLET nodalization for ISP33 by FRG/FZR.

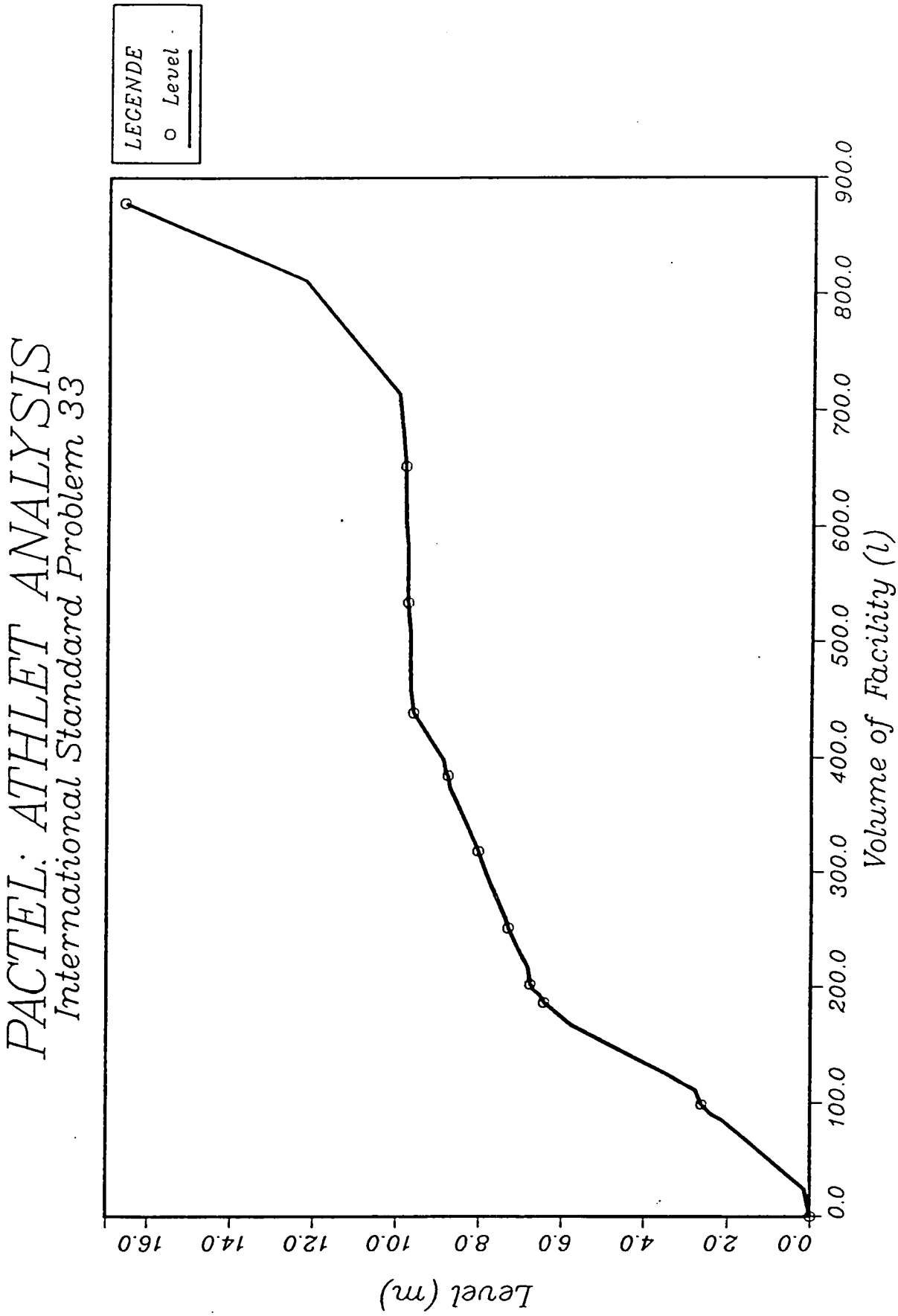

Figure 3.25 Coolant level versus coolant inventory (GRS).

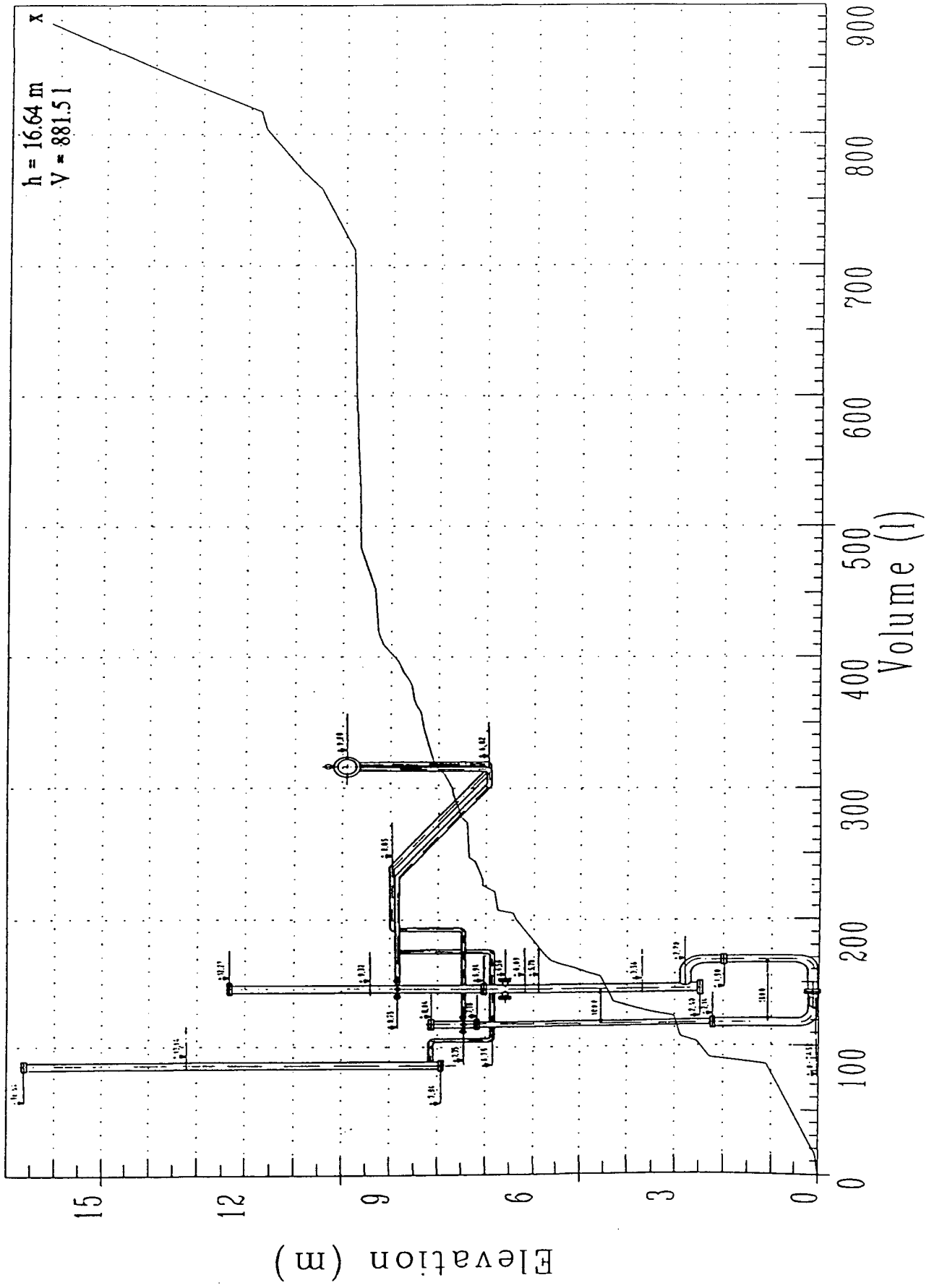

Figure 3.26 Coolant level versus coolant inventory (IJS).

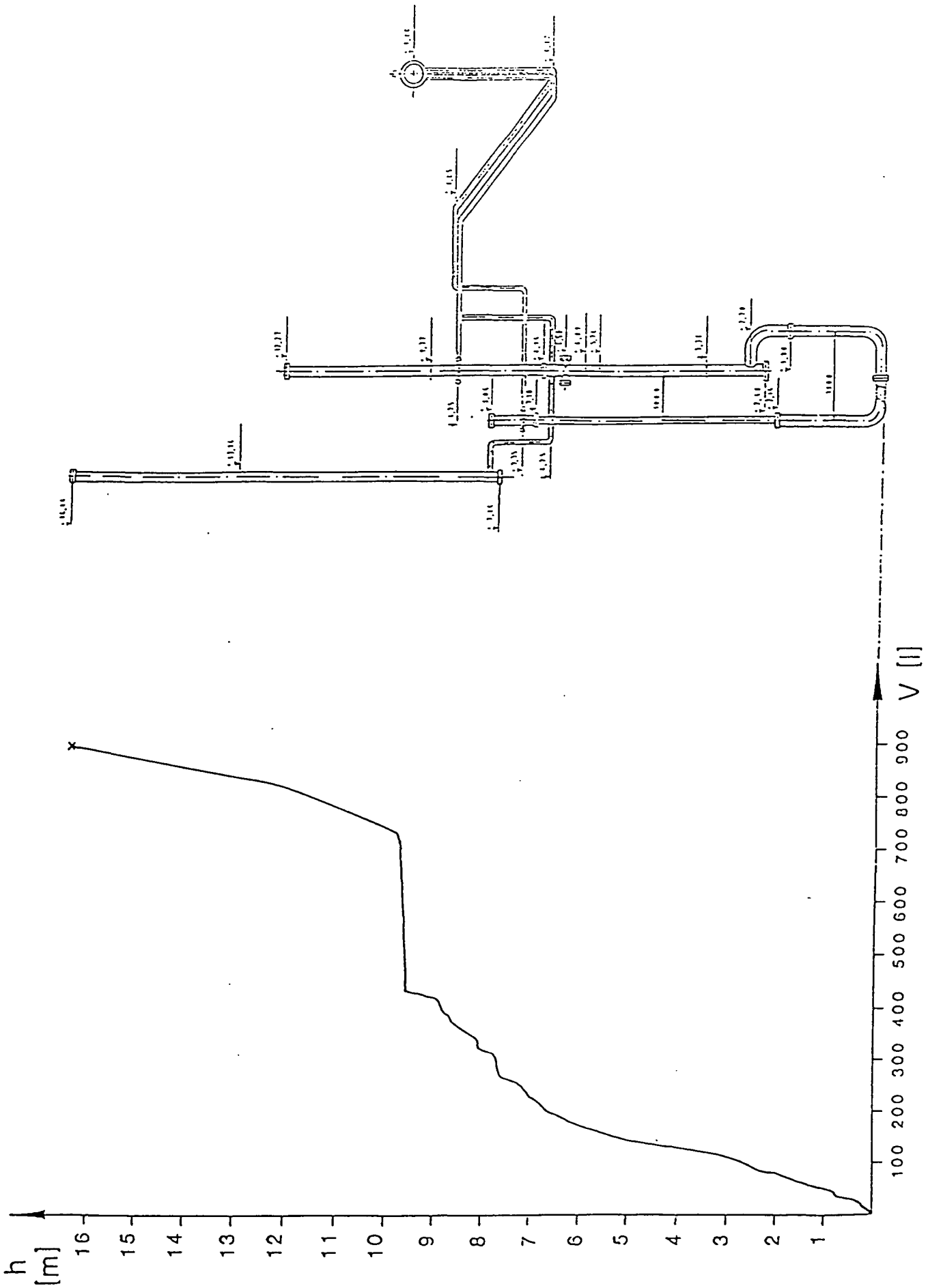

Figure 3.27 Coolant level versus coolant inventory (NRI Rez).

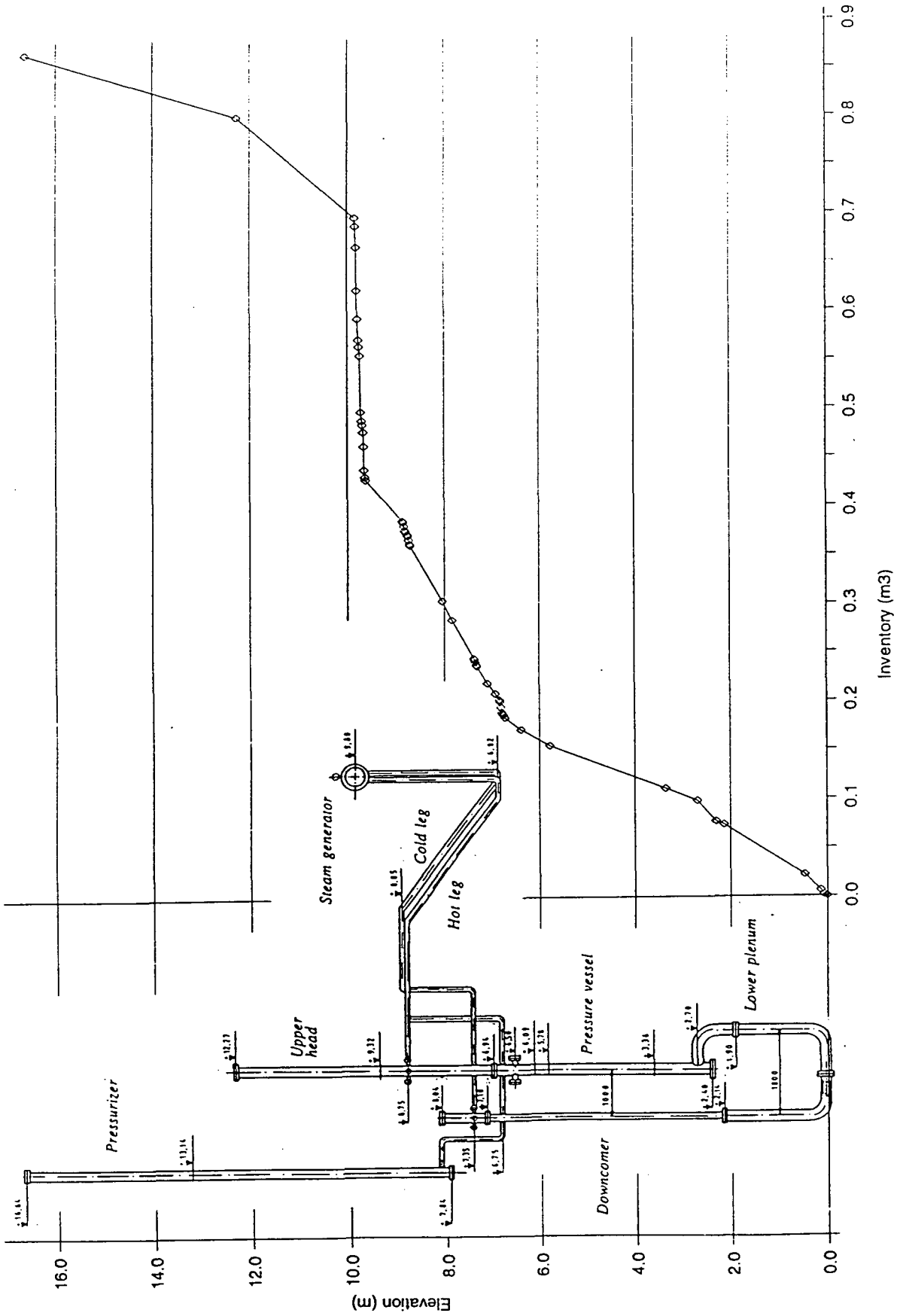

Figure 3.28 Coolant level versus coolant inventory (Studsvik).

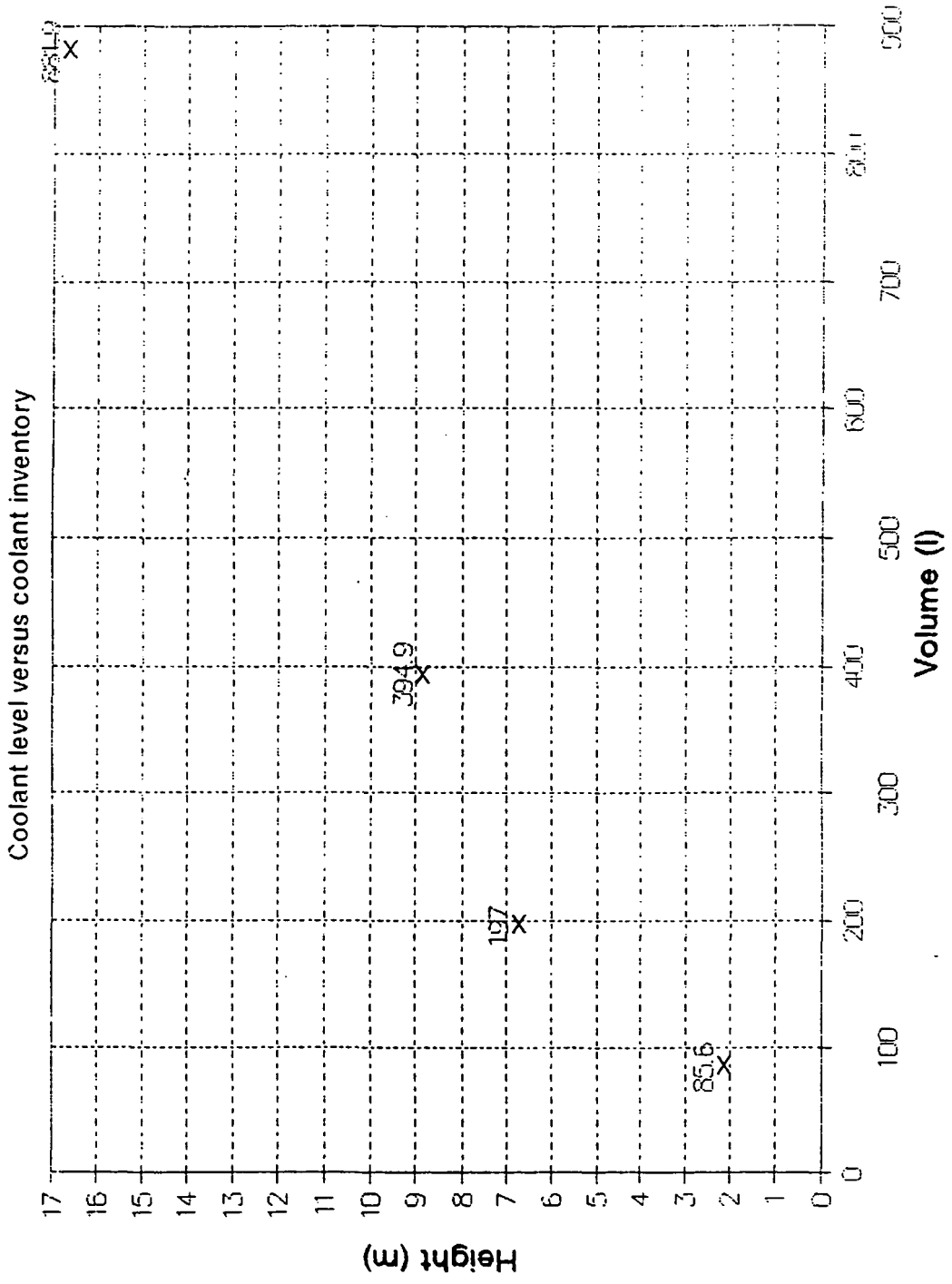

Figure 3.29 Coolant level versus coolant inventory (TAEK).

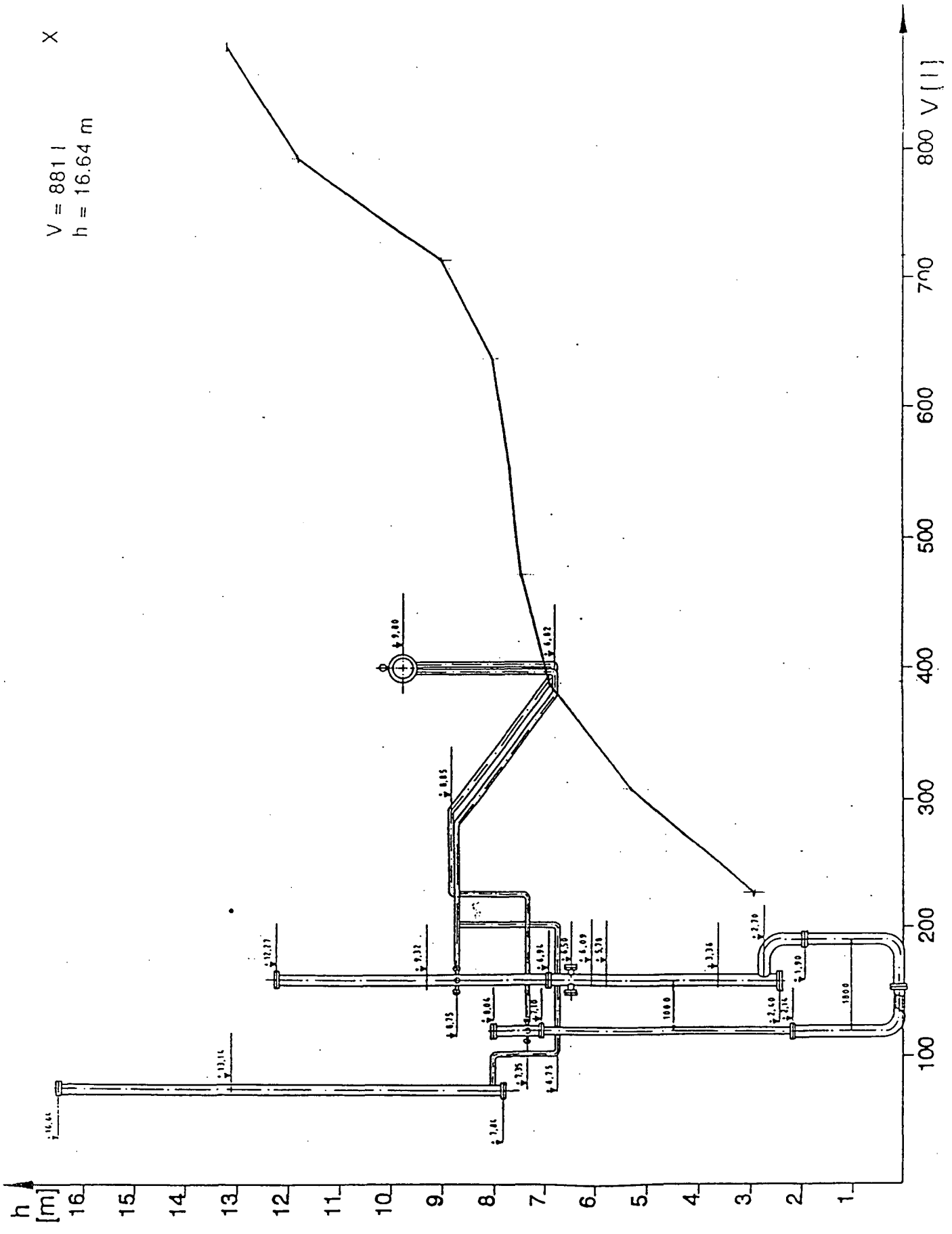

Figure 3.30 Coolant level versus coolant inventory (THZ).

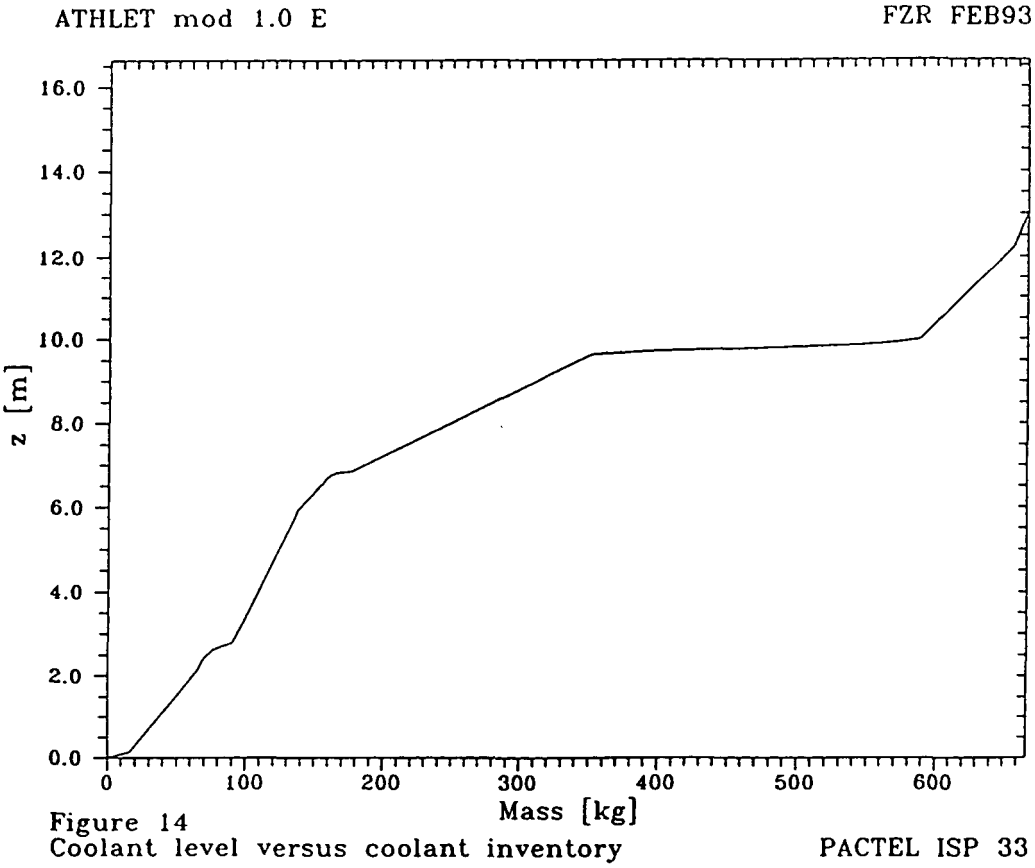

Figure 3.31 Coolant level versus coolant inventory (FZR).

References:

3.1 S. Nikonov, J. Steinborn, International Standard Problem 33, Results of Blind Pre-Test Calculation for PACTEL Test Facility with ATHLET Code, GRS, 1992.

3.2 W. Ambrosini et al, OECD/CSNI ISP 33: Pre-Test Prediction of the PACTEL Natural Circulation Experiment Performed by CATHARE2 V1.2E Code, NT 202 (92), Pisa, December 1992.

3.3 E. Laugier, L. Sabotinov. Papers submitted for ISP33.

3.4 RELAP4/MOD6, A Computer Program for Transient Thermal-Hydraulic Analysis of Nuclear Reactors and Related Systems, User's Manual, EG&G Idaho, Inc., January 1978.

3.5 V. H. Ransom et al, RELAP5/MOD2 Code Manual, Volume I. NUREG/CR-4312, EGG-2396, August 1985.

3.6 RELAP5/MOD3 Code Manual, Volume I. EG&G Idaho, Inc., June 1990.

3.7 SCDAP/RELAP5/MOD2 Code Manual. RELAP5 Code Structure, System Models and Solution Methods. V1 & V2, NUREG/CR-5273, EGG-2555, 1989.

4. COMPARISONS OF BLIND CALCULATIONS

4.1 Introduction

Twenty calculations were submitted before or soon after the deadline (November 30, 1992). One calculation result (FZR) was received in March 1993. Fifteen organizations pacticipated in the pretest calculations of ISP33, some of them in cooperation with other organizations.

The reports on the blind calculations submitted by the participants themselves are included in Volume II of this report. The comparisons of the calculated results and the experimental data are presented below.

4.2 Comparisons of Blind Calculations and Experimental Results

4.2.1 Comparison plots (ATHLET)

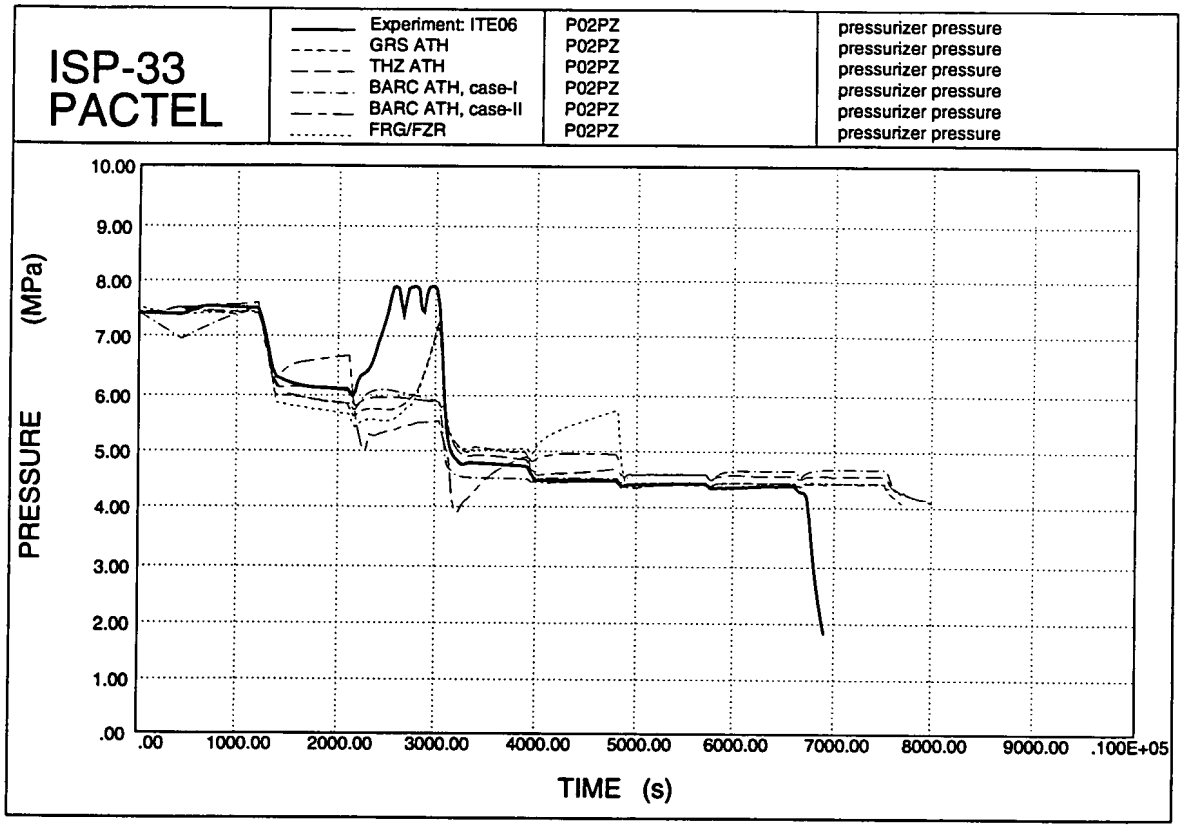

Figure 4.1. Pressurizer pressures.

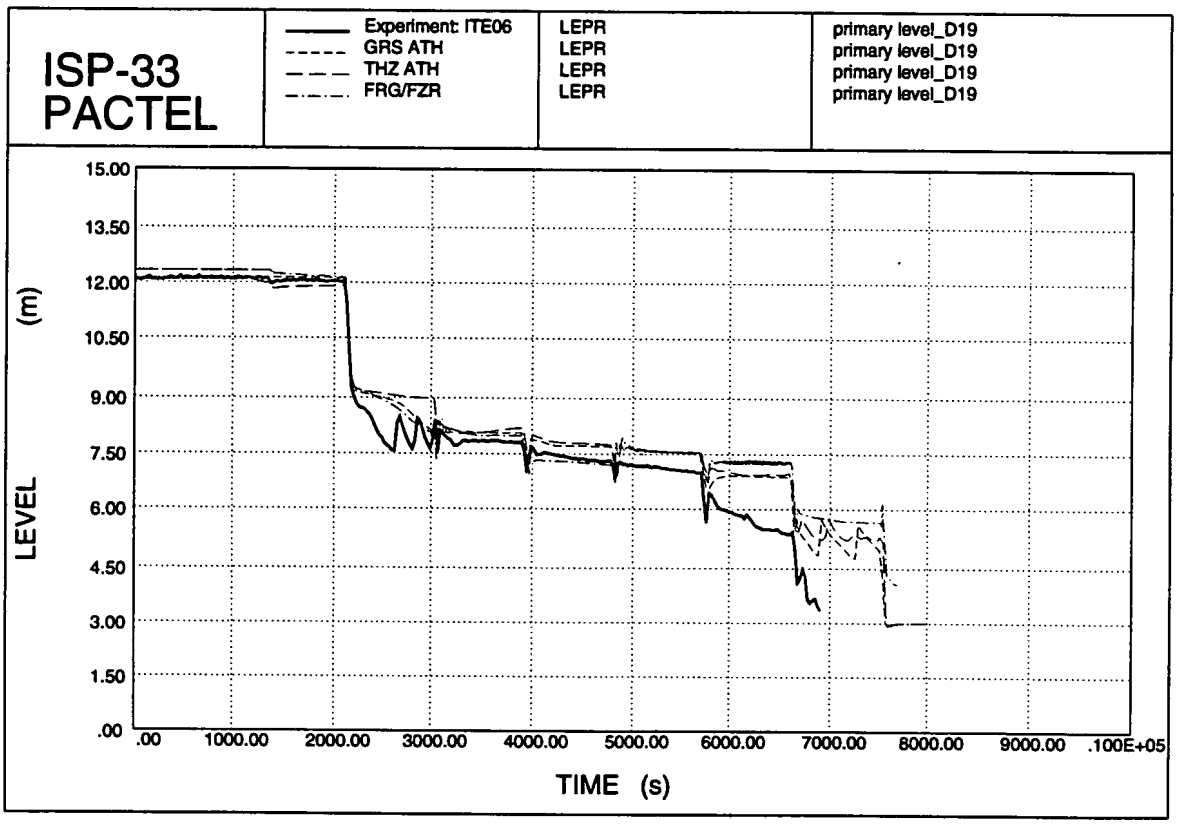

Figure 4.2. Primary levels.

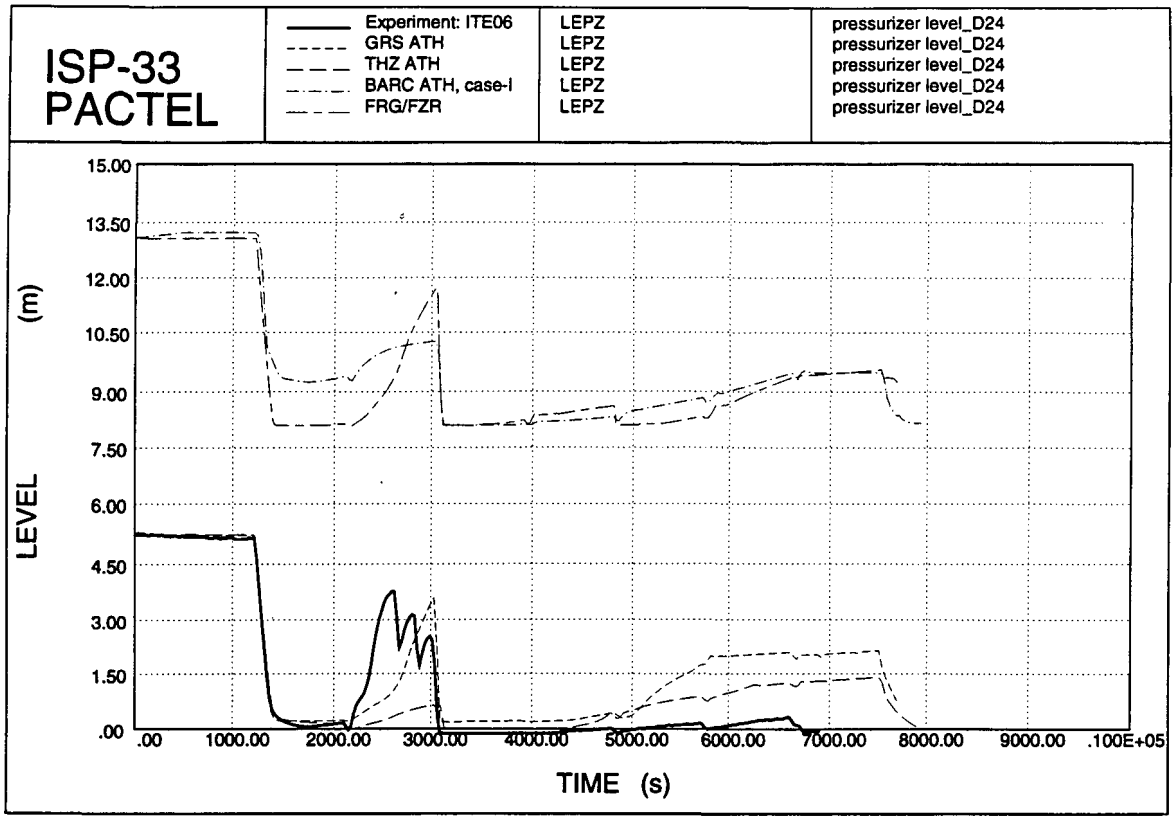

Figure 4.3. Pressurizer levels.

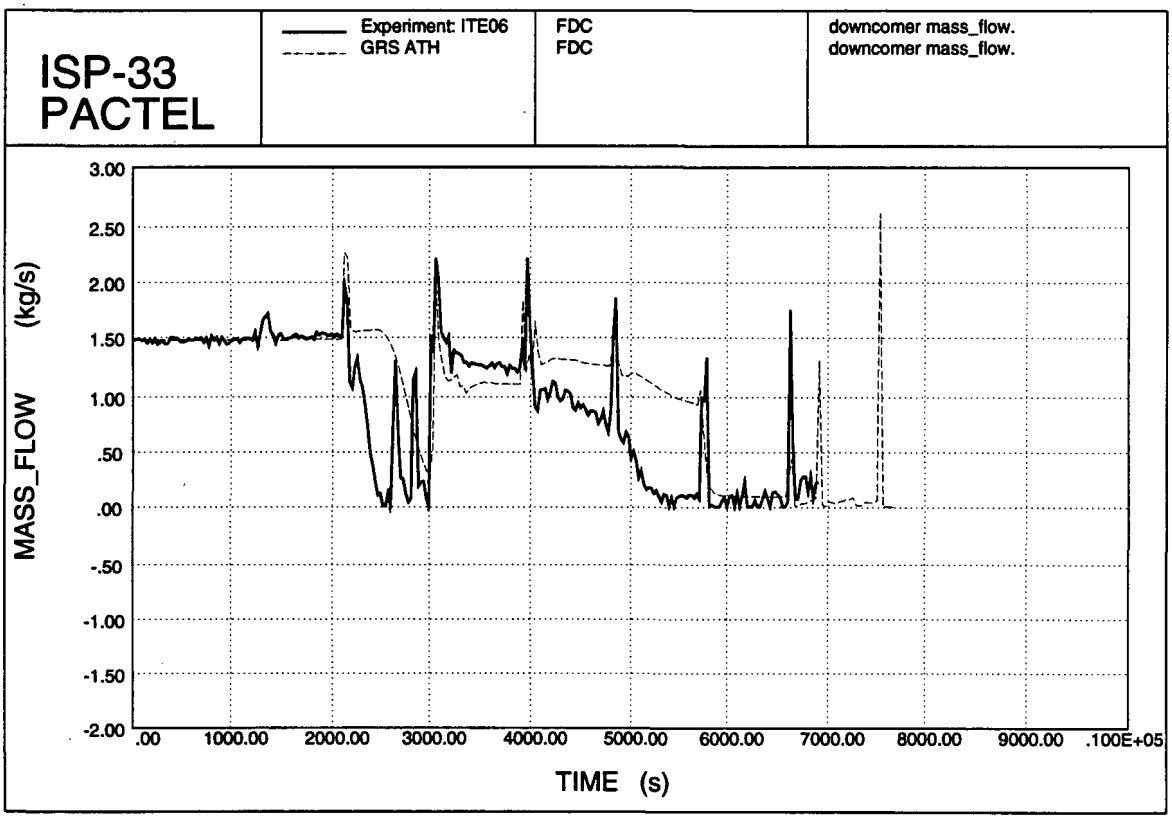

Figure 4.4. Downcomer mass flow.

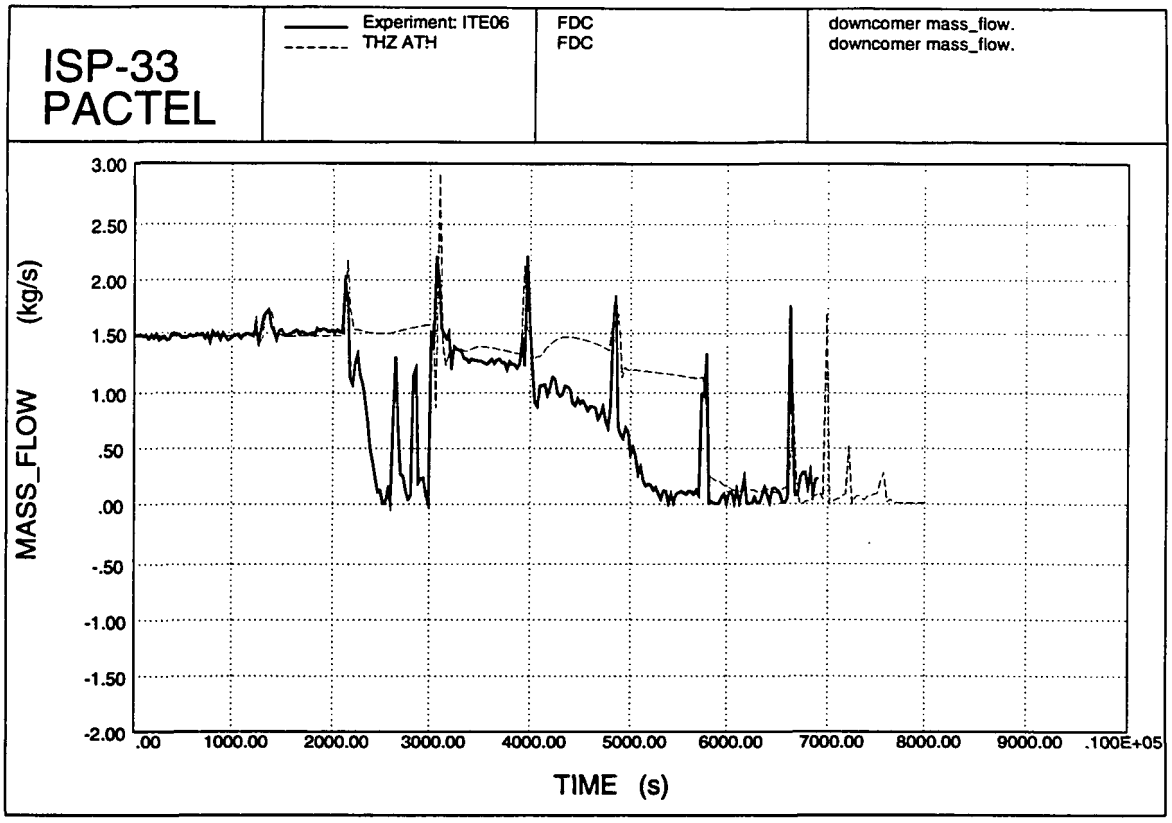

Figure 4.5. Downcomer mass flow.

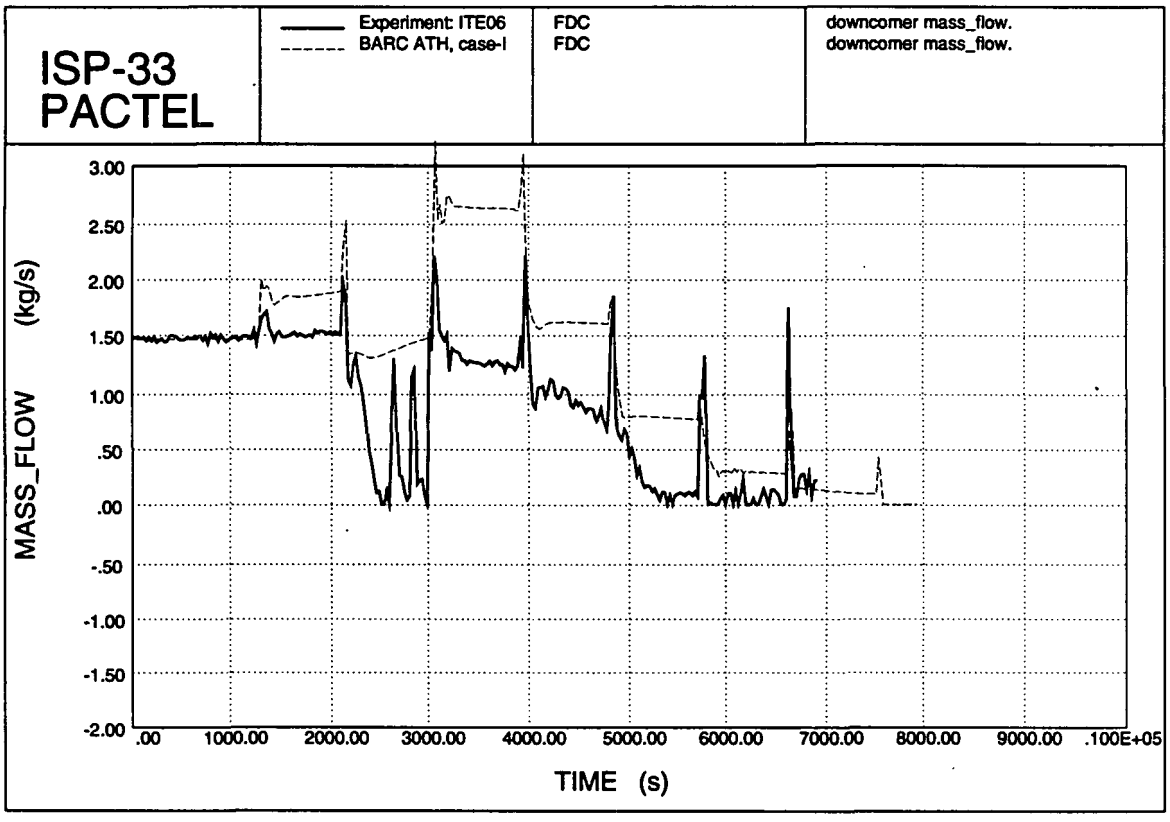

Figure 4.6. Downcomer mass flow.

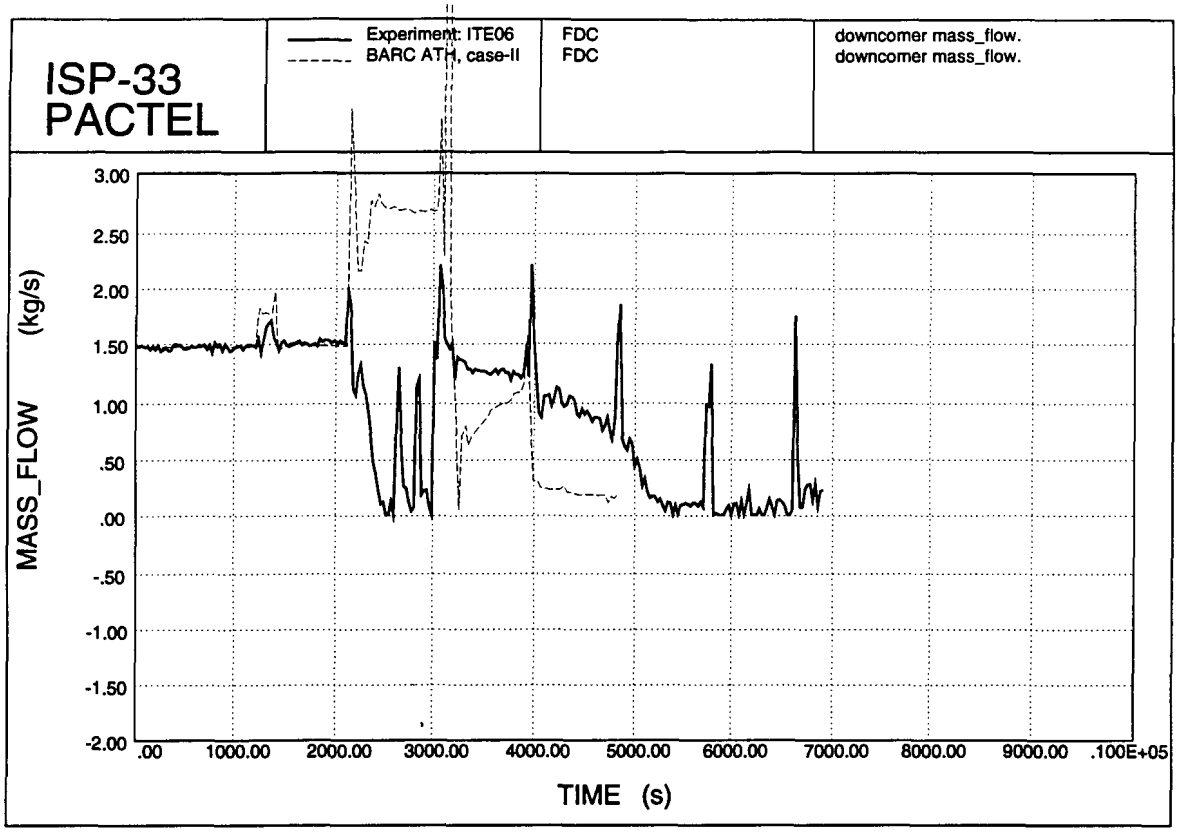

Figure 4.7. Downcomer mass flow.

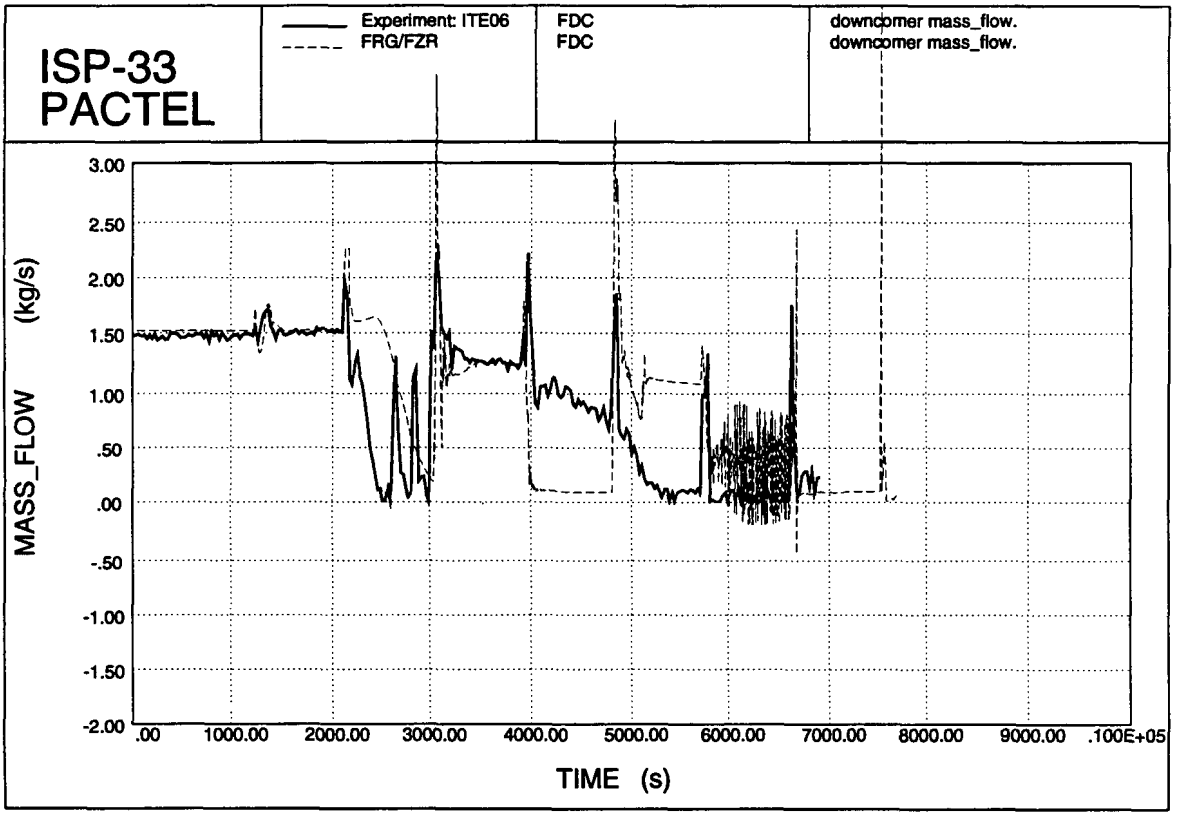

Figure 4.8. Downcomer mass flow.

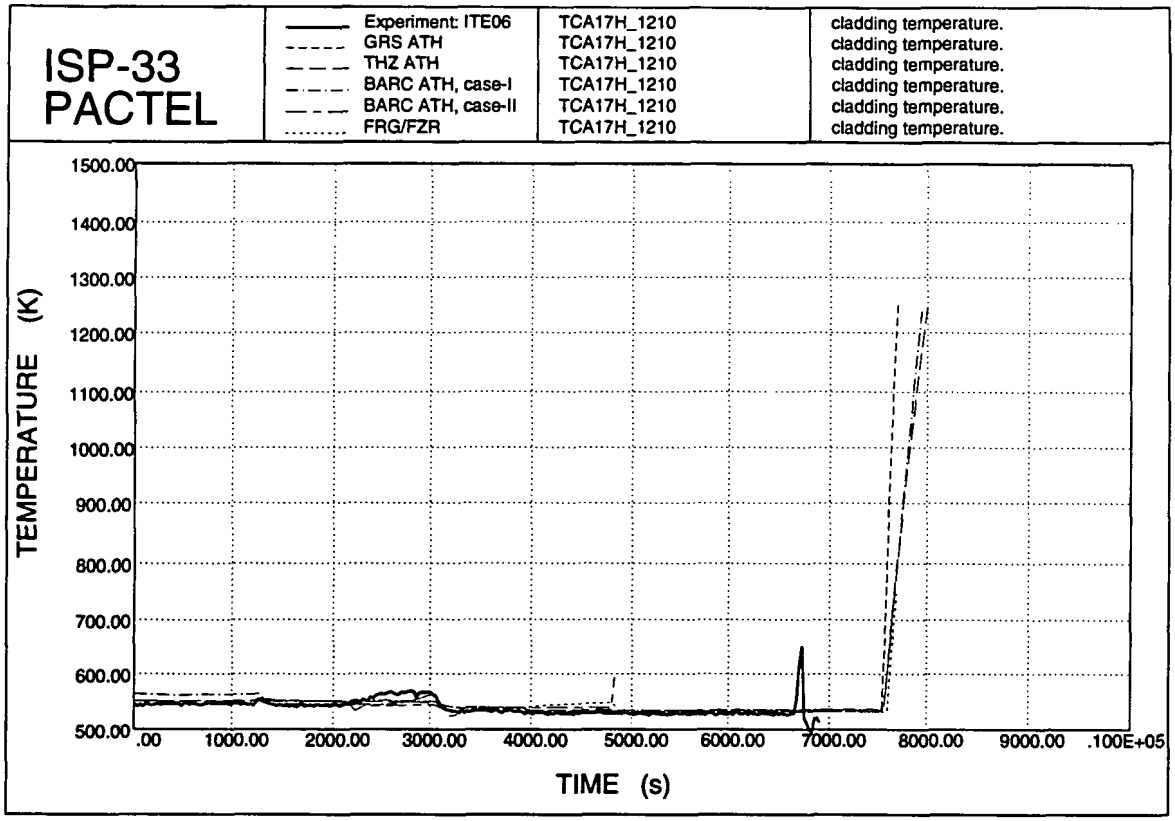

Figure 4.9. Cladding temperatures.

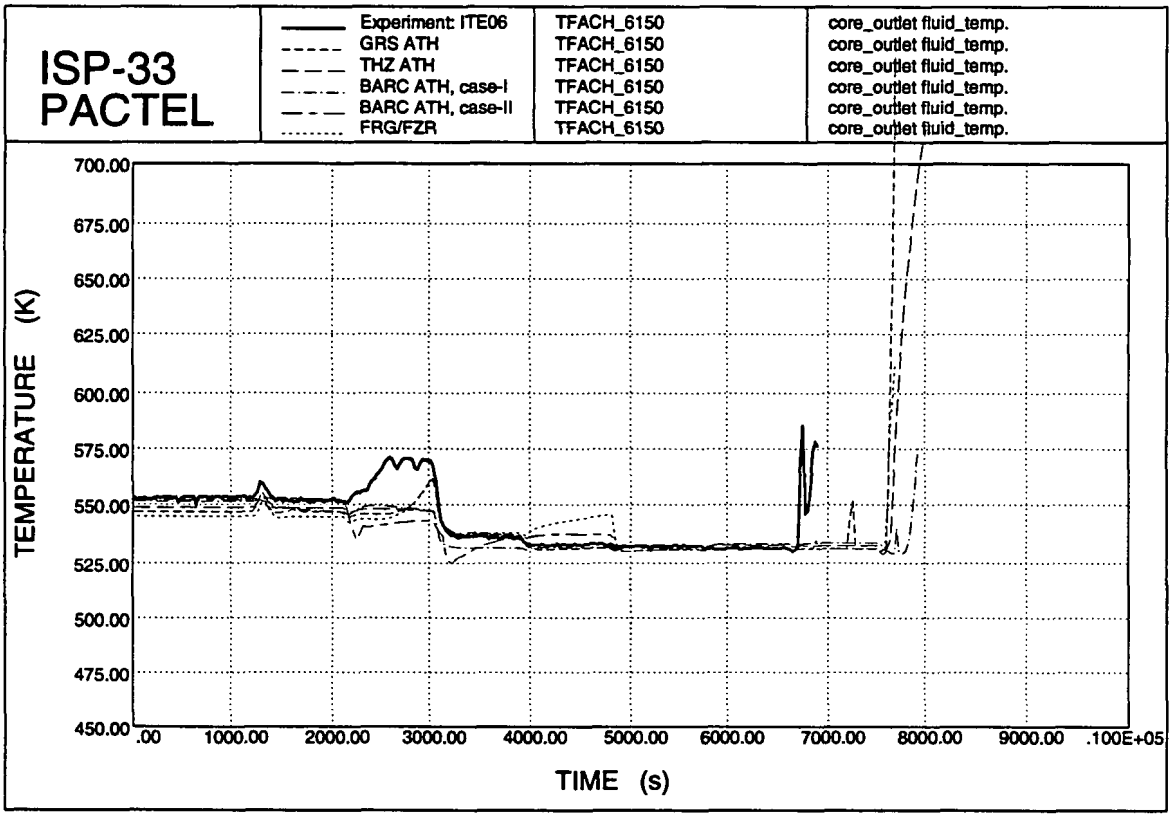

Figure 4.10. Core outlet coolant temperature.

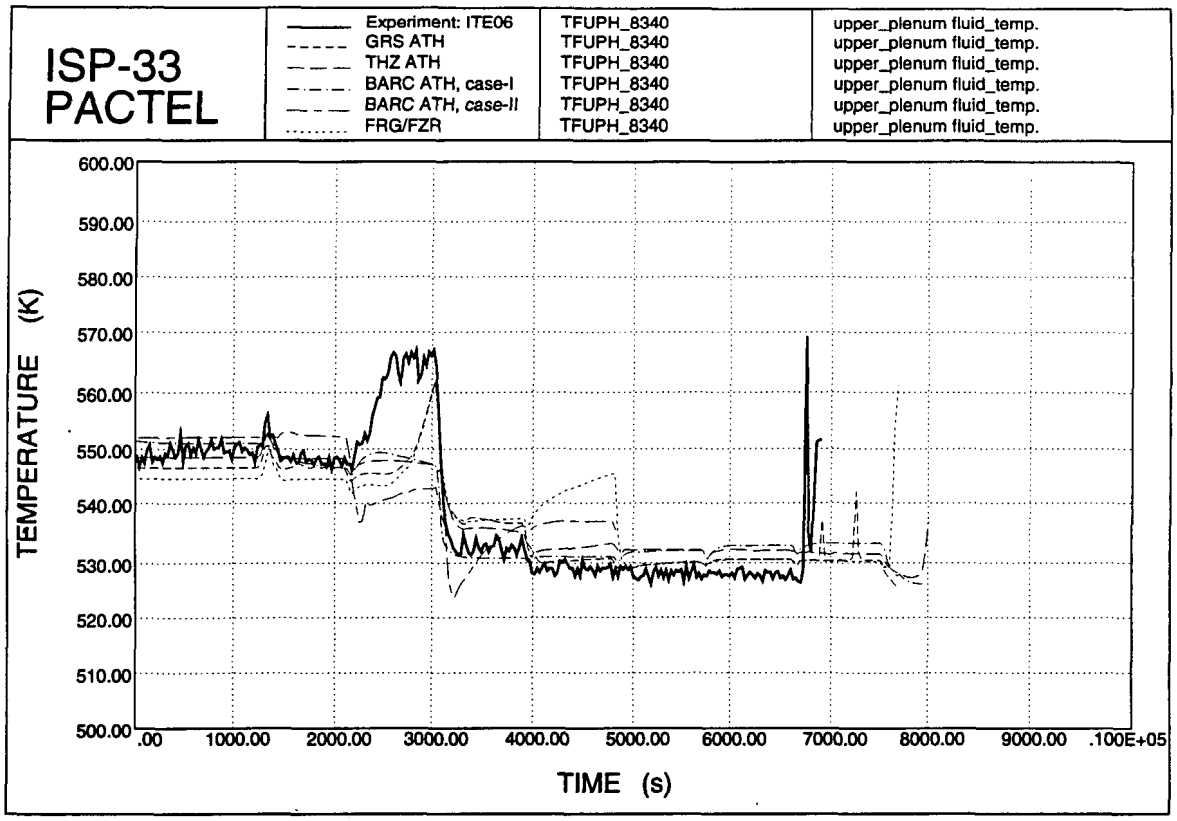

Figure 4.11. Upper plenum temperatures.

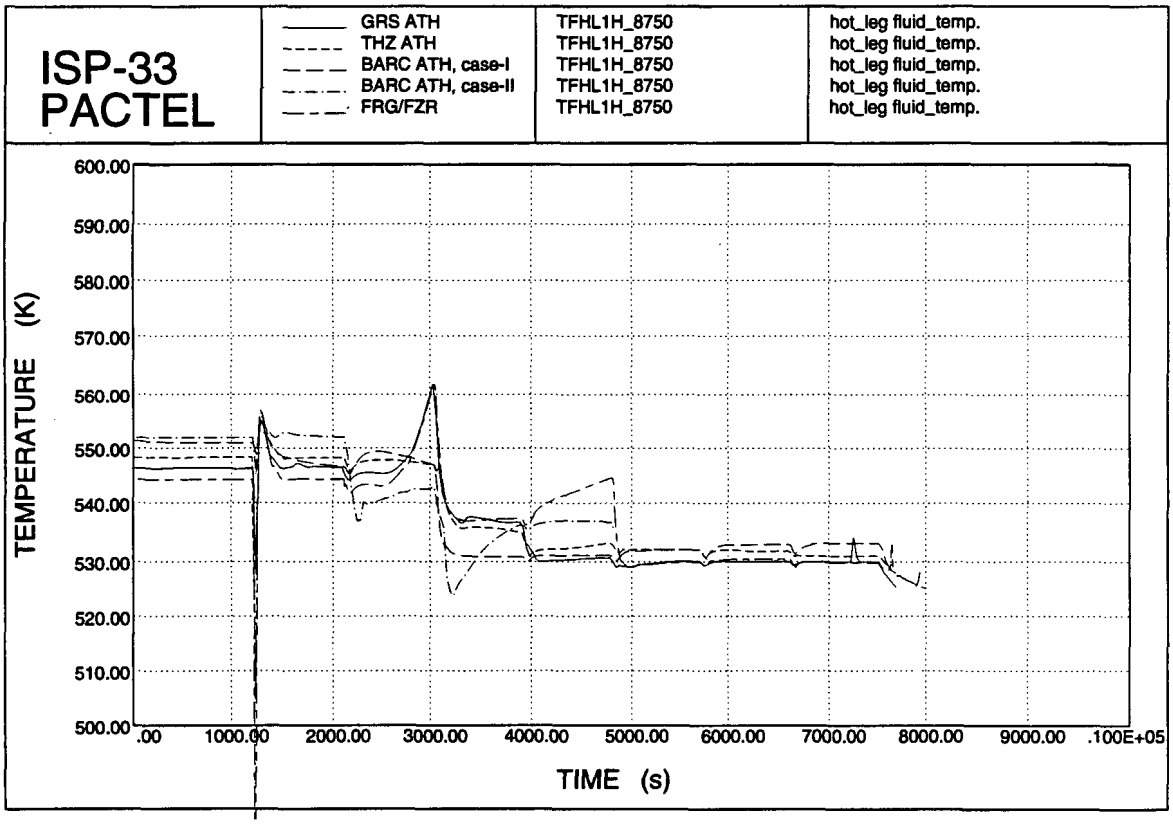

Figure 4.12. Hot leg coolant temperatures.

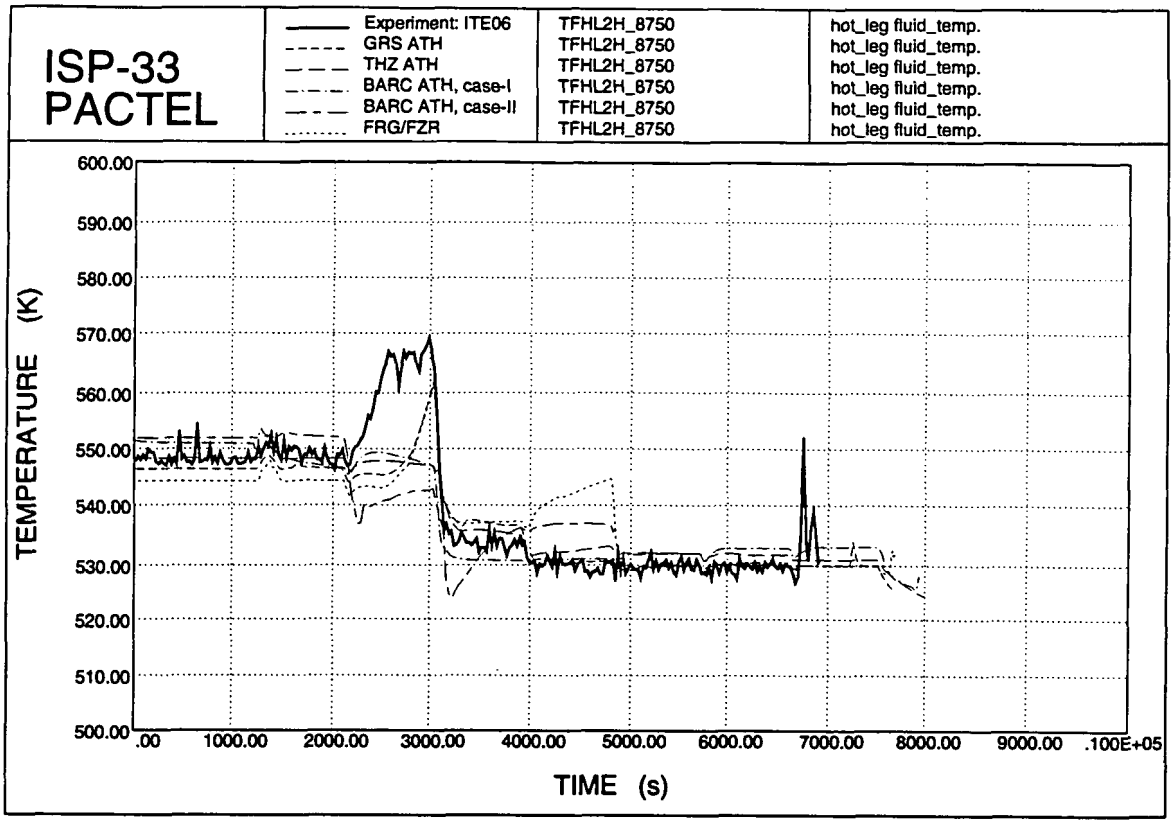

Figure 4.13. Hot leg temperatures.

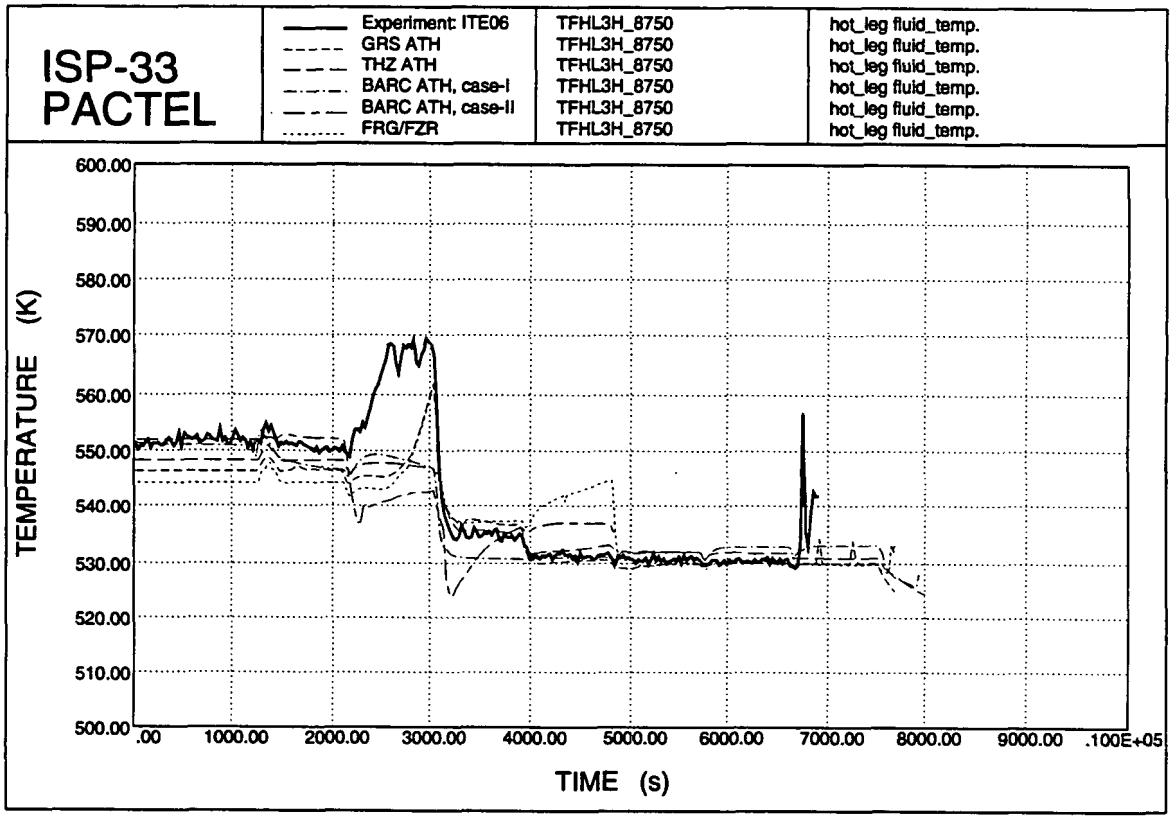

Figure 4.14. Hot leg coolant temperatures.

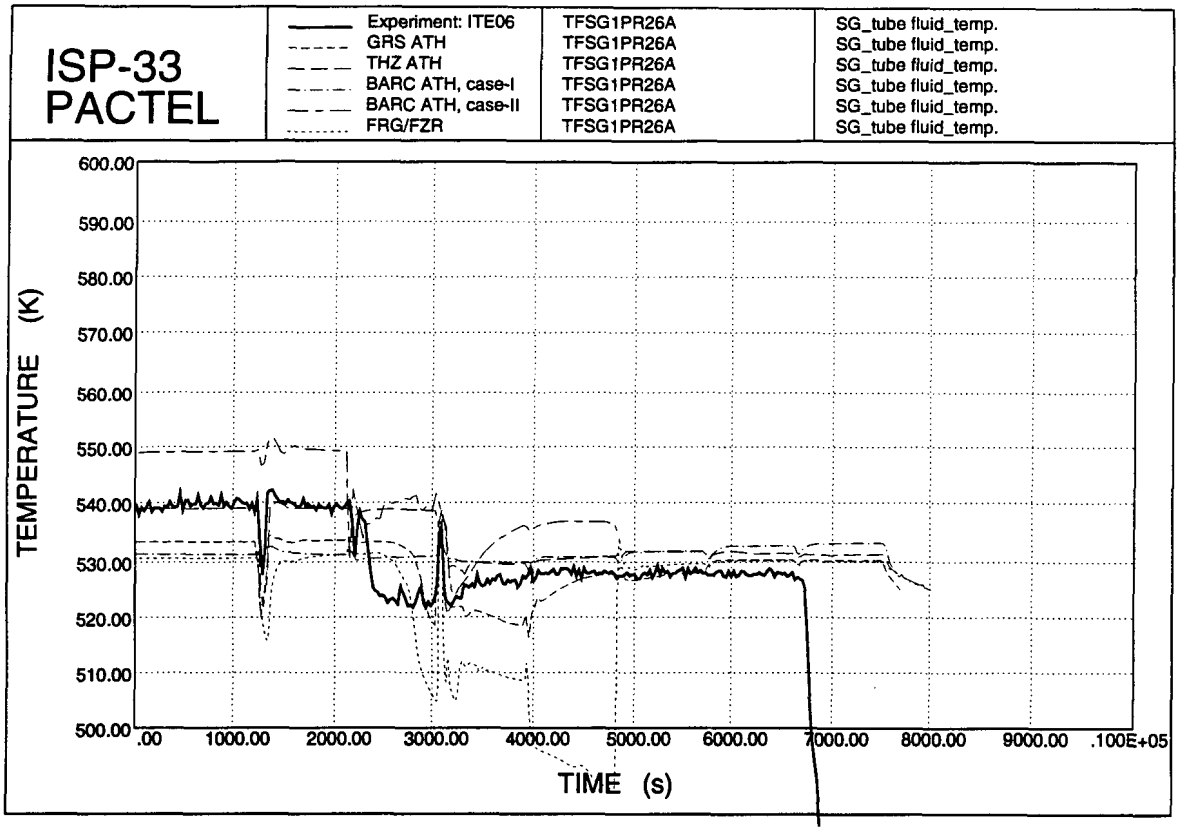

Figure 4.15. SG tube fluid temperatures.

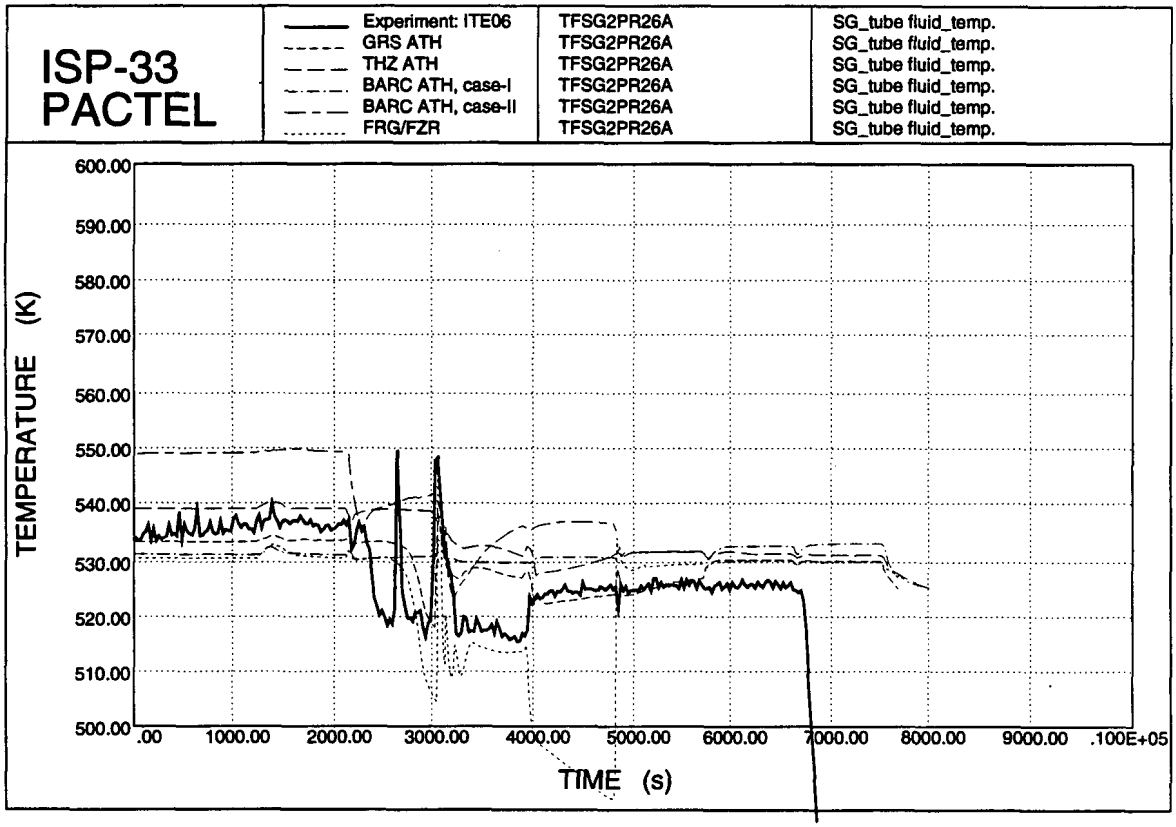

Figure 4.16. SG tube fluid temperatures.

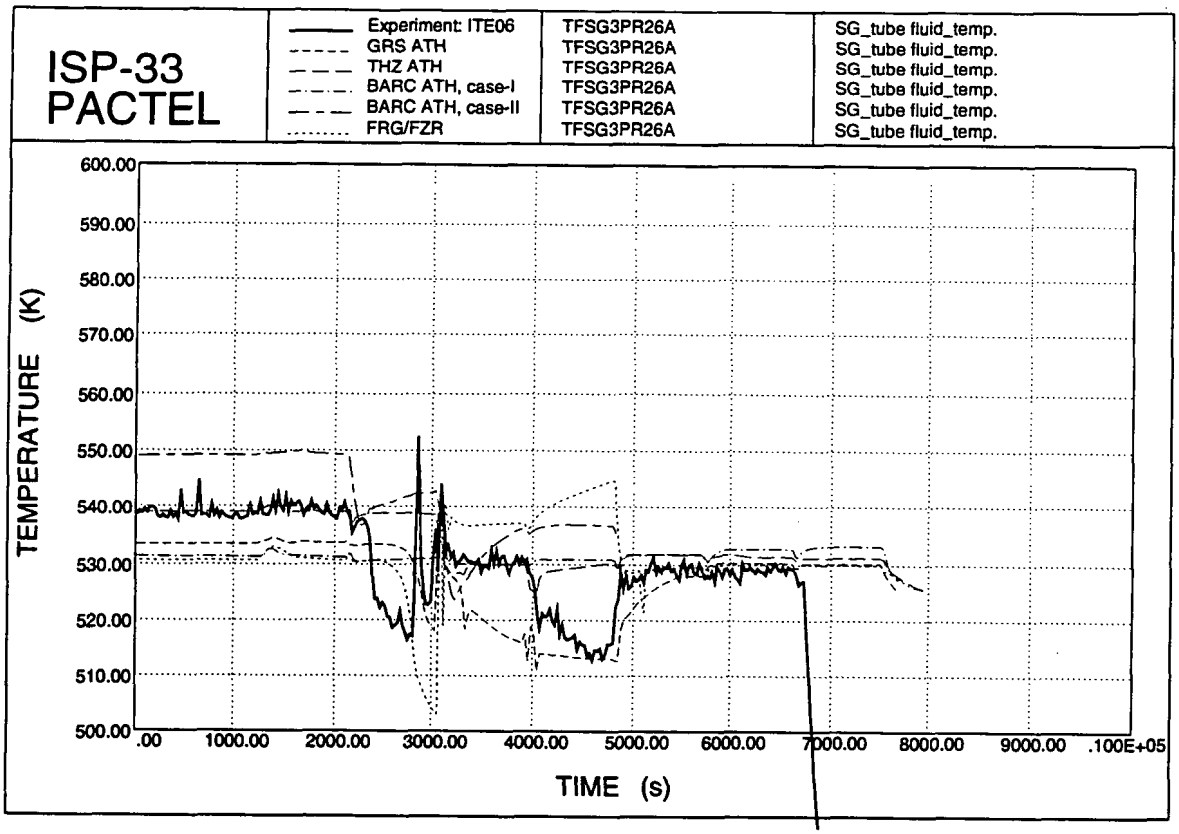

Figure 4.17. SG tube fluid temperatures.

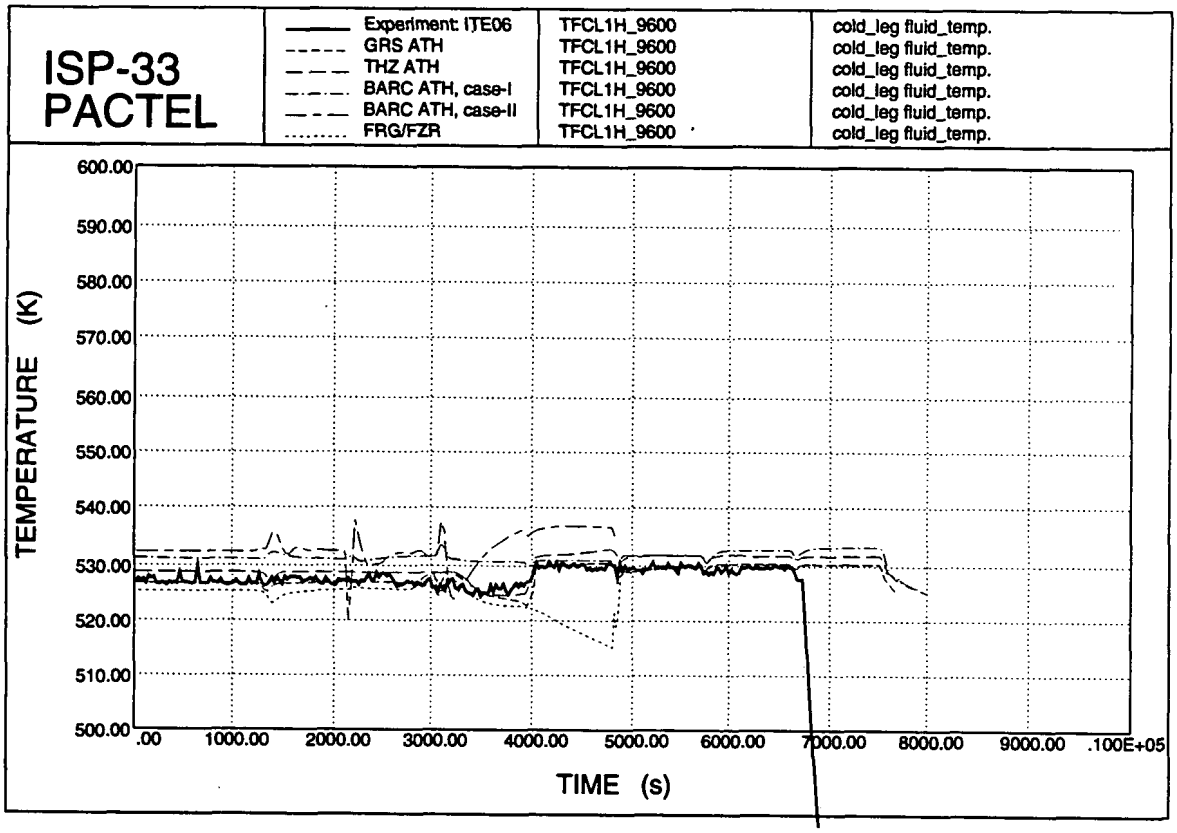

Figure 4.18. Cold leg temperatures.

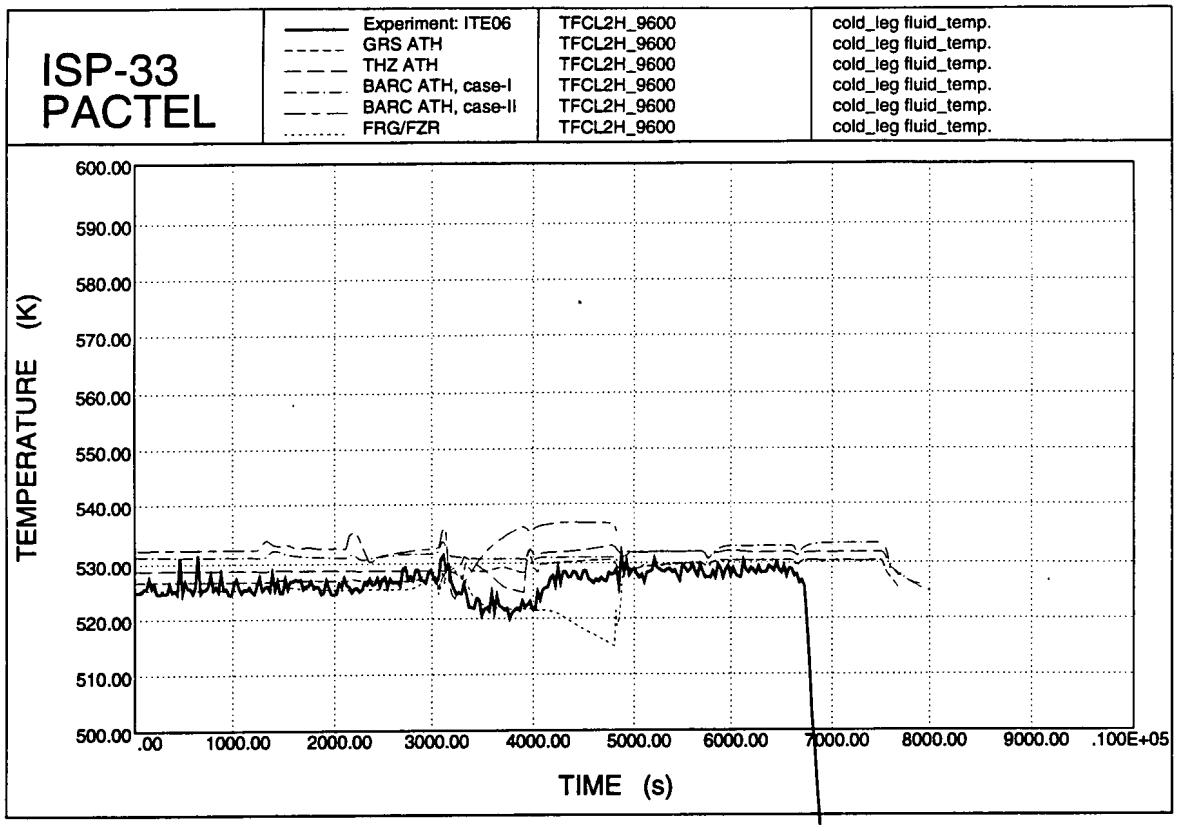

Figure 4.19. Cold leg coolant temperatures.

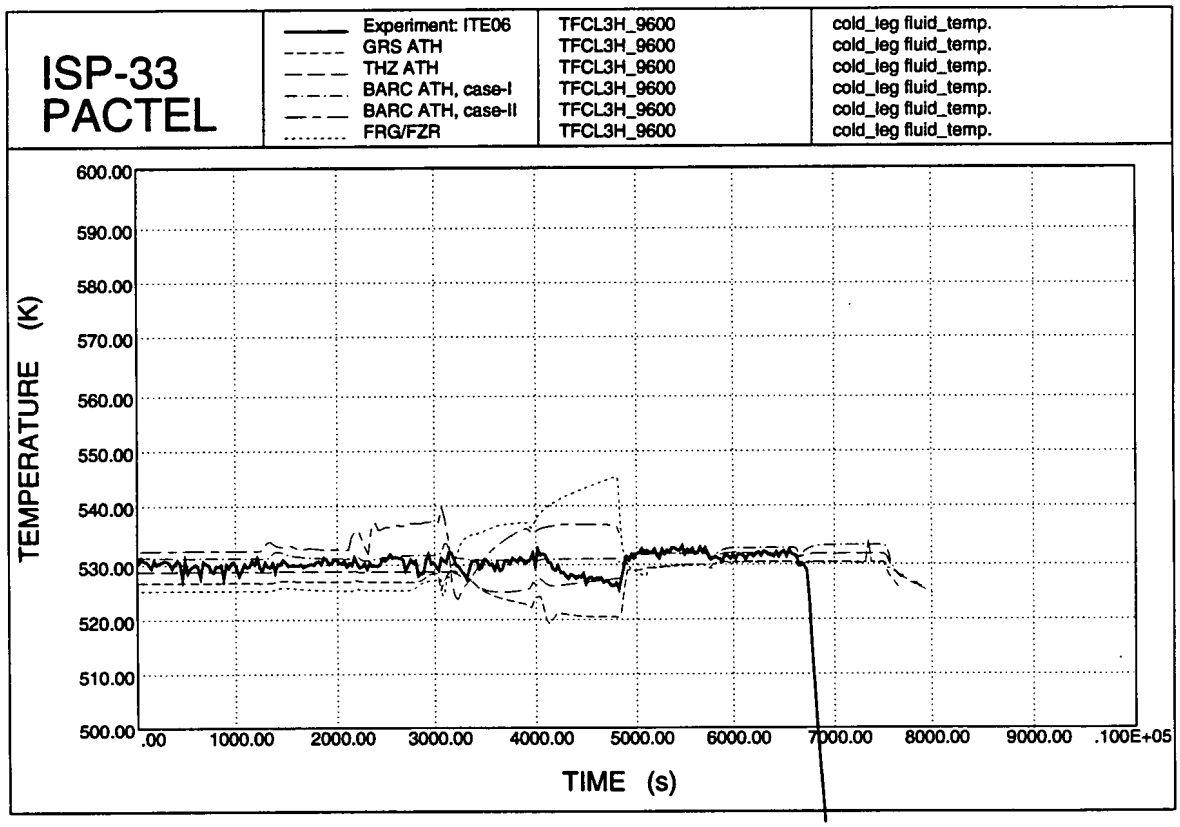

Figure 4.20. Cold leg temperatures.

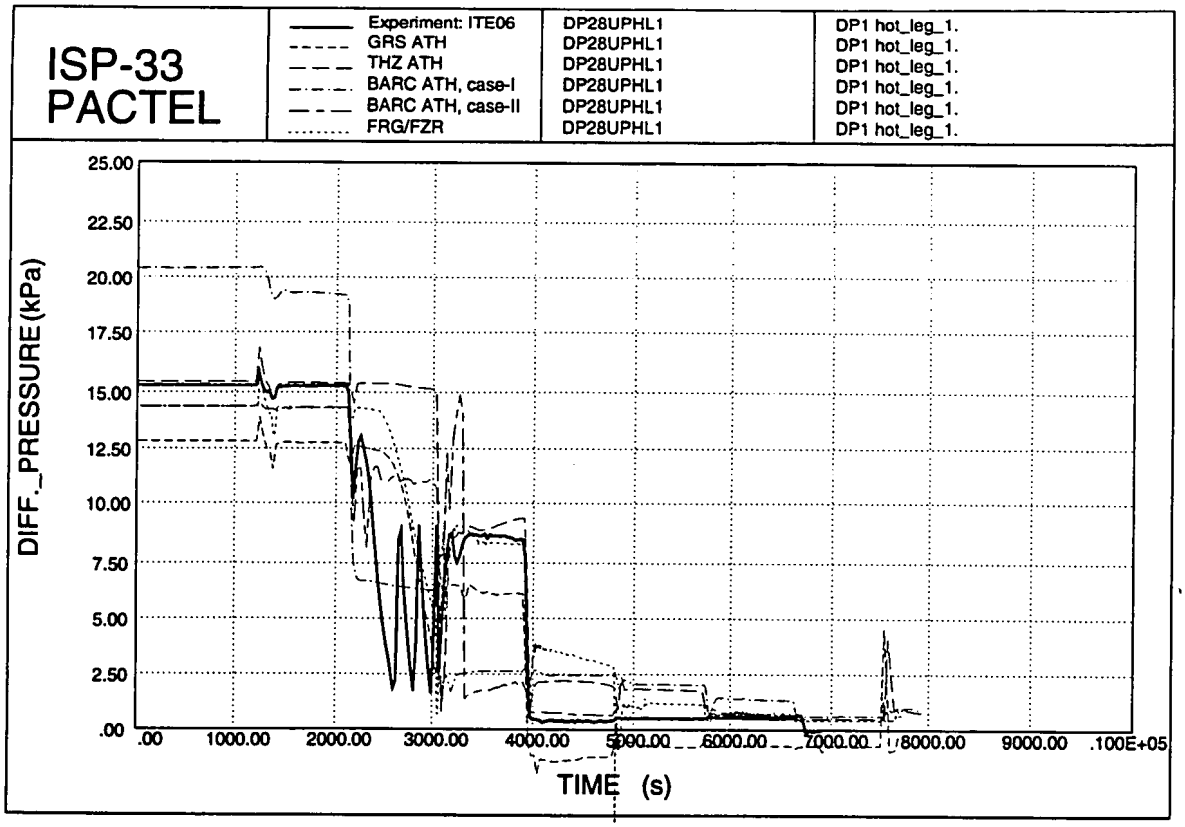

Figure 4.21. Hot leg 1 DP 1.

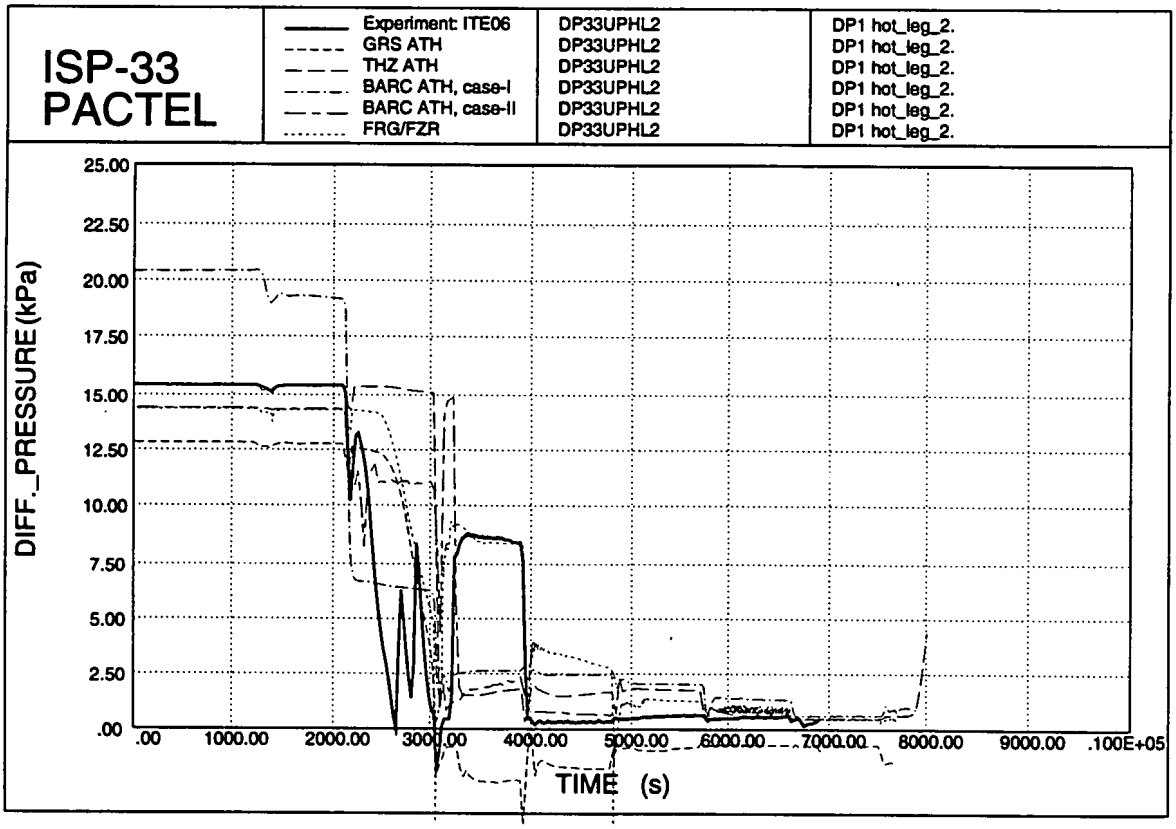

Figure 4.22. Hot leg 2 DP 1.

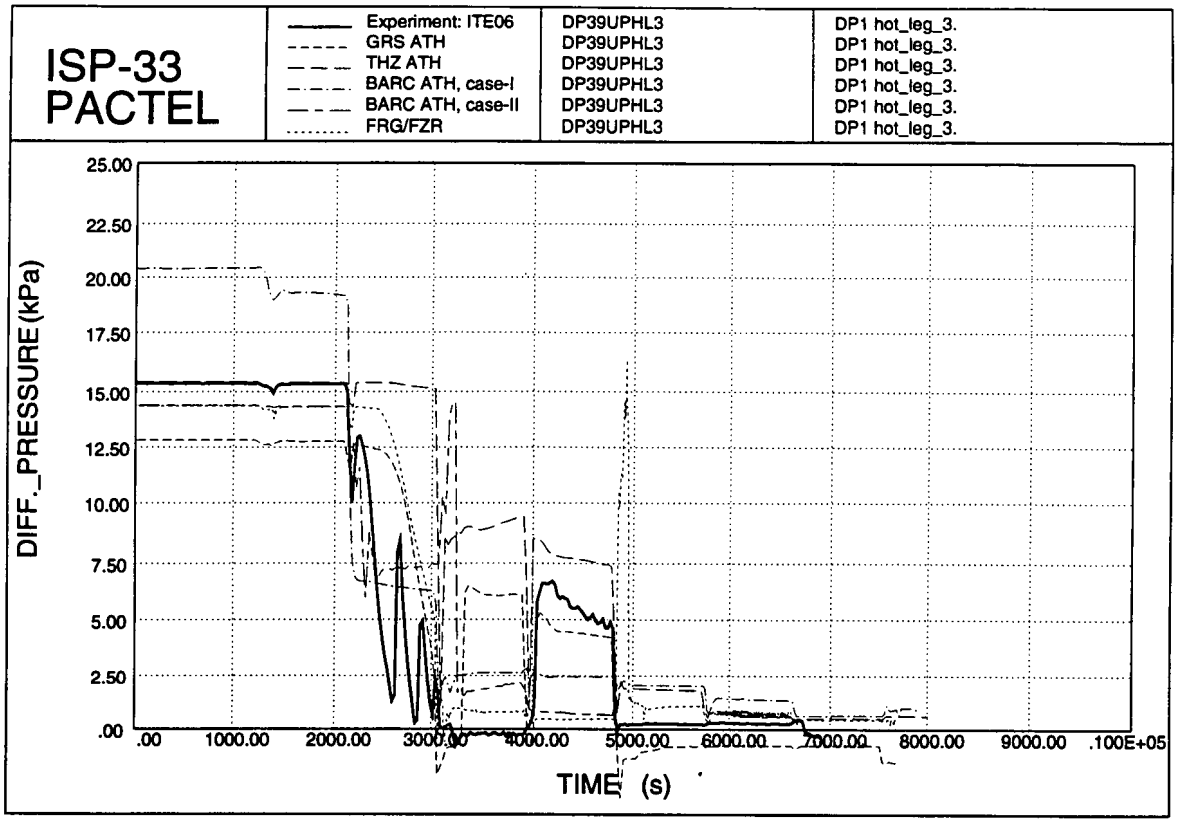

Figure 4.23. Hot leg 3 DP 1.

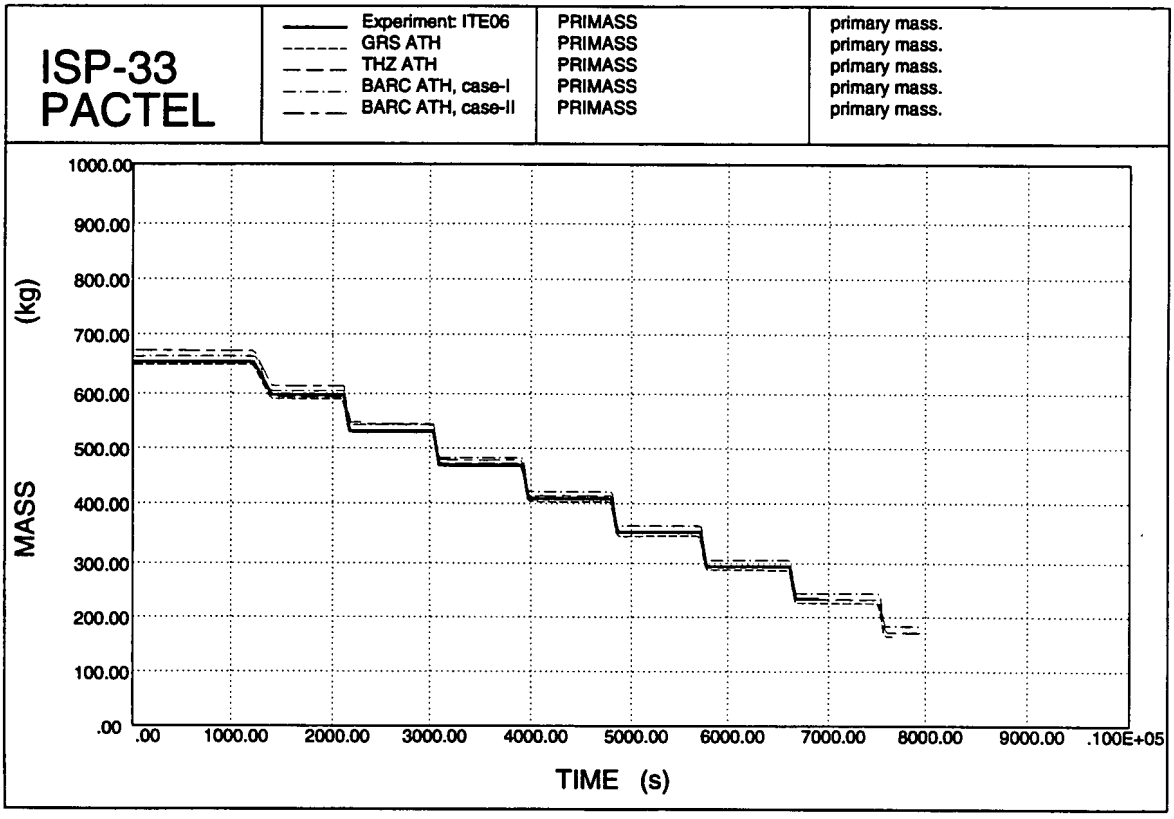

Figure 4.24. Primary mass inventory.

4.2.2 Comparison plots (CATHARE)

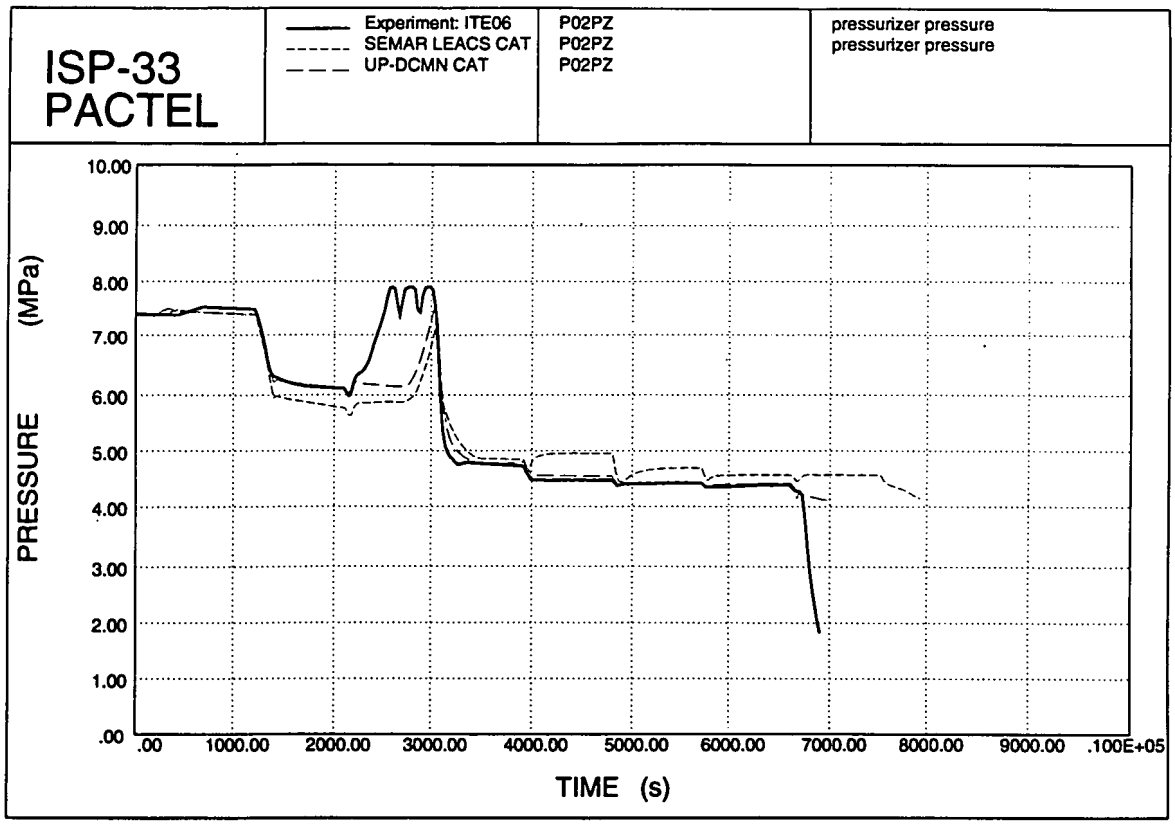

Figure 4.25. Pressurizer pressures.

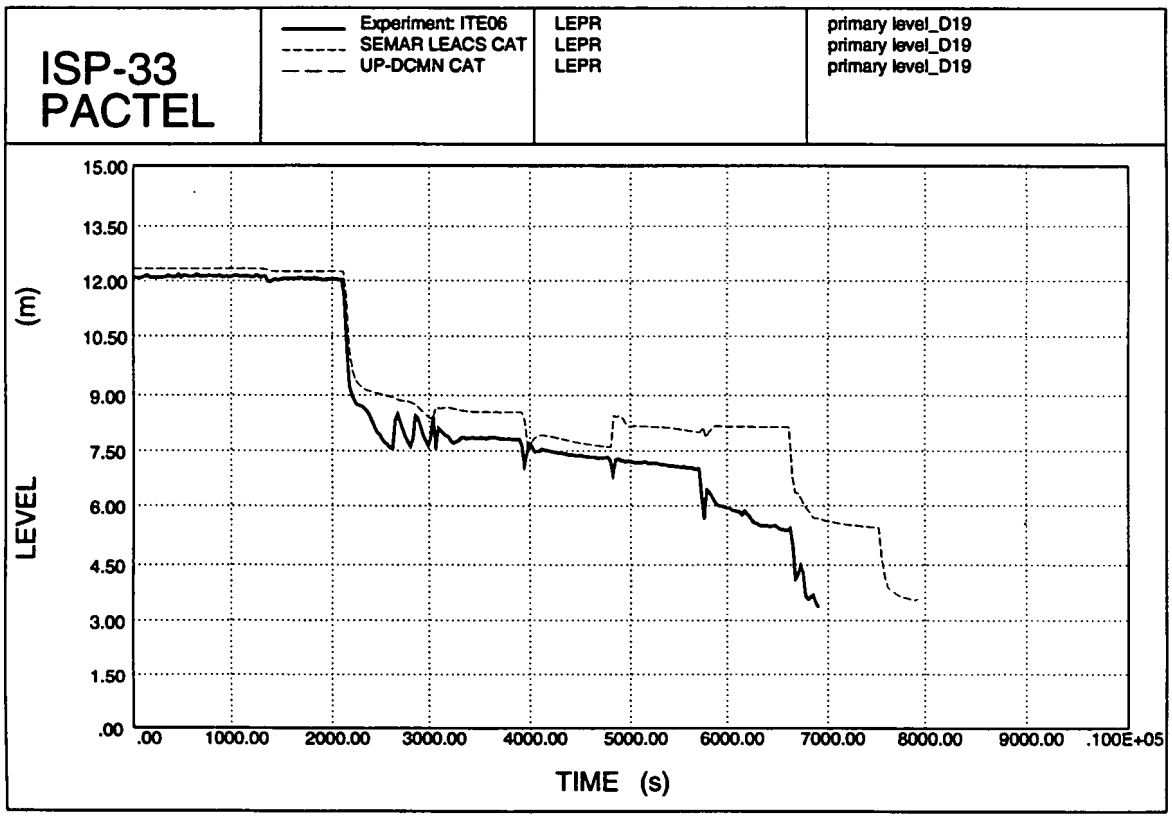

Figure 4.26. Primary levels.

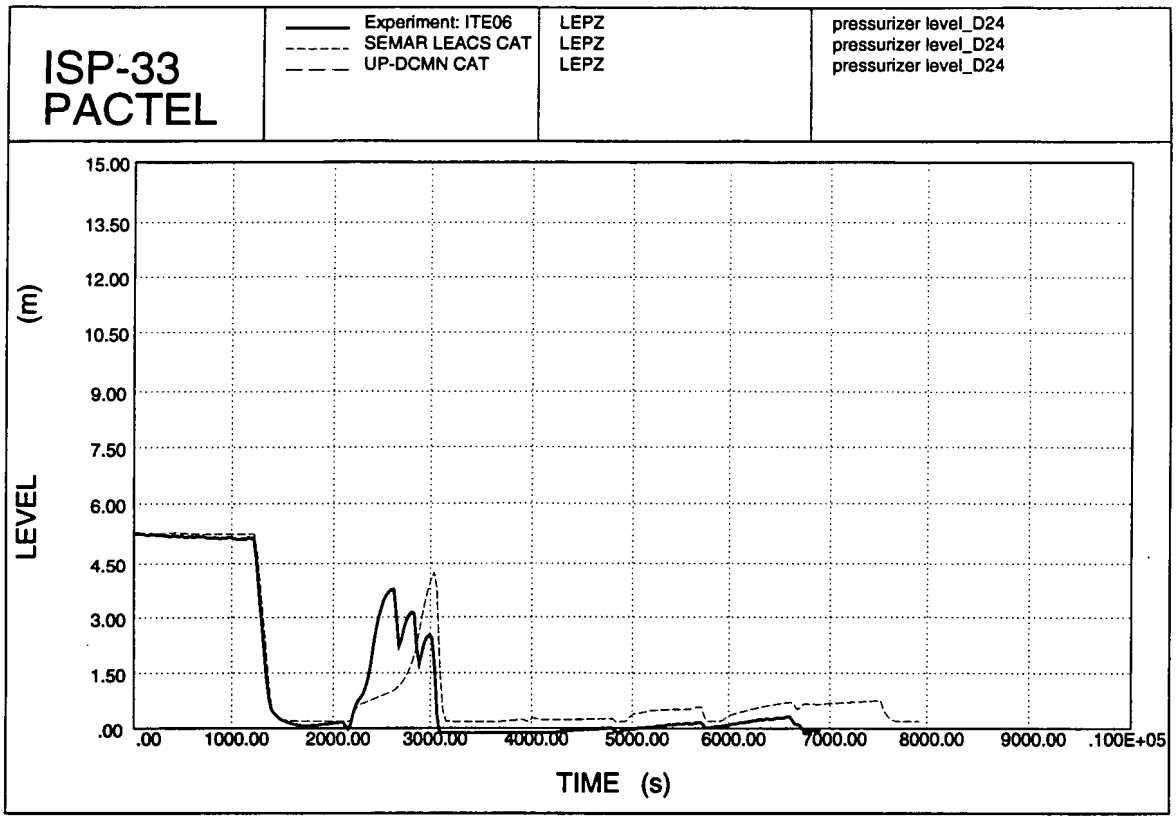

Figure 4.27. Pressurizer levels.

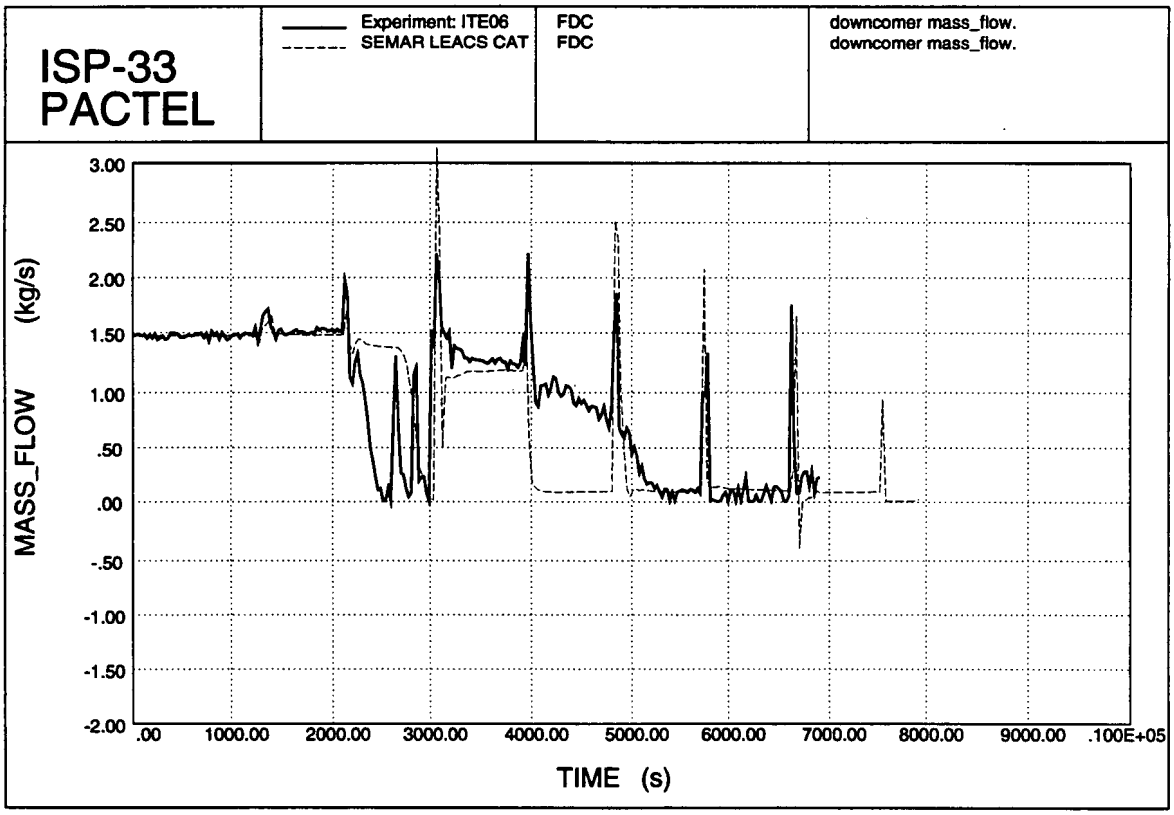

Figure 4.28. Downcomer mass flow.

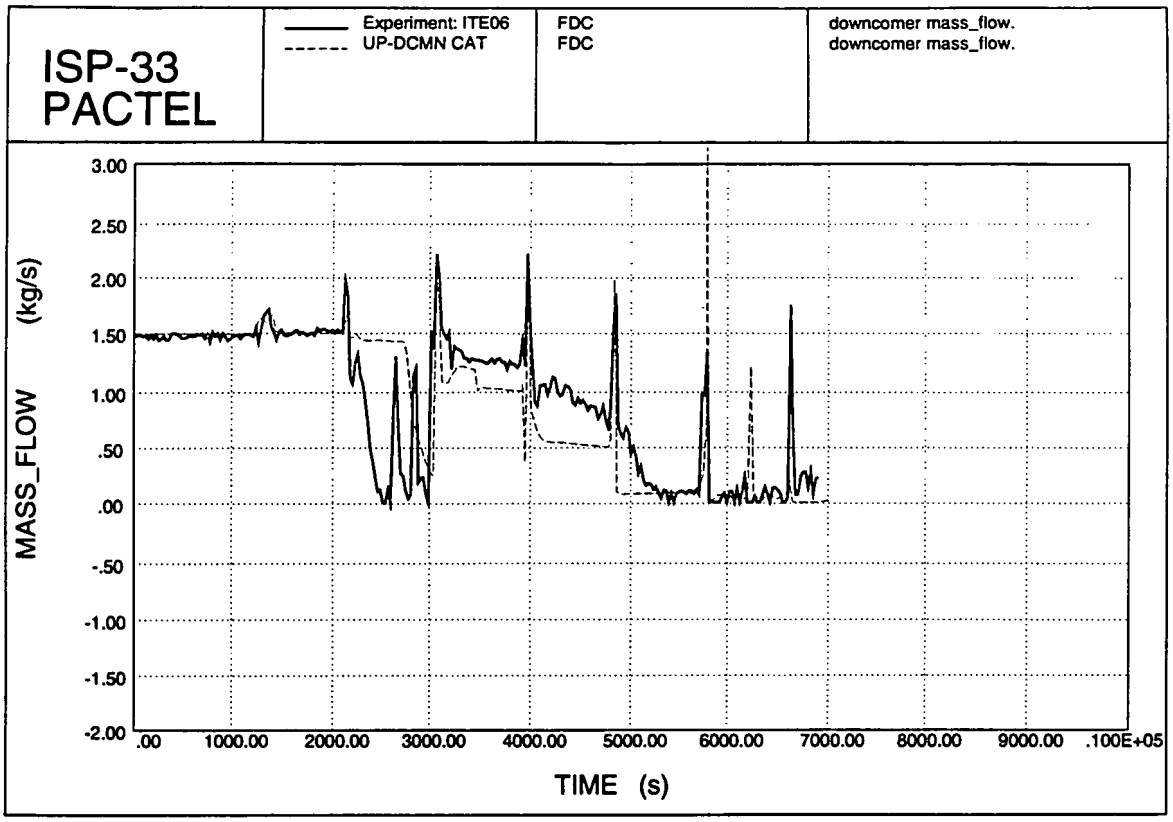

Figure 4.29. Downcomer mass flow.

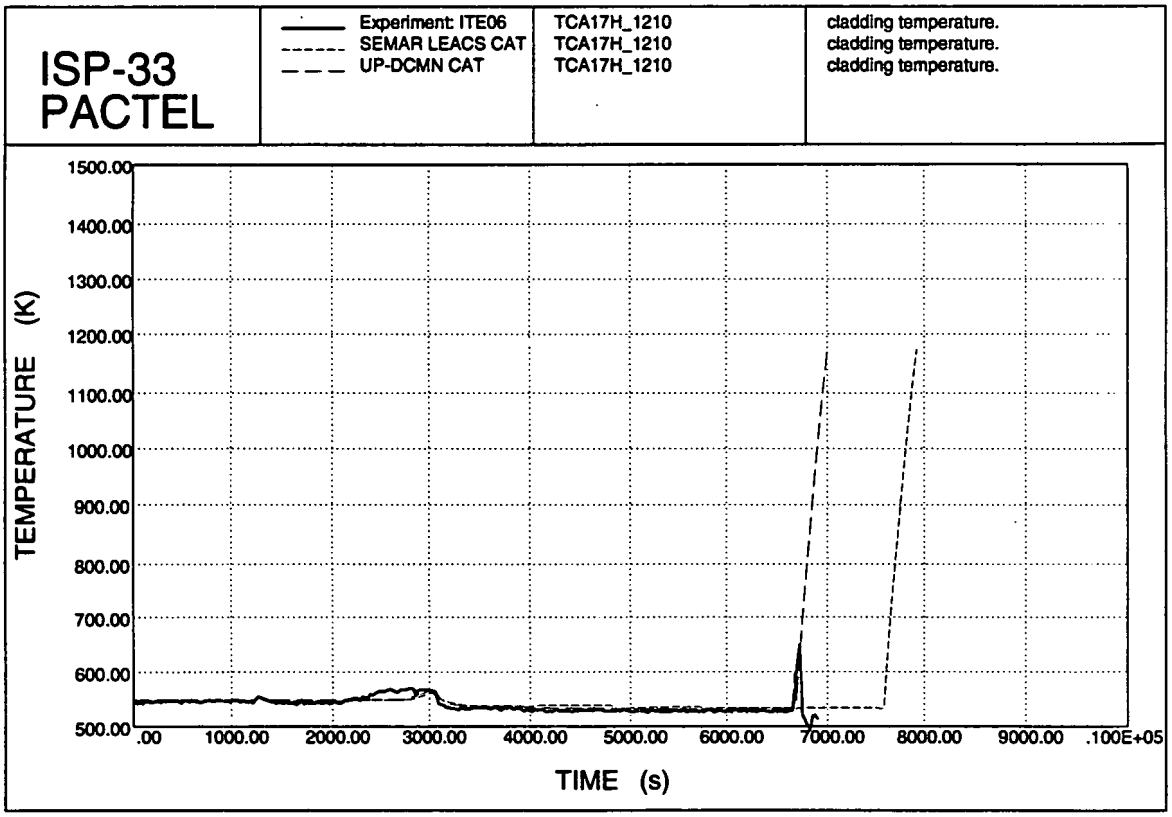

Figure 4.30. Cladding temperatures.

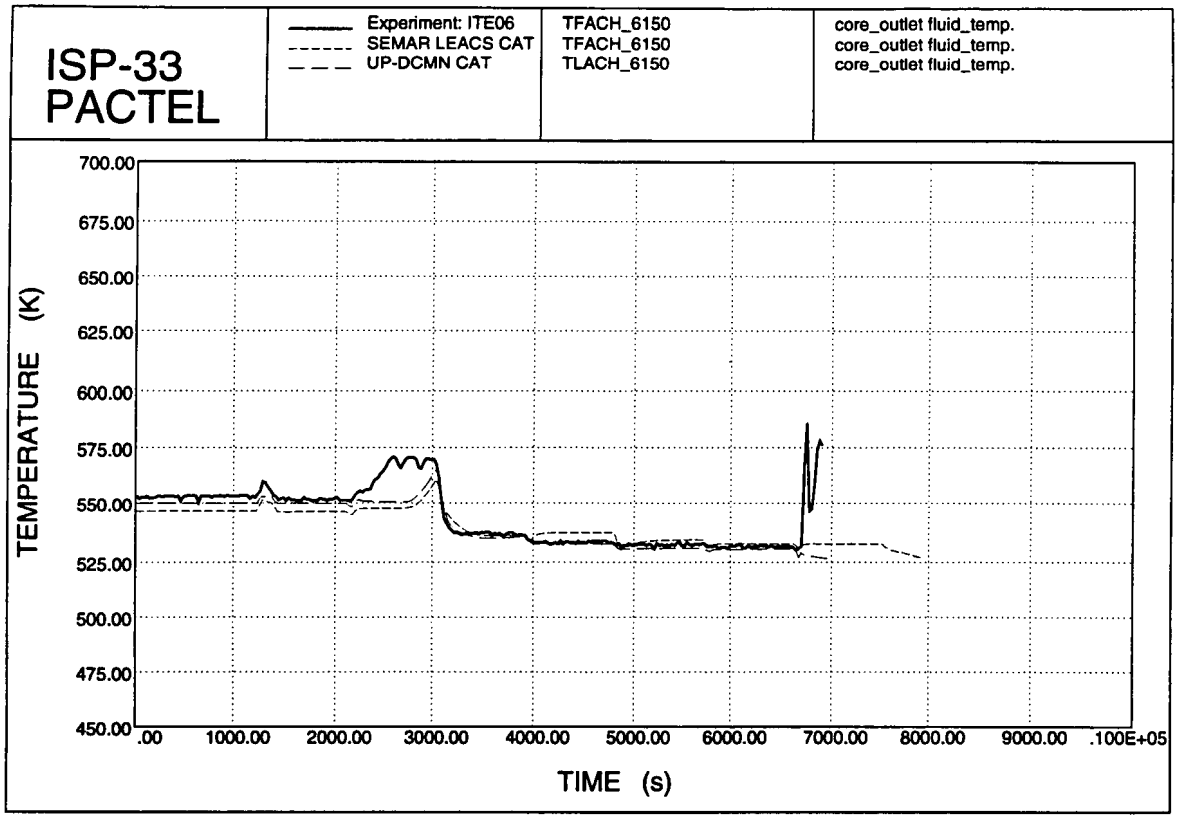

Figure 4.31. Core outlet coolant temperature.

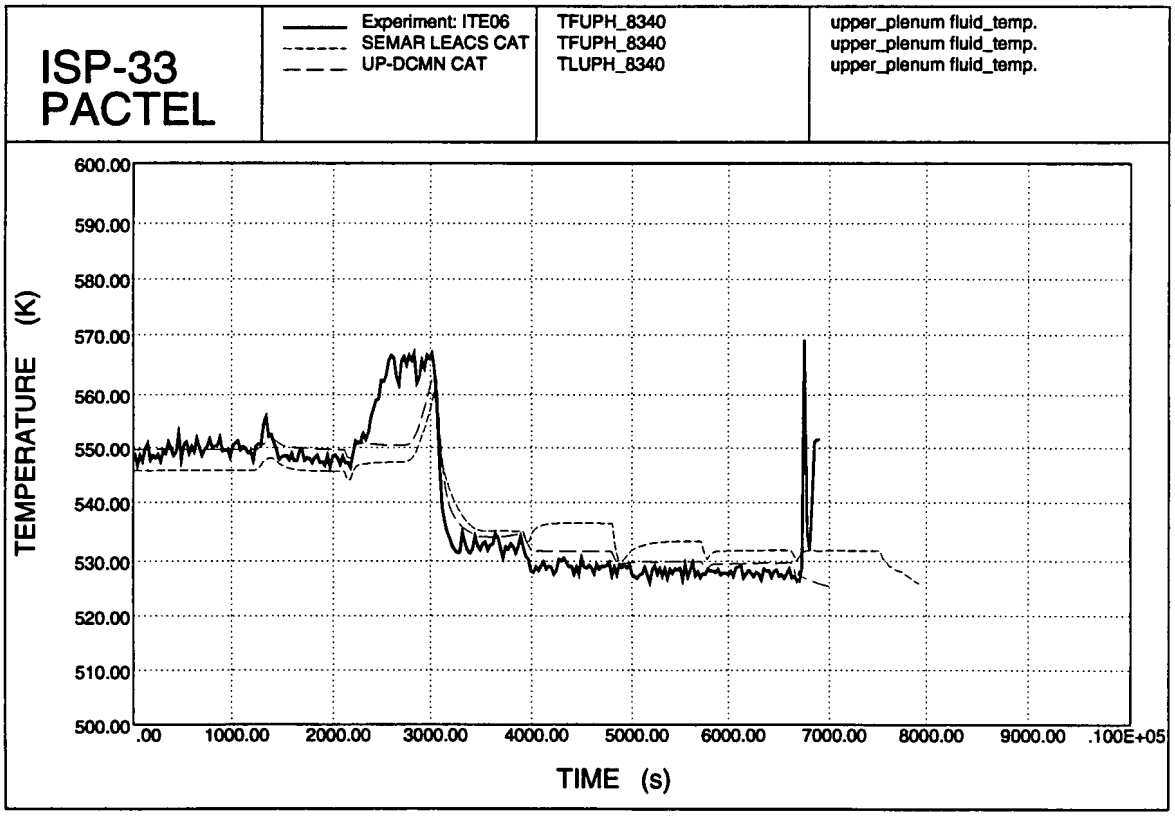

Figure 4.32. Upper plenum temperatures.

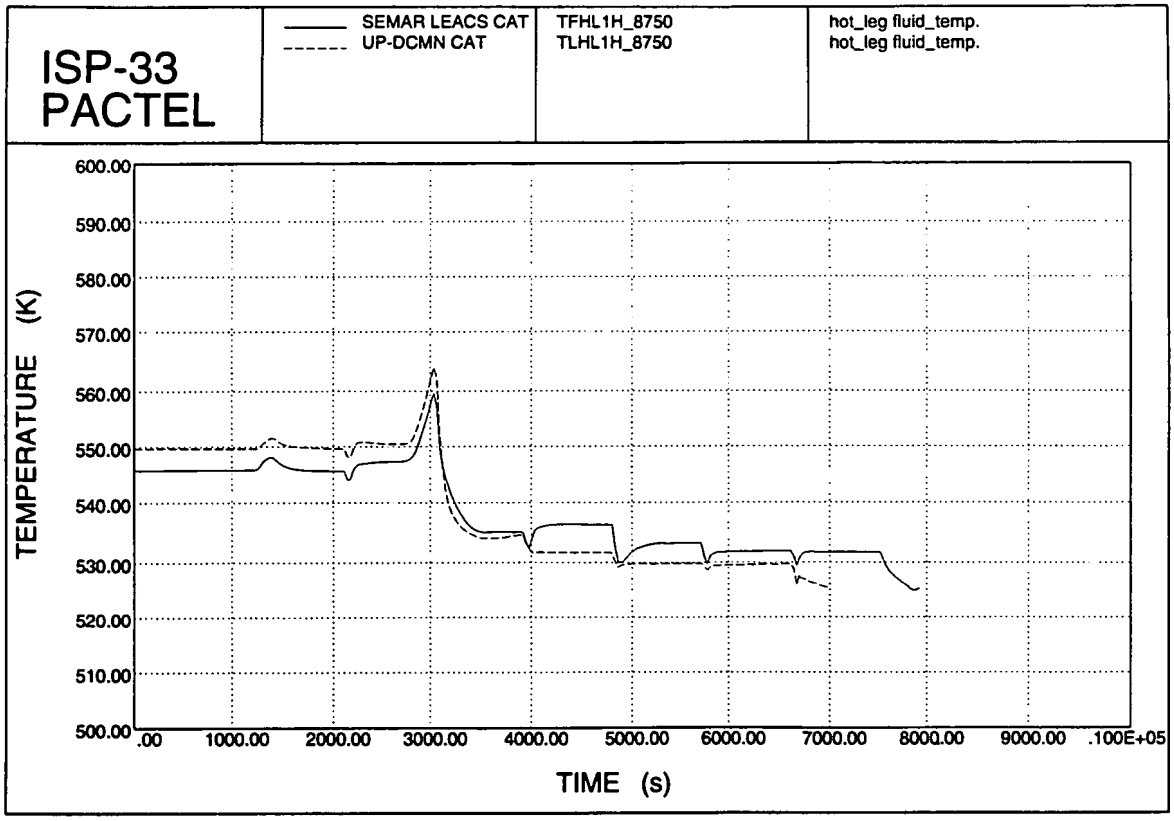

Figure 4.33. Hot leg coolant temperatures.

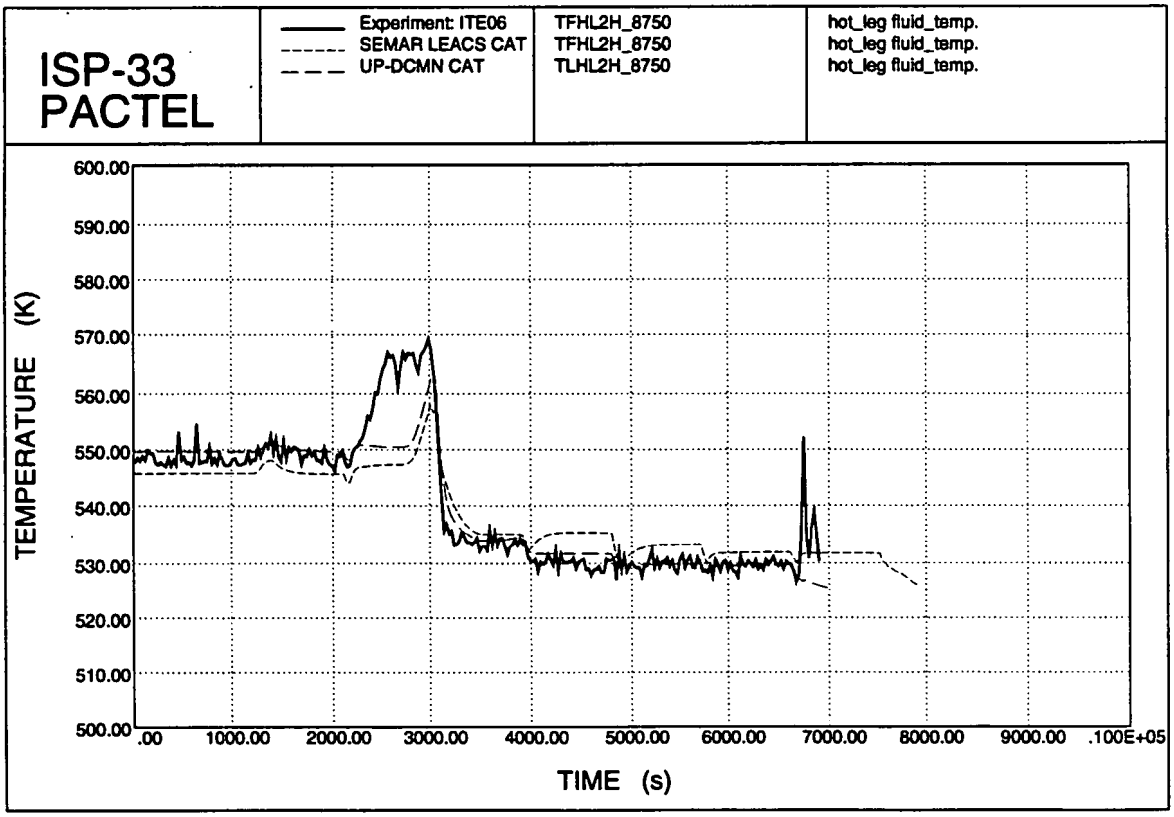

Figure 4.34. Hot leg temperatures.

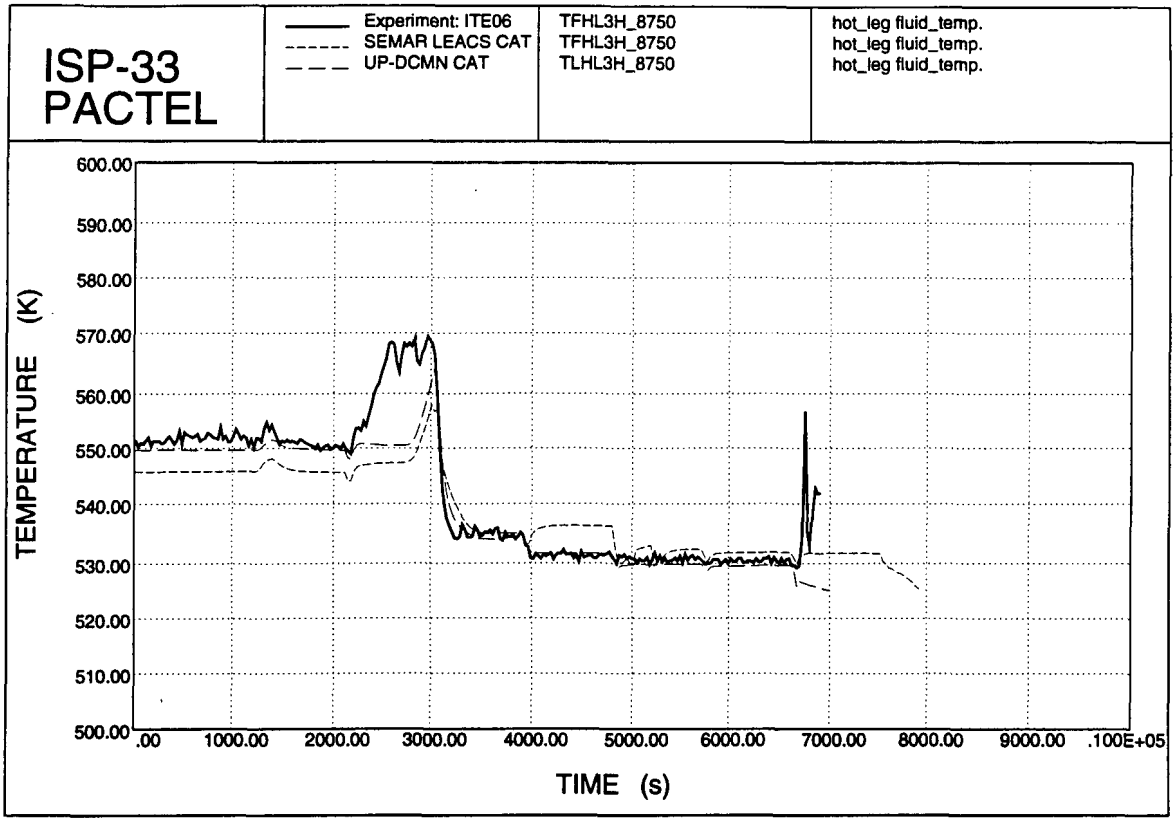

Figure 4.35. Hot leg coolant temperatures.

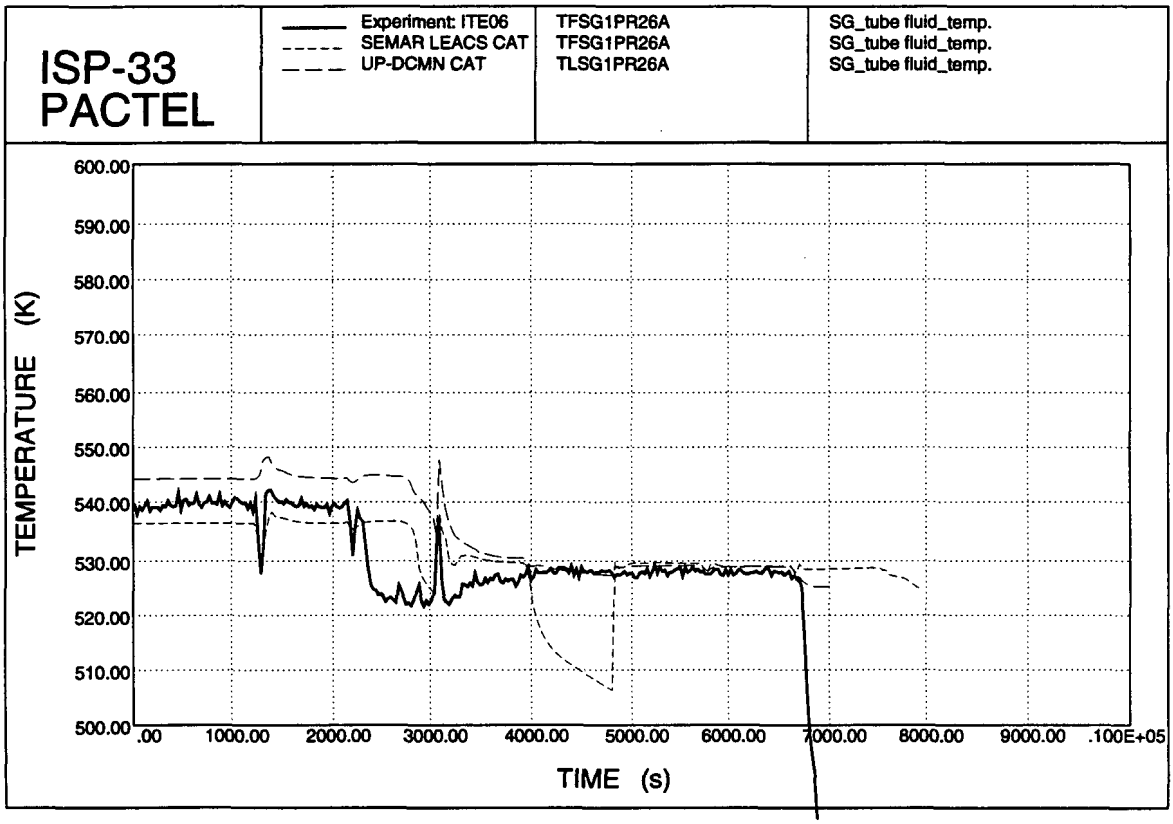

Figure 4.36. SG tube fluid temperatures.

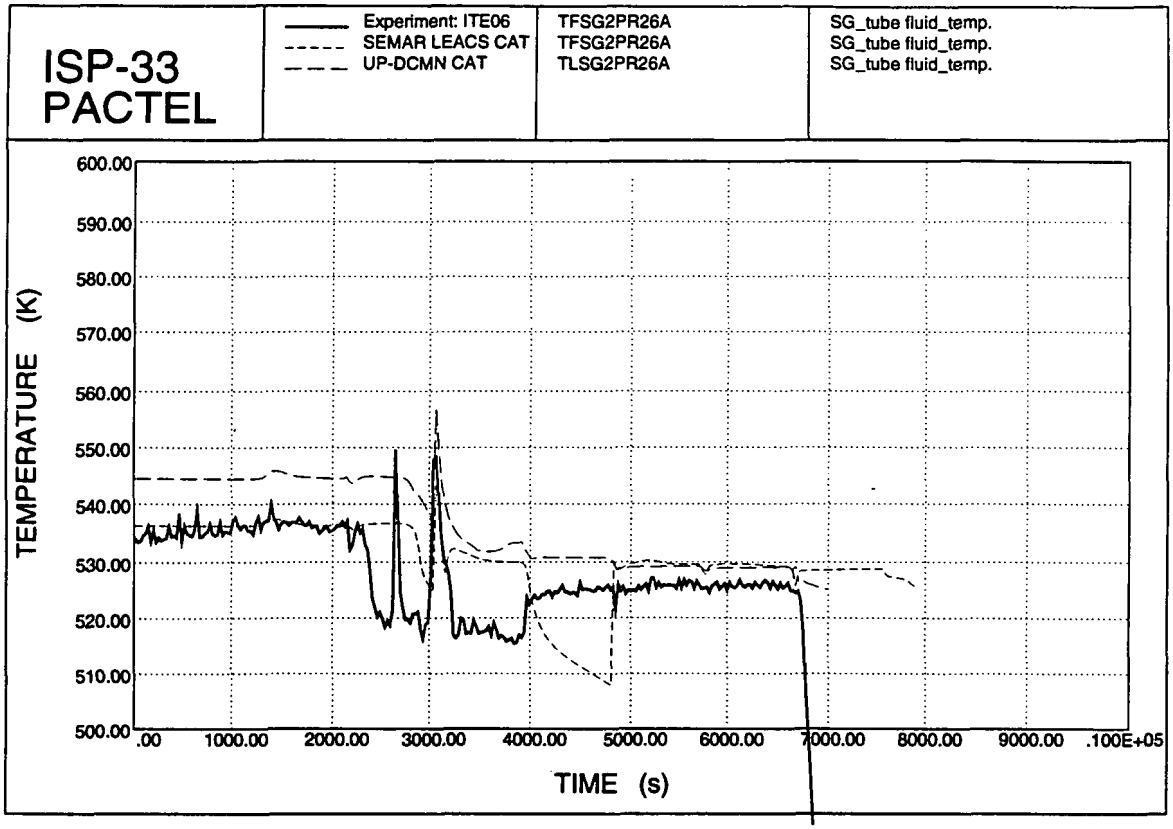

Figure 4.37. SG tube fluid temperatures.

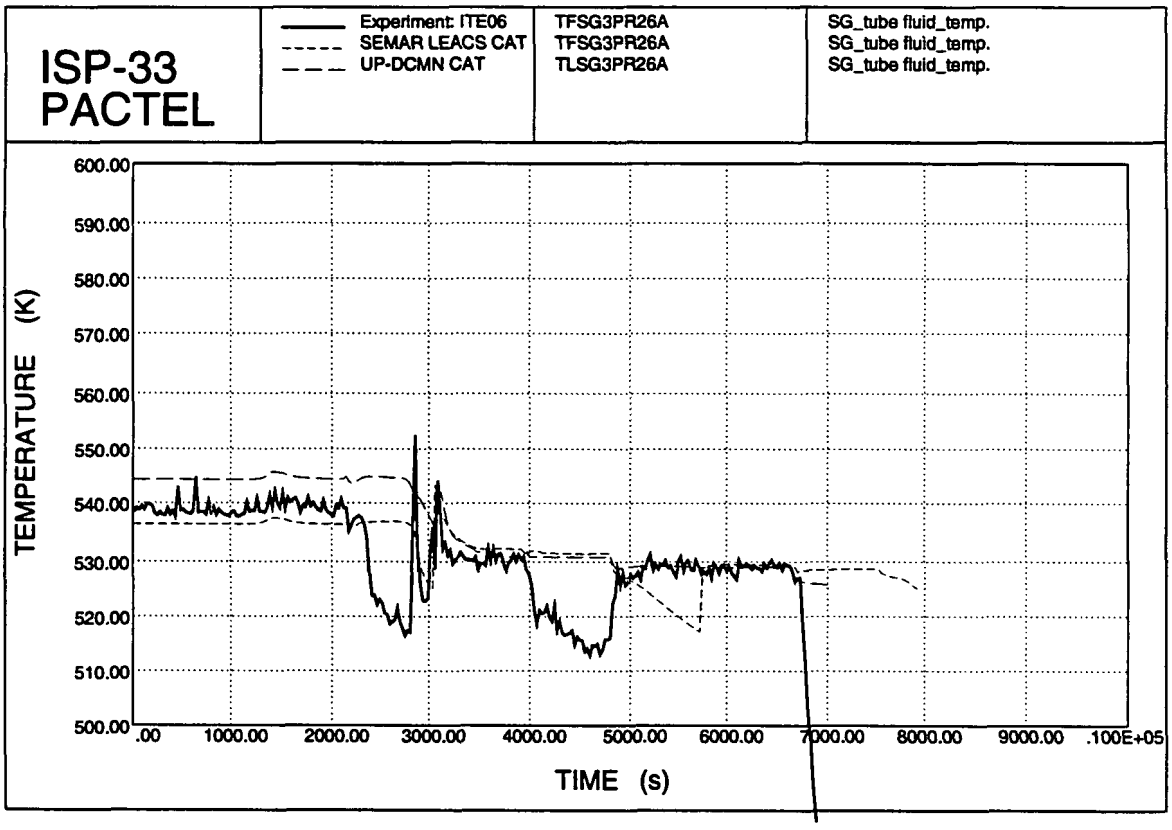

Figure 4.38. SG tube fluid temperatures.

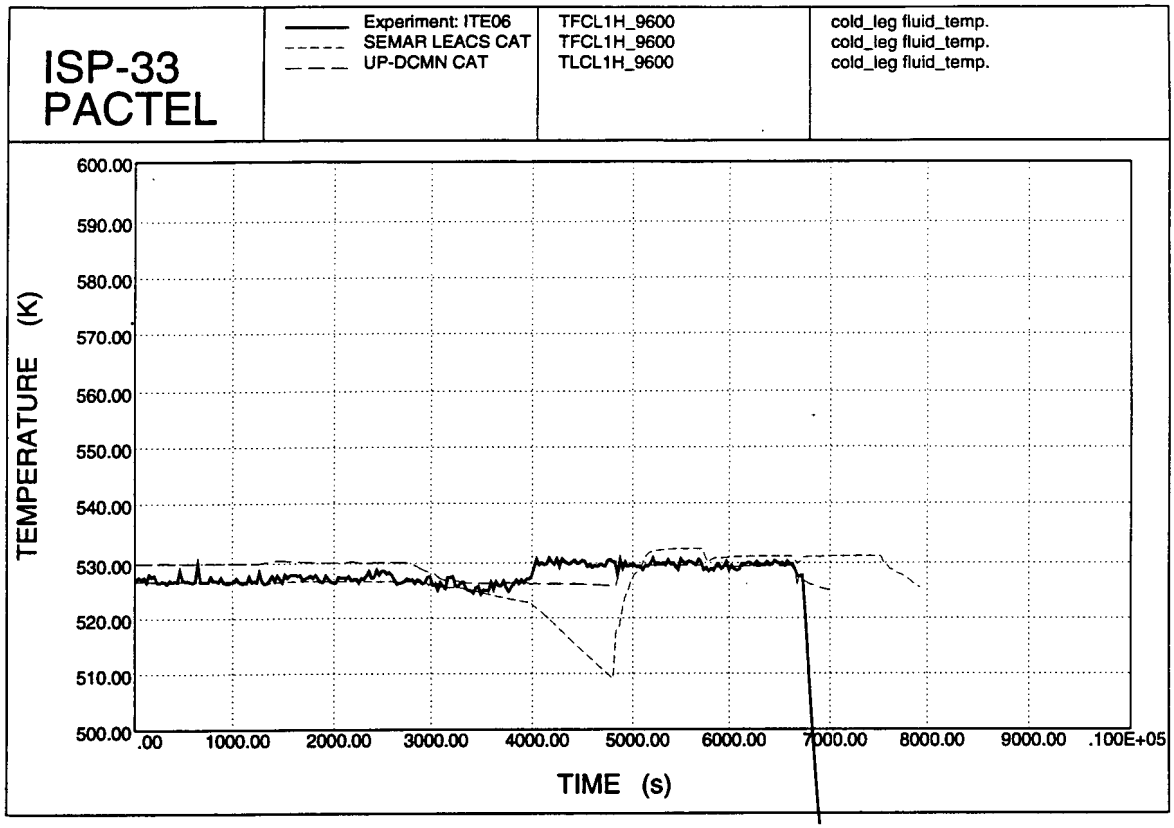

Figure 4.39. Cold leg temperatures.

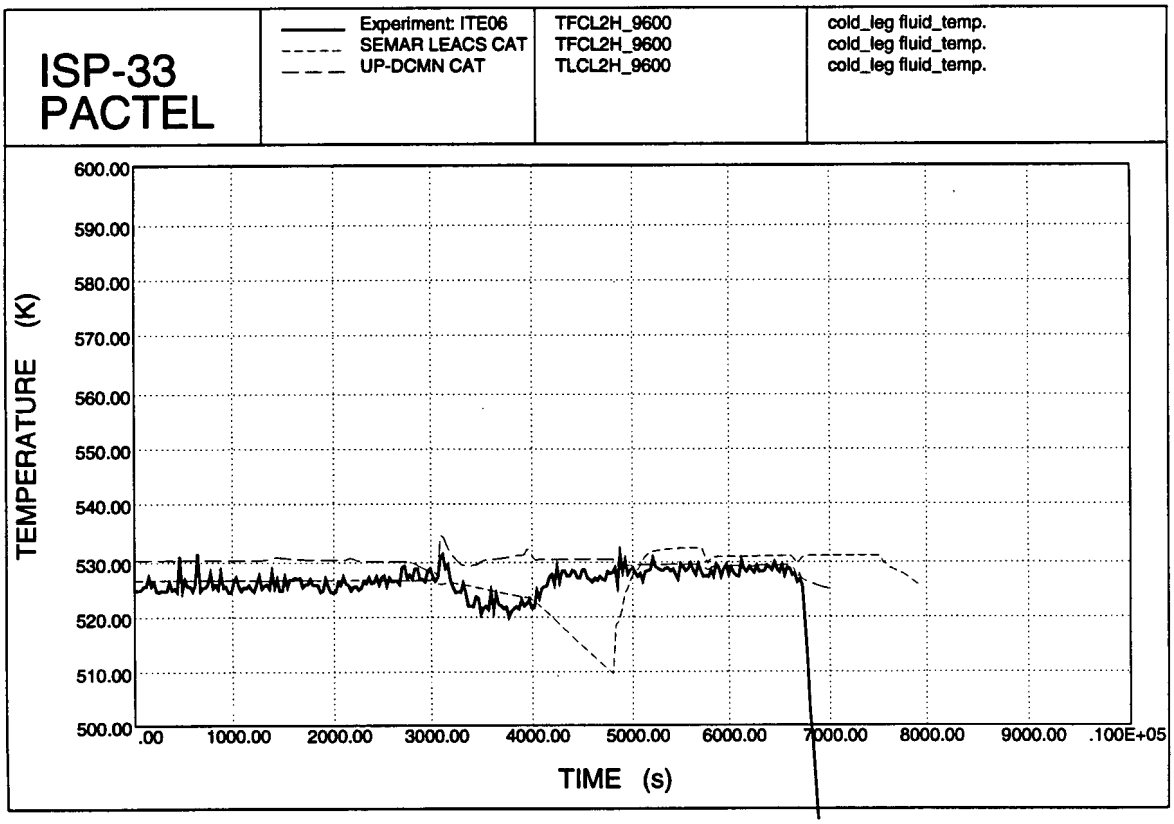

Figure 4.40. Cold leg coolant temperatures.

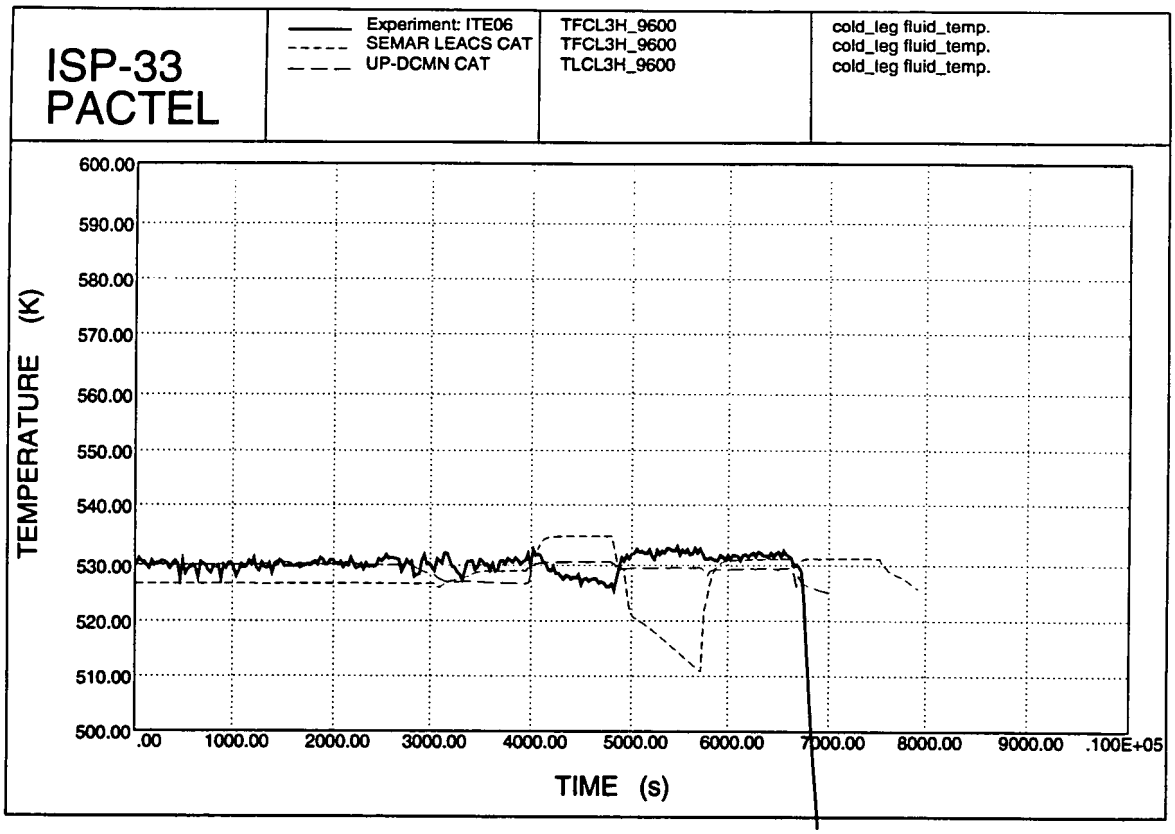

Figure 4.41. Cold leg temperatures.

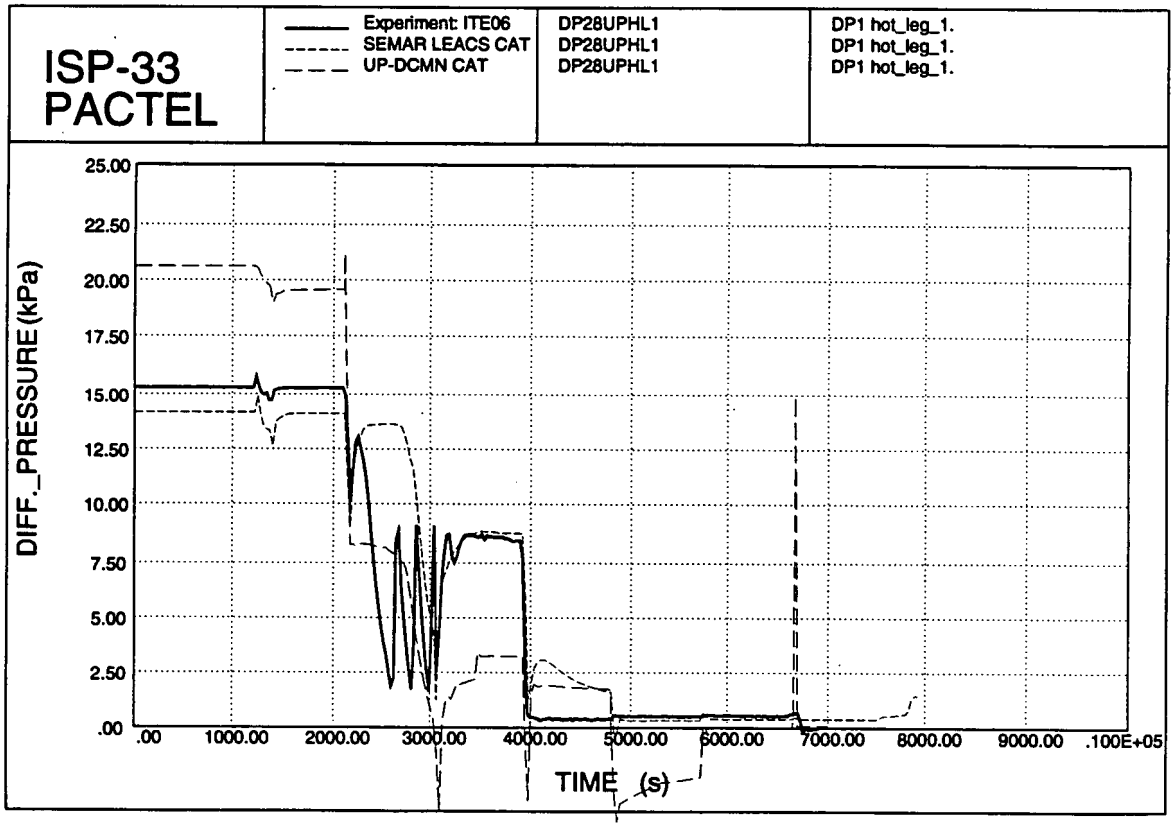

Figure 4.42. Hot leg 1 DP 1.

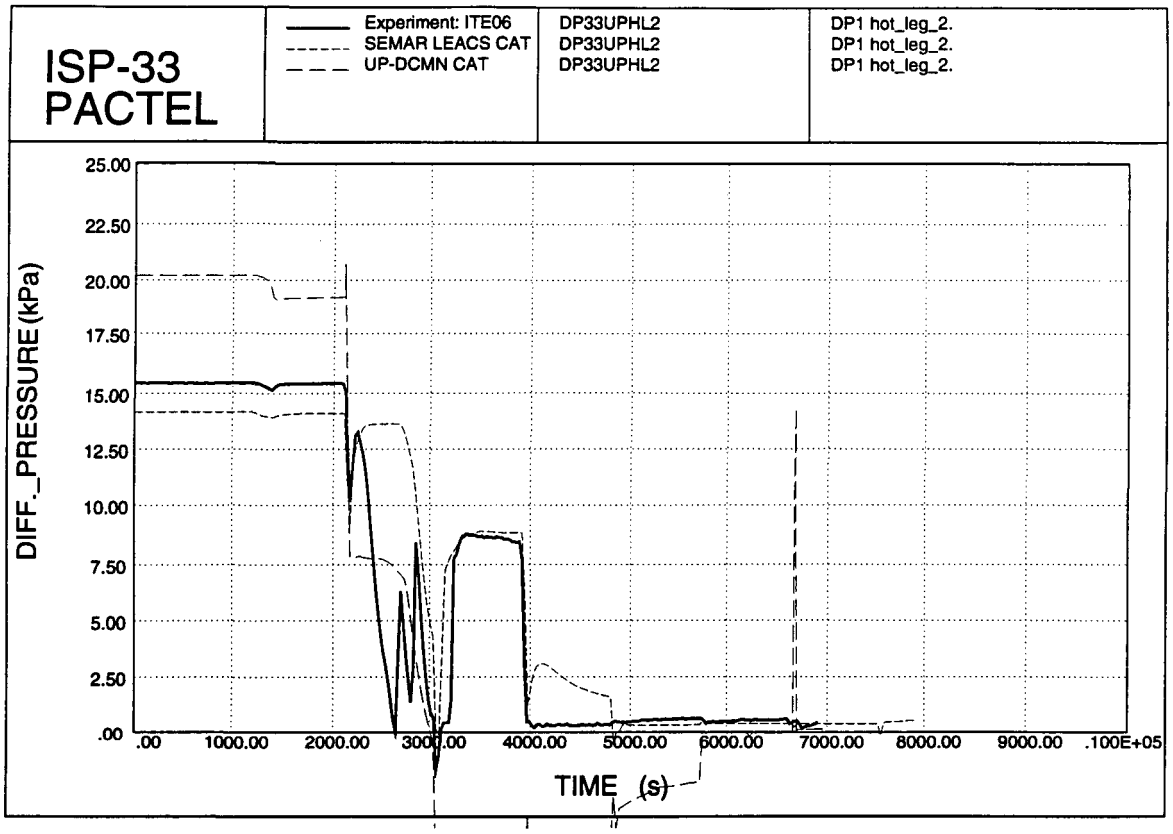

Figure 4.43. Hot leg 2 DP 1.

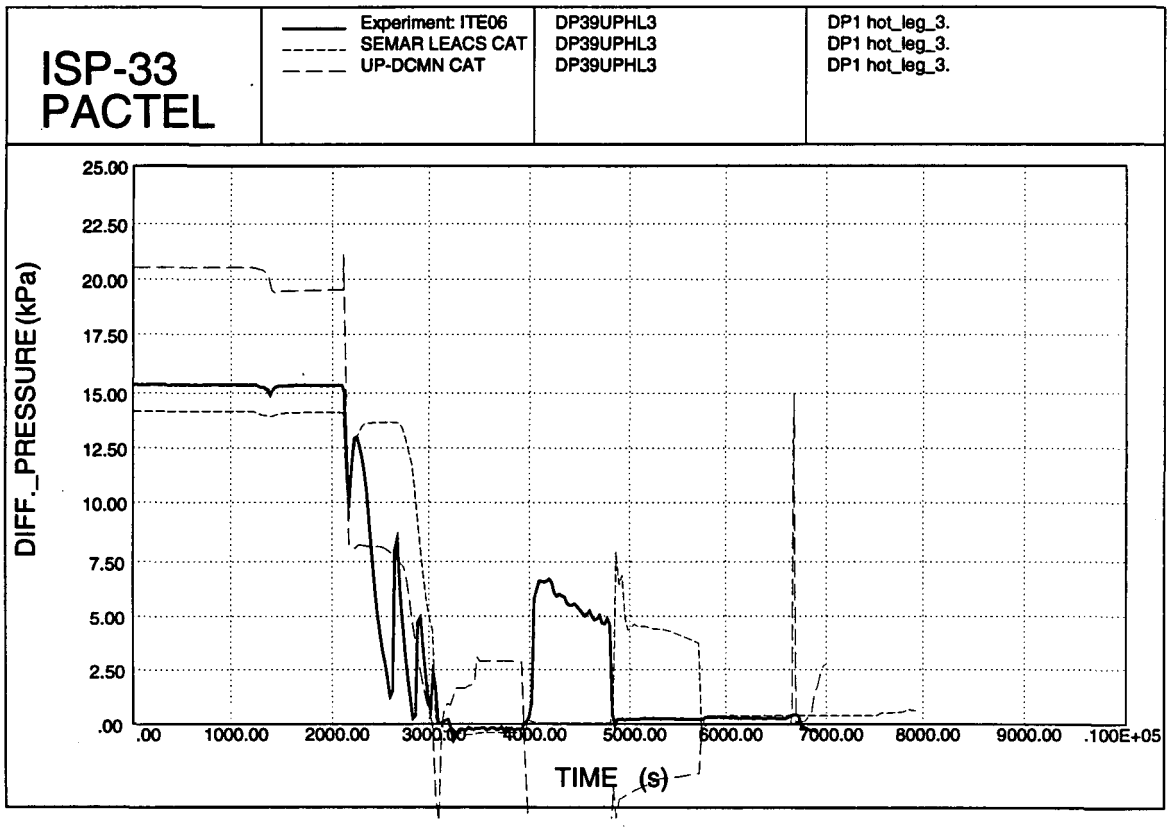

Figure 4.44. Hot leg 3 DP 1.

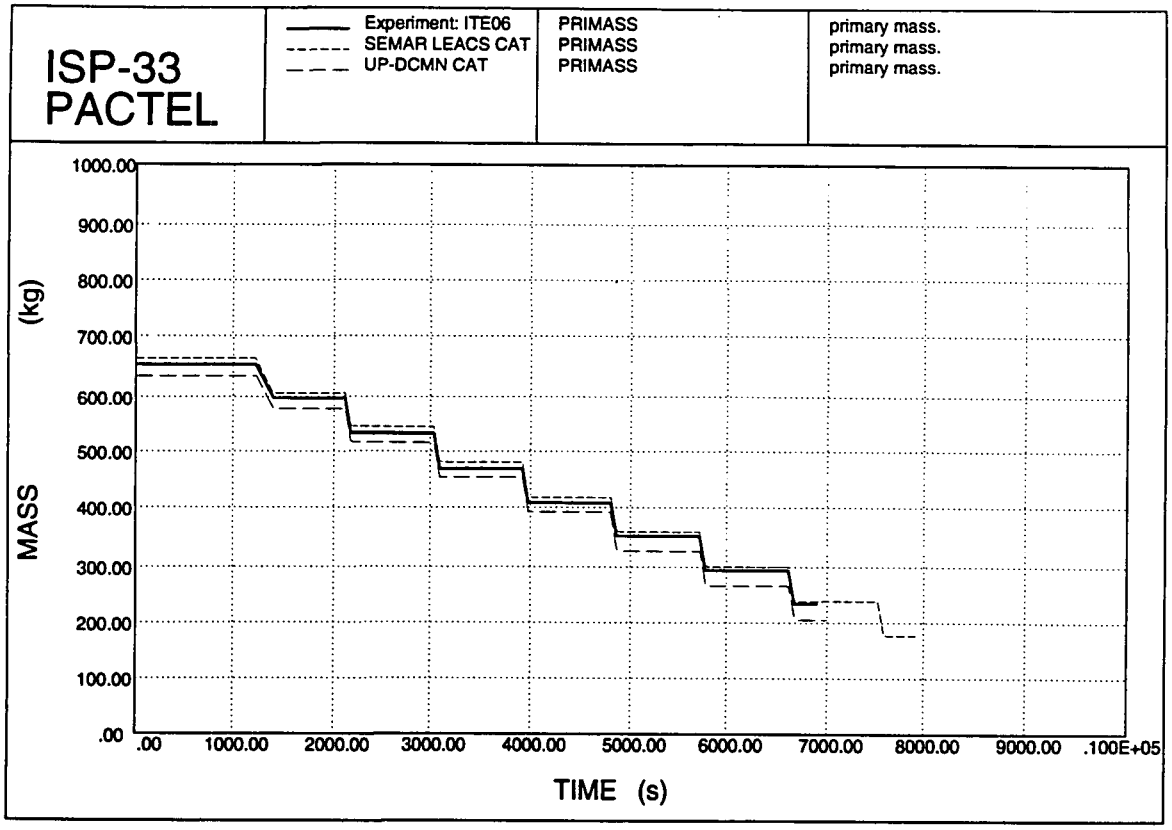

Figure 4.45. Primary mass inventory.

4.2.3 Comparison plots (RELAP5/MOD3)

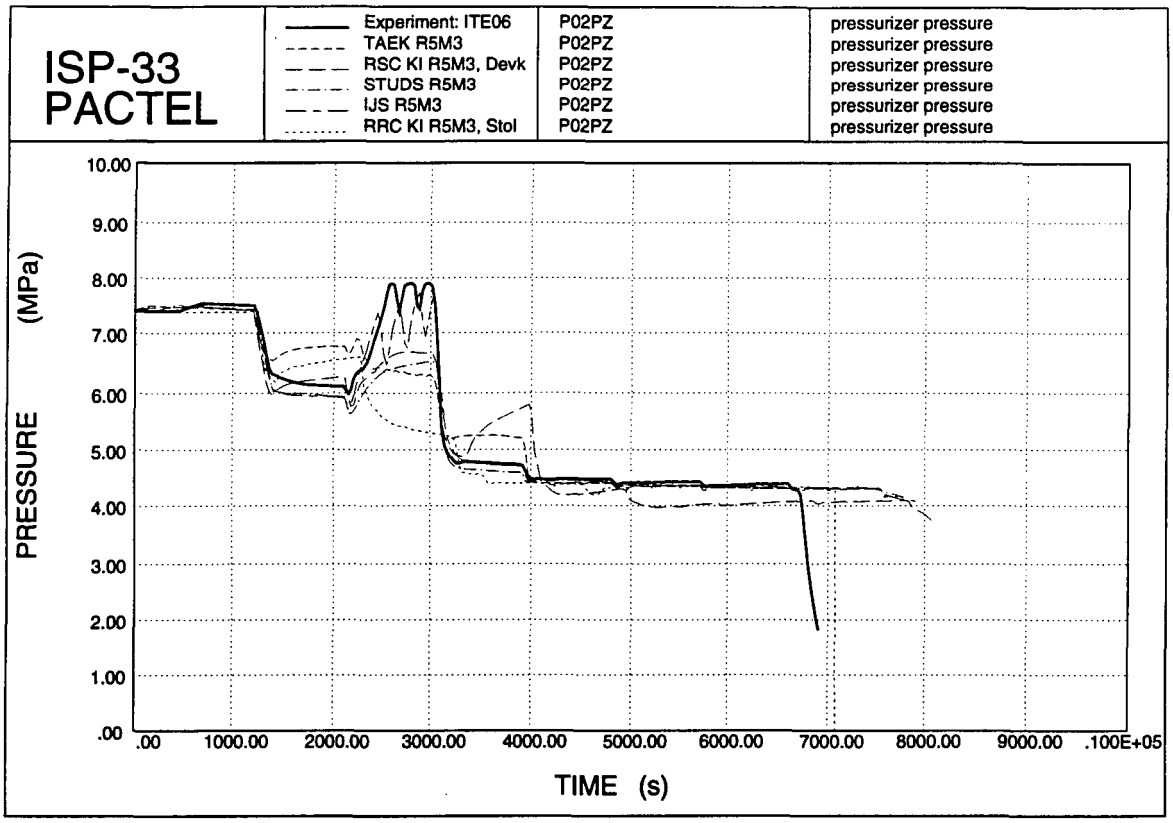

Figure 4.46. Pressurizer pressures.

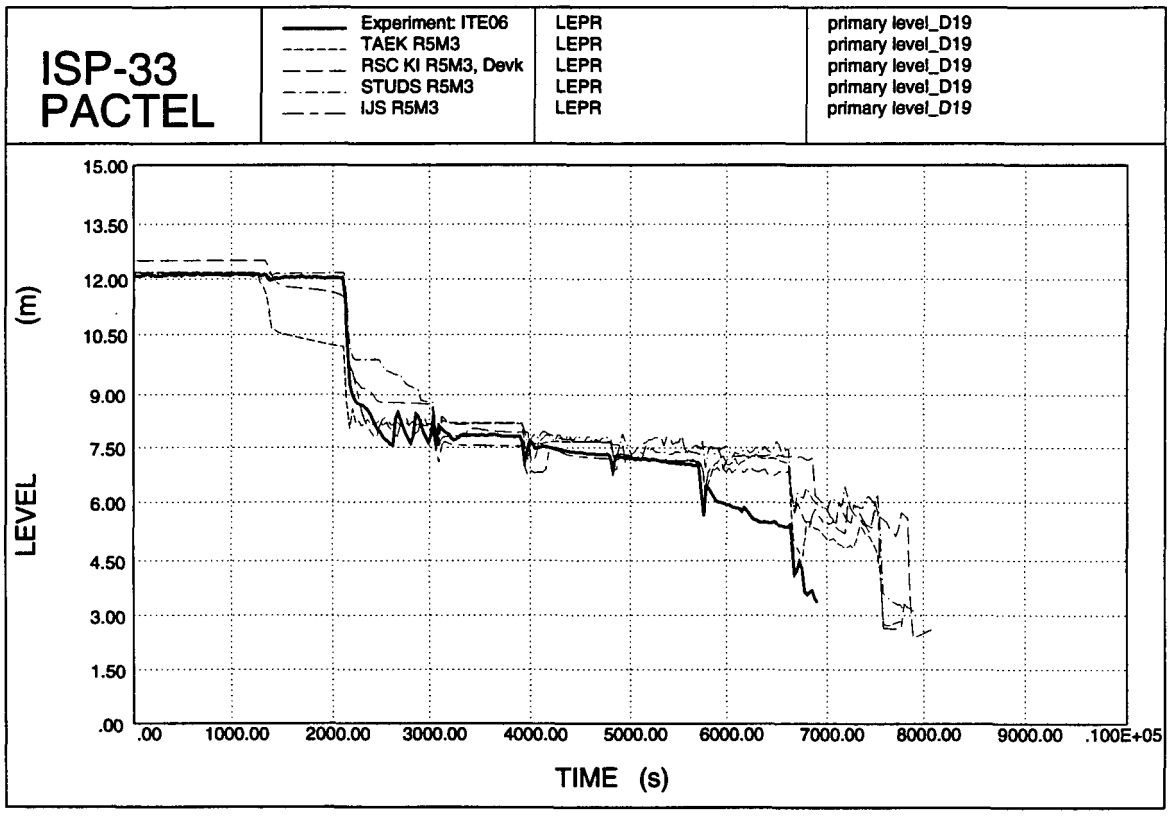

Figure 4.47. Primary levels.

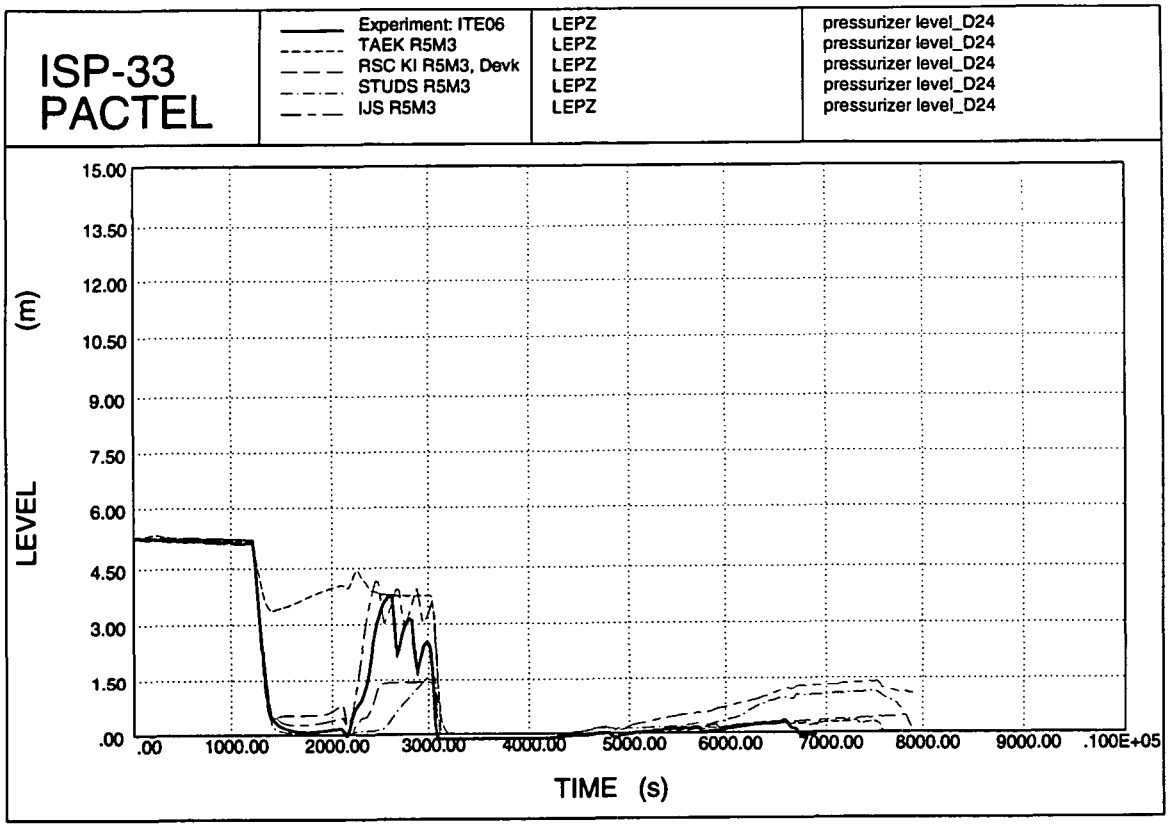

Figure 4.48. Pressurizer levels.

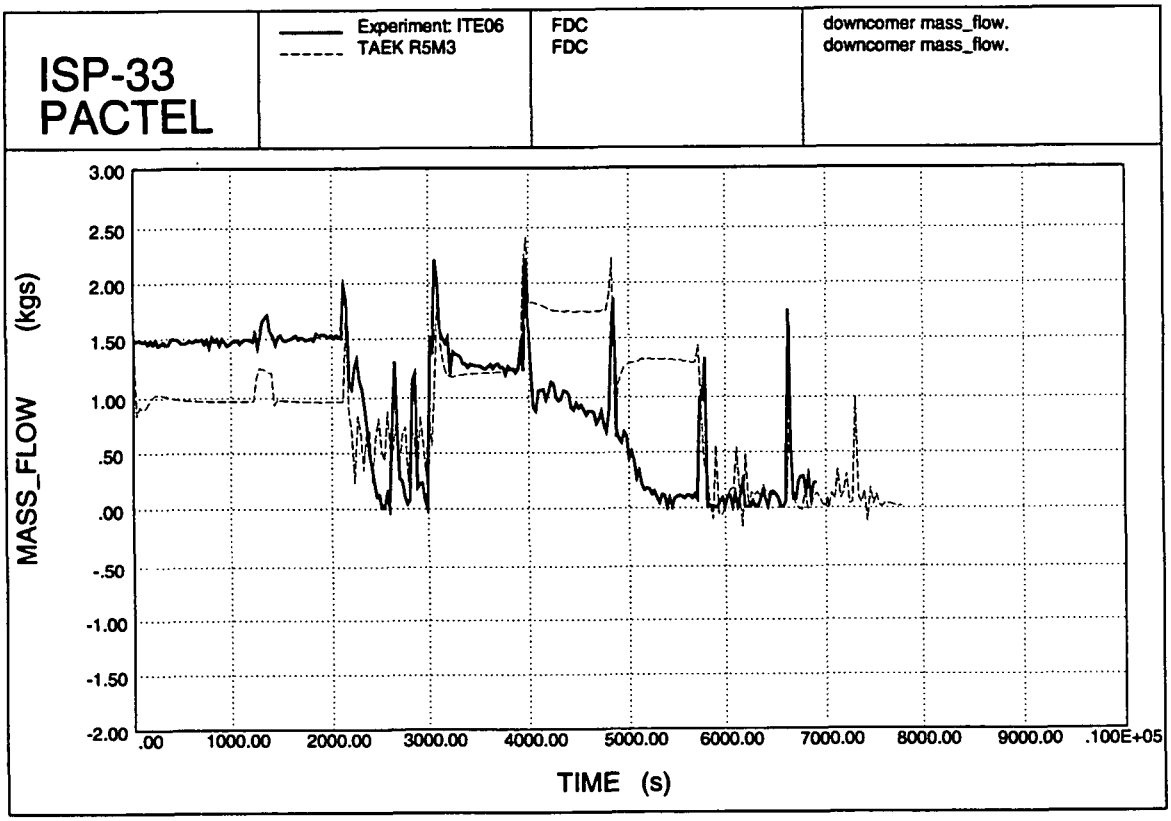

Figure 4.49. Downcomer mass flow.

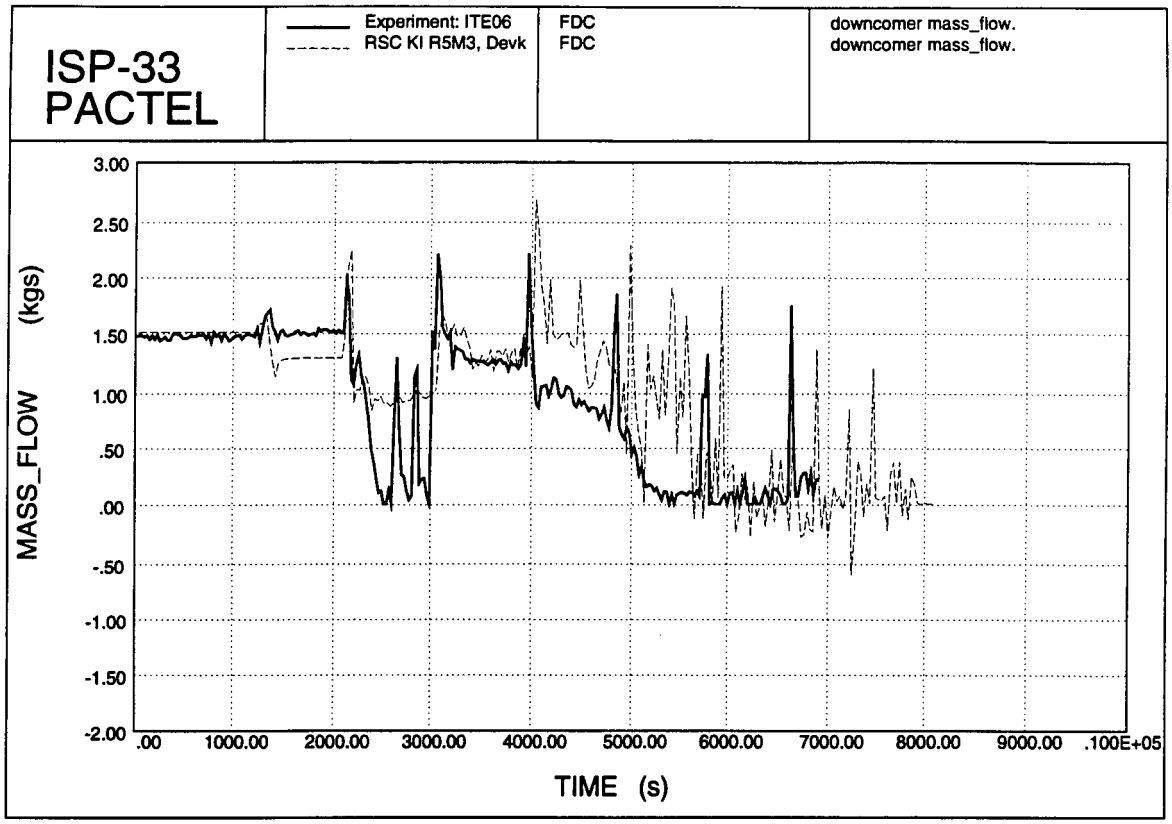

Figure 4.50. Downcomer mass flow.

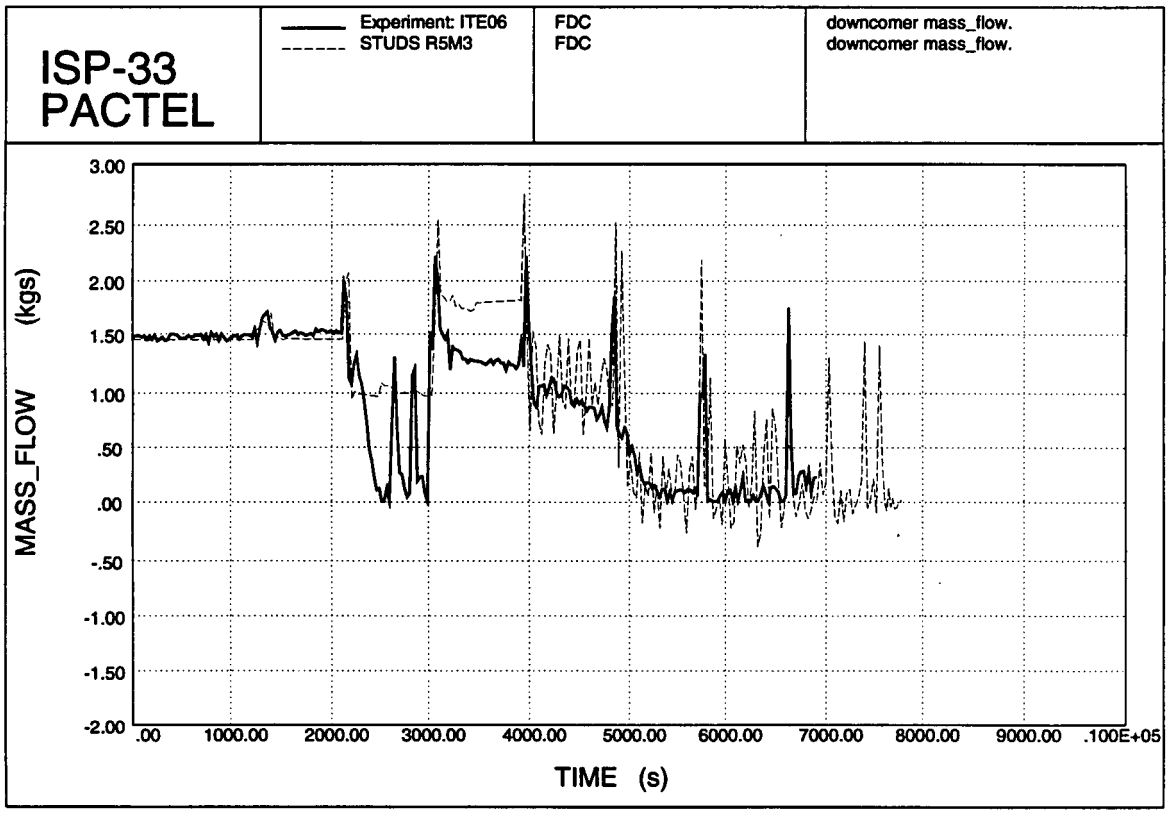

Figure 4.51. Downcomer mass flow.

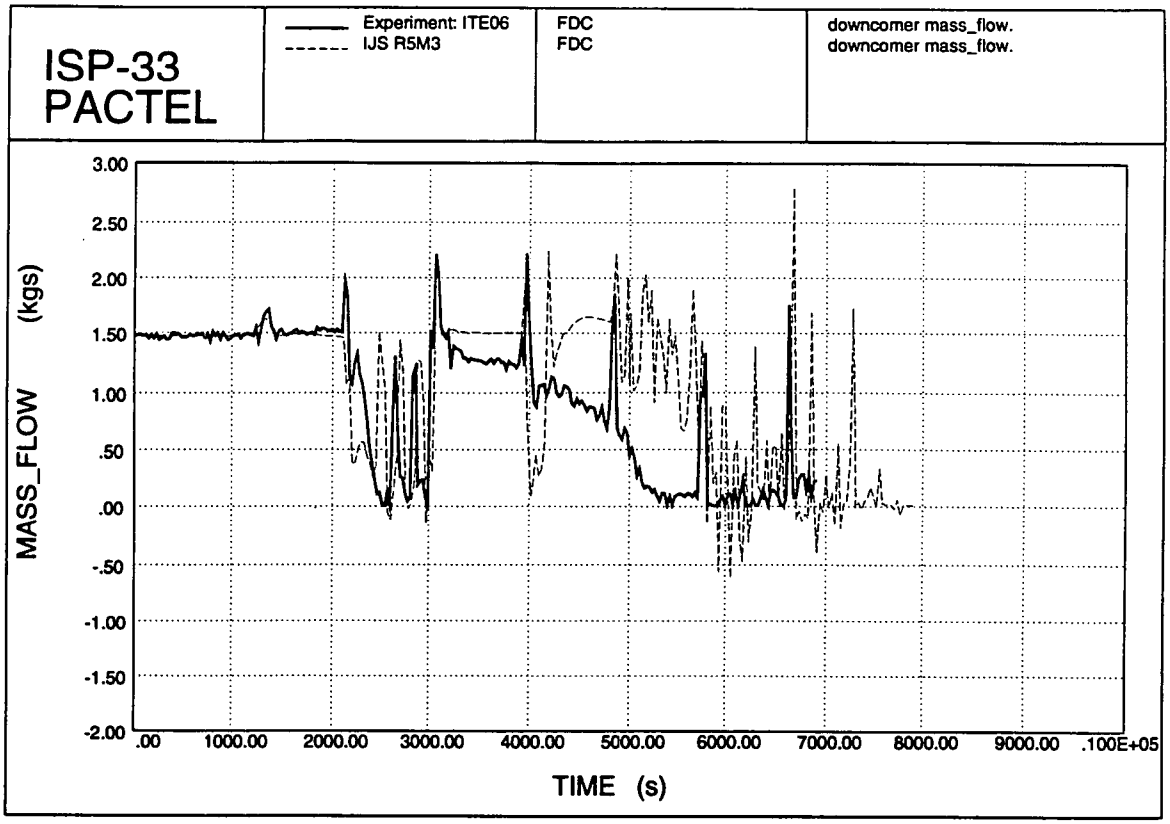

Figure 4.52. Downcomer mass flow.

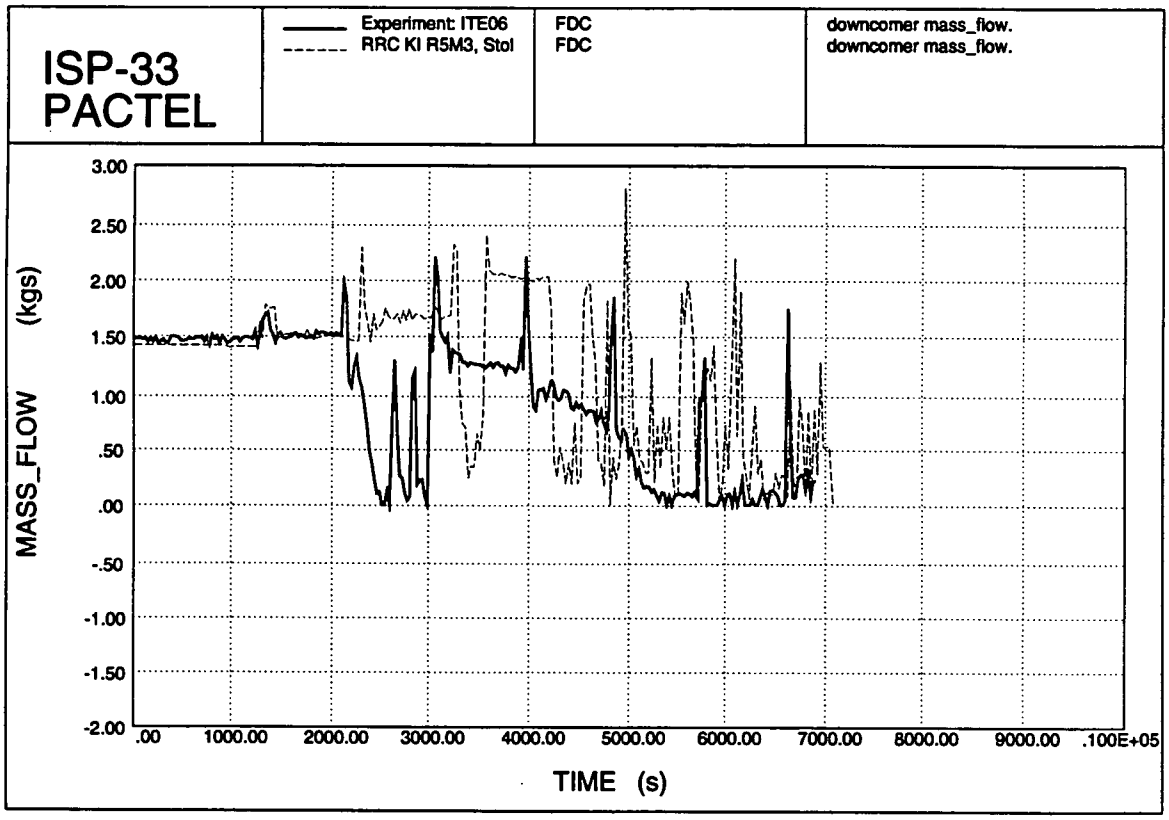

Figure 4.53. Downcomer mass flow.

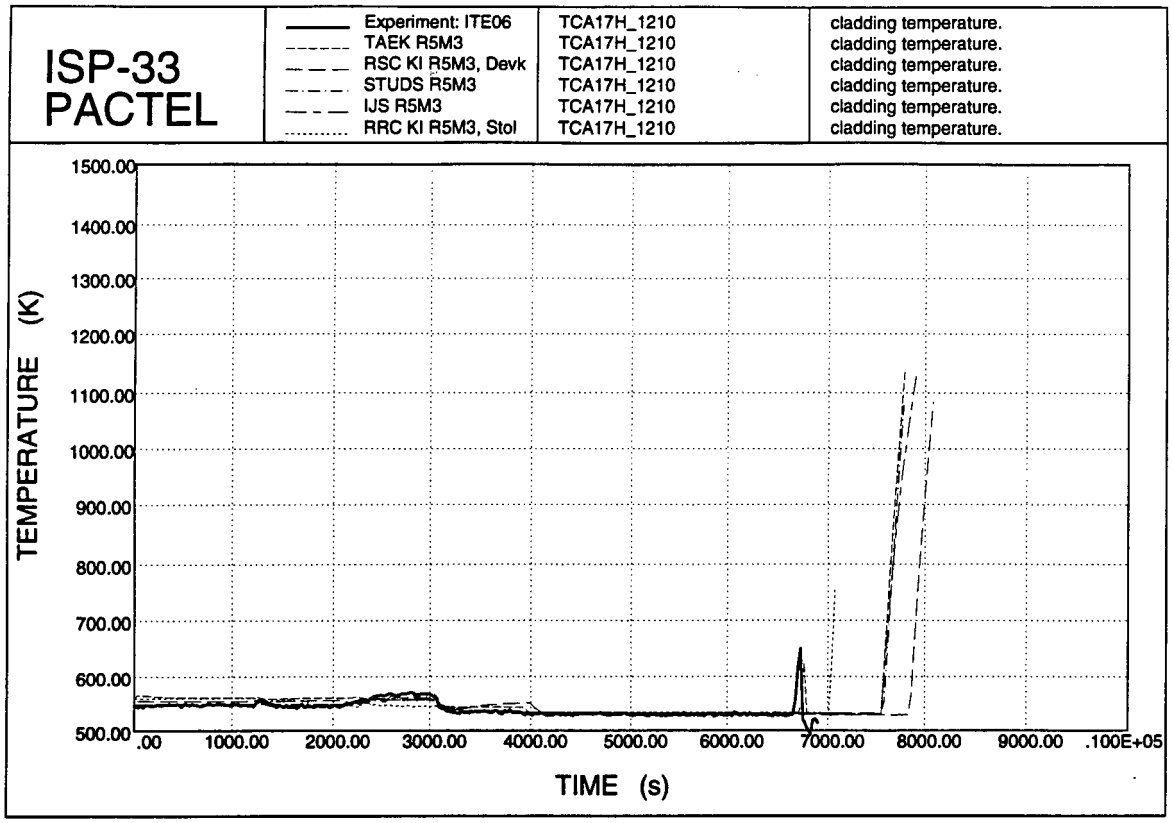

Figure 4.54. Cladding temperatures.

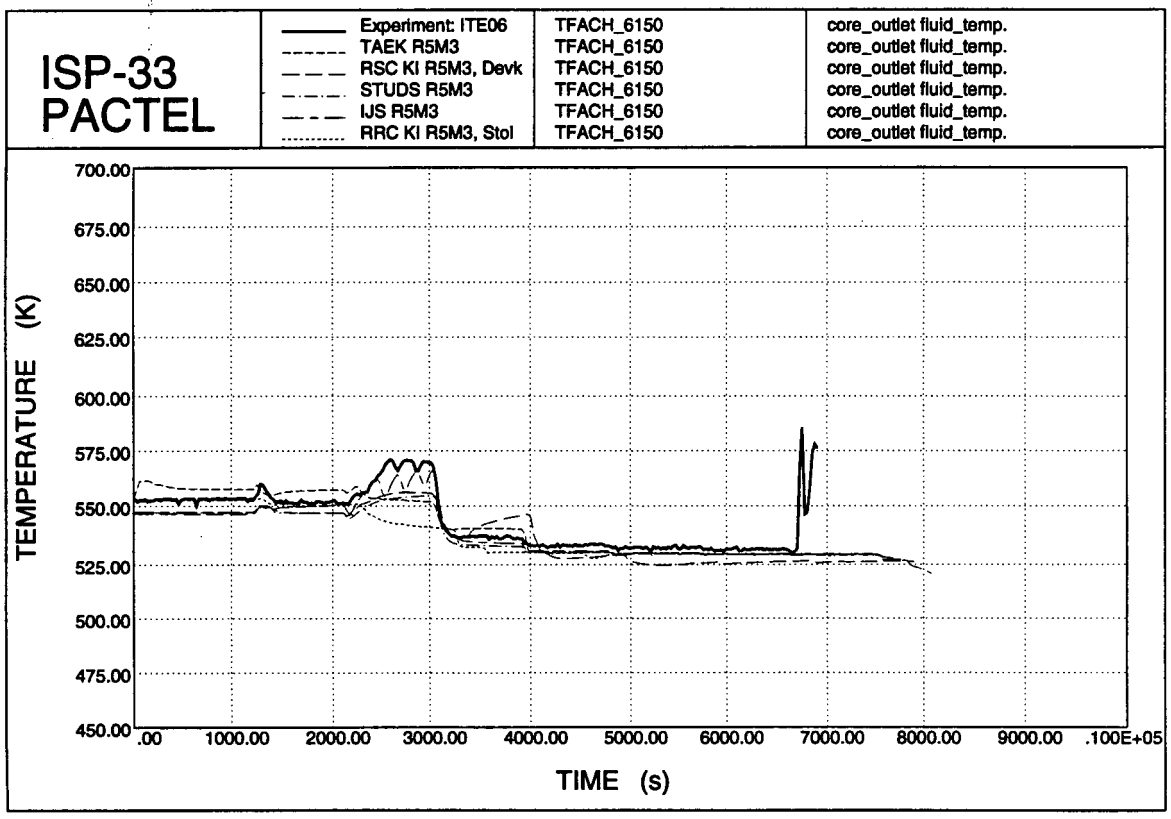

Figure 4.55. Core outlet coolant temperature.

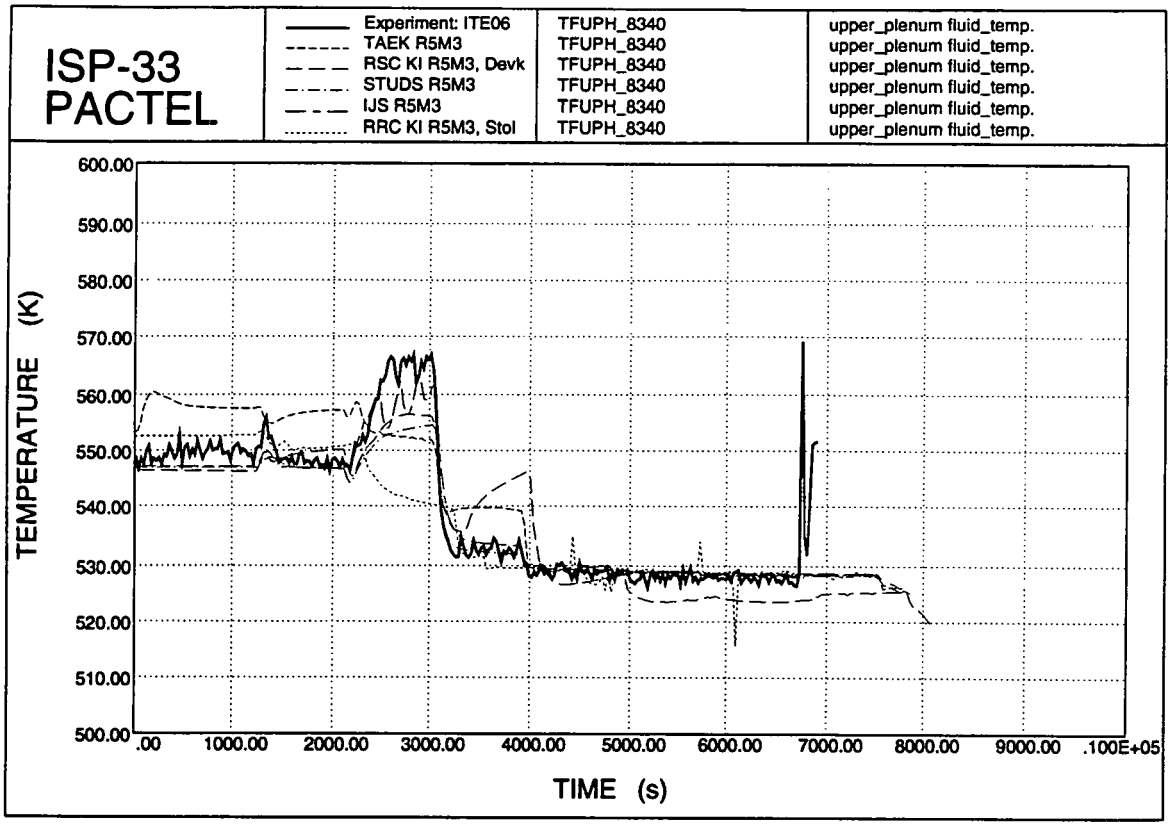

Figure 4.56. Upper plenum temperatures.

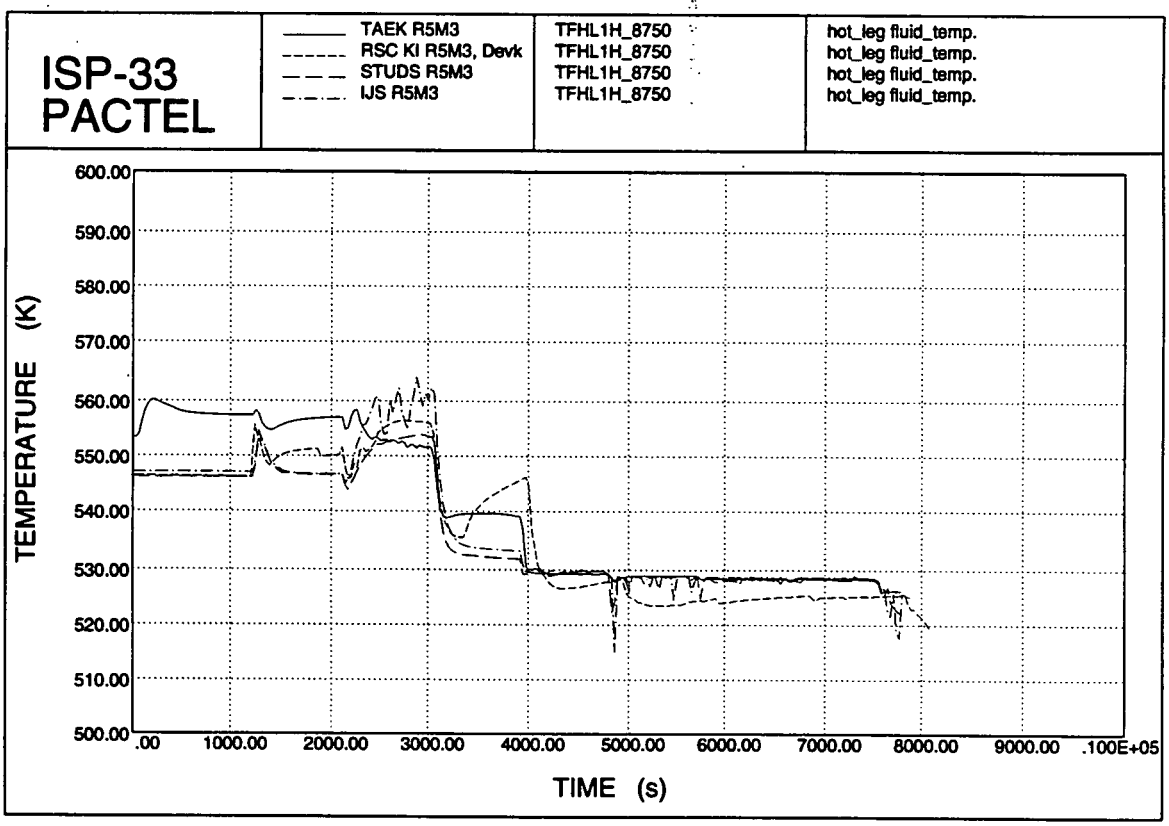

Figure 4.57. Hot leg coolant temperatures.

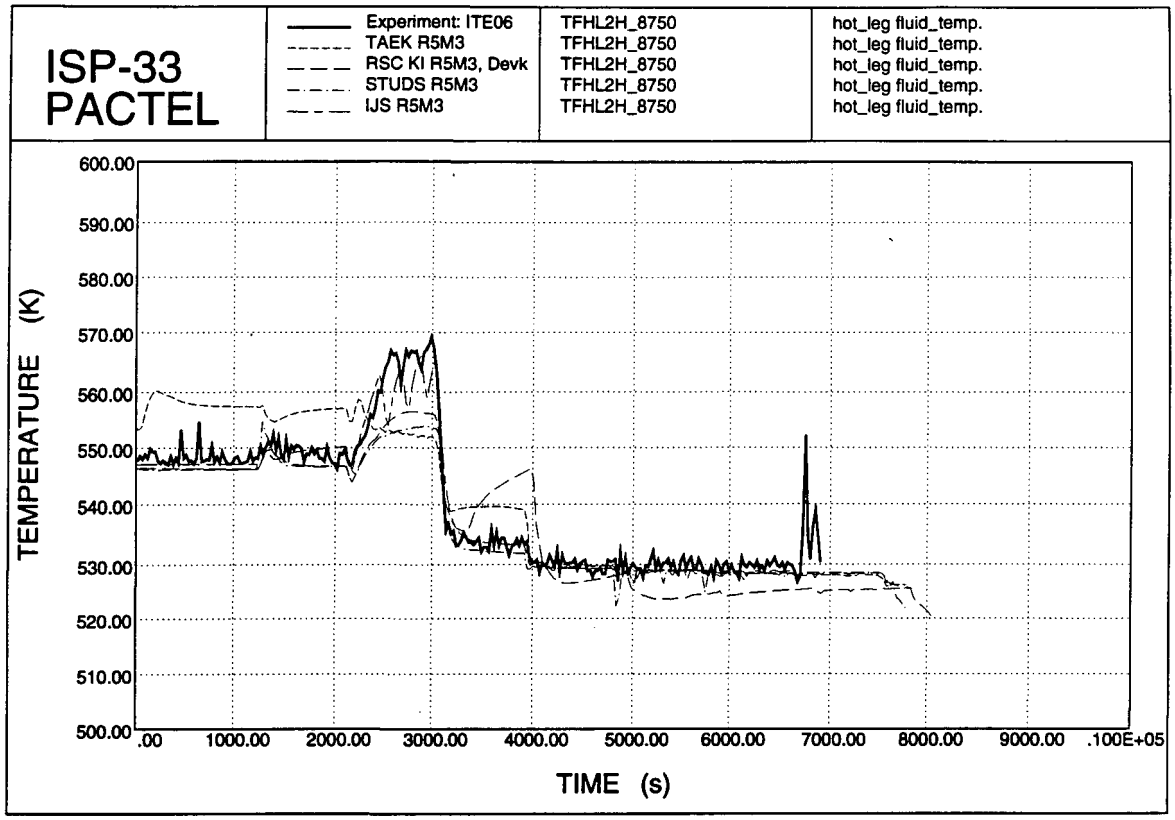

Figure 4.58. Hot leg temperatures.

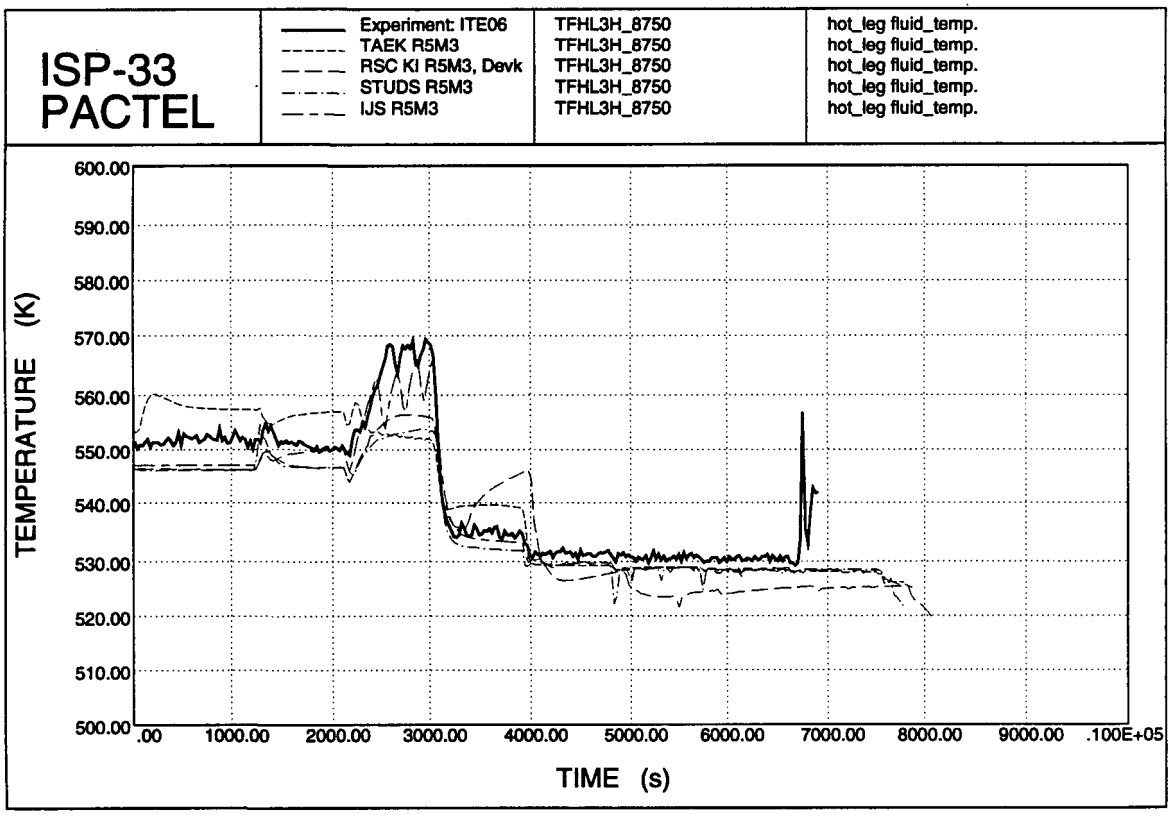

Figure 4.59. Hot leg coolant temperatures.

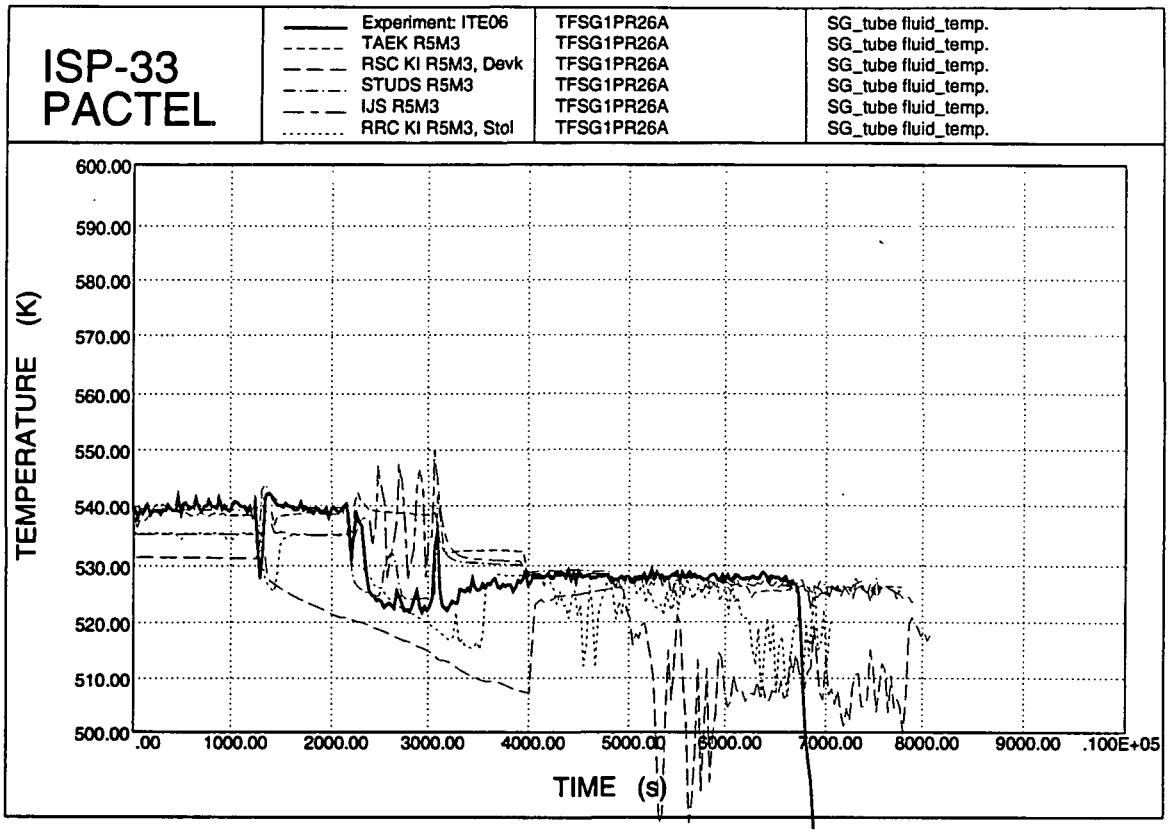

Figure 4.60. SG tube fluid temperatures.

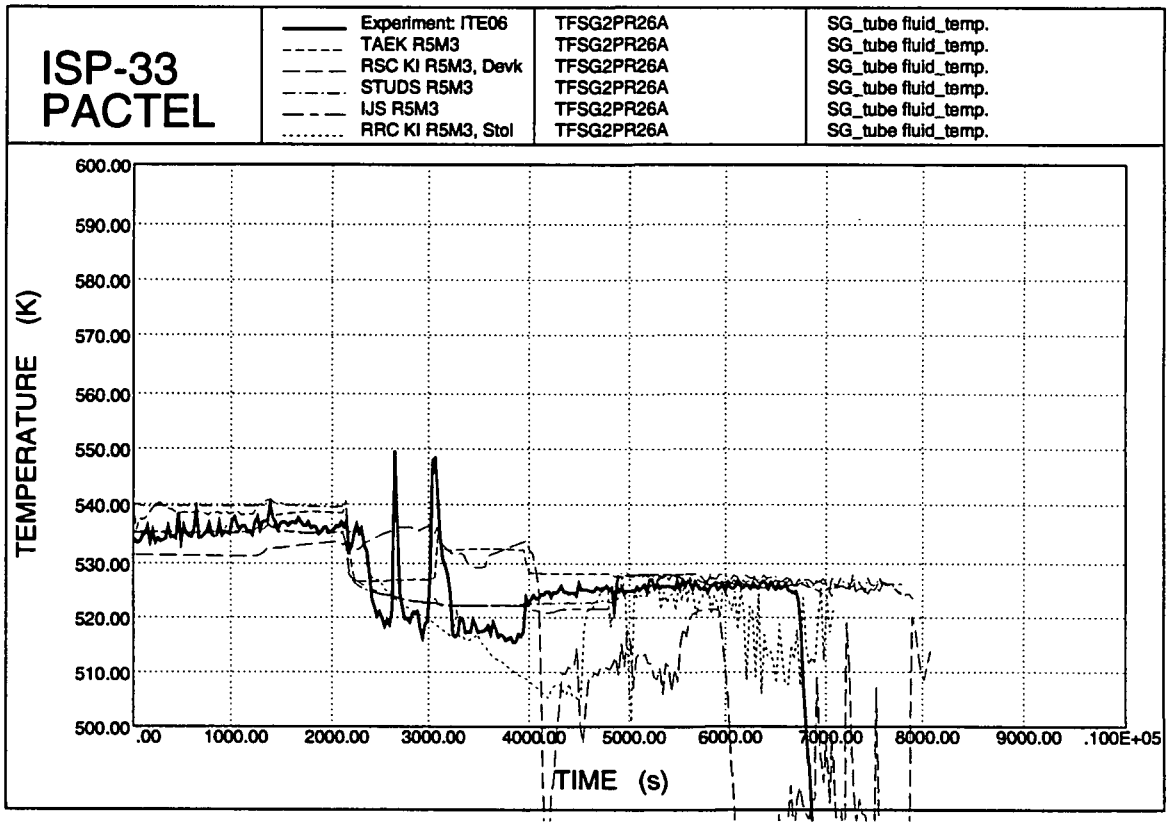

Figure 4.61. SG tube fluid temperatures.

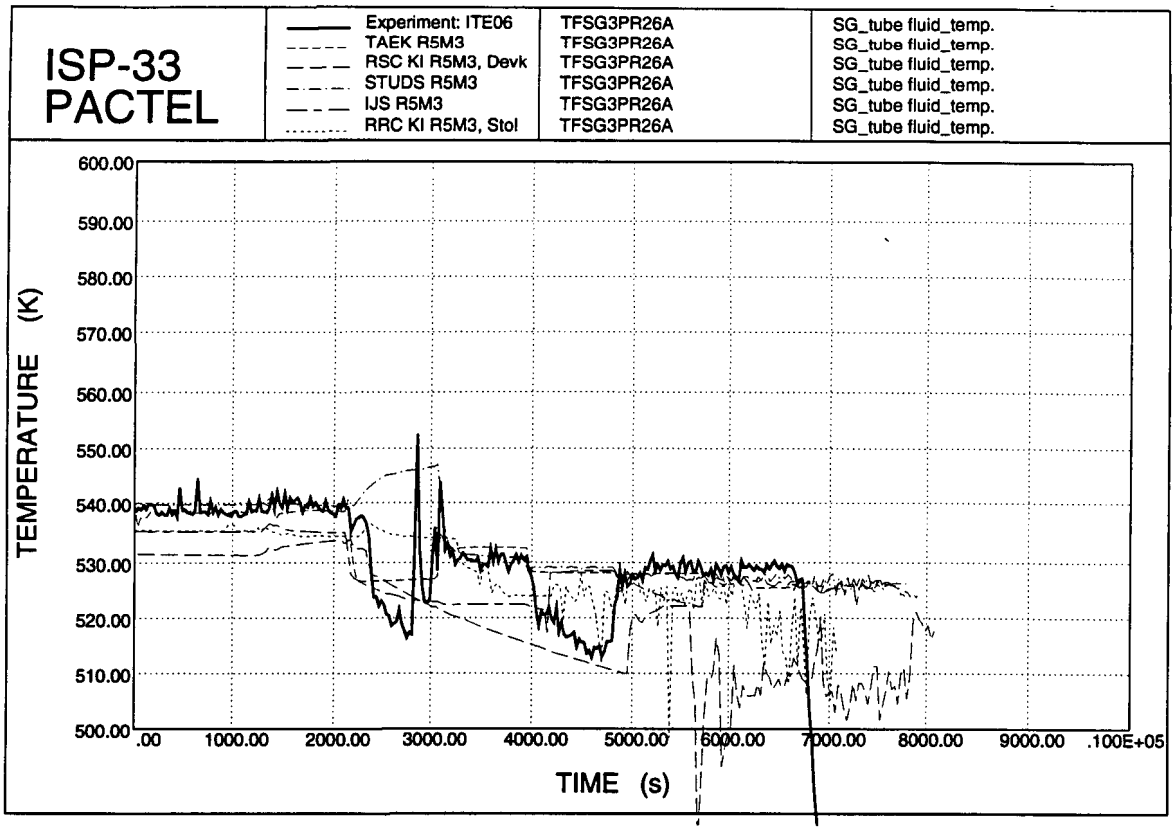

Figure 4.62. SG tube fluid temperatures.

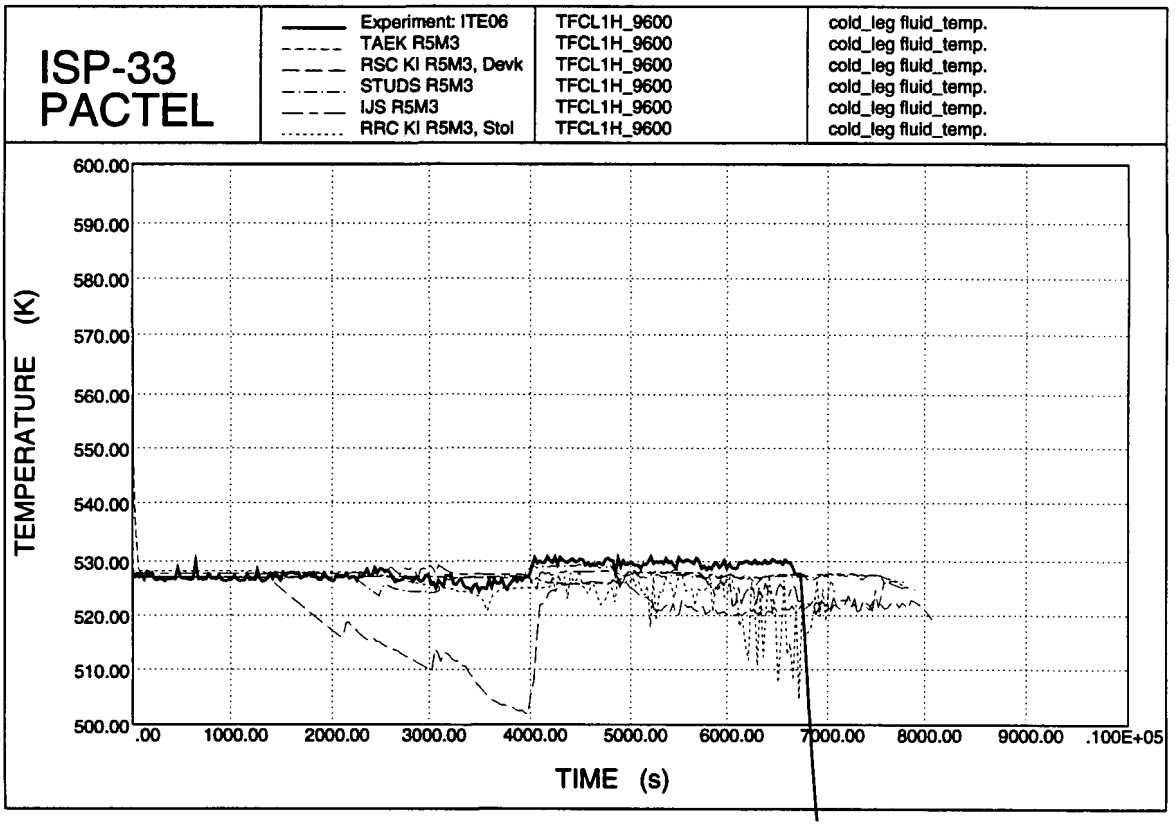

Figure 4.63. Cold leg temperatures.

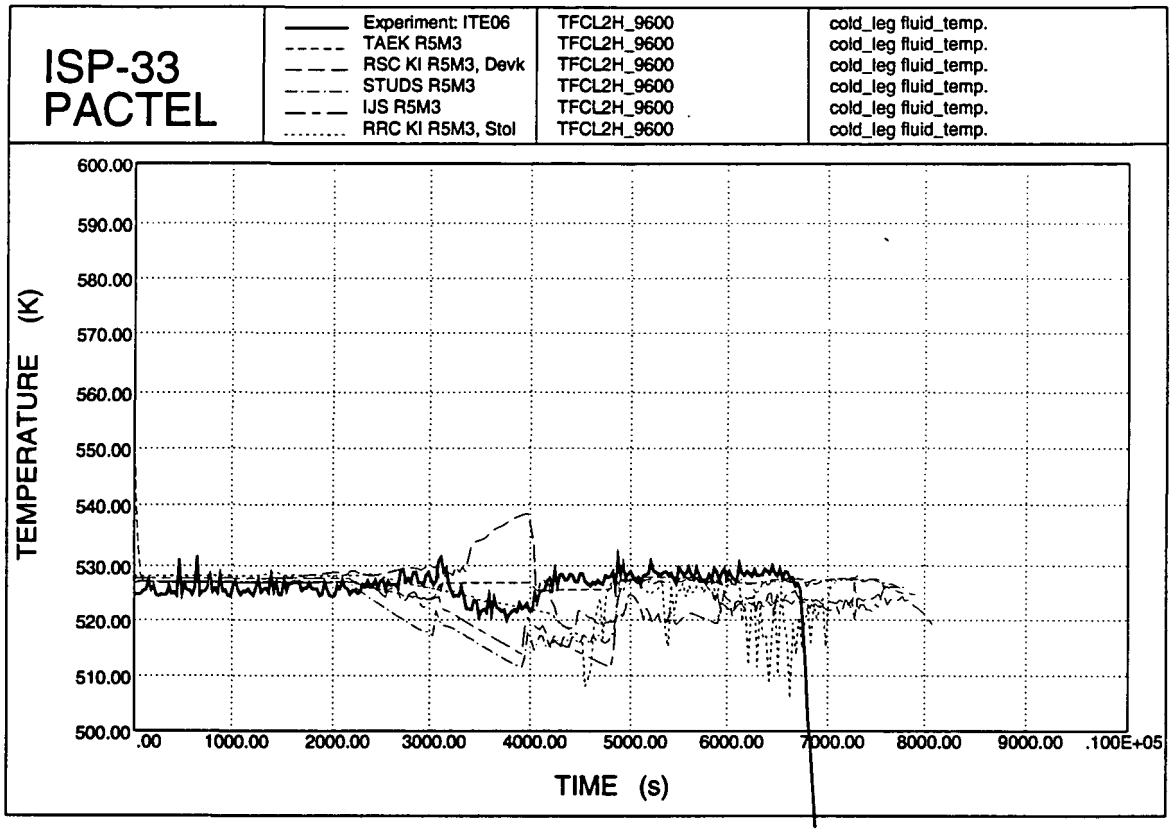

Figure 4.64. Cold leg coolant temperatures.

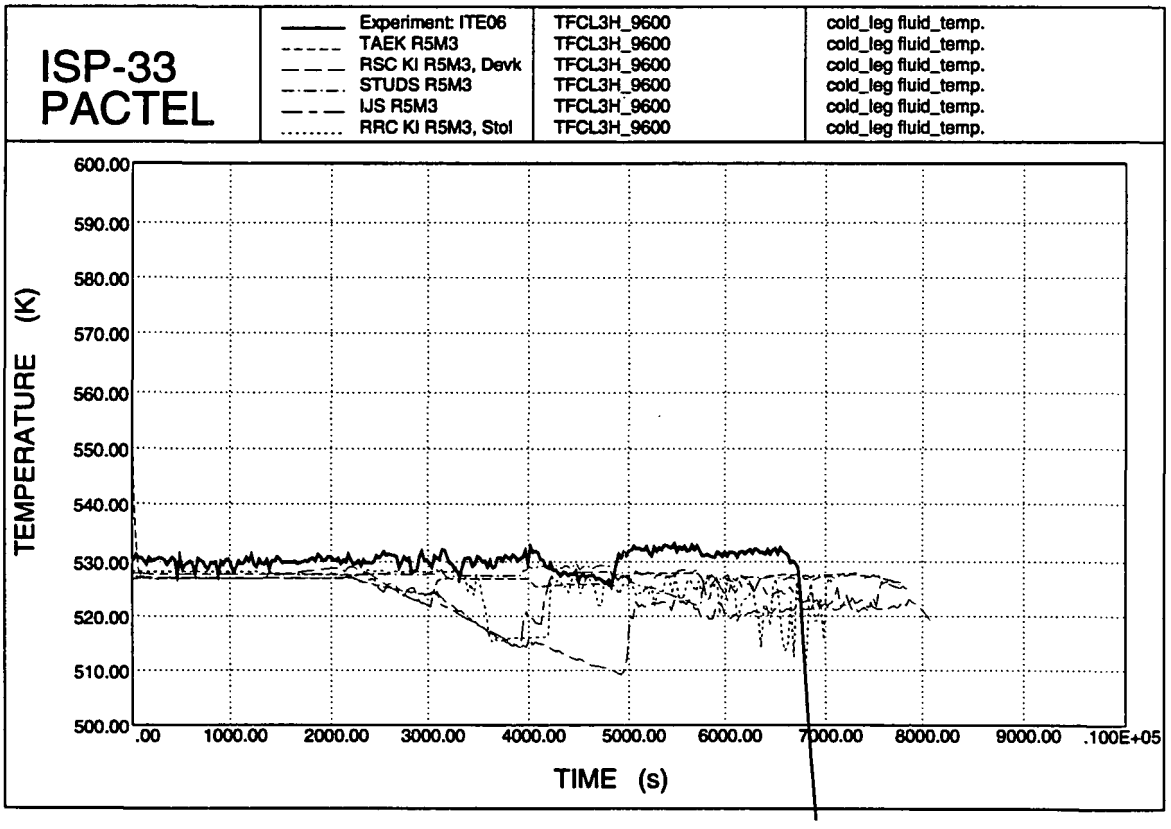

Figure 4.65. Cold leg temperatures.

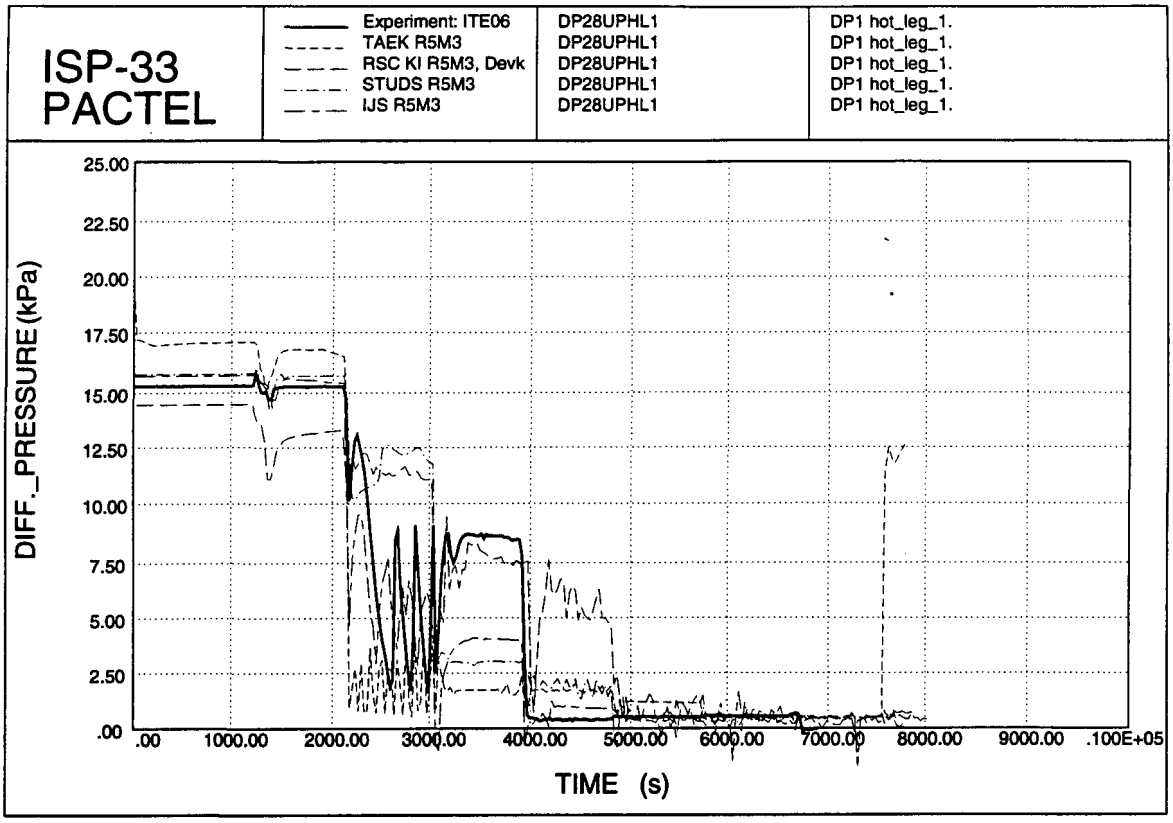

Figure 4.66. Hot leg 1 DP 1.

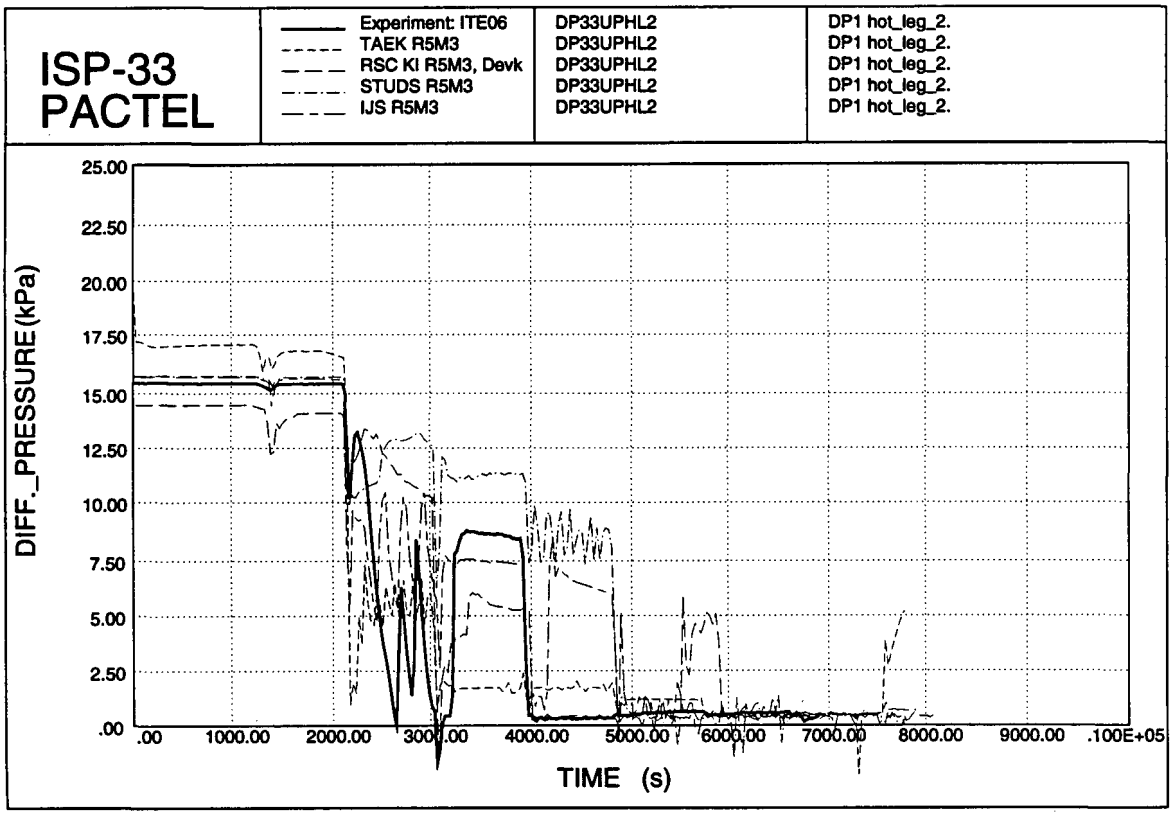

Figure 4.67. Hot leg 2 DP 1.

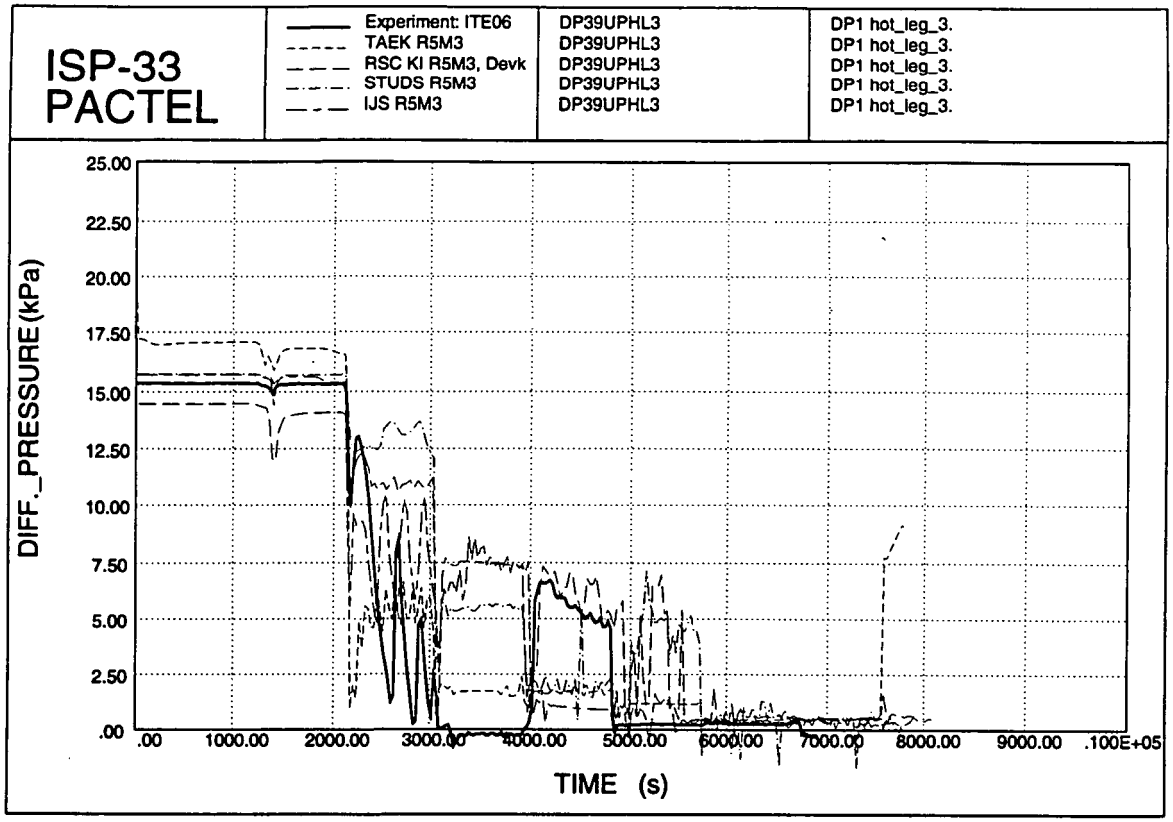

Figure 4.68. Hot leg 3 DP 1.

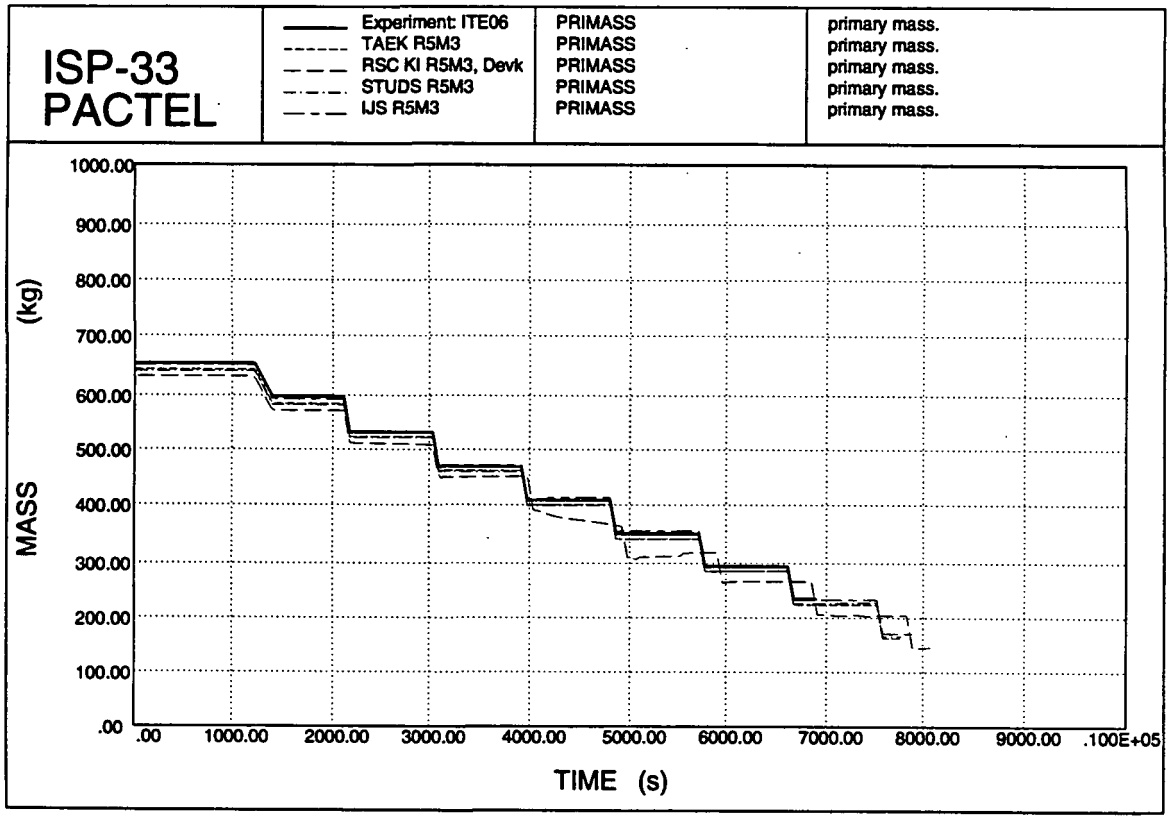

Figure 4.69. Primary mass inventory.

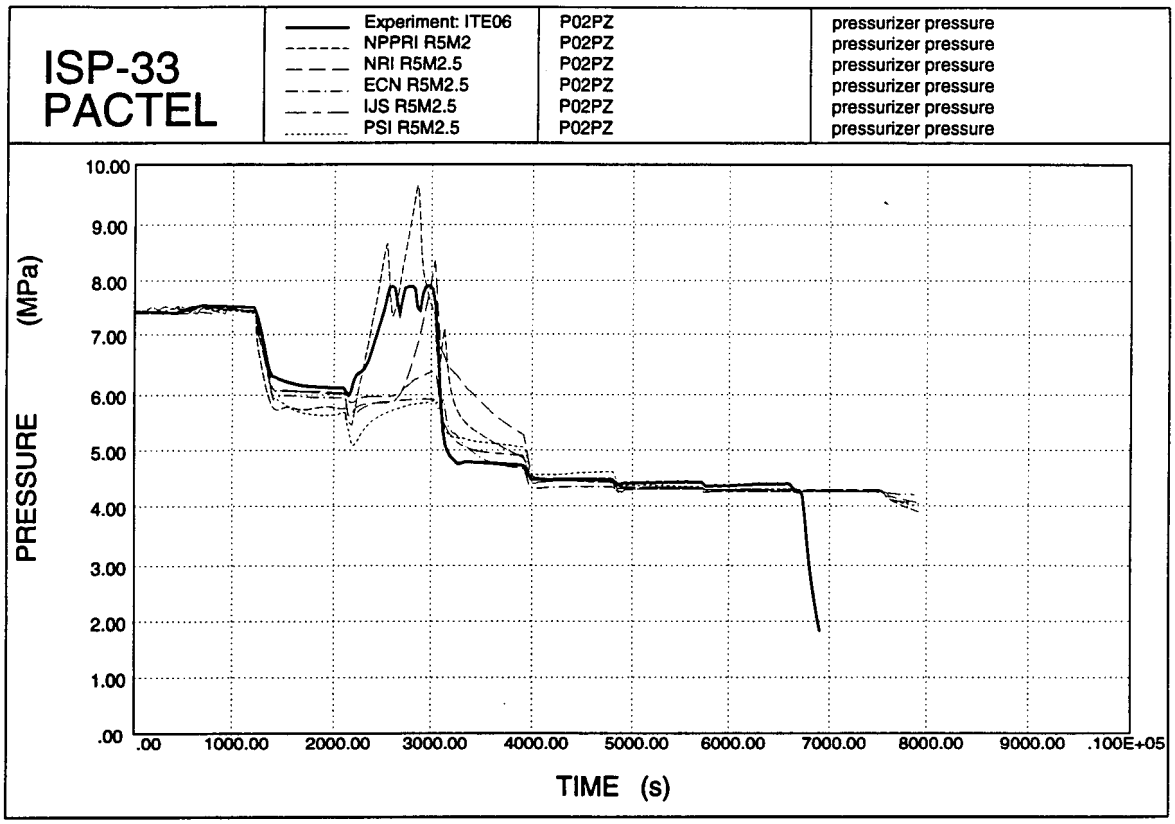

Figure 4.70. Pressurizer pressures.

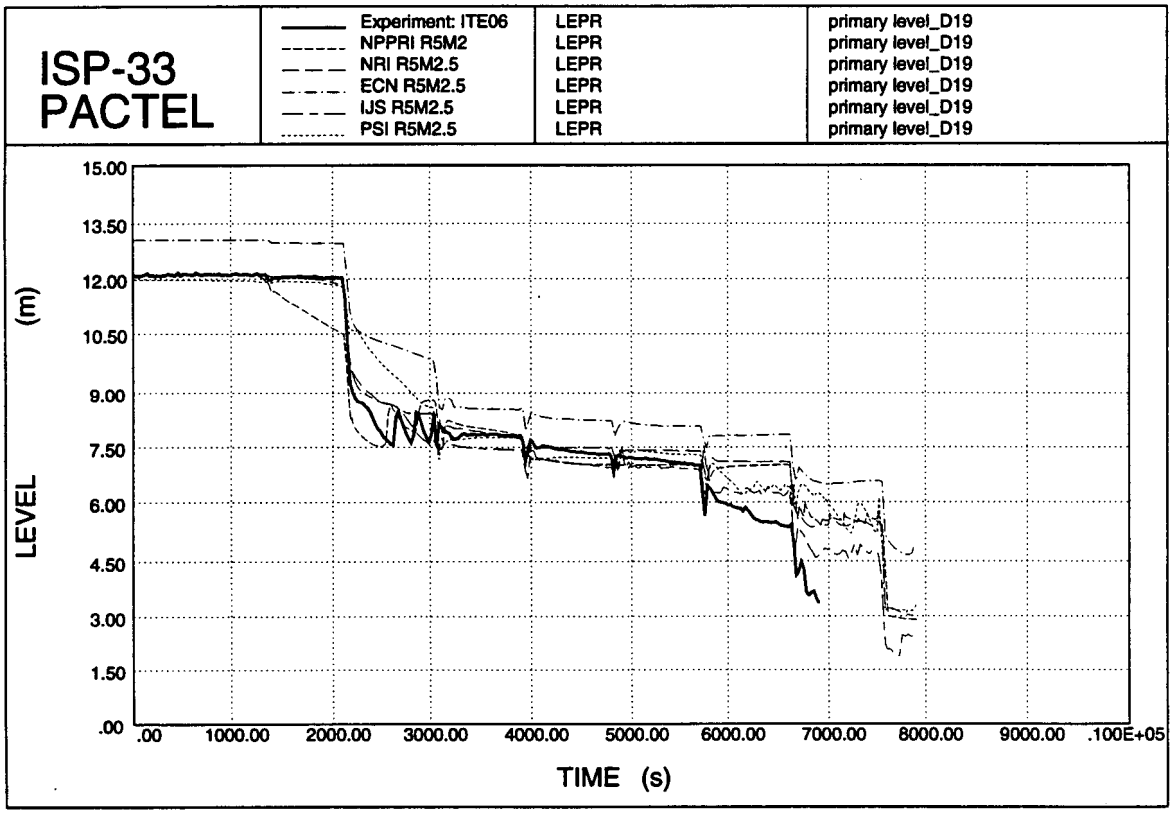

Figure 4.71. Primary levels.

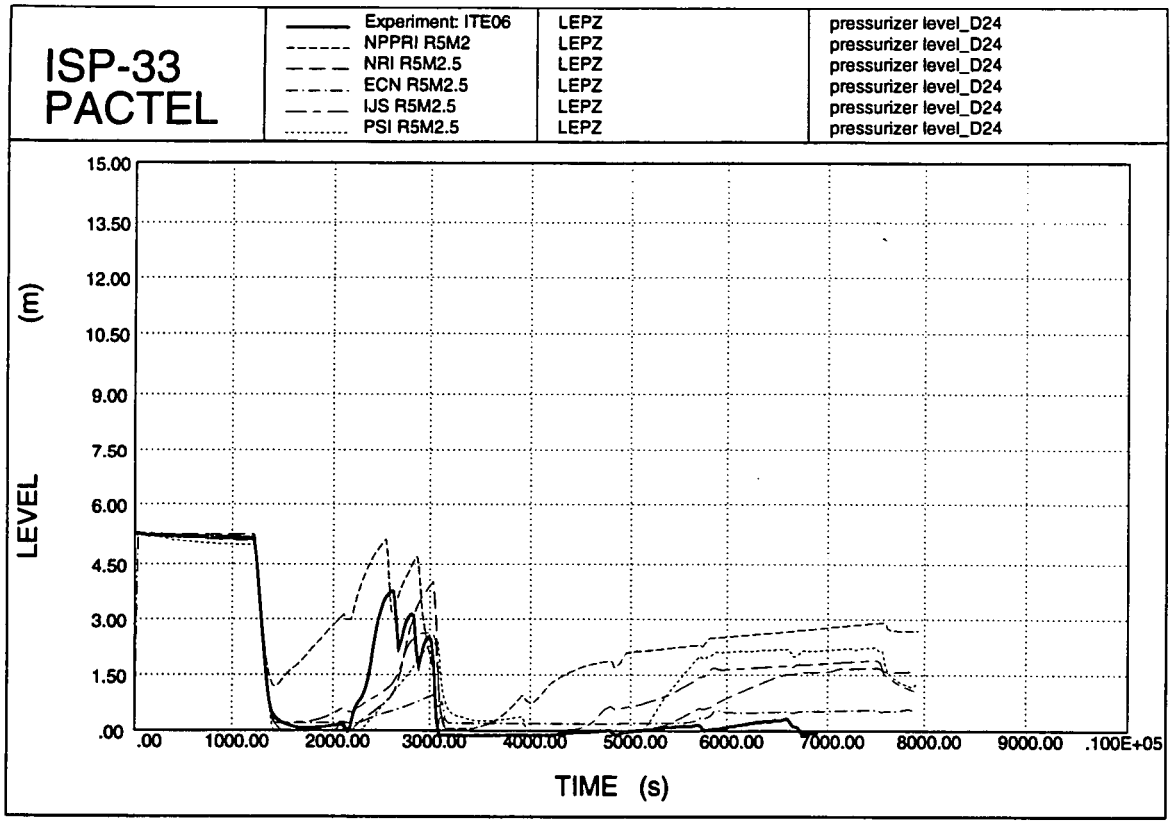

Figure 4.72. Pressurizer levels.

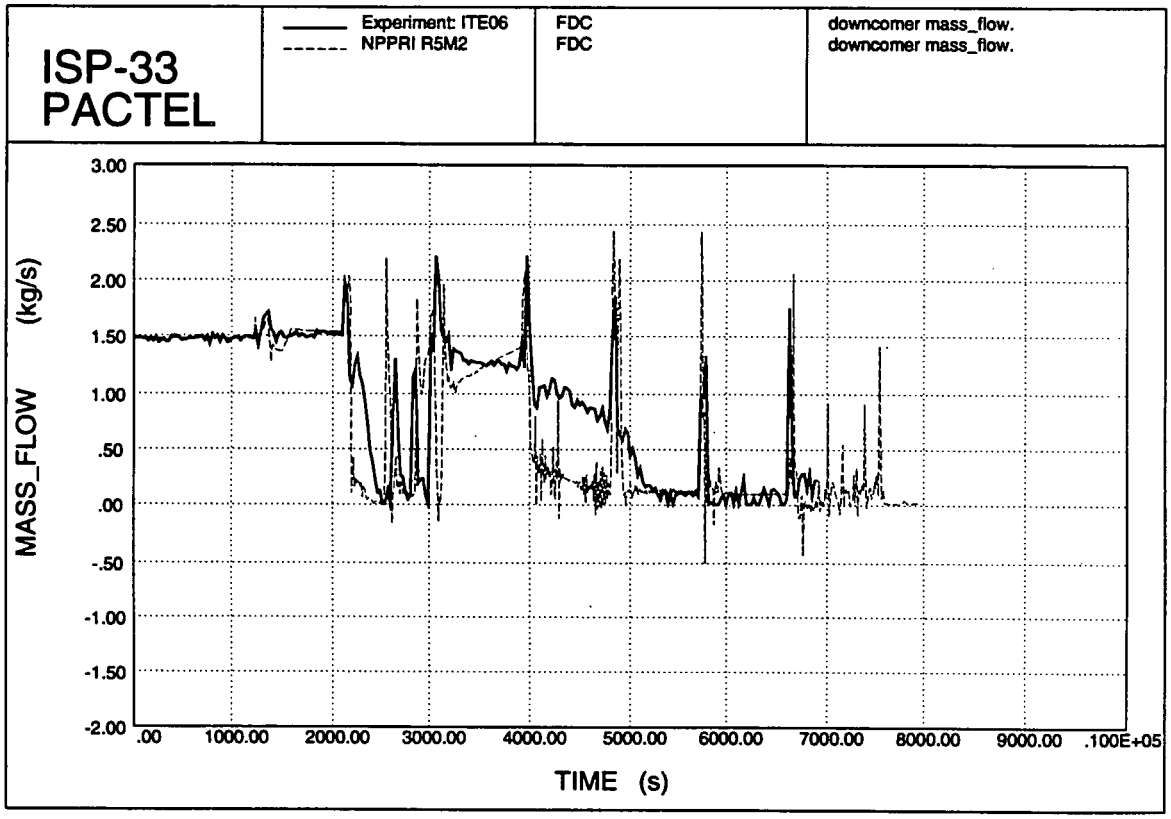

Figure 4.73. Downcomer mass flow.

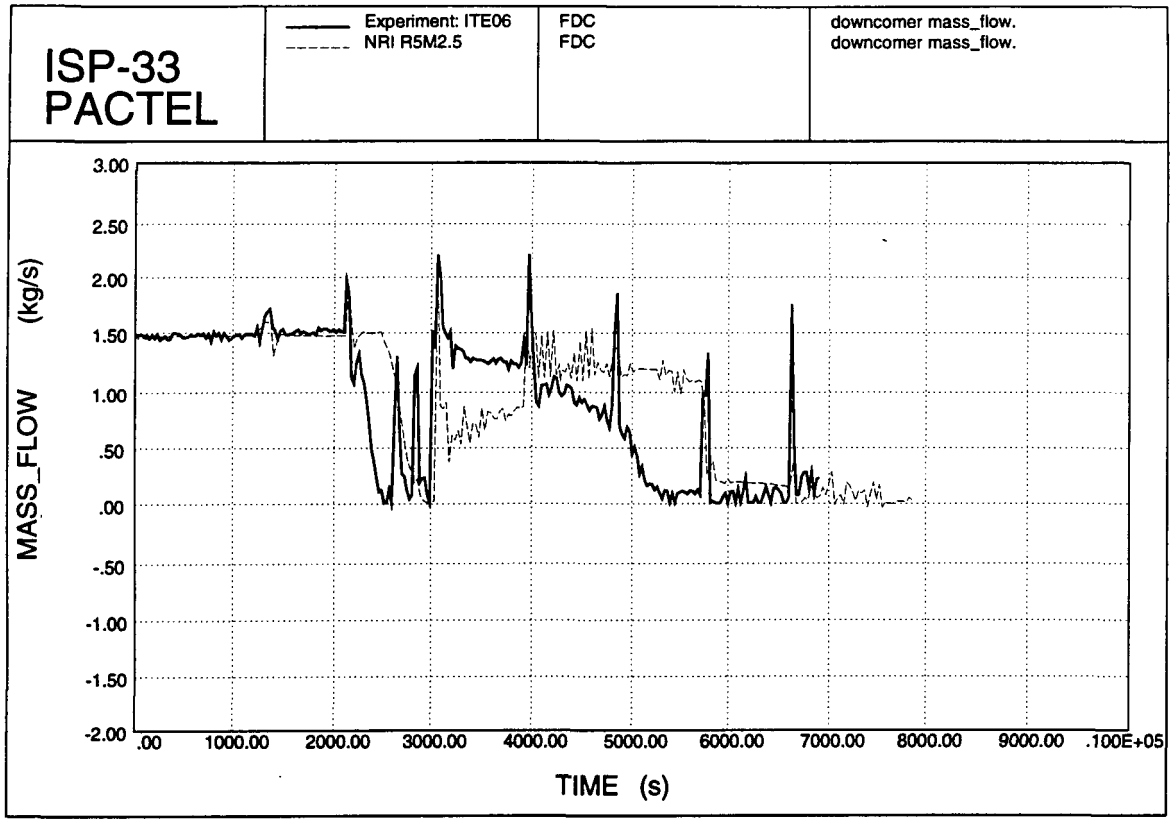

Figure 4.74. Downcomer mass flow.

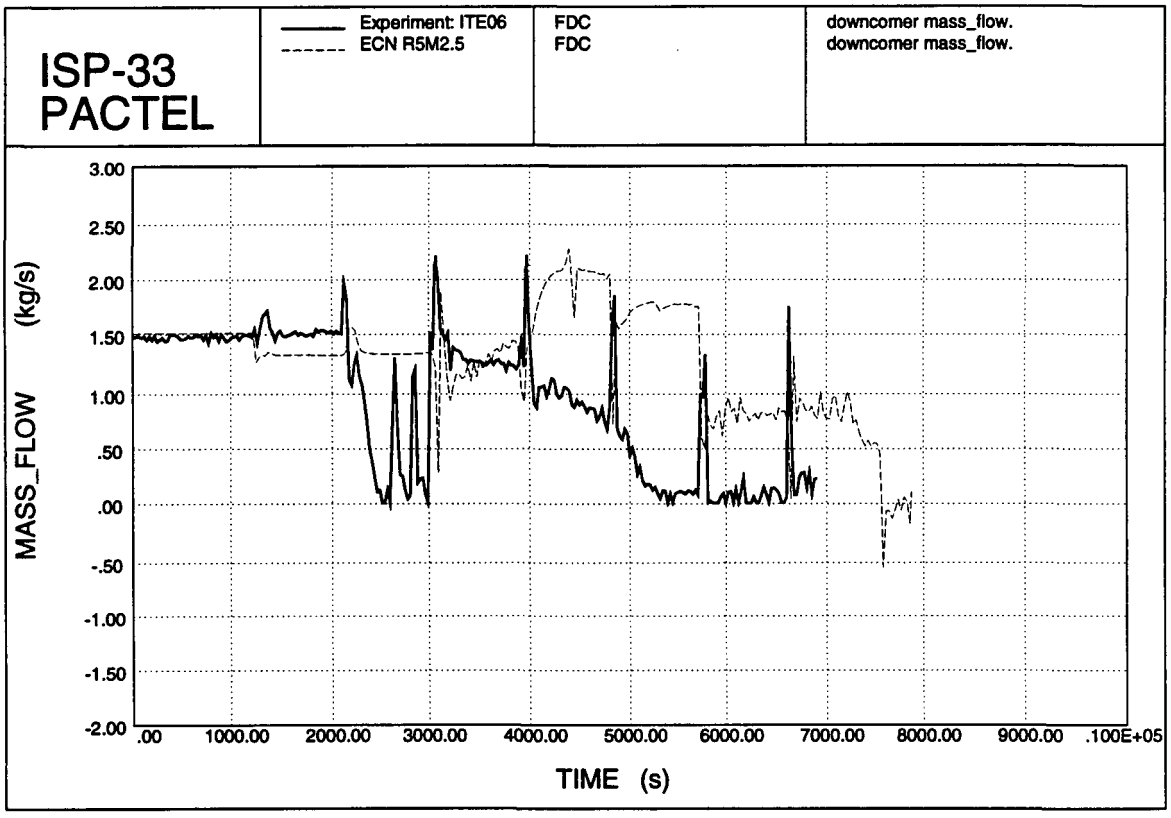

Figure 4.75. Downcomer mass flow.

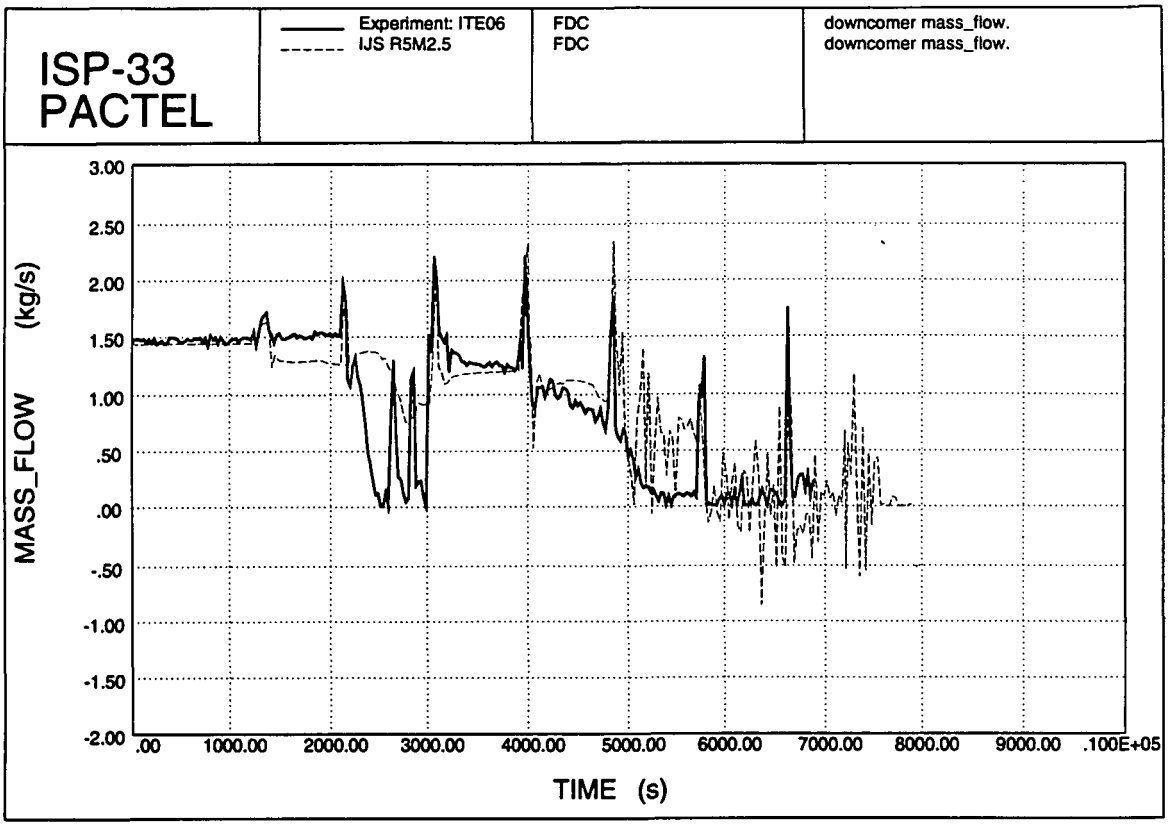

Figure 4.76. Downcomer mass flow.

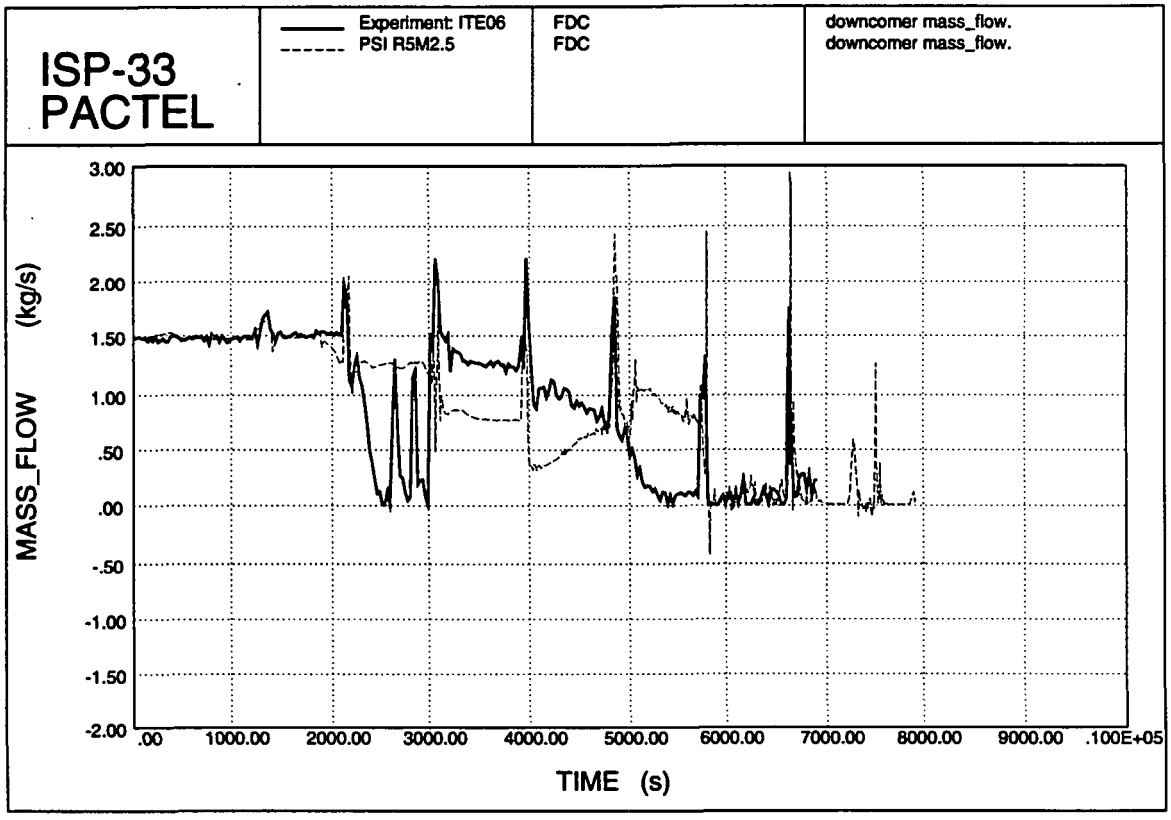

Figure 4.77. Downcomer mass flow.

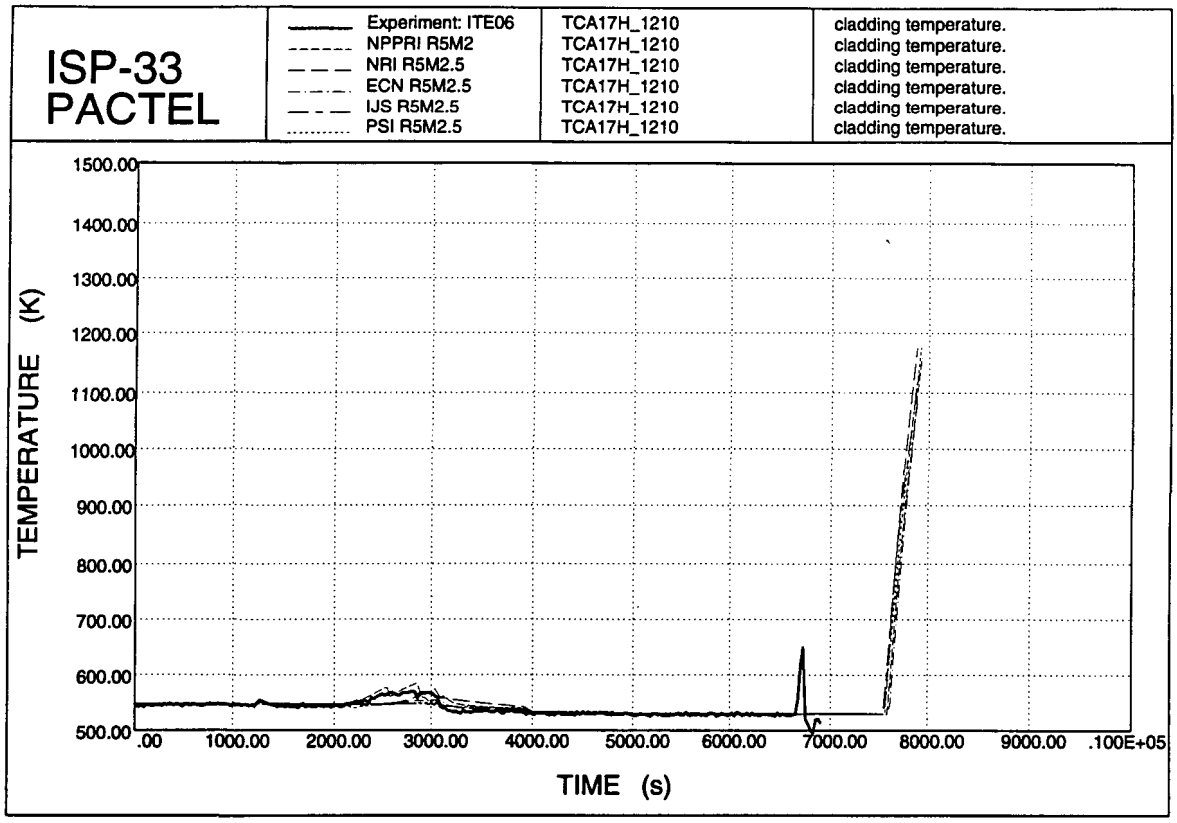

Figure 4.78. Cladding temperatures.

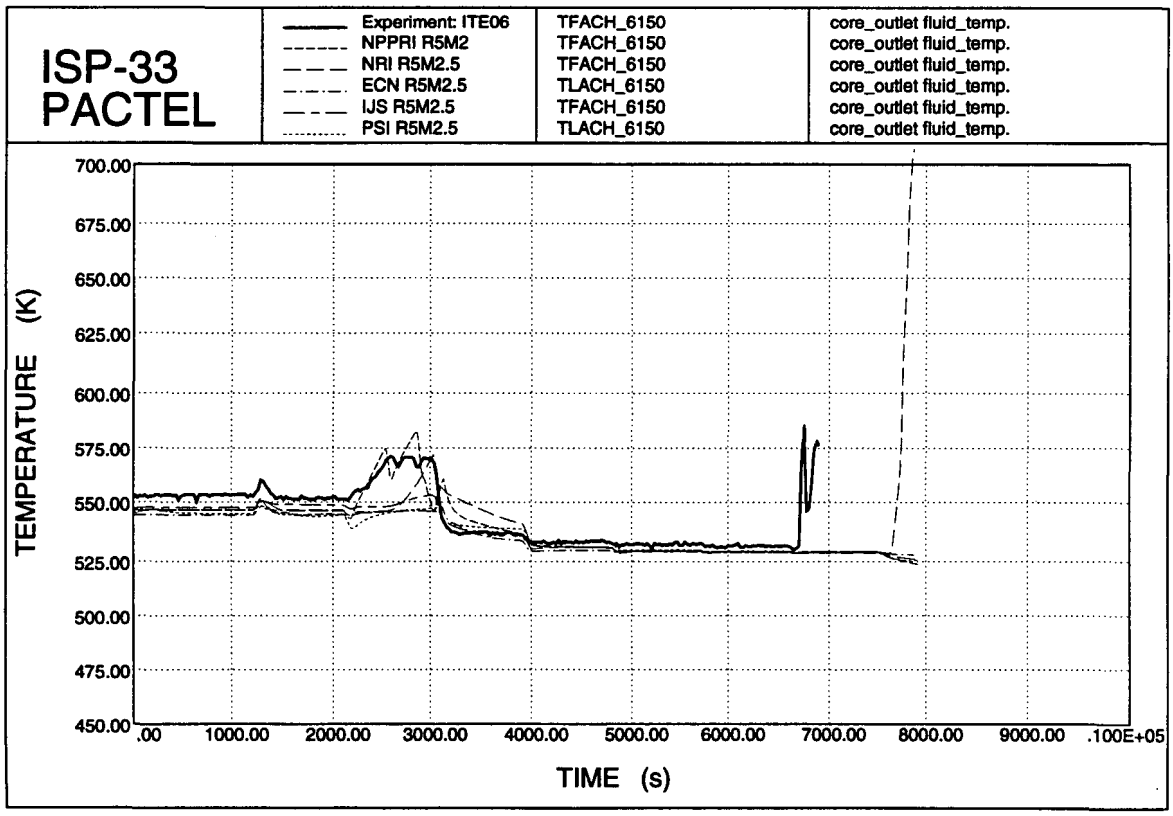

Figure 4.79. Core outlet coolant temperature.

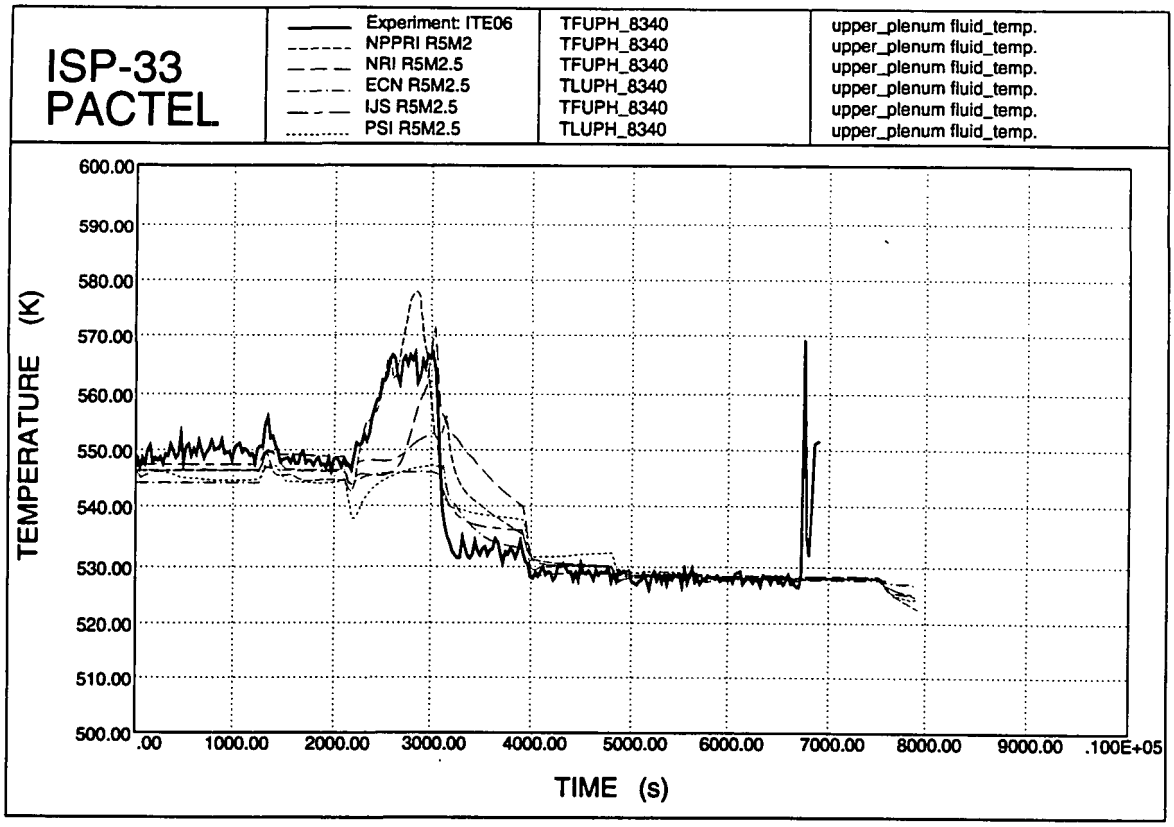

Figure 4.80. Upper plenum temperatures.

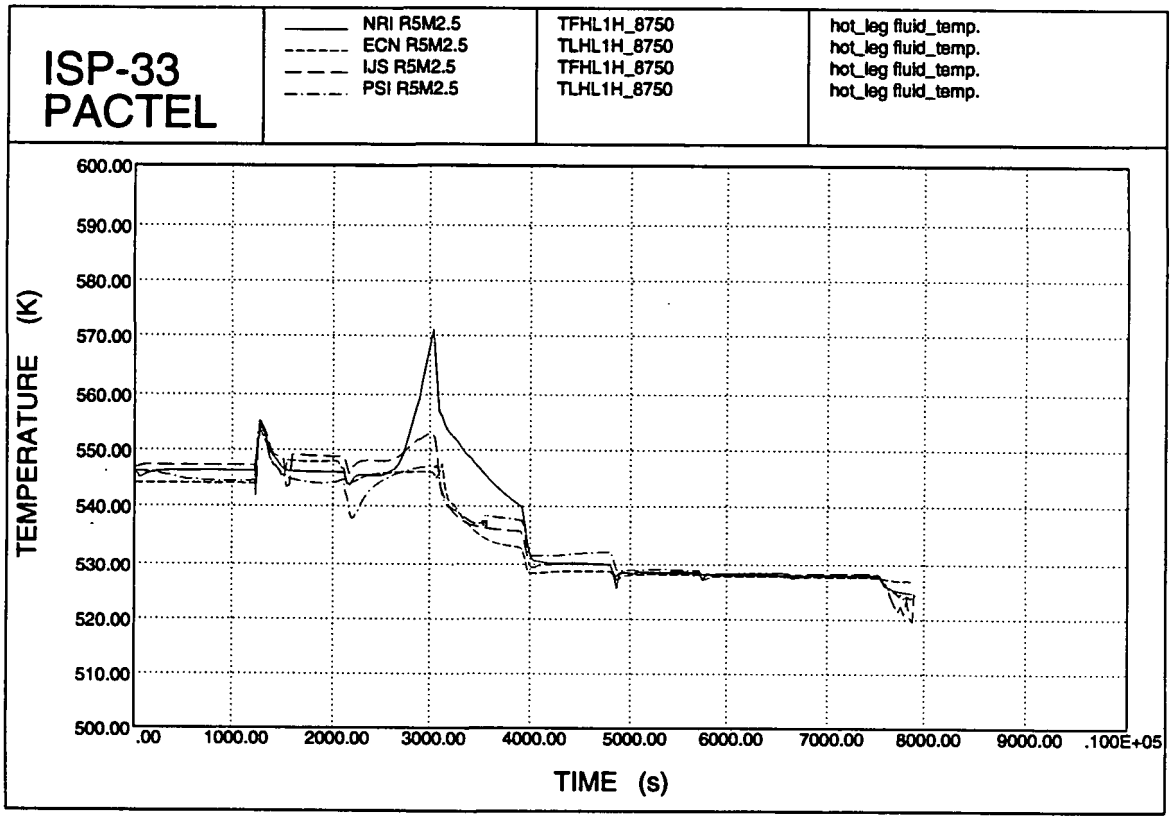

Figure 4.81. Hot leg coolant temperatures.

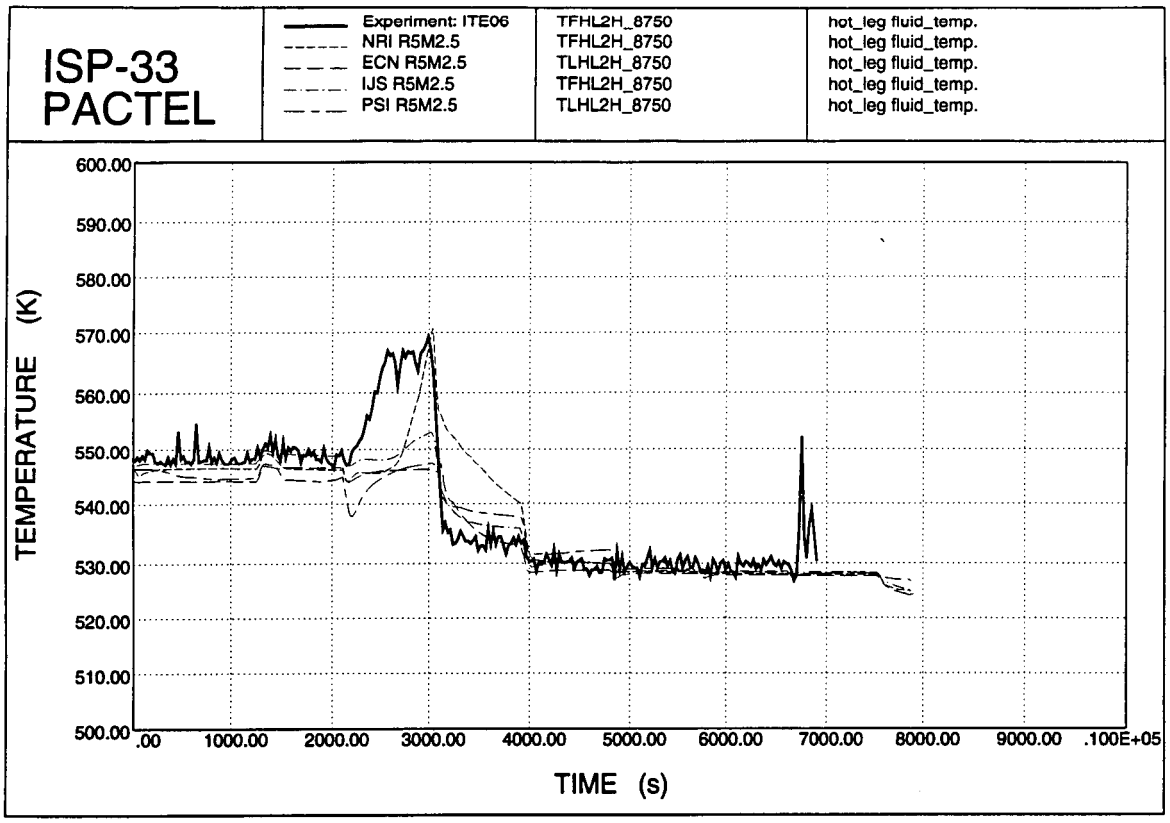

Figure 4.82. Hot leg temperatures.

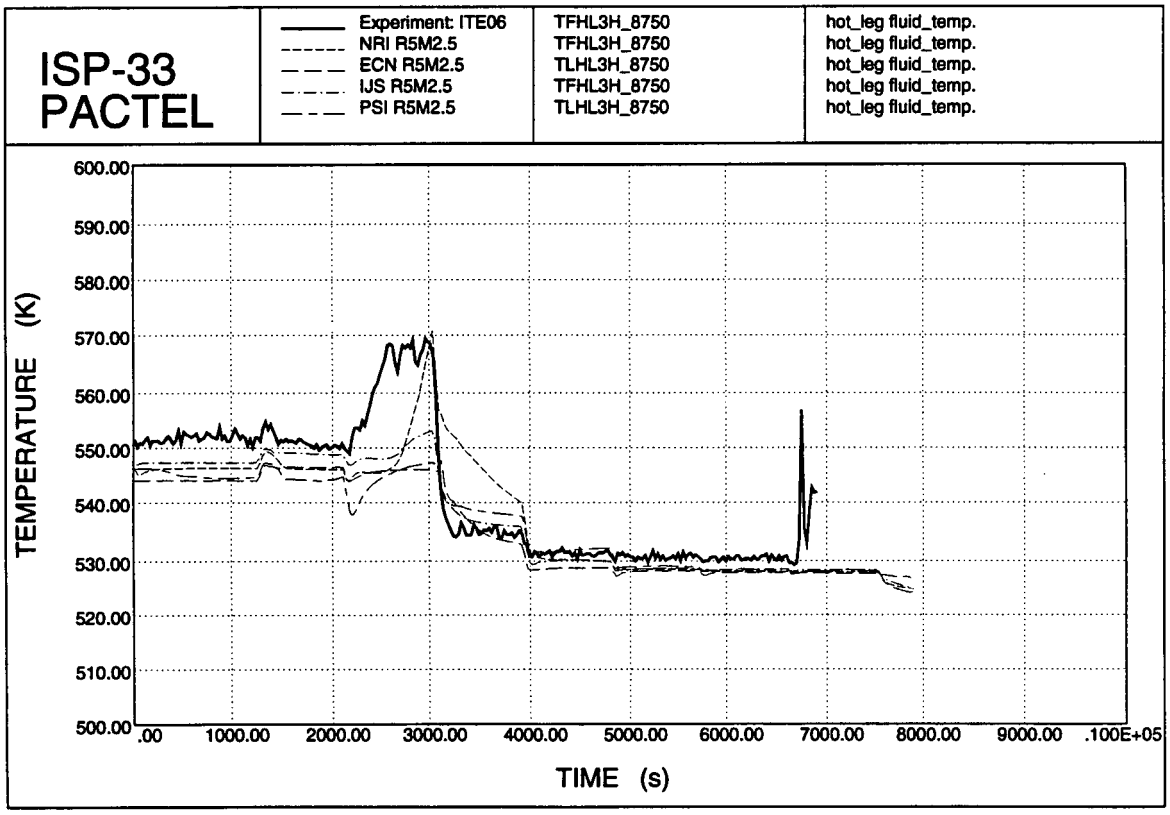

Figure 4.83. Hot leg coolant temperatures.

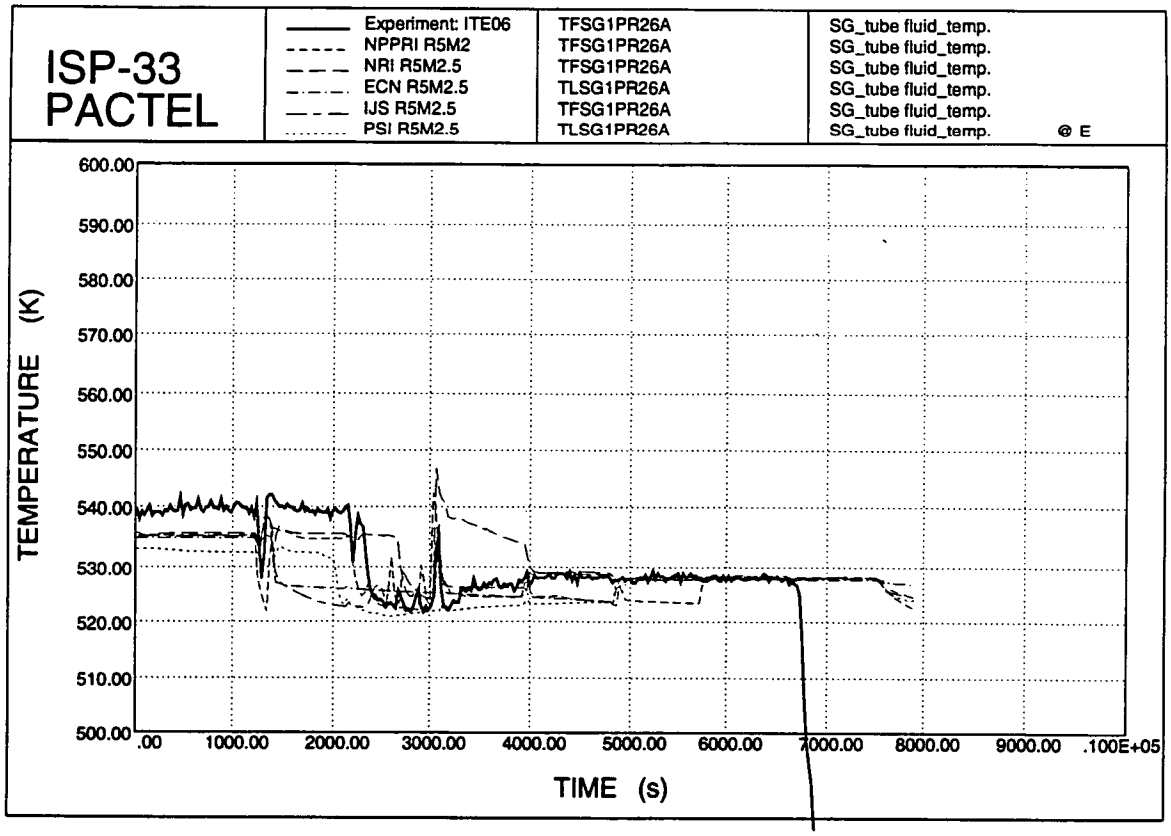

Figure 4.84. SG tube fluid temperatures.

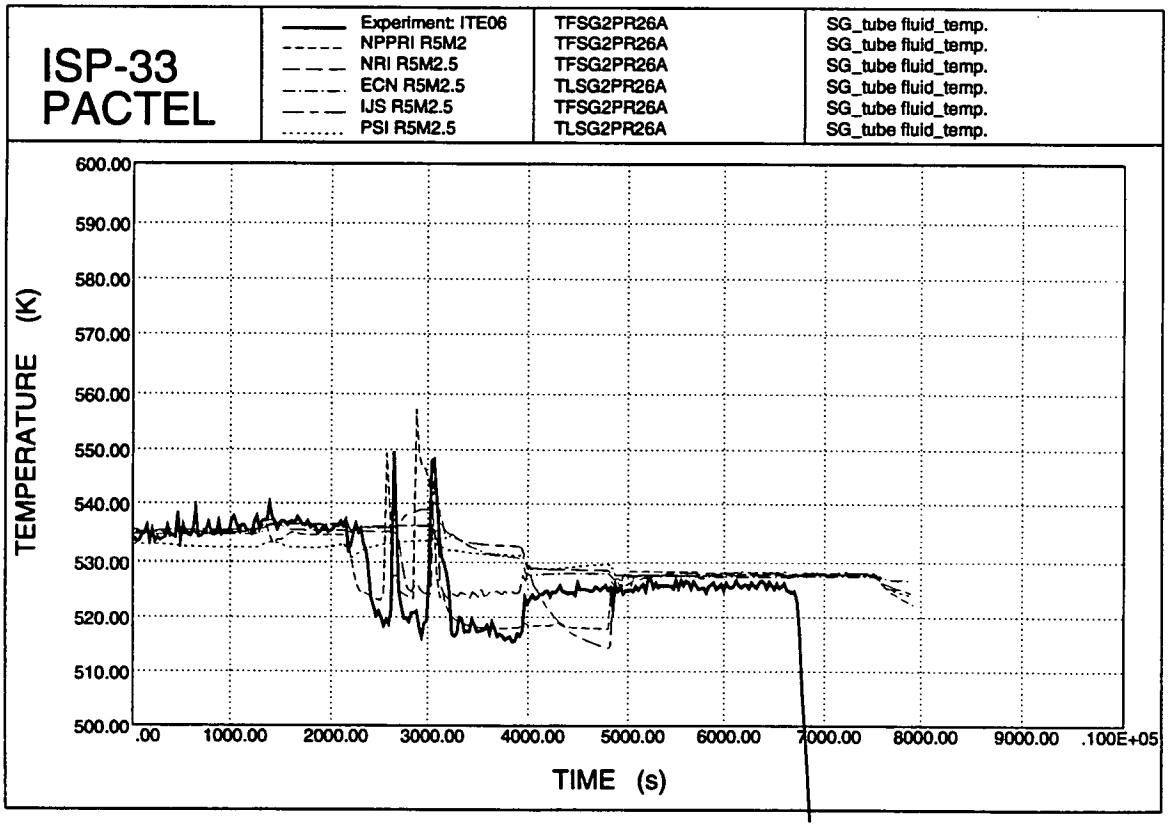

Figure 4.85. SG tube fluid temperatures.

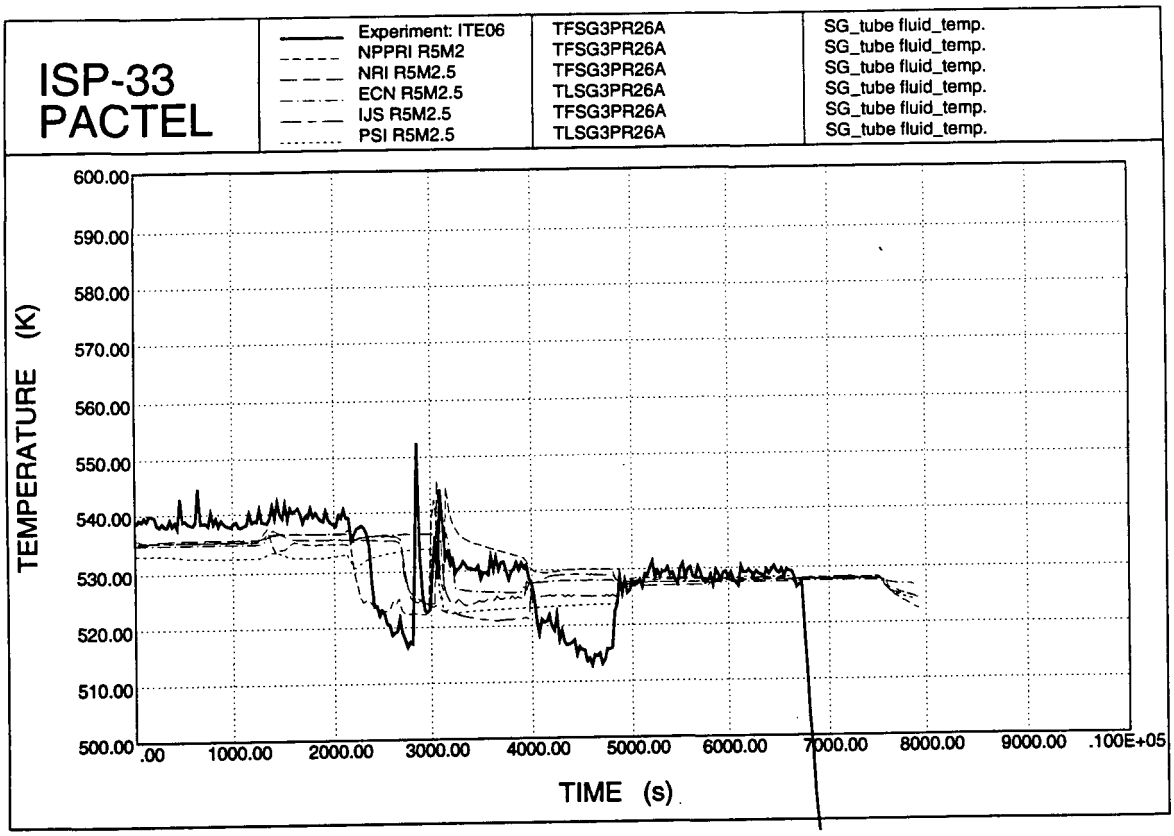

Figure 4.86. SG tube fluid temperatures.

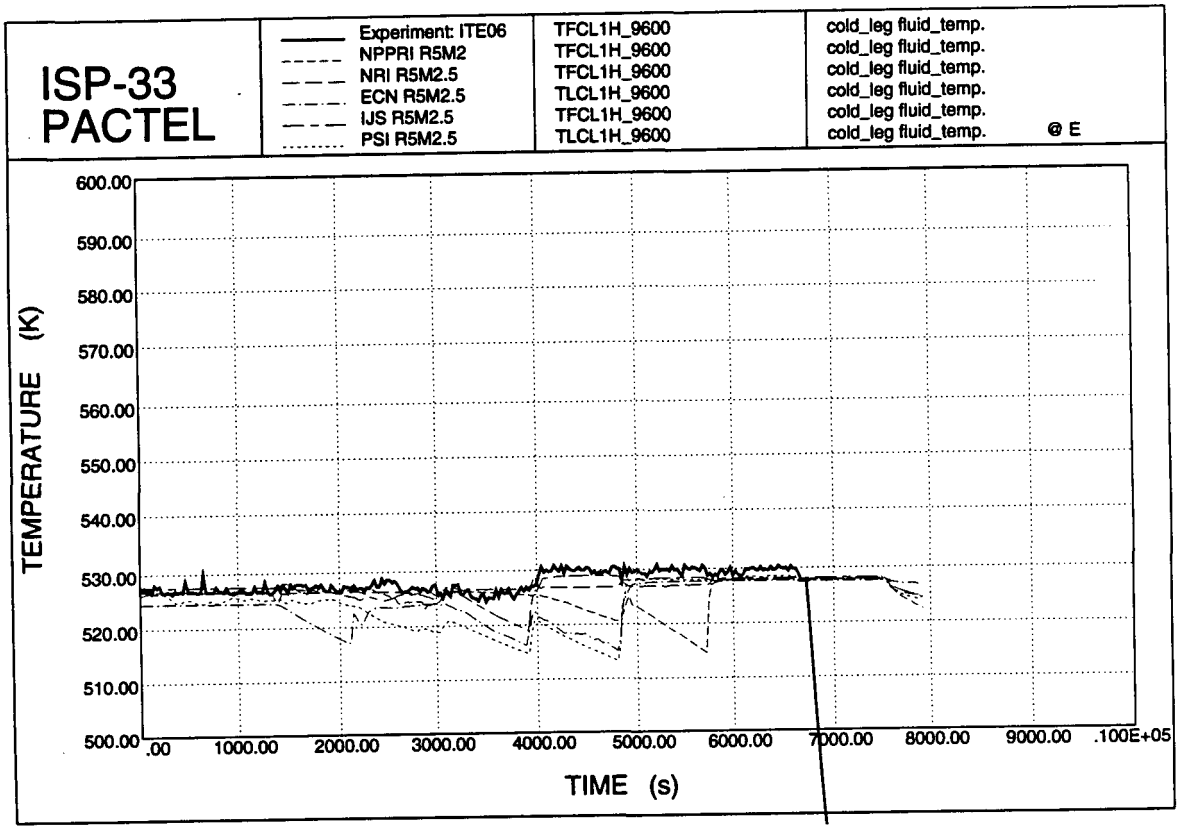

Figure 4.87. Cold leg temperatures.

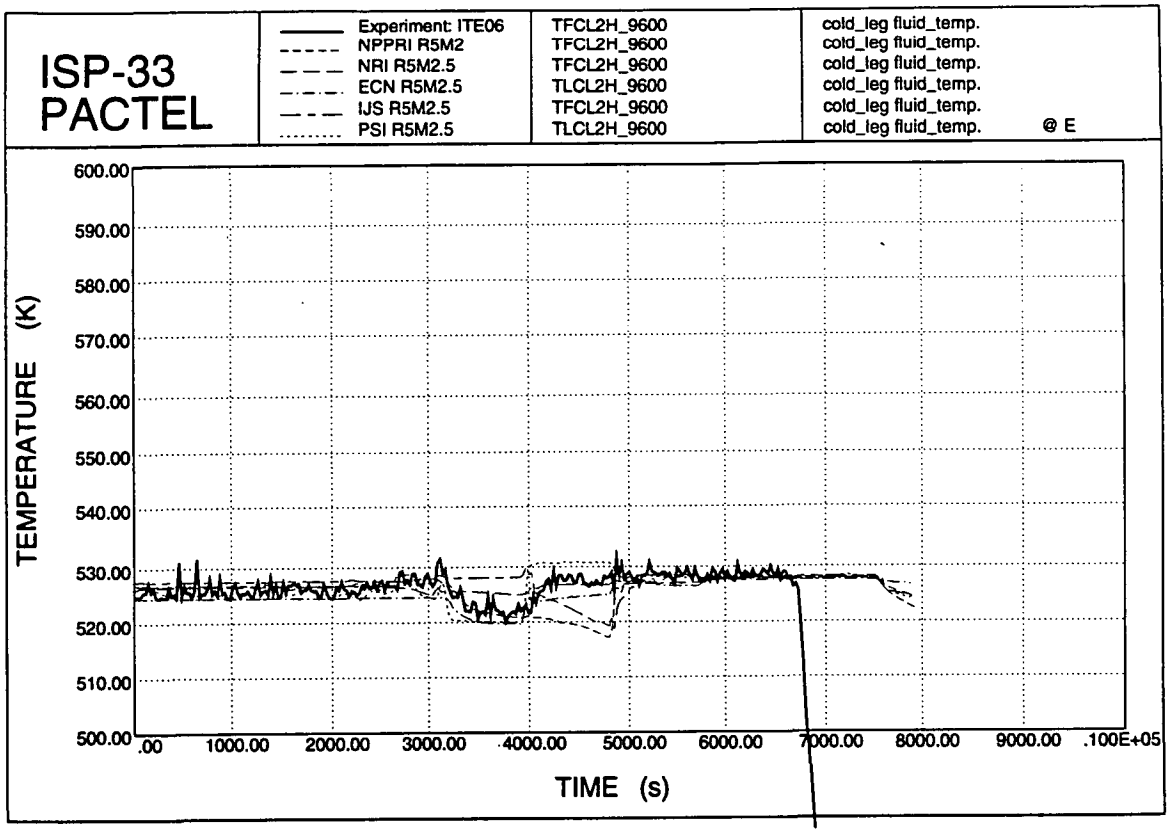

Figure 4.88. Cold leg coolant temperatures.

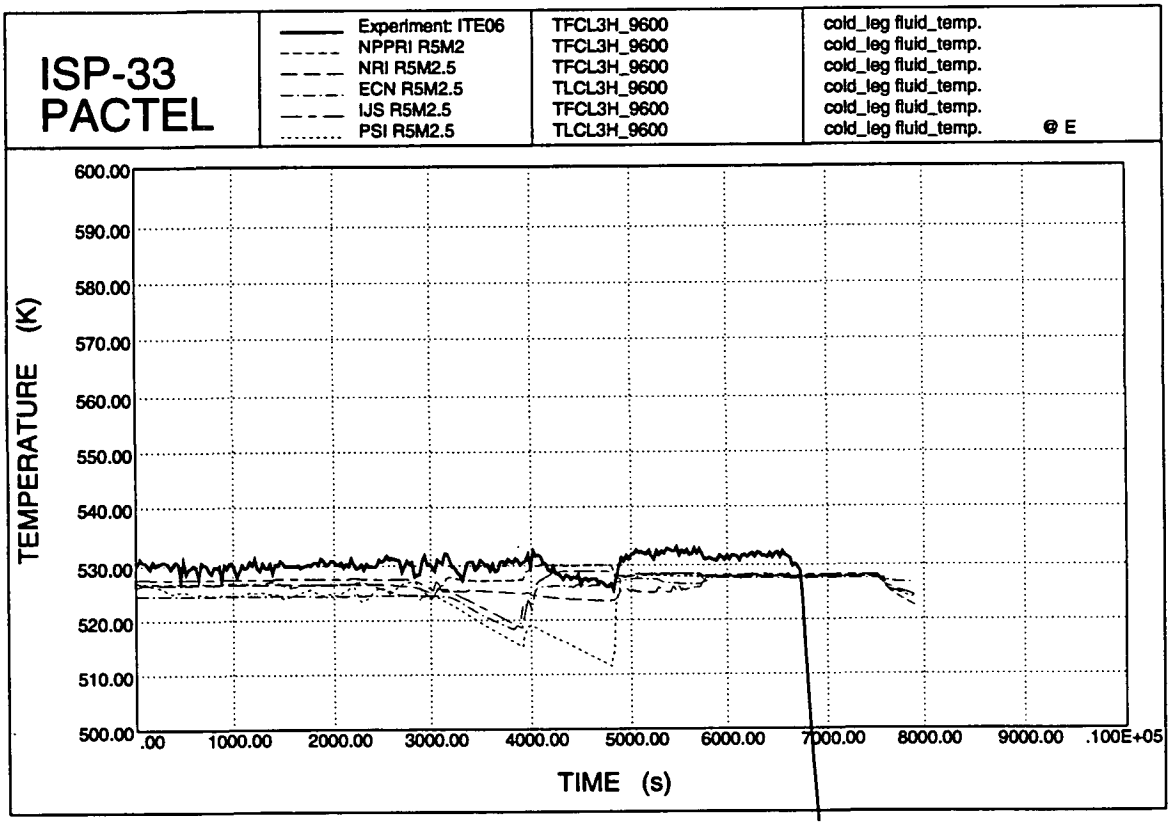

Figure 4.89. Cold leg temperatures.

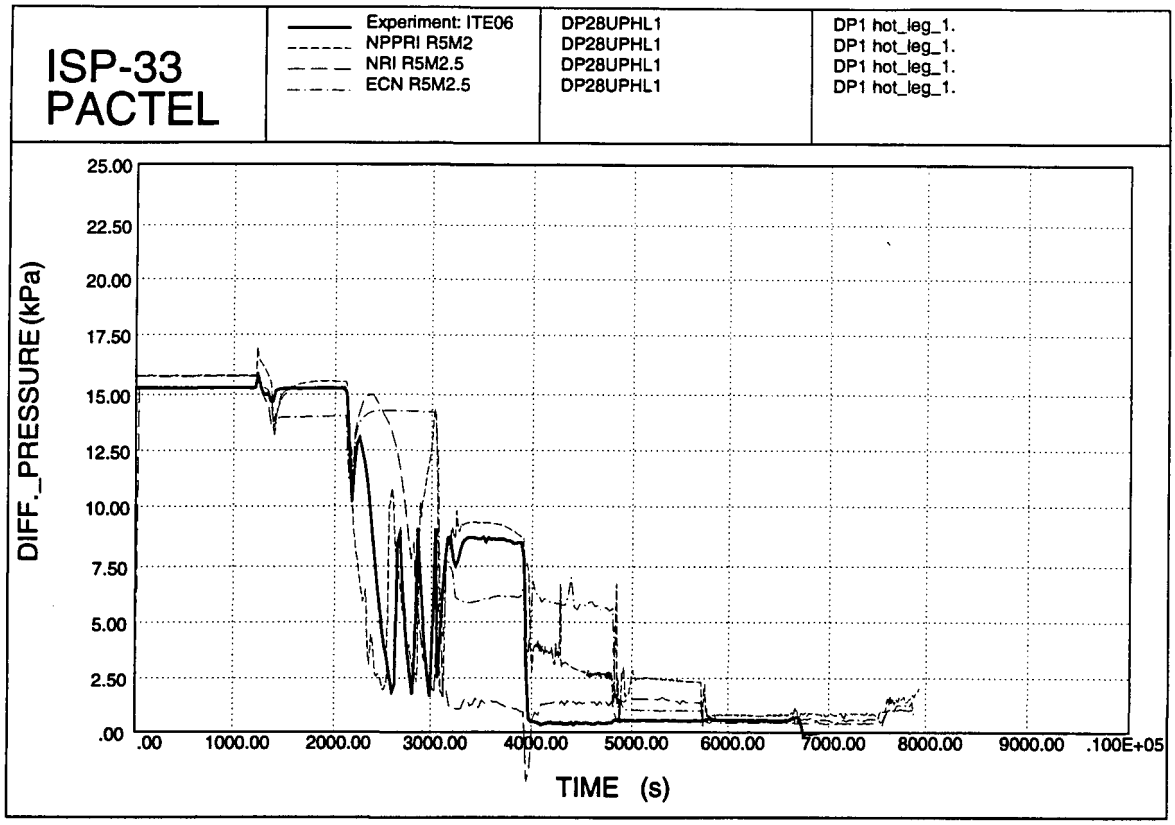

Figure 4.90. Hot leg 1 DP 1.

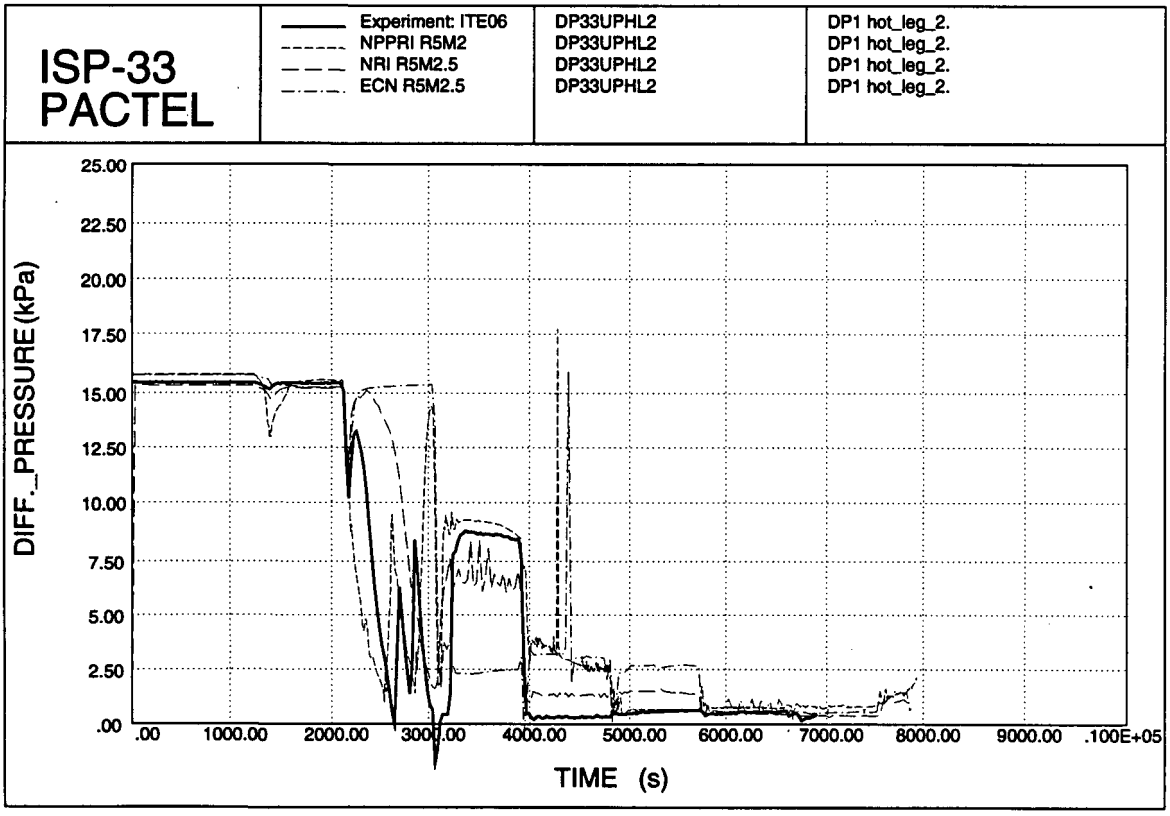

Figure 4.91. Hot leg 2 DP 1.

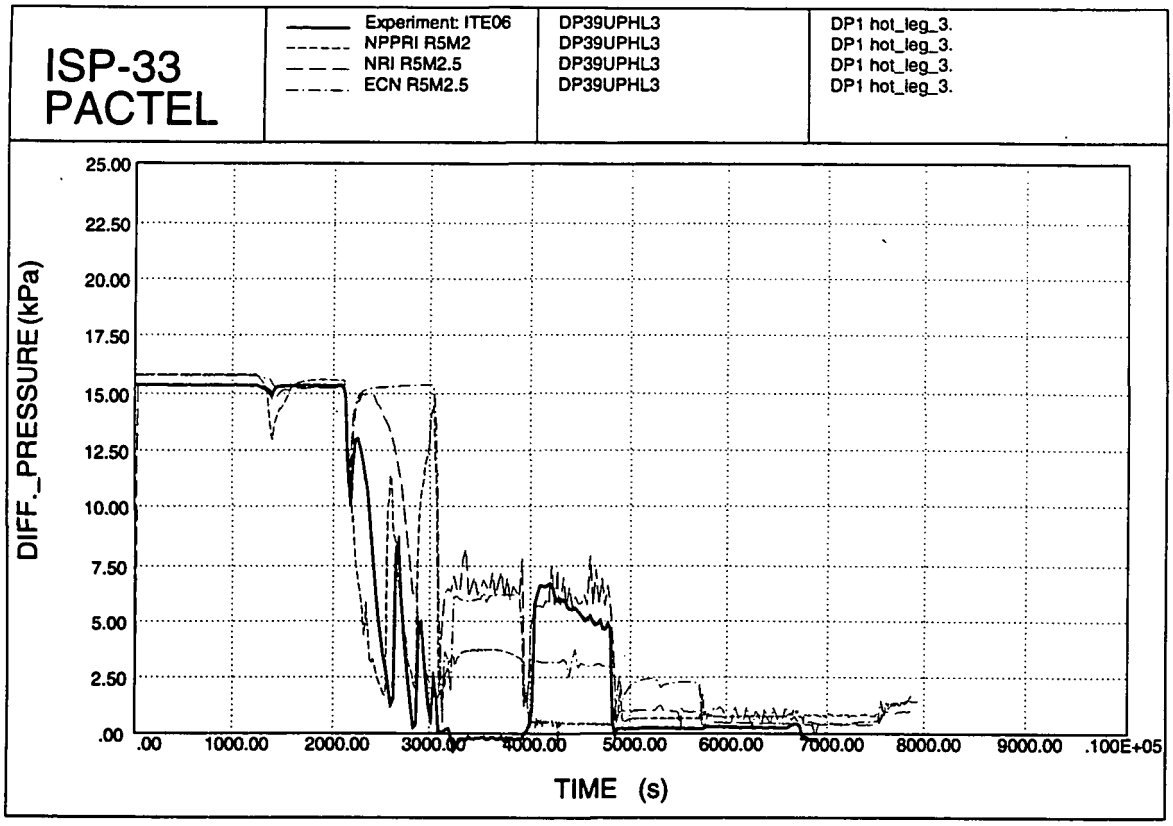

Figure 4.92. Hot leg 3 DP 1.

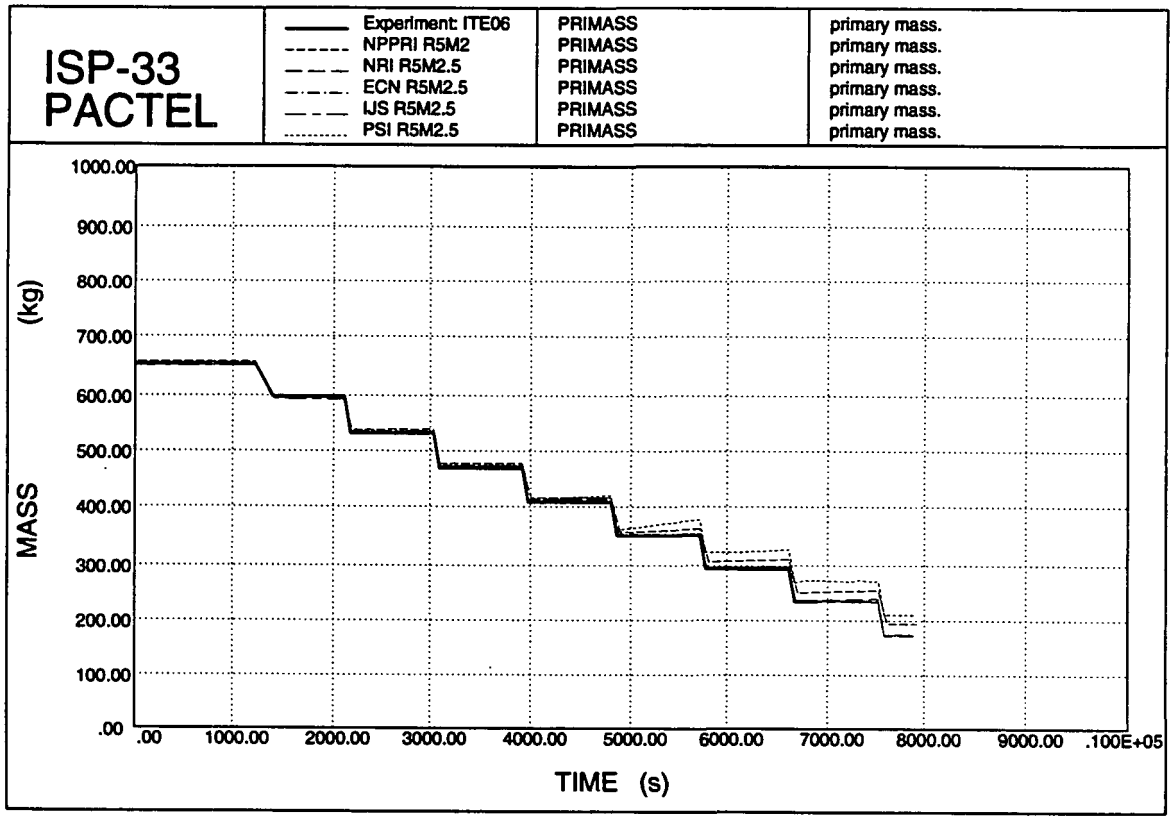

Figure 4.93. Primary mass inventory.

4.2.5 Comparison plots (SCDAP/RELAP5/MOD2, RELAP4/MOD6, DINAMIKA and TECH-M-4)

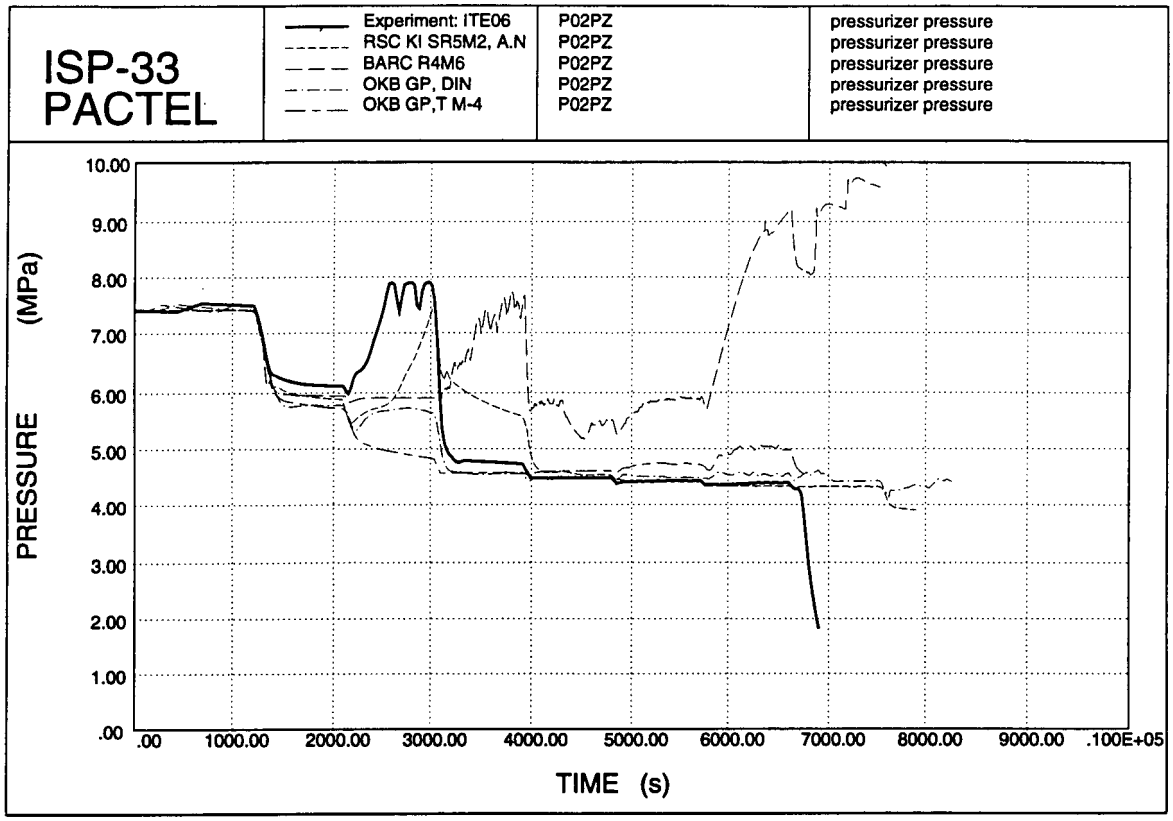

Figure 4.94. Pressurizer pressures.

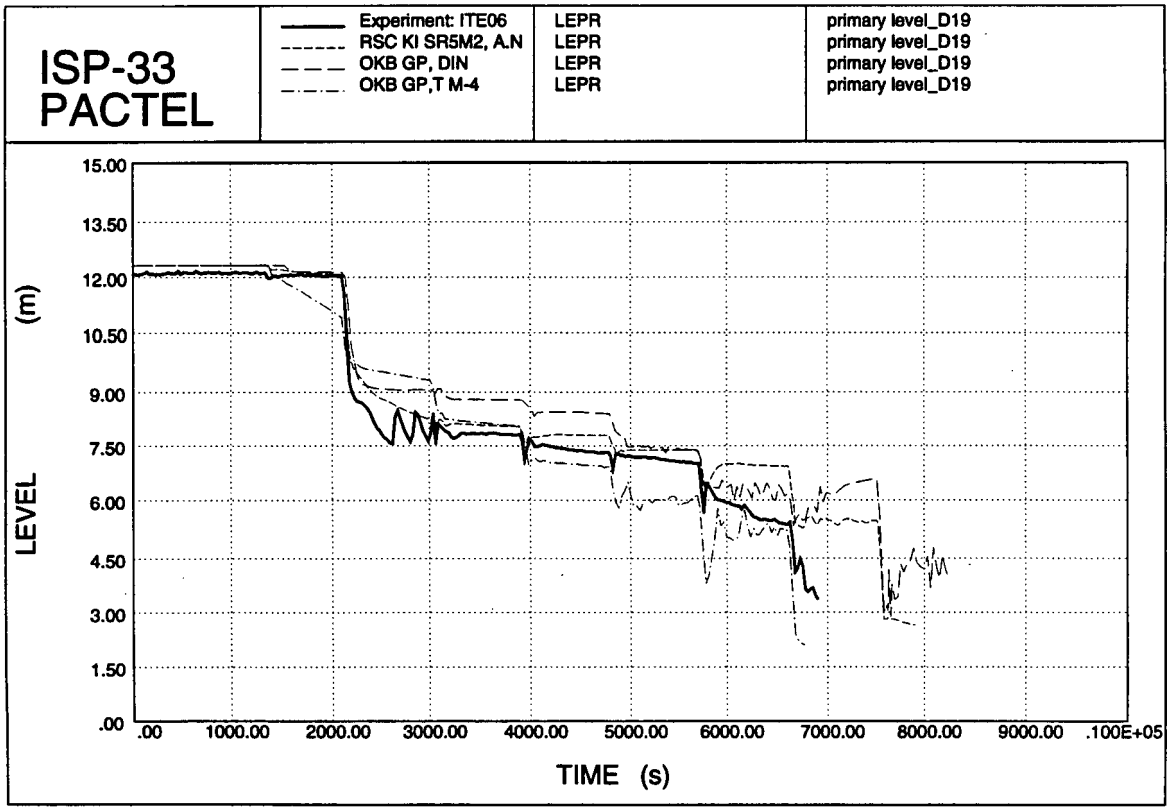

Figure 4.95. Primary levels.

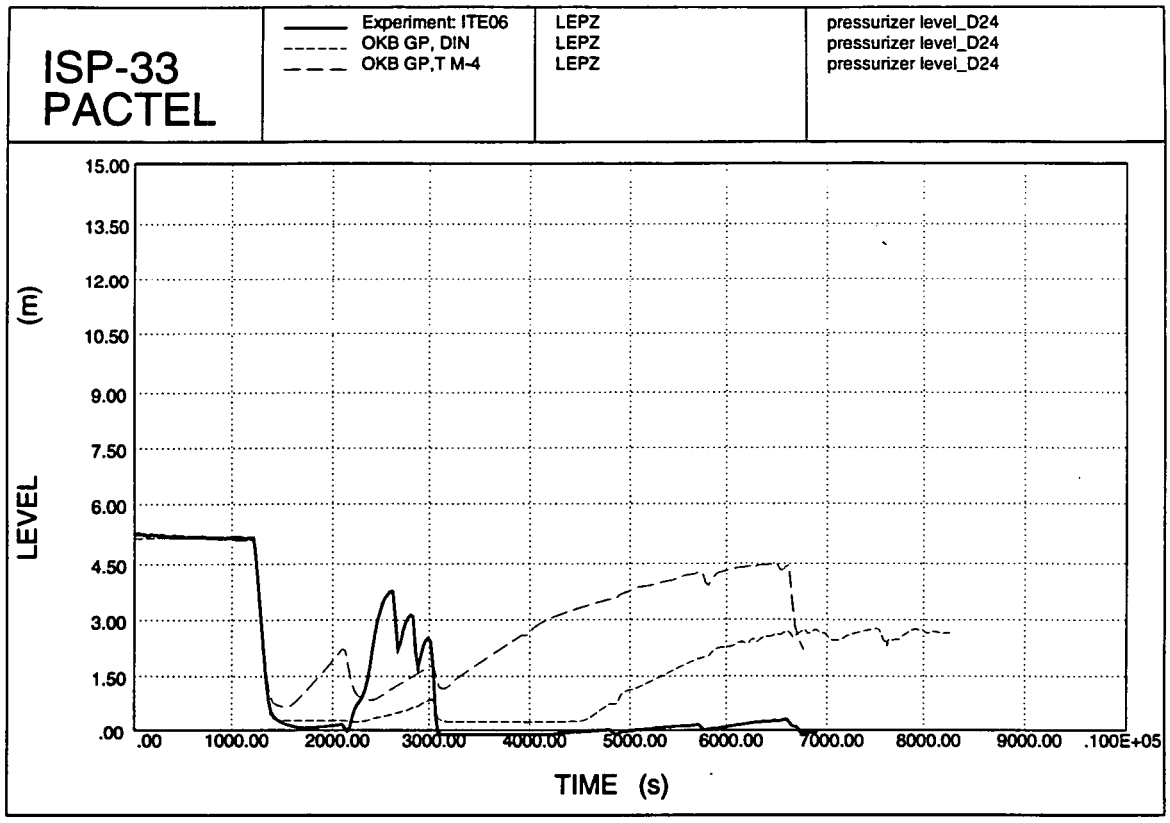

Figure 4.96. Pressurizer levels.

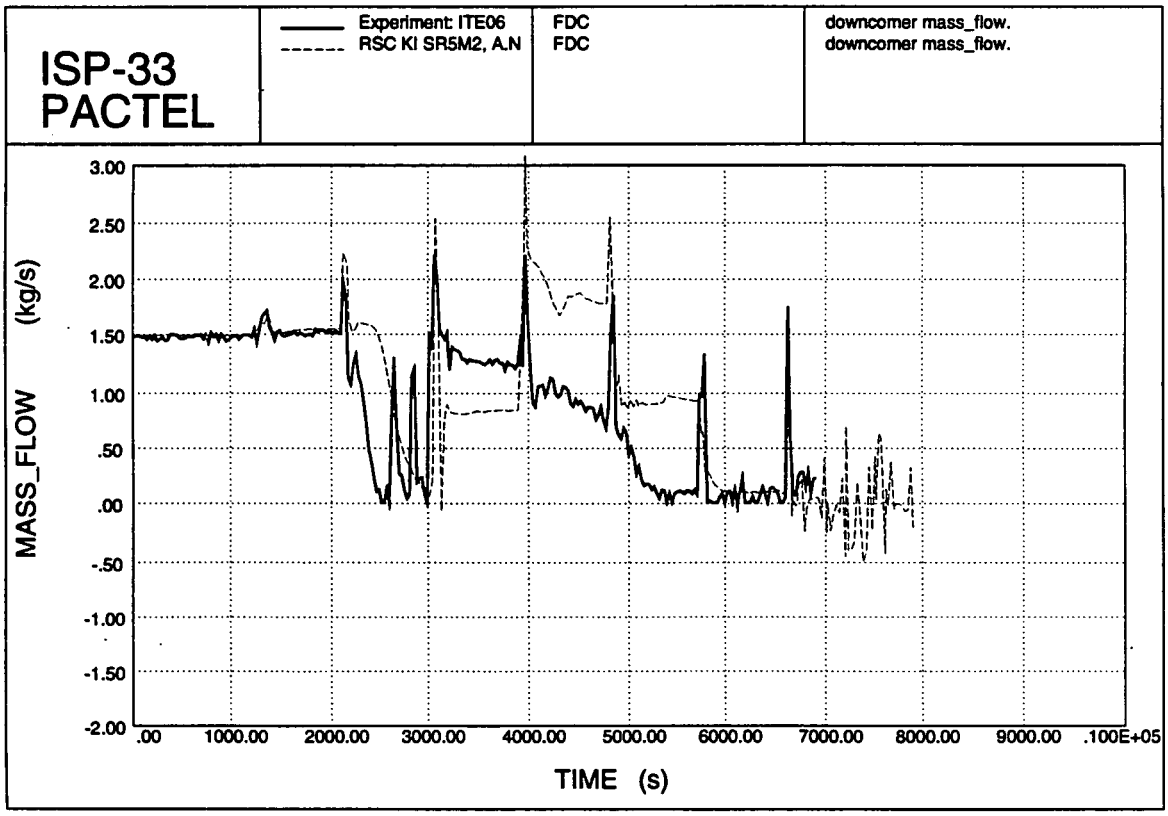

Figure 4.97. Downcomer mass flow.

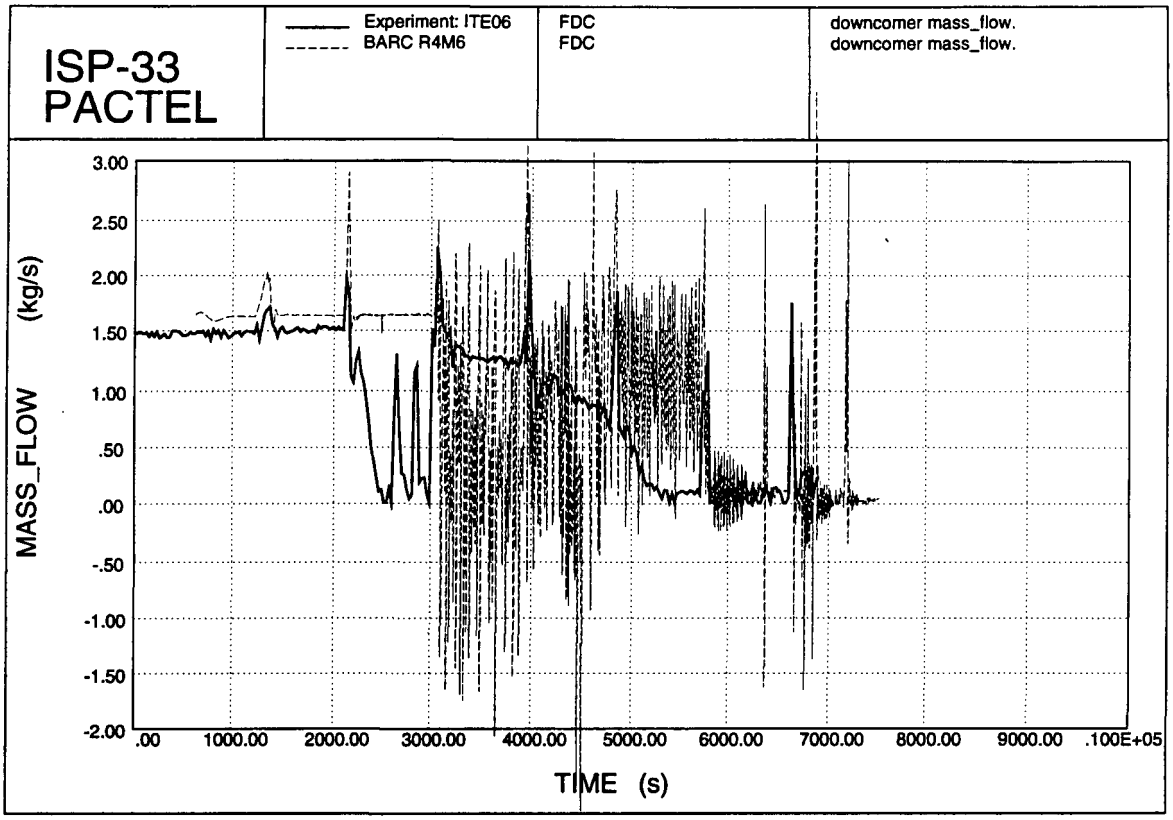

Figure 4.98. Downcomer mass flow.

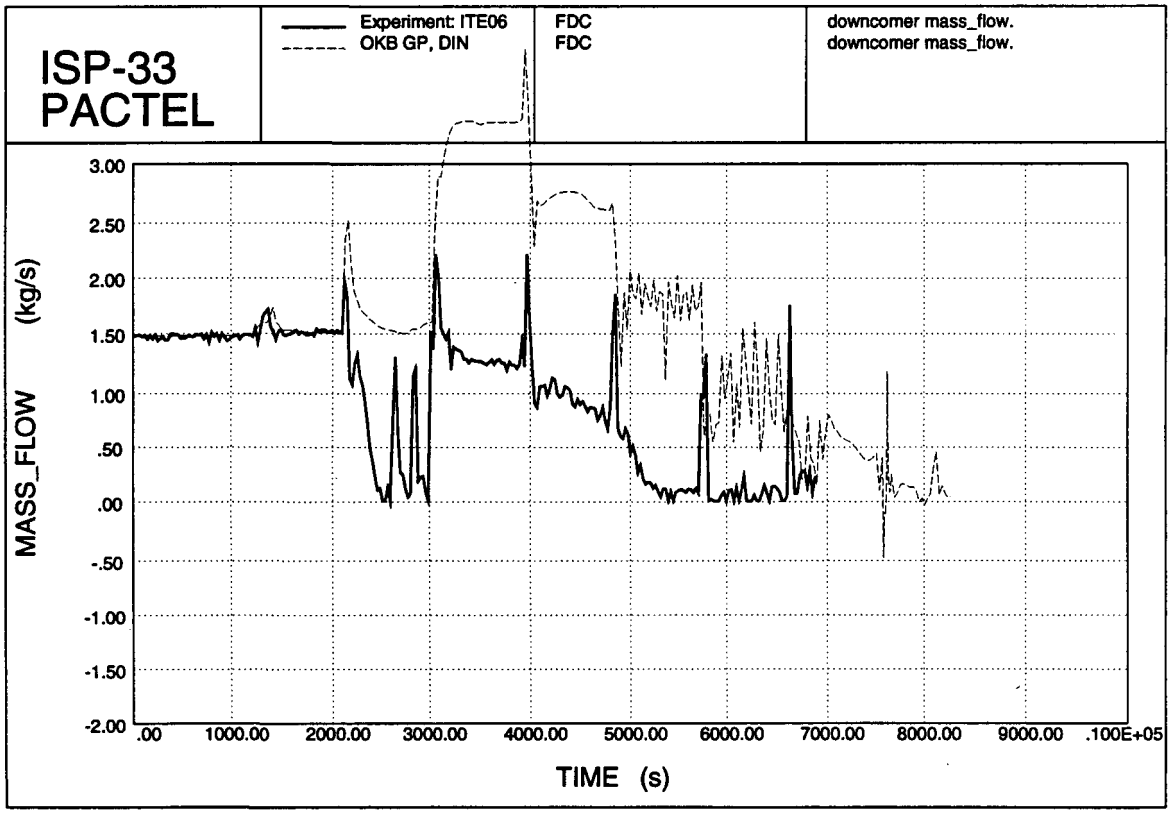

Figure 4.99. Downcomer mass flow.

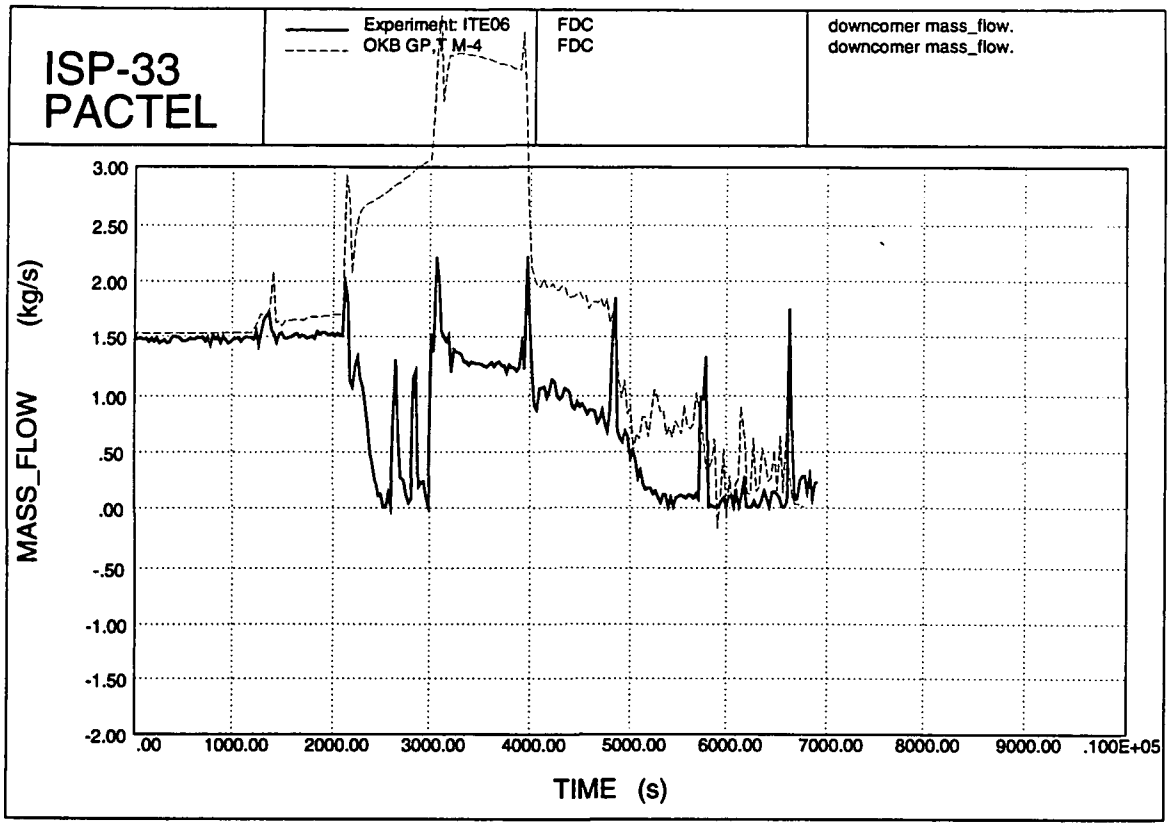

Figure 4.100. Downcomer mass flow.

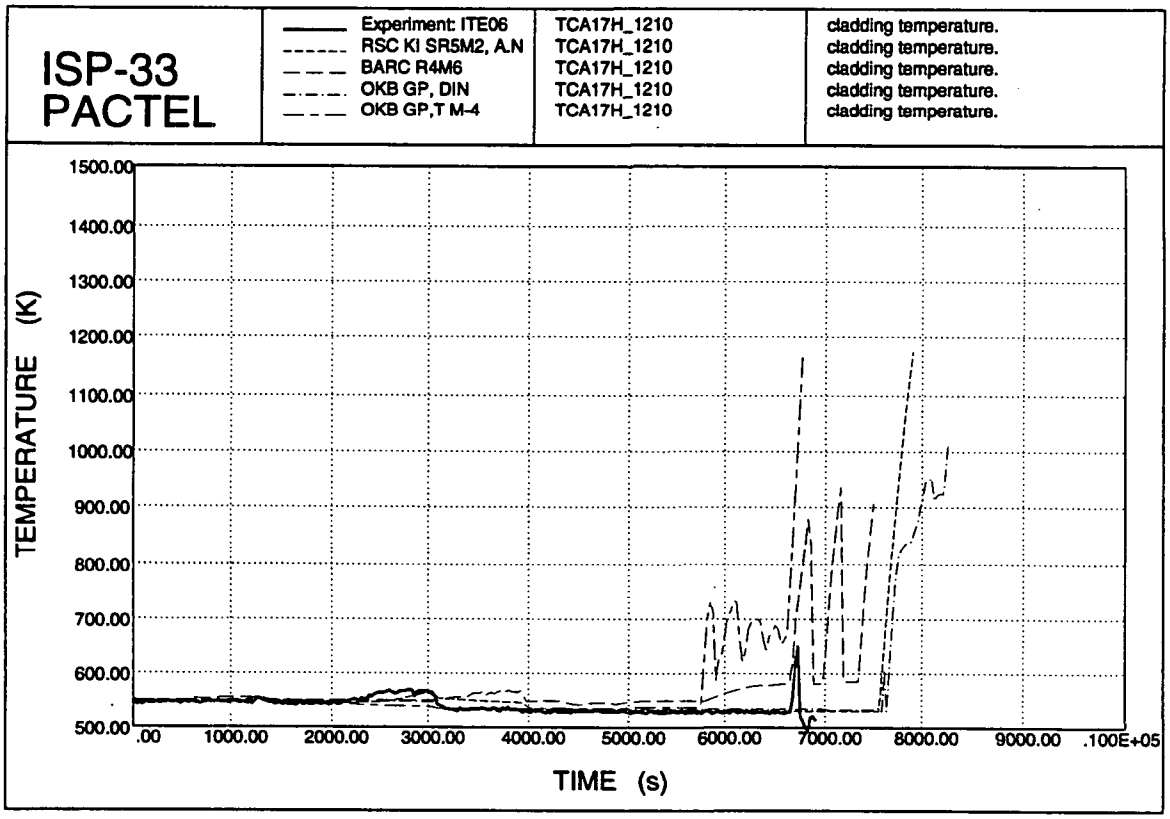

Figure 4.101. Cladding temperatures.

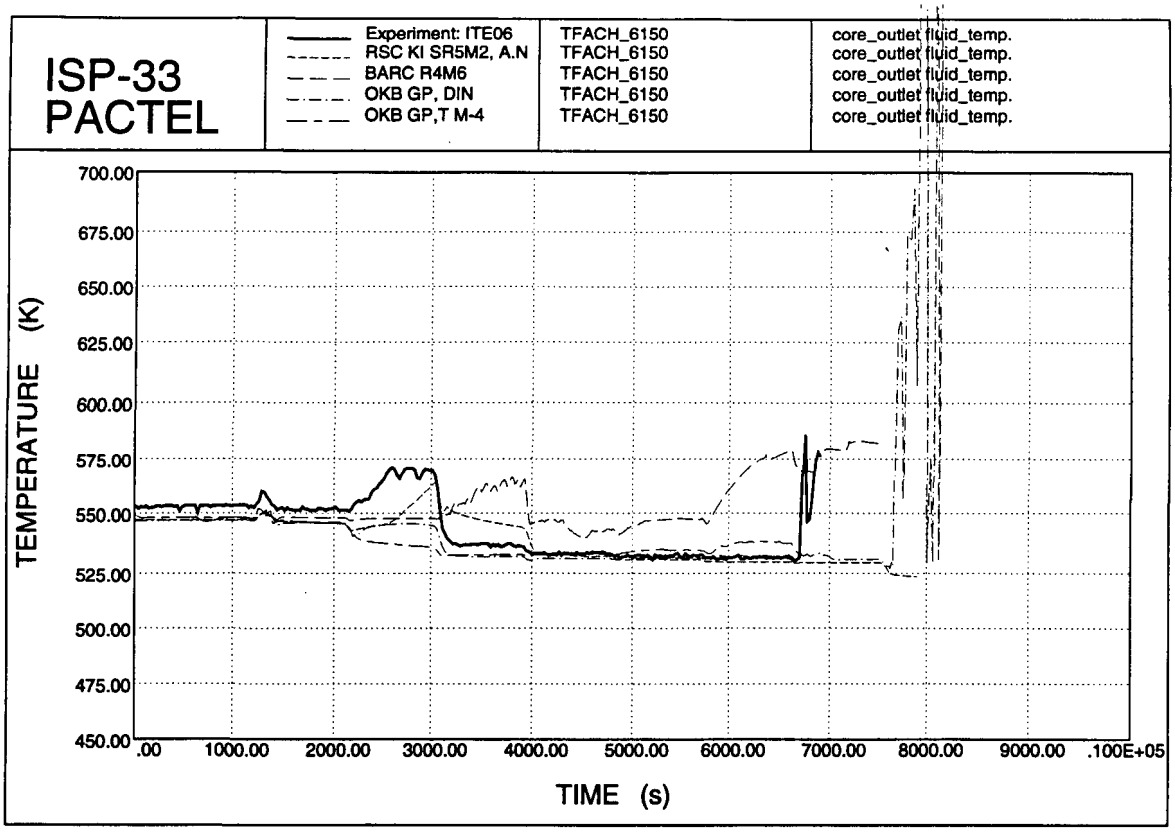

Figure 4.102. Core outlet coolant temperature.

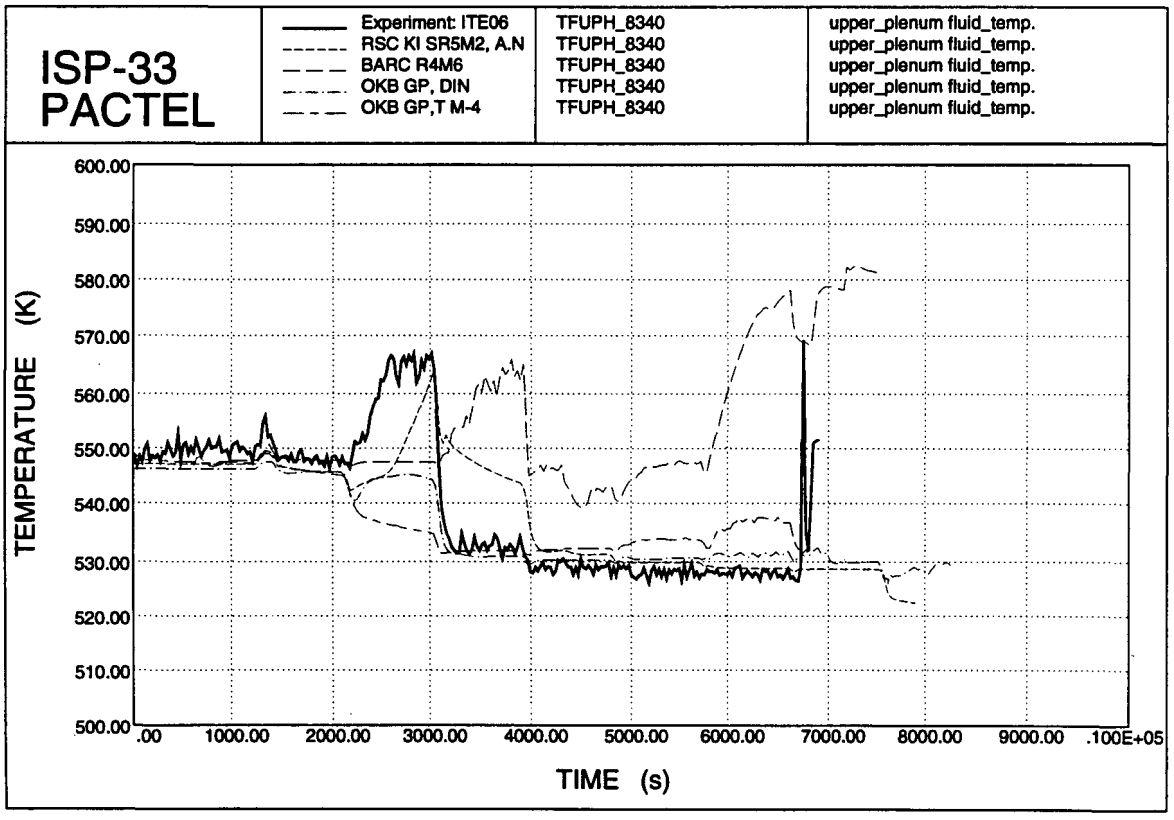

Figure 4.103. Upper plenum temperatures.

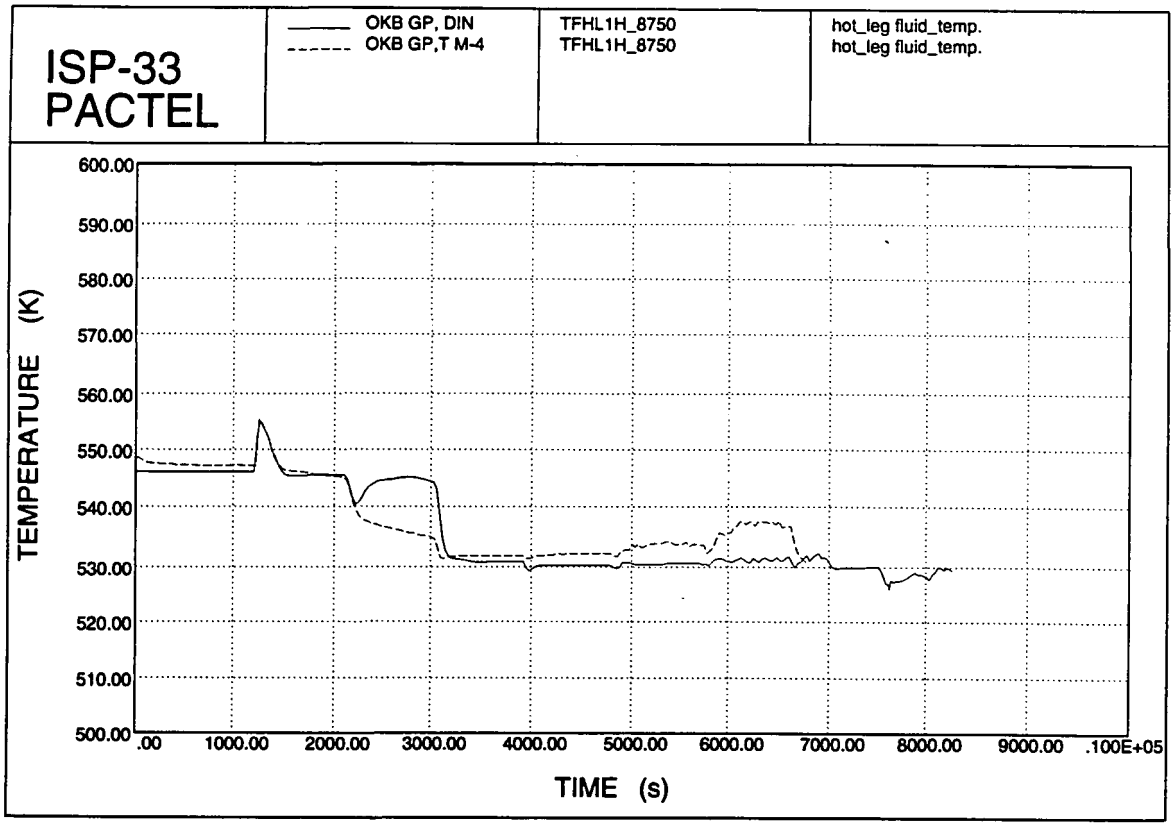

Figure 4.104. Hot leg coolant temperatures.

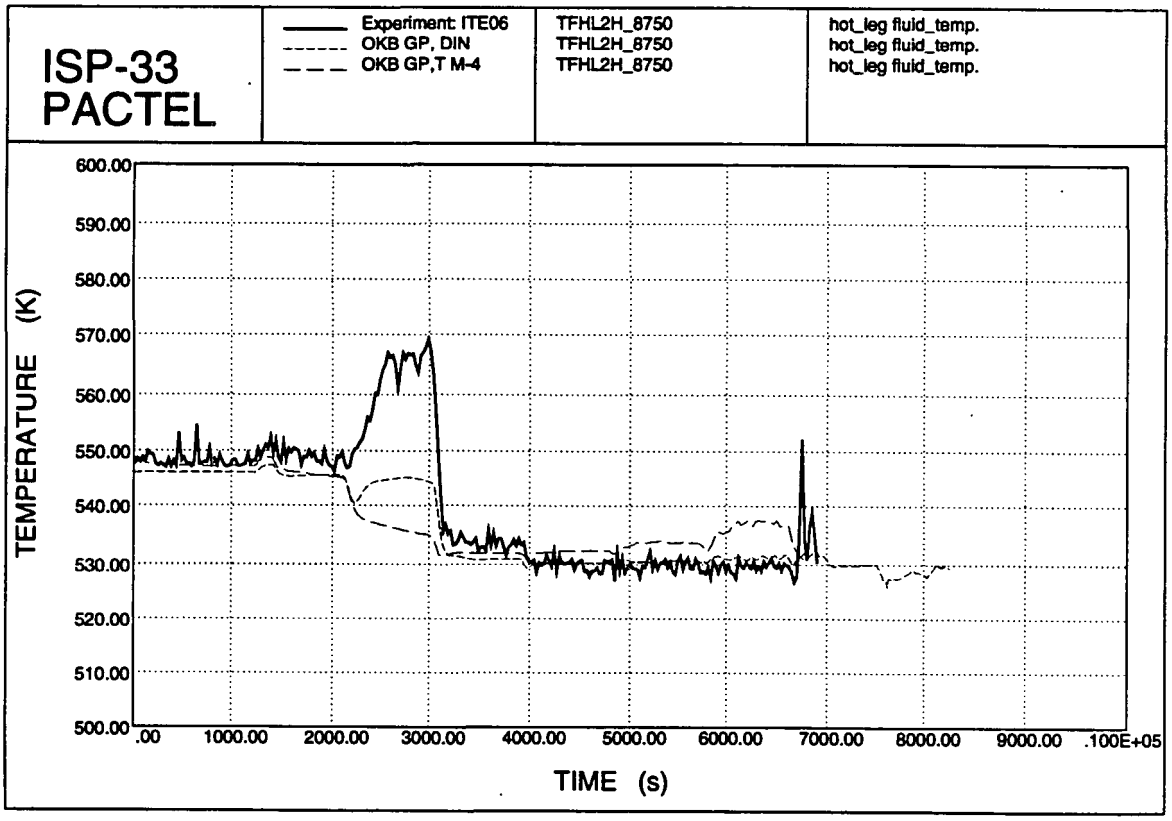

Figure 4.105. Hot leg temperatures.

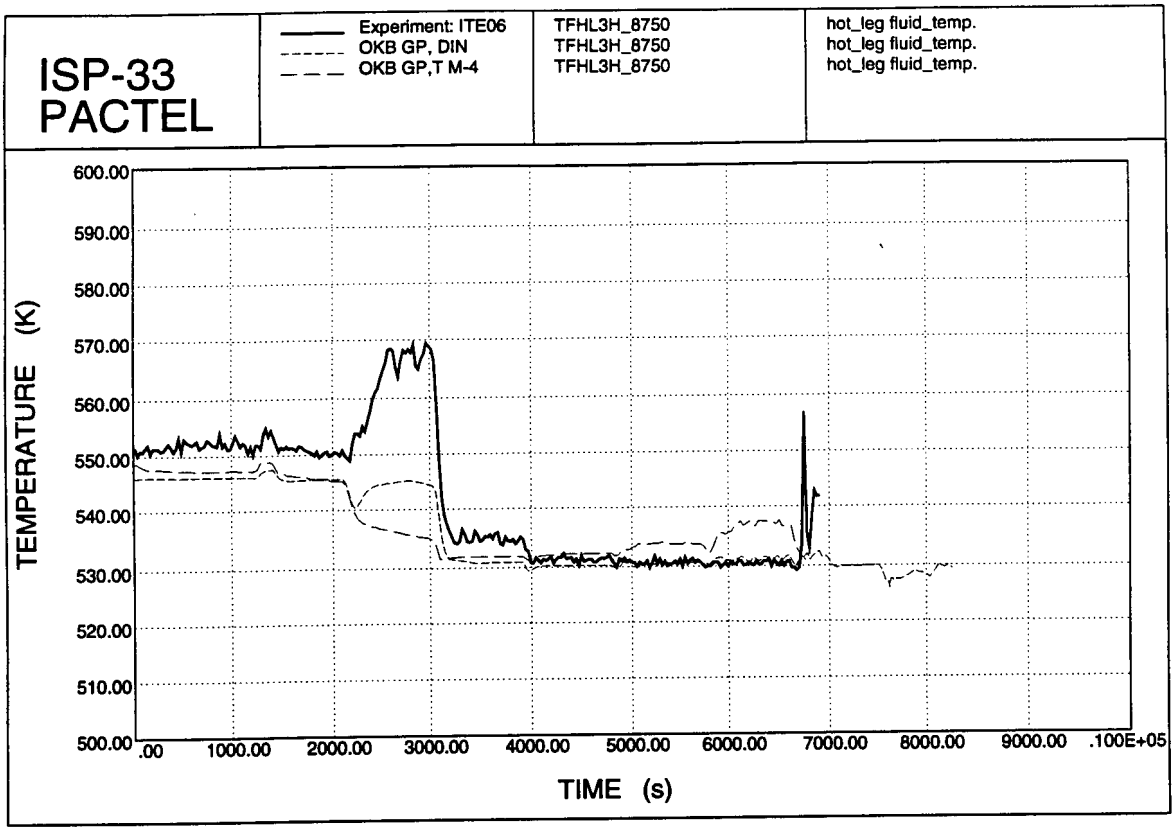

Figure 4.106. Hot leg coolant temperatures.

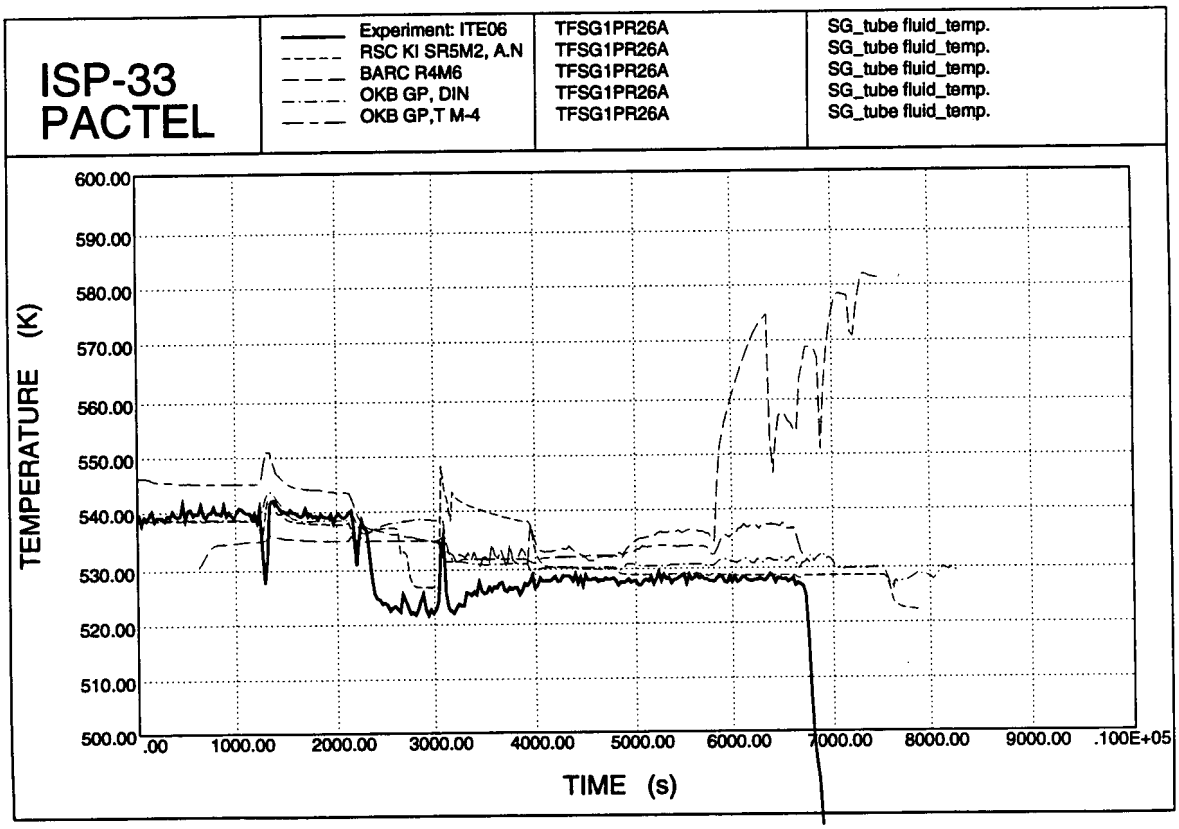

Figure 4.107. SG tube fluid temperatures.

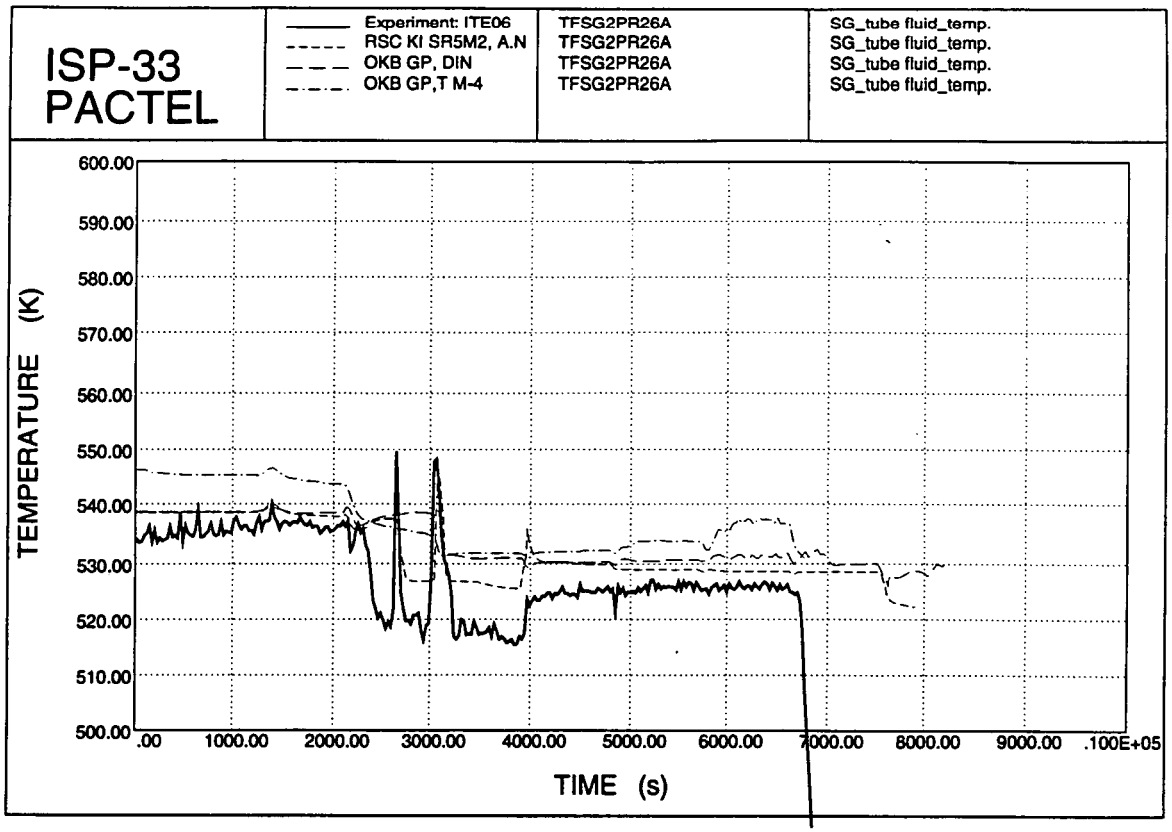

Figure 4.108. SG tube fluid temperatures.

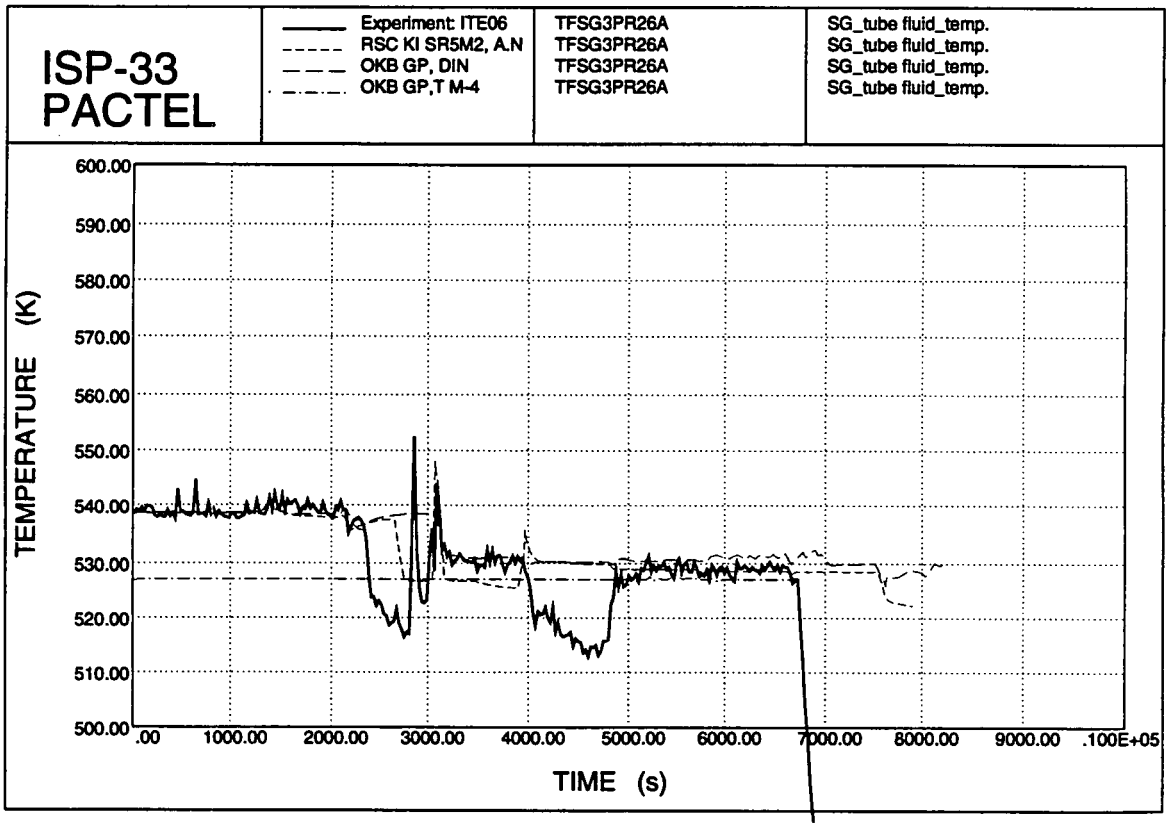

Figure 4.109. SG tube fluid temperatures.

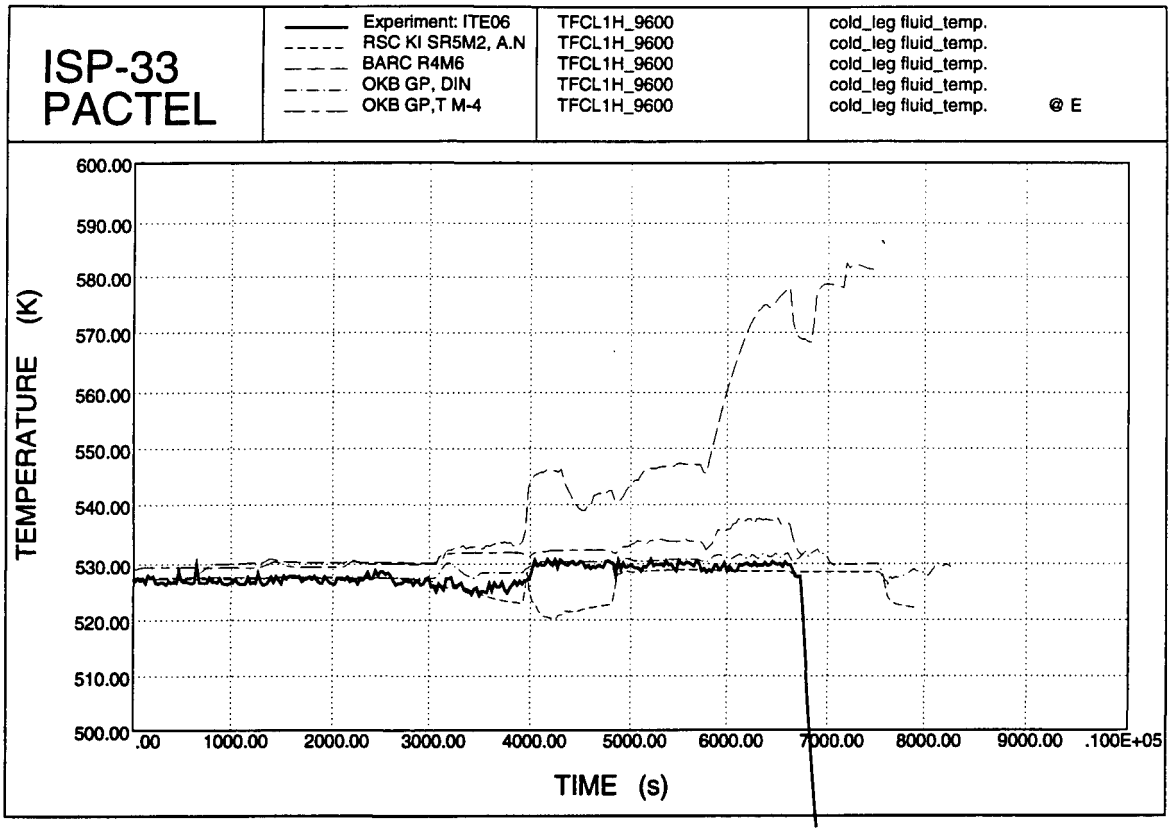

Figure 4.110. Cold leg temperatures.

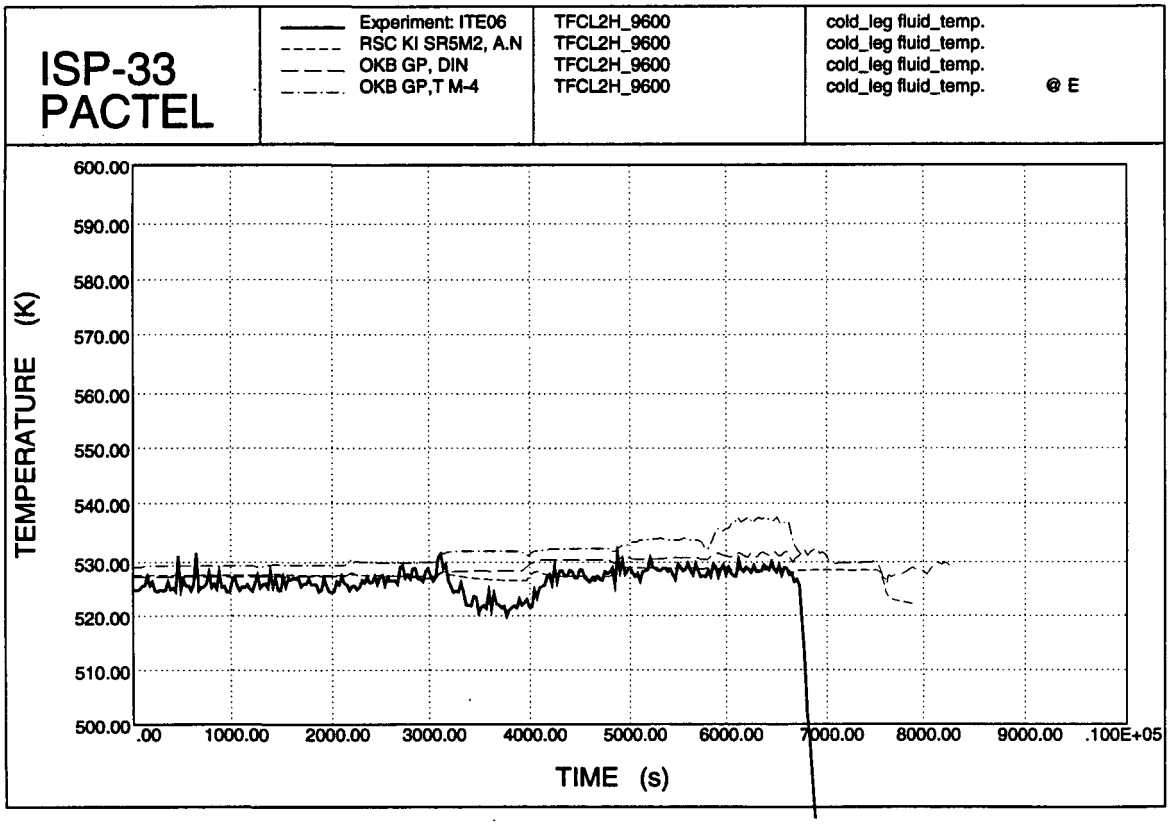

Figure 4.111. Cold leg coolant temperatures.

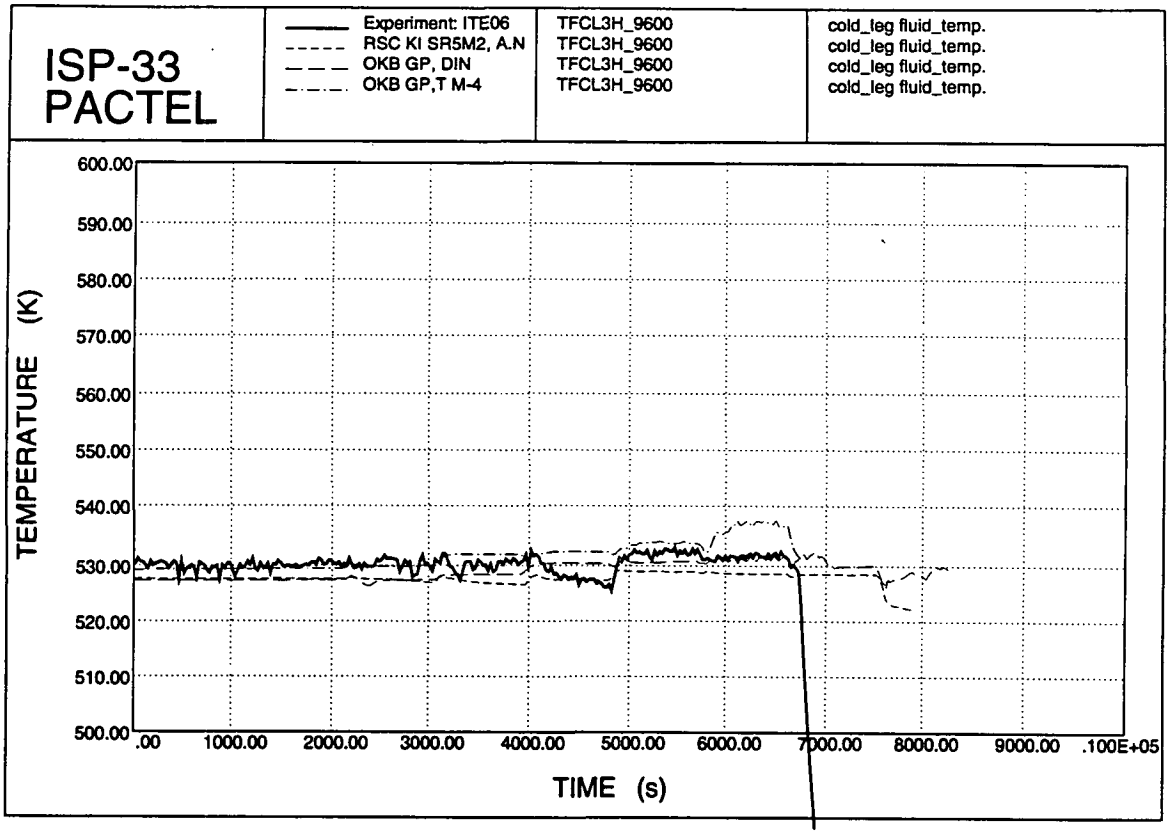

Figure 4.112. Cold leg temperatures.

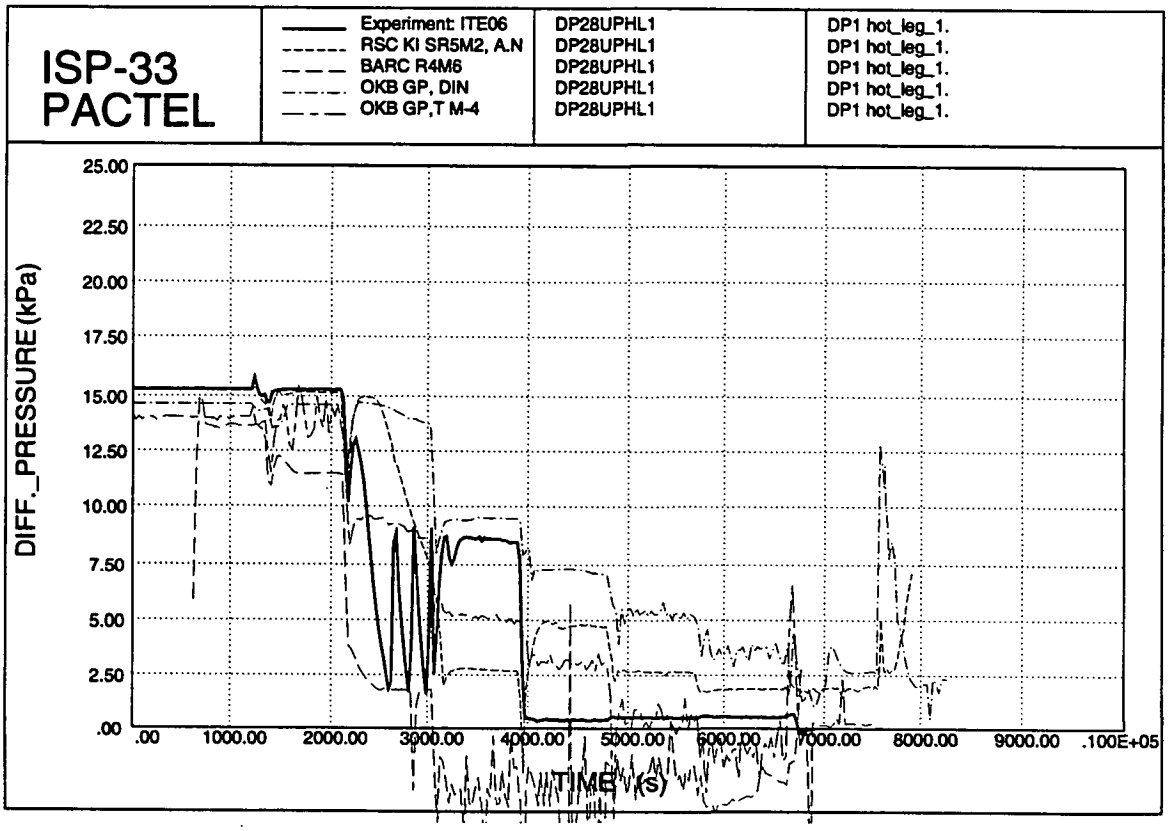

Figure 4.113. Hot leg 1 DP 1.

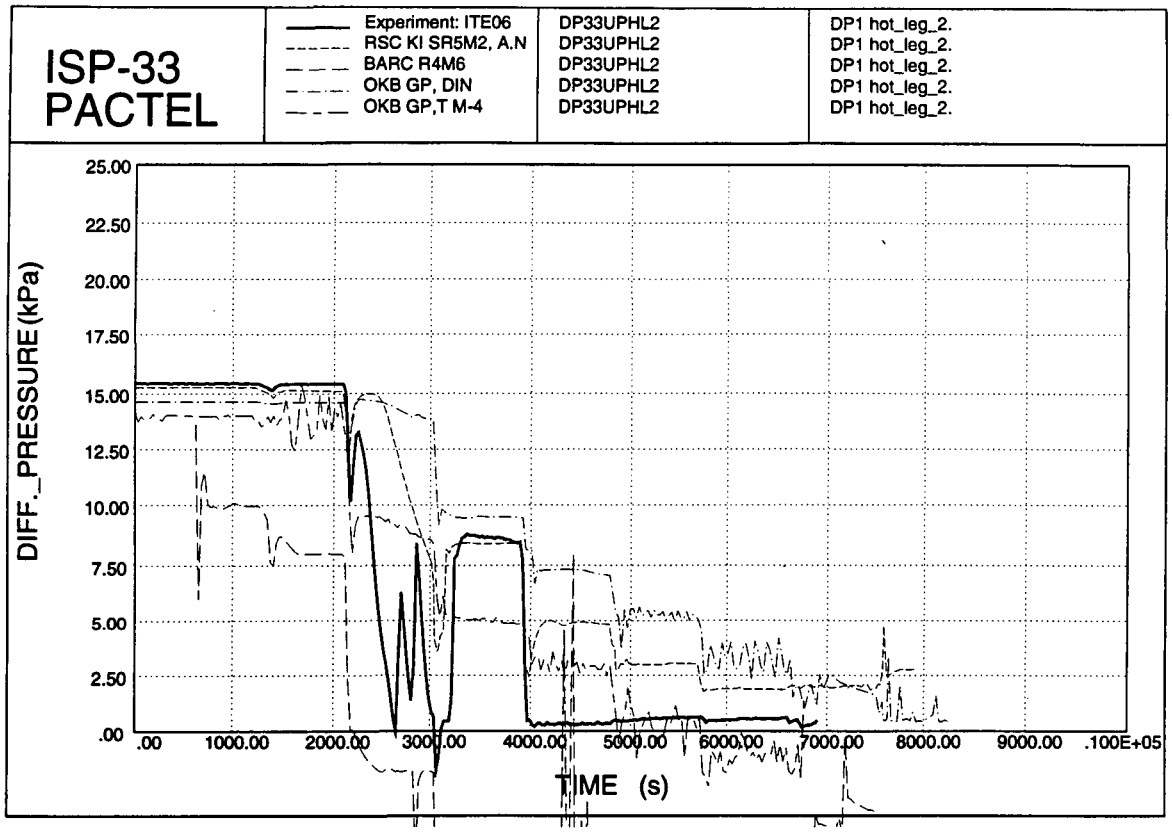

Figure 4.114. Hot leg 2 DP 1.

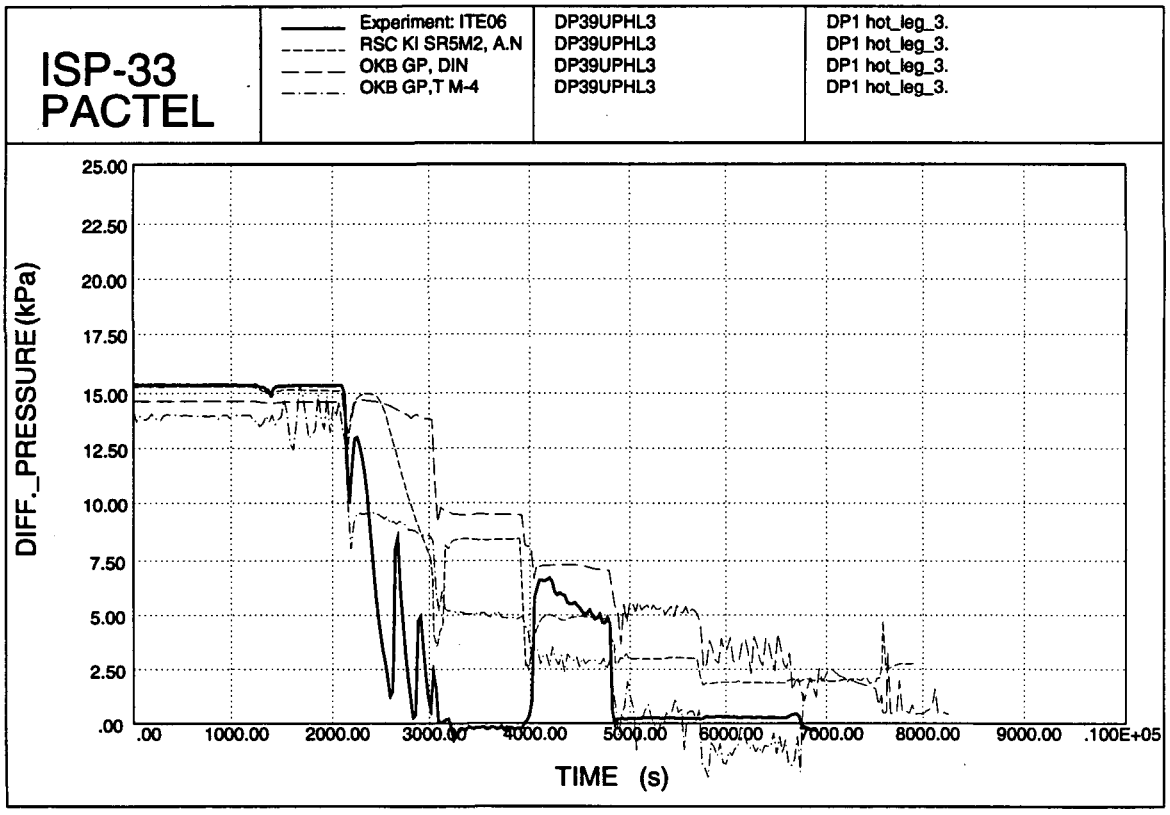

Figure 4.115. Hot leg 3 DP 1.

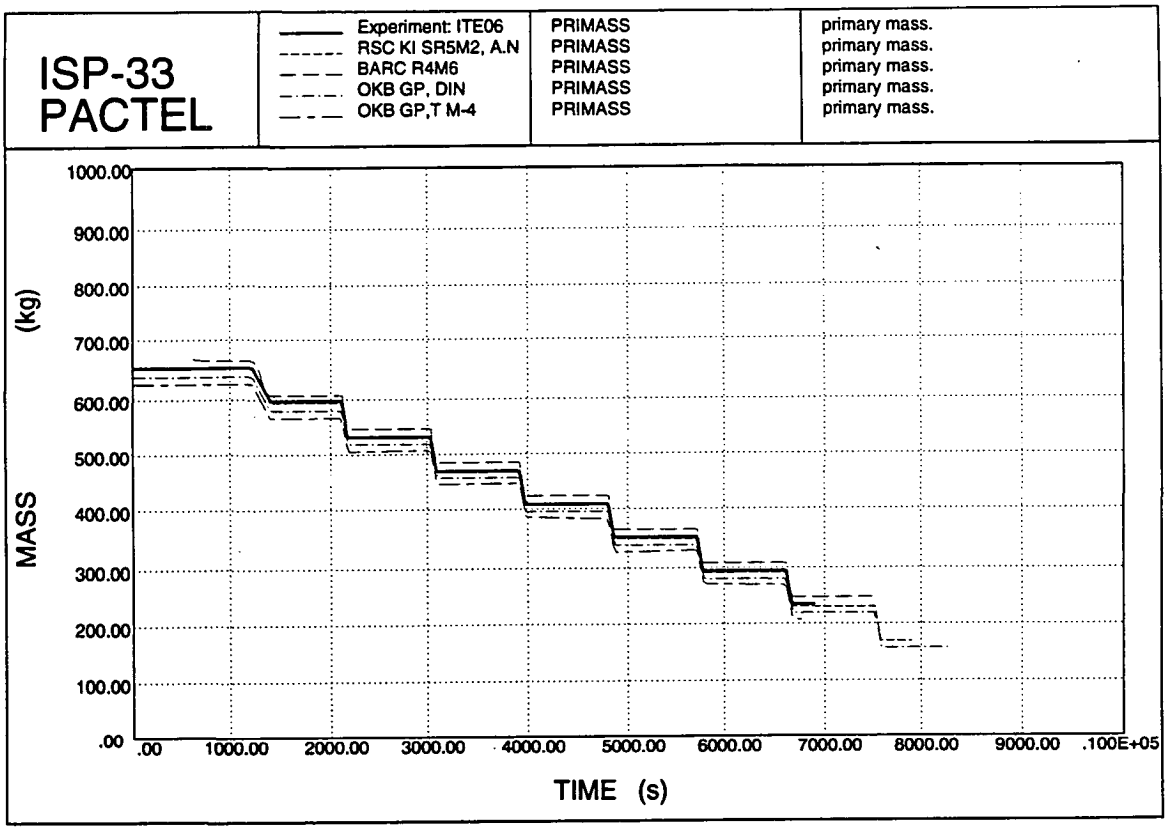

Figure 4.116. Primary mass inventory.

4.3 Comparison of blind calculations with the experimental results

The blind calculations were carried out using the characterization test data to tune the models and the initial conditions given in the specifiactions. The primary pressure in the experiment and the variation of pretest results are presented in Figure 4.117.

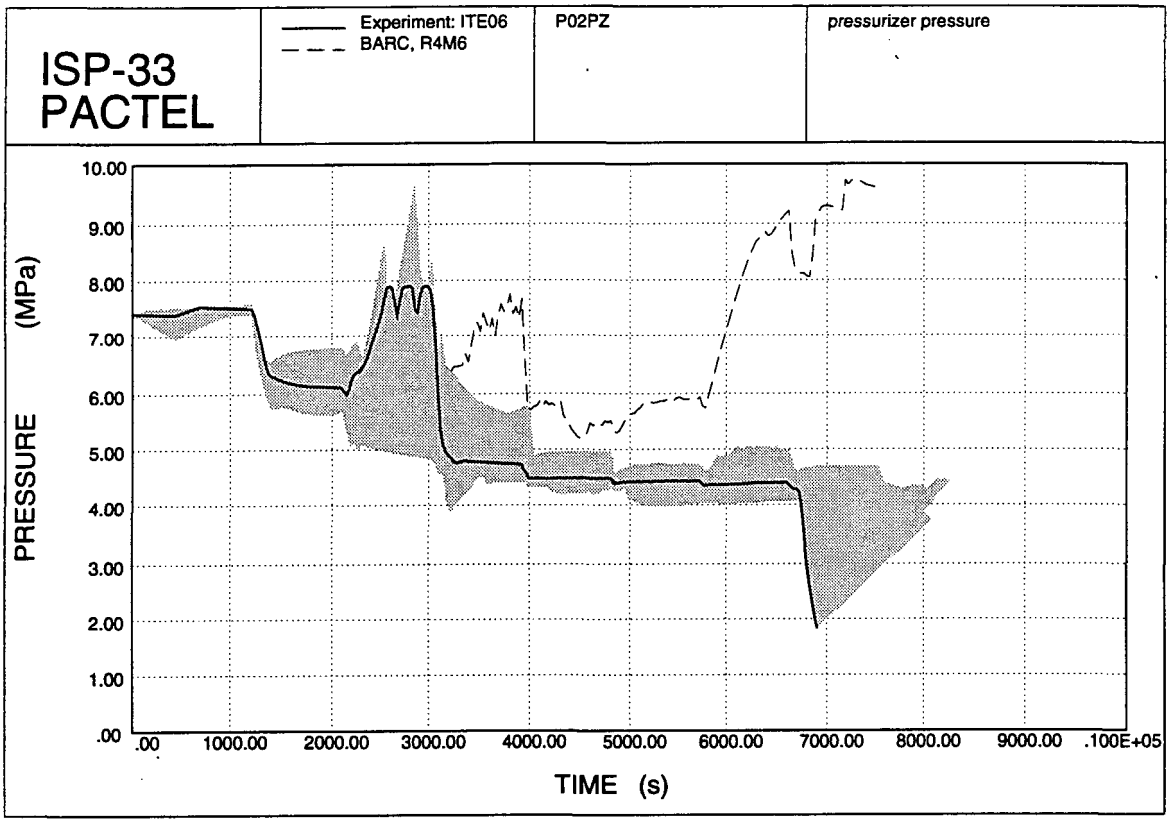

Figure 4.117. Primary pressure and the variation of pretest results.

4.3.1 ATHLET calculations

In all ATHLET calculations the initial conditions are in good agreement with the experimental results. However there are some variations in temperatures and differential pressures, which depend on the nodalization schemes and on the accuracy of tuning the model with the characterizing test.

Before the first draining the PACTEL facility operated 1200 s at nominal initial conditions. Behaviour of the primary pressure is close to the experimental data in all other calculations except in BARC (I) calculation. Primary pressure decreases more rapidly during the low heater power phase. Other parameters retain the initial values in all ATHLET calculations. The calculated mass flow rates and fluid temperatures stay absolutely constant.

First draining (at 1200 s) empties the pressurizer in GRS, THZ and FRG/FZR calculations, while, incorrectly, some water remains in BARC (I) calculation (all loops lumped together). The decrease of primary pressure down to the saturation pressure is well predicted in all calculations. Primary pressure is close to the experimental value after the draining in the THZ calculation and too low in GRS and BARC (I) calculations. BARC (II) calculation has an incorrect repressurization rate. The increase of downcomer mass flow rate during the draining period is predicted in all calculations. After the draining the mass flow returns to the initial value of the single phase natural circulation in all other ATHLET calculations except

in BARC (I), where 20% higher value is reached. The reasons for the peculiarities in BARC (I) and (II) calculations could not be found.

During the second draining (at 2100 s) the vessel water levels in GRS, THZ and FRG/FZR calculations do not decrease low enough to allow steam flow to hot legs. This is due to the calculated slow refilling of the pressurizer. The calculations do not show the continuous decrease of primary flow immediately after the draining. Instead, single phase natural circulation continuous at a constant rate. Both BARC calculations indicate voiding in the hot legs during draining, but they do not agree well with the decrease of experimental primary mass flow. BARC (II) calculation even predicts 80% higher downcomer mass flow rate compared to the initial nominal value. Depressurization that starts during the second draining, is long and deep in BARC (II) calculation. Primary pressure is partially recovered afterwards. In the GRS and FRG/FZR calculations the mass flow rate in the downcomer starts to decrease 300 s later than in the experiment, but the process is interrupted by the third draining before complete stagnation of the flow. Thus the ATHLET calculations (as most other blind calculations) miss the rapid repressurization of the primary side. Also the drop of collapsed water level in the vessel and the simultaneous coolant flow to the pressurizer occurs slower than in the experiment. The too low core power contributes to the erroneous behaviour after the second draining.

During the third draining (3000 s) the hot leg loop seals are emptied of water and steam is flowing to the steam generator leading to primary pressure decrease. The BARC (II) calculation experiences again an unrealistically steep depressurization and a partial pressure recovery during the stationary phase. Between the third and fourth drainings BARC (I) calculation shows very high mass flow rates in the downcomer compared to the experiment. Asymmetric two-phase flow takes place in GRS, THZ and FRG/FZR calculations after the third draining, one or more loop seals are practically cleared during stationary phases between drainings. Downcomer mass flow is overestimated in all calculations until initiation of the boiler-condenser mode. In BARC (II) calculation the boiler-condenser mode is begins too early after the fourth draining and core heat-up begins already after the fifth draining.

All other calculations except BARC (II) needed eight drainings before the beginning of core heat-up (one draining too much).

The BARC submission did not include all requested parameters.

4.3.2 CATHARE calculations

The initial conditions of both CATHARE calculations agree well with experimental data. SEMAR LEACS has 10 kg too high and UP-DCMN 20 kg too low initial coolant inventory.

The behaviour of pressure (combined effect of pressurizer heaters and heat losses) during the first 1200 s is very well predicted by both calculations.

The first 2100 s are generally well predicted by both participants. Pressures, mass flows, levels and temperatures agree well with measured values. After the second draining (2100 s) flow stagnation is delayed about 500 s in both calculations. The primary pressure never reaches the maximum operating pressure of the facility as a result of the third draining. One reason for this delay is too low core power (inaccurate value in the specifications).

Due to the clearance of one hot leg loop seal asymmetric flow takes place in both calculations after the third draining (3000 s). UP-DCMN also predicts extensive voiding in the uncleared loop seals.

In these calculations the primary mass flow in the late phase of the experiment is not predicted. Boiler-condenser mode is established earlier than in the experiment in both calculations, in SEMAR LEACS calculation after the fourth draining (3900 s) and in UP-DCMN calculation after the fifth draining (4800 s).

SEMAR LEACS calculation predicts one additional (the 8th) draining while the UP-DCMN core heat-up prediction agrees well with measured data. It should be noted that Pisa University used vertical SG tubes in its model and the initial coolant inventory was 20 kg lower than in the experiment.

The UP-DCMN submission did not include all requested parameters.

4.3.3 RELAP5/MOD3 calculations

The initial conditions are generally well calculated by all participants. However, TAEK did not calculate the initial steady state accurately and it has too low single-phase mass flow. Also the initial primary coolant inventory in RSC KI (Devkin) calculation is overestimated.

Pressure behaviour is well predicted by all participants except RRC KI (Stolchnev) having constant pressure and zero pressurizer heater power. Low primary mass flow in TAEK calculation predicts a too high core outlet temperature and excessive voiding in upper plenum after the first draining (1200 s). Thus, the pressurizer is not fully emptied.

After the second draining (2100 s) IJS and TAEK calculations predict sufficiently low primary water levels for flow stagnation. IJS predicts flow stagnations and periodic flows well in spite of using the too low core power. Also other calculations show a primary level decrease, but the level remains too high for steam to flow to the hot legs.

The third draining (3000 s) causes stable two-phase flow in all calculations, the mass flow rates are well predicted by TAEK and RSC KI (Devkin). Others have slightly too high mass flow rates. RSC KI (Devkin) calculation has a too strong repressurization after the third draining, which also affects the temperatures. In RRC KI (Stolchnev) calculation timing of the drainings is incorrect and causes several problems afterwards.

After the fourth draining (3900 s) Studsvik predicts downcomer mass flow well until the end of the test but with rather large oscillations. Other results are not as good. In RSC KI (Devkin) calculation the primary mass inventory is incorrectdue to the mass errors of the code. Also, timing of the later drainings is incorrectly predicted.

RRC KI (Stolchnev) submission did not include all requested parameters.

4.3.4 RELAP5/MOD2 and /MOD2.5 calculations

The initial conditions of the experiment were calculated well by all participants, but correct pressurizer cycling has not been reproduced in all calculations. The initial primary level in ECN calculation seems to have an incorrect reference level. Temperatures in the upper plenum are underestimated by all calculations. One reason for this is the too low core power.

The first draining (1200 s) empties the pressurizer in all calculations, except in NPPRI, which also predicts void in the upper plenum. Downcomer mass flow rates match the measured values well in three calculations. ECN and IJS predict slightly too low mass flows. NPPRI calculation begins to fill the pressurizer after the draining, although theupper plenum level is decreasing. In the other calculations pressurizer is discharged completely during draining as in the experiment.

The second draining (2100 s) brings the primary level near the hot leg connections in all calculations except those of ECN and PSI. Only NPPRI predicts periodic stagnations. In other calculations stagnations are more or less delayed, and ECN and PSI predicts no stagnations.

The mass flow rates during the rest of the transient are wellpredicted only by IJS calculation. NPPRI predicts the initiation of the boiler-condenser mode already after the fourth draining, while others need two more drainings. All participants need one additional draining (the 8th) before core heatup. Mass errors in some calculations have a significant influence on the mass inventory. Others, except ECN overestimate the pressurizer refill at the end of the experiment.

Some temperatures and differential pressures were missing from the submissions.

4.3.5 Other codes: (SCDAP/RELAP5/MOD2, RELAP4/MOD6, DINAMIKA, TECH-M-4)

The initial conditions were well calculated by all participants. BARC(R4M6) calculation starts from 605 s. The downcomer mass flow rate in BARC(R4M6) and the SG tube fluid temperatures in BARC(R4M6) and OKB GP (TM-4) calculations were not satisfactory. In BARC(R4M6) calculation all three loops are lumped together and in RSC KI (SR5M2) calculation the loops without pressurizer are lumped together.

During the first draining (1200 s) the coolant is discharged from the pressurizer in all calculations, and no significant void exists in the upper plenum. During the stationary phase OKB GP (TM-4) predicts that the pressurizer is refilled as void is accumulated in the upper plenum. The downcomer mass flow rate does not change after the first draining, except that it increases by 10% in OKB GP (TM-4) calculation.

The second draining (2100 s) causes delayed stagnation in RSC KI (SR5M2) calculation. Others do not indicate any stagnation. The reasons for this is the primary level, which does not reach the hot leg connections during this period. Mass flow predictions do not agree well with measured data during the rest of the transient.

After the third draining (3000 s) the calculated pressure behaviour is close to the measured data in both OKB GP calculations. In RSC KI (SR5M2) calculation the third draining does not decrease the primary pressure sufficiently, and in BARC(R4M6) calculation the primary pressure even increases after the draining.

Timing of the core heatup is well predicted only by OKB GP (TM-4).

Missing information on the water levels and differential pressures makes it difficult to compare all these results.

5. PARTICIPANTS OF POSTTEST CALCULATIONS

5.1 Participants

Thirteen foreign organizations participated in the second workshop of ISP33 on May 17-19 1993. This was also the dead-line for the posttest calculations. In addition, two organizations submitted their posttest results without participating the second workshop. A list of participants is presented in Table 5.1. This table also includes code and computer statistics, when available.

Twenty posttest calculations were received from fourteen organizations: HTWS Zittau (Germany), SEMAR LEACS (France), TAEK (Turkey) with two calculations, NRI Rez (Czech Republic), NPPRI (Slovakian Republic) with two calculations, FRG/FZR (Germany), IJS (Slovenia) with two calculations, Siemens (Germany), ECN (The Netherlands), GRS (Germany), PSI (Switzerland), UP-DCMN (Italy), JAERI (Japan) with two calculations and RRC KI (Russia) with three calculations. Numerical results from some organizations were not received to be included in the comparison plots. From organizations which submitted several results as sensitivity studies, only one result of a code is selected for comparison. Sensitivity studies are included in reports by participants in Volume II of this report.

The codes used for posttest calculations were ATHLET Mod 1.0, CATHARE2, RELAP5/MOD2, RELAP5/MOD3 and SCDAP/RELAP5/MOD2. Descriptions of these codes are presented in Chapter 3.2.

Table 5.1 ISP33 participants of posttest calculations (1/3)

Participant	ECN (The Netherlands), post	HTWS Zittau(Germany), post
Name	H. Roodbergen	B. Vandreier
Organization	Netherlands Energy Research	Hochschule für Technik, Wirtschaft und
	Foundation ECN	Sozialwesen Zittau/Görlitz (FH)
Address	P.O. Box 1	Theodor-Körner-Allee 16
City/State	1755 ZG Petten	FGE 7, Zittau
Zip Code		O-8800
Country	The Netherlands	Germany
Phone Number	+31 2246 4551	+03583 61674
Fax Number	+31 2246 3490	+03583 61627
Telex	57211 REACP NL	
Computer	**IBM RS6000, type 320H**	**IBM RISC 6000 MOD 320**
CPU / Real Time	54848 s/ 7846 s (6.99)	-
Code	**RELAP5/MOD2.5**	**ATHLET Mod 1.0 Cycle E**
Model Descr.		
Volumes	306	-
Junctions	313	-
Heat slabs	385	-
Received	28.Aug.93	17.May.93
Participant	**FRG/FZR (Germany), post**	**IJS (Slovenia),post**
Name	E. Krepper	I. Parzer, S. Petelin, O. Gortnar, B. Mavko,
Organization	Research Center Rossendorf Inc.	Institute "Jozef Stefan"
Address	POB 19	Jamova 39
City/State	D-O-8051 Dresden	61111 Ljubljana
Zip Code		
Country	Germany	Slovenia
Phone Number	(0351) 591/3460	+3861 371 321
Fax Number	(0351)4605812	+3861 374 919
Telex		31296 YU JOSTIN
Computer	**Sun-Workstation SPARC 10**	**SUN Sparc 2**
CPU / Real Time	400000s / 7850 s (50.45)	-
Code	**ATHLET mod 1.0 E**	**RELAP5/MOD2/36.05**
Model Descr.		
Volumes	316	220
Junctions	262	237
Heat slabs	256	259 (1263 Mesh points)
Mailing date	17.May.93	17.May.93
Participant	**GRS (Germany) & RSC KI (Russia)**	**IJS (Slovenia), post**
Name	J. Steinbom, S. Nikonov	I. Parzer, S. Petelin, O. Gortnar, B. Mavko,
Organization	Gesellschaft für Anlagen- und	Institute "Jozef Stefan"
	Reaktorsicherheit (GRS) mbH	
Address	Kurfürstendamm 200	Jamova 39
City/State	D-1000 Berlin 15	61111 Ljubljana
Zip Code		
Country	Germany	Slovenia
Phone Number	+0 30 88 41 89 27	+3861 371 321
Fax Number	+0 30 88 23 655	+3861 374 919
Telex		31296 YU JOSTIN
Computer	**IBM ES/9000**	**SUN Sparc 2**
CPU / Real Time	327000 s/ 7680.3 s (42.58)	-
Code	**ATHLET Mod 1.0 Cycle E**	**RELAP5/MOD3 5m5**
Model Descr.		
Volumes	212	220
Junctions	232	237
Heat slabs	228	259 (1263 Mesh points)
Mailing date	27.Aug.93	17.May.93

Table 5.1 ISP33 participants of posttest calculations (2/3)

Participant	JAERI (Japan), post	NRI (Czech Republic), post
Name	Y. Kukita	P. Král
Organization	Japan Atomic Energy Research Institute	Nuclear Research Institute
Address	Tokai-Mura	
City/State	Naga-Gun	25068 Rez
Zip Code	Ibaraki-Ken	
Country	319-11, Japan	Czech Republic
Phone Number	+(81) 292 82 5263	+42 2 685 8351
Fax Number	+(81) 292 82 5408	+42 2 685 7567
Telex		
Computer	**FACOM VP-2600**	**HP Apollo 720**
CPU / Real Time	2509 s/ 7000 s (0.36)	103587 s/ 9082s (11.40)
Code	**RELAP5/MOD2**	**RELAP5/MOD3/5m5**
Model Descr.		
Volumes	193	272
Junctions	208	317
Heat slabs	217	366 (1649 Mesh points)
Received	5.May.93	17.May.93
Participant	**NPPRI (Slovakia), post**	**PSI (Switzerland), post**
Name	P. Matejovic, L. Vranka	F. De Pasquale
Organization	Nuclear Power Plant Research Institute	Paul Scherrer Institute
		Thermal-Hydraulics Laboratory
Address	Okruzna 5	
City/State	918 64 Trnava	CH-5232 Villigen PSI
Zip Code		
Country	Slovakia	Switzerland
Phone Number	+42 805 41741	+056 99 27 26
Fax Number	+42 805 25396	+056 98 23 27
Telex	Cs-93851	827417 psi ch
Computer	**PC PPS (INTEL486/33)**	**CRAY-X/MP**
CPU / Real Time	120361 s/ 7590 s (15.85)	-
Code	**RELAP5/MOD3/5M5**	**RELAP5/Mod2.5**
Model Descr.		
Volumes	287	-
Junctions	304	-
	317 (1921 Mesh points)	-
Received	17.May.93	12.Jul.93
Participant	**NPPRI (Slovakia), post**	**RRC KI (Russia), post**
Name	P. Matejovic, L. Vranka	A. Nikonov, S. Spolitak
Organization	Nuclear Power Plant Research Institute	Russian Research Center Kurchatov Institute
		RRC KI
Address	Okruzna 5	Nuclear Reactors Institute, Kurchatov Square, 1
City/State	918 64 Trnava	123182 Moscow
Zip Code		
Country	Slovakia	Russia
Phone Number	+42 805 41741	+7 095 196 61 72
Fax Number	+42 805 25396	+7 095 196 61 72
Telex	Cs-93851	411594 shuga
Computer	**PC PPS (INTEL486/33)**	**Cyber-963**
CPU / Real Time	105148 s/ 7570 s (13.89)	48189 s/7827 s (6.16)
Code	**RELAP5/MOD2/RMA**	**SCDAP/RELAP5/MOD2**
Model Descr.		
Volumes	287	149
Junctions	304	153
Heat slabs	317 (1921 Mesh points)	183 (549 Mesh points)
Received	17.May.93	25.Apr.93

Table 5.1 ISP33 participants of posttest calculations (3/3)

Participant	RRC KI (Russia), post	TAEK (Turkey), post
Name	A. S. Devkin, E.D. Derbyshire	A. Tanrikut
Organization	Russian Research Center Kurchatov Institute	Turkish Atomic Energy Authority
	RRC KI	
Address	Nuclear Reactors Institute, Kurchatov Square, 1	PK 249, Kavaklidere
City/State	123182 Moscow	06693 Ankara
Zip Code		
Country	Russia	Turkey
Phone Number	+7 095 196 61 72	+90 312 212 76 65
Fax Number	+7 095 196 66 39	+90 312 223 44 39
Telex	411594 shuga	ATOM TR 46459
Computer	**IBM PC/AT-386 "GEO" model**	**IBM RISC 6000 - Model 320**
CPU / Real Time	458588 s/ 8819 s (52.00)	100270 s/ 7785 s (12.88)
Code	**RELAP5/MOD3 version 5m5**	**RELAP5/MOD3 (v5m5)**
Model Descr.		
Volumes	265	176
Junctions	284	186
Heat slabs	223 (1030 Mesh points)	176
Received	17.May.93	17.May.93
Participant	**SEMAR LEACS (France), post**	**UP-DCMN (Italy), post**
Name	E. Laugier, L. Sabotinov	W. Ambrosini, S. Belsito,
		F. D'Auria, M. Frogheri
Organization	Centre de Cadarache	University of Pisa, Department of
		Mechanical and Nuclear Engineering
Address	13108 Saint-Paul -Lez-Durance CEDEX	Via Diotisalvi 2
City/State		56126 Pisa
Zip Code		
Country	France	Italy
Phone Number	+33 42 25 39 47, +33 42 25 78 60	+39 50 585 253
Fax Number	+33 42 25 63 99	+39 50 585 265
Telex	440 678 F	500104 (I)
Computer	-	**IBM 9121/440**
CPU / Real Time		128350 s/ 6942 s (18.49)
Code	**CATHARE2 V1.3e**	**CATHARE 2 V1.3E**
Model Descr.		
Volumes	-	47 hydr. compon. 644 hydr. meshes
Junctions	-	50
Heat slabs	-	42
Received	17.May.93	17.May.93
Participant	**Siemens (Germany), post**	**VTT (Finland), post**
Name	M. Protze	V. Riikonen
Organization	Siemens AG/ Power Generation Group (KWU)	Technical Research Centre of Finland
		Nuclear Engineering Laboratory
Address	Hammerbacherstrasse 12 + 14, P.O.Box 3220	P.O. Box 20
City/State	8520 Erlangen	53851 Lappeenranta
Zip Code		
Country	Germany	Finland
Phone Number	+49 9131 18 - 5474	+358 53 571 2376
Fax Number	+49 9131 18 - 4345	+358 53 571 2379
Telex	62929 slk d	
Computer	**HP Apollo 730**	**HP 9000/735**
CPU / Real Time	56000 s/ 7800 s (7.18)	-s/ 7905 s (-)
Code	**RELAP5/MOD2.5**	**RELAP5/MOD3**
Model Descr.		
Volumes	345	224
Junctions	358	185
Heat slabs	367 (1807 Mesh points)	381
Received	6.Apr.93	-

6. COMPARISONS OF POSTTEST CALCULATIONS

6.1 Introduction

Twenty posttest calculations were submitted. The reports are included in Volume II of this report. The comparisons of the calculated results and the experimental data are presented below.

6.2 Comparisons of Posttest Calculations with the Experimental Results

6.2.1 Comparison plots (ATHLET)

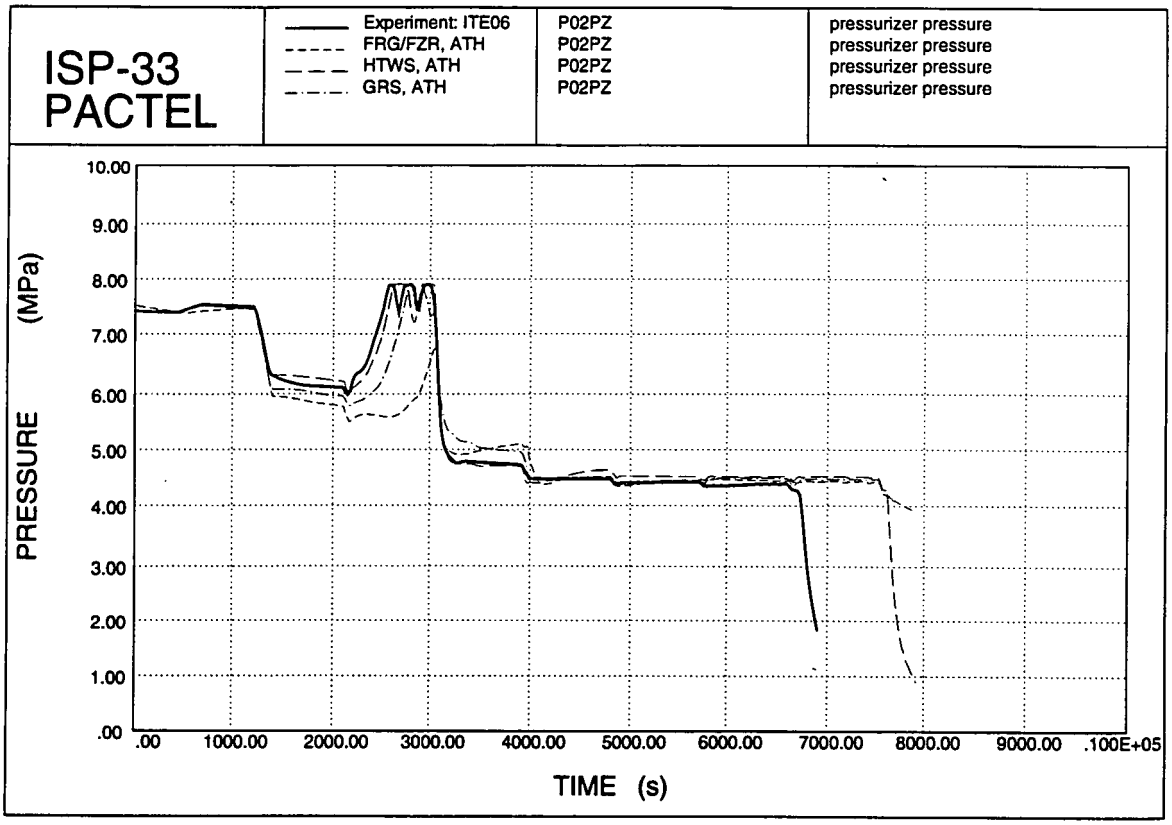

Figure 6.1. Pressurizer pressures.

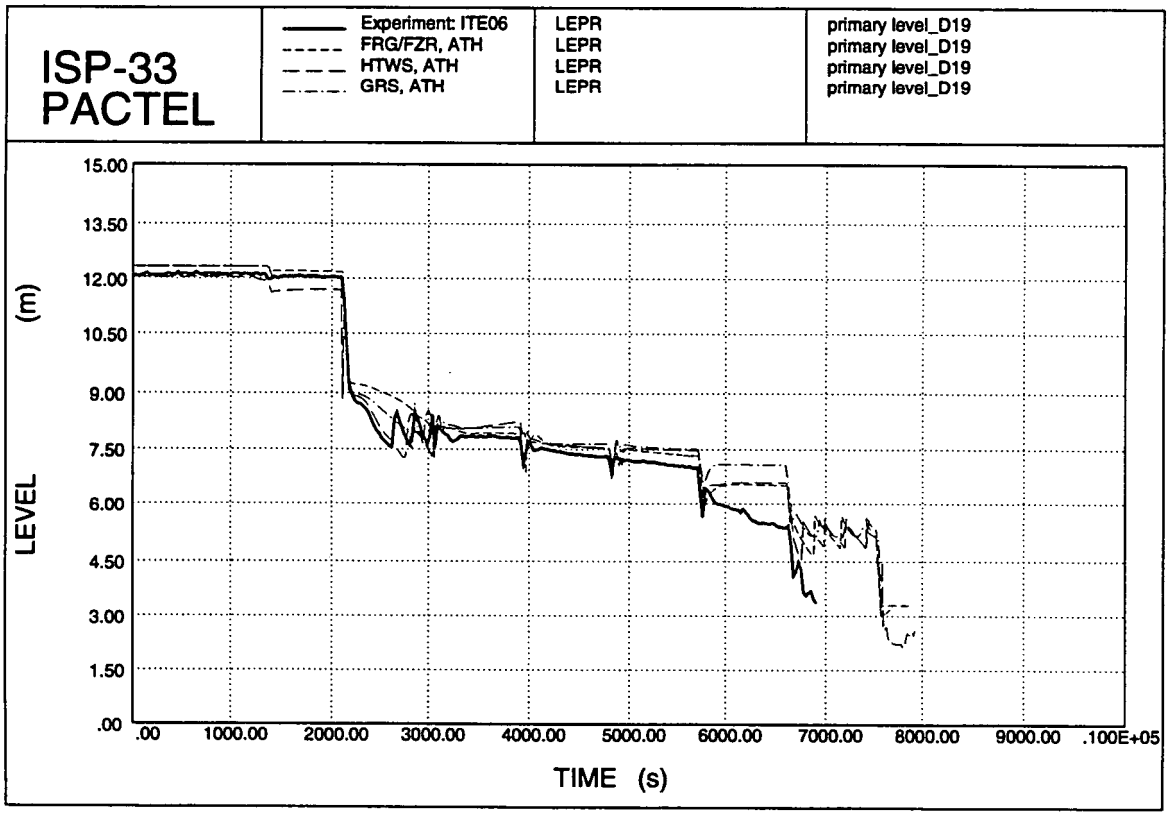

Figure 6.2. Primary levels.

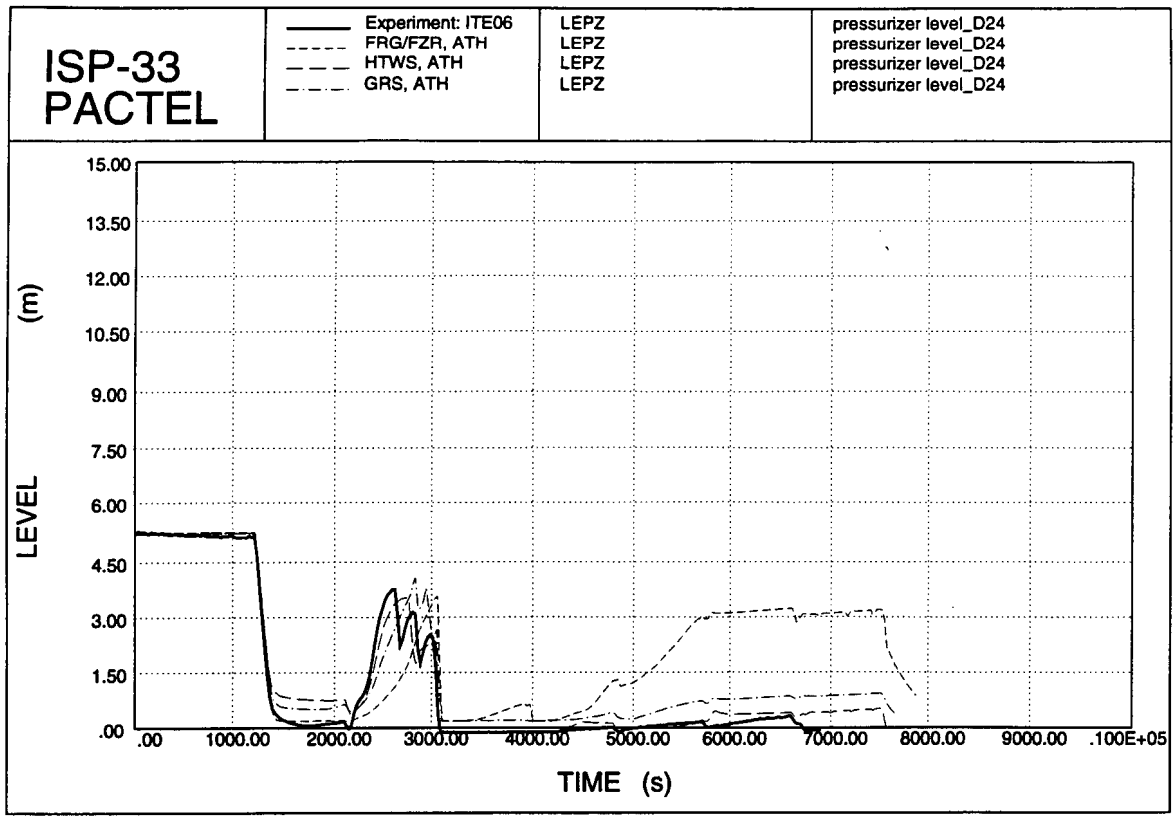

Figure 6.3. Pressurizer levels.

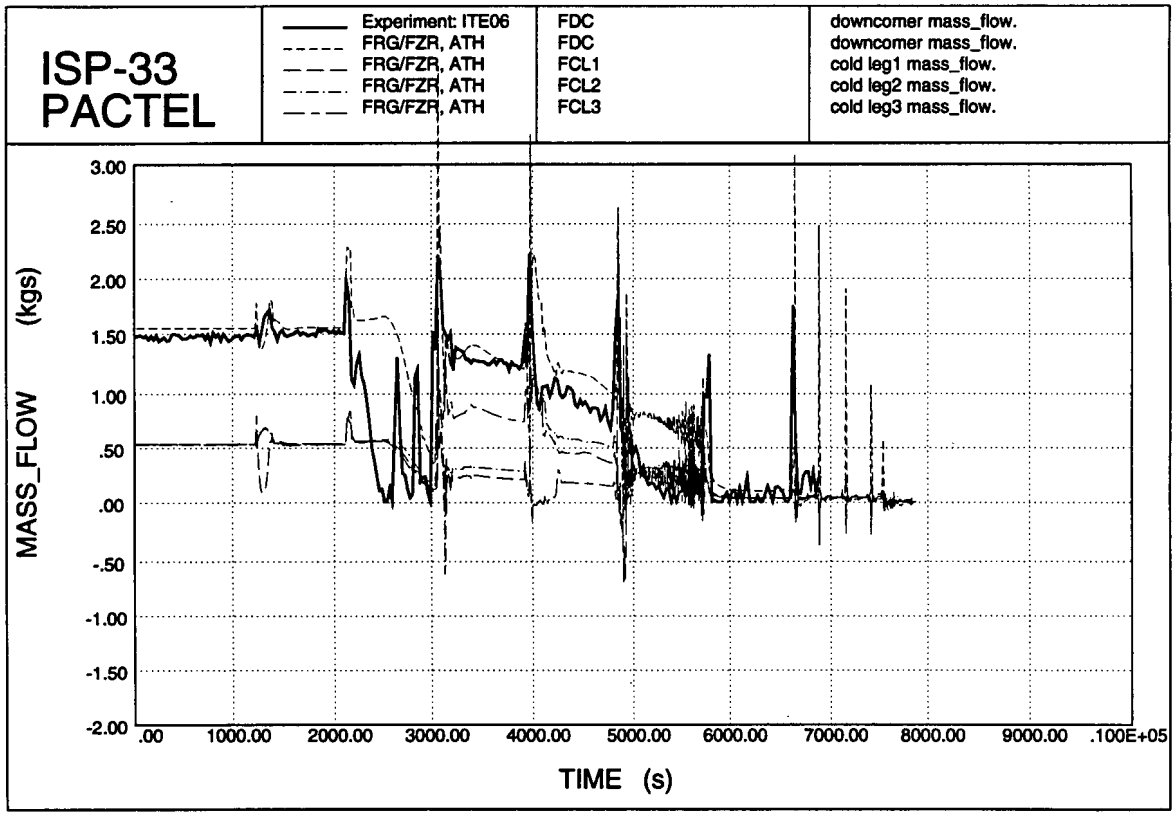

Figure 6.4. Primary mass flows.

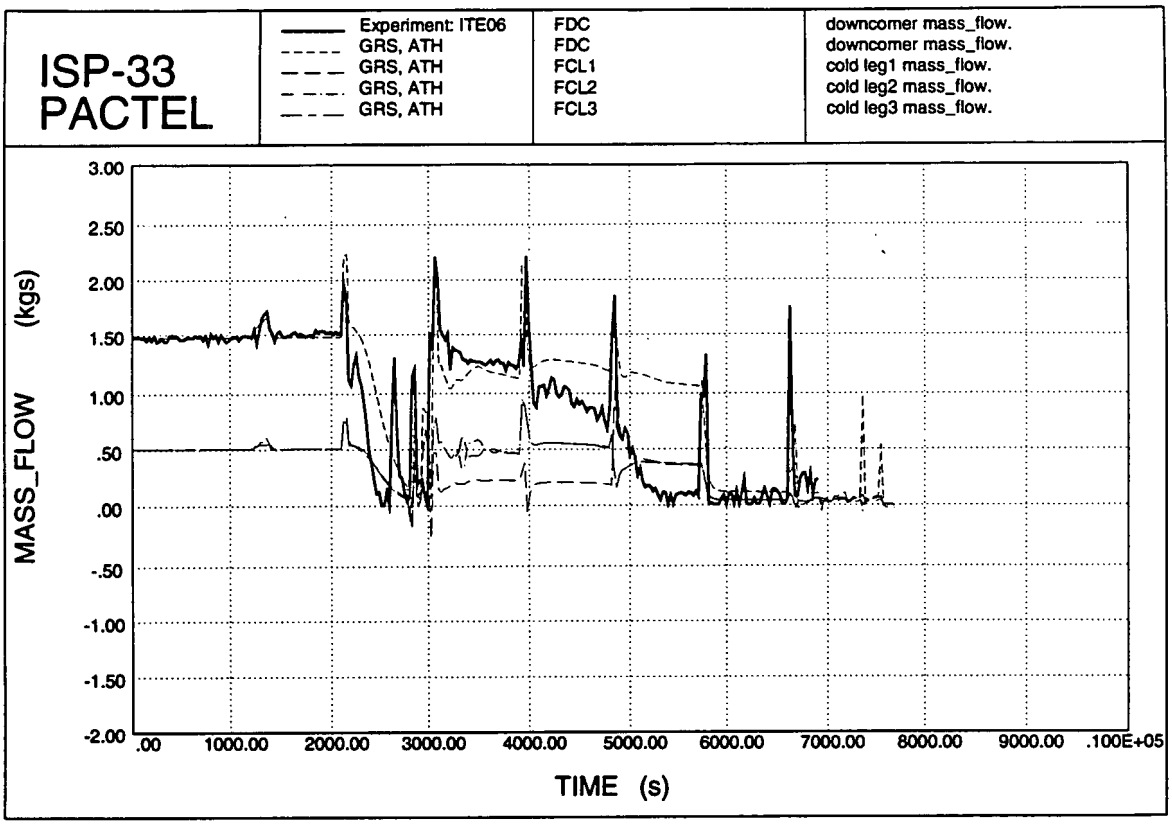

Figure 6.5. Primary mass flows.

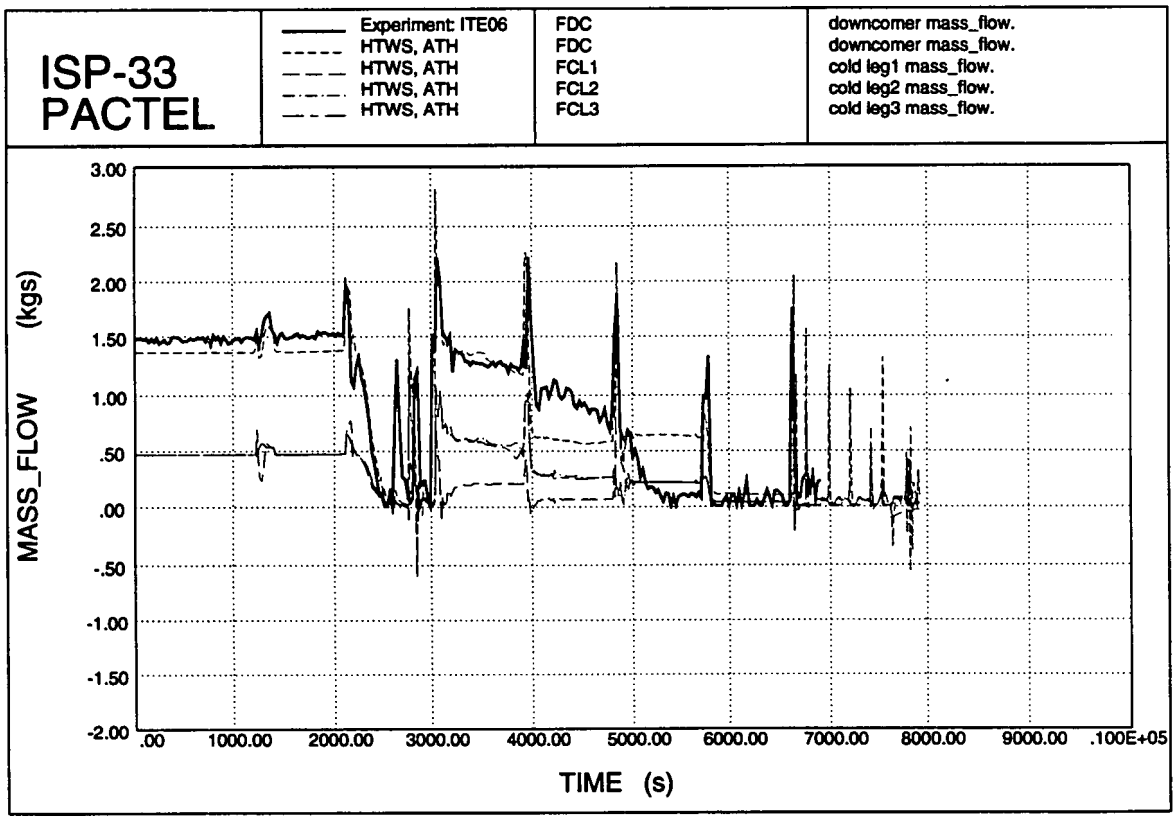

Figure 6.6. Primary mass flows.

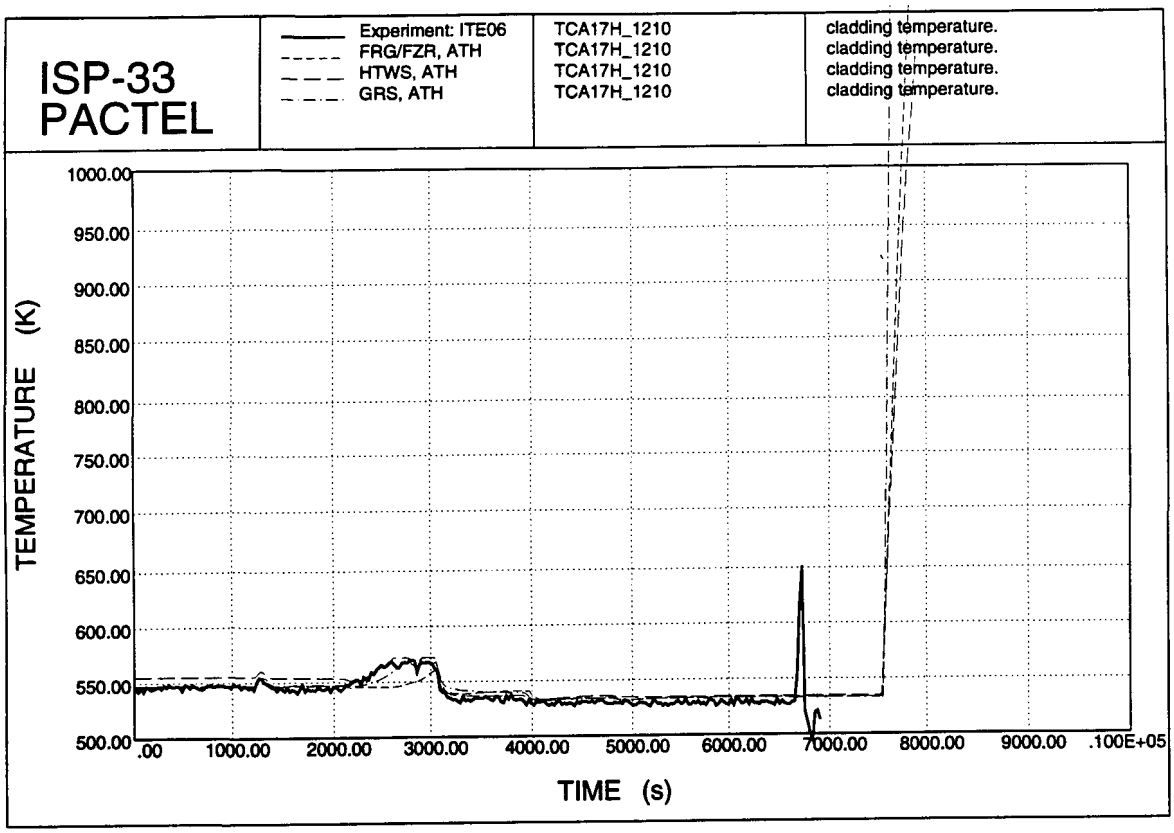

Figure 6.7. Cladding temperatures.

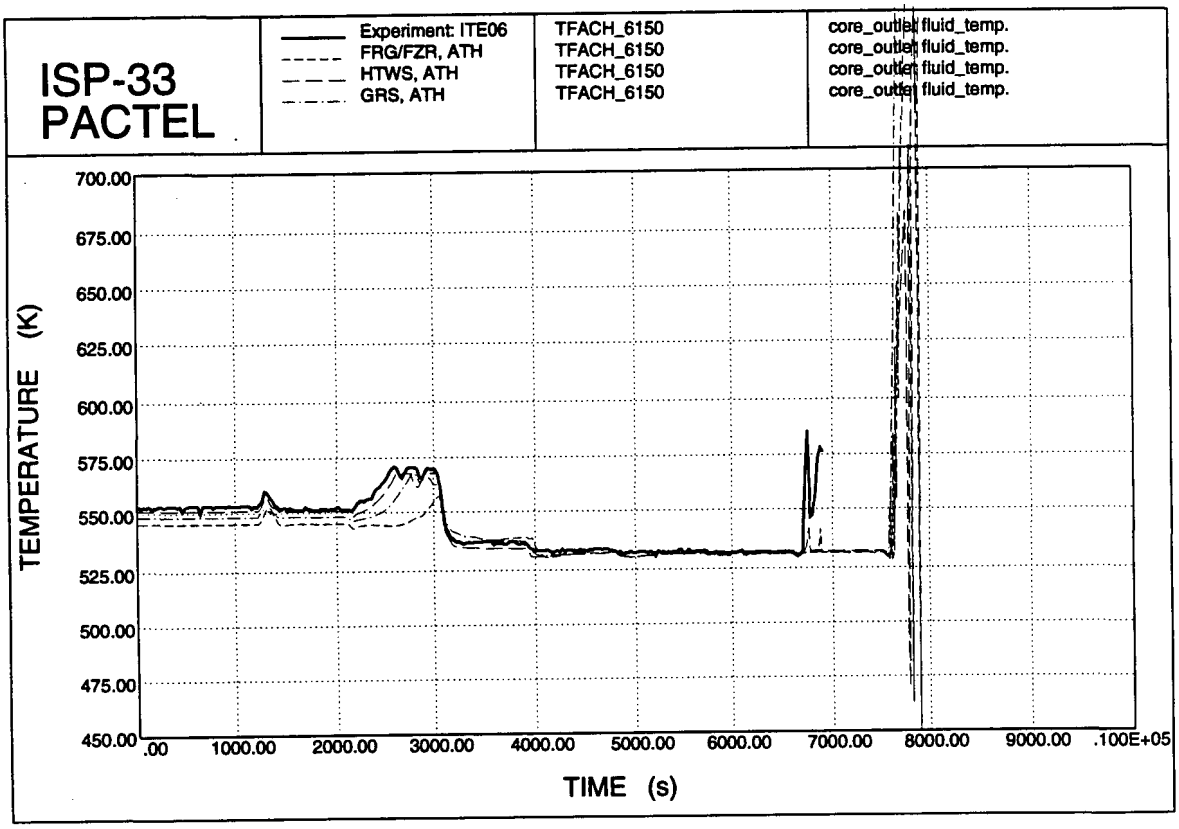

Figure 6.8. Core outlet coolant temperature.

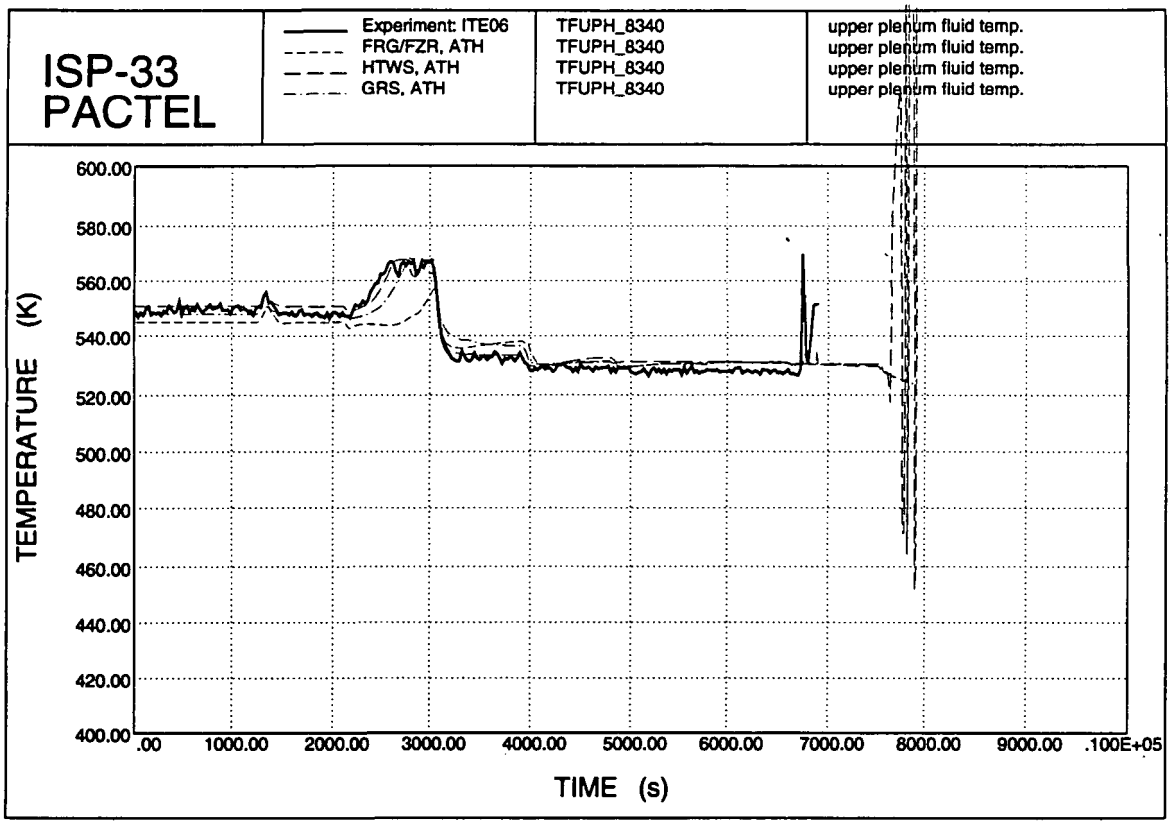

Figure 6.9. Upper plenum temperatures.

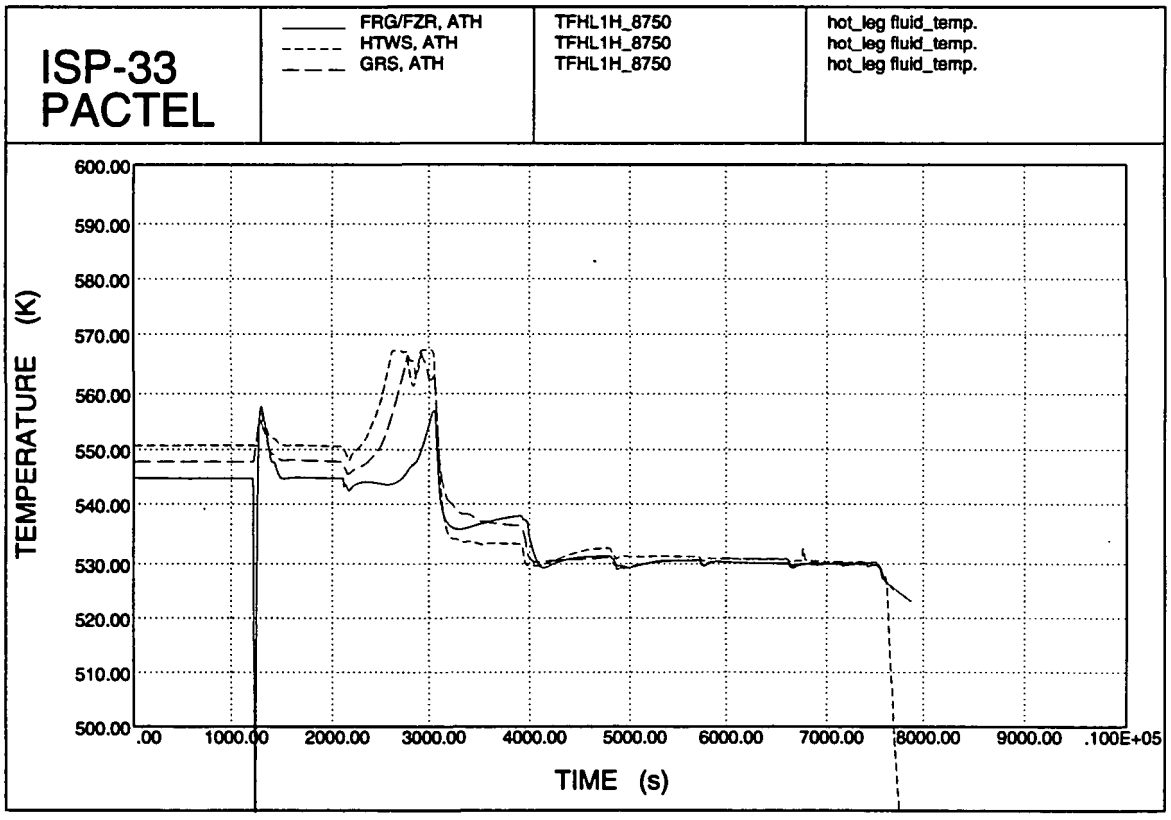

Figure 6.10. Hot leg temperatures.

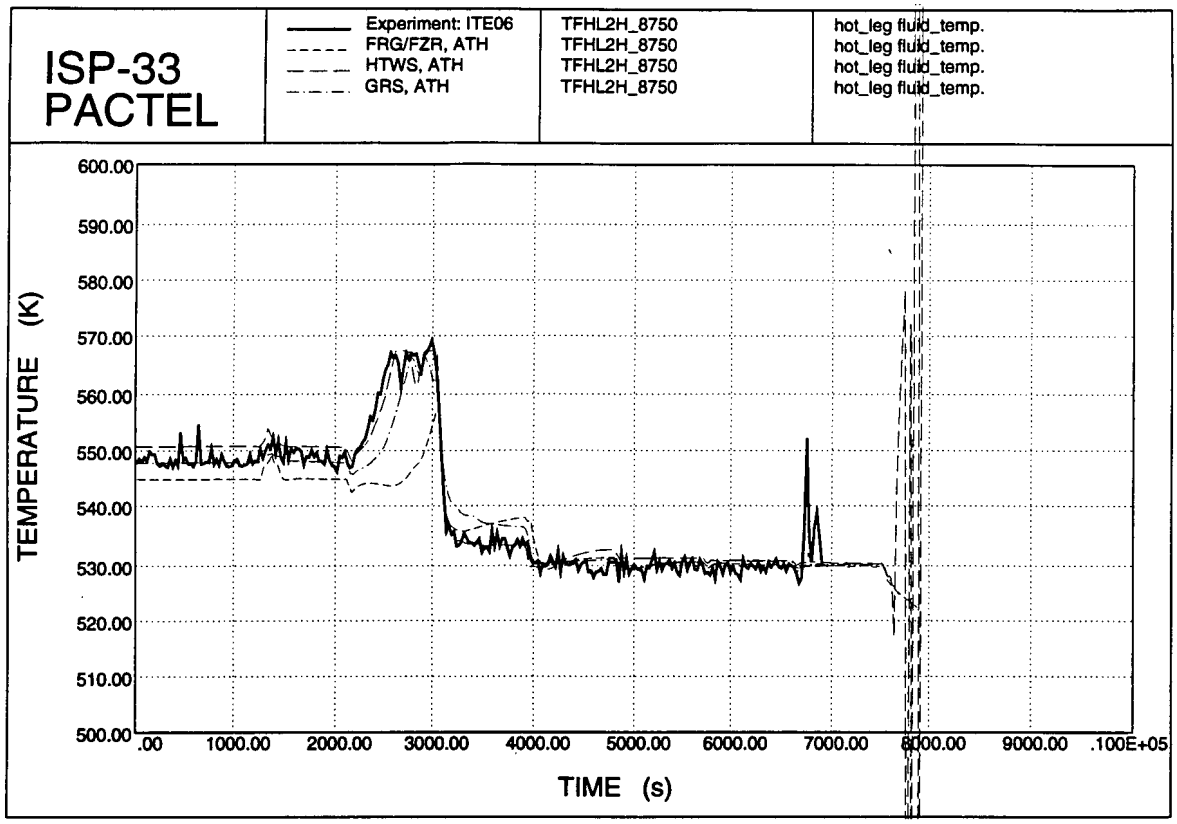

Figure 6.11. Hot leg temperatures.

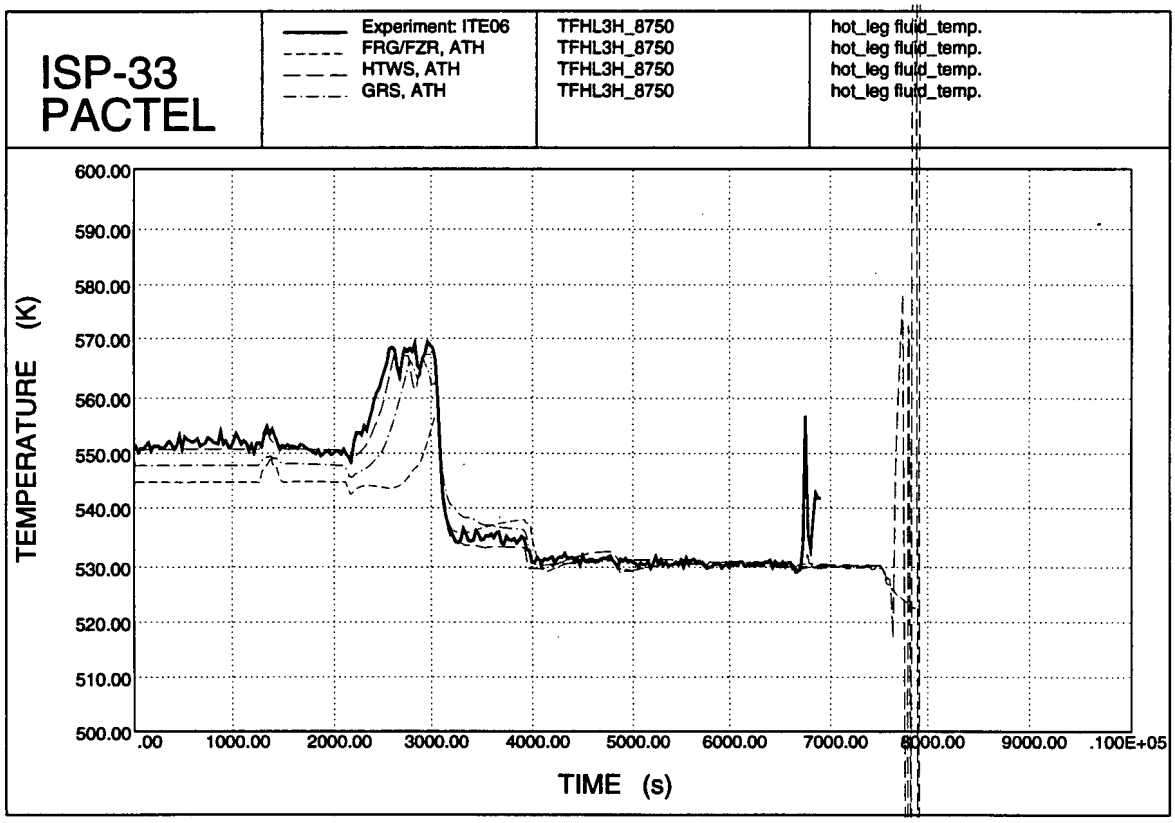

Figure 6.12. Hot leg temperatures.

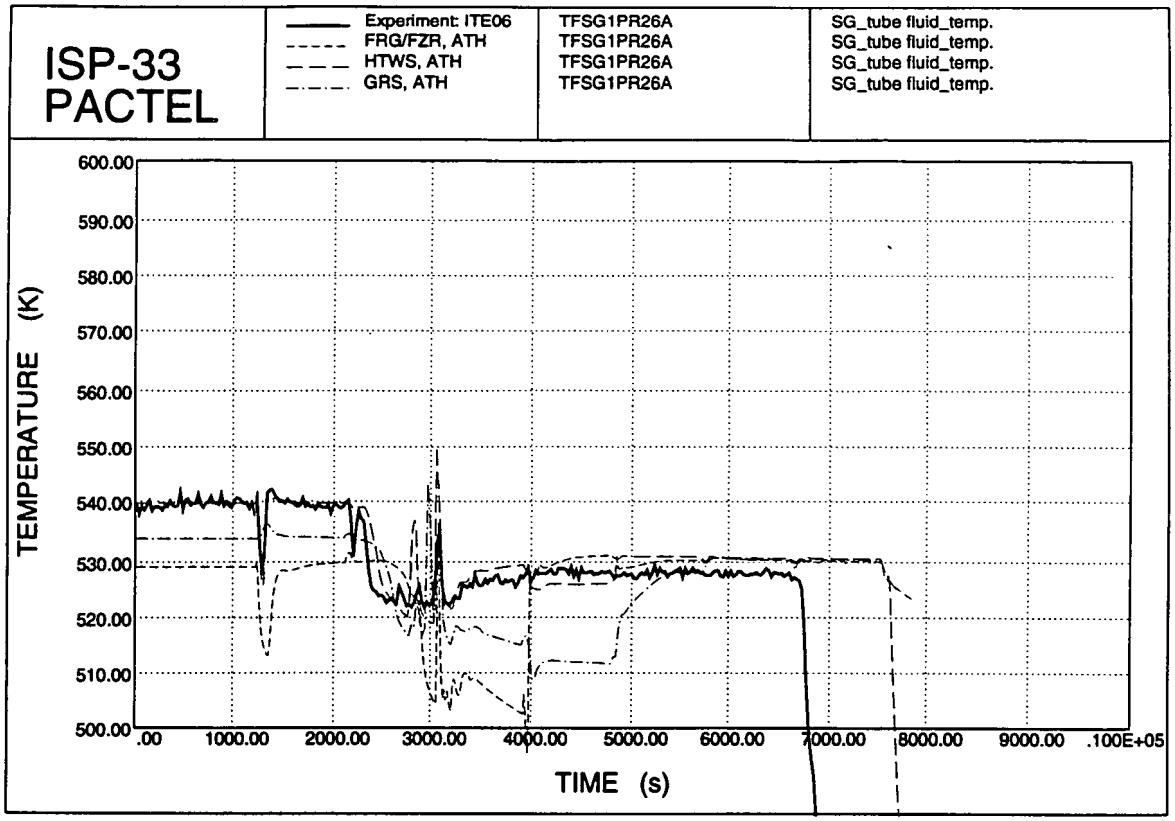

Figure 6.13. SG tube fluid temperatures.

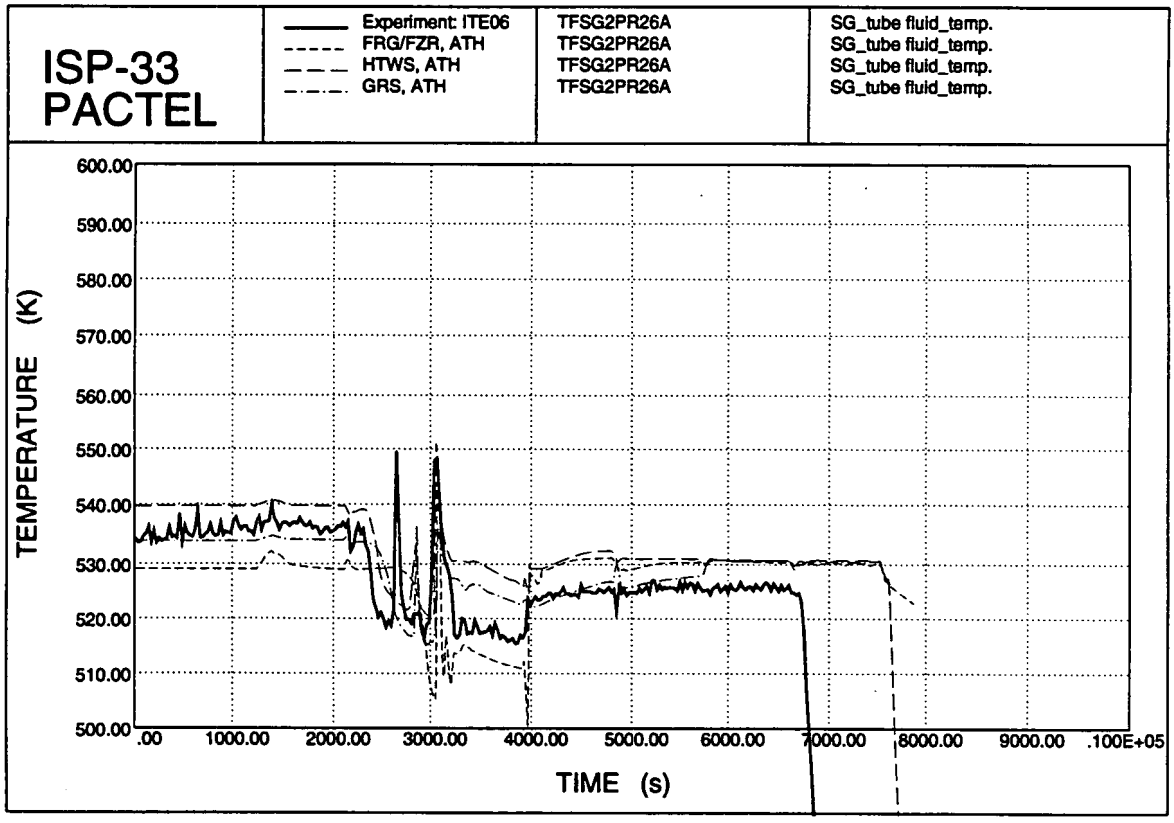

Figure 6.14. SG tube fluid temperatures.

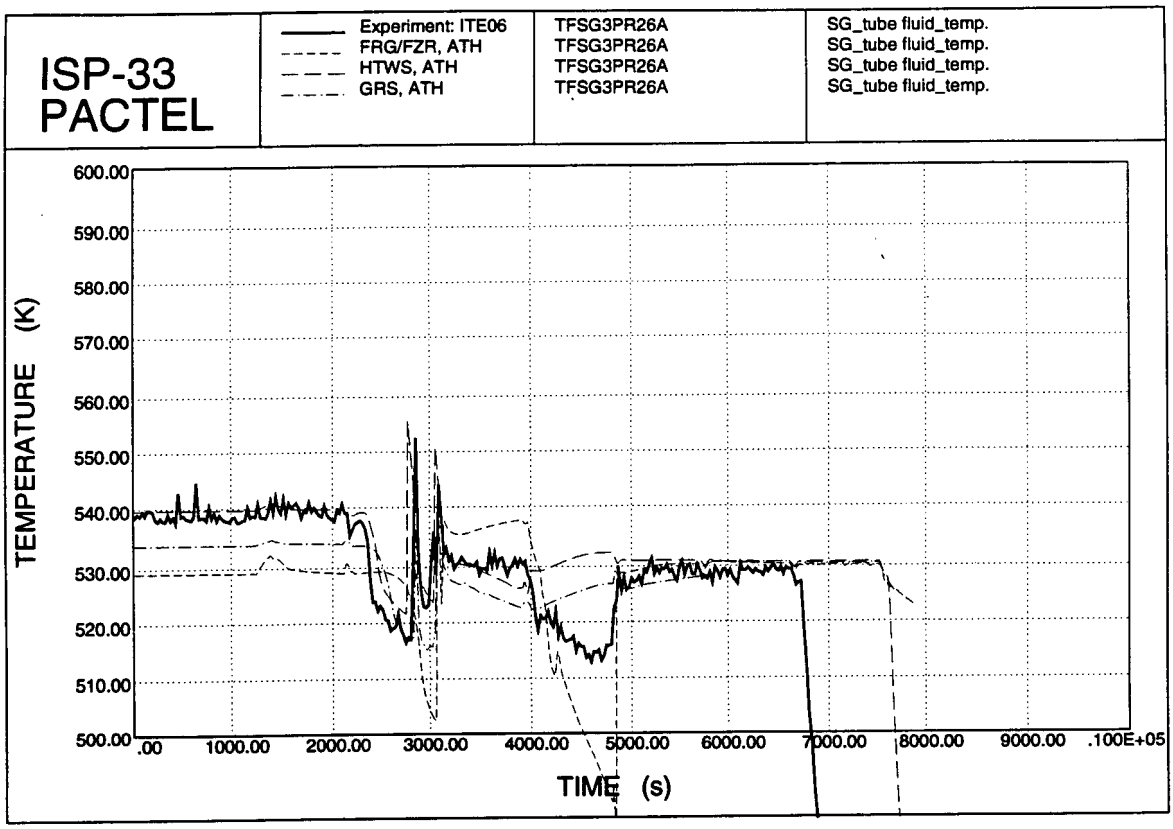

Figure 6.15. SG tube fluid temperatures.

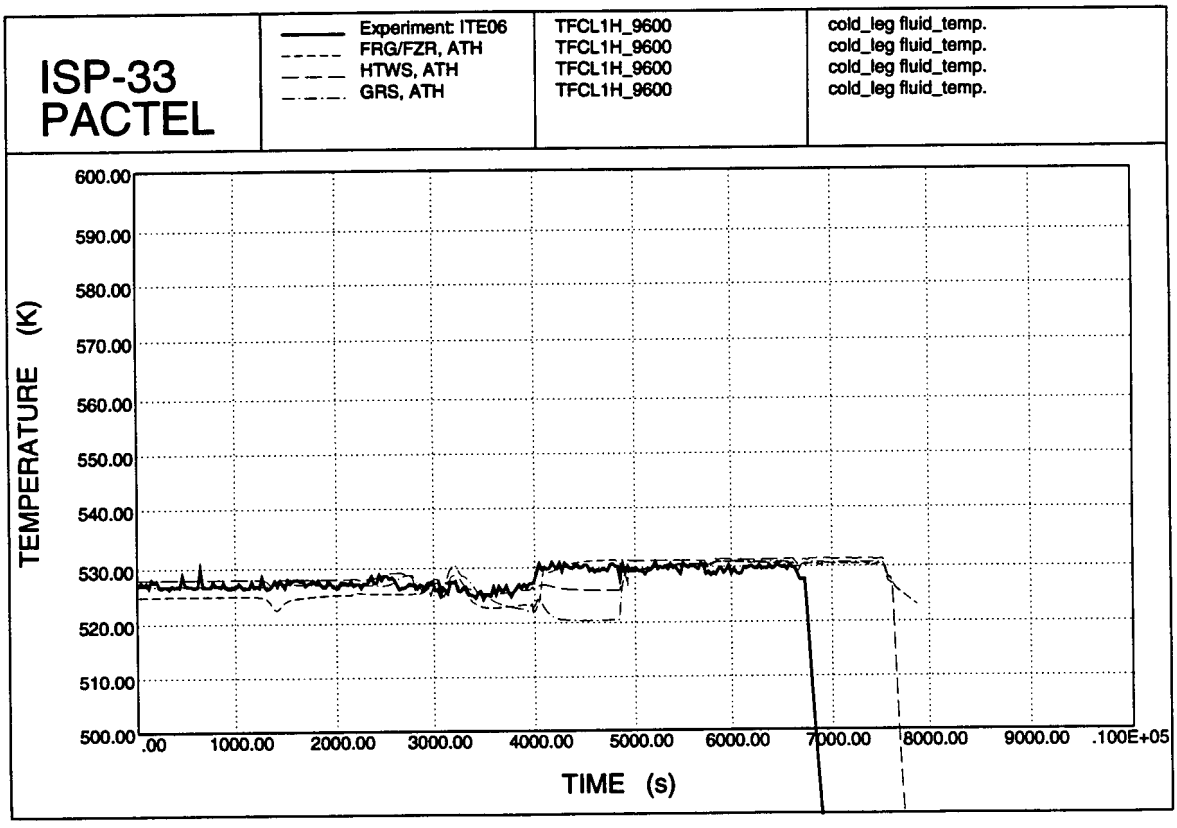

Figure 6.16. Cold leg temperatures.

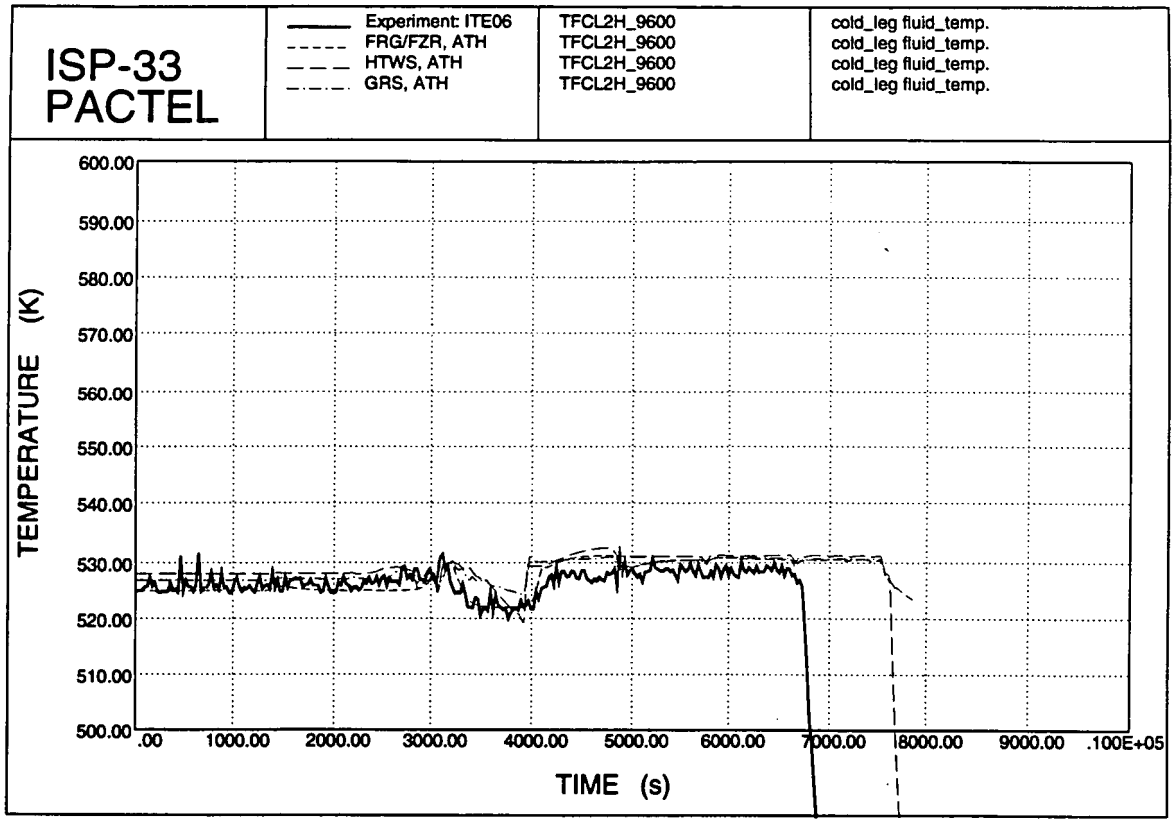

Figure 6.17. Cold leg temperatures.

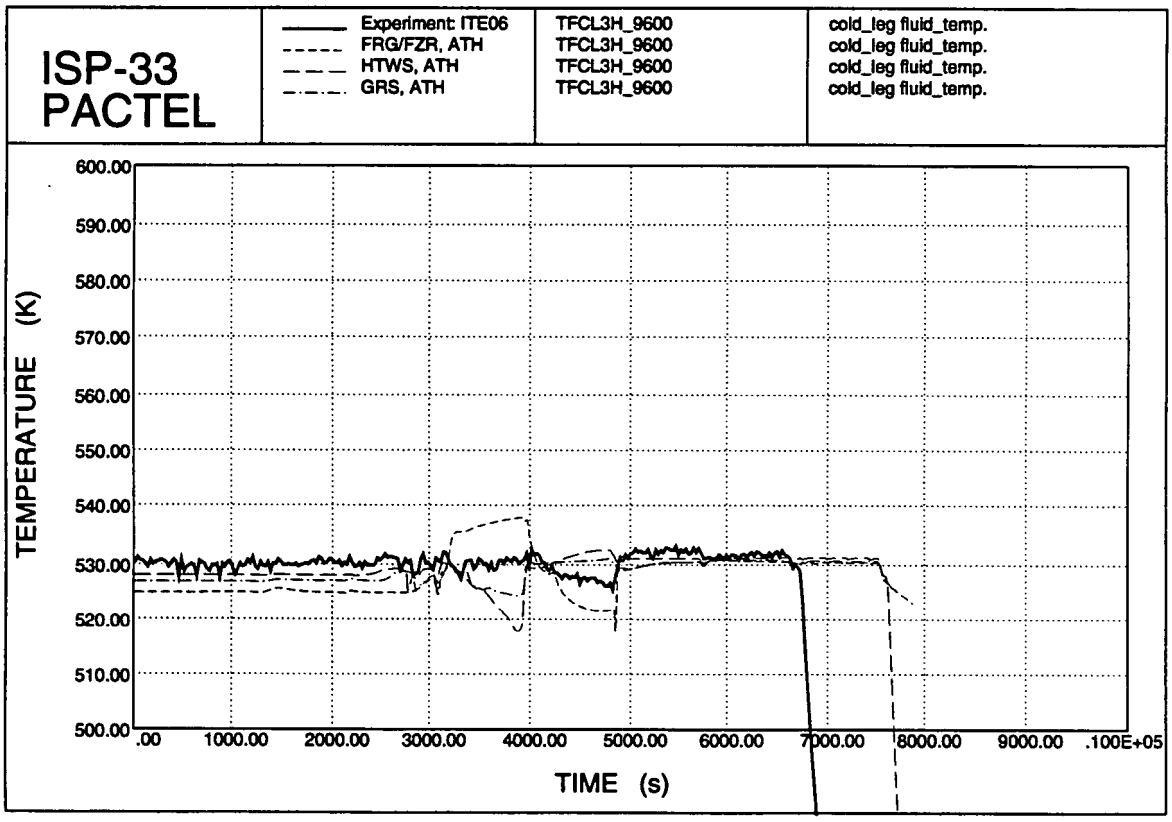

Figure 6.18. Cold leg temperatures.

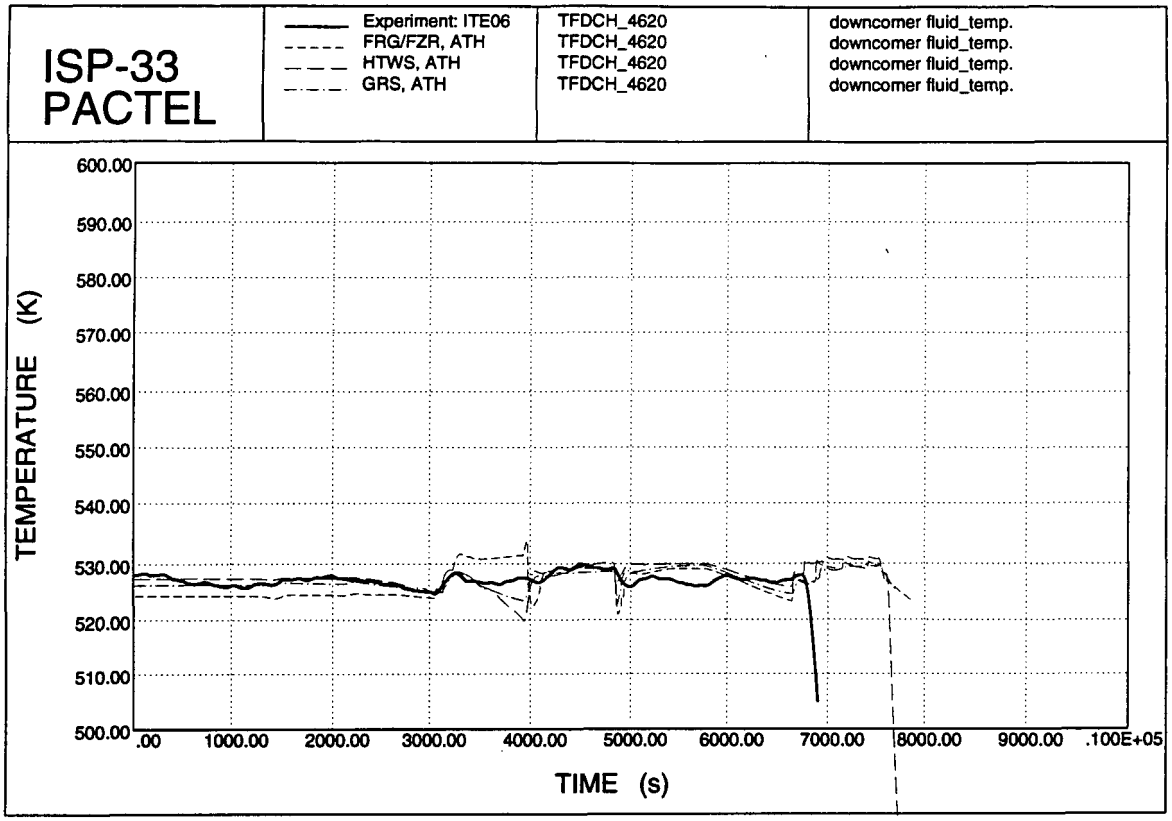

Figure 6.19. Downcomer temperatures.

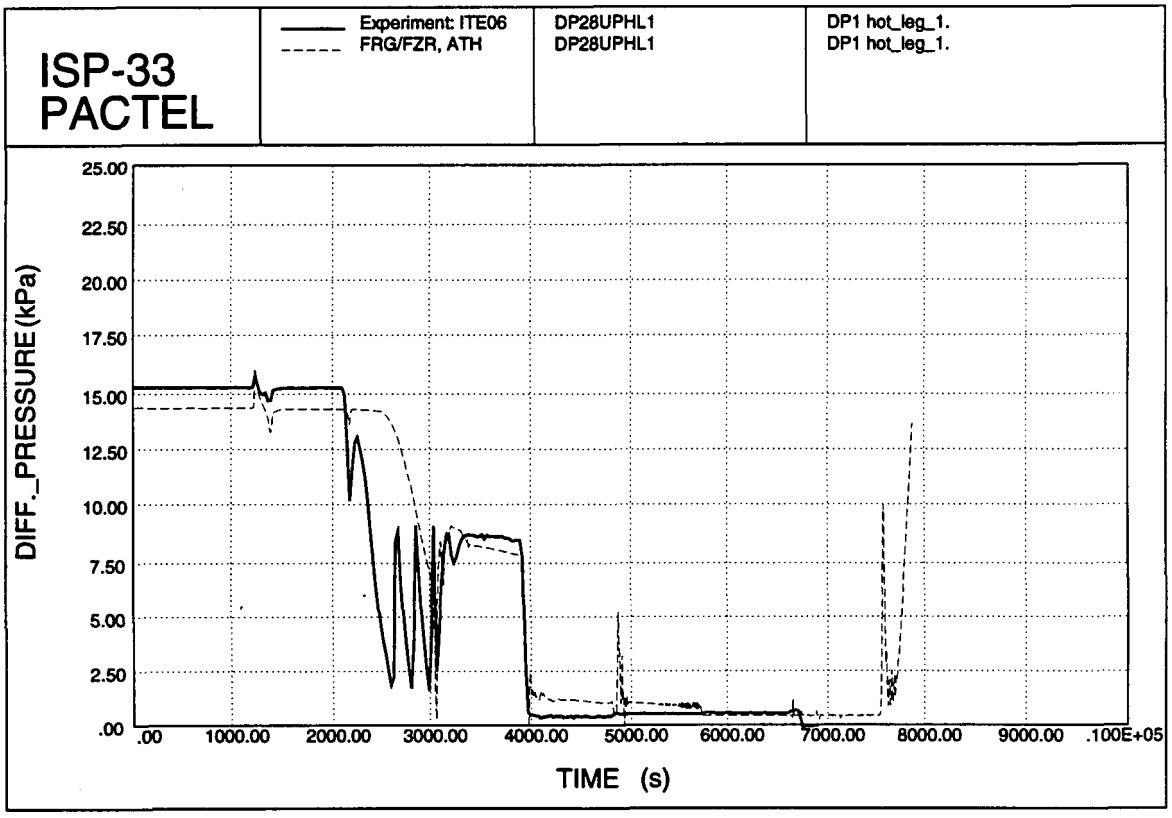

Figure 6.20. Hot leg 1 DP 1.

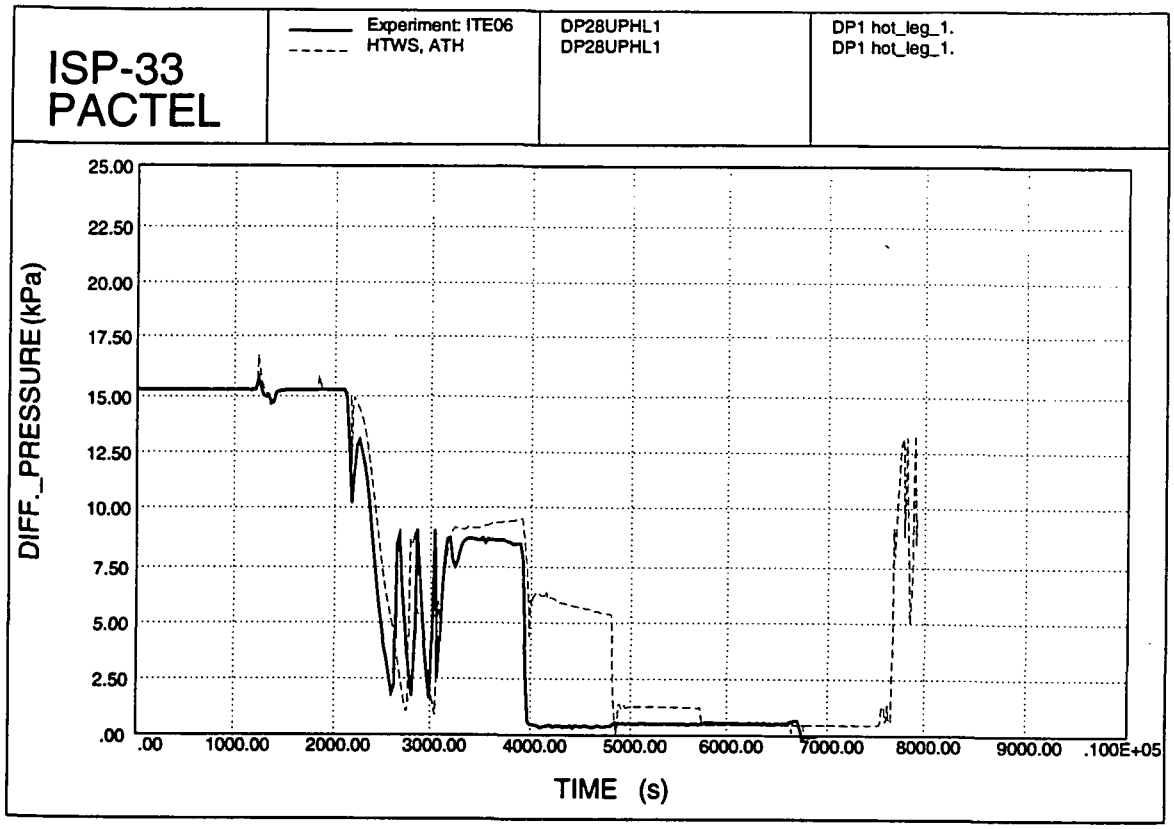

Figure 6.21. Hot leg 1 DP 1.

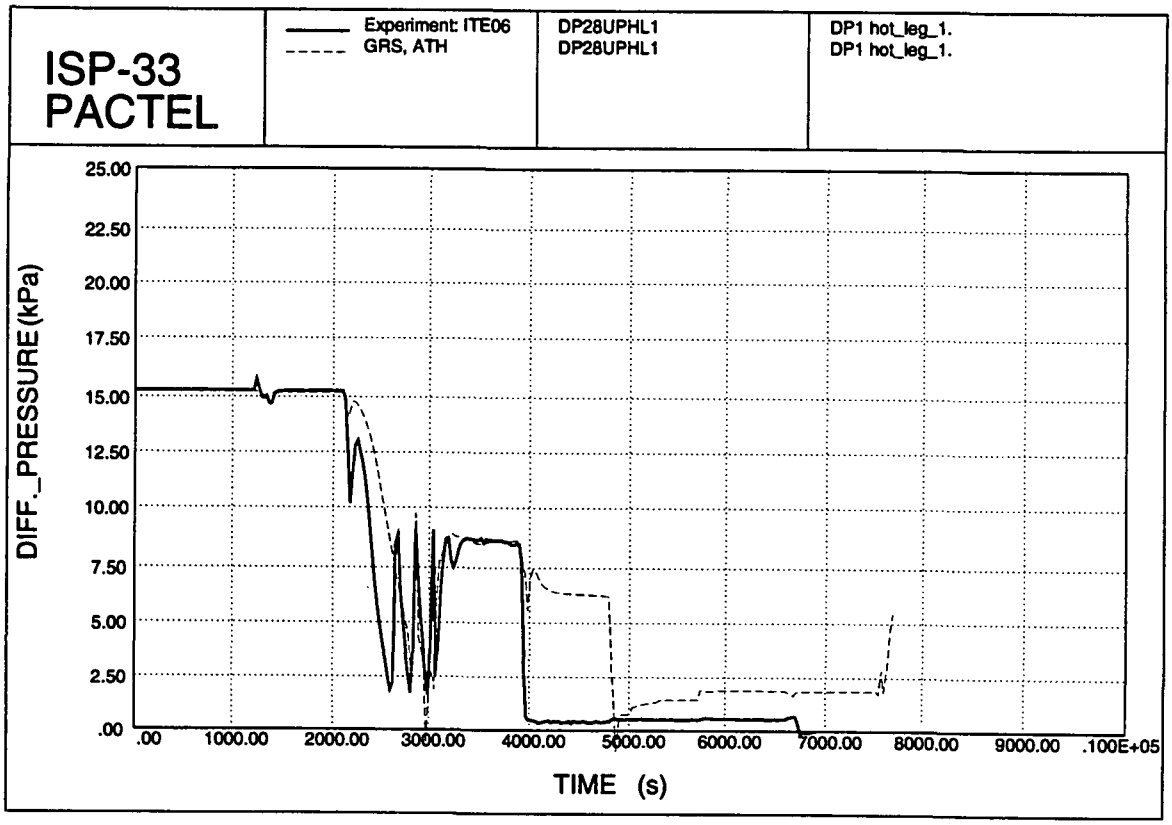

Figure 6.22. Hot leg 1 DP 1.

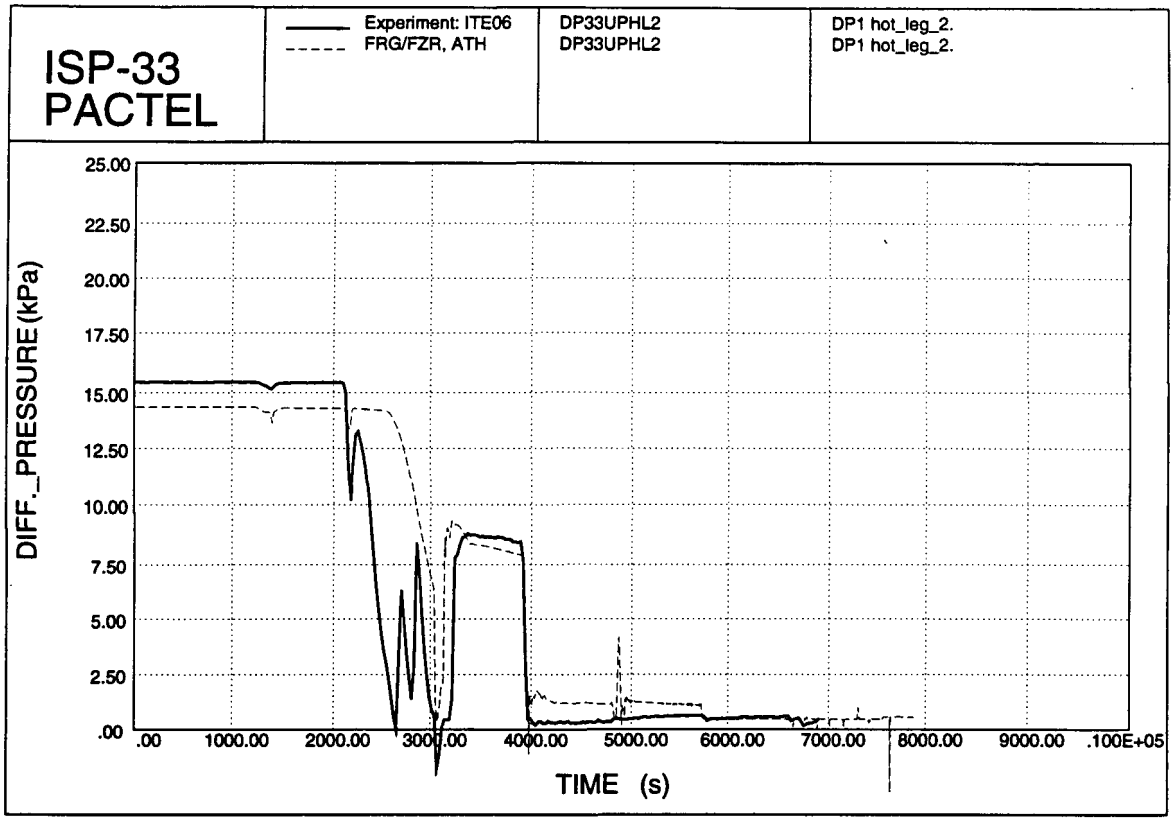

Figure 6.23. Hot leg 2 DP 1.

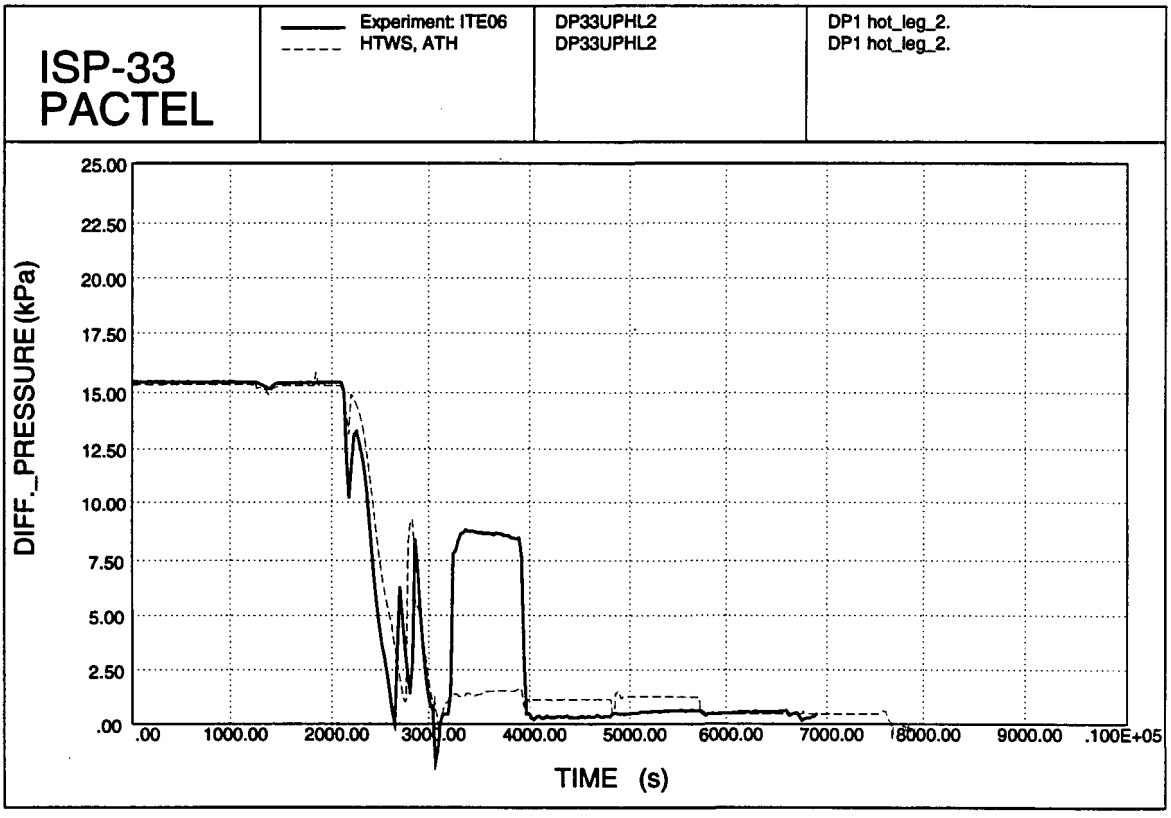

Figure 6.24. Hot leg 2 DP 1.

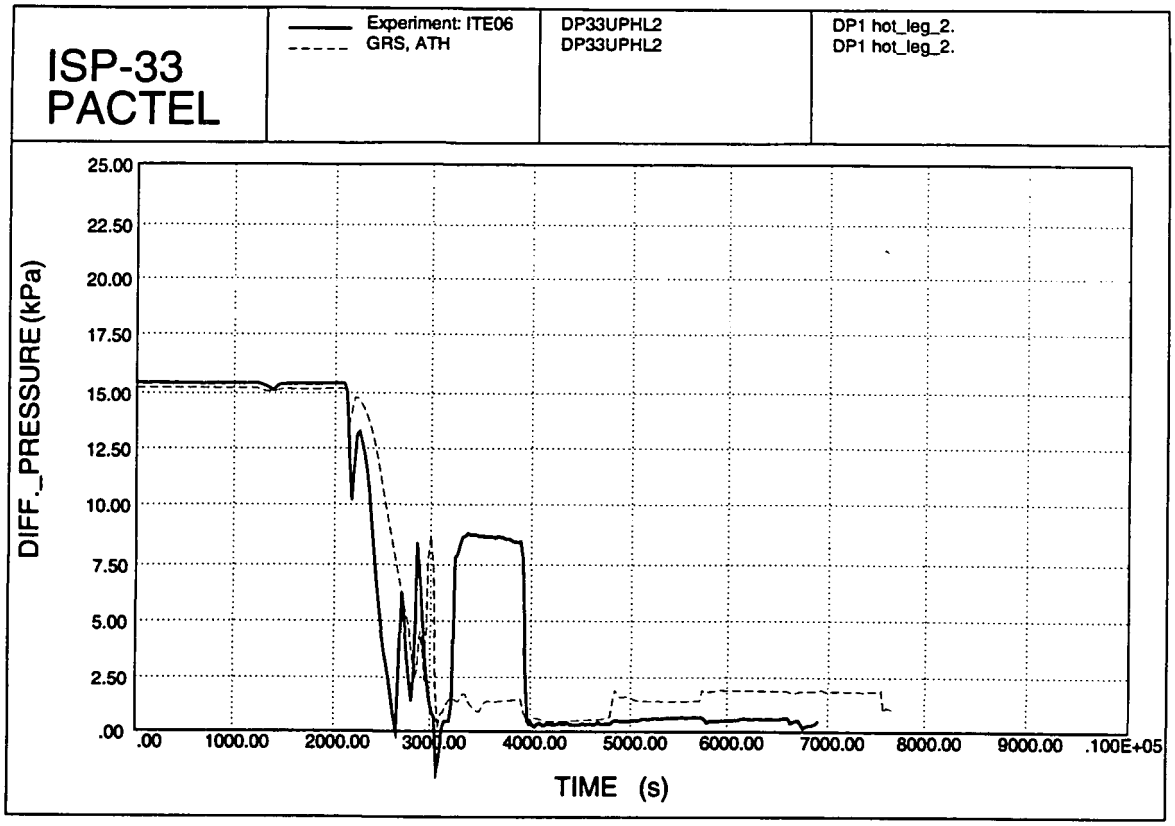

Figure 6.25. Hot leg 2 DP 1.

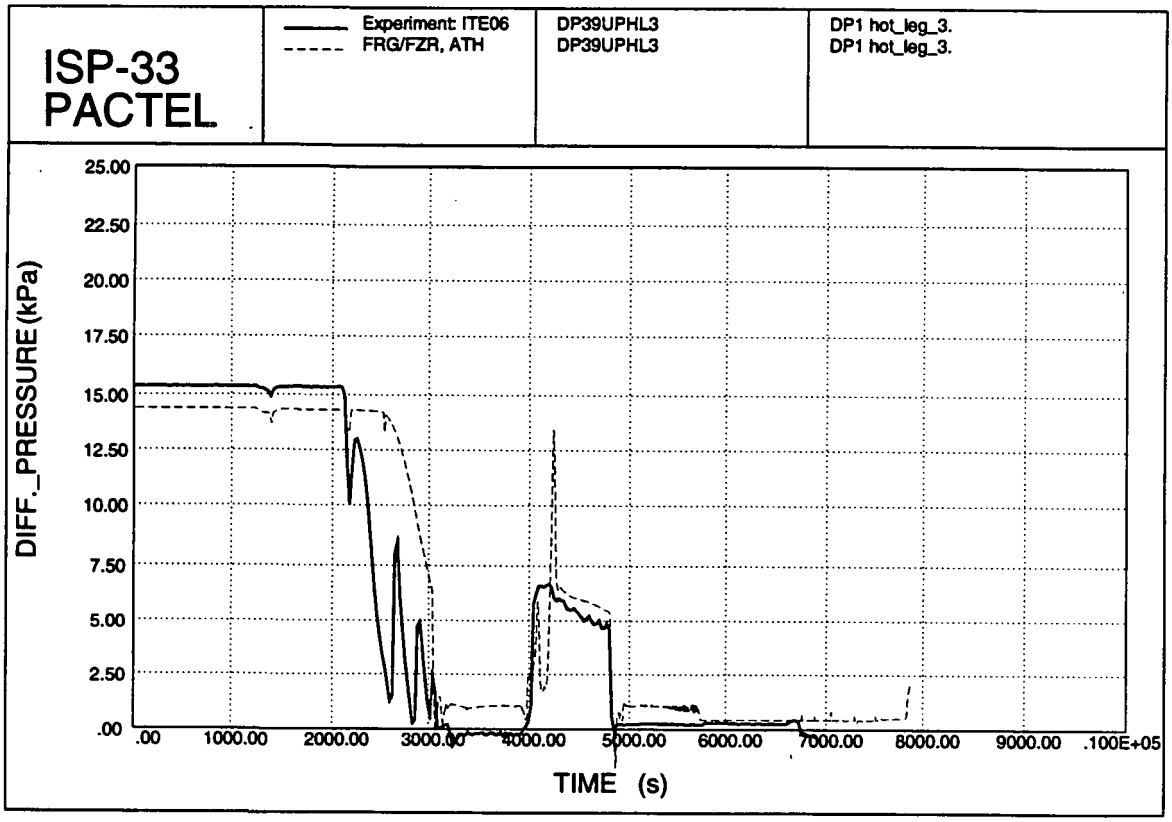

Figure 6.26. Hot leg 3 DP 1.

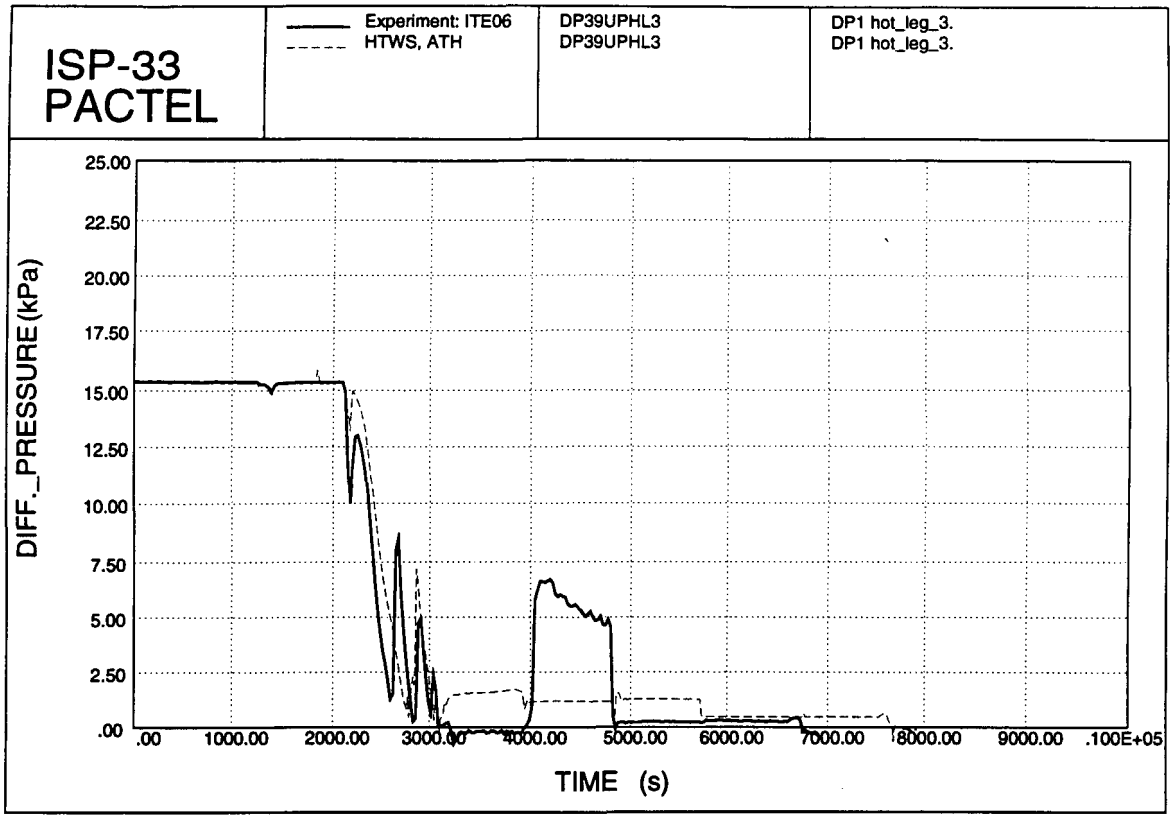

Figure 6.27. Hot leg 3 DP 1.

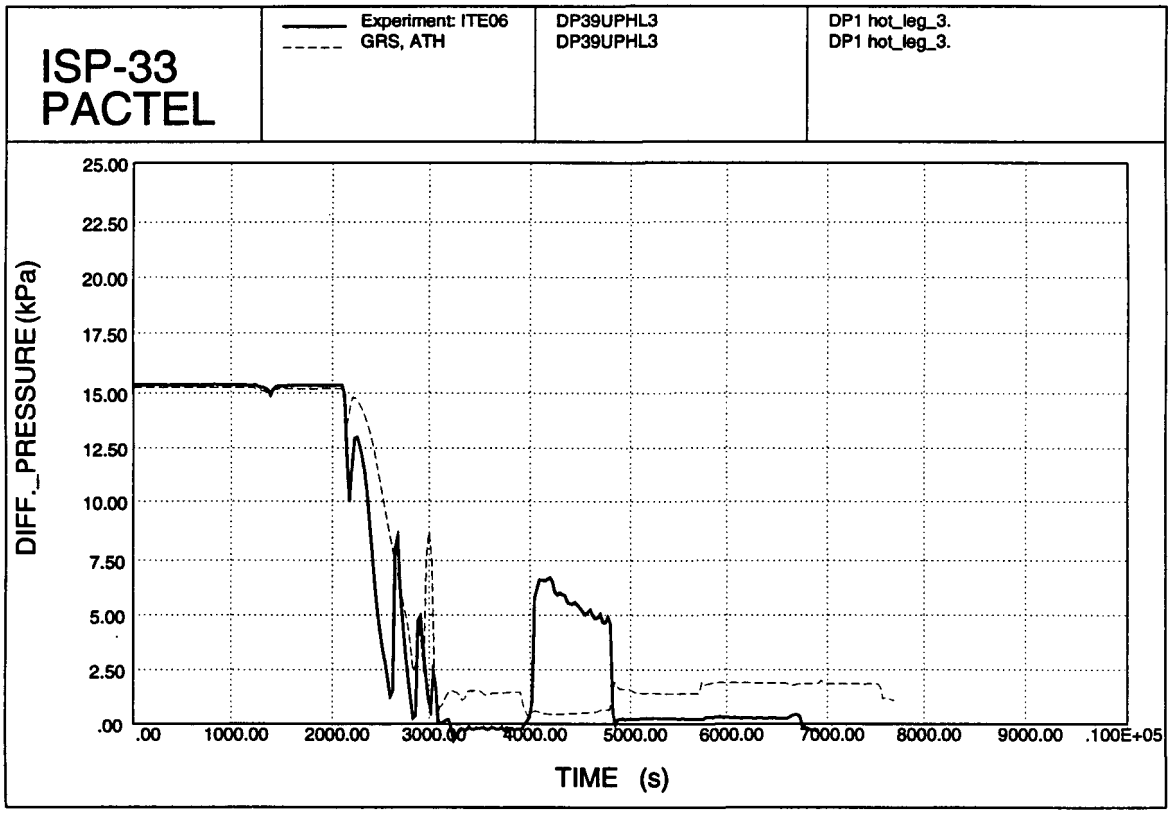

Figure 6.28. Hot leg 3 DP 1.

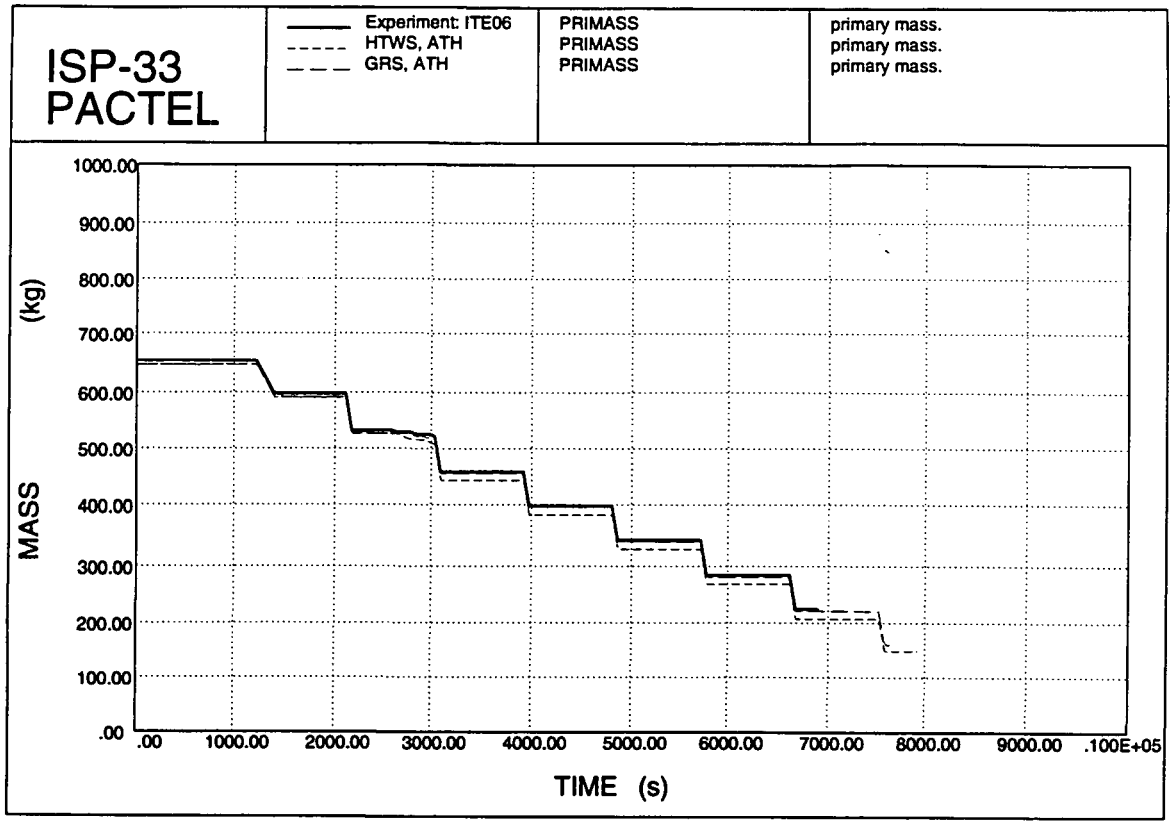

Figure 6.29. Primary mass inventory.

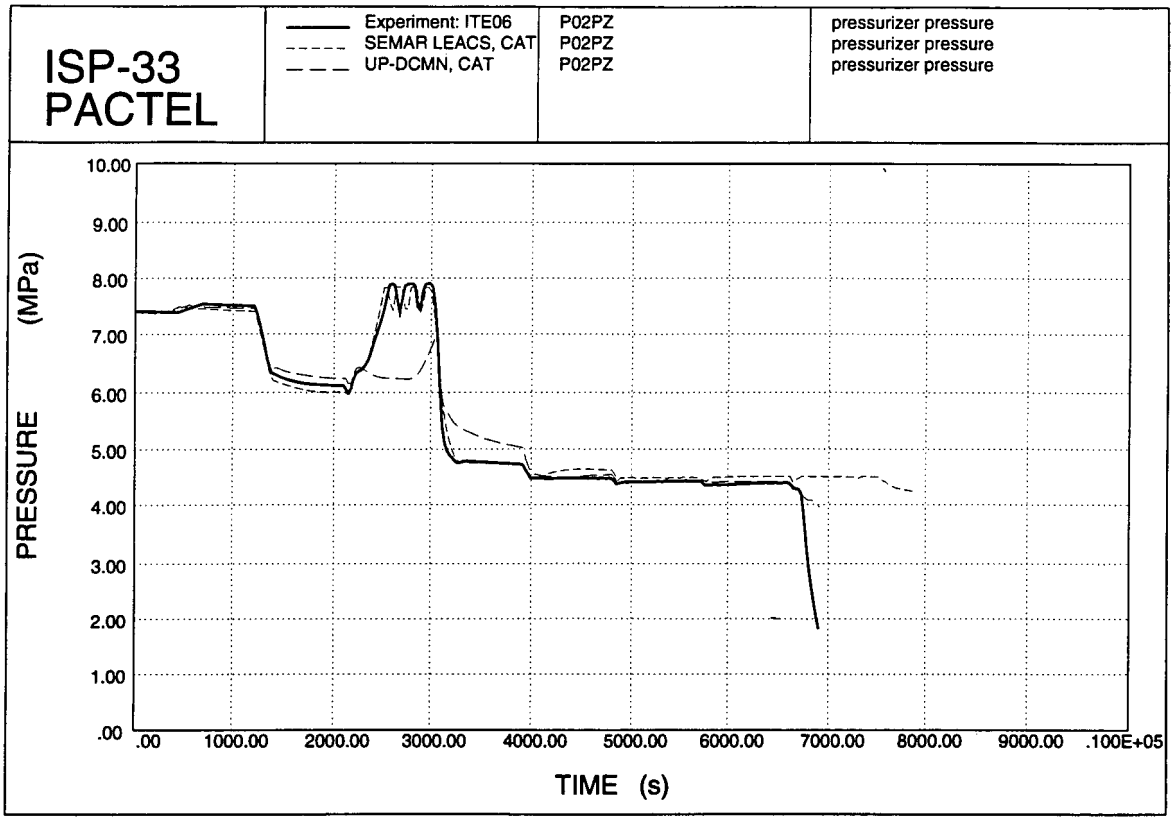

Figure 6.30. Pressurizer pressures.

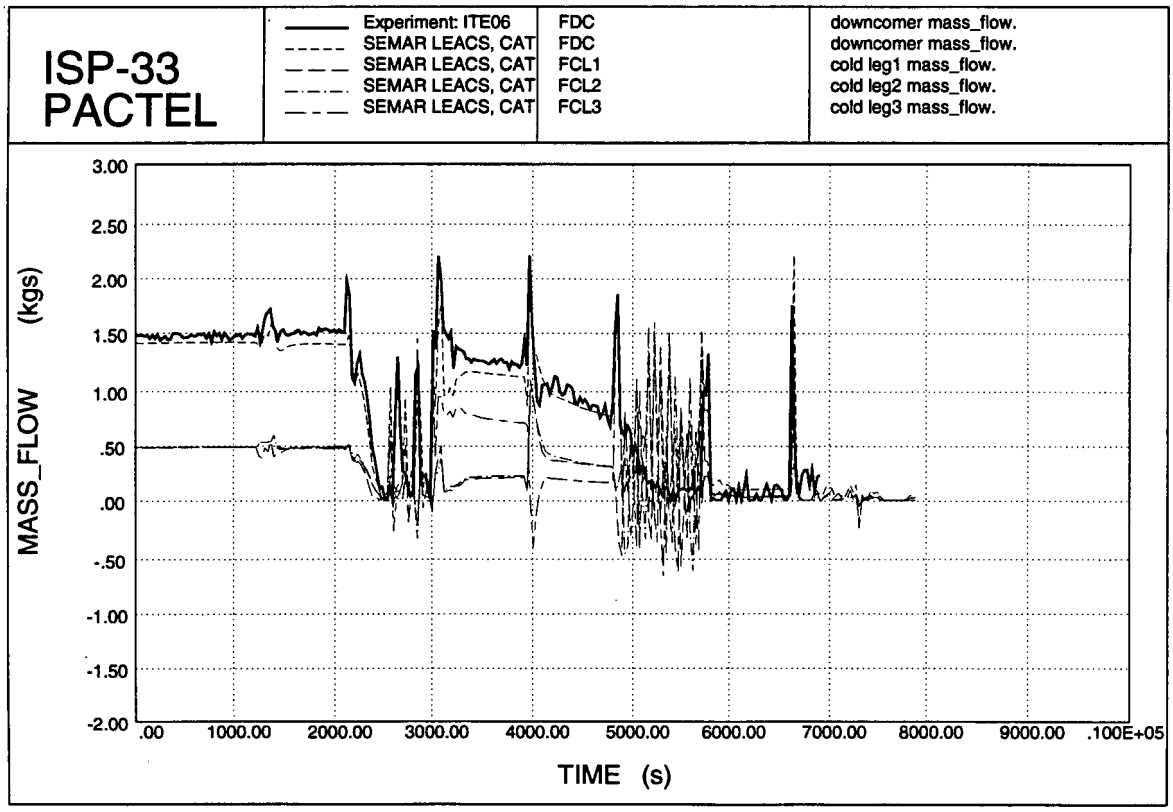

Figure 6.31. Primary mass flows.

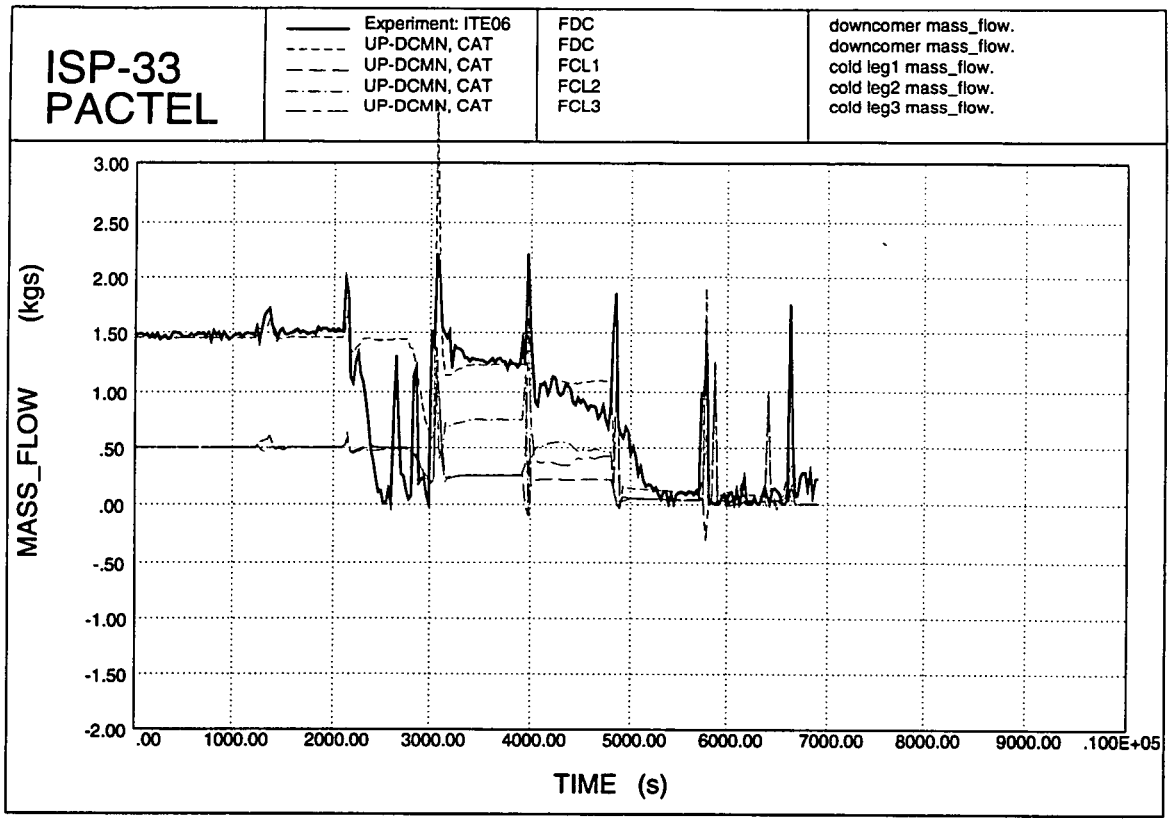

Figure 6.32. Primary mass flows.

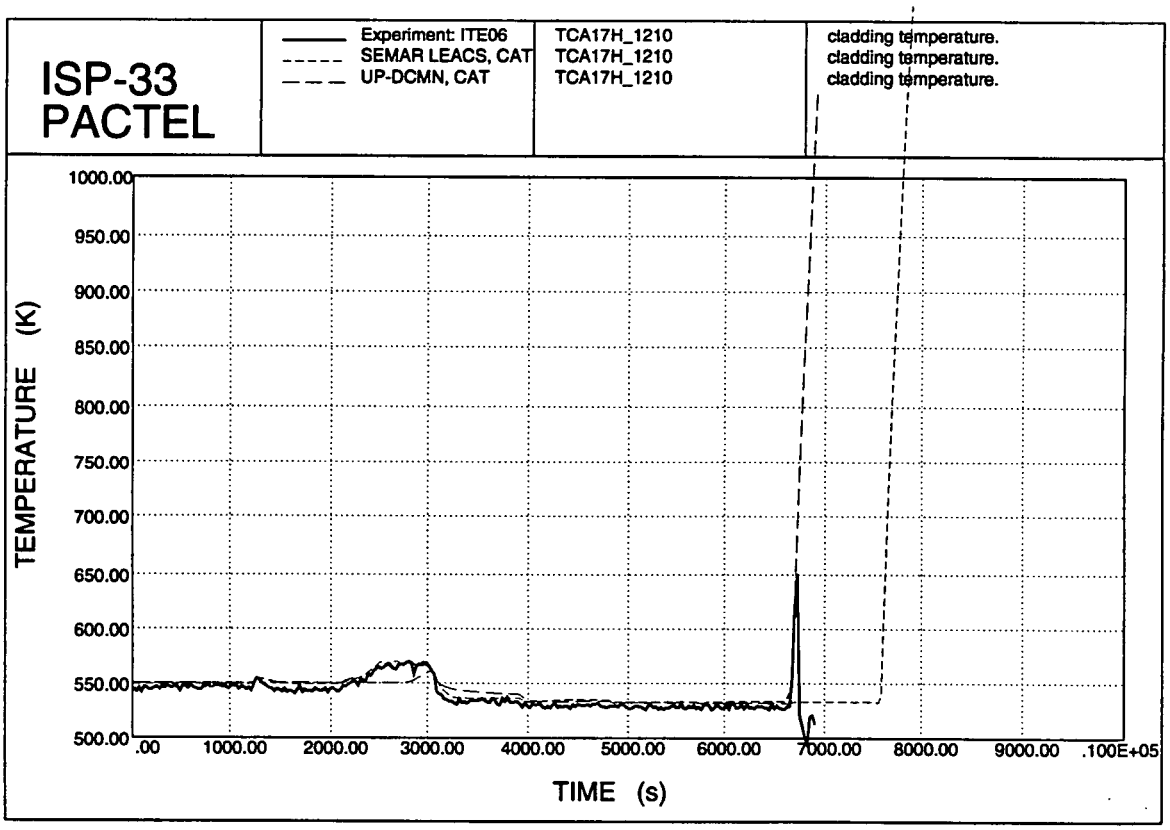

Figure 6.33. Cladding temperatures.

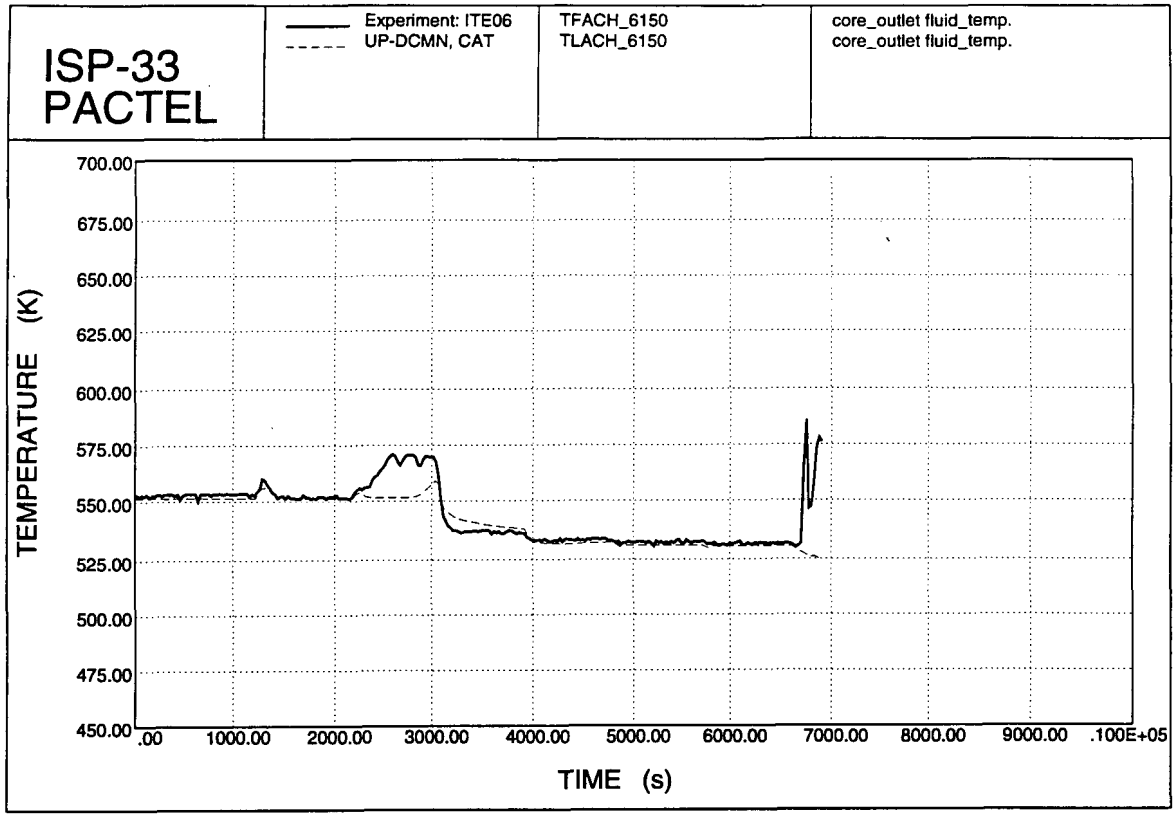

Figure 6.34. Core outlet coolant temperature.

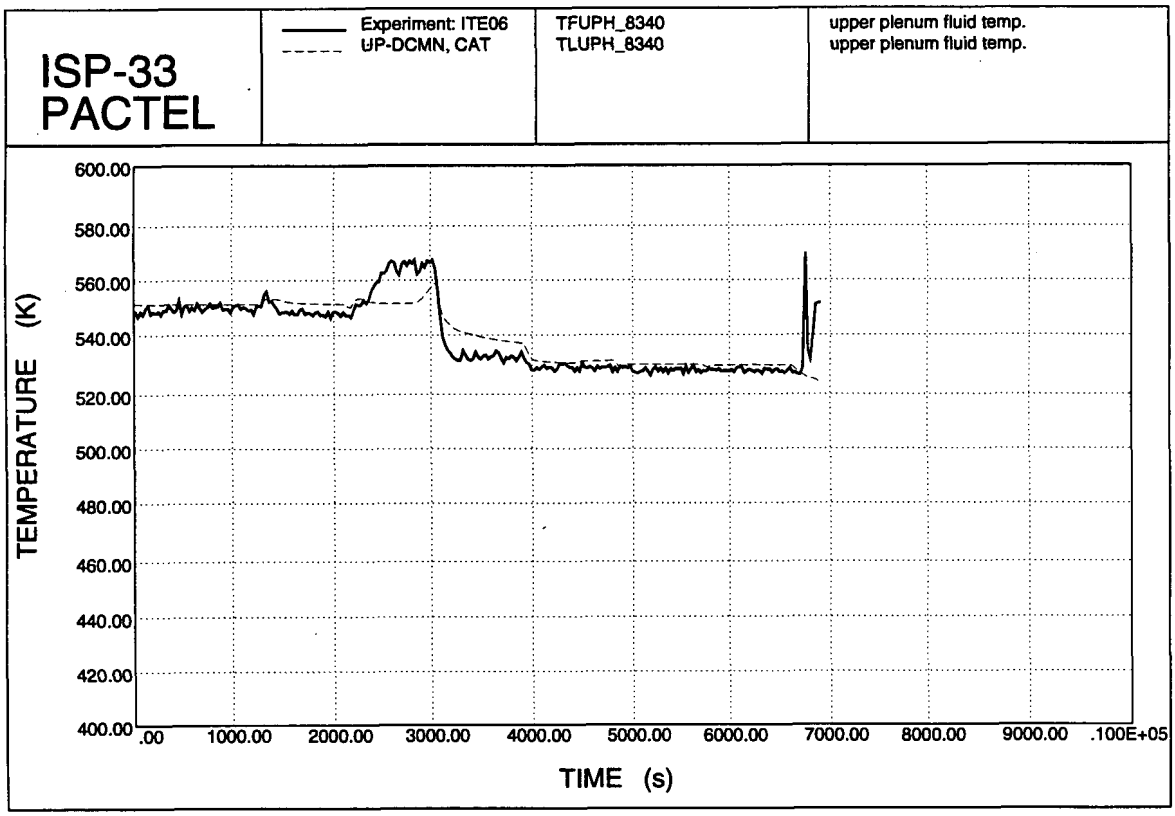

Figure 6.35. Upper plenum temperatures.

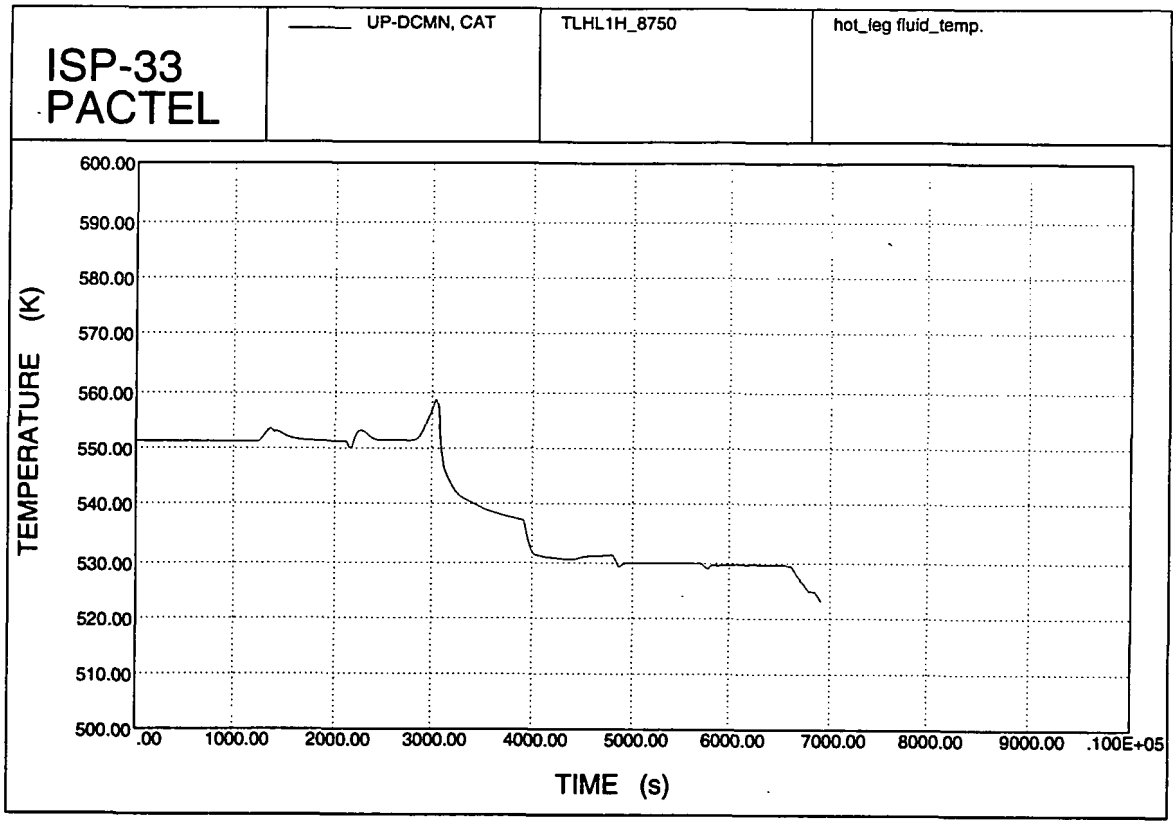

Figure 6.36. Hot leg coolant temperatures.

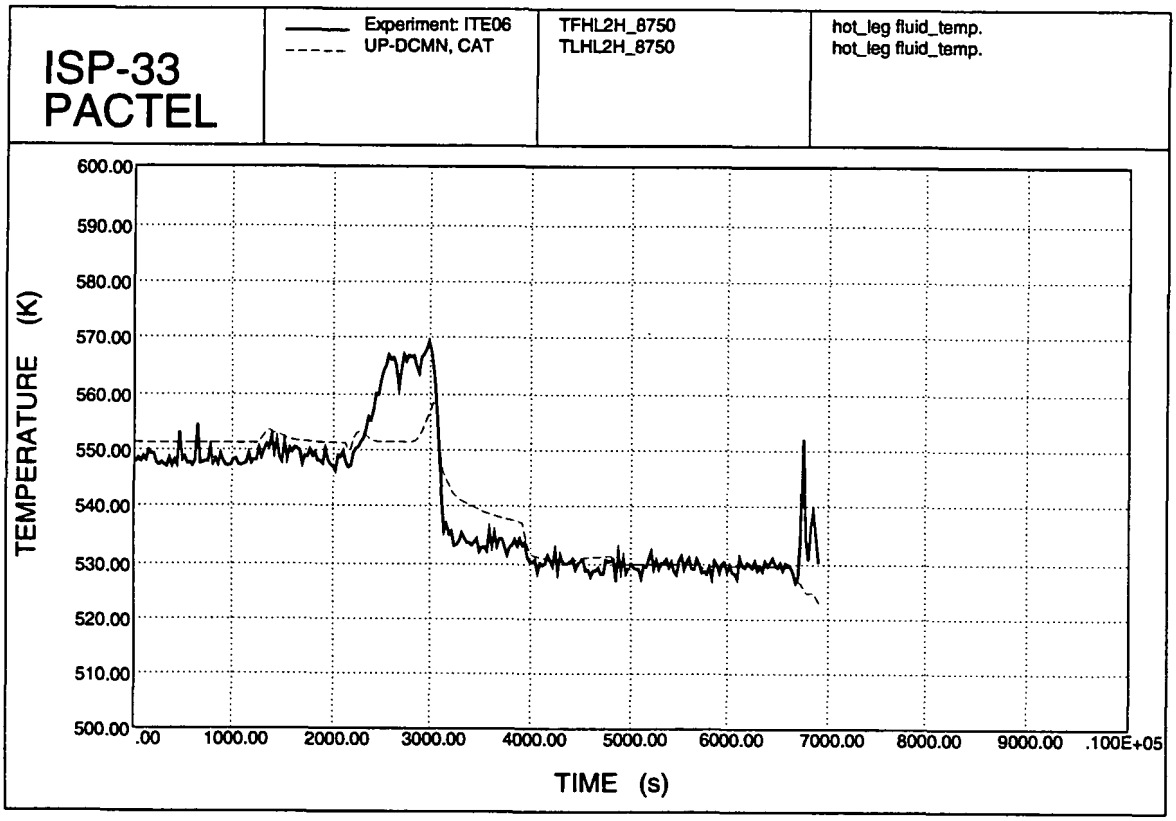

Figure 6.37. Hot leg temperatures.

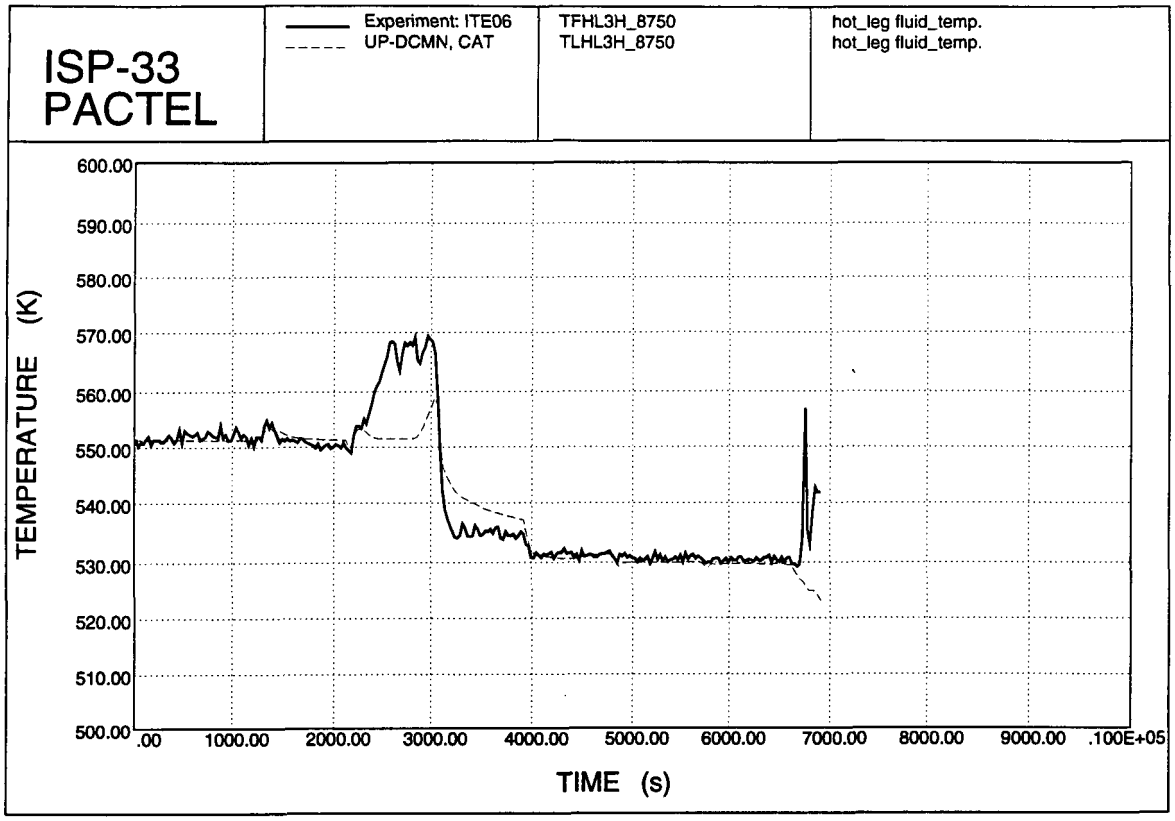

Figure 6.38. Hot leg coolant temperatures.

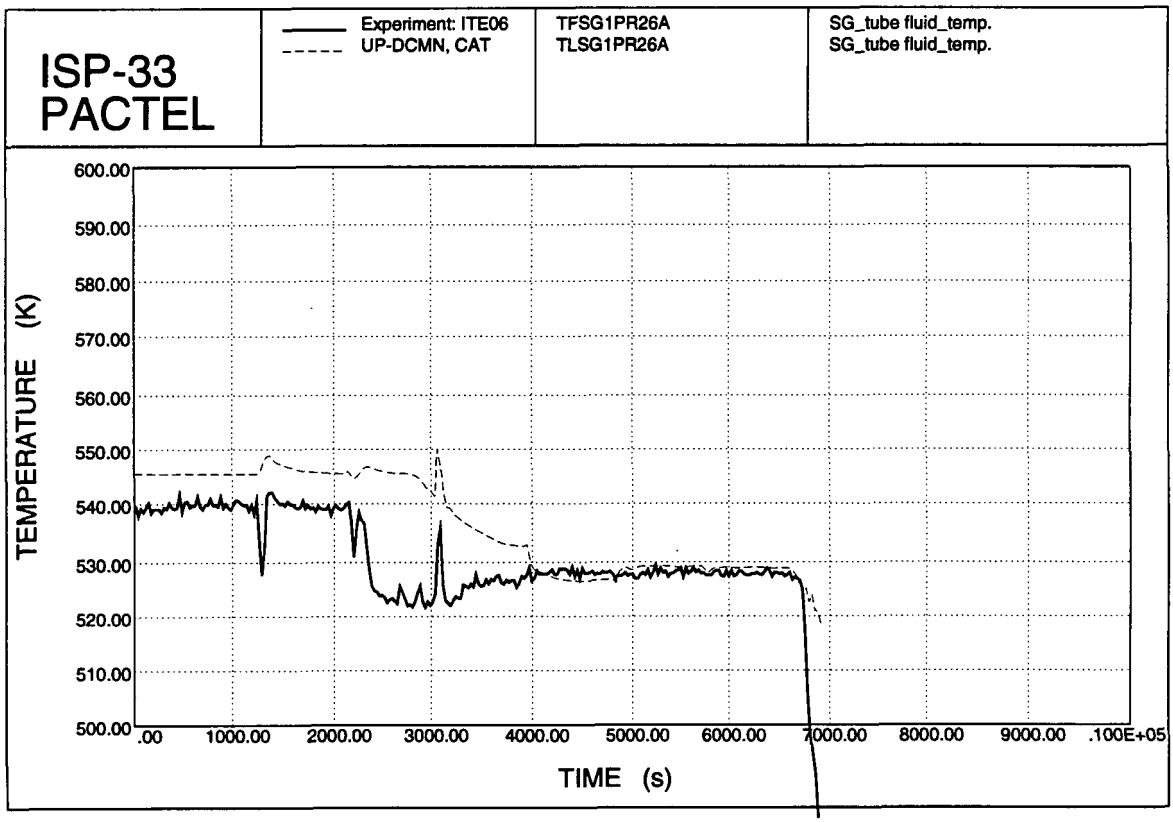

Figure 6.39. SG tube fluid temperatures.

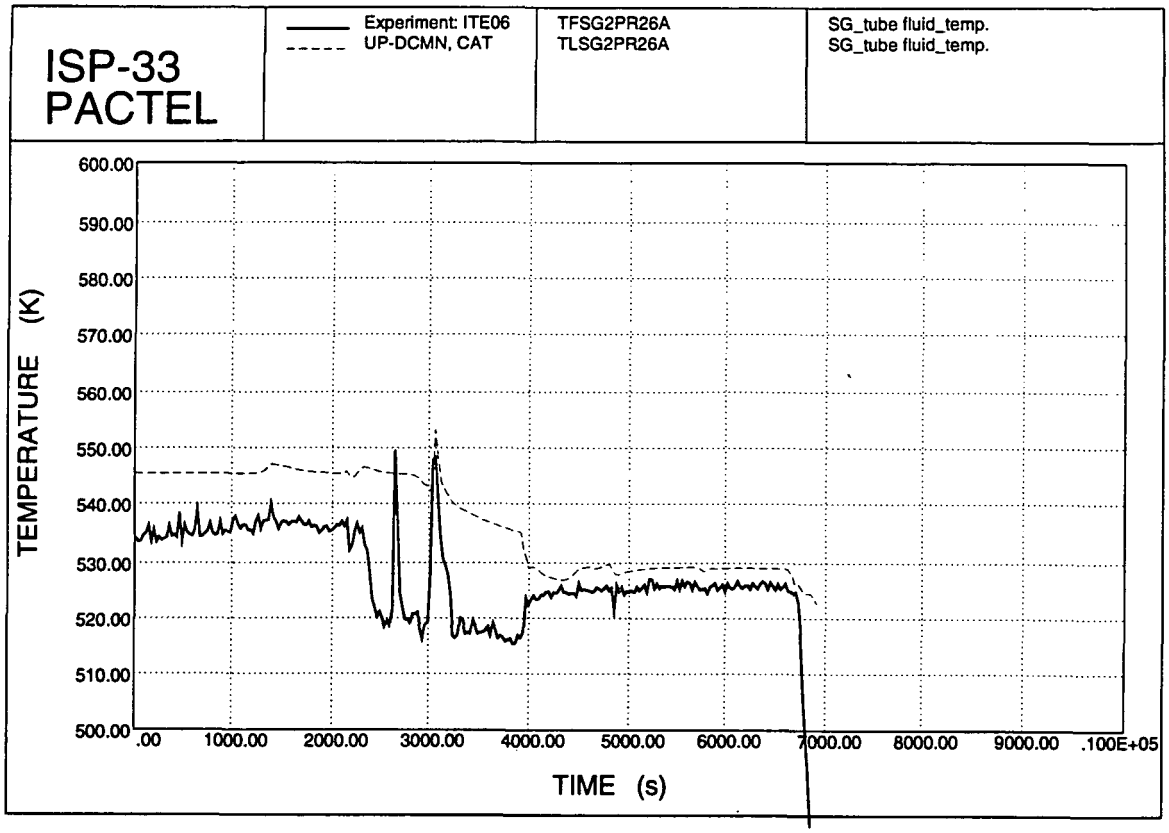

Figure 6.40. SG tube fluid temperatures.

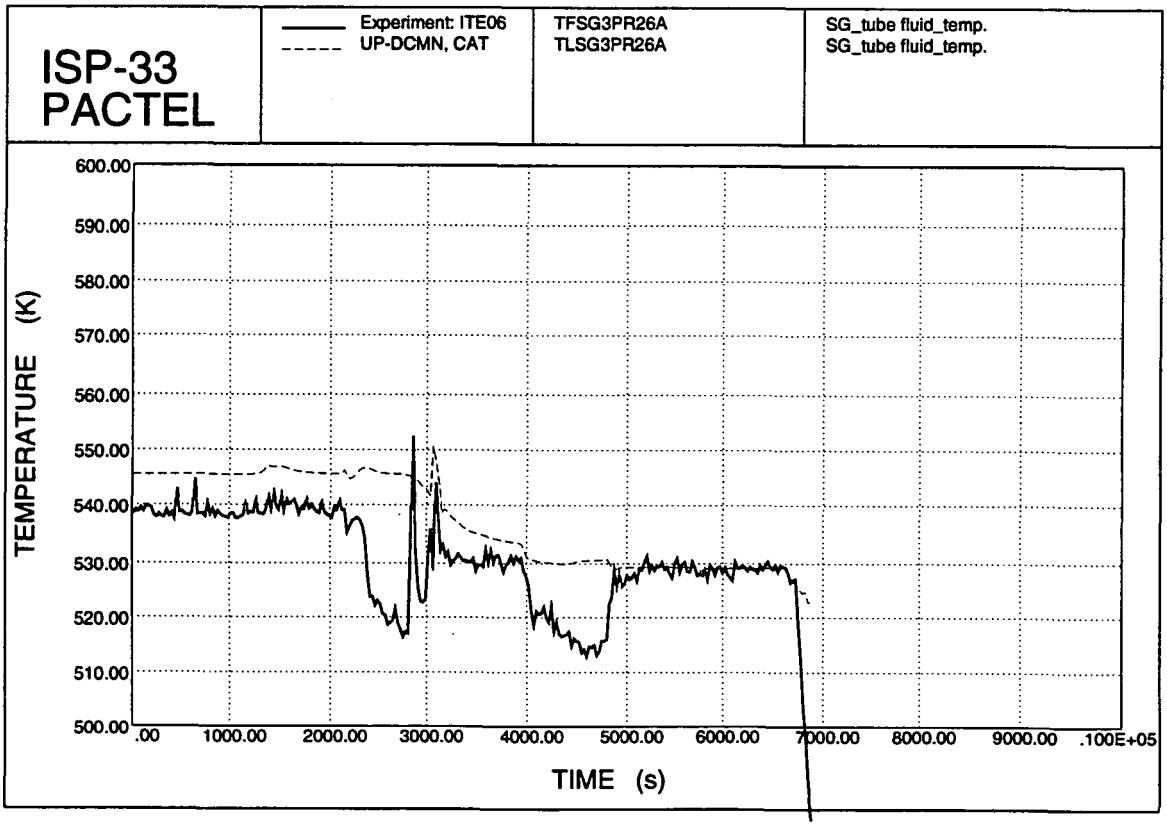

Figure 6.41. SG tube fluid temperatures.

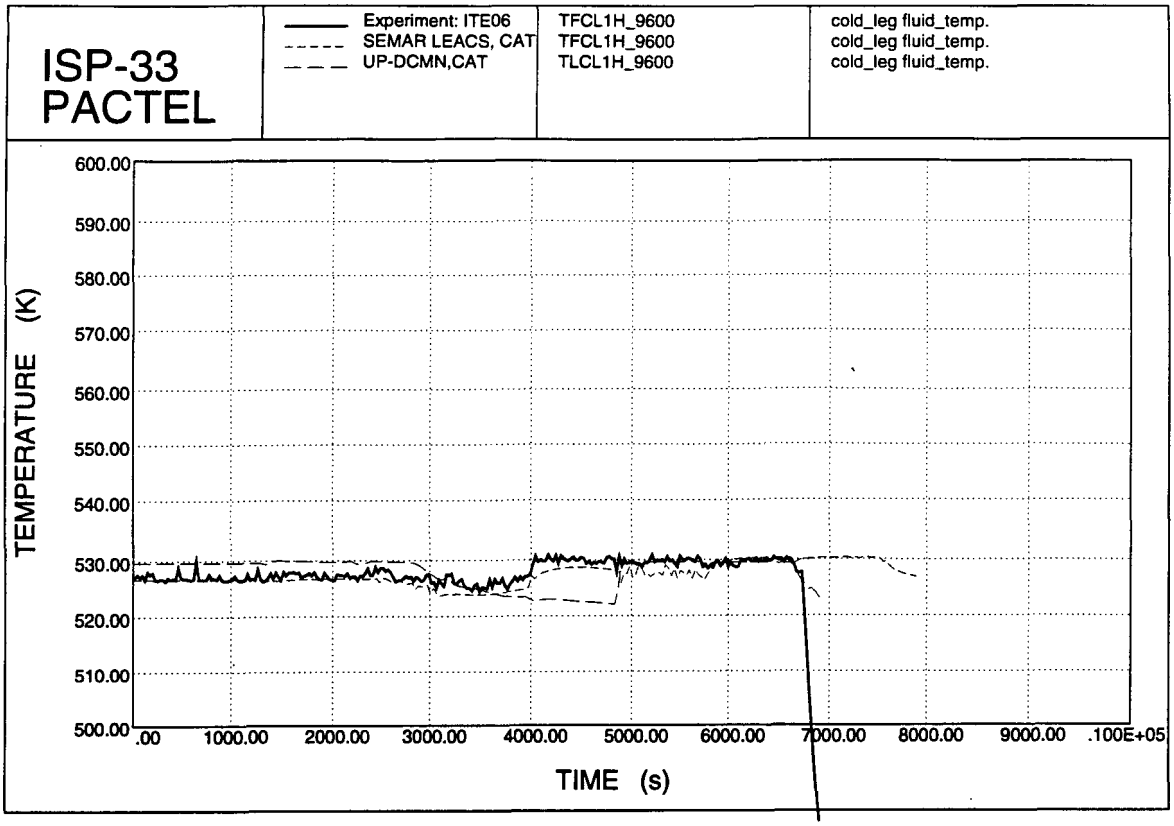

Figure 6.42. Cold leg temperatures.

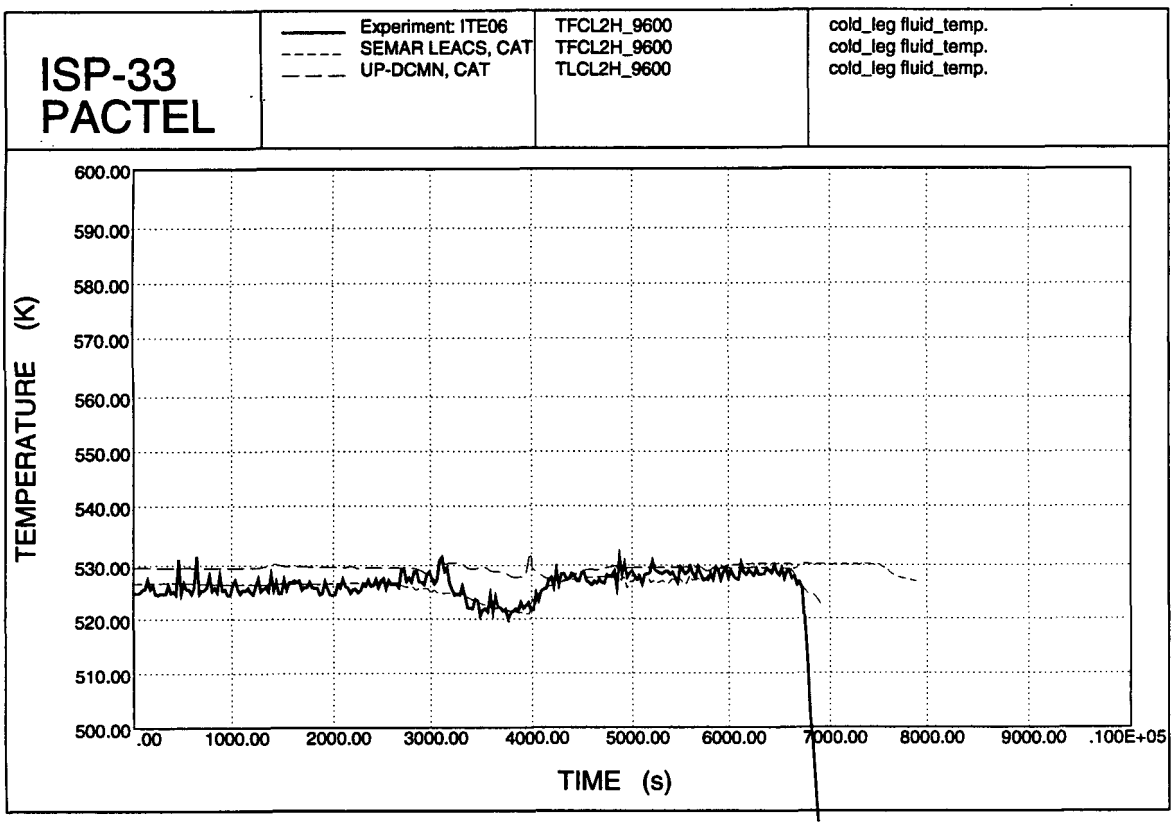

Figure 6.43. Cold leg temperatures.

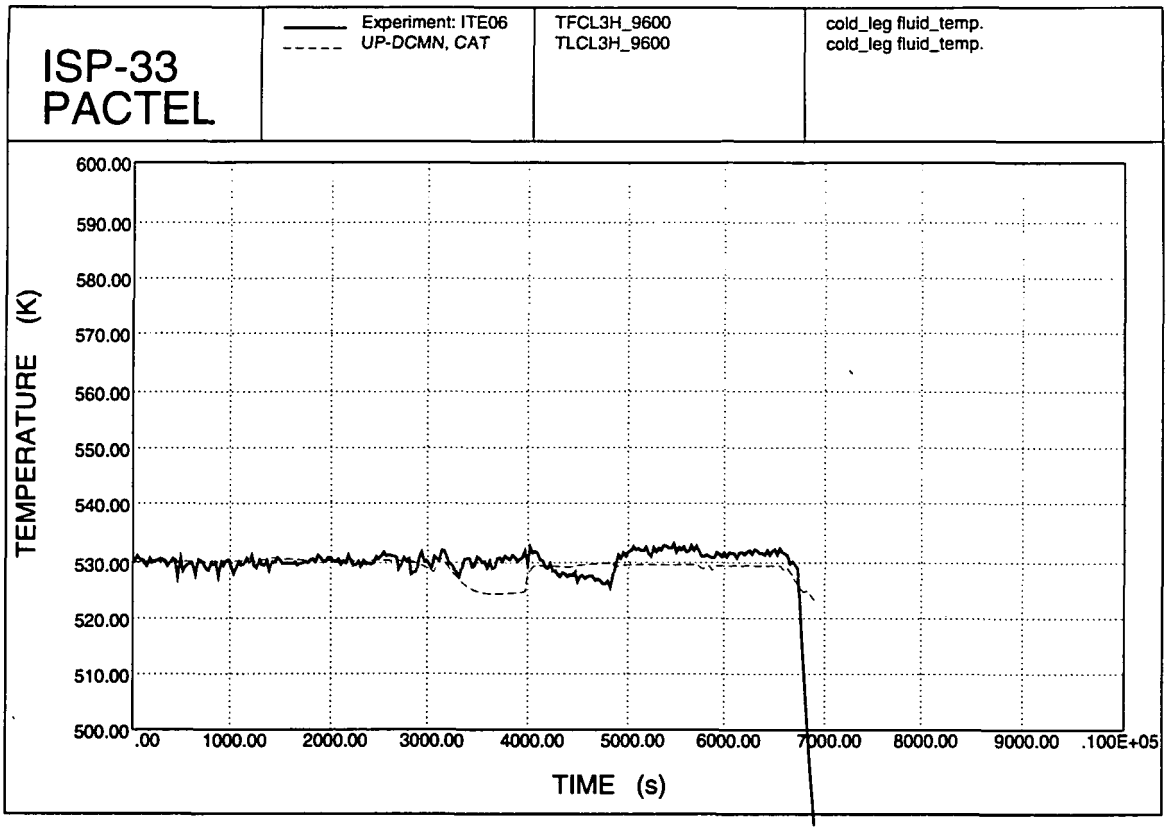

Figure 6.44. Cold leg temperatures.

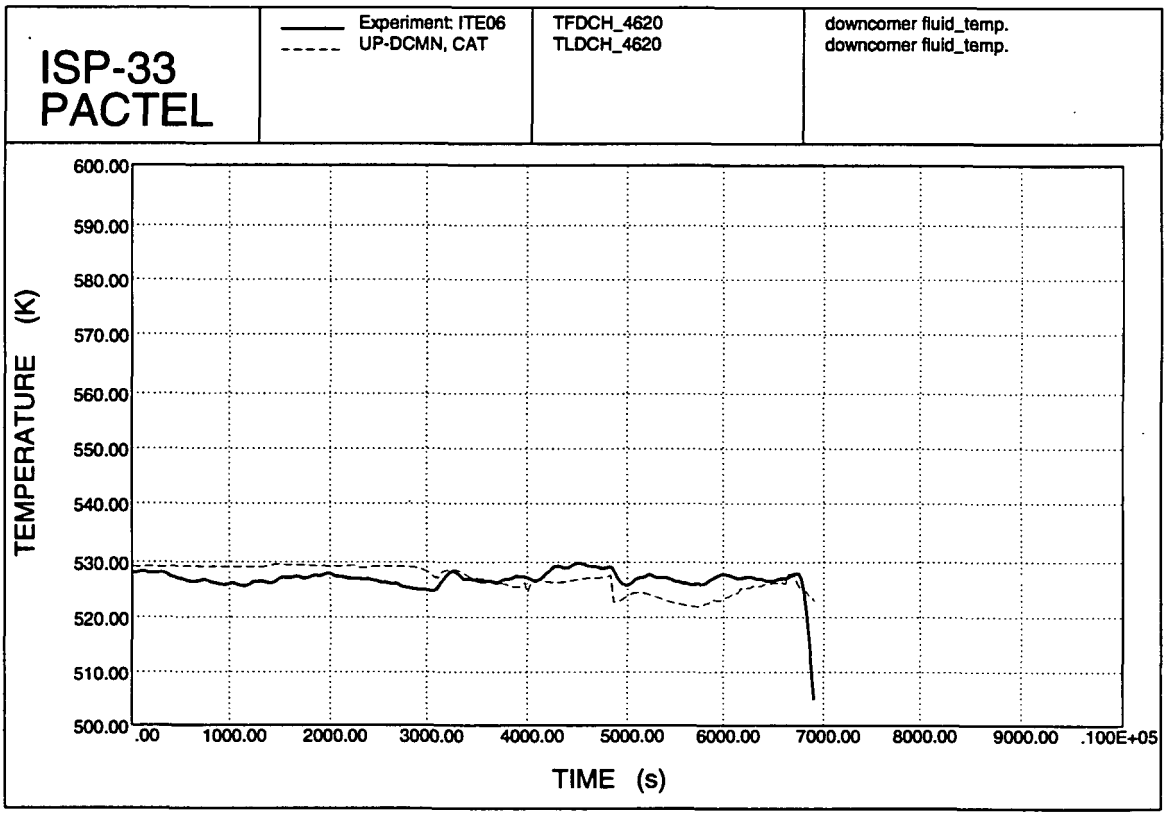

Figure 6.45. Downcomer temperatures.

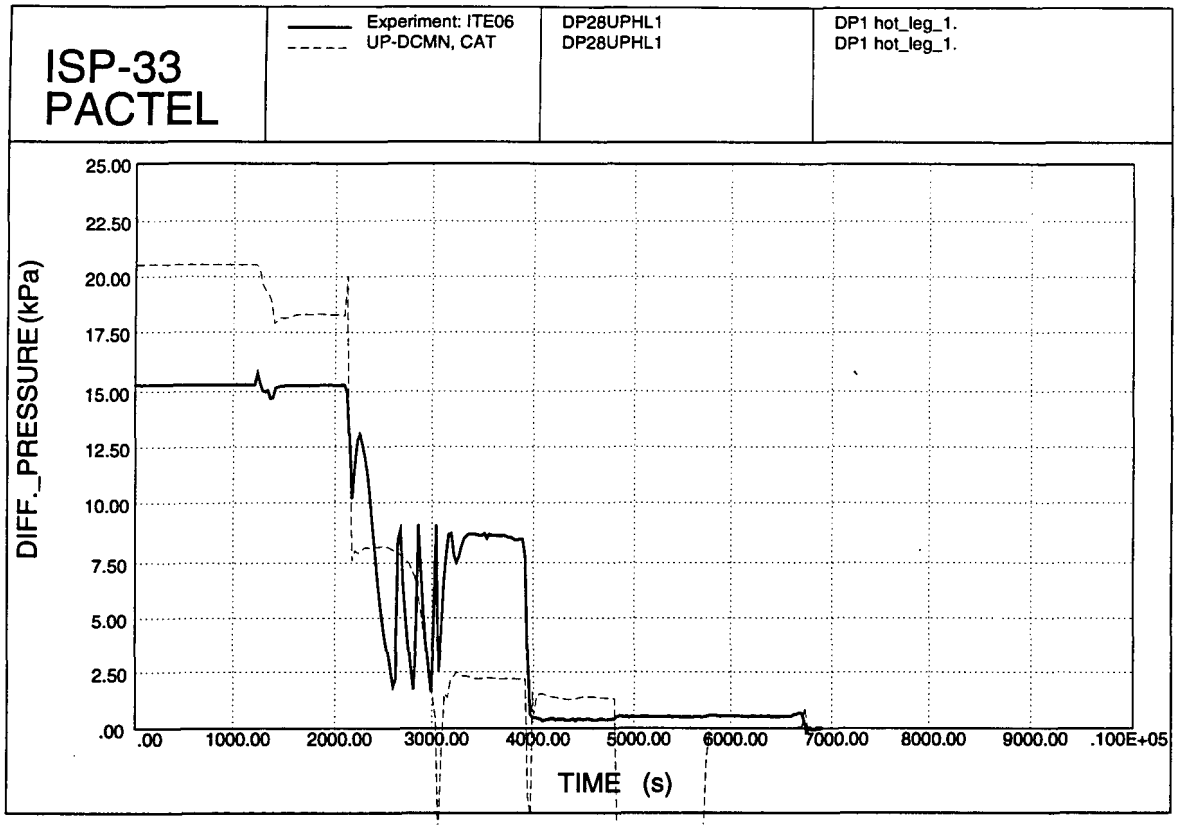

Figure 6.46. Hot leg 1 DP 1.

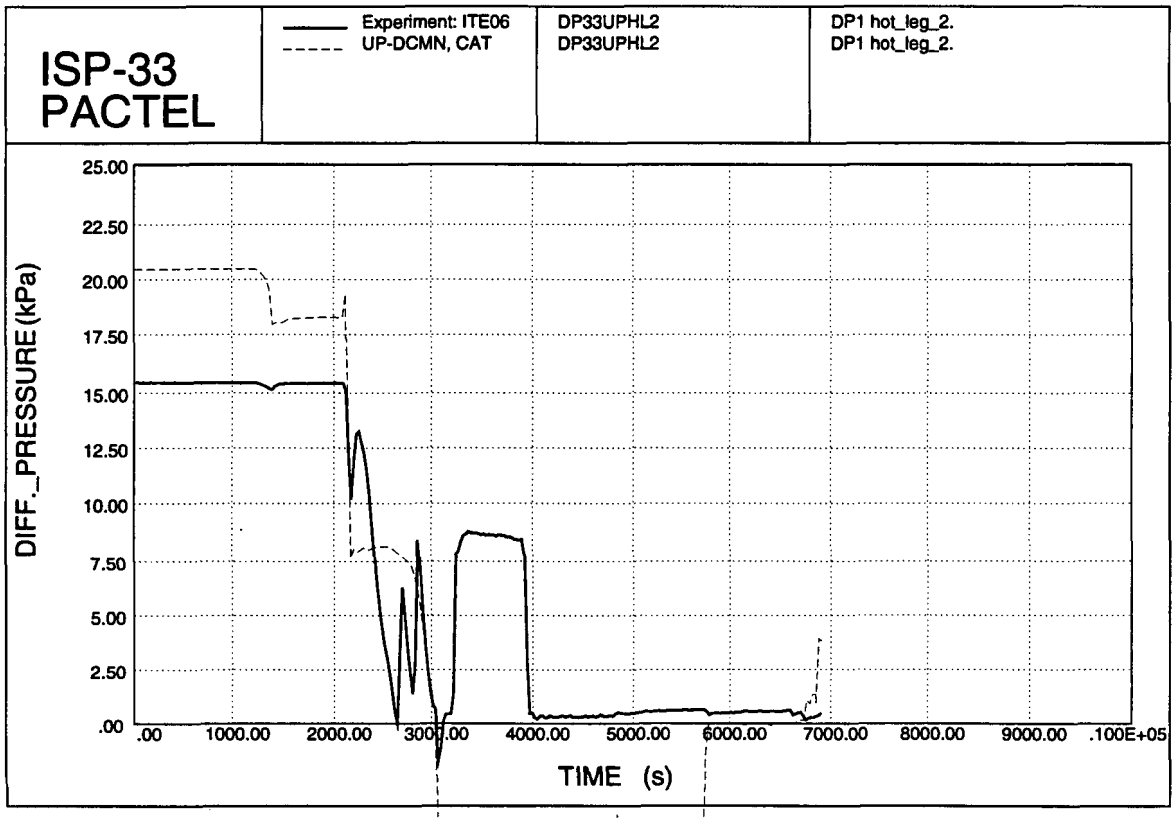

Figure 6.47. Hot leg 2 DP 1.

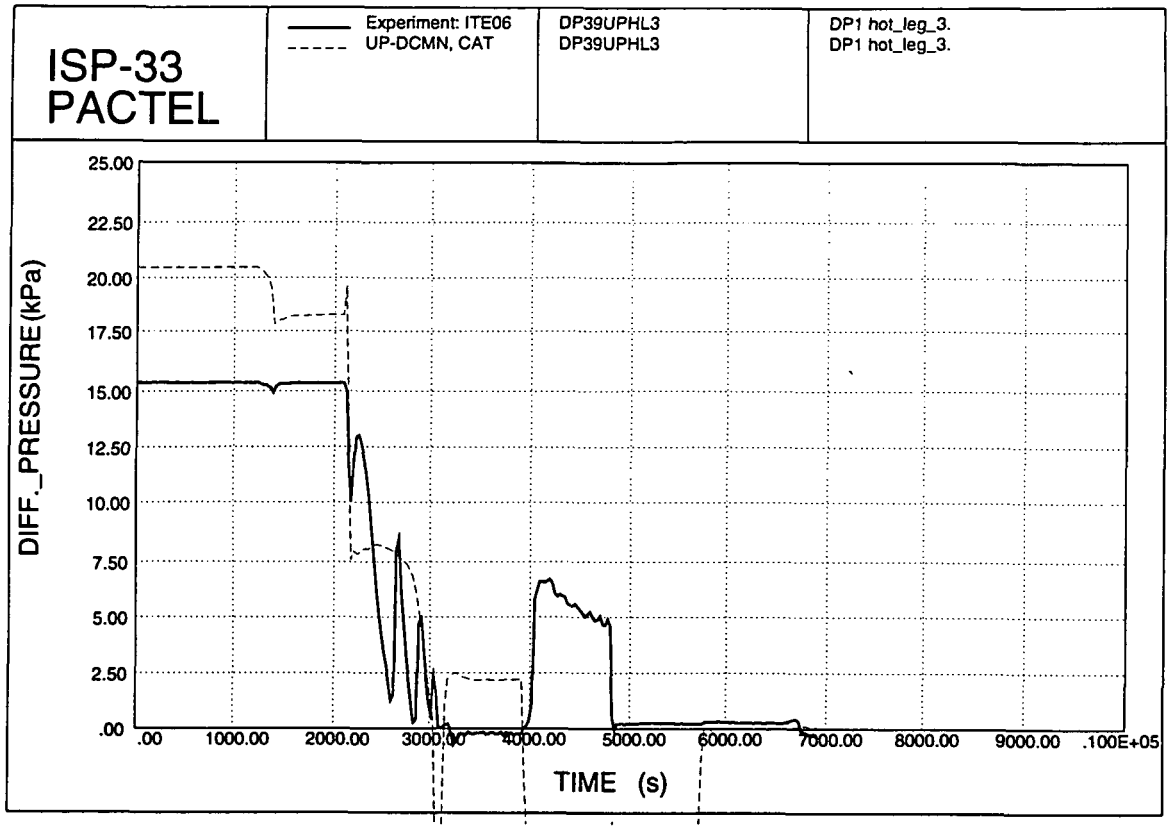

Figure 6.48. Hot leg 3 DP 1.

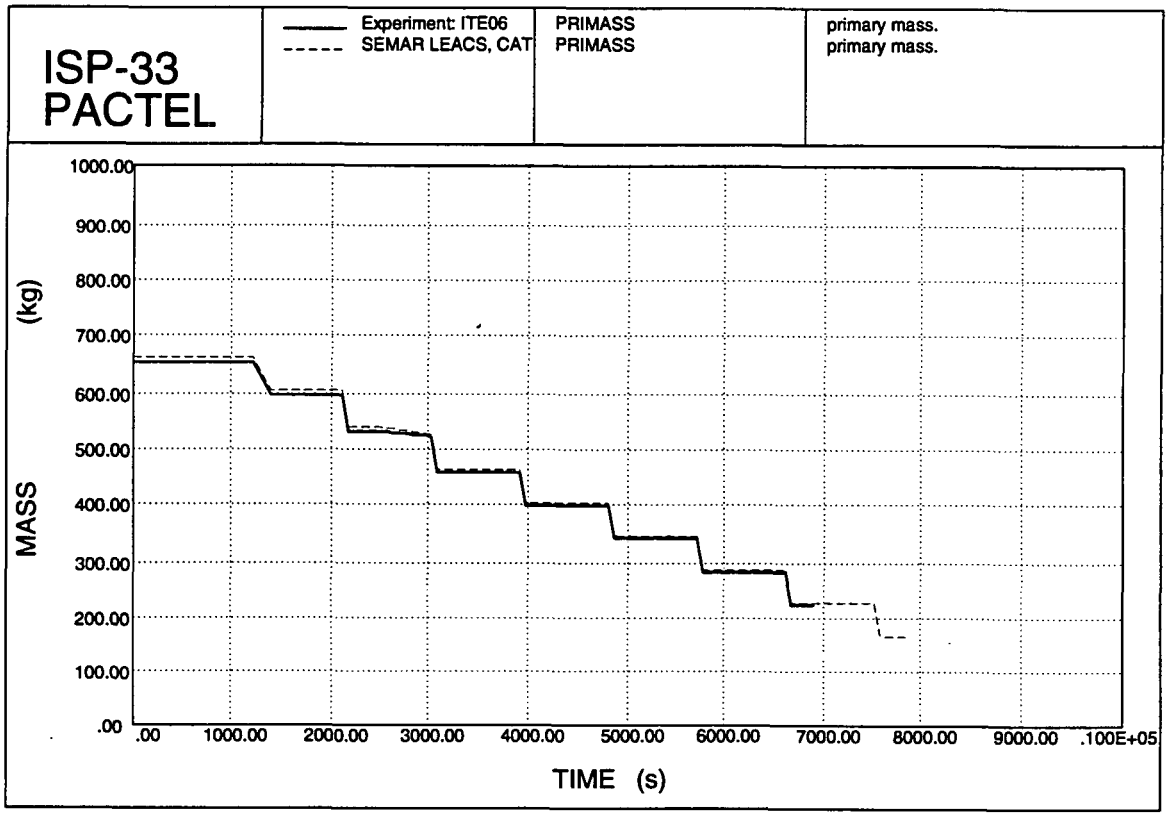

Figure 6.49. Primary mass inventory.

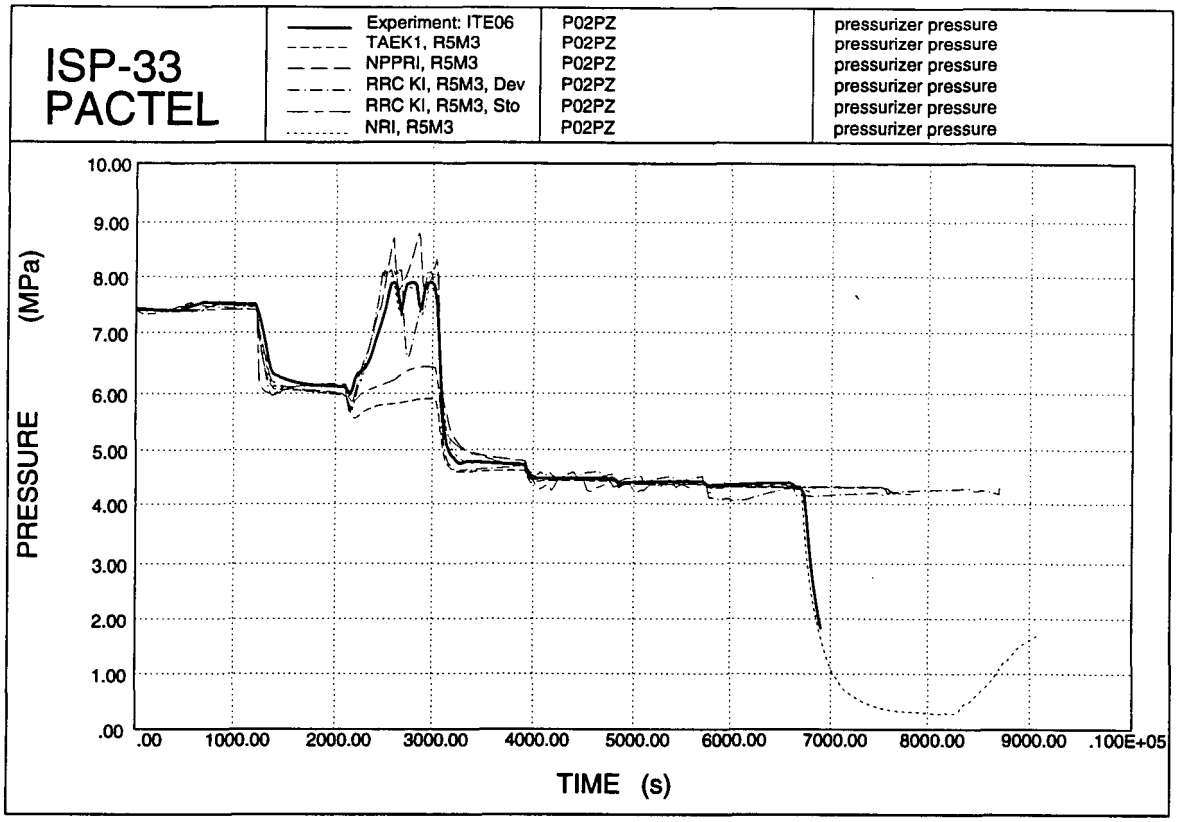

Figure 6.50. Pressurizer pressures.

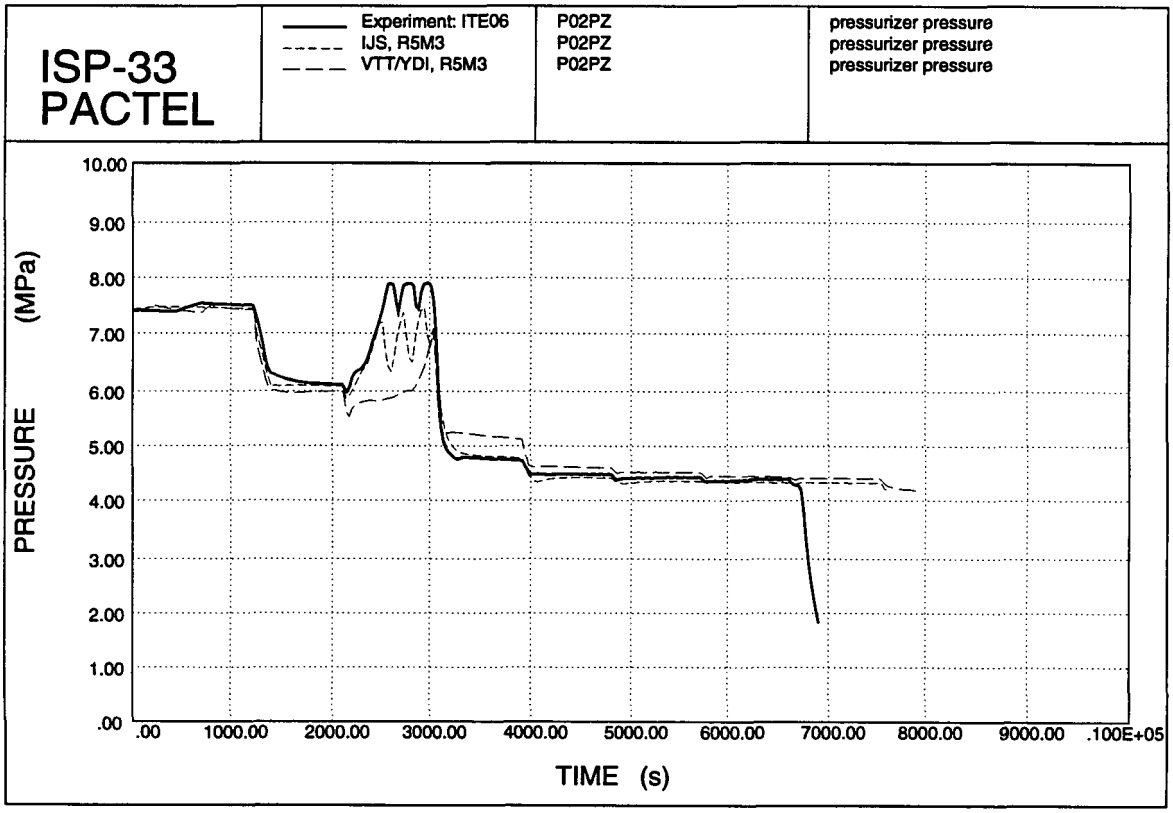

Figure 6.51. Pressurizer pressures.

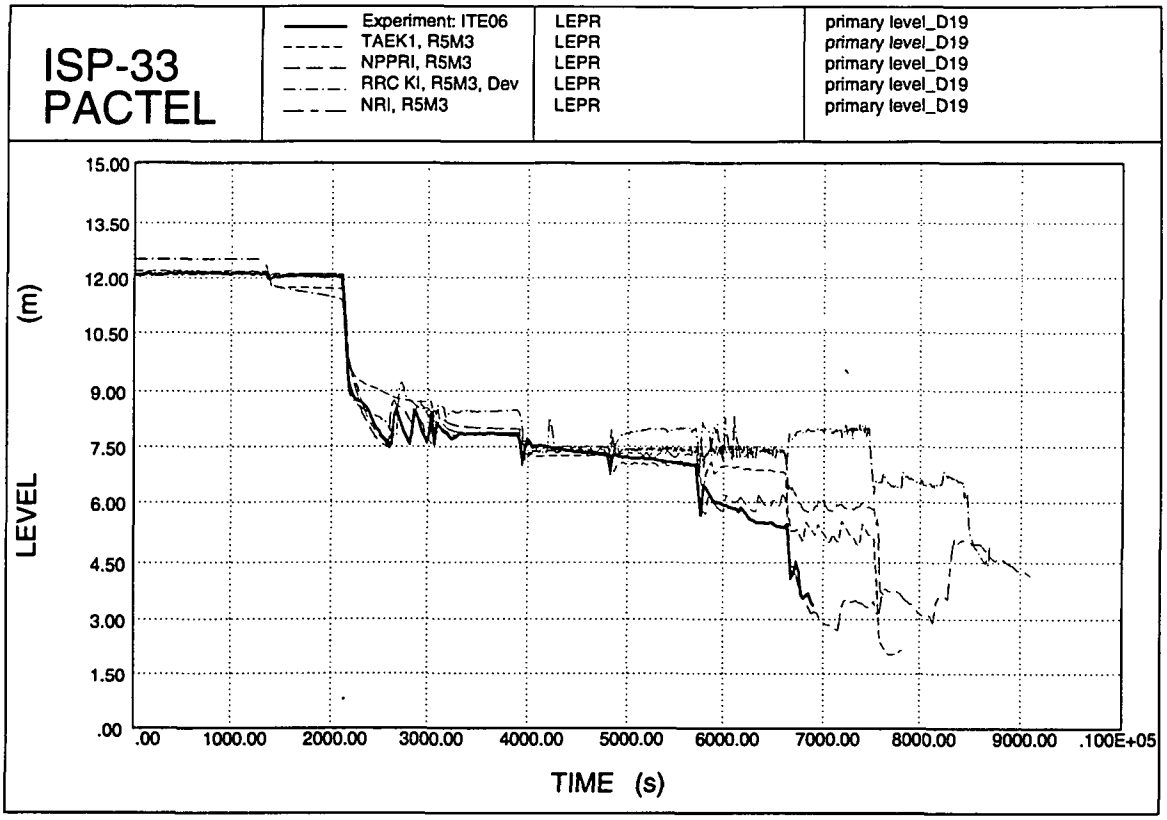

Figure 6.52. Primary levels.

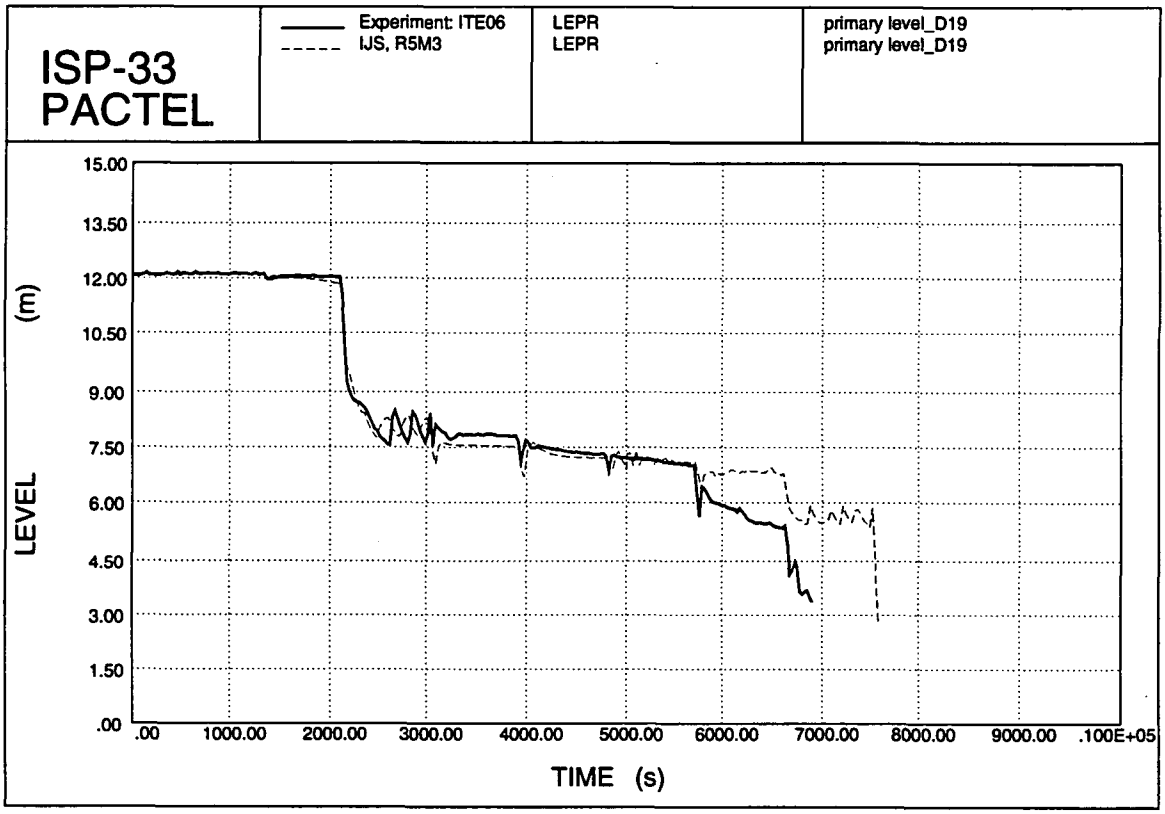

Figure 6.53. Primary levels.

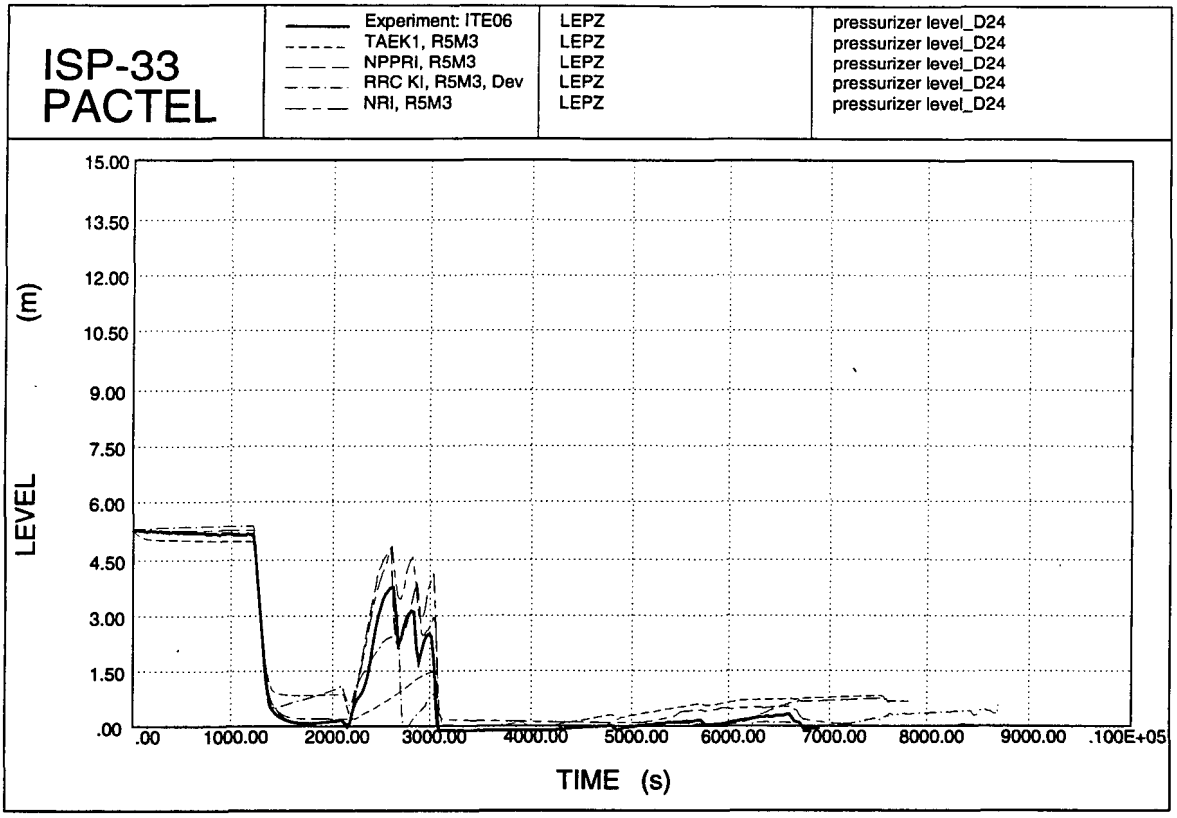

Figure 6.54. Pressurizer levels.

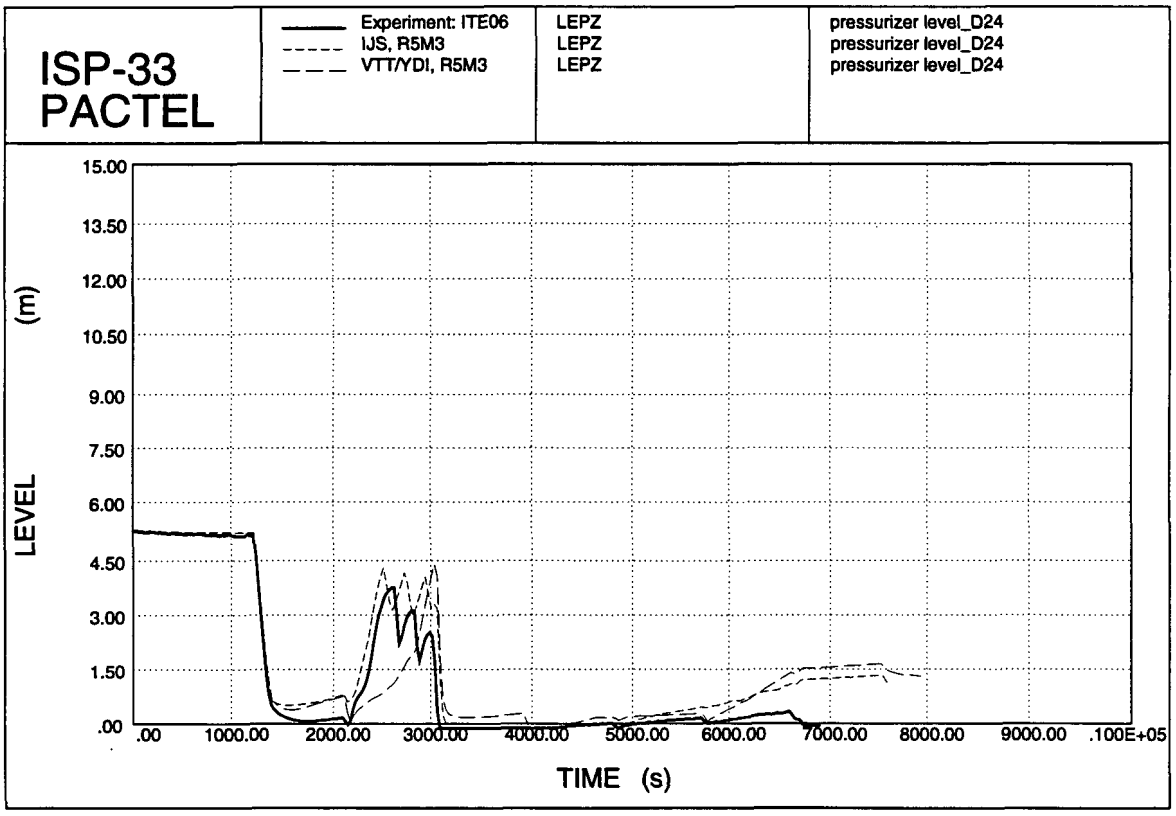

Figure 6.55. Pressurizer levels.

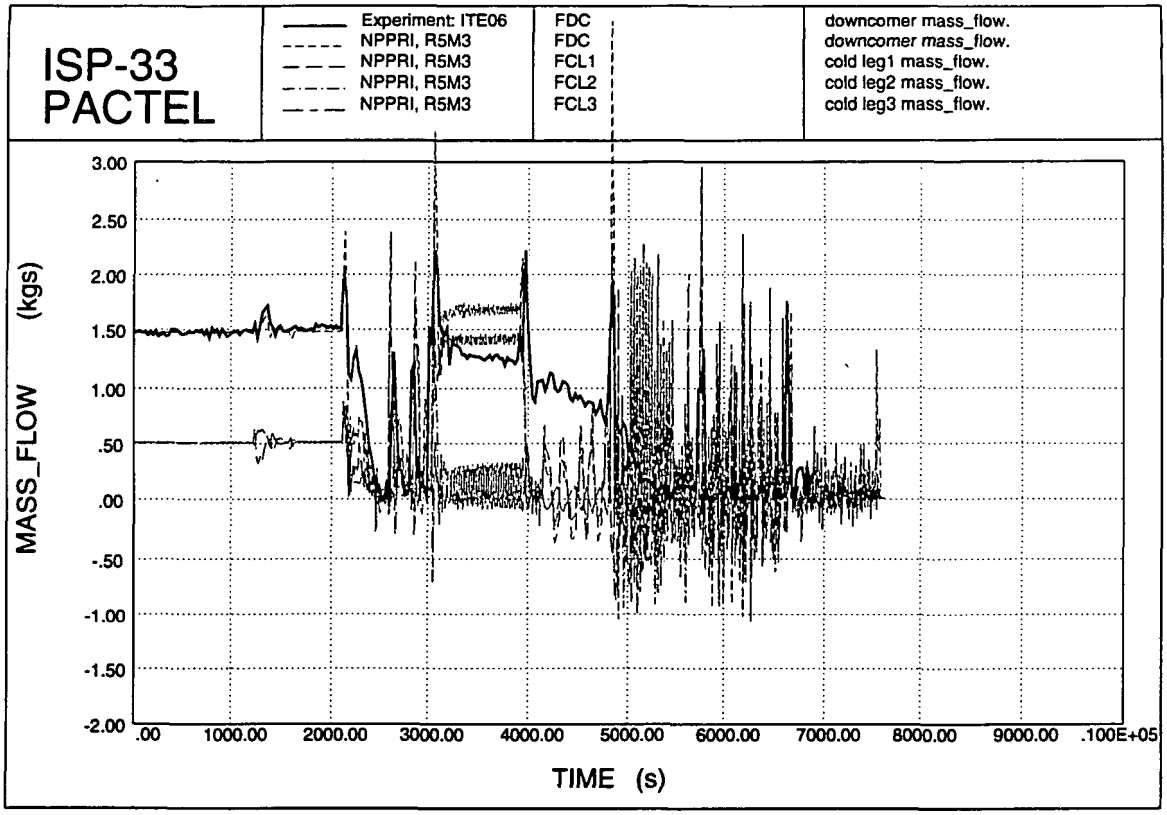

Figure 6.56. Primary mass flows.

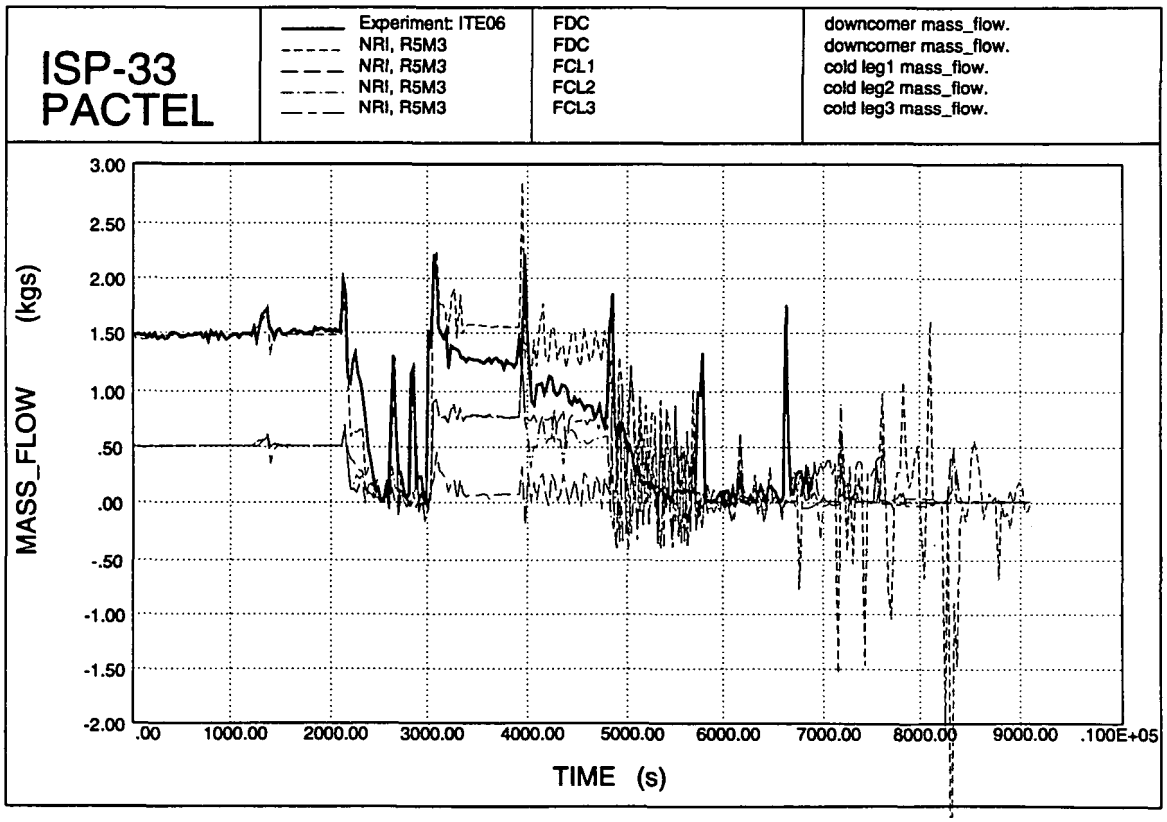

Figure 6.57. Primary mass flows.

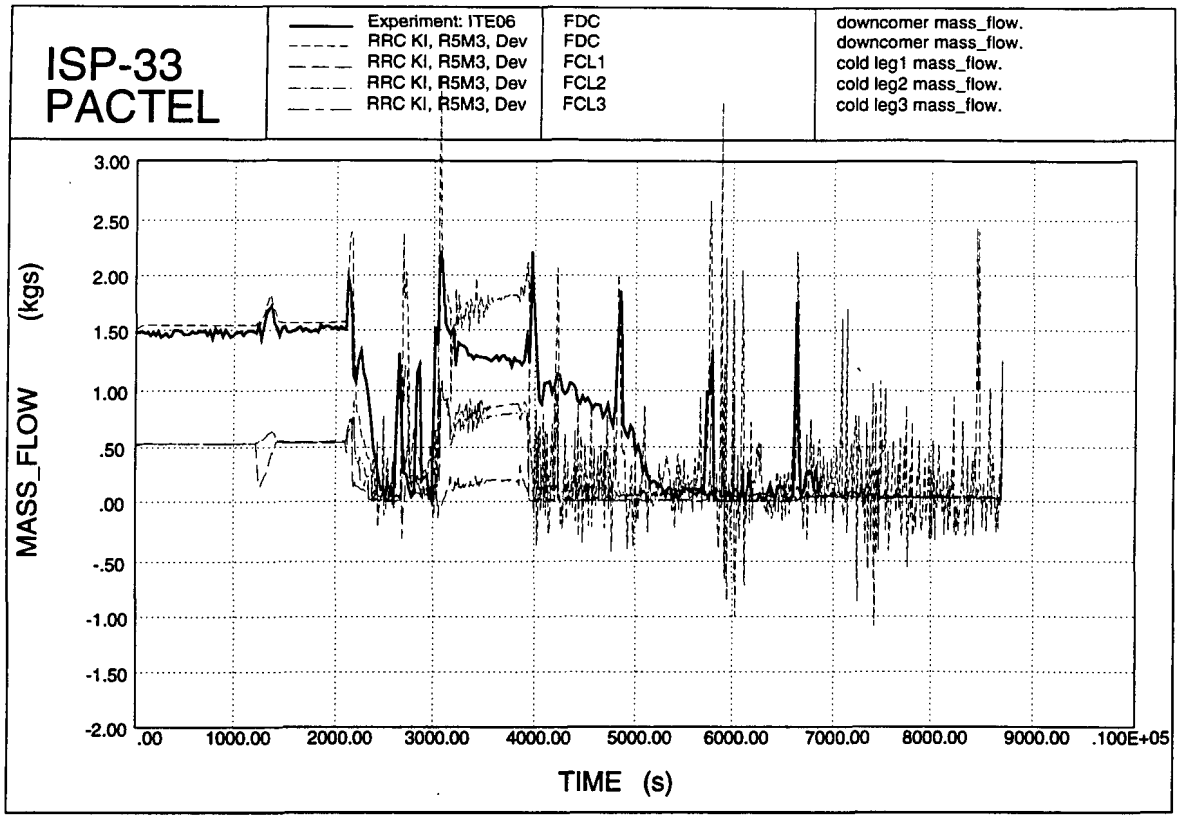

Figure 6.58. Primary mass flows.

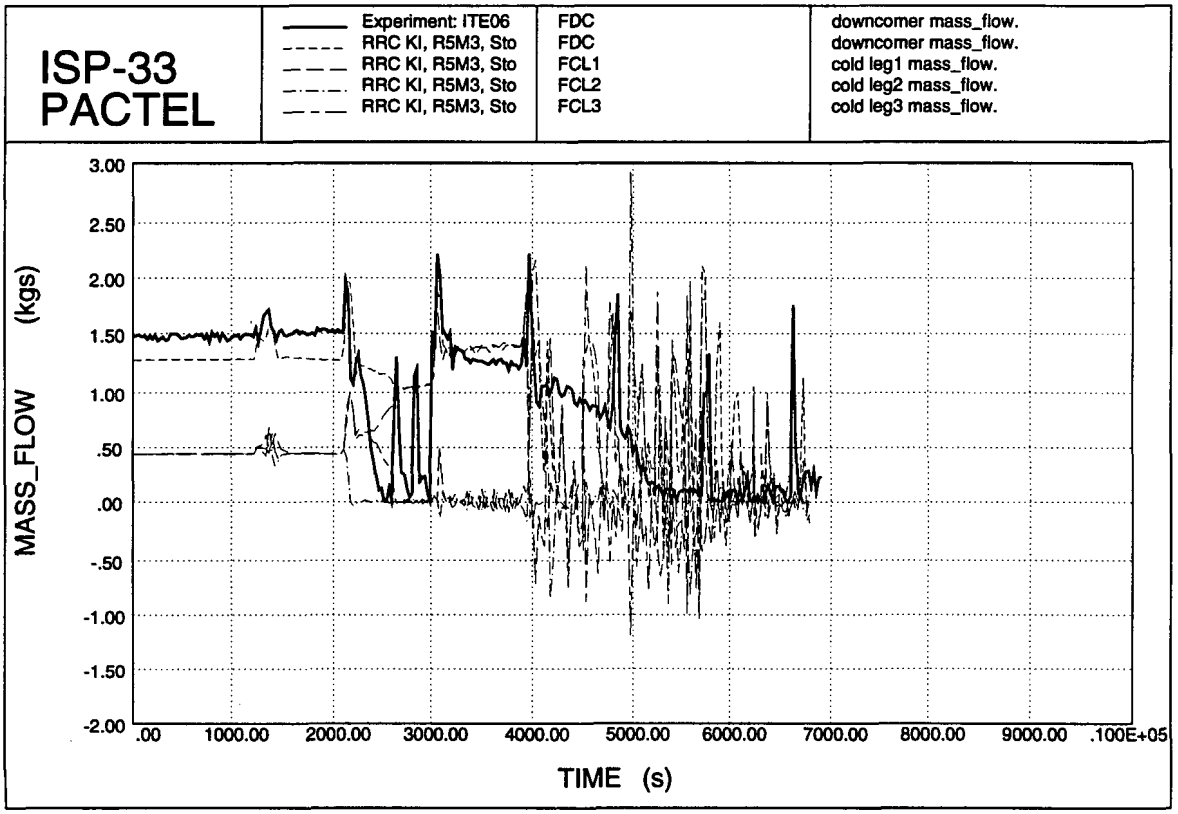

Figure 6.59. Primary mass flows.

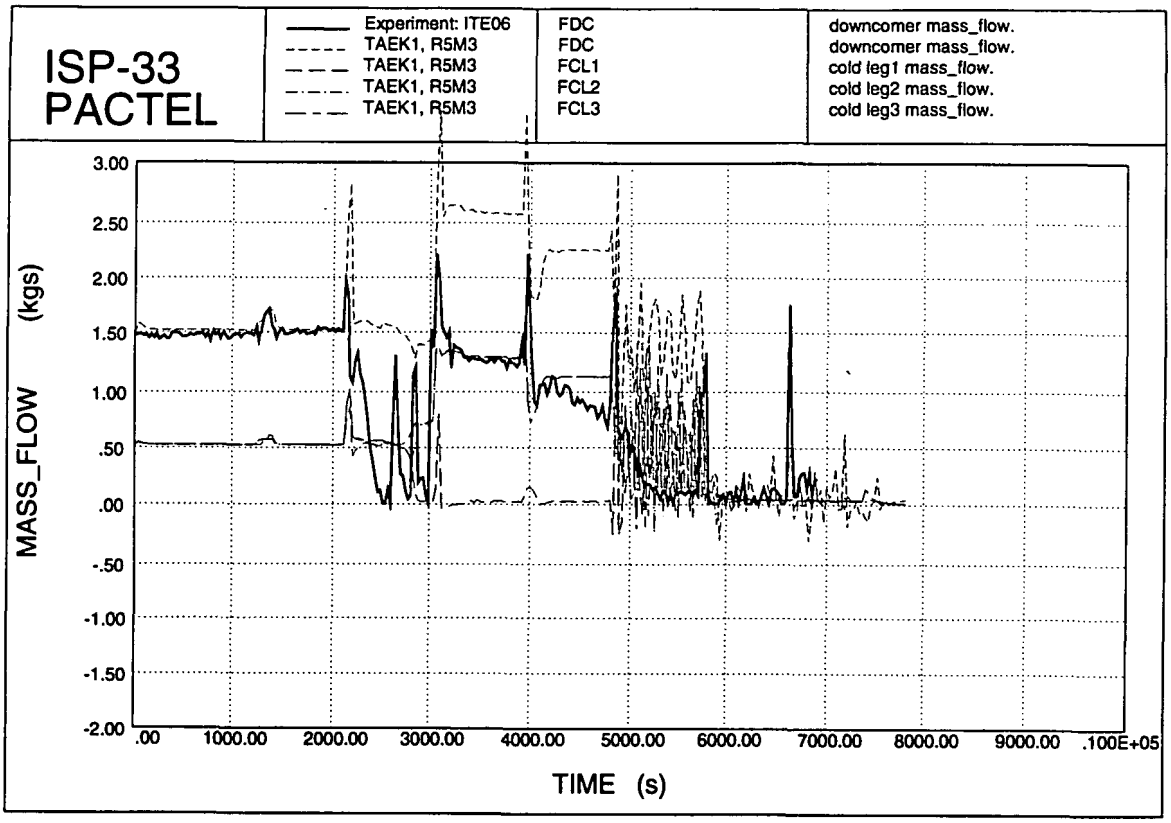

Figure 6.60. Primary mass flows.

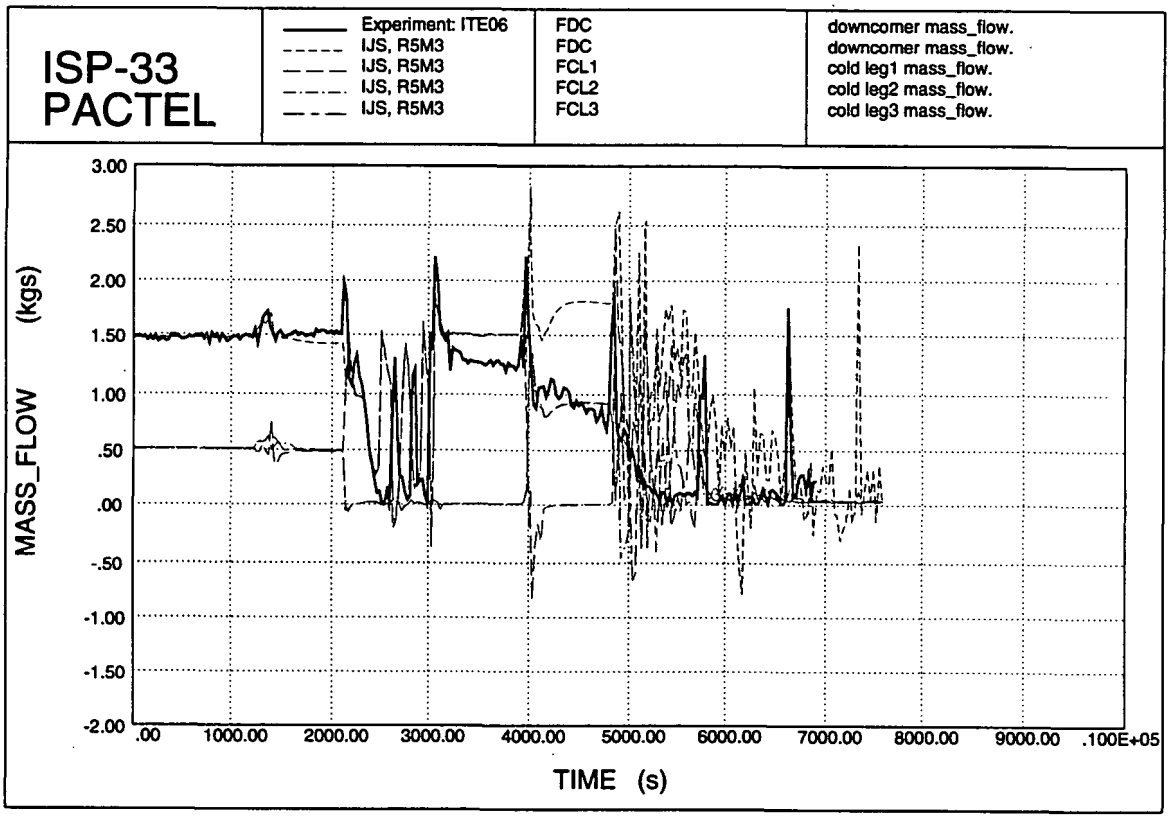

Figure 6.61. Primary mass flows.

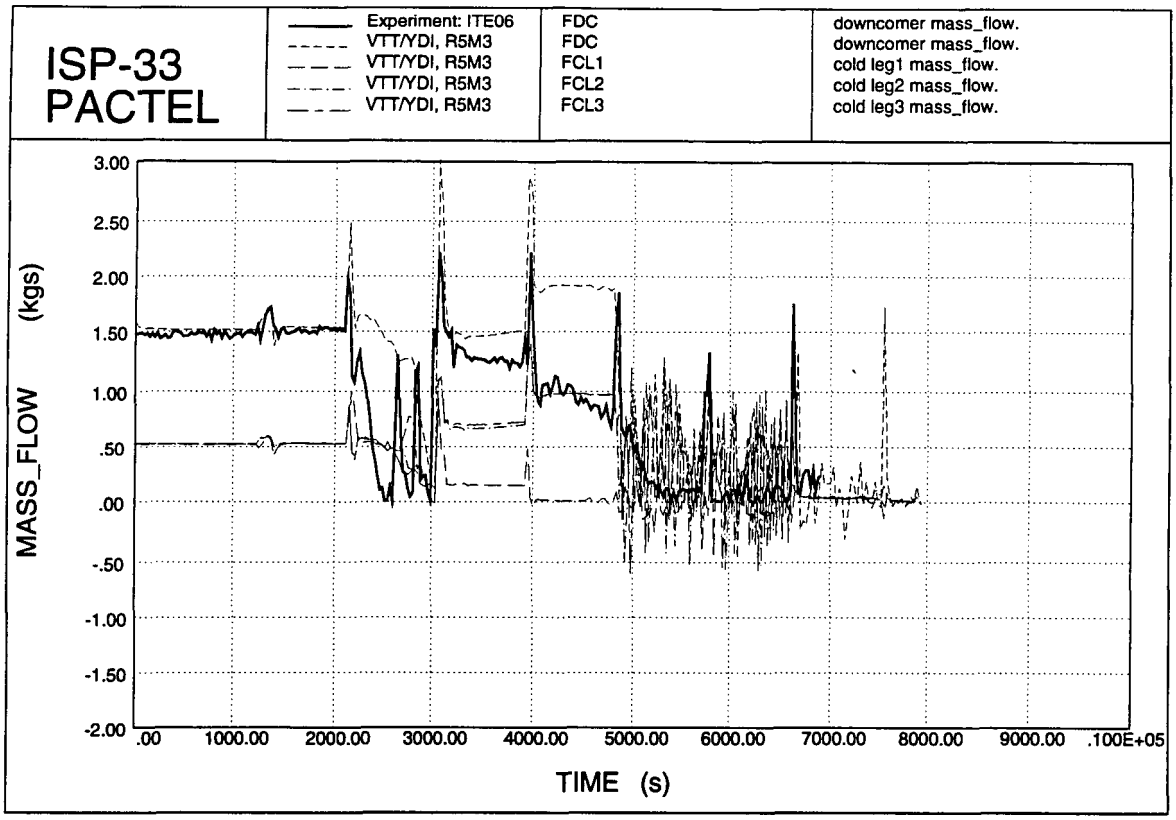

Figure 6.62. Primary mass flows.

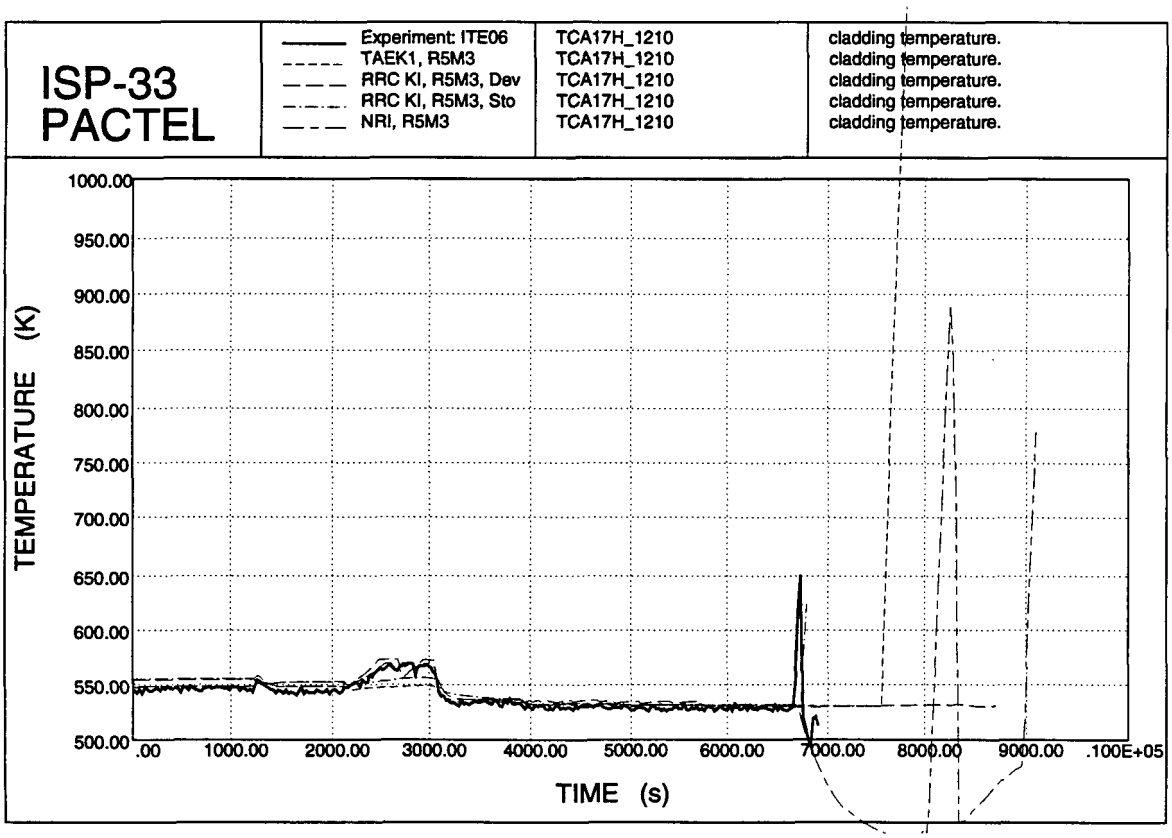

Figure 6.63. Cladding temperatures.

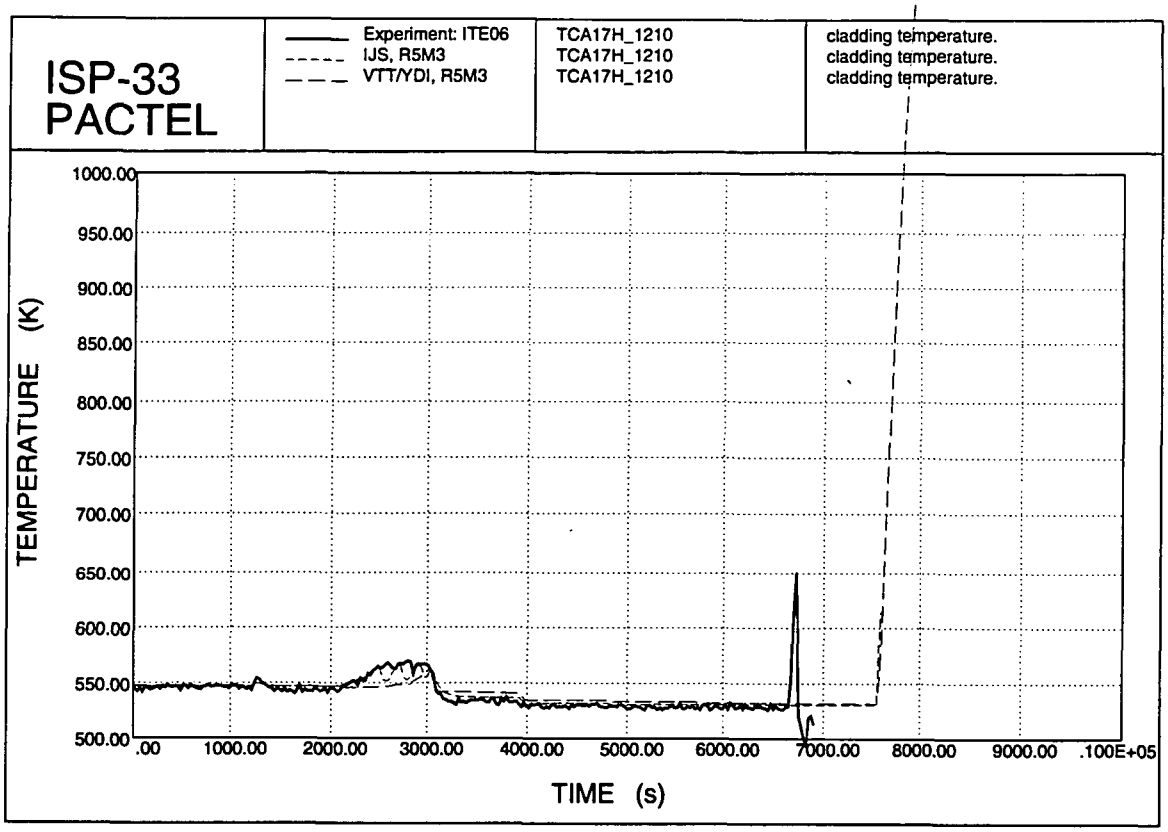

Figure 6.64. Cladding temperatures.

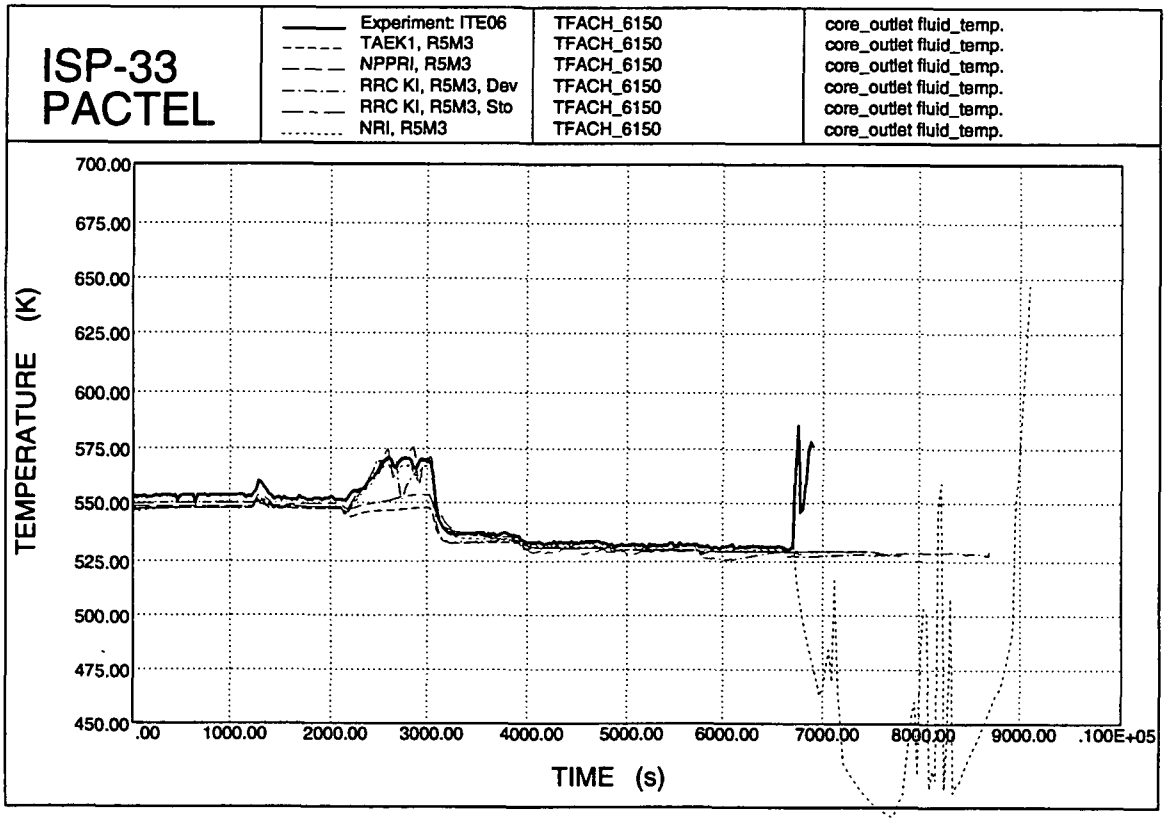

Figure 6.65. Core outlet coolant temperature.

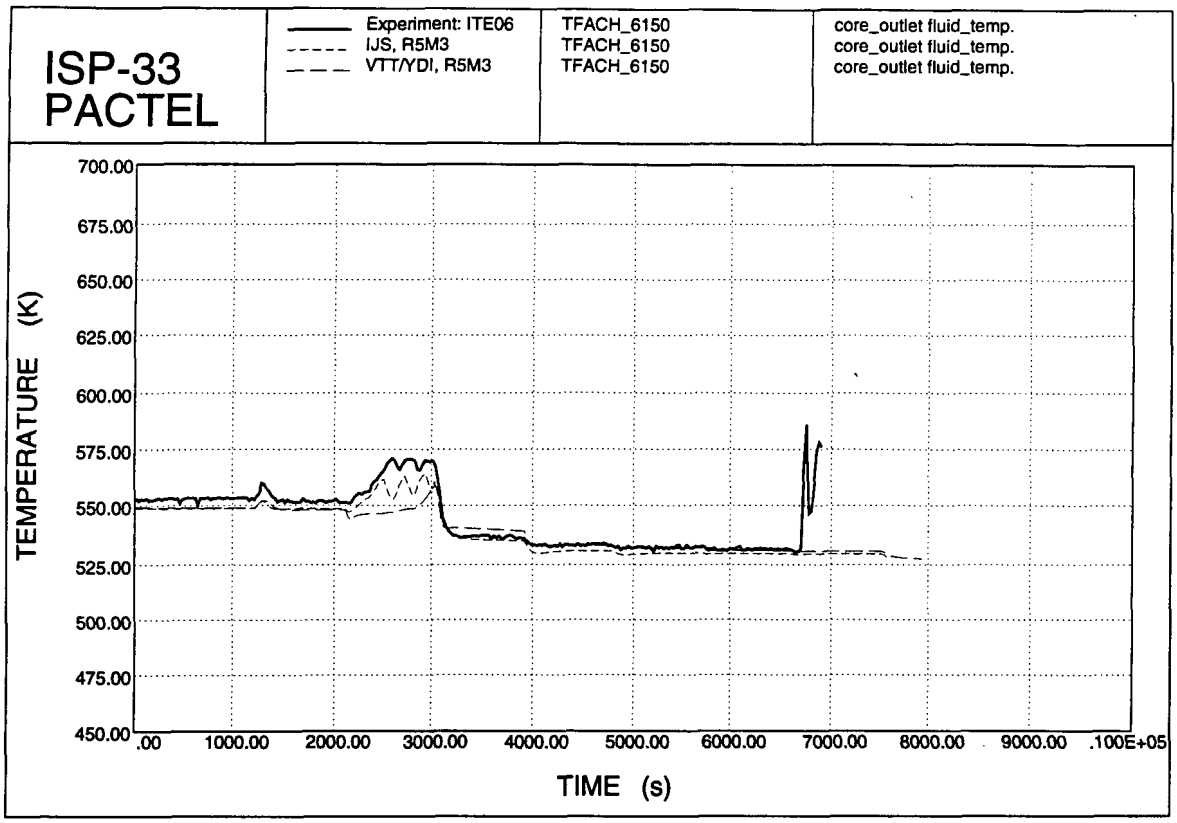

Figure 6.66. Core outlet coolant temperature.

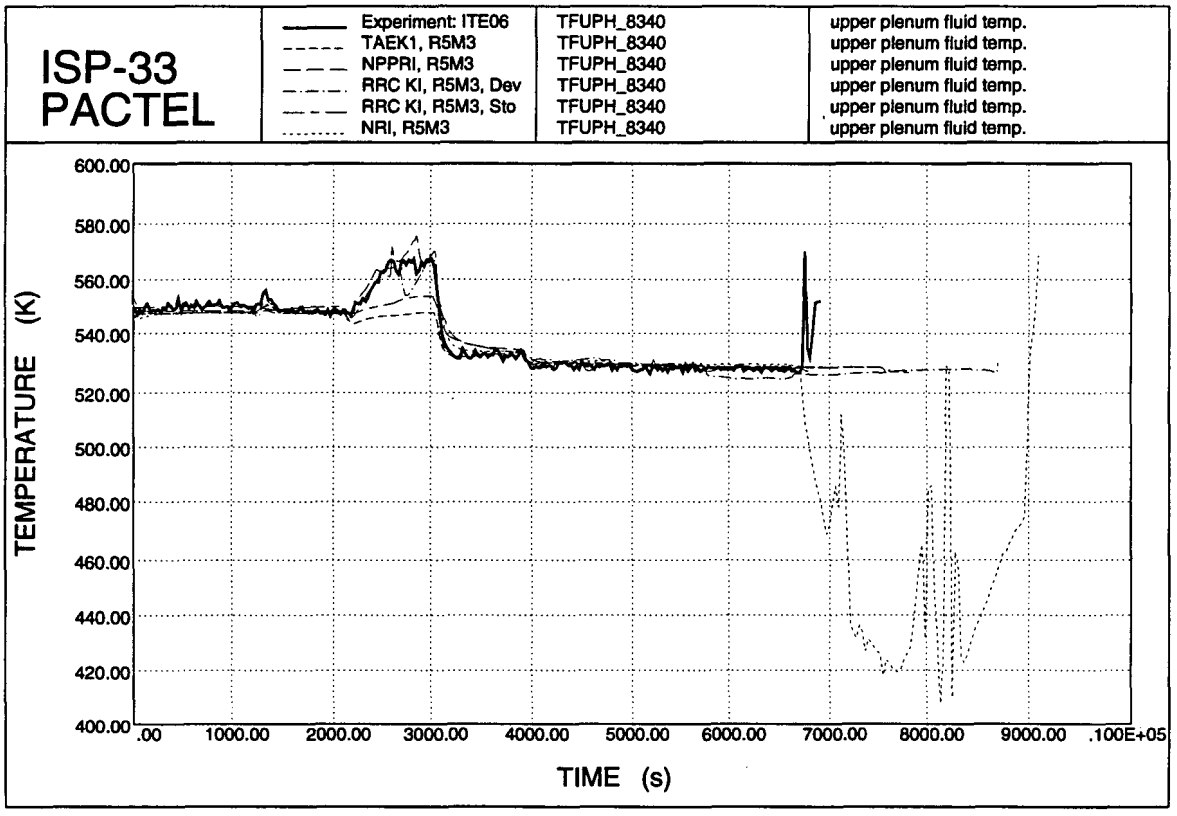

Figure 6.67. Upper plenum temperatures.

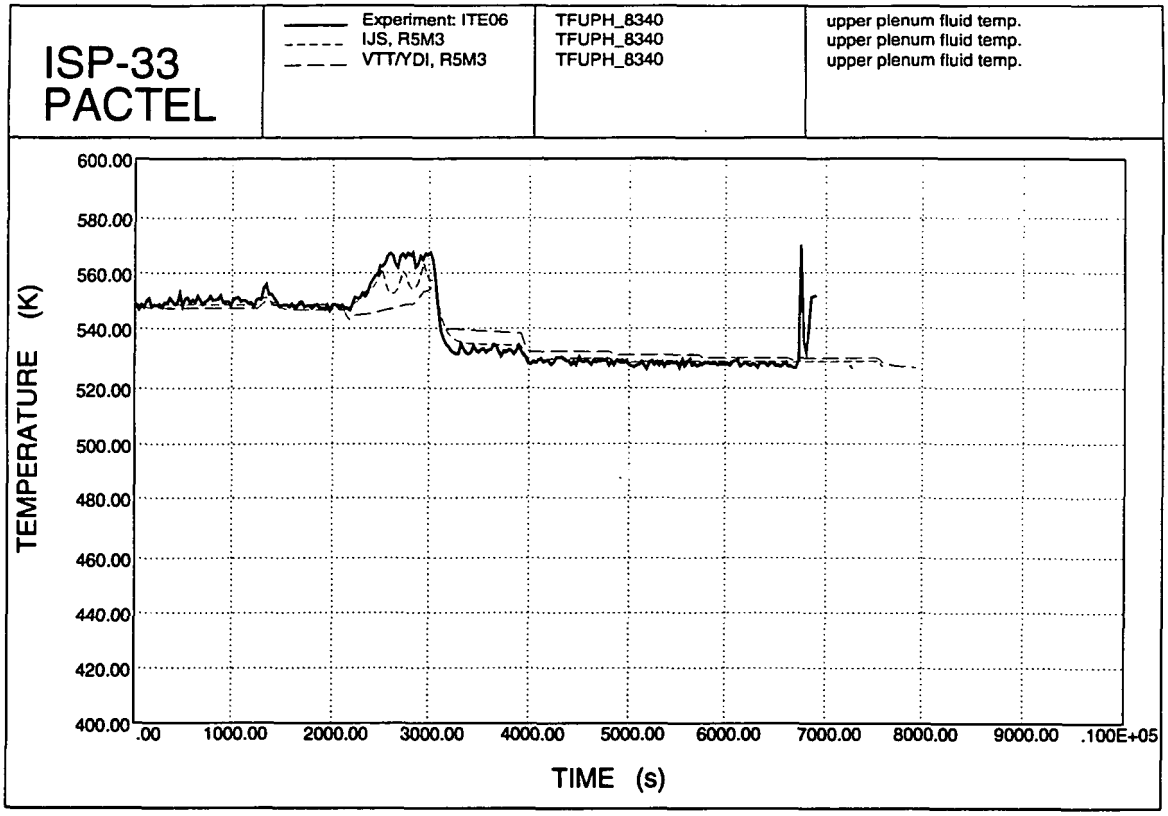

Figure 6.68. Upper plenum temperatures.

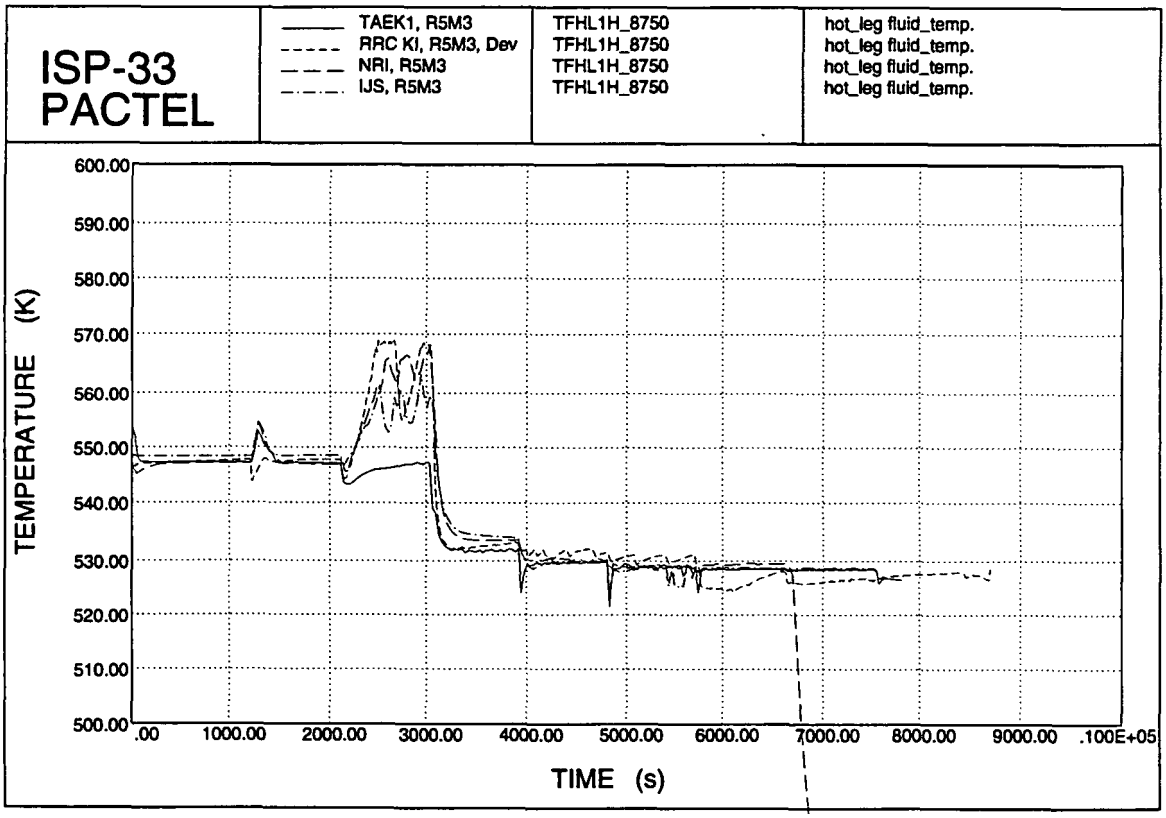

Figure 6.69. Hot leg coolant temperatures.

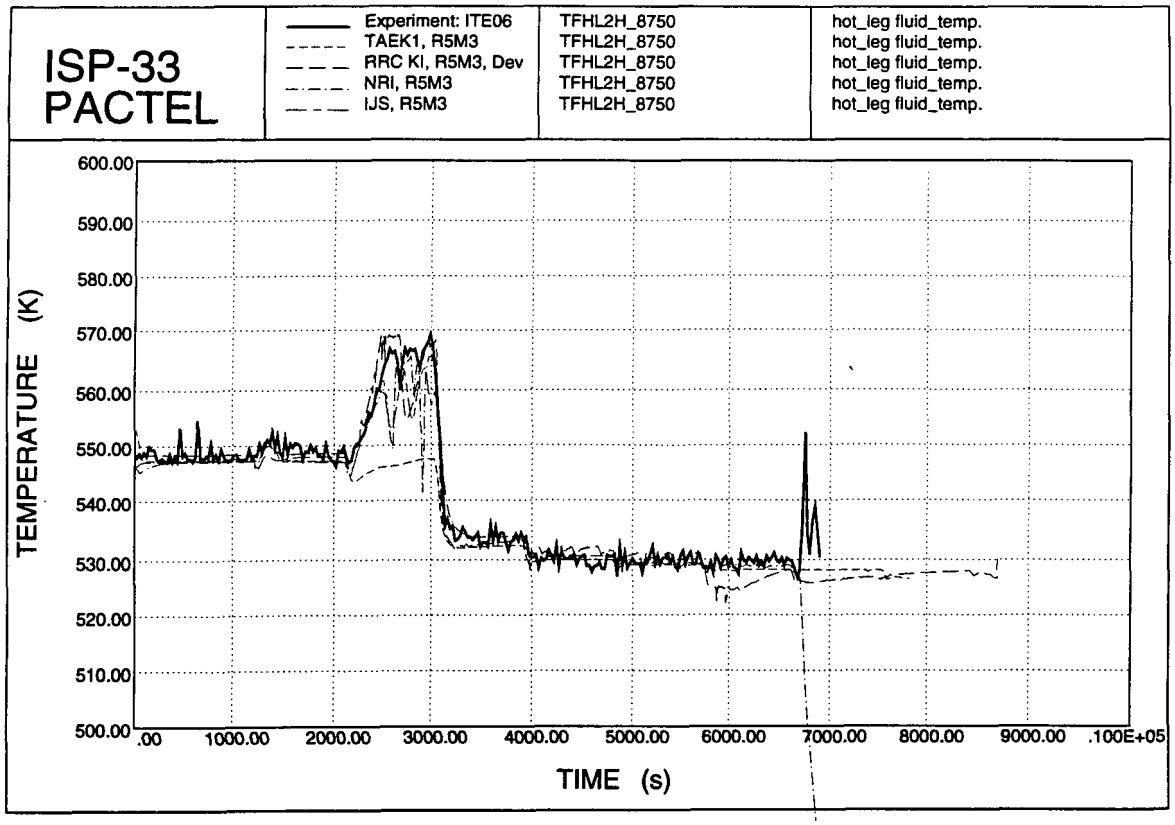

Figure 6.70. Hot leg temperatures.

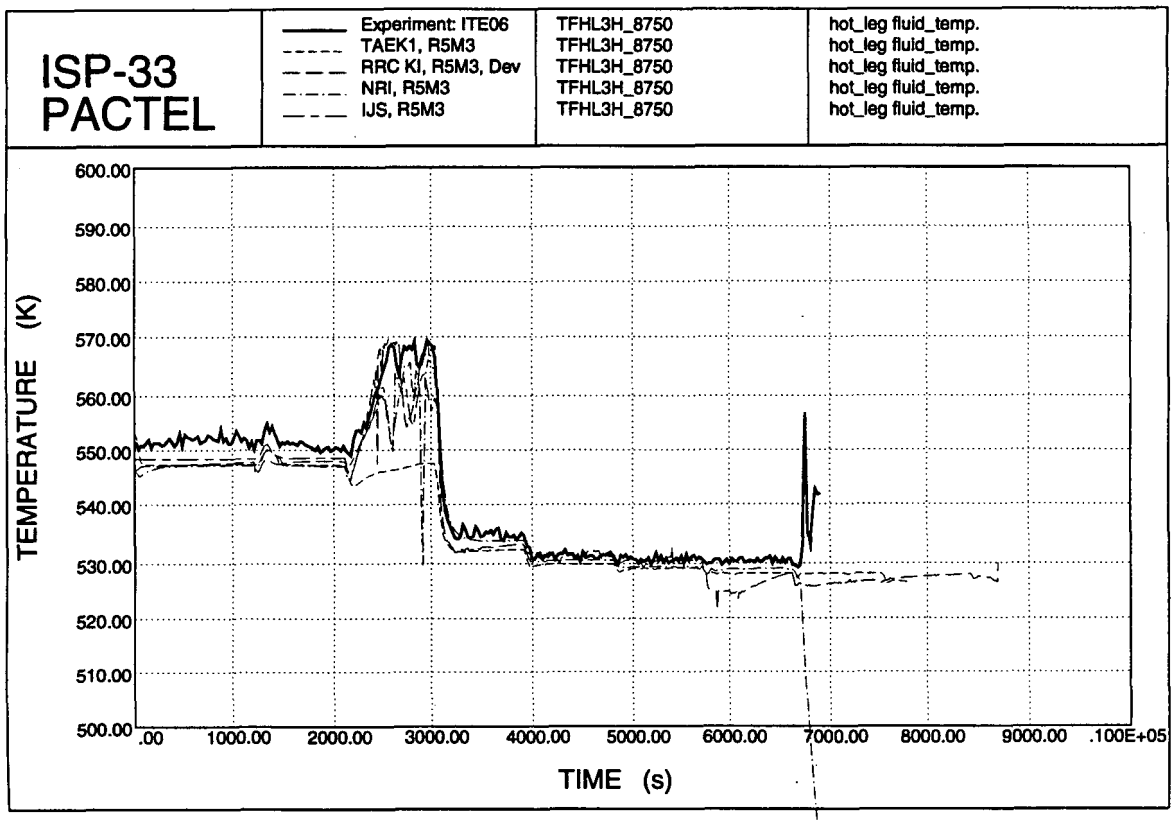

Figure 6.71. Hot leg coolant temperatures.

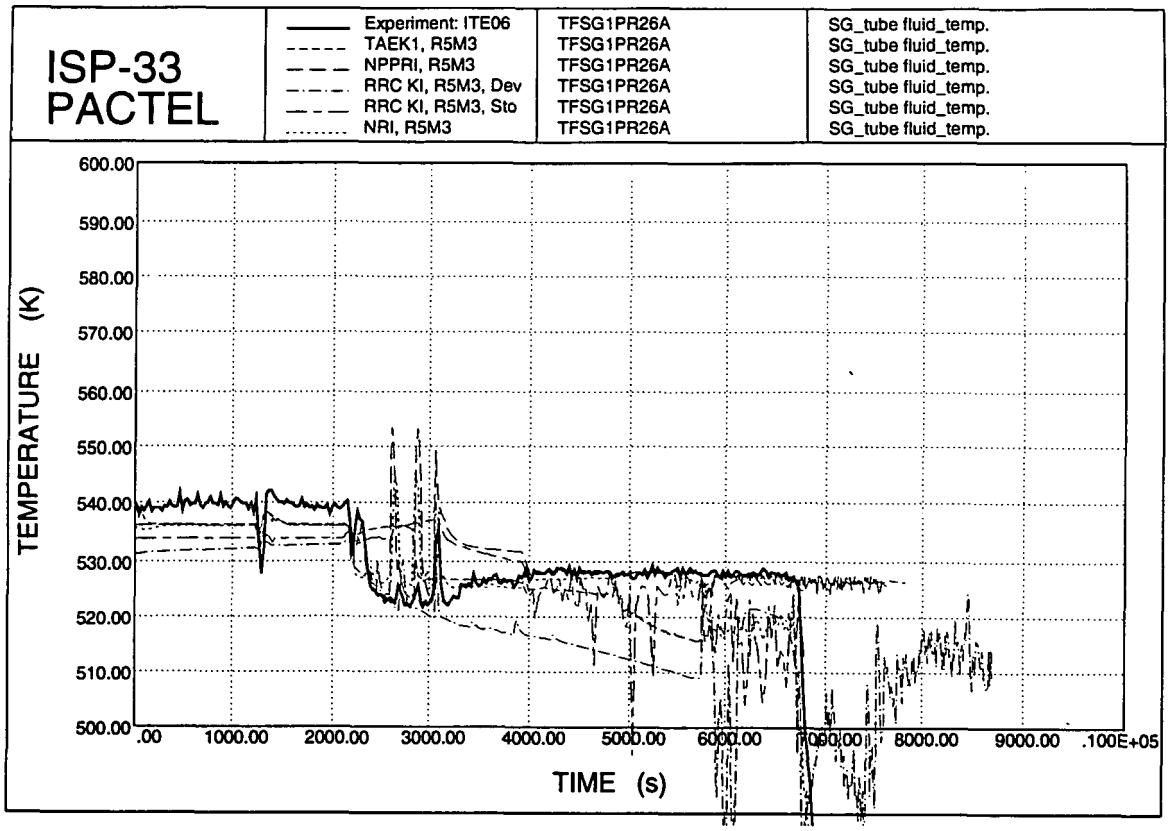

Figure 6.72. SG tube fluid temperatures.

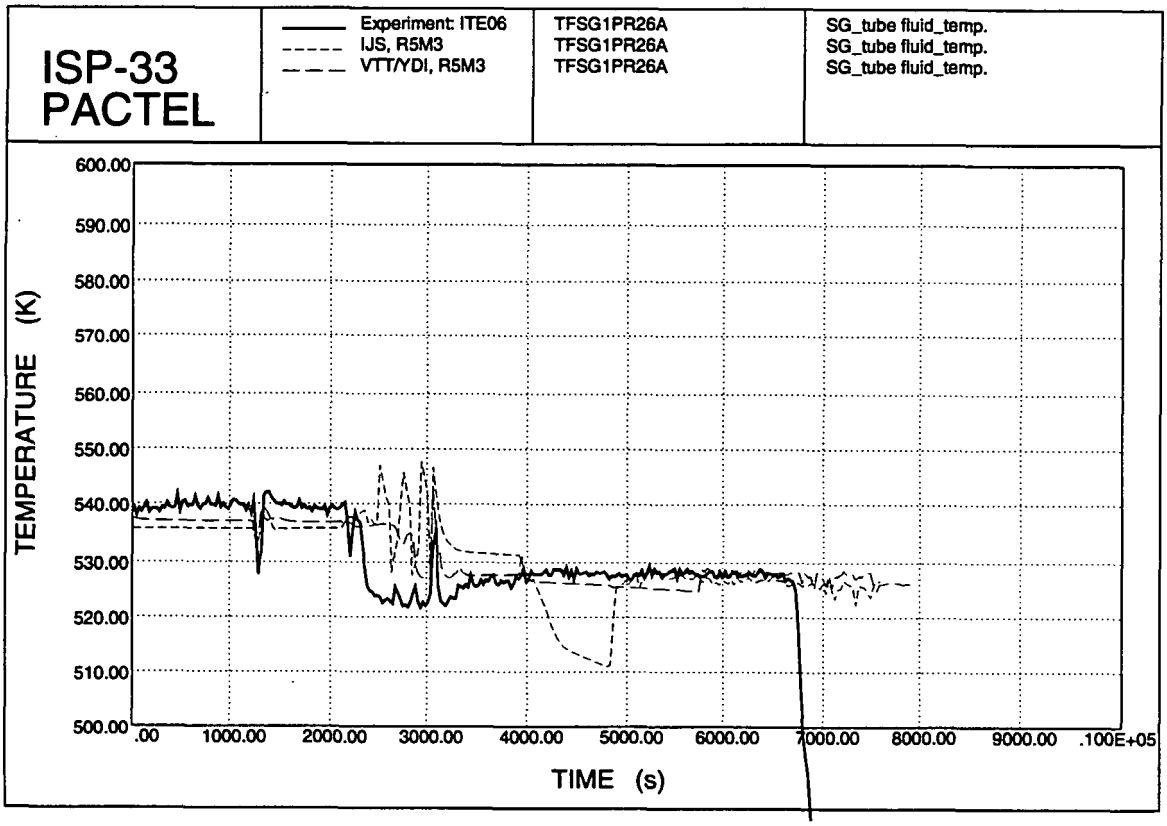

Figure 6.73. SG tube fluid temperatures.

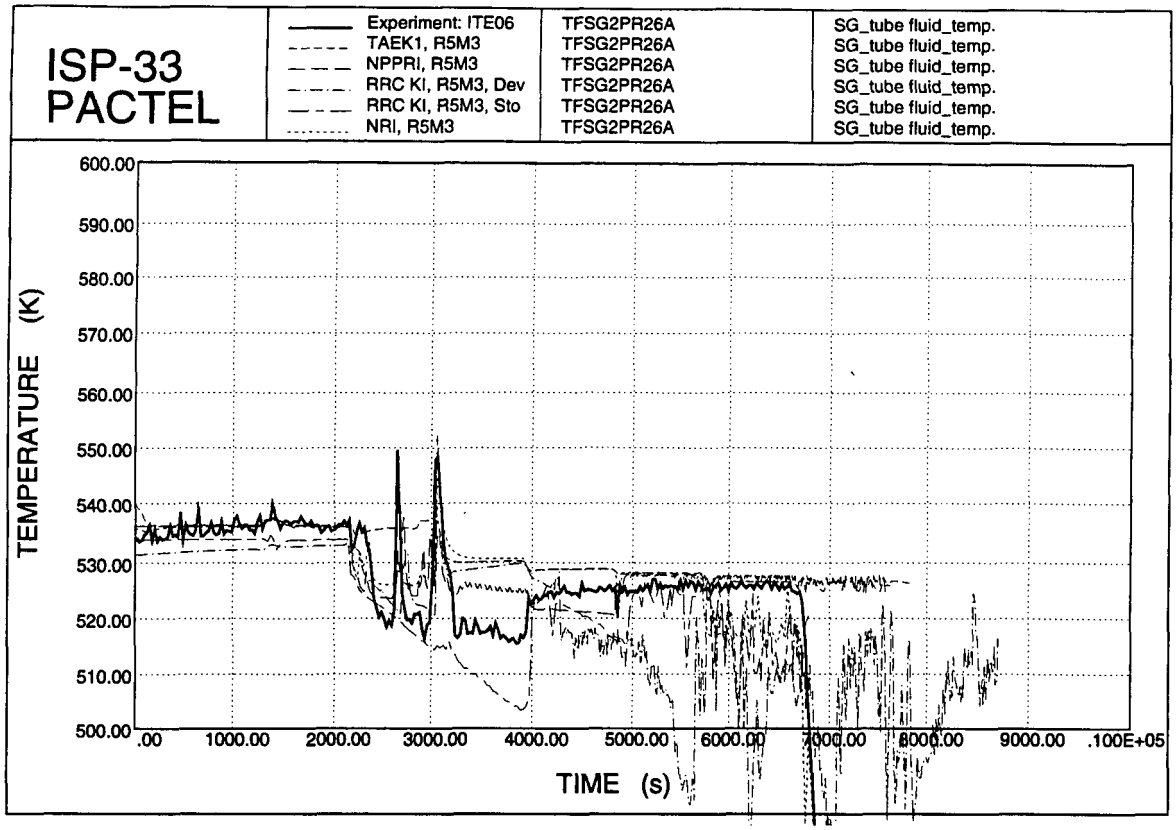

Figure 6.74. SG tube fluid temperatures.

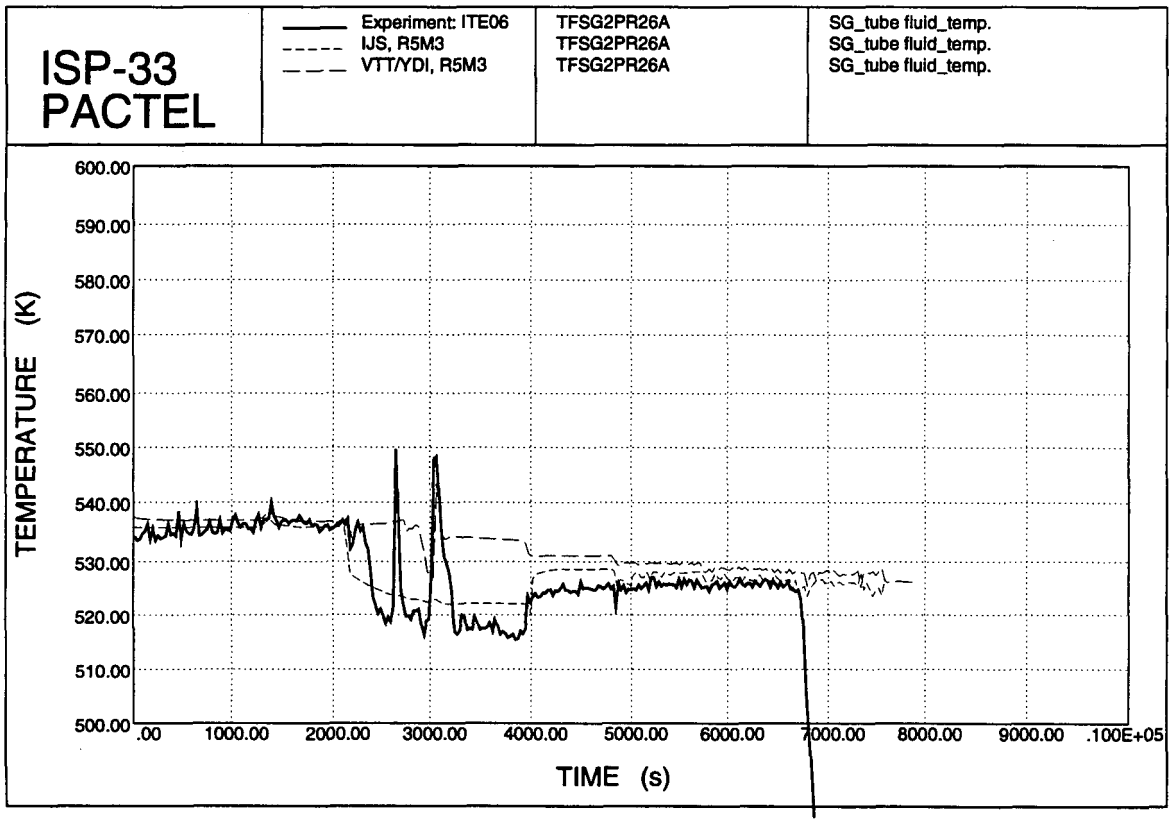

Figure 6.75. SG tube fluid temperatures.

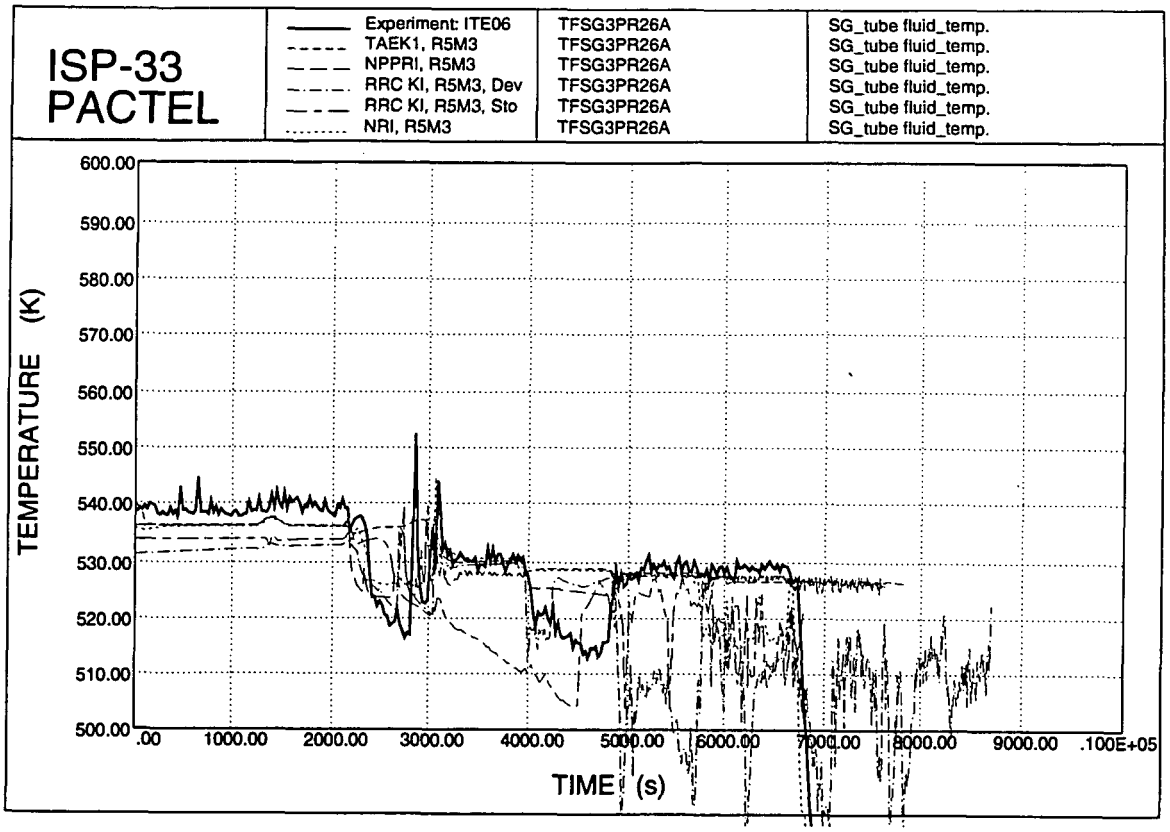

Figure 6.76. SG tube fluid temperatures.

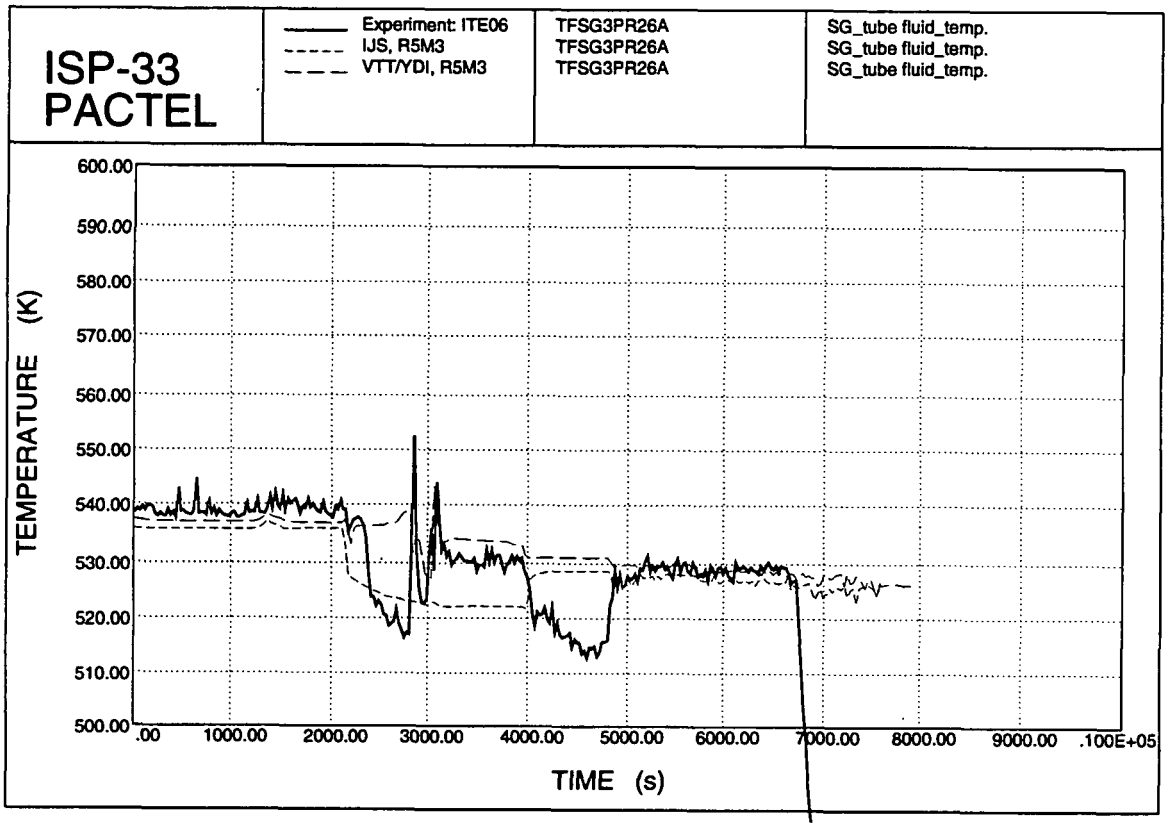

Figure 6.77. SG tube fluid temperatures.

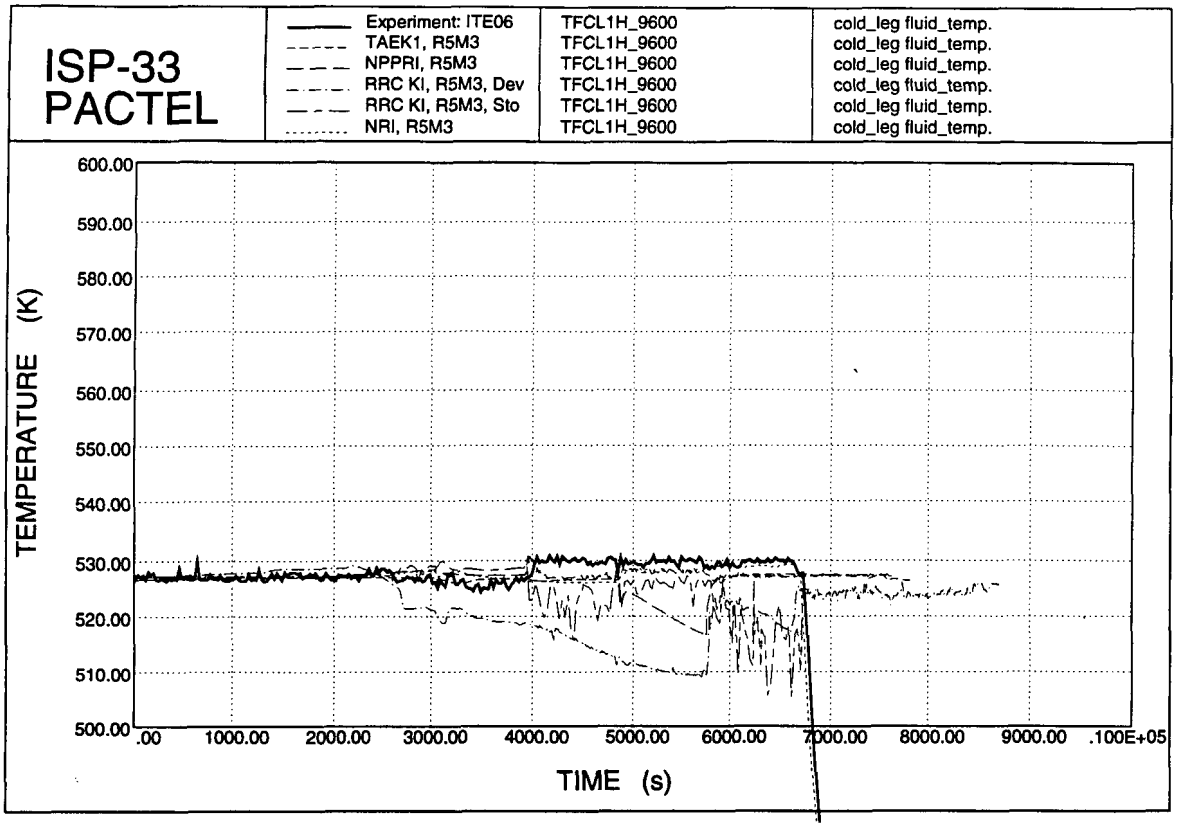

Figure 6.78. Cold leg temperatures.

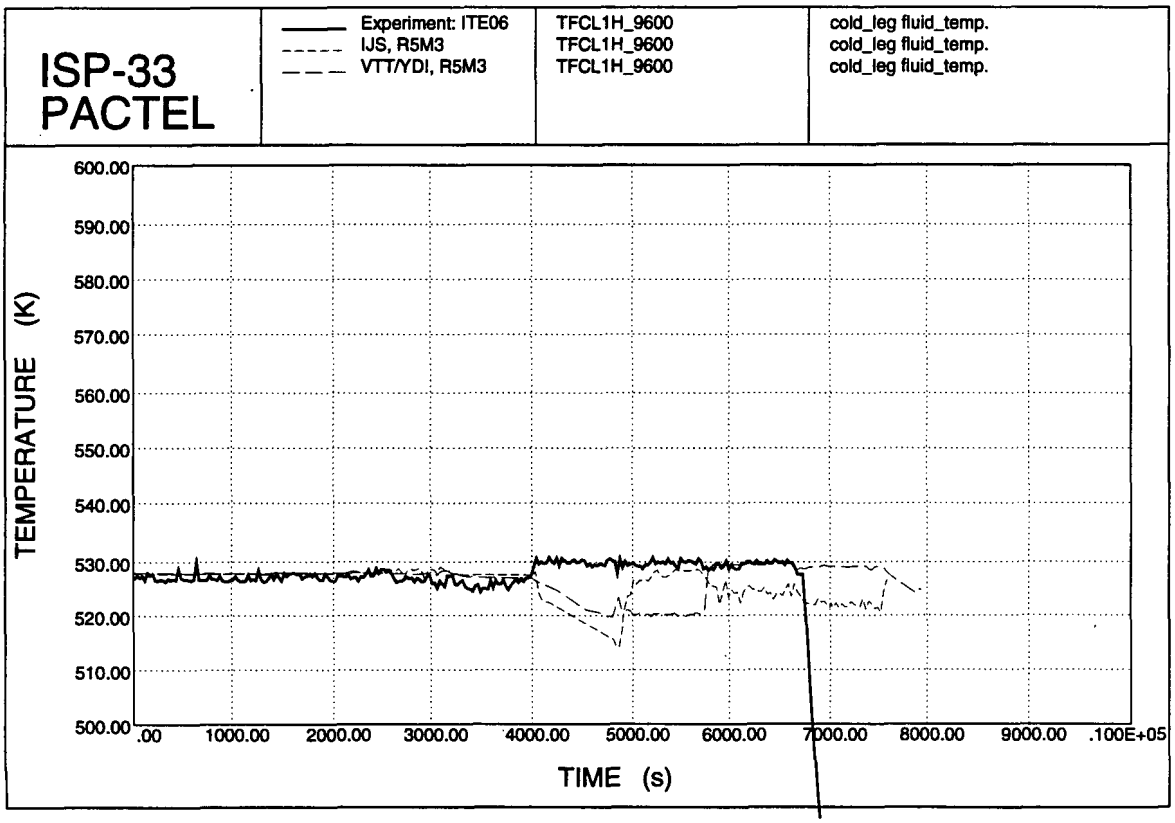

Figure 6.79. Cold leg temperatures.

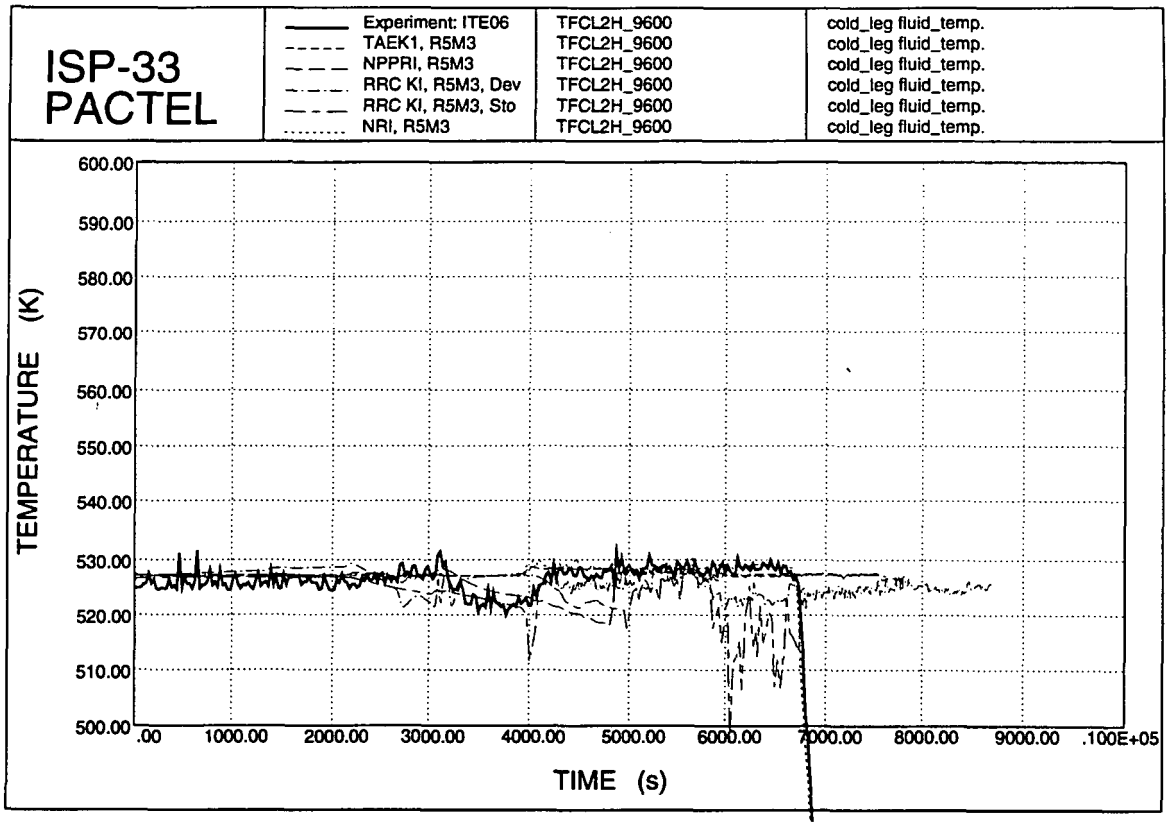

Figure 6.80. Cold leg coolant temperatures.

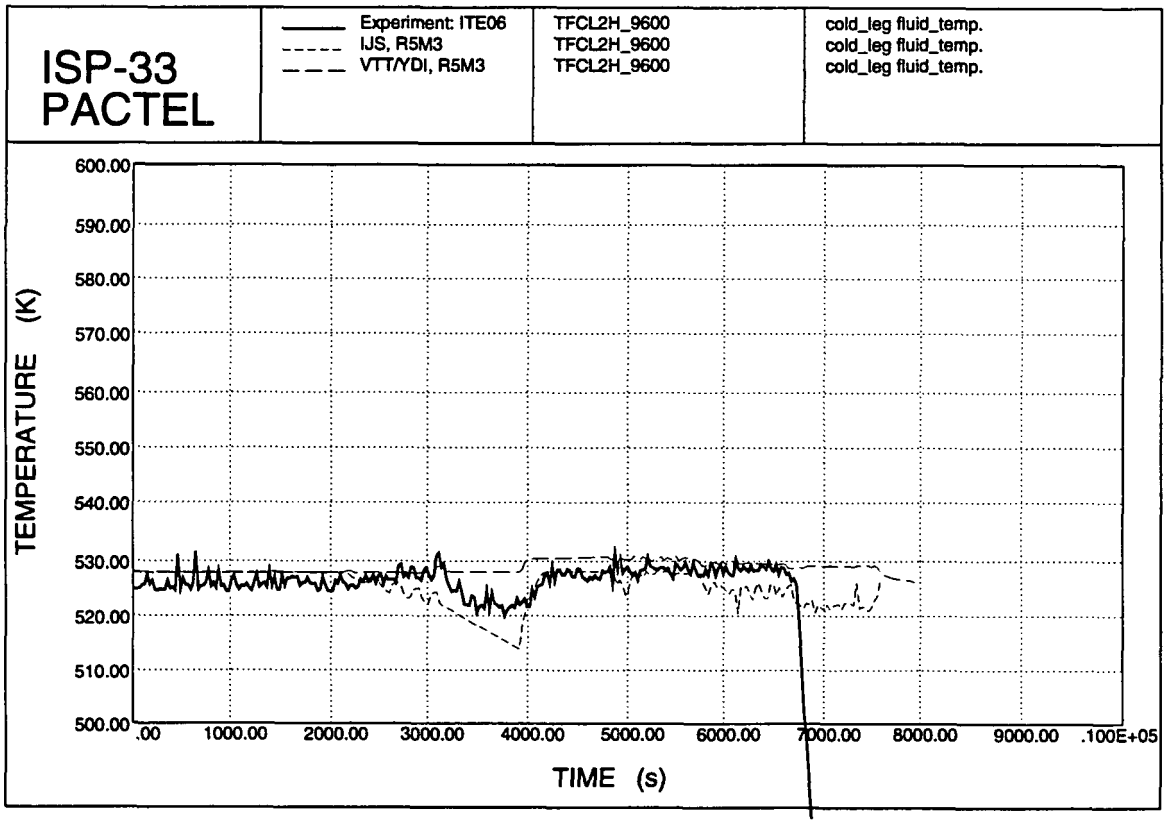

Figure 6.81. Cold leg coolant temperatures.

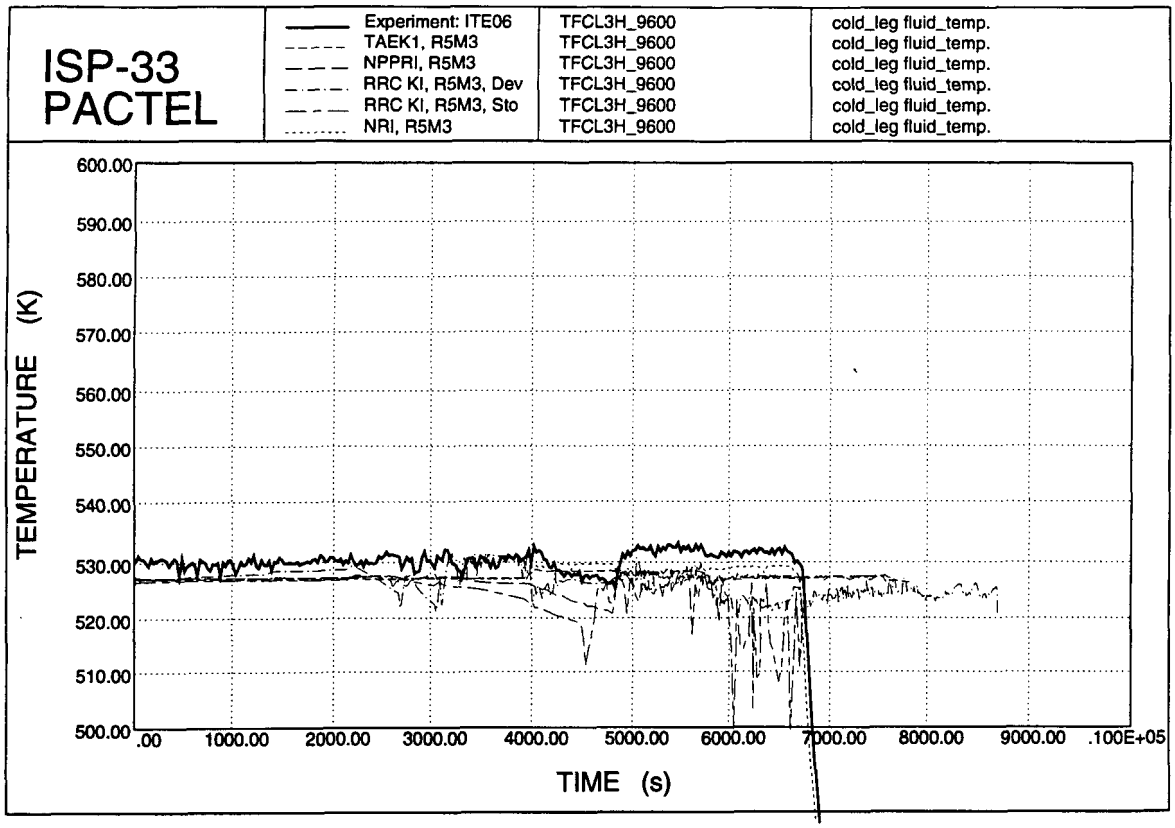

Figure 6.82. Cold leg temperatures.

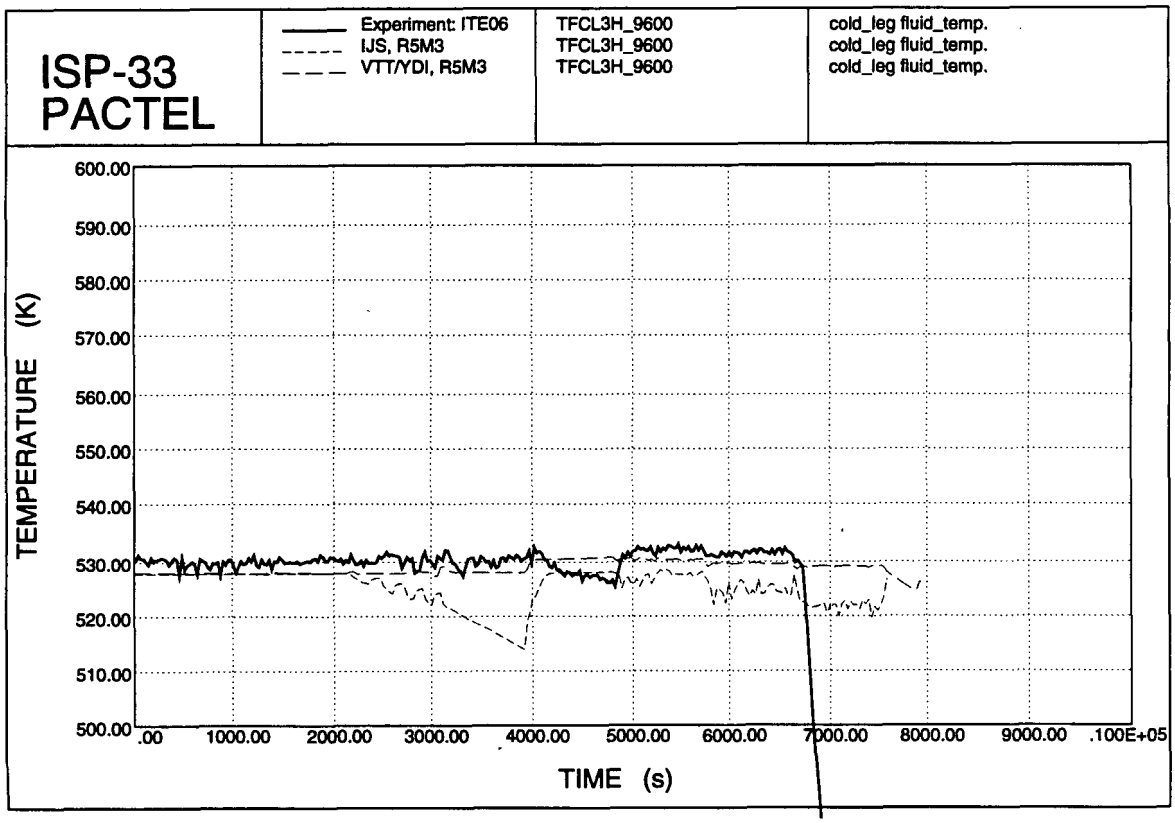

Figure 6.83. Cold leg temperatures.

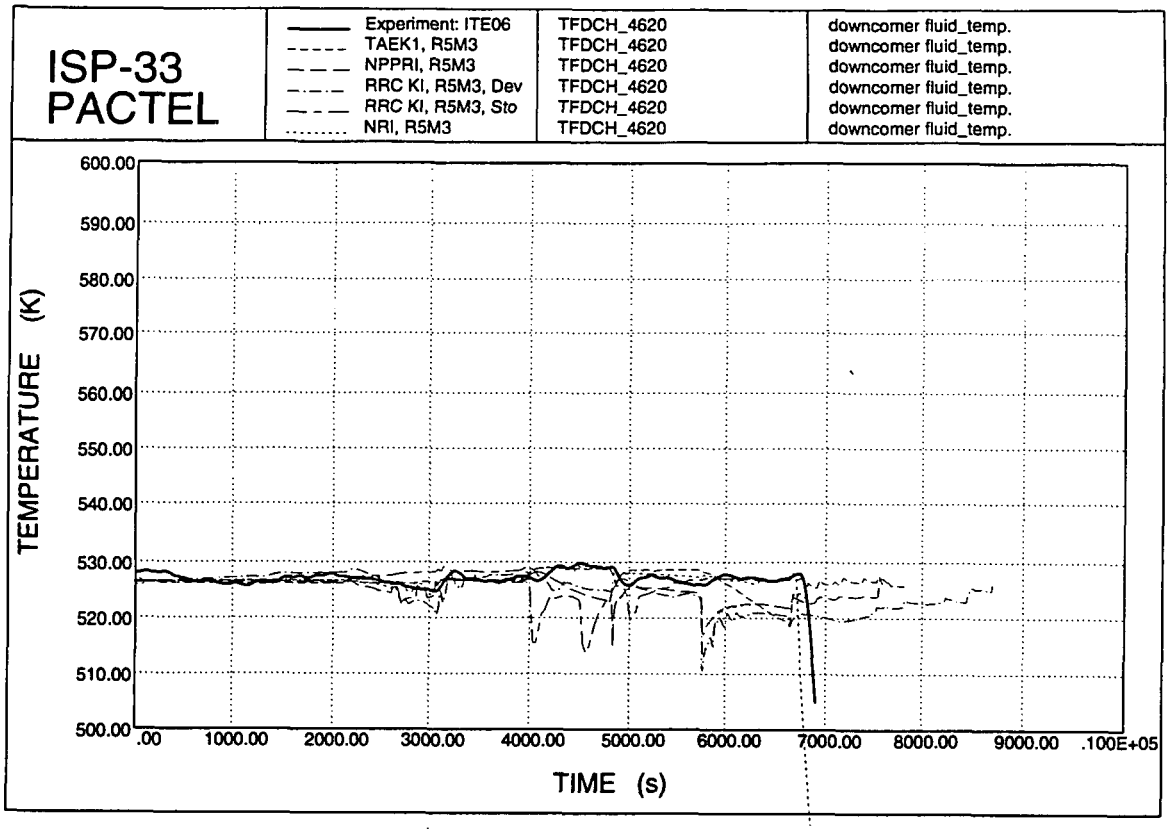

Figure 6.84. Downcomer temperatures.

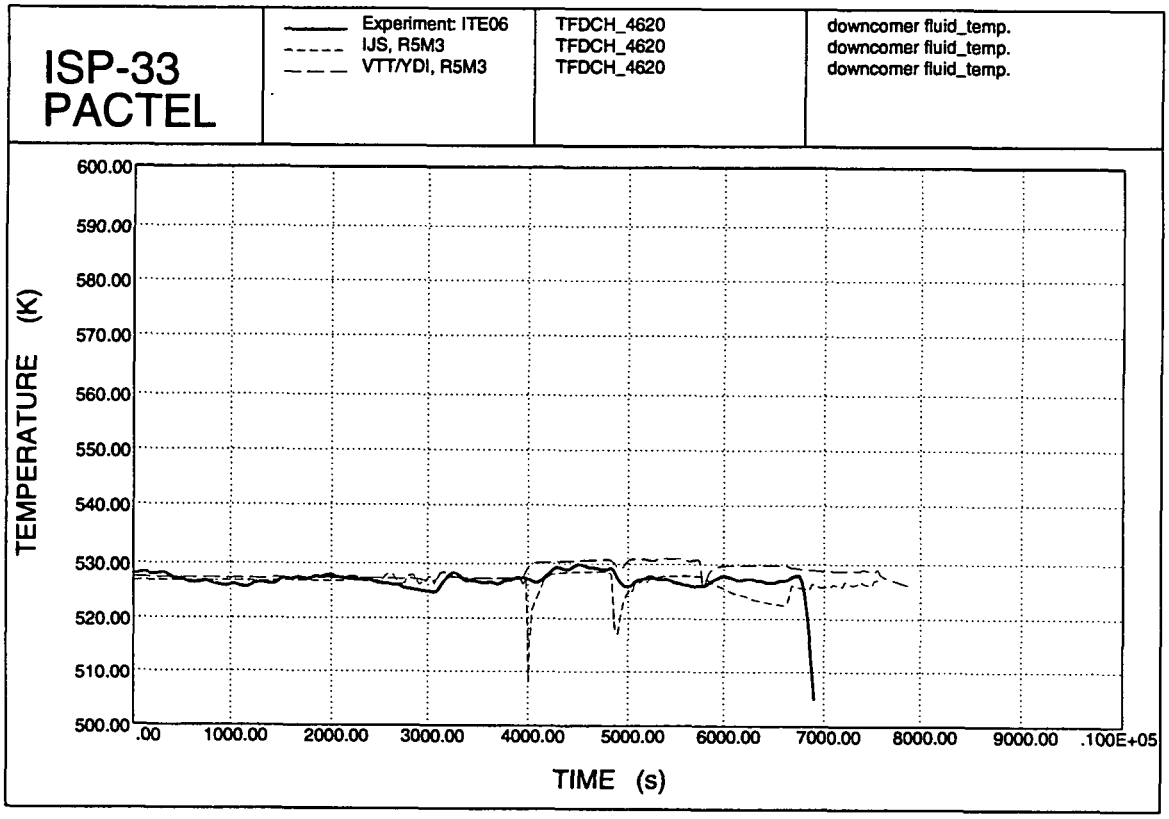

Figure 6.85. Downcomer temperatures.

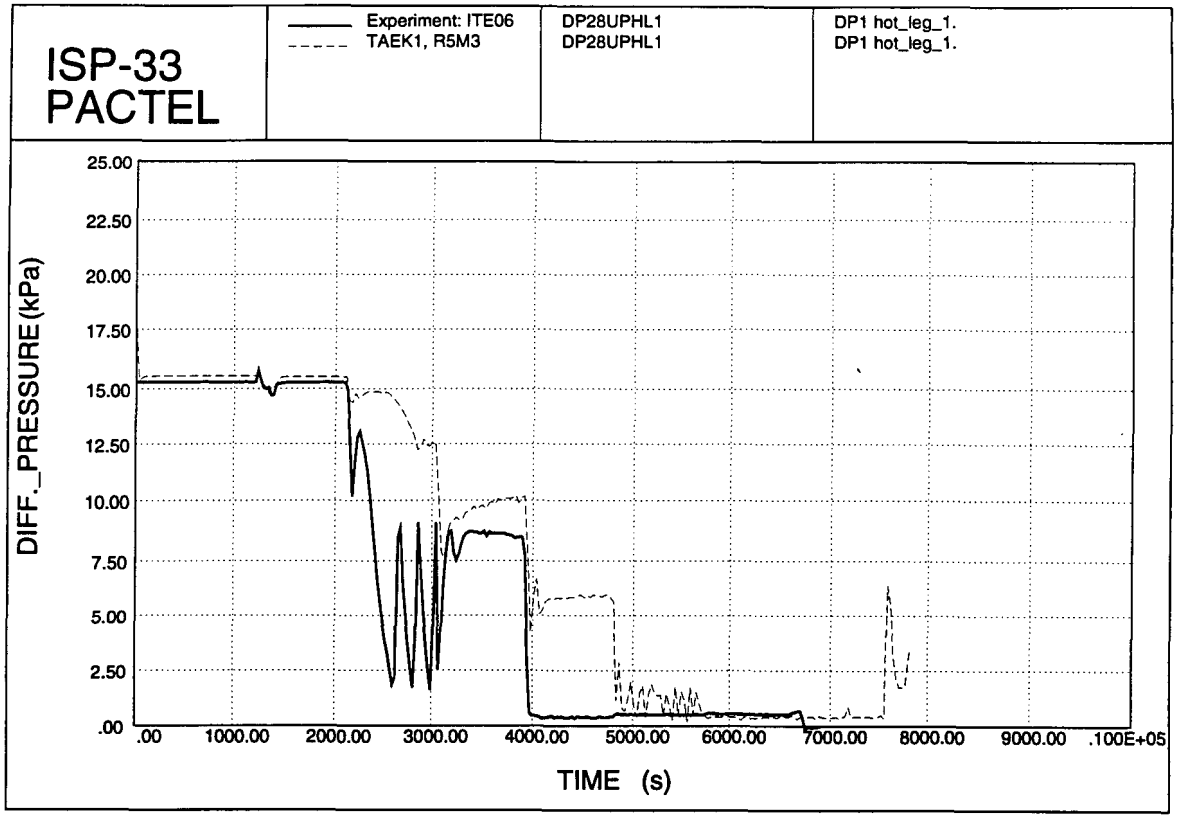

Figure 6.86. Hot leg 1 DP 1.

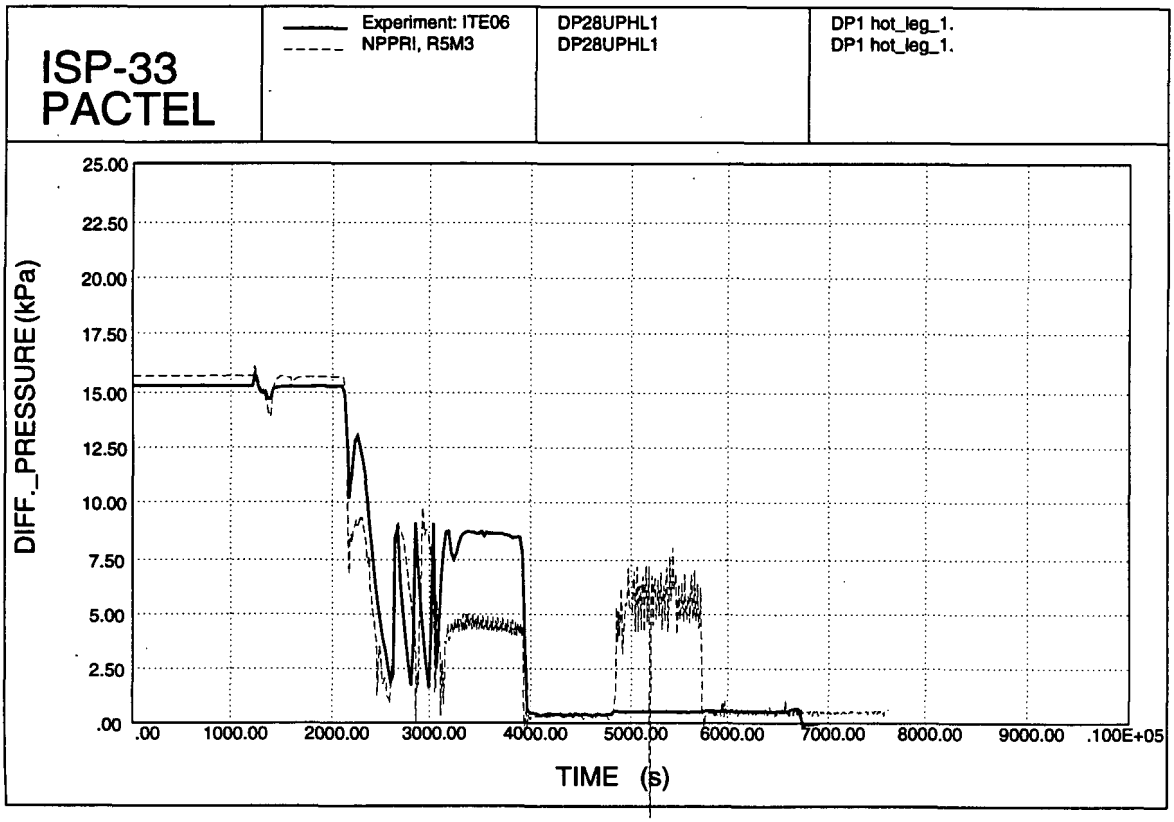

Figure 6.87. Hot leg 1 DP 1.

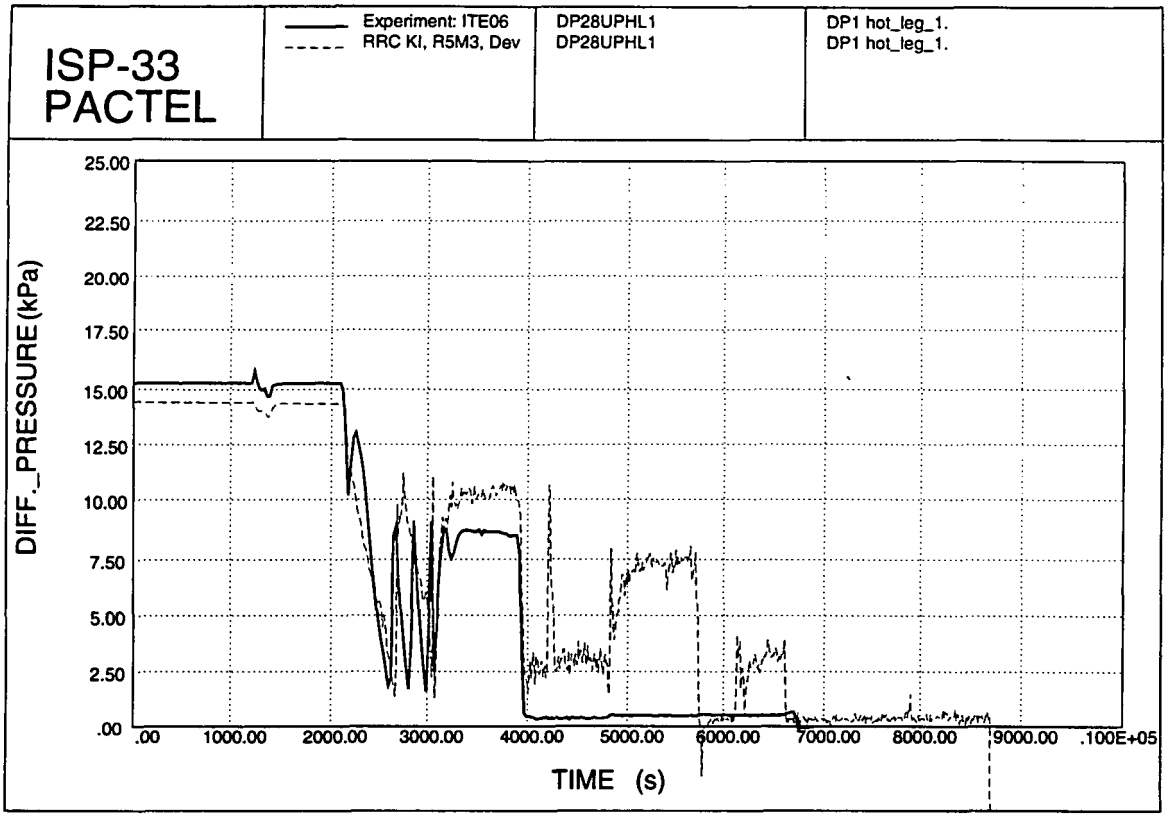

Figure 6.88. Hot leg 1 DP 1.

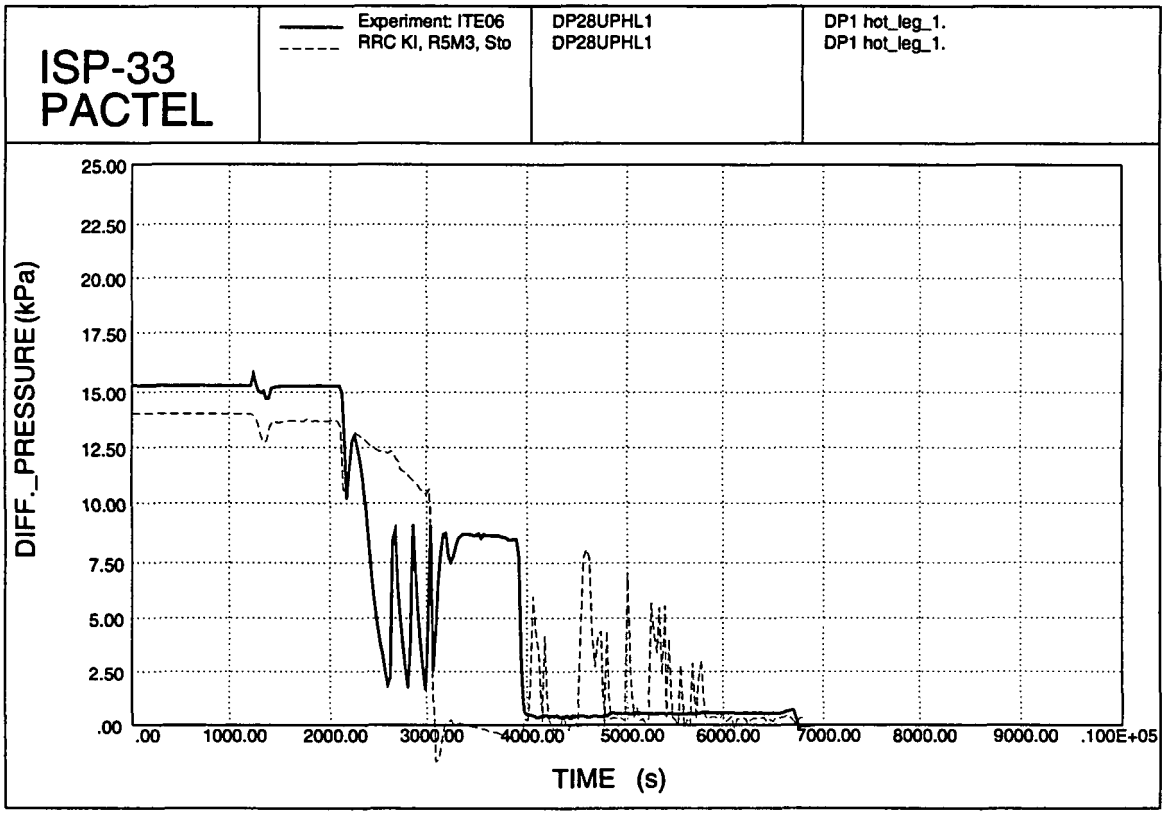

Figure 6.89. Hot leg 1 DP 1.

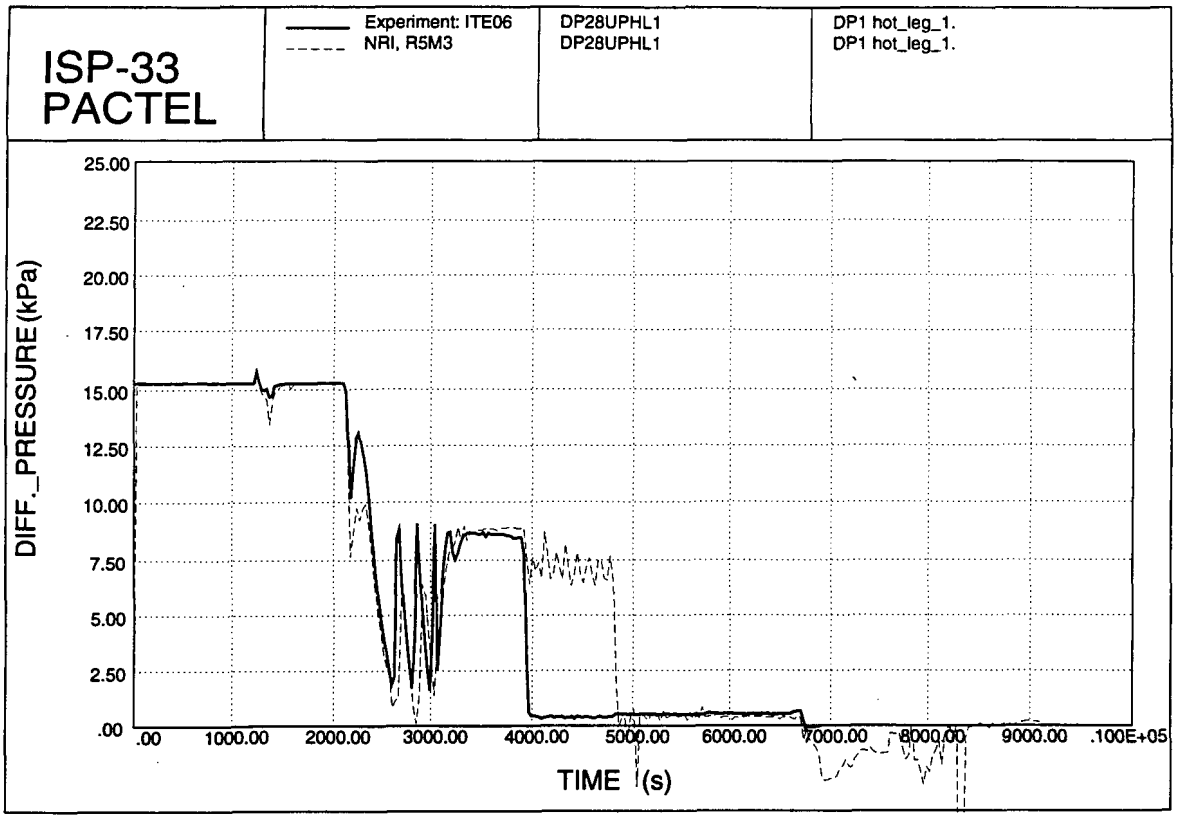

Figure 6.90. Hot leg 1 DP 1.

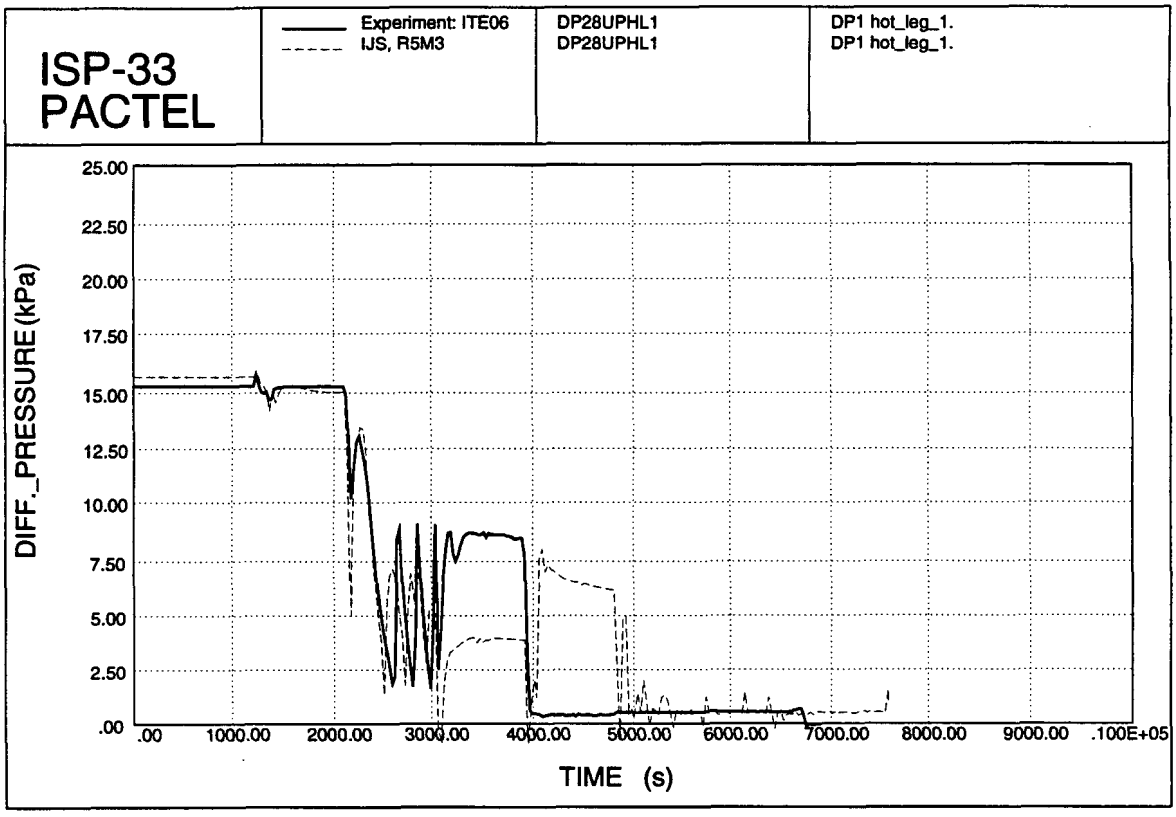

Figure 6.91. Hot leg 1 DP 1.

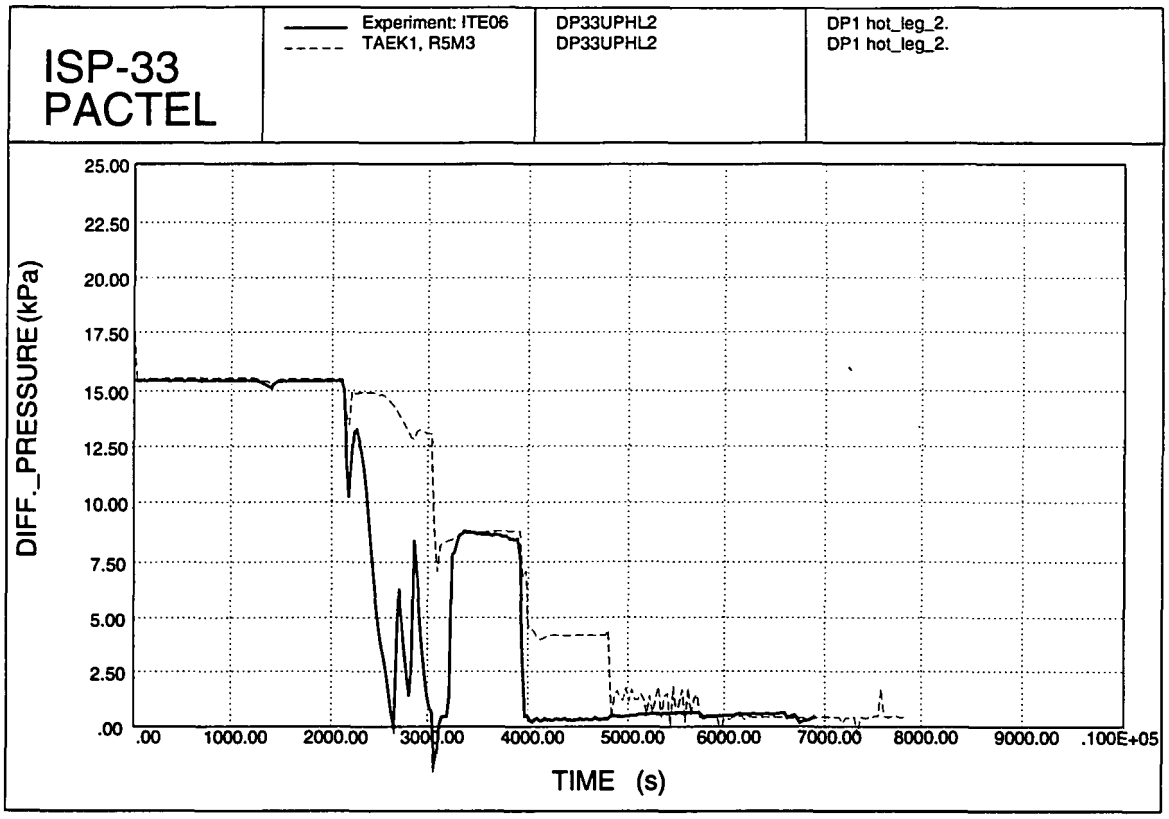

Figure 6.92. Hot leg 2 DP 1.

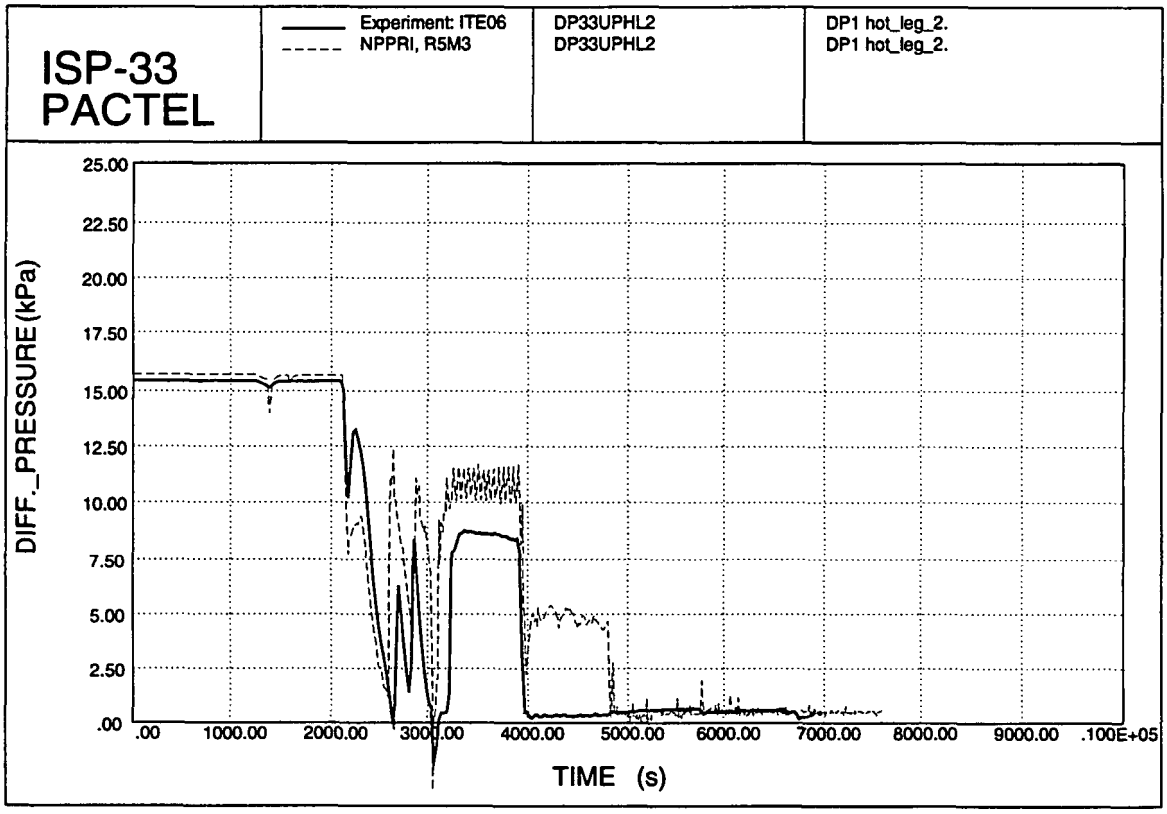

Figure 6.93. Hot leg 2 DP 1.

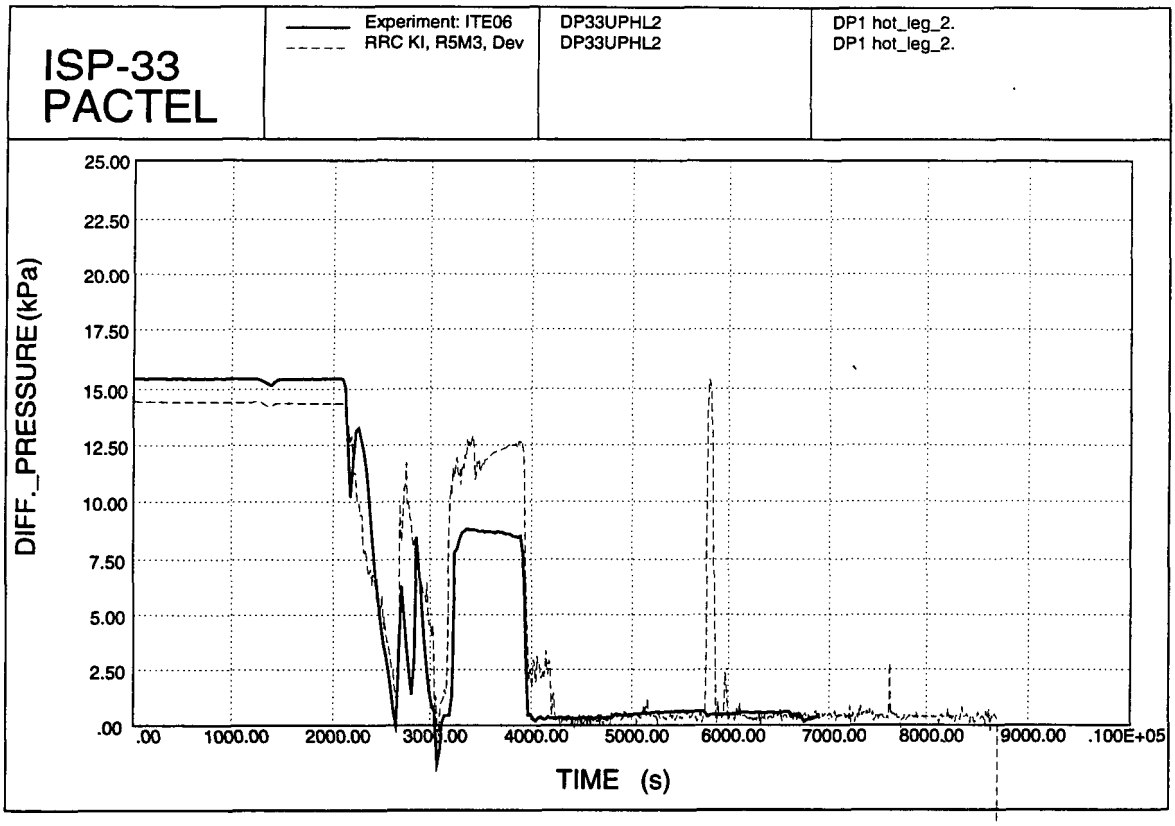

Figure 6.94. Hot leg 2 DP 1.

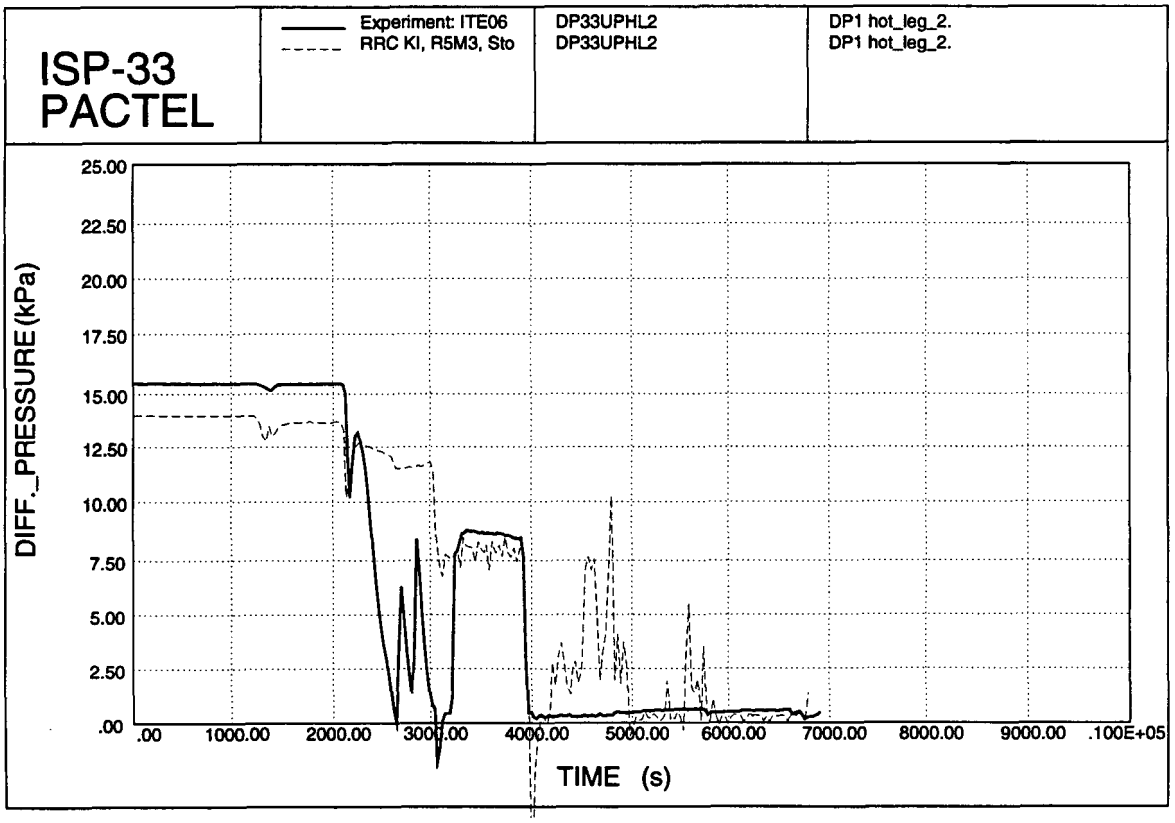

Figure 6.95. Hot leg 2 DP 1.

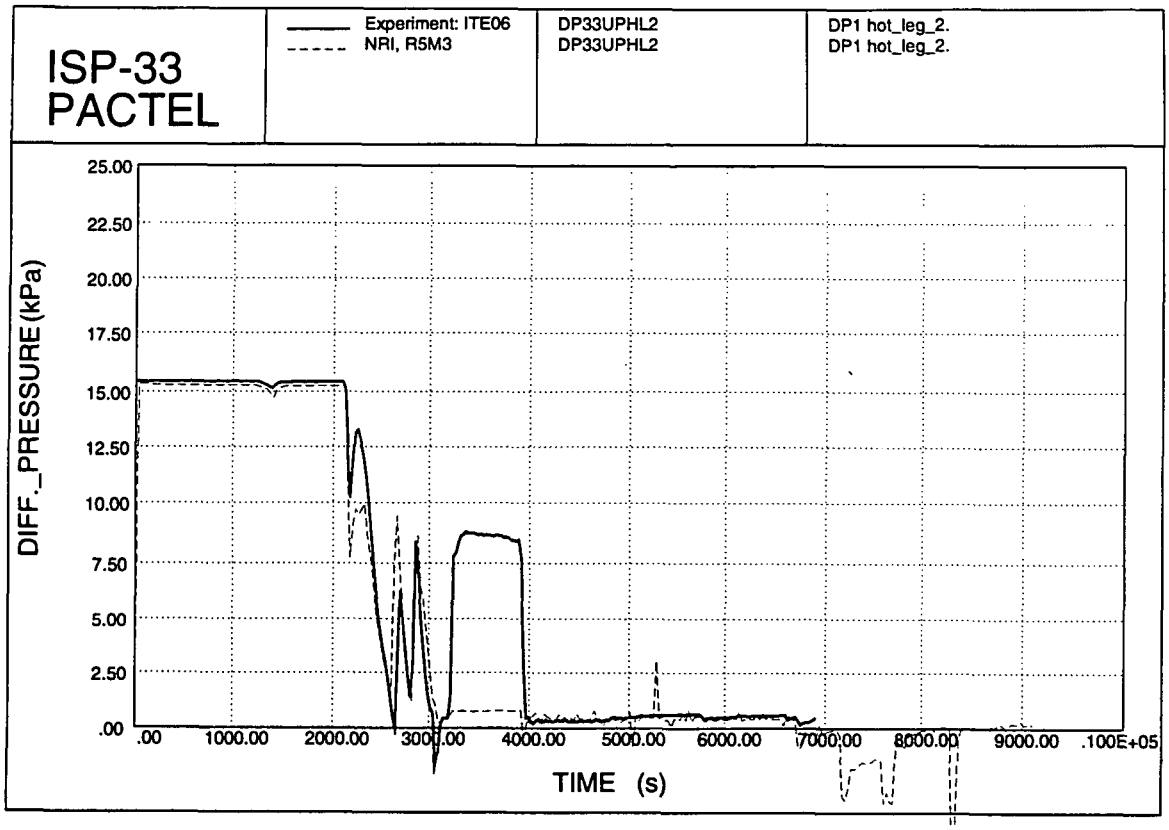

Figure 6.96. Hot leg 2 DP 1.

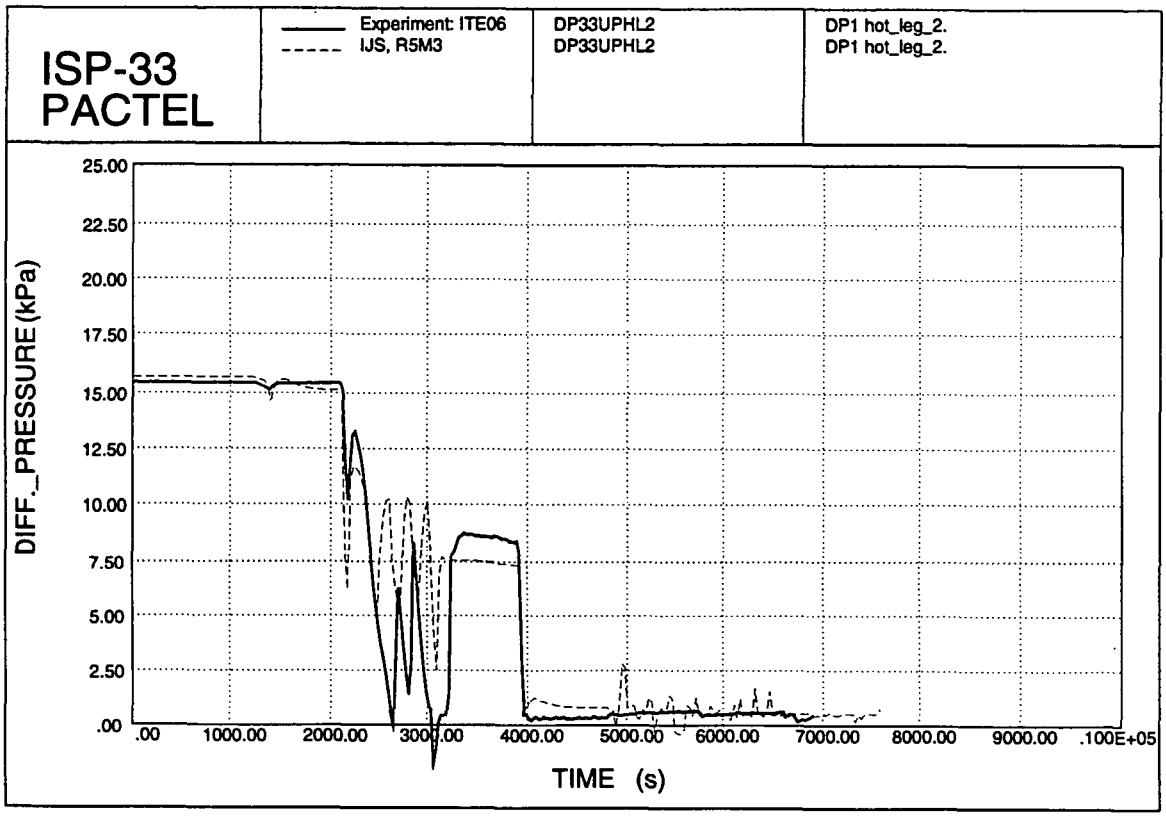

Figure 6.97. Hot leg 2 DP 1.

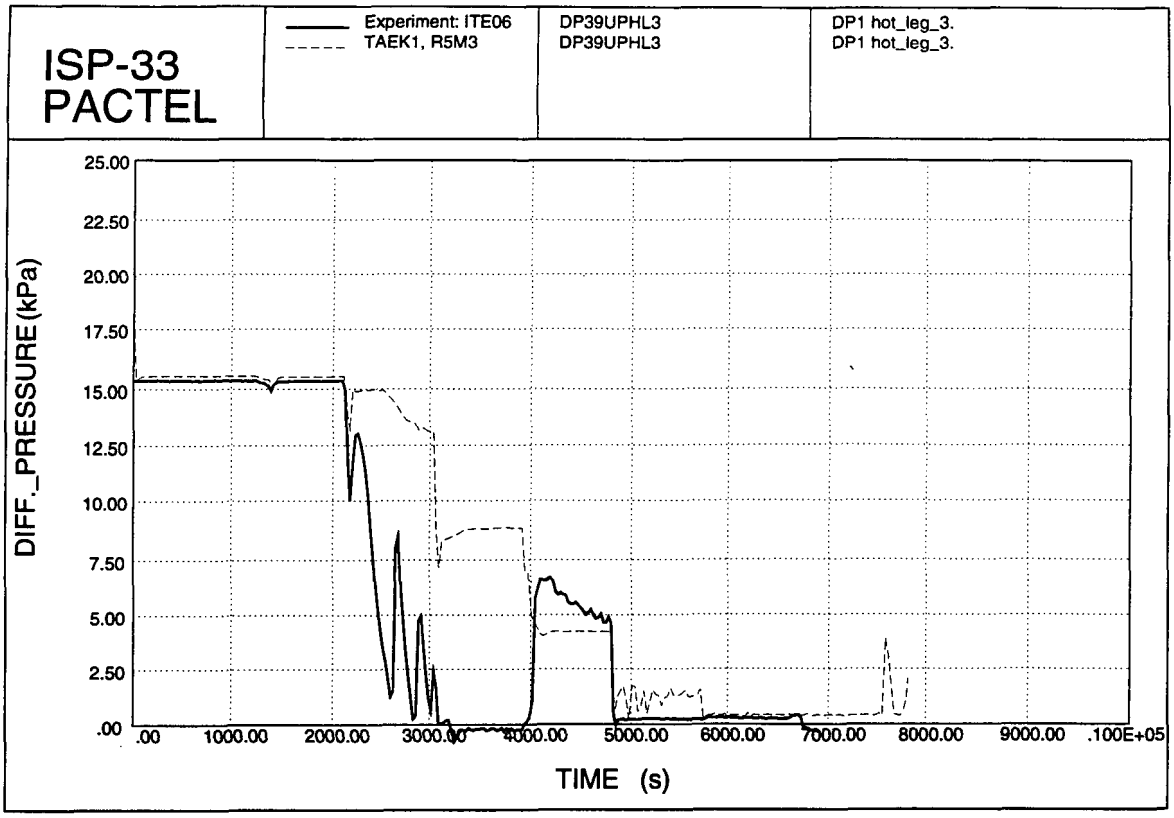

Figure 6.98. Hot leg 3 DP 1.

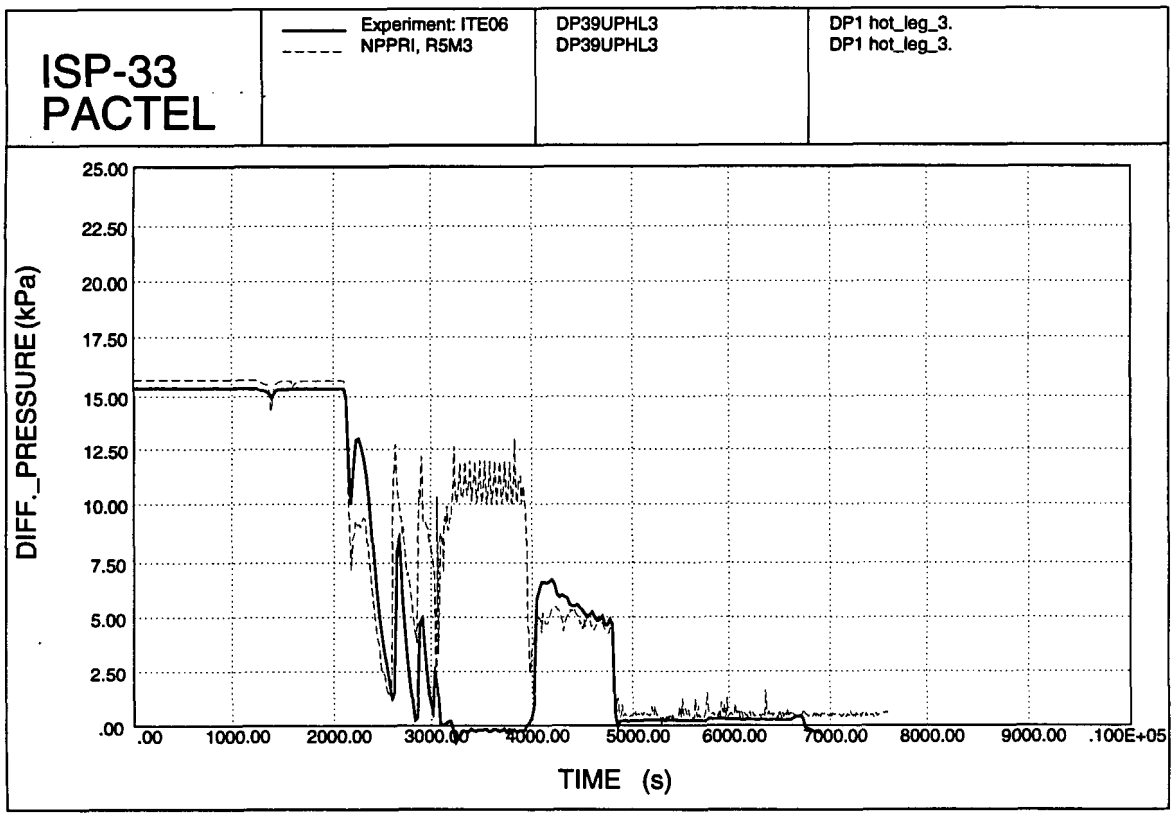

Figure 6.99. Hot leg 3 DP 1.

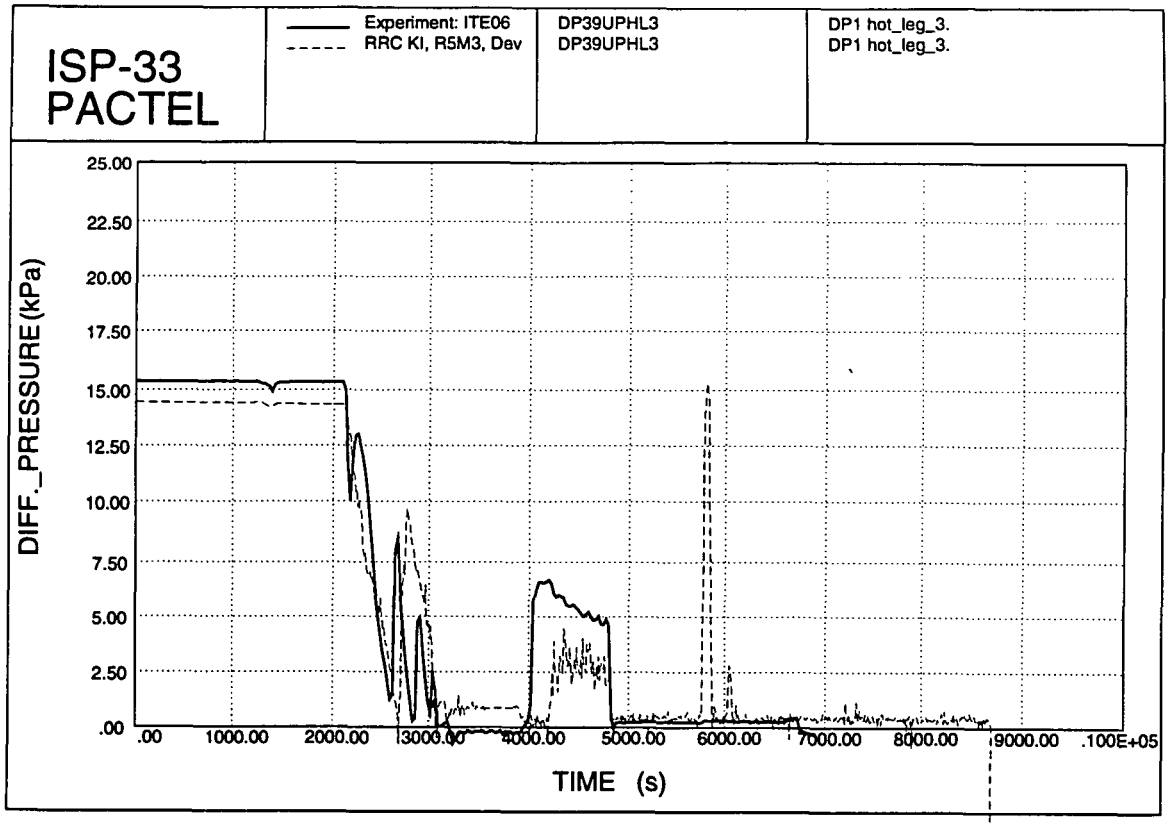

Figure 6.100. Hot leg 3 DP 1.

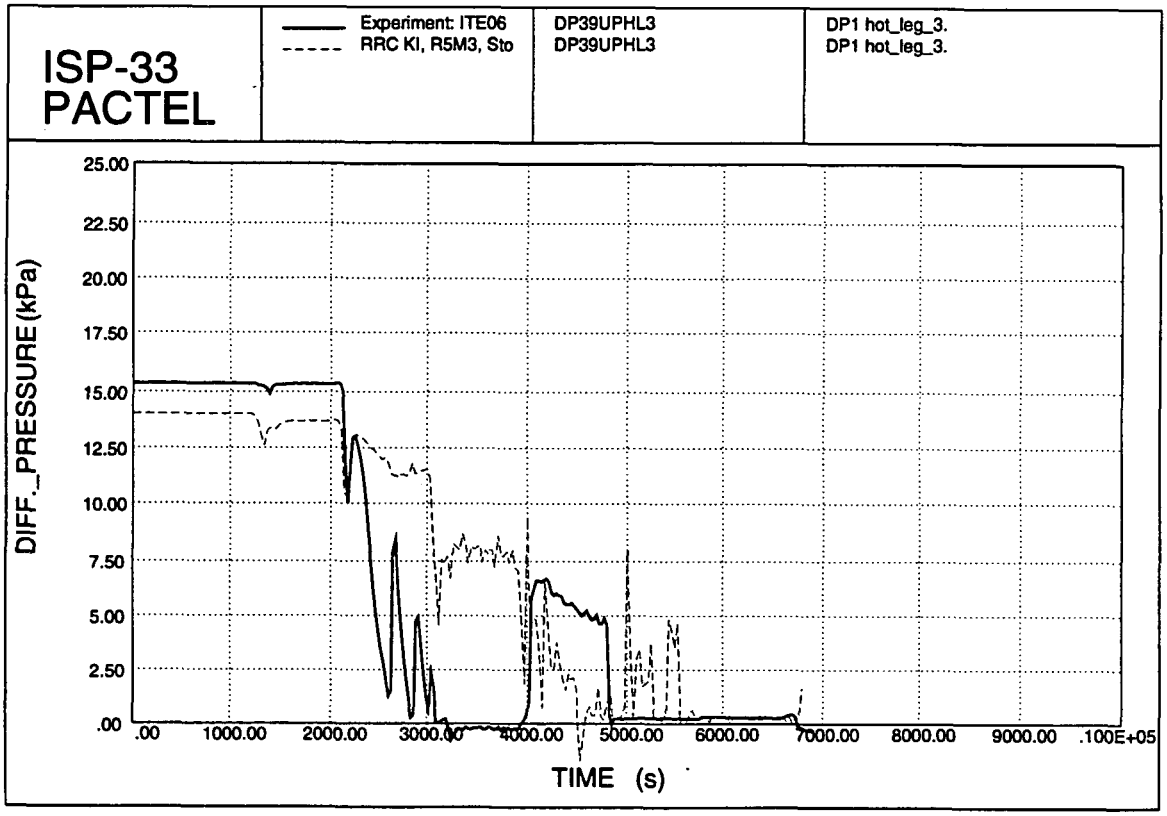

Figure 6.101. Hot leg 3 DP 1.

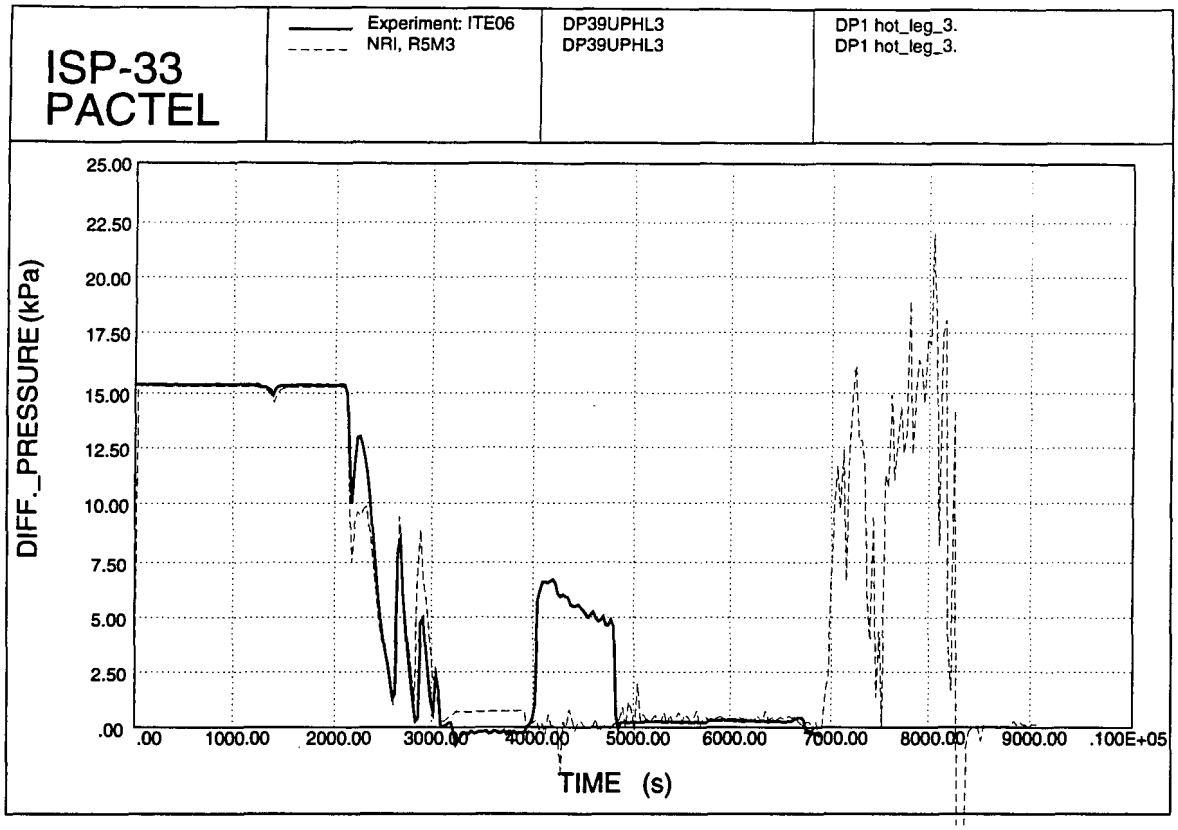

Figure 6.102. Hot leg 3 DP 1.

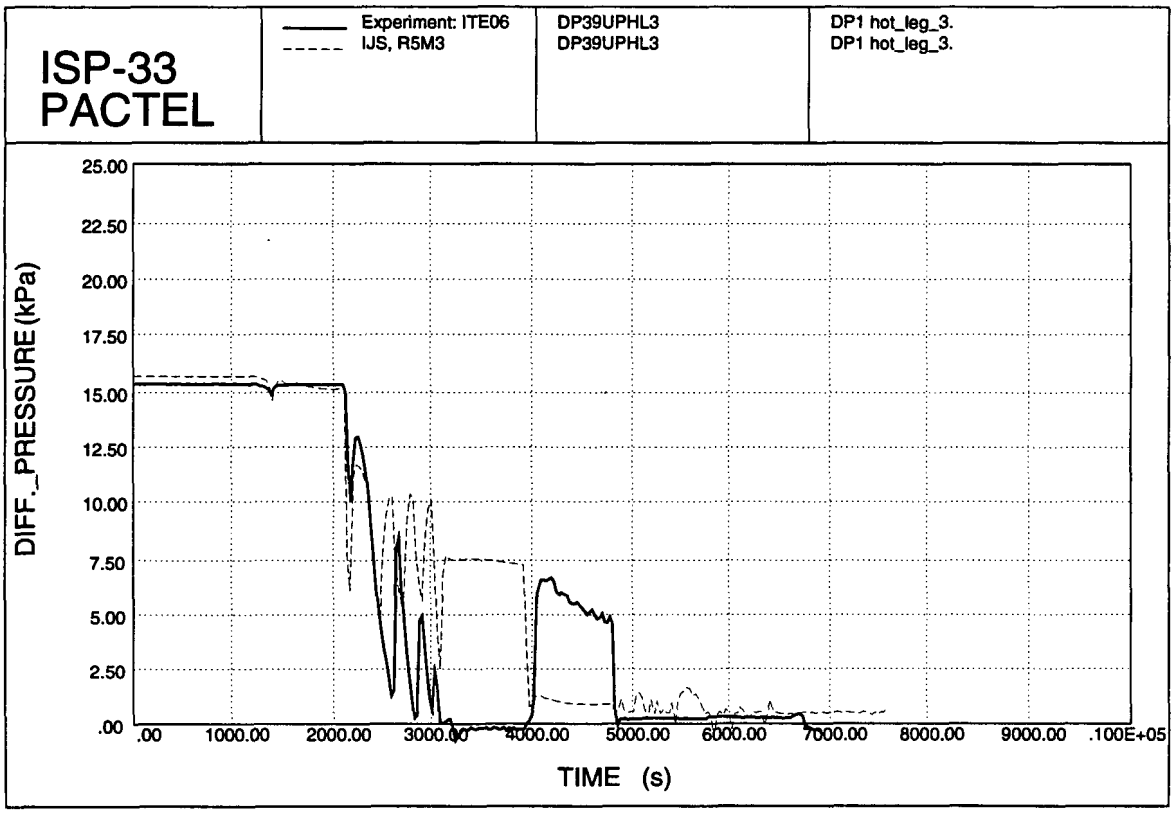

Figure 6.103. Hot leg 3 DP 1.

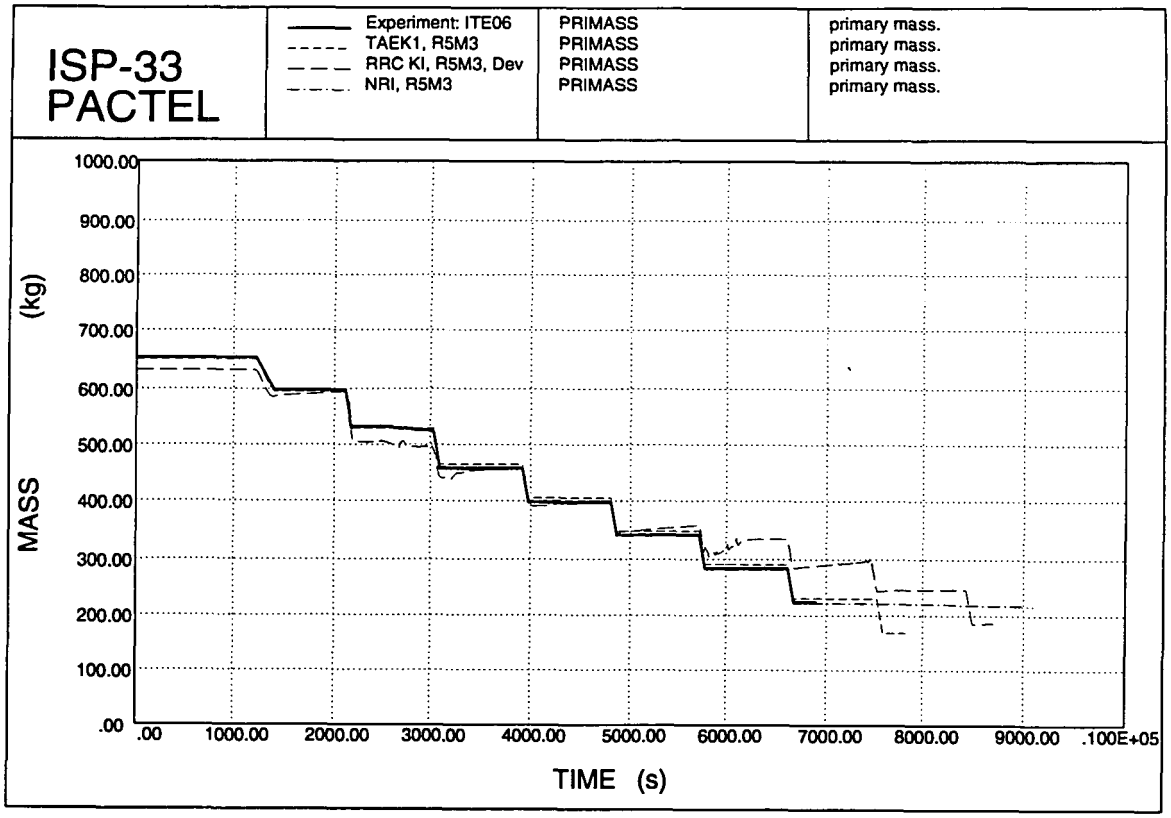

Figure 6.104. Primary mass inventory.

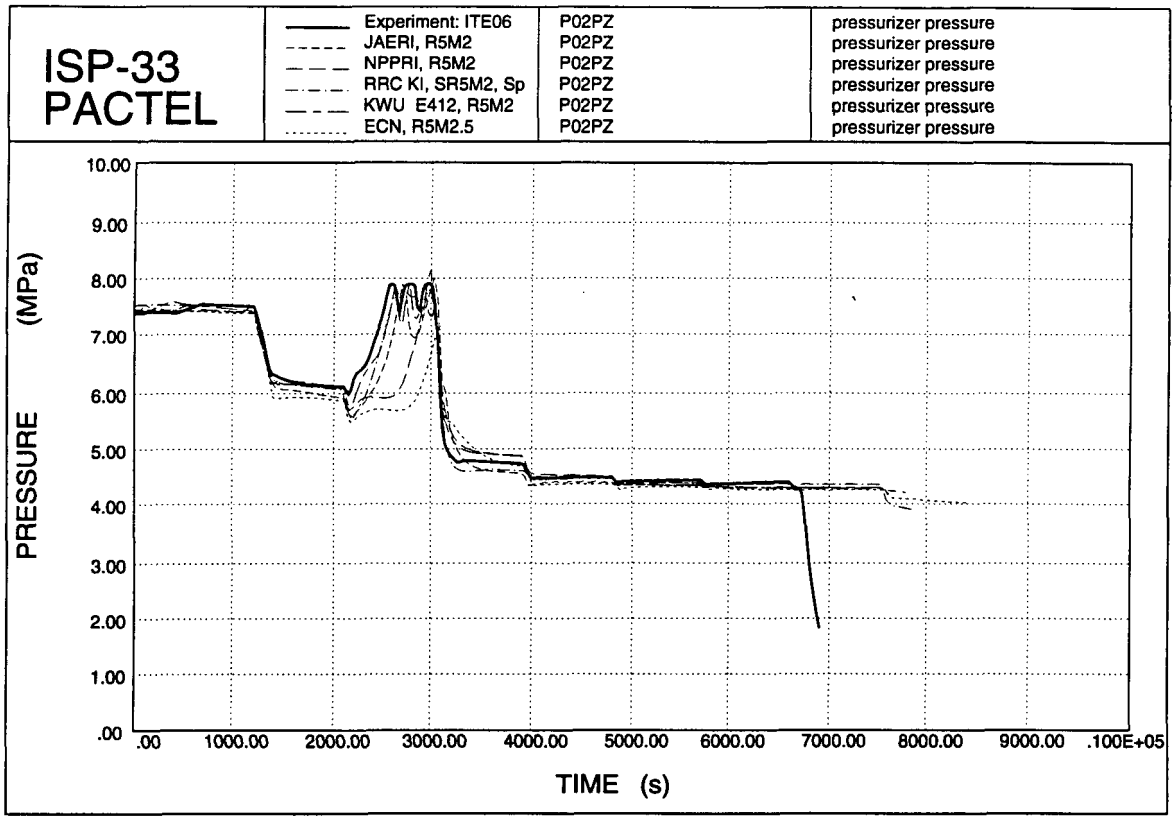

Figure 6.105. Pressurizer pressures.

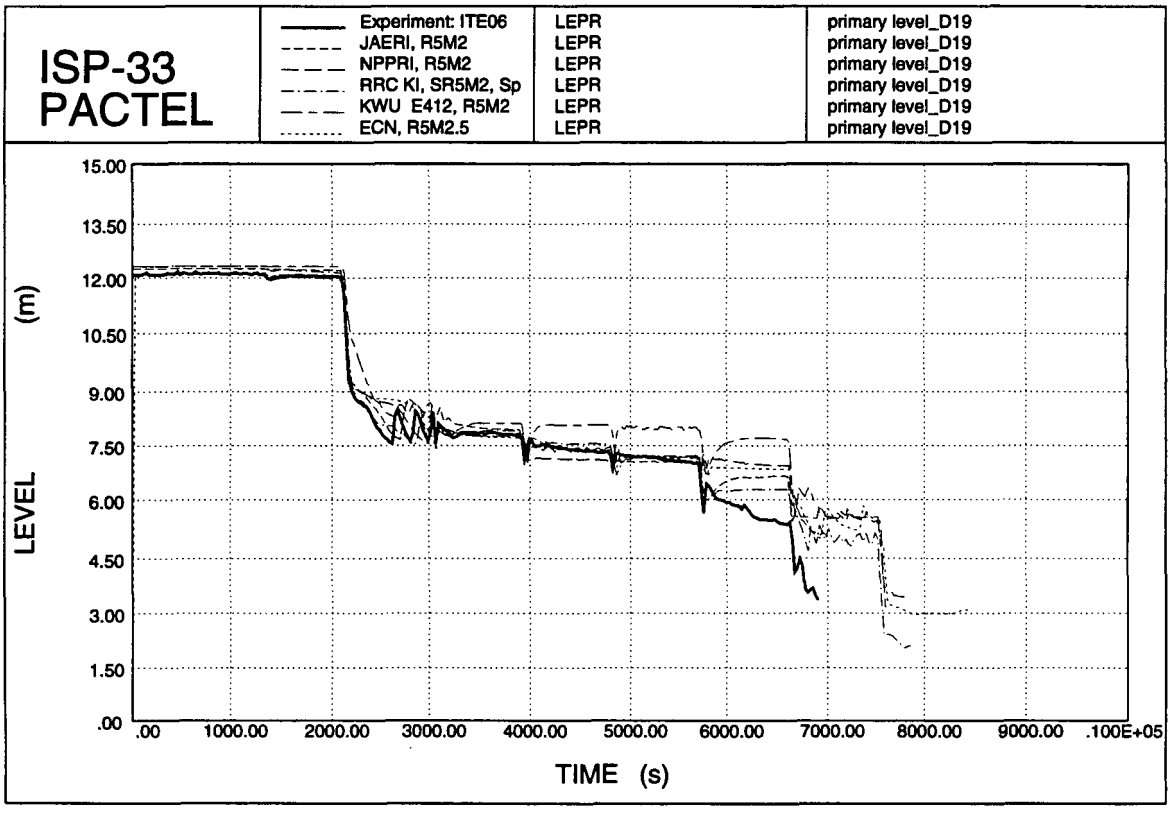

Figure 6.106. Primary levels.

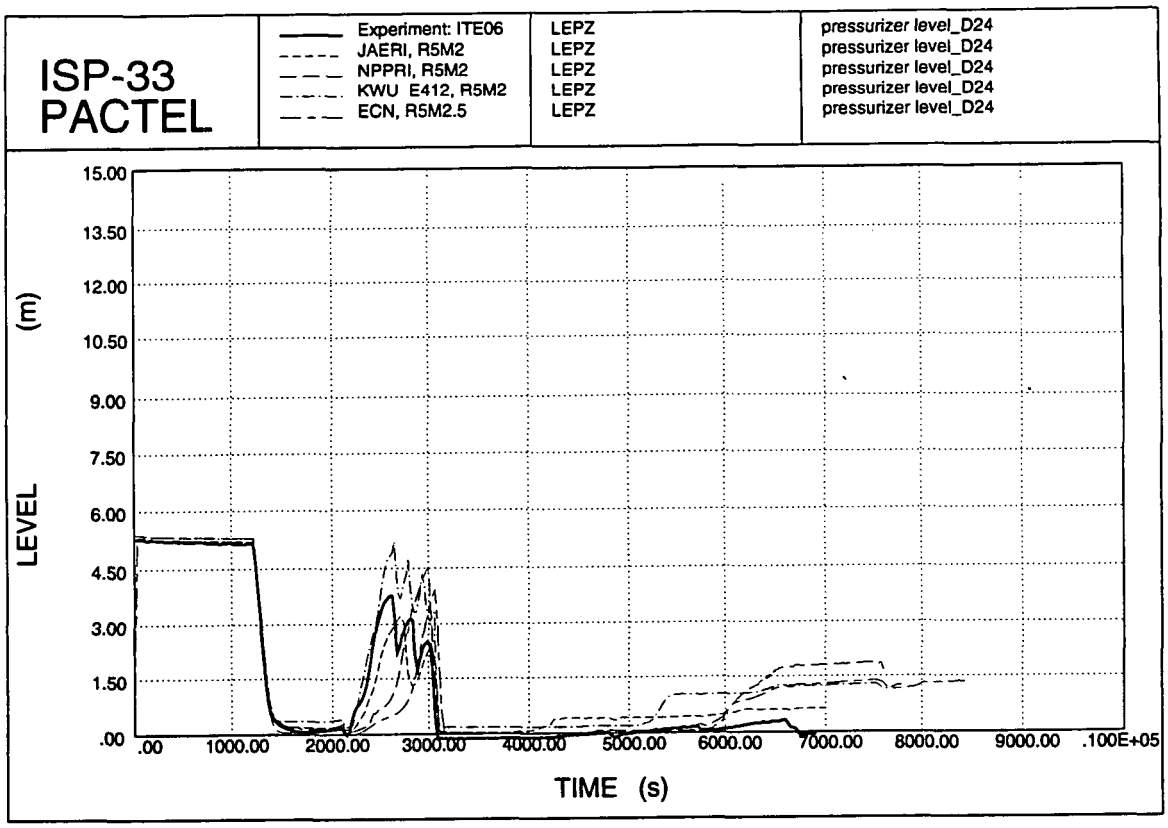

Figure 6.107. Pressurizer levels.

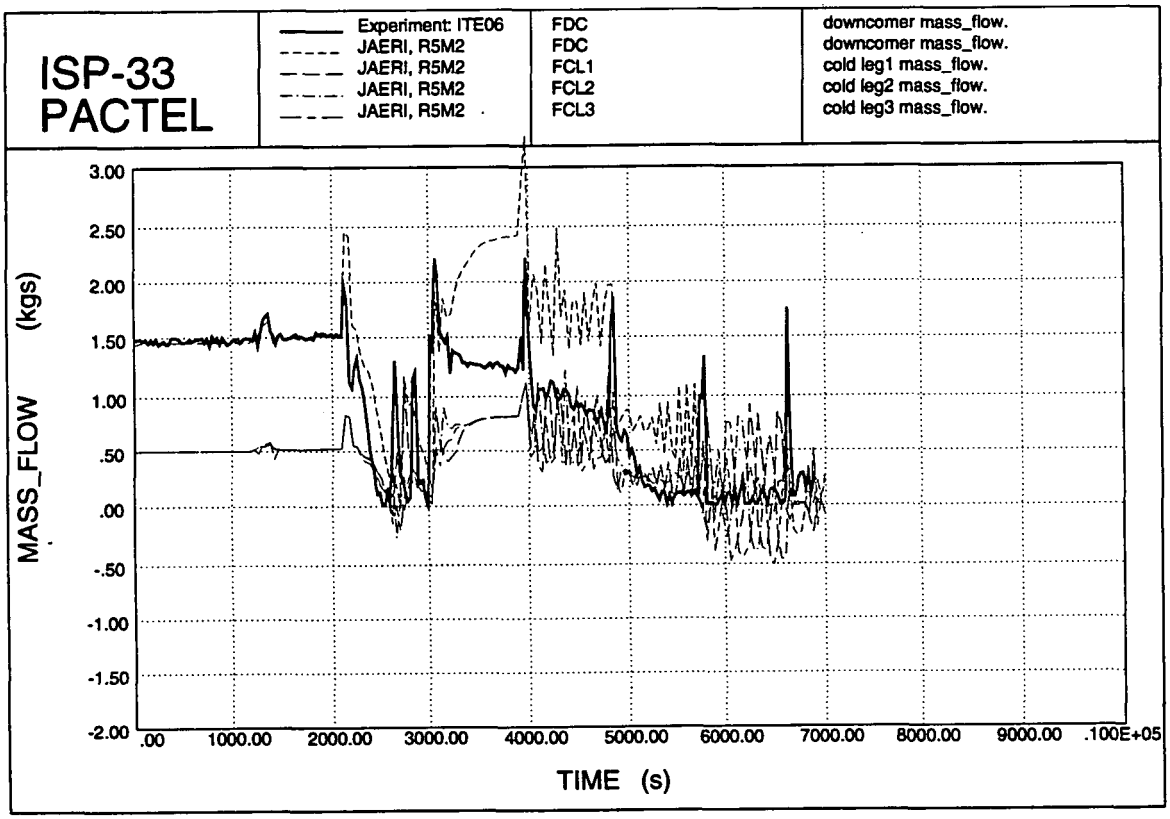

Figure 6.108. Primary mass flows.

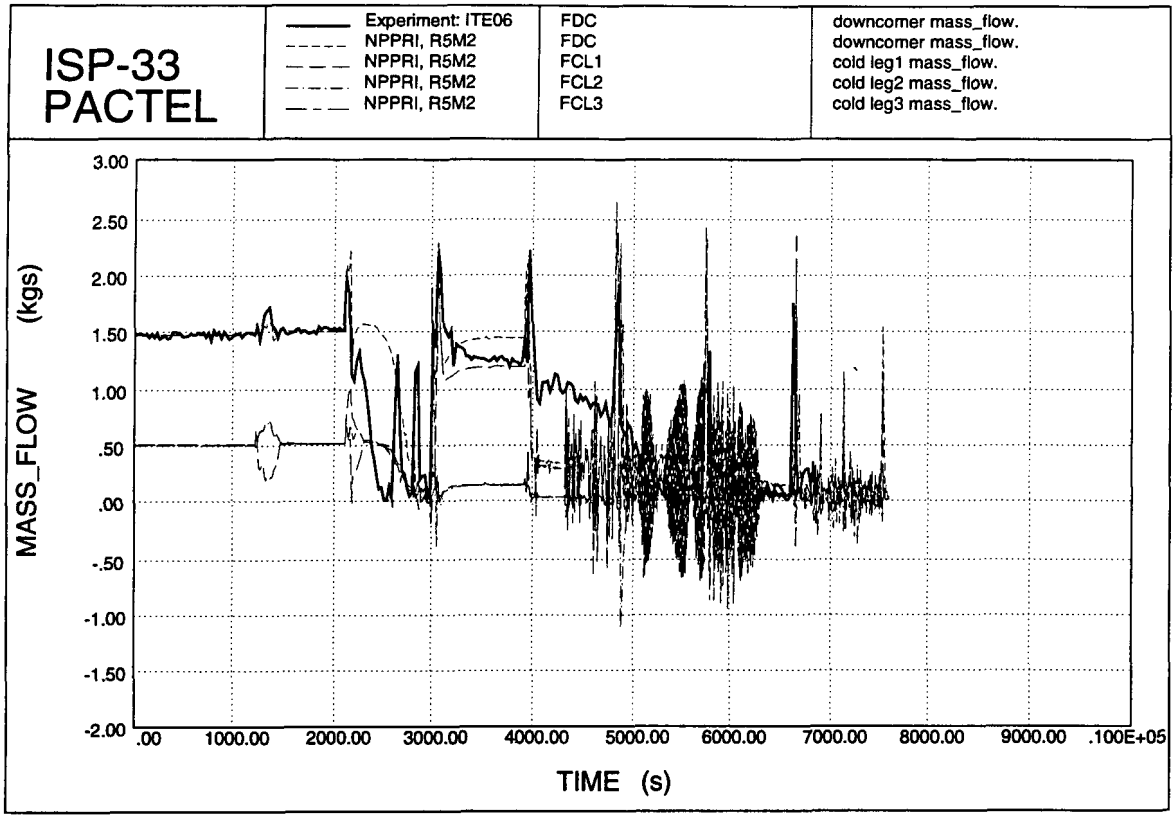

Figure 6.109. Primary mass flows.

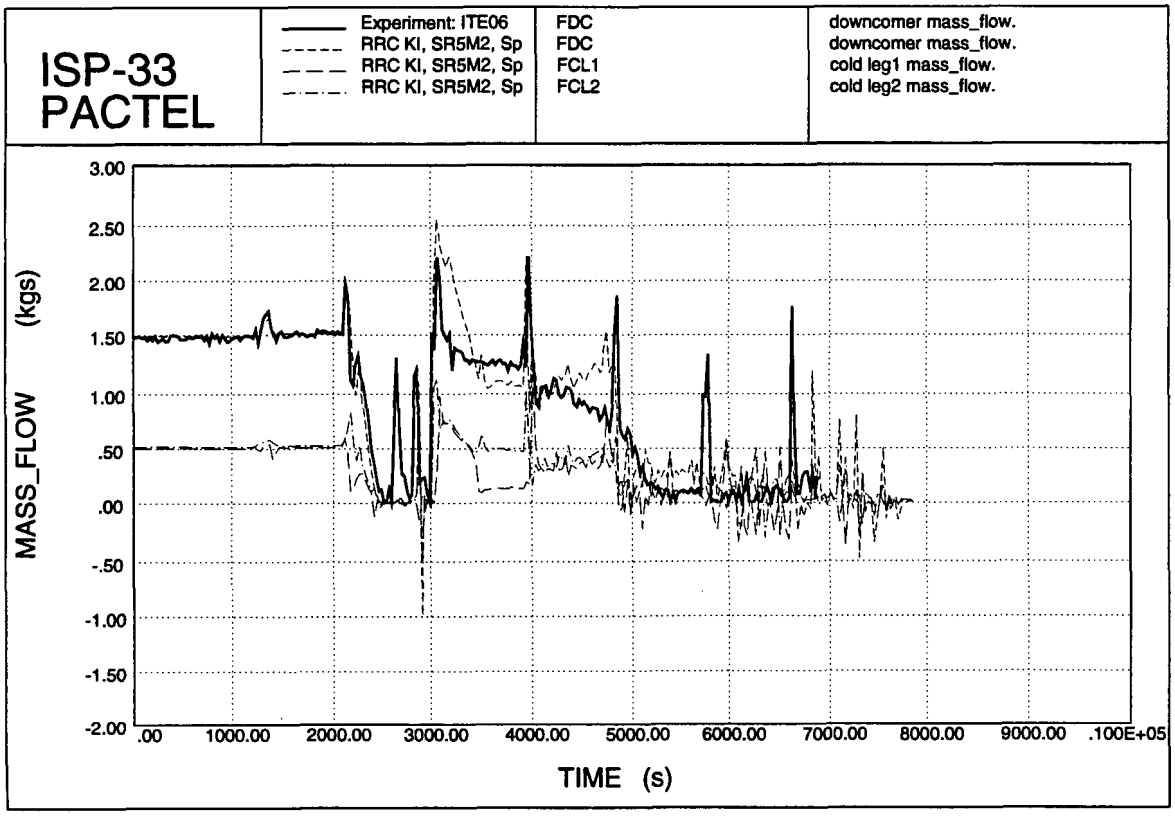

Figure 6.110. Primary mass flows.

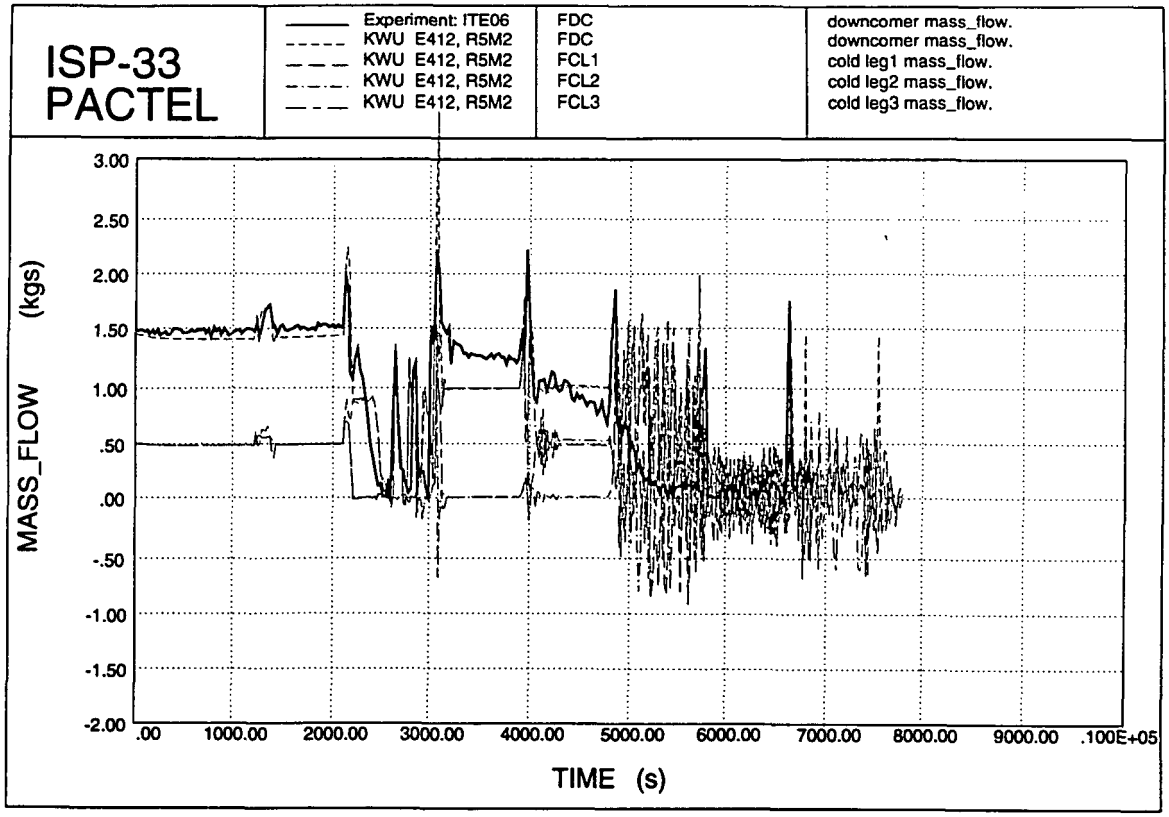

Figure 6.111. Primary mass flows.

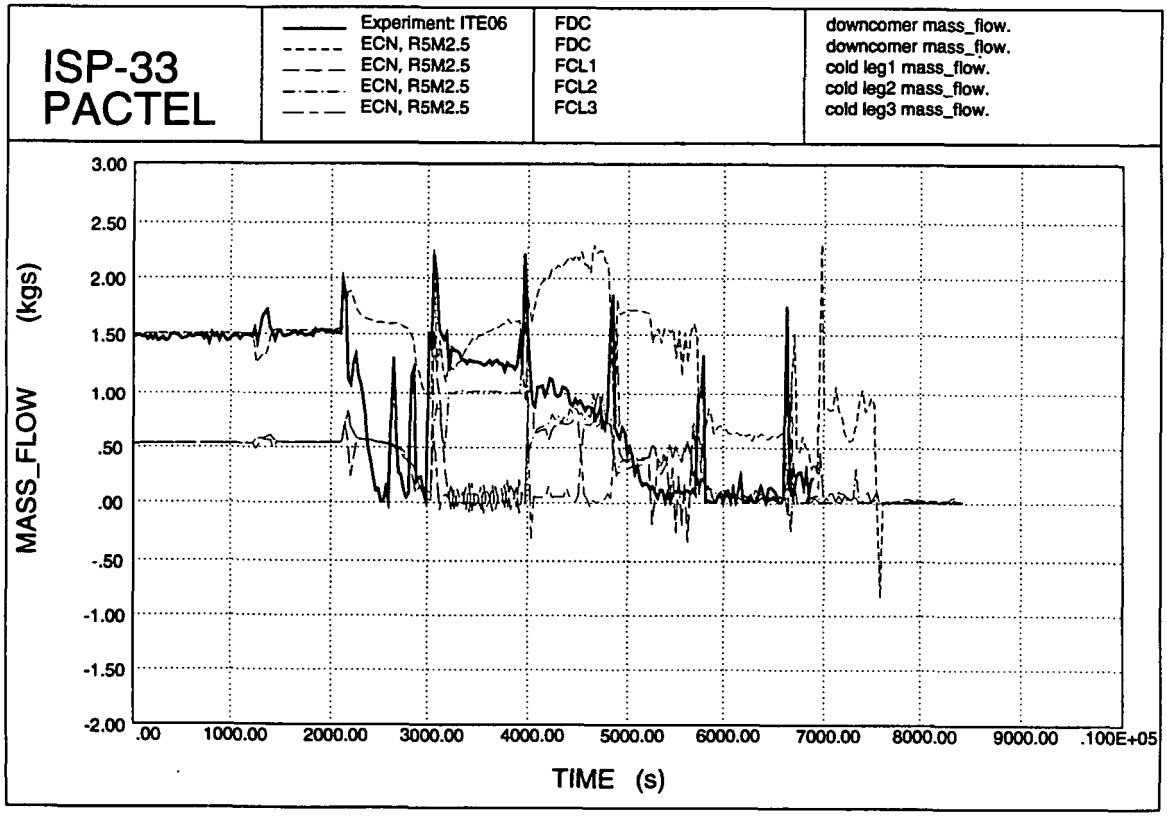

Figure 6.112. Primary mass flows.

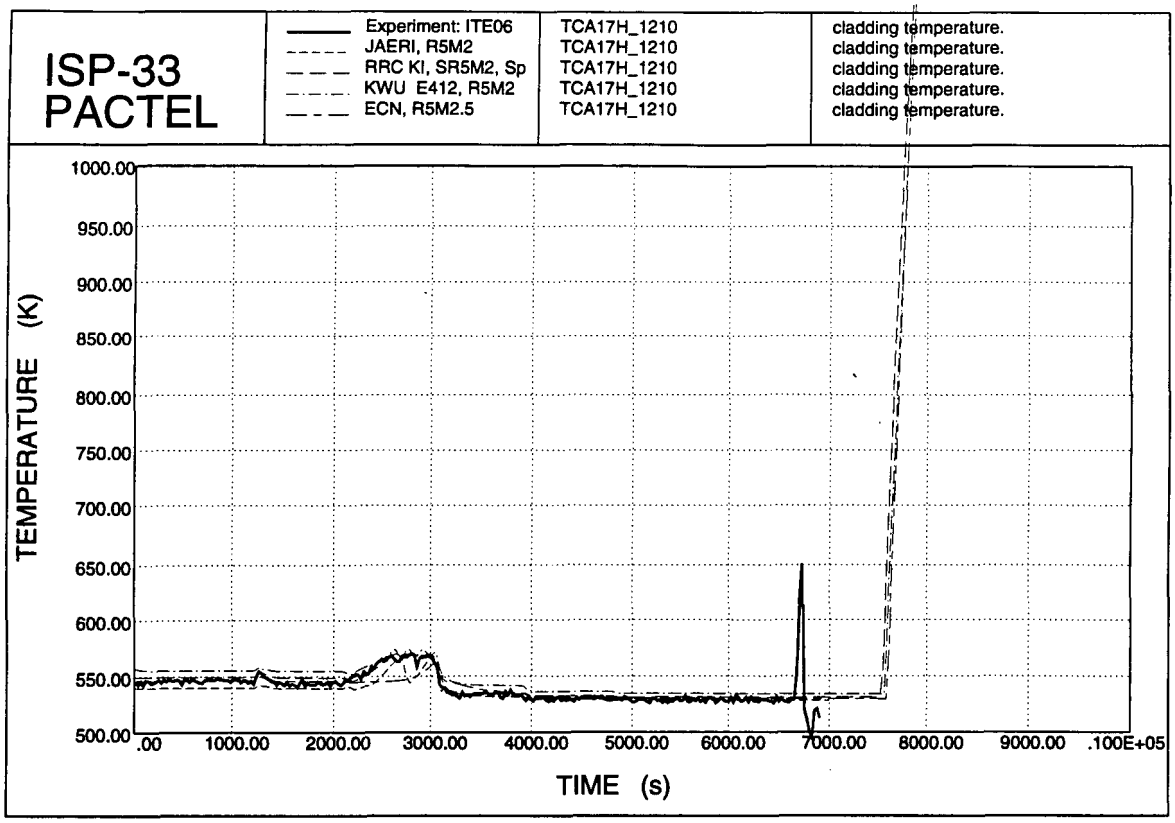

Figure 6.113. Cladding temperatures.

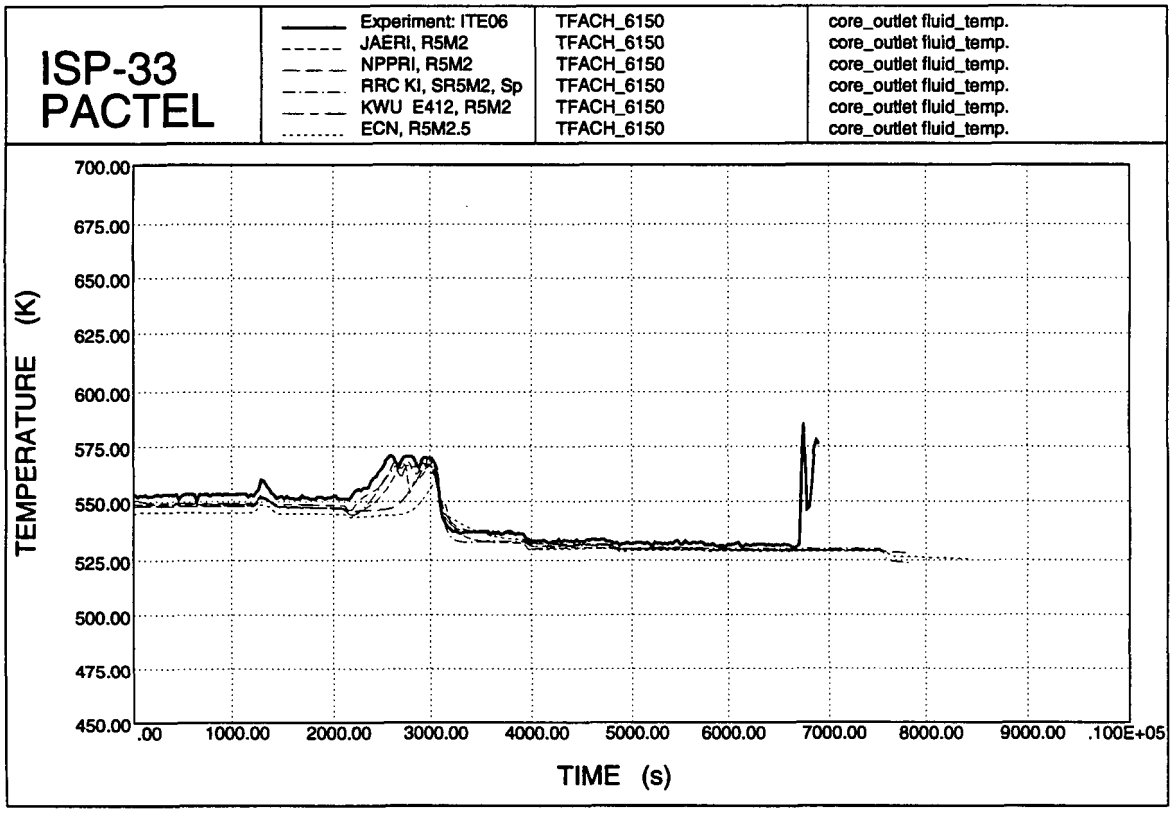

Figure 6.114. Core outlet coolant temperature.

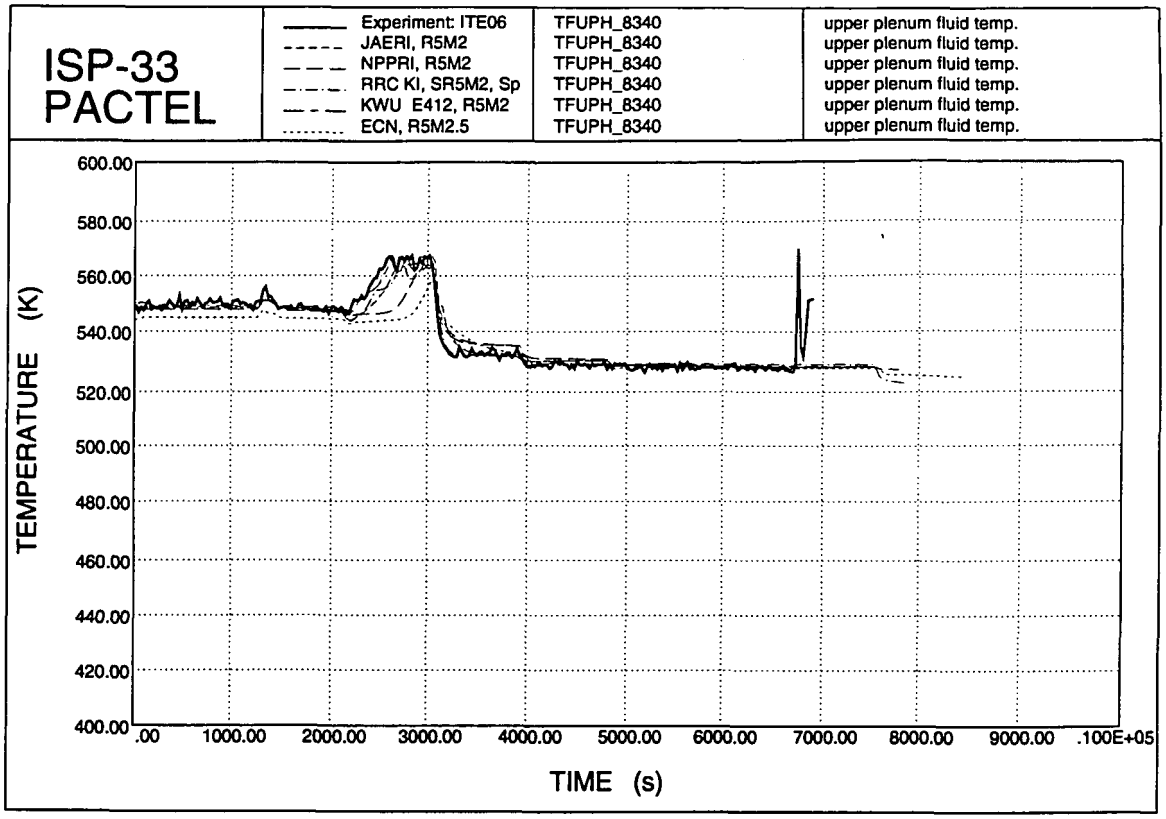

Figure 6.115. Upper plenum temperatures.

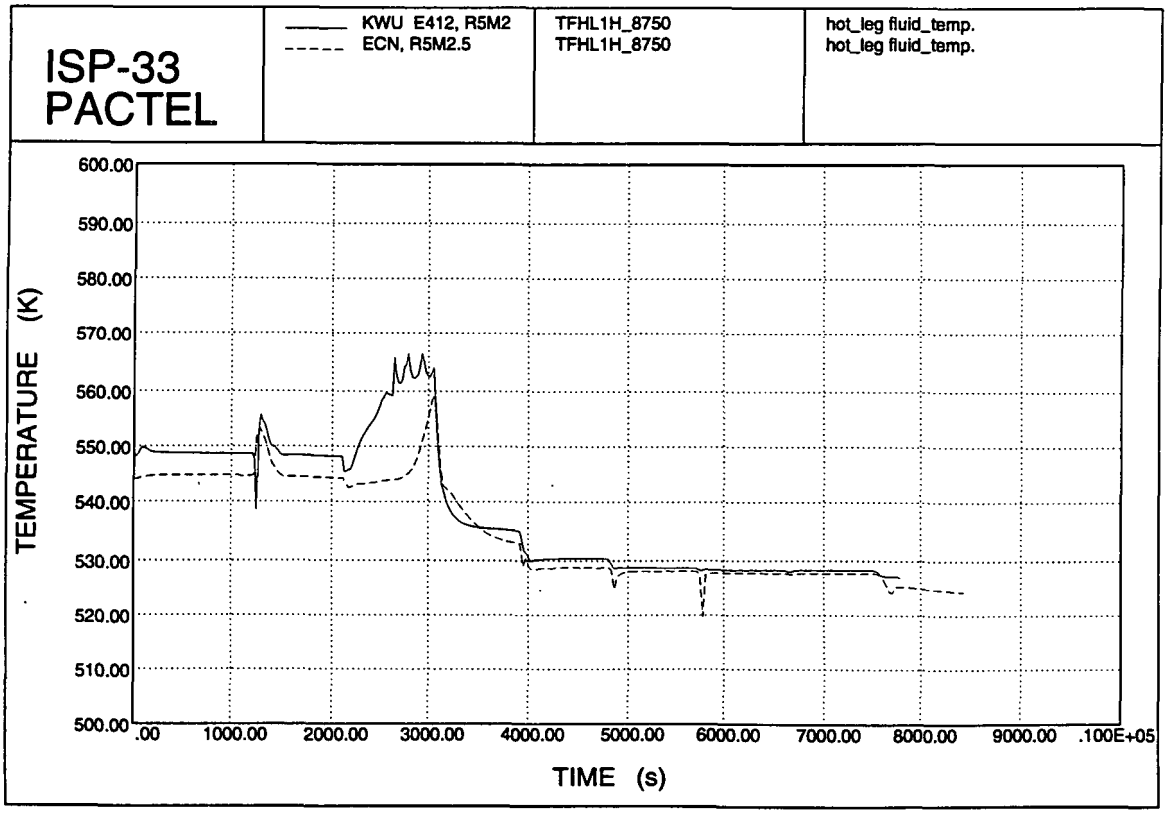

Figure 6.116. Hot leg coolant temperatures.

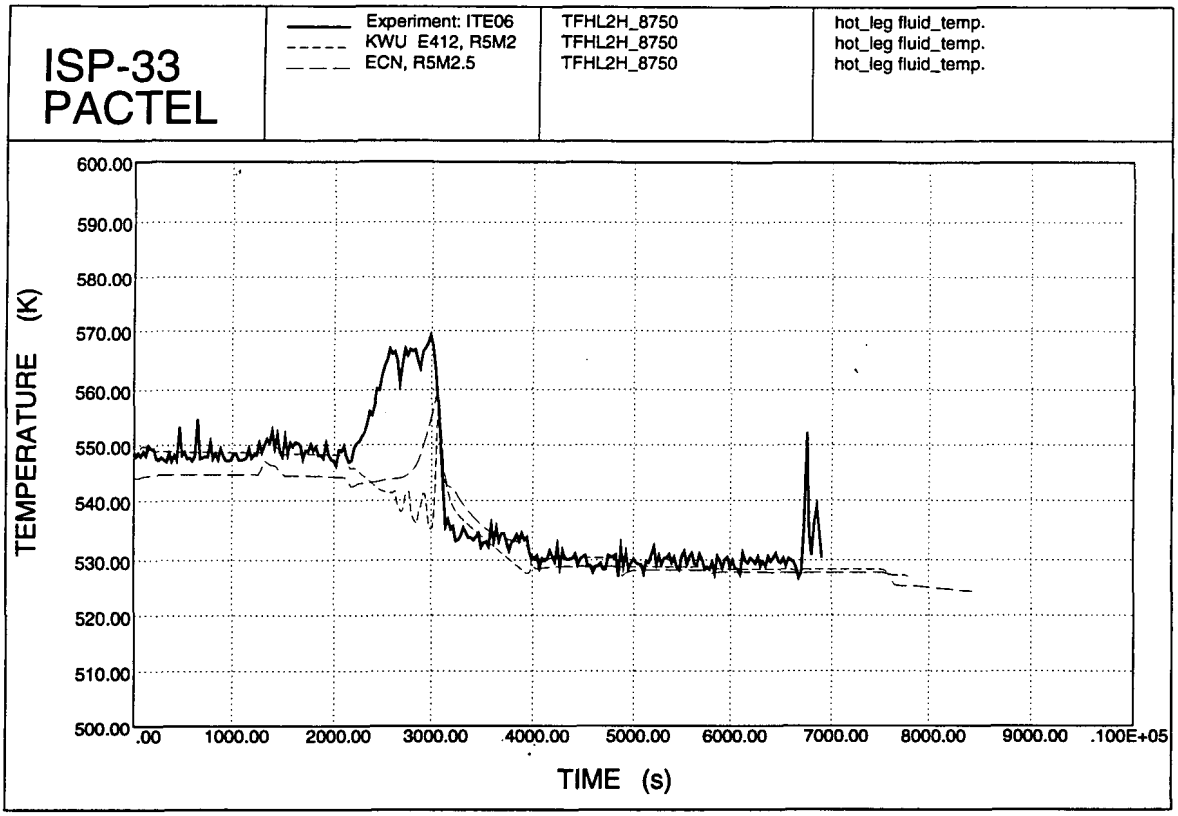

Figure 6.117. Hot leg temperatures.

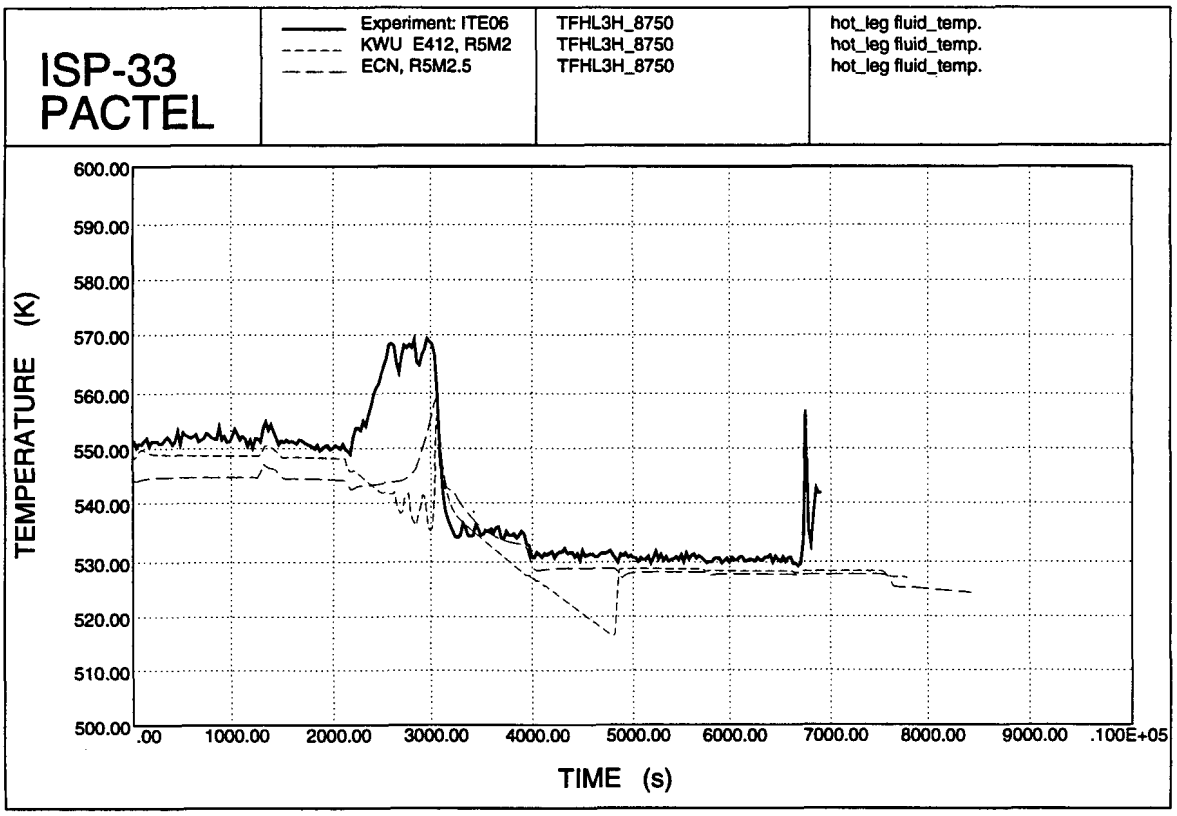

Figure 6.118. Hot leg coolant temperatures.

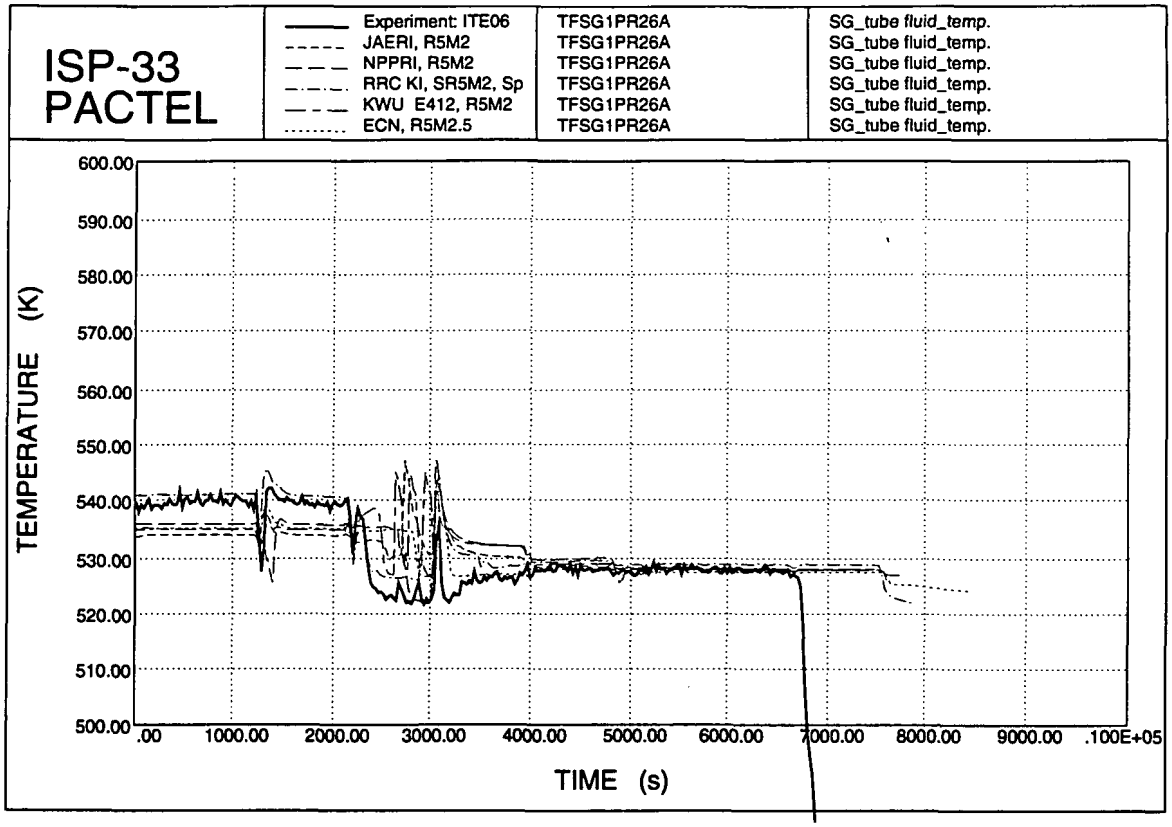

Figure 6.119. SG tube fluid temperatures.

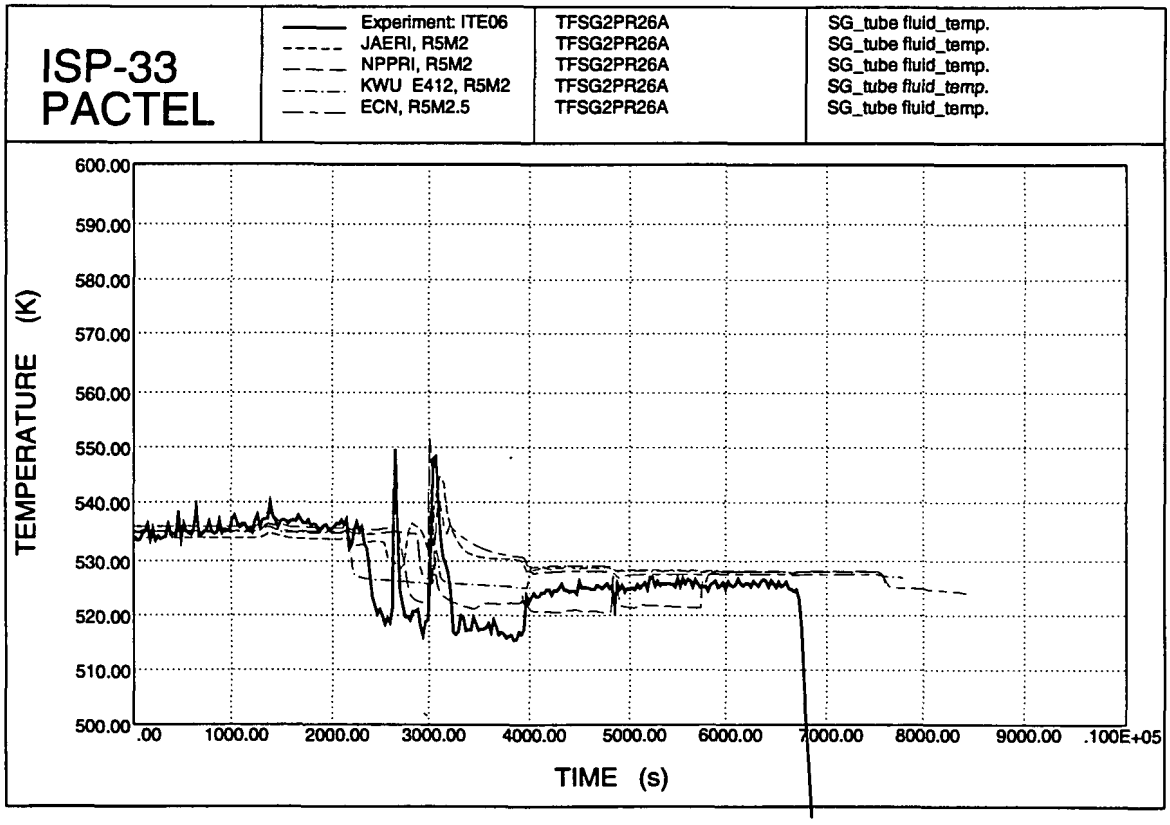

Figure 6.120. SG tube fluid temperatures.

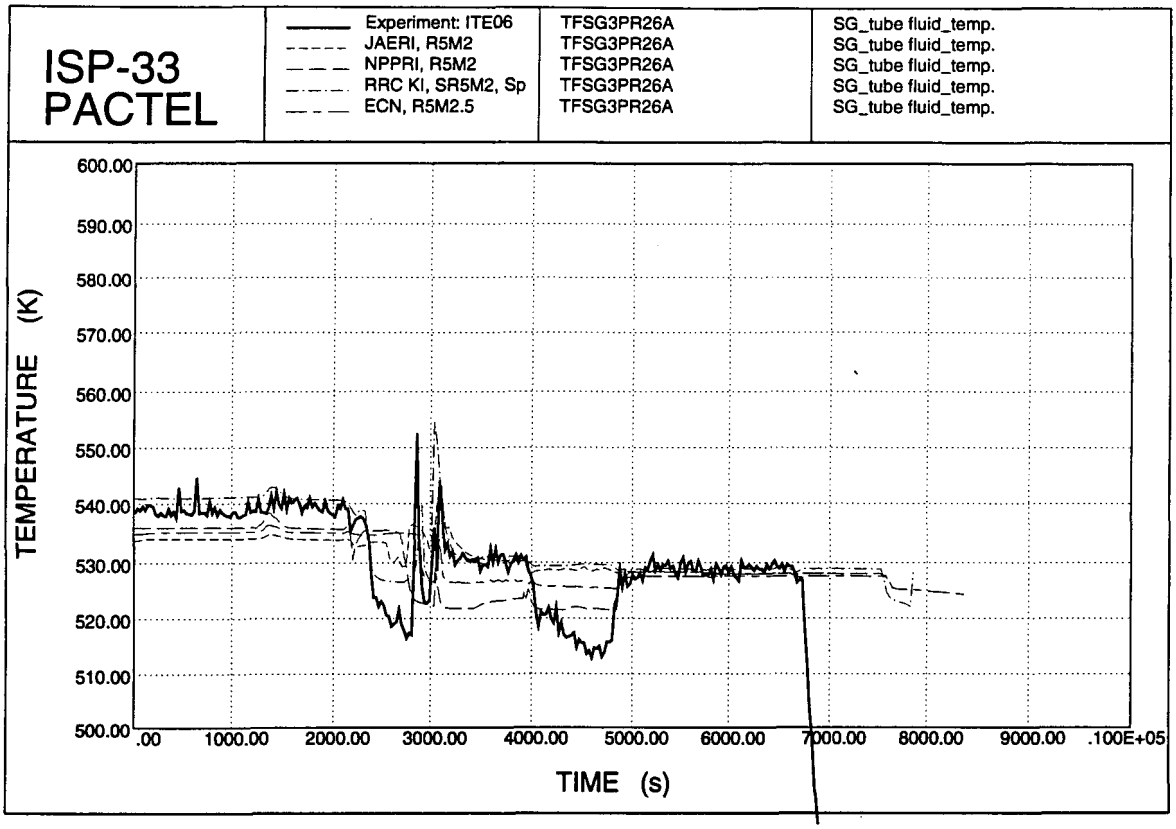

Figure 6.121. SG tube fluid temperatures.

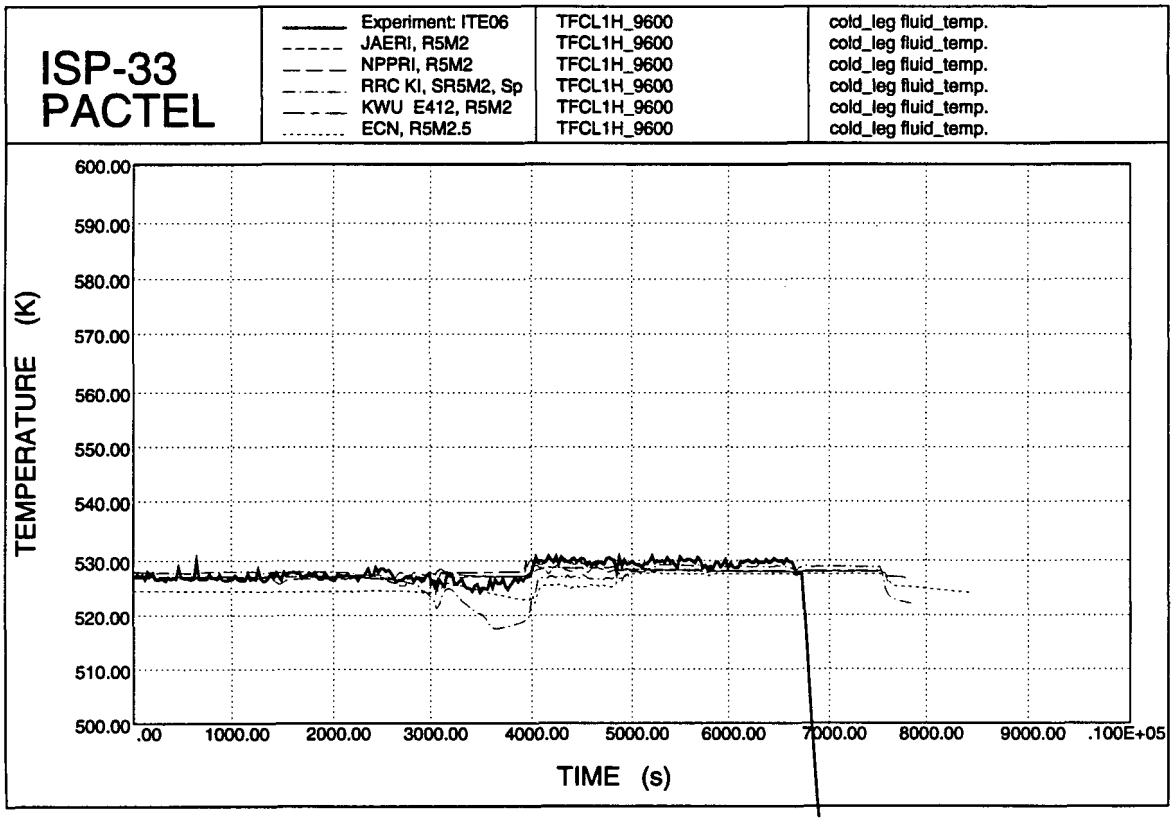

Figure 6.122. Cold leg temperatures.

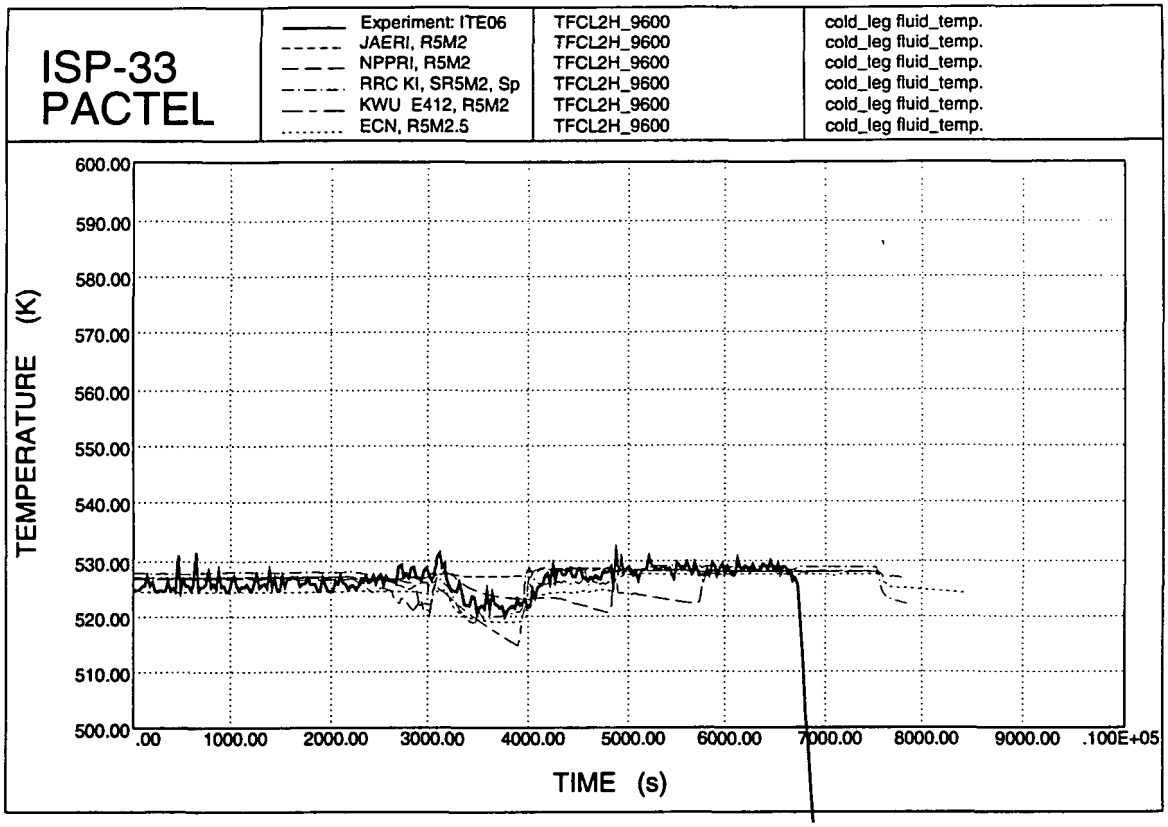

Figure 6.123. Cold leg coolant temperatures.

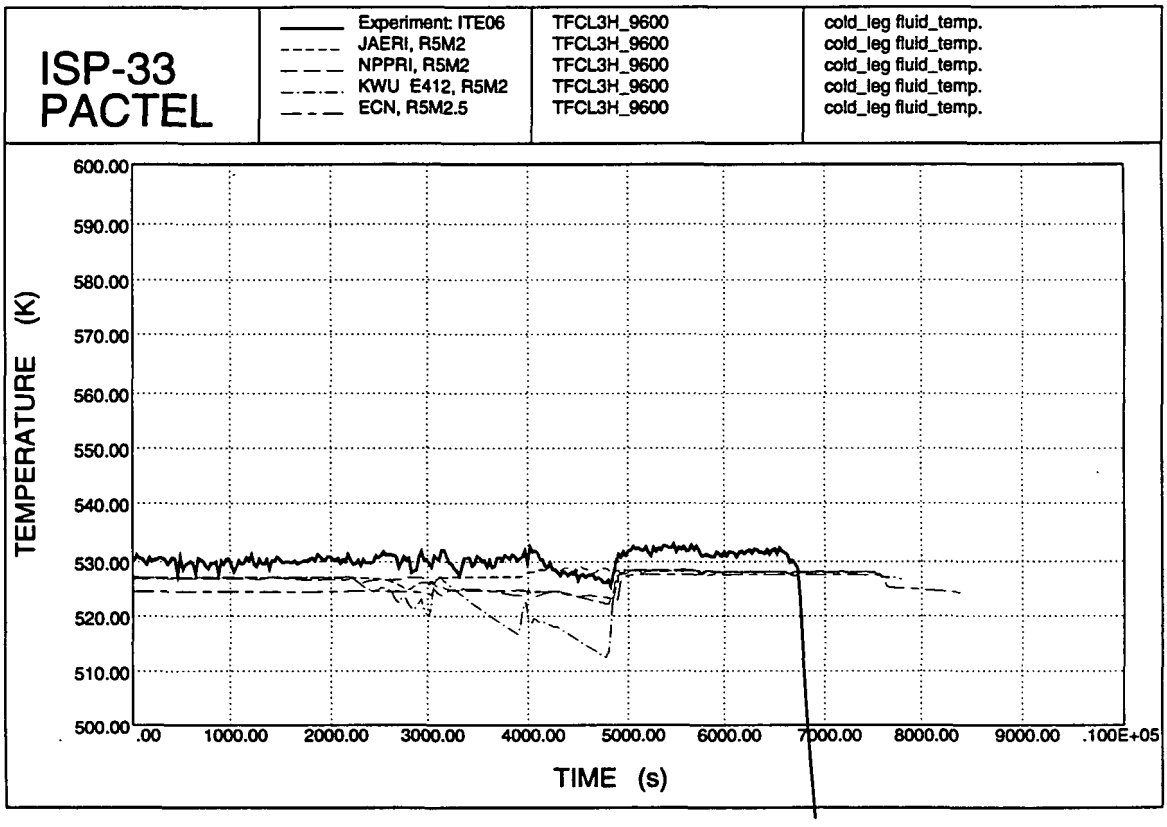

Figure 6.124. Cold leg temperatures.

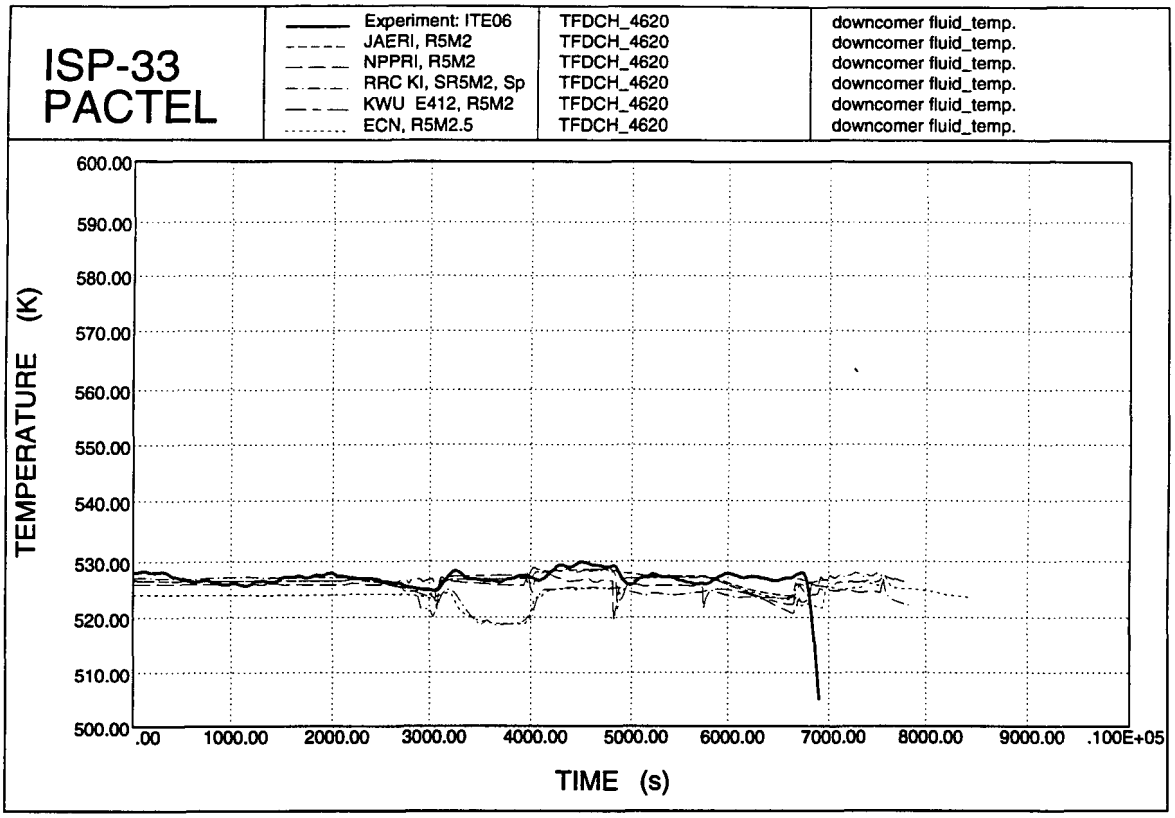

Figure 6.125. Downcomer temperatures.

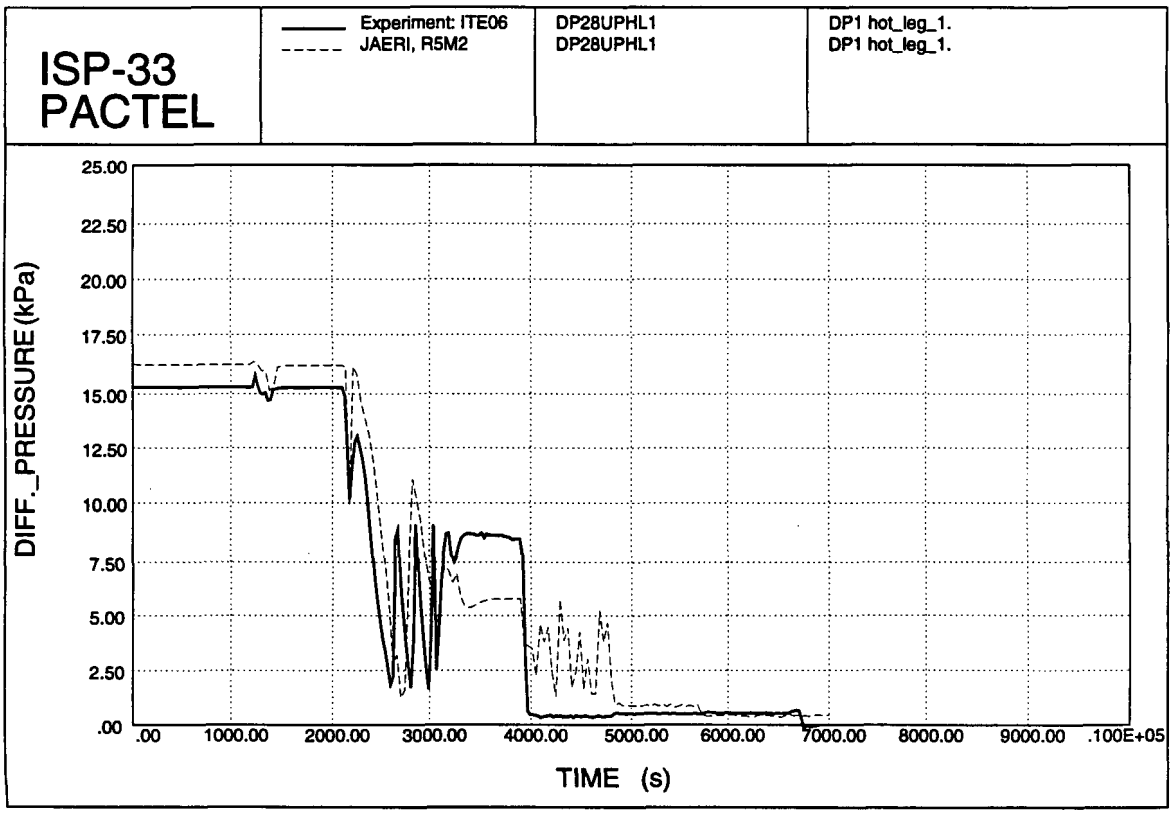

Figure 6.126. Hot leg 1 DP 1.

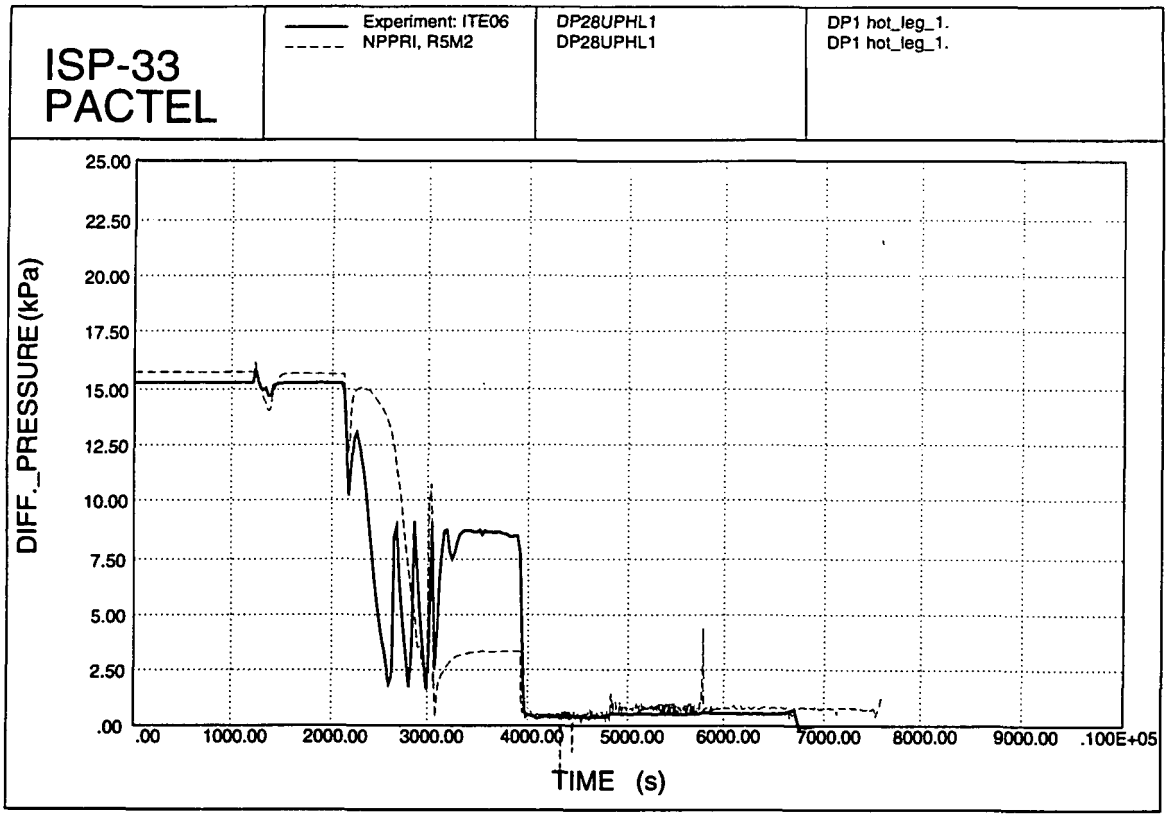

Figure 6.127. Hot leg 1 DP 1.

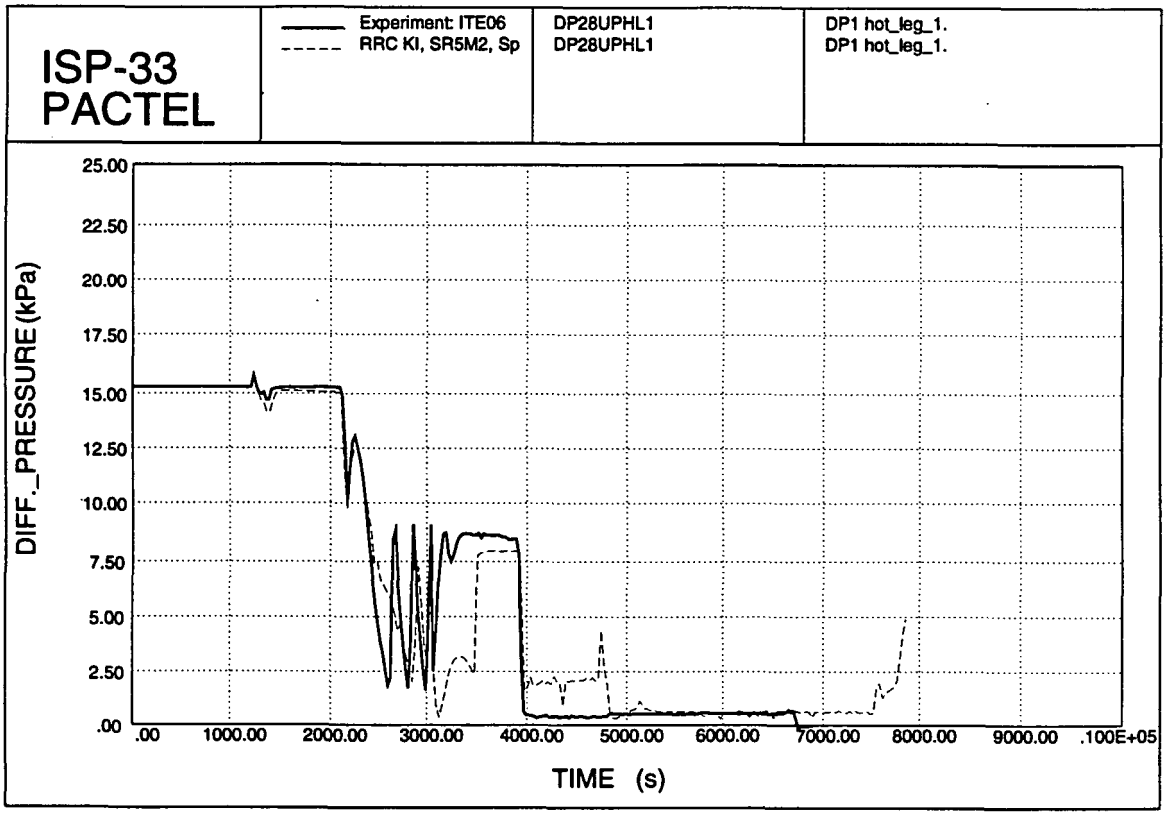

Figure 6.128. Hot leg 1 DP 1.

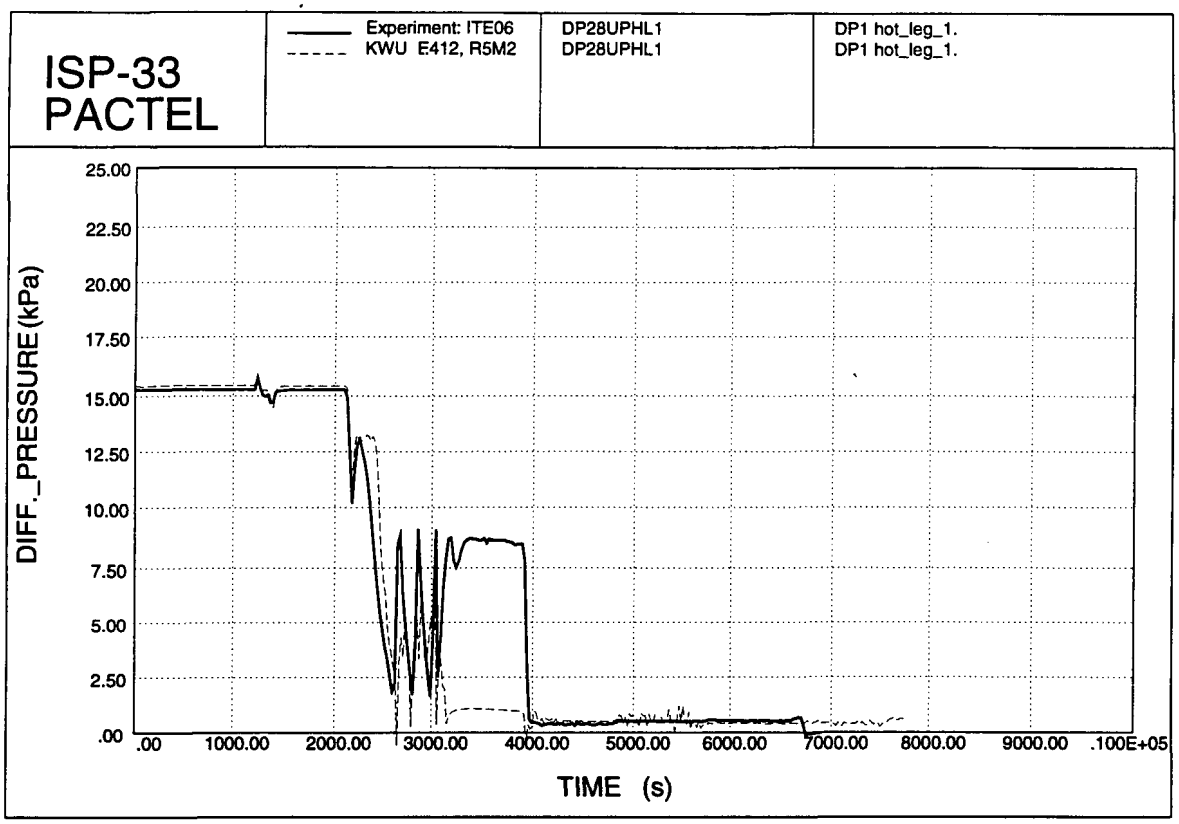

Figure 6.129. Hot leg 1 DP 1.

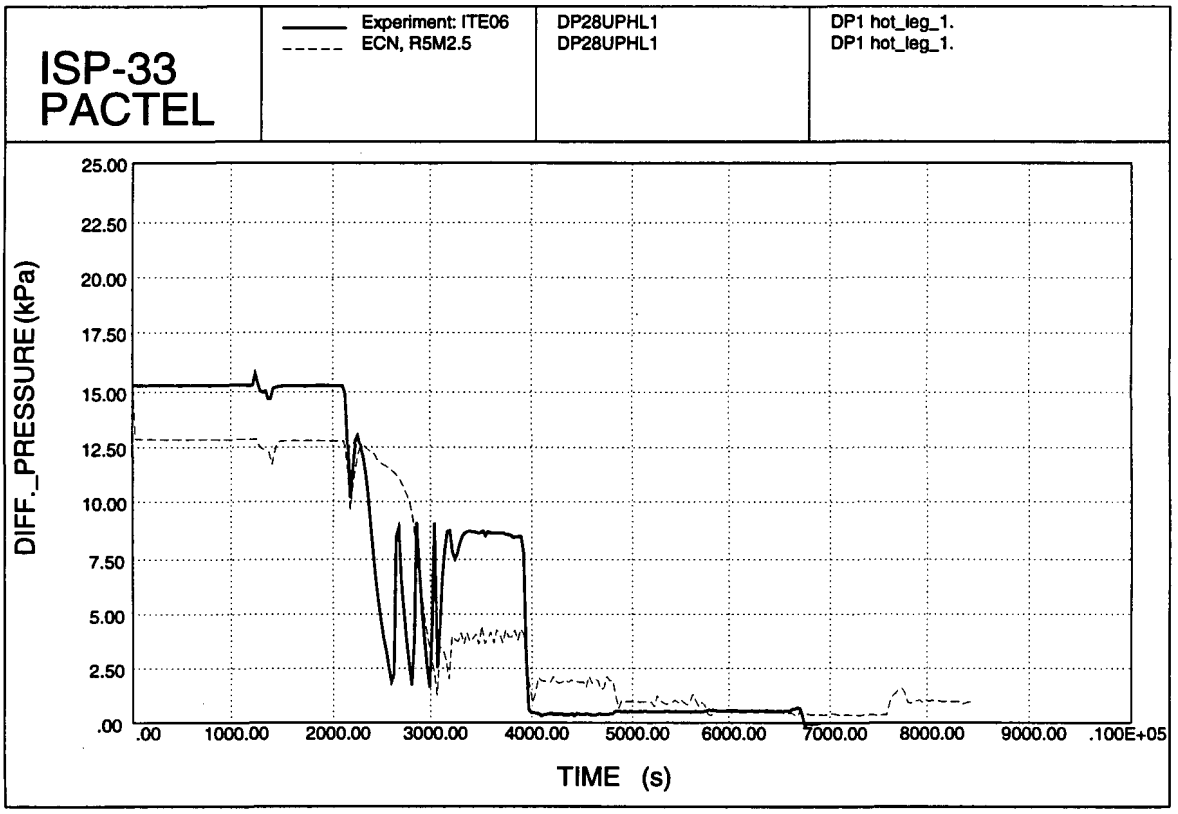

Figure 6.130. Hot leg 1 DP 1.

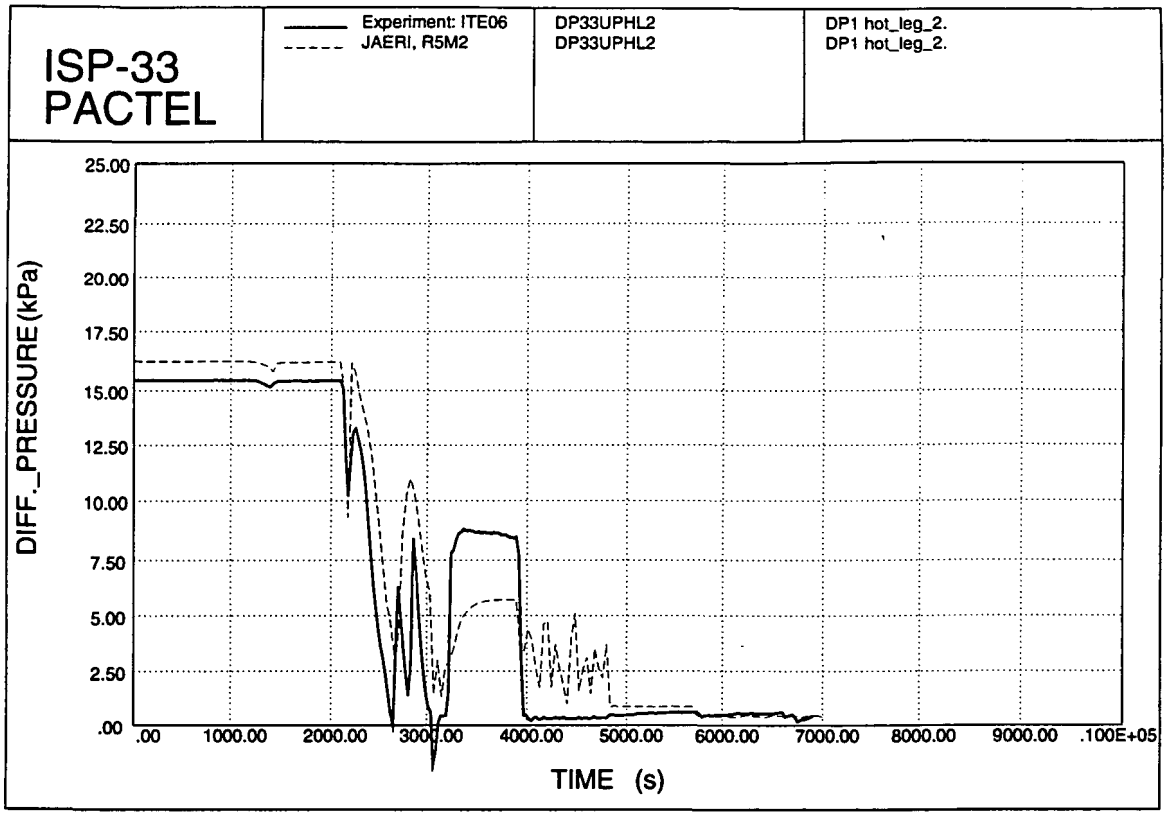

Figure 6.131. Hot leg 2 DP 1.

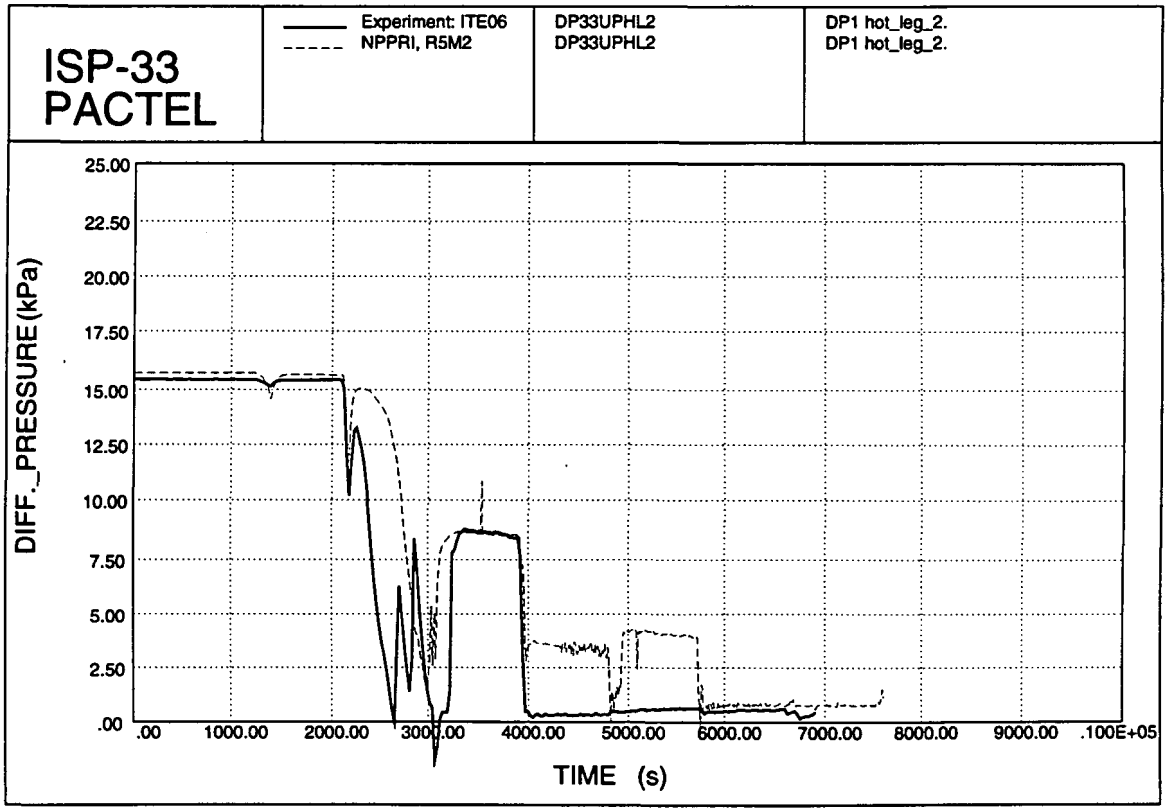

Figure 6.132. Hot leg 2 DP 1.

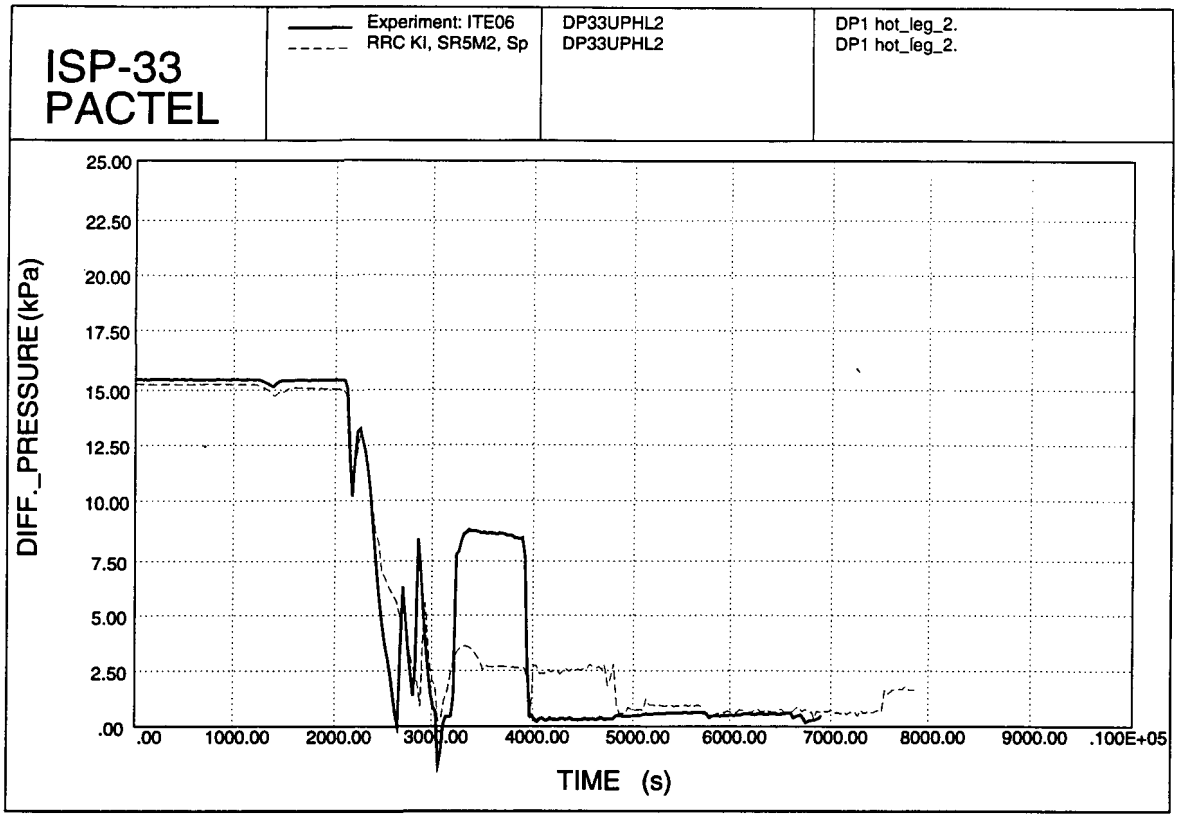

Figure 6.133. Hot leg 2 DP 1.

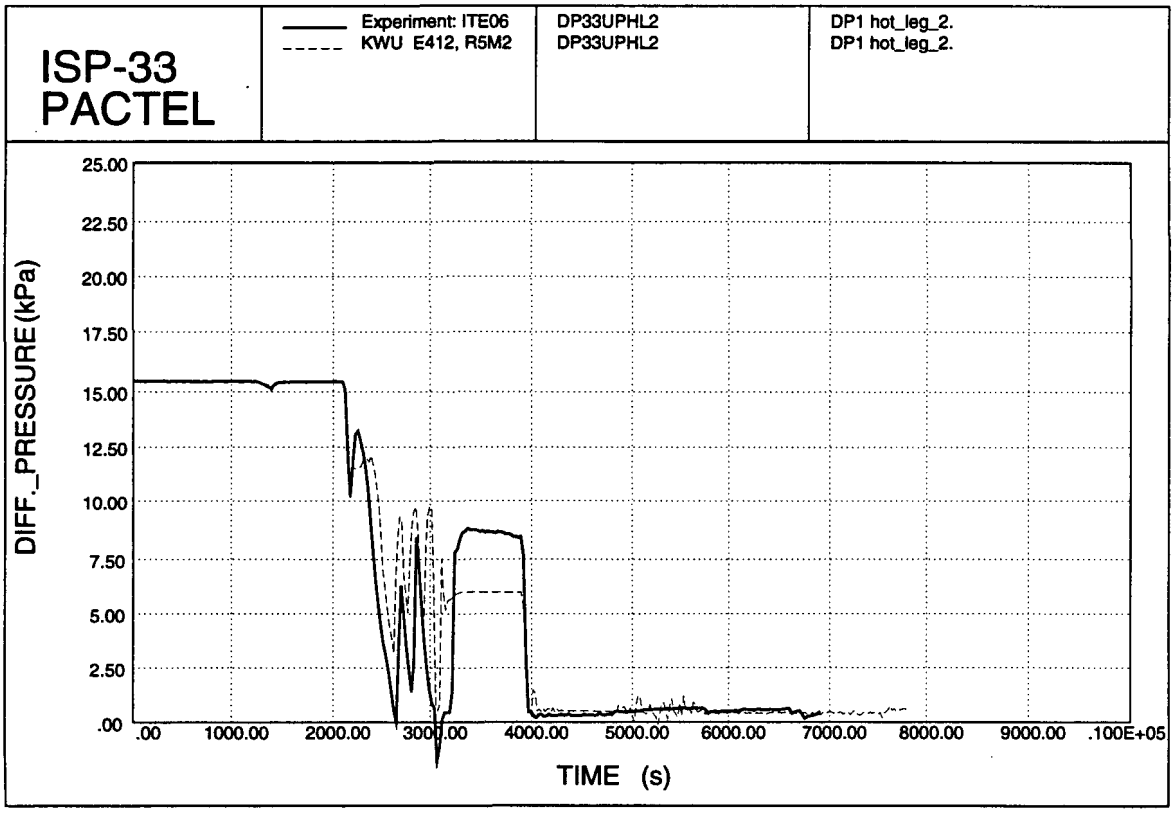

Figure 6.134. Hot leg 2 DP 1.

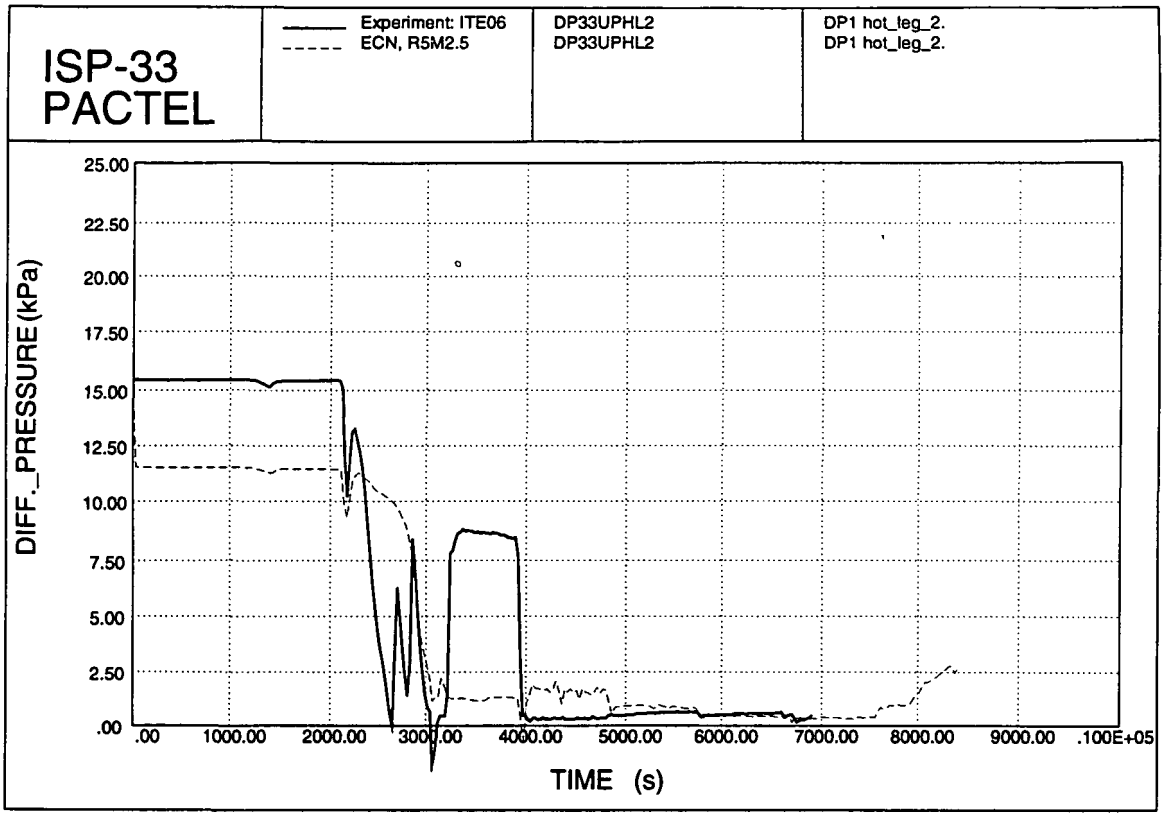

Figure 6.135. Hot leg 2 DP 1.

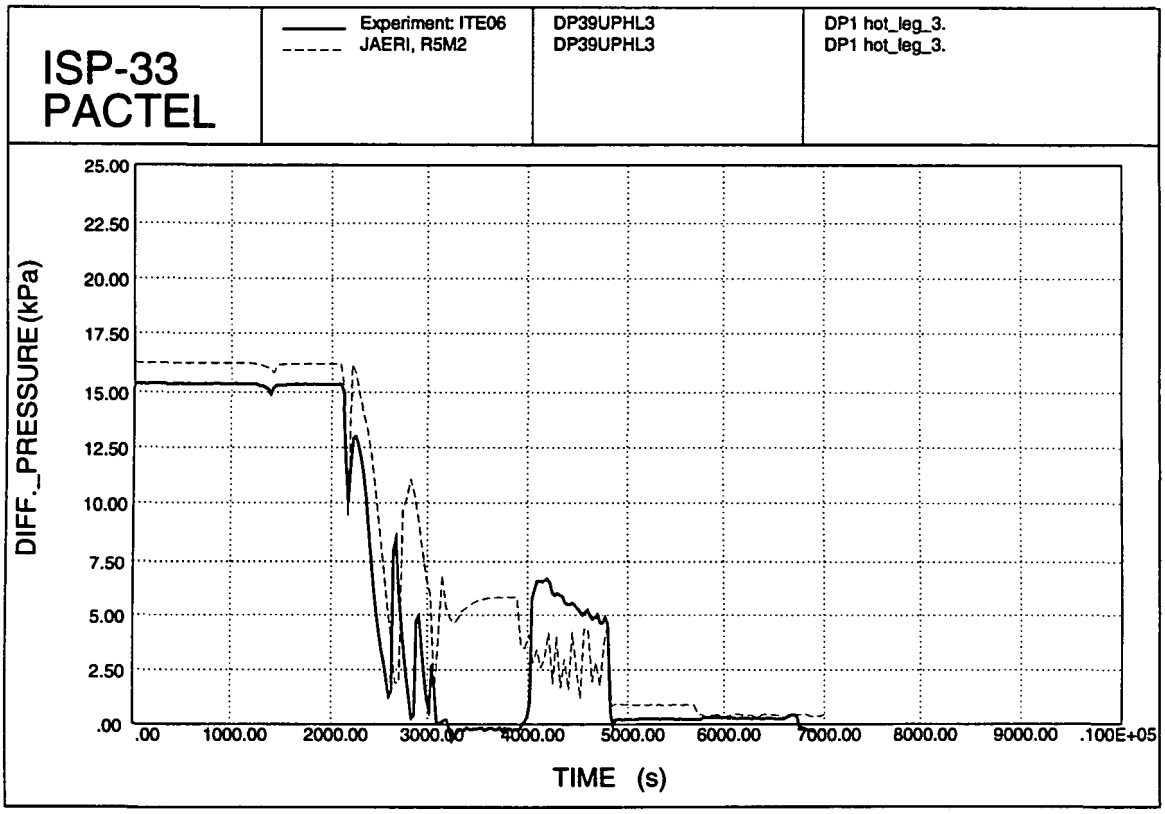

Figure 6.136. Hot leg 3 DP 1.

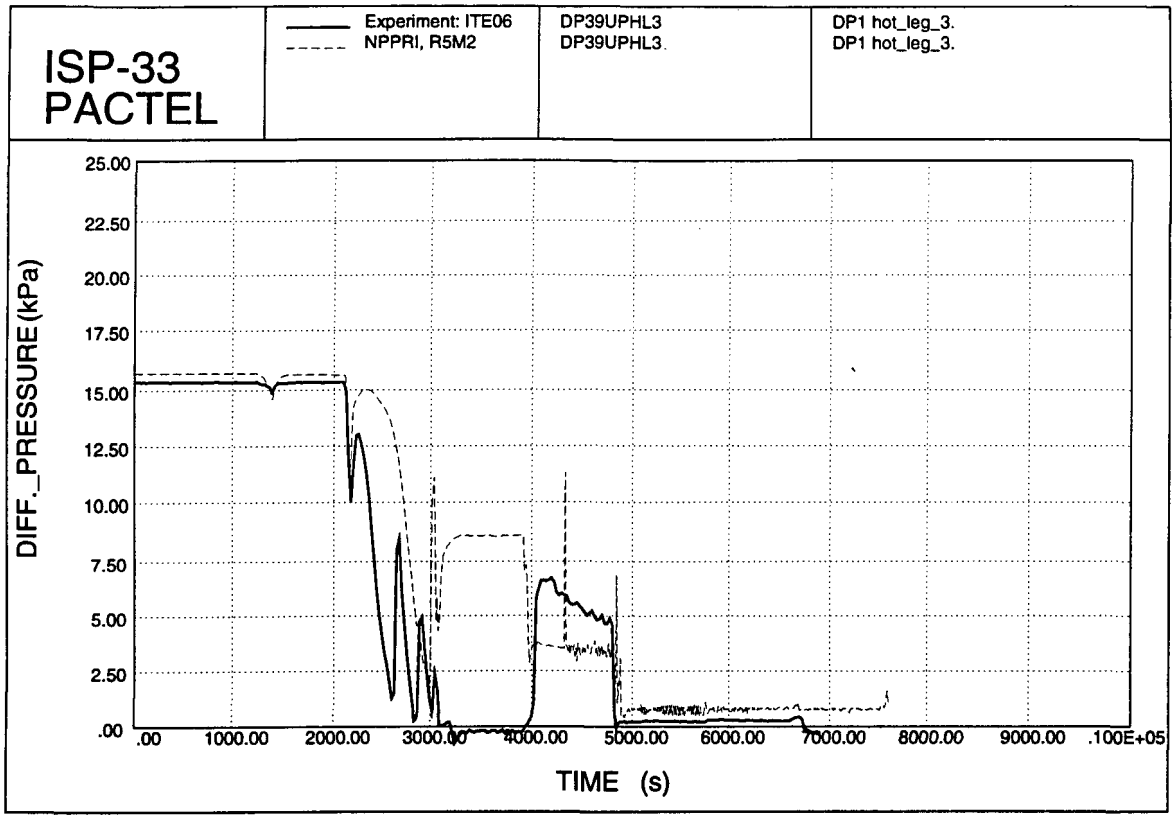

Figure 6.137. Hot leg 3 DP 1.

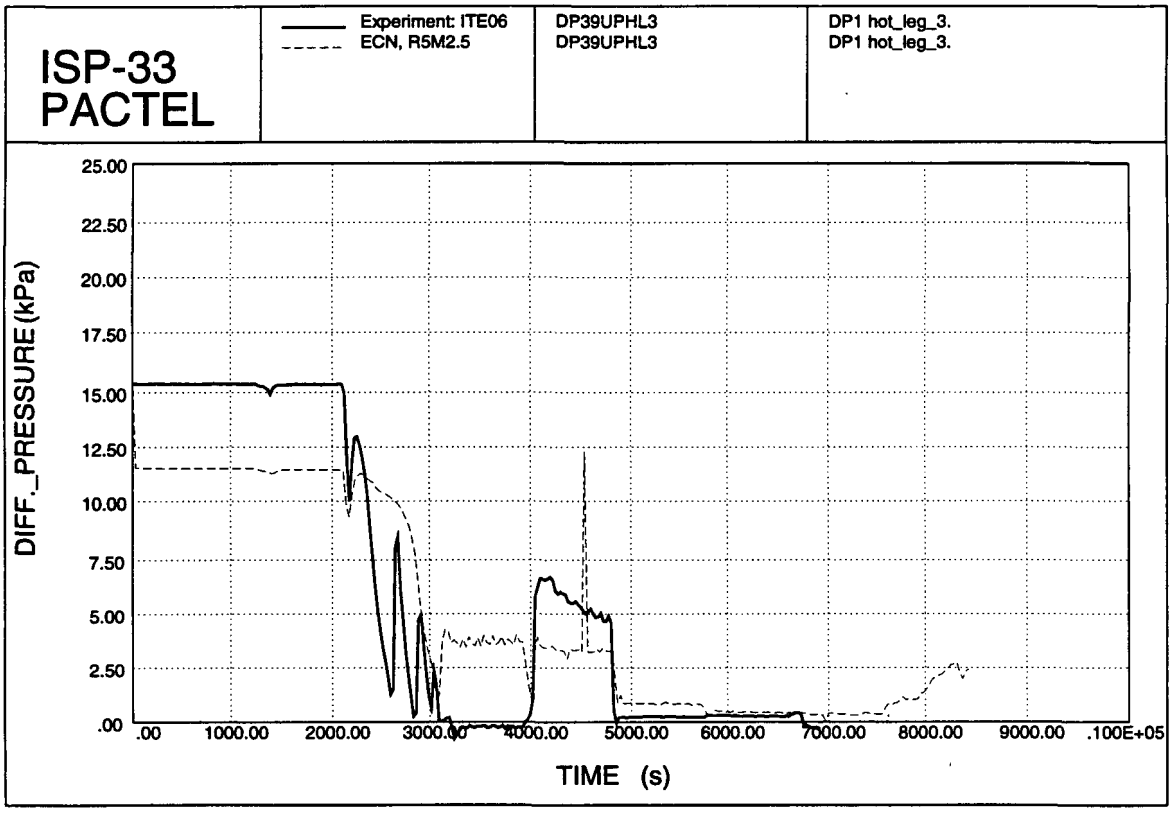

Figure 6.138. Hot leg 3 DP 1.

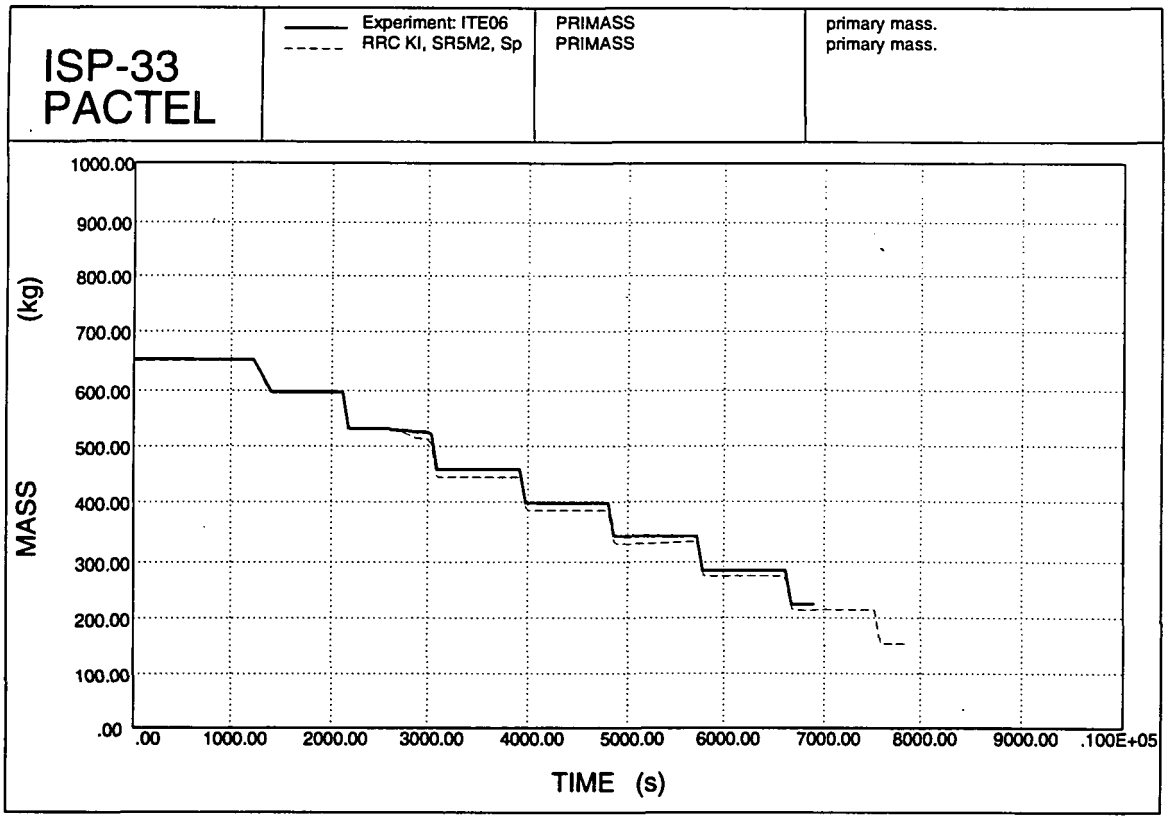

Figure 6.139. Primary mass inventory.

6.3 Conclusions of Posttest Calculations

All participants used the recommended 10 kW higher core power (165 kW) than originally specified. Also, the leakage of the safety valve at the top of the upper plenum was taken into the account in all the calculations. Other changes compared to the blind calculations included the corrections of the initial coolant inventory, renodalization of the upper plenum and the pressurizer to achieve circulation, reduction of heat losses and modifications in condensation correlations. The primary pressure in the experiment and the variation of posttest results are presented in Figure 6.140.

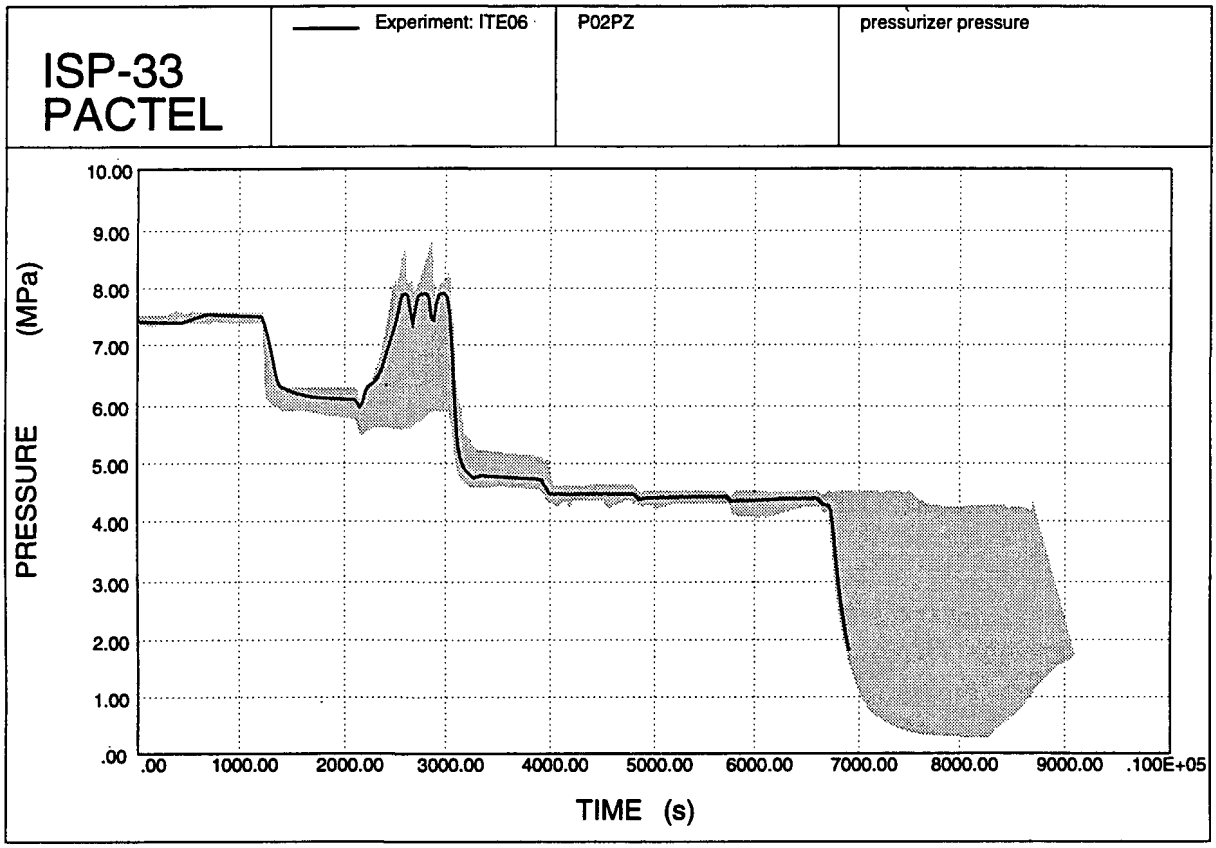

Figure 6.140 Primary pressure and the variation of posttest results.

6.3.1 ATHLET calculations

In all ATHLET calculations the initial conditions and loop behaviour before the first draining are in good agreement with experimental results. In HTWS and GRS calculations primary pressure behaviour is identical to the experiment, in FRG/FZR results the primary pressure changes are somewhat slow. Hot leg loop temperatures differ from the experimental values only a little bit. Downcomer mass flow rate in HTWS calculation is about 1.4 kg/s instead of the measured 1.5 kg/s.

After the first draining (at 1200 s) the mass flow rates and the temperatures remain the same as before the draining. Some steam exists in the upper plenum in HTWS calculation due to the higher temperature. The pressurizer level also stays a bit higher than in the experiment. Other parameters agree well with measured results.

The second draining (at 2100 s) brings the primary level close to hot leg connections in HTWS and GRS calculations but in FRG/FZR results the coolant level remains somewhat too high.

After the draining the primary level decreases further and reaches the hot leg connections while pressurizer is refilling in all calculations. The amount of steam increases in hot leg loop seals and causes flow stagnation and repressurization. In HTWS calculation the transient behaviour is well predicted but with only two pressure peaks. GRS results deviate a bit more from experimental results having also two pressure peaks. In FRG/FZR calculation repressurization is delayed due to the higher primary level, but stagnation still takes place before the next draining.

After the third draining (at 3000 s) all results agree well with measured values. Asymmetric flow takes place in all calculations and downcomer mass flow rates are well predicted.

The next two drainings (at 3900 s and 4800 s) both cause slight decrease in downcomer mass flow rate in experimental data. This is very well predicted only in FRG/FZR calculation. GRS predicts that the mass flow rate maintains previous higher values. In HTWS calculation the downcomer mass flow rate is underestimated, but stays almost constant until the boiler-condenser mode begins. The boiler-condenser mode takes place after the sixth draining in all three calculations. Core heat-up is calculated to begin after the 8th draining (one too many).

6.3.2 CATHARE calculations

The initial conditions and the first 2100 s in both CATHARE calculations agree well with experimental data, except the differential pressure values in loops are not well predicted by UP-DCMN calculation. Fluid temperatures in the SG tubes are overestimated by UP-DCMN results.

After the second draining (at 2100 s) the flow stagnation is delayed in UP-DCMN calculation, and the repressurization takes place too late. The primary pressure and the downcomer mass flow rates in SEMAR LEACS calculation agree well with experimental data.

The pressure decrease after the third draining (at 3000 s) is well predicted by SEMAR-LEACS calculation, but underestimated by UP-DCMN. The mass flow rates are in good agreement with experimental data, and asymmetric loop flow takes place in both calculations.

The primary pressure and the temperatures after the fourth draining (at 3900 s) are well predicted by UP-DCMN calculation for the rest of the transient. The core heat-up also occurs correctly after the seventh draining. SEMAR-LEACS needs one additional draining (the 8th) to reach the beginning of core heat-up.

UP-DCMN modelled the steam generator with vertical u-tubes. SEMAR LEACS used predefined secondary feedwater injection mass flow rates, (not actual injection to control secondary level). This could lead to a situation, where the secondary coolant temperature, rather than the behaviour of the loop seals, determines the asymmetric behaviour of the loops. Missing information on the level and differential pressures makes it difficult to compare both results.

6.3.3 RELAP5/MOD3 calculations

The initial conditions and first 2100 s of transient are well calculated by all participants. RRC KI (Devkin) calculation overestimates the primary level. The initial downcomer mass flow rate is underestimated by 0.2 kg/s in RSC KI (Stolchnev) calculation. The primary pressure and pressurizer heater behaviour is predicted reasonably well. RRC KI (Stolchnev) uses constant primary pressure. The primary level drops already during the first draining (at 1200 s) in both RRC KI (Devkin) and TAEK calculations. Pressurizer level stays too high in both calculations.

The second draining (at 2100 s) brings the primary level to the hot leg connection region in all calculations, except in TAEK calculation. RRC KI (Stolchnev) results include no level information. NPPRI, RRC KI (Devkin), NRI and IJS have reproduced the stagnations and pressure peaks. The leakage through the upper plenum safety valve does not have much influence on the transient behaviour. However, modelling the leakage gives somewhat better results during this phase.

After the third draining (at 3000 s) asymmetric loop flow takes place according to all calculations, but the mass flow rates are overestimated by all participants. For the rest of the transient mass flows deviate more from the measured values. NRI results agree well with experimental data, but NPPRI and both RRC KI calculations reach the boiler-condenser mode already after the fourth draining (at 3900 s). Others overestimate the downcomer flow rate by a factor of two.

NRI and RRC KI (Stolchnev) calculate the core heat-up to begin after the seventh draining, others need one or two additional drainings. A mass error in RRC KI (Devkin) calculation increased the coolant inventory and delayed the core heat-up. Coolant distribution in the circuit has been improved by declining the horizontal steam generator tubes in NRI calculation. This artificial way of modelling seems to confirm the ability of the horizontal tubes to retain coolant in the tubes.

6.3.4 RELAP5/MOD2, RELAP5/MOD2.5 and SCDAP/RELAP5/MOD2.5 calculations

The initial conditions of the experiment have been well calculated by all participants, but pressurizer heater cycling is not predicted by all calculations. KWU (Siemens) has a slightly too low downcomer coolant mass flow rate. Generally, the first 2100 s has been calculated well by all participants. The behaviour of primary and pressurizer levels agree well with the experimental data.

After the second draining (at 2100 s) primary level is close to the hot leg connections. In KWU calculation primary level decrease is too slow. All calculations predict at least one flow stagnation. ECN predicts stagnation just before the next draining.

The third draining (at 3000 s) empties the pressurizer again, and steady two-phase flow takes place in all calculations. In JAERI results the loop flows are asymmetric at first, but change to symmetric flow after 3400 s. Also the downcomer mass flow rate is increasing and overestimated by factor of two. Other participants predict asymmetric loop flow, and the measured flow rates are closer to the measured values.

After the fourth draining (at 3900 s) the overall transient behaviour is well predicted although there are some differences in loop flow and differential pressures in the loops. ECN predicts incorrectly that downcomer flow rate is increasing after this draining.

The core heat-up is not calculated to occur soon after the seventh draining as in the experiment.

7. CONCLUSIONS

ISP33 is the first CSNI standard problem related to VVER type of pressurized water reactors. The reference reactors of the PACTEL test facility, which was used for carrying out the ISP33 experiment, are the two VVER-440 units, which are located near the Finnish city of Loviisa.

The objective of the ISP33 Test was to study the natural circulation behaviour of VVER-440 reactors at different coolant inventories, and to study the effect of opening a relief valve in the secondary side. The ISP was conducted as a double-blind problem.

Natural circulation was considered as a particularly suitable phenomenon to focus on by the first VVER related ISP due to its fundamental importance in most accidents and transients, and due to the expected different behaviour compared to Western type of PWRs. The difference is mainly due to the effect of horizontal steam generators and the hot leg loop seals.

The experiment was started with single-phase liquid flow at full coolant inventory. The inventory was reduced stepwise at about 900 second intervals draining 60 kg each time from the bottom of the lower plenum. The core power was about 3.7 % of the nominal value. The test was terminated soon after the cladding temperatures began to rise. After the experiment had been performed it was discovered that the safety valve at the top of the upper plenum had probably leaked (approximately 10 kg of coolant was lost), and that the correct value for the power was somewhat larger than originally given, 165 kW instead of 155 kW (±9 kW). This information was not available for the blind calculations, but apparently did not have a major effect.

The results of 21 double-blind calculations from 15 organizations in 12 countries (Finland not included) were submitted. Five of the countries were not members of the OECD/NEA. Eight codes were used: ATHLET 1.0, CATHARE2, RELAP5 (MODs 3, 2.5 and 2), RELAP4/MOD6, DINAMIKA5 and TECH-M4.

The overall transient was reasonably well calculated by all codes except by RELAP4/MOD6 indicating the limitations of the old conservative codes. However, some shortcomings were also encountered with respect the capabilities of the advanced best-estimate codes.

The main discrepancies were noticed in the prediction of the flow stagnations and the three pressure spikes after the second draining, and the time of the core heat-up at the end of the test. The heat-up was calculated to occur more or less too late. These problems were mainly due to the inability to calculate accurately the behaviour of the hot leg loop seals and the accumulation of water in the horizontal steam generator tubes. The 2-phase natural circulation flow rate and the refilling rate of the pressurizer at the end of the test were generally overpredicted. The stagnations were predicted well by two participants (Institute "Jozef Stefan", Slovenia, and NPP Research Institute, Slovakia, using RELAP5/MOD3 and MOD2 respectively). The correct time of the core heat-up was predicted by only one participant (University of Pisa DCMN, using CATHARE). According to both a quantitative accuracy evaluation using the Fast Fourier Transform (FFT) method of the University of Pisa and a qualitative evaluation the best overall results were obtained by Institute "Jozef Stefan". The scatter within the RELAP5/MOD2 results were larger than the scatter within other code results.

The results of 20 open (posttest) calculations from 14 organizations in 11 countries (four of them non-OECD) were submitted after the deadline for the blind result submittals. Five codes were used this time: ATHLET 1.0, CATHARE2 and RELAP5 (MODs 3, 2.5 and 2).

Compared to the blind calculations the results were improved. Some of the posttest calculations can be considered excellent. Only a few problem areas remain. According to both the quantitative and the qualitative accuracy evaluations the best overall results were obtained by the Nuclear Research Institute, Czech Republic, using RELAP5/MOD3, and by GRS, Germany, using ATHLET. Judging qualitatively the results of the posttest calculation by IPSN Cadarache (SEMAR LEACS) were also excellent, but due to some missing parameters they were not evaluated quantitatively. This time the scatter within the RELAP5/MOD3 results was larger than the scatter within the other code results.

The input modifications for the posttest calculations included addition of a model for the safety valve and allowing for a leak through it, increase of the power from 155 kW to 165 kW, decrease of the pressurizer heat losses and corrections to the coolant mass, the pressure losses etc.

In addition, there were some artificial changes. The Nuclear Research Institute, Czech Republic, tilted the steam generator tubes in order to investigate whether the assumption of accumulation of water in the steam generator tubes was a proper one. Two participants added a circulation in the pressurizer. Several participants used a circulation in the upper plenum in both blind and open calculations.

The remaining problems have to do with the accurate calculation of the loop seal behaviour and accumulation of water inside the steam generators leading to a too late core heat-up. Also, the codes tend to overpredict 2-phase natural circulation flow rate in case of small gravitational driving heads. As expected, the accuracy of the calculated results decreases clearly with time as the deviations from reality accumulate.

In summary, despite of some inaccuracies in the original specifications ISP33 proved to be a successful and valuable exercise with a wider than expected participation. The reasons for the observed discrepancies were easier to investigate than in most ISPs, because the experiment was not excessively complicated. Due to large number of participants the effort for the (small) hosting team was again rather excessive, although the experience surely warranted it.